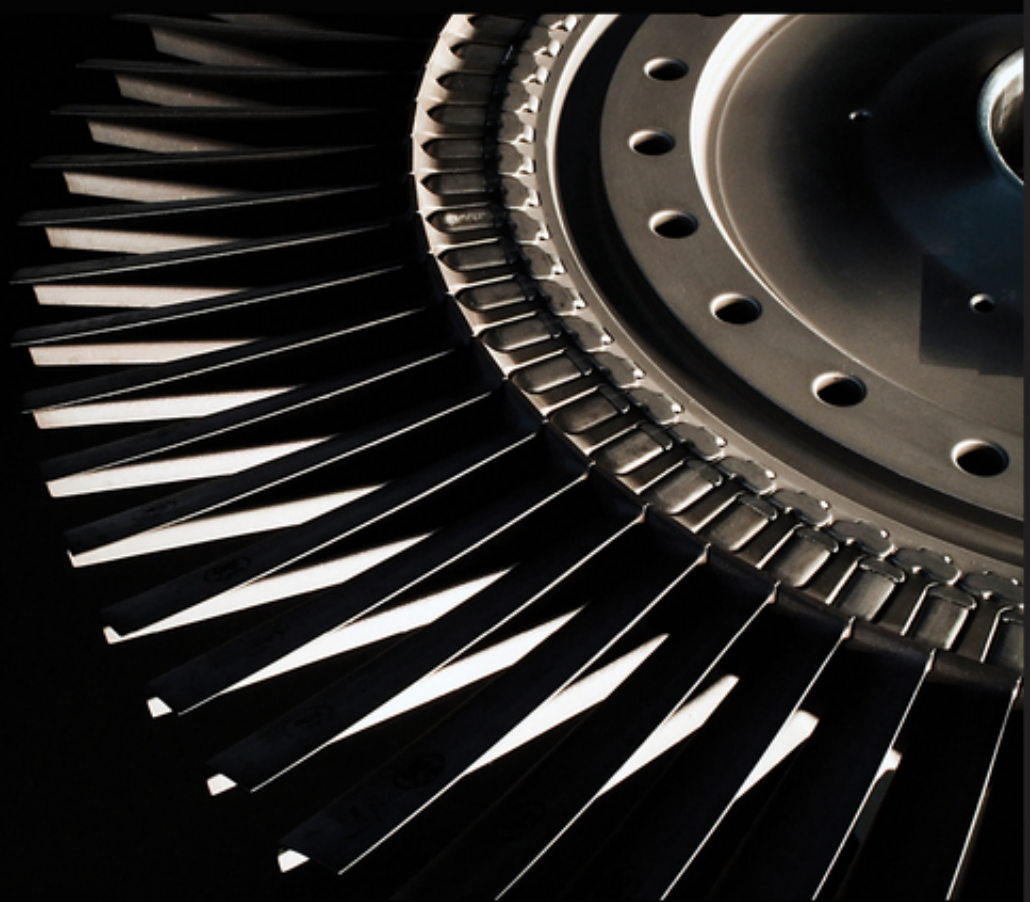


PRINCIPLES OF **TURBOMACHINERY**

SECOND EDITION

SEPPO A. KORPELA



WILEY

PRINCIPLES OF TURBOMACHINERY

PRINCIPLES OF TURBOMACHINERY

Second Edition

Seppo A. Korpela
The Ohio State University

WILEY

This edition first published 2020
© 2020 John Wiley & Sons, Inc.

Edition History

“John Wiley & Sons Inc. (1e, 2010)”.

All rights reserved. No part of this publication may be reproduced, stored in a retrieval system, or transmitted, in any form or by any means, electronic, mechanical, photocopying, recording or otherwise, except as permitted by law. Advice on how to obtain permission to reuse material from this title is available at <http://www.wiley.com/go/permissions>.

The right of Seppo A. Korpela to be identified as the author of this work has been asserted in accordance with law.

Registered Office

John Wiley & Sons, Inc., 111 River Street, Hoboken, NJ 07030, USA

Editorial Office

111 River Street, Hoboken, NJ 07030, USA

For details of our global editorial offices, customer services, and more information about Wiley products visit us at www.wiley.com.

Wiley also publishes its books in a variety of electronic formats and by print-on-demand. Some content that appears in standard print versions of this book may not be available in other formats.

Limit of Liability/Disclaimer of Warranty

In view of ongoing research, equipment modifications, changes in governmental regulations, and the constant flow of information relating to the use of experimental reagents, equipment, and devices, the reader is urged to review and evaluate the information provided in the package insert or instructions for each chemical, piece of equipment, reagent, or device for, among other things, any changes in the instructions or indication of usage and for added warnings and precautions. While the publisher and authors have used their best efforts in preparing this work, they make no representations or warranties with respect to the accuracy or completeness of the contents of this work and specifically disclaim all warranties, including without limitation any implied warranties of merchantability or fitness for a particular purpose. No warranty may be created or extended by sales representatives, written sales materials or promotional statements for this work. The fact that an organization, website, or product is referred to in this work as a citation and/or potential source of further information does not mean that the publisher and authors endorse the information or services the organization, website, or product may provide or recommendations it may make. This work is sold with the understanding that the publisher is not engaged in rendering professional services. The advice and strategies contained herein may not be suitable for your situation. You should consult with a specialist where appropriate. Further, readers should be aware that websites listed in this work may have changed or disappeared between when this work was written and when it is read. Neither the publisher nor authors shall be liable for any loss of profit or any other commercial damages, including but not limited to special, incidental, consequential, or other damages.

Library of Congress Cataloging-in-Publication Data

Names: Korpela, S. A., author.

Title: Principles of turbomachinery / Seppo A. Korpela, The Ohio State University.

Description: Second edition. | Hoboken, NJ, USA : John Wiley & Sons, Inc., 2019. | Includes bibliographical references and index. |

Identifiers: LCCN 2019001992 (print) | LCCN 2019002189 (ebook) | ISBN 9781119518112 (Adobe PDF) | ISBN 9781119518099 (ePub) | ISBN 9781119518082 (hardback)

Subjects: LCSH: Turbomachines.

Classification: LCC TJ267 (ebook) | LCC TJ267 .K57 2019 (print) | DDC 621.406—dc23

LC record available at <https://lcn.loc.gov/2019001992>

Cover design by Wiley

Cover image: © Fertnig/Getty Images

Set in 10/12pt NimbusRomNo9L by SPi Global, Chennai, India

Printed in the United States of America

10 9 8 7 6 5 4 3 2 1

*To my wife Terttu,
to our daughter Liisa,
and to the memory of our
daughter Katja*

CONTENTS

| | |
|---|----------|
| Foreword | xv |
| Acknowledgments | xvii |
| About the Companion Website | xix |
| 1 Introduction | 1 |
| 1.1 Energy and Fluid Machines | 1 |
| 1.1.1 Energy conversion of fossil fuels | 1 |
| 1.1.2 Steam turbines | 2 |
| 1.1.3 Gas turbines | 3 |
| 1.1.4 Hydraulic turbines | 4 |
| 1.1.5 Wind turbines | 5 |
| 1.1.6 Compressors | 5 |
| 1.1.7 Pumps and blowers | 5 |
| 1.1.8 Other uses and issues | 6 |
| 1.2 Historical Survey | 7 |
| 1.2.1 Water power | 7 |
| 1.2.2 Wind turbines | 8 |
| 1.2.3 Steam turbines | 9 |
| 1.2.4 Jet propulsion | 10 |
| 1.2.5 Industrial turbines | 11 |

| | | |
|----------|--|-----------|
| 1.2.6 | Pumps and compressors | 11 |
| 1.2.7 | Note on units | 12 |
| 2 | Principles of Thermodynamics and Fluid Flow | 15 |
| 2.1 | Mass Conservation Principle | 15 |
| 2.2 | First Law of Thermodynamics | 17 |
| 2.3 | Second Law of Thermodynamics | 19 |
| 2.3.1 | Tds -equations | 19 |
| 2.4 | Equations of State | 20 |
| 2.4.1 | Properties of steam | 21 |
| 2.4.2 | Ideal gases | 27 |
| 2.4.3 | Air tables and isentropic relations | 29 |
| 2.4.4 | Ideal gas mixtures | 32 |
| 2.4.5 | Incompressibility | 36 |
| 2.4.6 | Stagnation state | 37 |
| 2.5 | Efficiency | 37 |
| 2.5.1 | Efficiency measures | 37 |
| 2.5.2 | Thermodynamic losses | 43 |
| 2.5.3 | Incompressible fluid | 45 |
| 2.5.4 | Compressible flows | 46 |
| 2.6 | Momentum Balance | 48 |
| | Exercises | 56 |
| 3 | Compressible Flow | 63 |
| 3.1 | Mach Number and The Speed of Sound | 63 |
| 3.1.1 | Mach number relations | 65 |
| 3.2 | Isentropic Flow with Area Change | 67 |
| 3.2.1 | Converging nozzle | 71 |
| 3.3 | Influence of Friction on Flow Through Nozzles | 73 |
| 3.3.1 | Polytropic efficiency | 73 |
| 3.3.2 | Loss coefficients | 77 |
| 3.3.3 | Nozzle efficiency | 81 |
| 3.3.4 | Combined Fanno flow and area change | 82 |
| 3.4 | Supersonic Nozzle | 87 |
| 3.5 | Normal Shocks | 90 |
| 3.5.1 | Rankine–Hugoniot relations | 95 |
| 3.6 | Moving Shocks | 98 |
| 3.7 | Oblique Shocks and Expansion Fans | 100 |
| 3.7.1 | Mach waves | 100 |
| 3.7.2 | Oblique shocks | 101 |
| 3.7.3 | Supersonic flow over a rounded concave corner | 107 |
| 3.7.4 | Reflected shocks and shock interactions | 108 |

| | | |
|----------|---|------------|
| 3.7.5 | Mach reflection | 110 |
| 3.7.6 | Detached oblique shocks | 110 |
| 3.7.7 | Prandtl–Meyer theory | 112 |
| | Exercises | 124 |
| 4 | Gas Dynamics of Wet Steam | 131 |
| 4.1 | Compressible Flow of Wet Steam | 132 |
| 4.1.1 | Clausius–Clapeyron equation | 132 |
| 4.1.2 | Adiabatic exponent | 133 |
| 4.2 | Conservation Equations for Wet Steam | 137 |
| 4.2.1 | Relaxation times | 139 |
| 4.2.2 | Conservation equations in their working form | 144 |
| 4.2.3 | Sound speeds | 146 |
| 4.3 | Relaxation Zones | 149 |
| 4.3.1 | Type I wave | 149 |
| 4.3.2 | Type II wave | 154 |
| 4.3.3 | Type III wave | 157 |
| 4.3.4 | Combined relaxation | 157 |
| 4.3.5 | Flow in a variable area nozzle | 159 |
| 4.4 | Shocks in Wet Steam | 161 |
| 4.4.1 | Evaporation in the flow after the shock | 164 |
| 4.5 | Condensation Shocks | 167 |
| 4.5.1 | Jump conditions across a condensation shock | 169 |
| | Exercises | 174 |
| 5 | Principles of Turbomachine Analysis | 177 |
| 5.1 | Velocity Triangles | 178 |
| 5.2 | Moment of Momentum Balance | 181 |
| 5.3 | Energy Transfer in Turbomachines | 182 |
| 5.3.1 | Trothalpy and specific work in terms of velocities | 186 |
| 5.3.2 | Degree of reaction | 189 |
| 5.4 | Utilization | 191 |
| 5.5 | Scaling and Similitude | 198 |
| 5.5.1 | Similitude | 198 |
| 5.5.2 | Incompressible flow | 199 |
| 5.5.3 | Shape parameter or specific speed and specific diameter | 202 |
| 5.5.4 | Compressible flow analysis | 206 |
| 5.6 | Performance Characteristics | 208 |
| 5.6.1 | Compressor performance map | 208 |
| 5.6.2 | Turbine performance map | 209 |
| | Exercises | 210 |

| | | |
|----------|--|------------|
| 6 | Steam Turbines | 215 |
| 6.1 | Introduction | 215 |
| 6.2 | Impulse Turbines | 217 |
| 6.2.1 | Single-stage impulse turbine | 217 |
| 6.2.2 | Pressure compounding | 226 |
| 6.2.3 | Blade shapes | 230 |
| 6.2.4 | Velocity compounding | 233 |
| 6.3 | Stage with Zero Reaction | 238 |
| 6.4 | Loss Coefficients | 241 |
| | Exercises | 243 |
| 7 | Axial Turbines | 247 |
| 7.1 | Introduction | 247 |
| 7.2 | Turbine Stage Analysis | 249 |
| 7.3 | Flow and Loading Coefficients and Reaction Ratio | 253 |
| 7.3.1 | Fifty percent (50%) stage | 258 |
| 7.3.2 | Zero percent (0%) reaction stage | 262 |
| 7.3.3 | Off-design operation | 263 |
| 7.3.4 | Variable axial velocity | 265 |
| 7.4 | Three-Dimensional Flow and Radial Equilibrium | 267 |
| 7.4.1 | Free vortex flow | 269 |
| 7.4.2 | Fixed blade angle | 273 |
| 7.4.3 | Constant mass flux | 273 |
| 7.5 | Turbine Efficiency and Losses | 276 |
| 7.5.1 | Soderberg loss coefficients | 276 |
| 7.5.2 | Stage efficiency | 277 |
| 7.5.3 | Stagnation pressure losses | 279 |
| 7.5.4 | Performance charts | 285 |
| 7.5.5 | Zweifel correlation | 290 |
| 7.5.6 | Further discussion of losses | 291 |
| 7.5.7 | Ainley–Mathieson correlation | 293 |
| 7.5.8 | Secondary loss | 296 |
| 7.6 | Multistage Turbine | 302 |
| 7.6.1 | Reheat factor in a multistage turbine | 302 |
| 7.6.2 | Polytropic or small-stage efficiency | 304 |
| | Exercises | 305 |
| 8 | Axial Compressors | 311 |
| 8.1 | Compressor Stage Analysis | 312 |
| 8.1.1 | Stage temperature and pressure rise | 313 |
| 8.1.2 | Analysis of a repeating stage | 315 |

| | | |
|----------|---|------------|
| 8.2 | Design Deflection | 321 |
| 8.2.1 | Compressor performance map | 324 |
| 8.3 | Radial Equilibrium | 326 |
| 8.3.1 | Modified free vortex velocity distribution | 327 |
| 8.3.2 | Velocity distribution with zero-power exponent | 330 |
| 8.3.3 | Velocity distribution with first-power exponent | 331 |
| 8.4 | Diffusion Factor | 333 |
| 8.4.1 | Momentum thickness of a boundary layer | 335 |
| 8.5 | Efficiency and Losses | 339 |
| 8.5.1 | Efficiency | 339 |
| 8.5.2 | Parametric calculations | 342 |
| 8.6 | Cascade Aerodynamics | 343 |
| 8.6.1 | Blade shapes and terms | 344 |
| 8.6.2 | Blade forces | 345 |
| 8.6.3 | Other losses | 347 |
| 8.6.4 | Diffuser performance | 348 |
| 8.6.5 | Flow deviation and incidence | 349 |
| 8.6.6 | Multi-stage compressor | 351 |
| 8.6.7 | Compressibility effects | 352 |
| 8.6.8 | Design of a compressor | 353 |
| | Exercises | 359 |
| 9 | Centrifugal Compressors and Pumps | 363 |
| 9.1 | Compressor Analysis | 364 |
| 9.1.1 | Slip factor | 365 |
| 9.1.2 | Pressure ratio | 367 |
| 9.2 | Inlet Design | 374 |
| 9.2.1 | Choking of the inducer | 379 |
| 9.3 | Exit Design | 381 |
| 9.3.1 | Performance characteristics | 381 |
| 9.3.2 | Diffusion ratio | 384 |
| 9.3.3 | Blade height | 385 |
| 9.4 | Vaneless Diffuser | 387 |
| 9.5 | Centrifugal Pumps | 391 |
| 9.5.1 | Specific speed and specific diameter | 395 |
| 9.6 | Fans | 403 |
| 9.7 | Cavitation | 404 |
| 9.8 | Diffuser and Volute Design | 406 |
| 9.8.1 | Vaneless diffuser | 406 |
| 9.8.2 | Volute design | 407 |
| | Exercises | 411 |

| | | |
|-----------|--|------------|
| 10 | Radial Inflow Turbines | 415 |
| 10.1 | Turbine Analysis | 416 |
| 10.2 | Efficiency | 421 |
| 10.3 | Specific Speed and Specific Diameter | 425 |
| 10.4 | Stator Flow | 431 |
| 10.4.1 | Loss coefficients for stator flow | 436 |
| 10.5 | Design of the Inlet of a Radial Inflow Turbine | 440 |
| 10.5.1 | Minimum inlet Mach number | 441 |
| 10.5.2 | Blade stagnation Mach number | 447 |
| 10.5.3 | Inlet relative Mach number | 449 |
| 10.6 | Design of the Exit | 450 |
| 10.6.1 | Minimum exit Mach number | 450 |
| 10.6.2 | Radius ratio r_{3s}/r_2 | 453 |
| 10.6.3 | Blade height-to-radius ratio b_2/r_2 | 454 |
| 10.6.4 | Optimum incidence angle and the number of blades | 455 |
| | Exercises | 460 |
| 11 | Hydraulic Turbines | 463 |
| 11.1 | Hydroelectric Power Plants | 463 |
| 11.2 | Hydraulic Turbines and their Specific Speed | 465 |
| 11.3 | Pelton Wheel | 467 |
| 11.4 | Francis Turbine | 475 |
| 11.5 | Kaplan Turbine | 483 |
| 11.6 | Cavitation | 486 |
| | Exercises | 488 |
| 12 | Hydraulic Transmission of Power | 491 |
| 12.1 | Fluid Couplings | 491 |
| 12.1.1 | Fundamental relations | 492 |
| 12.1.2 | Flow rate and hydrodynamic losses | 494 |
| 12.1.3 | Partially filled coupling | 496 |
| 12.2 | Torque Converters | 497 |
| 12.2.1 | Fundamental relations | 497 |
| 12.2.2 | Performance | 500 |
| | Exercises | 504 |
| 13 | Wind Turbines | 507 |
| 13.1 | Horizontal-Axis Wind Turbine | 508 |
| 13.2 | Momentum Theory of Wind Turbines | 509 |
| 13.2.1 | Axial momentum | 509 |
| 13.2.2 | Ducted wind turbine | 514 |

| | | |
|---|--|-----|
| 13.2.3 | Wake rotation | 516 |
| 13.2.4 | Irrotational wake | 518 |
| 13.3 | Blade Element Theory | 522 |
| 13.3.1 | Nonrotating wake | 522 |
| 13.3.2 | Wake with rotation | 525 |
| 13.3.3 | Ideal wind turbine | 530 |
| 13.3.4 | Prandtl's tip correction | 532 |
| 13.4 | Turbomachinery and Future Prospects for Energy | 535 |
| | Exercises | 536 |
| Appendix A: Streamline Curvature and Radial Equilibrium | | 539 |
| A.1 | Streamline Curvature Method | 539 |
| A.1.1 | Fundamental equations | 539 |
| A.1.2 | Formal solution | 543 |
| Appendix B: Thermodynamic Tables | | 545 |
| References | | 559 |
| Index | | 565 |

Foreword

Turbomachines are important machines in our industrial civilization. Steam turbines are used to generate electricity at central station power plants, whether fueled by coal or uranium. Gas turbines and axial compressors are found in jet engines. Aero-derivative gas turbines are used to generate electricity with natural gas as fuel. Same technology is used to drive centrifugal compressors for transmission of natural gas across continents. Blowers and fans are in use for mine and industrial ventilation. Large pumps provide feed-water to boilers and move wastewater in sanitation plants. Hydraulic turbines generate electricity from water stored in reservoirs, and wind turbines do the same from the blowing wind.

This is a textbook on turbomachines. It aims for a unified treatment of the subject matter, with consistent notation and concepts. Chapter 4 is new to this edition. It consists of an account of droplet laden flows of steam that is relevant to the flow in the low pressure end of a steam turbine. It is quite specialized and ought to be left for an advanced course, or later self-study. Similarly, the new section on oblique shocks in Chapter 3 is included as background material for understanding phenomena in transonic compressors. Those with a background on thermodynamics and gas dynamics, may just glance through Chapter 2 and early parts of Chapter 3. Some sample computer codes are given in the text. They are based on MATLAB and its equivalent GNU-OCTAVE. The latter is free software and tailored to be compatible with MATLAB. In the Appendix B is a script that can be used in the calculations of air with variable specific heats. The program XSTEAM by Magnus Holmgren is used when the properties of steam are needed. It is available from Mathworks website. <https://www.mathworks.com/matlabcentral/profile/authors/870351-magnus-holmgren>.

Acknowledgments

In preparing this second edition, I have benefitted from discussions with professor Anestis Kalfas, at the Aristotle University of Thessaloniki and with my former student V. Babu, a professor of Mechanical Engineering of the Indian Institute of Technology, Madras. Professor Kemeswararao Anupindi, also from IIT Madras, provided a long list of corrections. I am grateful for their help. I welcome the publication of this second edition, for it has given me the opportunity to include these corrections and many that I have been able to discover. Undoubtedly, few errors remain in the book, and I will be thankful to readers who take the time to point them out to me by e-mail at the address: korpela.1@osu.edu.

I am grateful for permission to use graphs and figures from various published works and wish to acknowledge the generosity of the various organization for granting the permission to use them. These include Figures 1.1 and 1.2 from Siemens press photo, Siemens AG; Figure 1.3, from Schmalenberger Strömungstechnologie AG; Figures 1.6 and 8.1 are by courtesy of MAN Diesel & Turbo SE, and Figures 5.12 and 5.13 are published by permission of BorgWarner Turbo Systems. Figure 3.11 is courtesy of Professor D. Papamaschou; Figures 11.3 and 11.11 are published under the GNU Free Documentation licenses with original courtesy of Voith Siemens Hydro. The Figure 11.9 is reproduced under the Gnu Free Documentation licence, with the original photo by Audrius Meskauskas. Figure 11.5 is also published under Gnu Free Documentation licence, and so is Figure 1.4 and by permission from Aermotor. The Institution of Mechanical Engineers has granted permission to reproduce Figures 4.10, 7.16, 8.6, 8.7, and 8.17. Figure 5.11 is published under agreement with NASA. The *Journal of the Royal Aeronautical Society* granted permission to publish Figure 7.11. Figures 7.19 and 7.20 are published under the Crown Stationary Office's Open Government Licence of UK. Figure 3.8 has been adapted from J. H. Keenan, *Thermodynamics*, MIT Press and Figure 10.6 from O. E. Balje, *Turbo*

machines – A guide to Selection and Theory. Permission to use Figures 13.13 and 13.15 from *Wind Turbine Handbook* by T. Burton, N. Jenkins, D. Sharpe, and E. Bossanyi has been granted by John Wiley & Sons.

I wish also to thank the editorial team at John Wiley & Sons, Bob Esposito, Martin Preuss, Michael Leventhal, Beryl Mesiahdas, Vishnu Priya and others, as well as belated thanks Christine Punzo, who edited the first edition.

I have been lucky to have Terttu as a wife and a companion in my life. She has been and continues to be very supportive of all my efforts.

S. A. K.

About the Companion Website

This book is accompanied by a companion website:



www.wiley.com/go/Korpela/PrinciplesTurbomachinery_2e

The website contains Solutions Manual for Principles of Turbomachinery

CHAPTER 1

INTRODUCTION

1.1 ENERGY AND FLUID MACHINES

The rapid development of modern industrial societies was made possible by the large-scale extraction of fossil fuels buried in the earth's crust. Today, oil makes up 33% of world's energy mix, coal's share is 30%, and that of natural gas is 24%, for a total of 87%. Hydropower contributes 7%, and nuclear's share is about 4%, and these increase the total from these sources to 98%. The final 2% is supplied by wind, geothermal energy, waste products, and solar energy [101]. Most of the biomass is excluded from these, for it is used largely locally, and thus, its contribution is difficult to calculate. The best estimates put its use at 10% of the total, in which case, the other percentages need to be adjusted downward appropriately [61].

1.1.1 Energy conversion of fossil fuels

Over the last two centuries, engineers have invented methods to convert the chemical energy stored in fossil fuels into usable forms. Foremost among them are methods for converting this energy into electricity. This is done in steam power plants, in which combustion of coal is used to vaporize steam, and the thermal energy of the steam is then converted to shaft work in a steam turbine. The shaft turns a generator that produces electricity. Nuclear power plants work on the same principle, with uranium, and in rare cases thorium, as the fuel.

Oil is used sparingly this way, and it is mainly refined to gasoline and diesel fuel. The refinery stream also yields residual heating oil, which goes to industry and to winter heating of houses. Gasoline and diesel oil are used in internal-combustion engines for transportation needs, mainly in automobiles and trucks, but also in trains. Ships are powered by diesel fuel and aircraft by jet fuel.

Natural gas is largely methane, and in addition to its importance in the generation of electricity, it is also used in some parts of the world as a transportation fuel. A good fraction of natural gas goes to winter heating of residential and commercial buildings and to chemical process industries as raw material.

Renewable energy sources include the potential energy of water behind a dam in a river and the kinetic energy of blowing winds. Both are used for generating electricity. Water waves and ocean currents also fall into the category of renewable energy sources, but their contributions are negligible today.

In all the aforementioned methods, conversion of energy to usable forms takes place in a *fluid machine*, and in these instances, they are *power-producing* machines. There are also *power-absorbing* machines, such as pumps and compressors, in which energy is transferred into a fluid stream.

In both power-producing and power-absorbing machines, energy transfer takes place between a fluid and a moving machine part. In *positive-displacement machines*, the interaction is between a fluid at high pressure and a reciprocating piston. Spark ignition and diesel engines are well-known machines of this class. Others include piston pumps, reciprocating and screw compressors, and vane pumps.

In *turbomachines*, energy transfer takes place between a *continuously flowing fluid stream* and a *set of blades rotating about a fixed axis*. The blades in a pump are part of an *impeller* that is fixed to a shaft. In an axial compressor, they are attached to a compressor *wheel*. In steam and gas turbines, the blades are fastened to a disk, which is fixed to a shaft, and the assembly is called a turbine *rotor*. Fluid is guided into the rotor by *stator vanes* that are fixed to the *casing* of the machine. The inlet stator vanes are also called *nozzles*, or in hydraulic turbines *inlet guide vanes*.

Examples of power-producing turbomachines are steam and gas turbines and water and wind turbines. The power-absorbing turbomachines include pumps, for which the working fluid is a liquid, and fans, blowers, and compressors, which transfer energy to gases.

Methods derived from the principles of thermodynamics and fluid dynamics have been developed to analyze the design and operation of these machines. These subjects, and heat transfer, are the foundation of *energy engineering*, a discipline central in the program of study of mechanical engineering.

1.1.2 Steam turbines

Central station power plants, fueled either by coal or uranium, employ steam turbines to convert the thermal energy of steam to shaft power to run electric generators. During the year 2016, coal provided 30%, and nuclear fuels 20%, of the electricity production in the United States. For the world, the corresponding numbers are 40% and 11%, respectively. It is clear from these figures that steam turbine manufacture and service are major industries in both the United States and the world.

Figure 1.1 shows a 100-MW steam turbine manufactured by Siemens AG of Germany. Steam enters the turbine through the nozzles near the center of the machine, which direct the flow to a rotating set of blades. On leaving the first stage, steam flows (in the sketch toward the top right corner) through the rest of the 12 stages of the high-pressure section

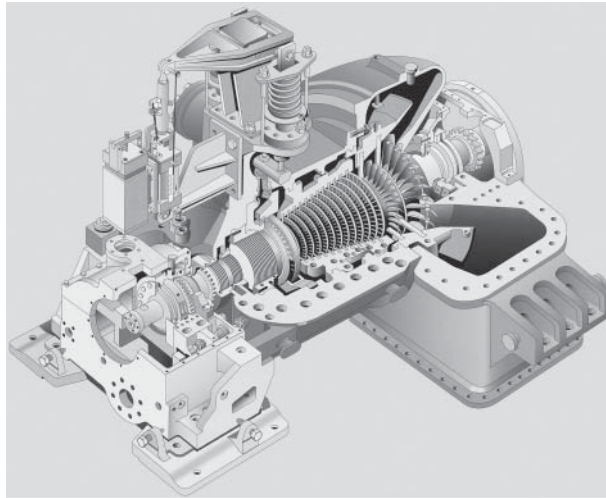


Figure 1.1 The Siemens SST-600 industrial steam turbine with a capacity of up to 100 MW. Source: Courtesy Siemens press picture, Siemens AG.

in this turbine. Each stage consists of a set of rotor blades, preceded by a set of stator vanes. The stators, fixed to the casing (of which one-quarter is removed in the illustration), are not clearly visible in this figure. After leaving the high-pressure section, steam flows into a two-stage low-pressure turbine, and from there, it leaves the machine and enters a condenser located on the floor below the turbine bay. Temperature of the entering steam is near 540°C , and its pressure is close to 140 bar. Angular speed of the shaft is generally in the range 3500–15000 rpm (rev/min). In this turbine, there are five bleed locations for the steam. The steam extracted from the bleeds enters feed-water heaters and from them back to a boiler. The large regulator valve in the inlet section controls the steam flow rate through the machine.

In order to increase the plant efficiency, new designs operate at supercritical pressures. Critical pressure for steam is 220.9 bar, and its critical temperature is 373.14°C . In an ultra-supercritical plant, the boiler pressure can reach 600 bar and turbine inlet temperature, 620°C .

1.1.3 Gas turbines

Major manufacturers of gas turbines produce both jet engines and industrial turbines. Since the 1980s, gas turbines, with clean-burning natural gas as a fuel, have also become important in electricity production. Their use in combined cycle power plants has increased the plant's overall thermal efficiency to just under 60%. They have also been employed for stand-alone power generation. In fact, most of the power plants in the United States since 1998 have been fueled by natural gas, and they now account for 34% of the electricity production. Unfortunately, production from the old natural gas fields of North America is strained, even if new resources have been developed from shale deposits. Projections show increasing use of natural gas in the energy mix in the United States, although it is still unclear how long the new deposits last since these wells deplete rapidly.

Figure 1.2 shows a gas turbine manufactured also by Siemens AG. The flow is from the back toward the front. The rotor is equipped with advanced single-crystal turbine

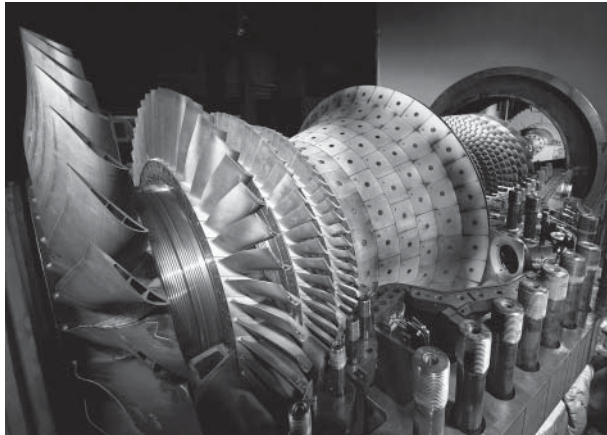


Figure 1.2 An open rotor and combustion chamber of an SGT5-4000F gas turbine. Source: Courtesy Siemens press picture, Siemens AG.

blades, with thermal barrier coatings and film cooling. Flow enters a three-stage turbine from an annular combustion chamber, which has 24 burners and walls made from ceramic tiles. These turbines power the 15 axial compressor stages that feed compressed air to the combustor. The fourth turbine stage, called a *power turbine*, drives an electric generator in a combined cycle power plant for which this turbine has been designed. The plant delivers a power output of 292 MW.

1.1.4 Hydraulic turbines

In those areas of the world with large rivers, water turbines are used to generate electric power. At the turn of the millennium, hydropower represented 17% of the total electrical energy generated in the world. The installed capacity at the end of year 2016 was 1064000 MW, but generation was 451000MW; therefore, their ratio, called a *capacity factor*, comes to 0.38.

With the completion of the 22500-MW Three Gorges Dam, China has now the world's largest installed capacity of 319000 MW and generated 28000 MW of power, based on year 2014 statistics. Canada, owing to its expansive landmass, is the world's second largest producer of hydroelectric power, with generation at 44000 MW from installed capacity of 76000 MW. Hydropower accounts for 58% of Canada's electricity needs. The sources of this power are the great rivers of British Columbia and Quebec. The next largest producer is Brazil, which obtains 43000 MW from an installed capacity of 89000 MW. Over 80% of Brazil's energy is obtained by water power. The Itaipu plant on the Paraná River, which borders Brazil and Paraguay, generates 12600 MW of power at full capacity. Of nearly the same size is Venezuela's Guri dam power plant with a rated capacity of 10200 MW, based on 20 generators.

The two largest power stations in the United States are the Grand Coulee station in the Columbia River and the Hoover Dam station in the Colorado River. The capacity of the Grand Coulee is 6480 MW and that of Hoover is 2000 MW. Tennessee Valley Authority operates a network of dams and power stations in the Southeastern parts of the country. Many small hydroelectric power plants can also be found in New England. Hydroelectric power in the United States today provides 282 billion kilowatt-hours (kwh) a year, or

33000 MW, but this represents only 6% of the total energy used in the United States. Fossil fuels still account for 86% of the US energy needs.

Next on the list of largest producers of hydroelectricity are Russia and Norway. With its small and thrifty population, Norway ships its extra generation to the other Scandinavian countries, and now with completion of a high-voltage powerline under the North Sea, also to western Europe. Norway and Iceland both obtain nearly all their electricity from hydropower.

1.1.5 Wind turbines

The Netherlands has been identified historically as a country of windmills. She and Denmark have seen a rebirth of wind energy generation since 1985 or so. These countries are relatively small in land area, and both are buffeted by winds from the North Sea. Since the 1990s, Germany has embarked on a quest to harness its winds. By 2015, its installed wind turbine's capacity was 45000 MW. It was exceeded only by China and the United States. China's installed capacity was 145400 MW and that of the United States was 74500 MW. They were followed by India and Spain with installed capacity of 27100 MW in India and 23000 MW in Spain. Although Denmark has fallen from the leaders, it still generates a larger percentage of its energy from wind than the others.

For the world, the capacity factor for wind power averages about 0.20, thus even lower than for hydropower. But for the United States, it is about 0.32, and wind constitutes about 2% of the country's total energy needs. It is the fastest-growing of the renewable energy systems. The windy plains of North and South Dakota and of West and North Texas offer great potential for wind power generation.

1.1.6 Compressors

Compressors find many applications in industry. An important use is in the transmission of natural gas across continents. Natural-gas production in the United States is centered in Texas and Louisiana as well as offshore in the Gulf of Mexico. In addition to Texas, there are tight gas formations in North Dakota, Colorado, Pennsylvania, and Ohio. The main users are the midwestern cities, in which natural gas is used in industry and for winter heating. Pipelines also cross the Canadian border with gas supplied to the west coast and to the northern states from Alberta.

Russia has 18% of world's natural-gas reserves, and much of its gas is transported to Europe through Ukraine. China has constructed a natural-gas pipeline to transmit the gas produced in the western provinces to the eastern cities. Extensions to Turkmenistan have been completed, and extensions to Iran are in the planning stage. Both have large natural-gas reserves.

Another important application of compressors is in the jet engines as previously mentioned.

1.1.7 Pumps and blowers

Pumps are used to increase pressure of liquids. Compressors, blowers, and fans do the same for gases. In steam power plants, condensate pumps return water to feed-water heaters, from which the water is pumped to boilers. Pumps are also used for cooling water flows in these power plants.



Figure 1.3 A centrifugal pump. Source: Courtesy Schmalenberger GmbH.

Figure 1.3 shows a centrifugal pump manufactured by Schmalenberger Strömungstechnologie GmbH. Flow enters through the eye of an impeller and leaves through a spiral volute. This pump is designed to handle a flow rate of $100 \text{ m}^3/\text{h}$, with a 20 m increase in its head.

In the mining industry, blowers circulate fresh air into mines and exhaust stale and contaminated air from them. In oil, chemical, and process industries, there is a need for large blowers and pumps. Pumps are also used in great numbers in agricultural irrigation and municipal sanitary facilities.

Offices, hospitals, schools, and other public buildings have heating, ventilating, and air conditioning (HVAC) systems, in which conditioned air is moved by large fans. Pumps provide chilled water to cool the air and for other needs.

1.1.8 Other uses and issues

Small turbomachines are present in all households. In fact, it is safe to say that in most homes, only electric motors are more common than turbomachines. A pump is needed in a dishwasher, a washing machine, and the sump. Fans are used in the heating system and as window and ceiling fans. Exhaust fans are installed in kitchens and bathrooms. Both an air conditioner and a refrigerator is equipped with a compressor, although it may be a screw compressor (which is not a turbomachine) in an air conditioner. In a vacuum cleaner, a fan creates suction. In a car there is a water pump, a fan, and, in some models, a turbocharger. All are turbomachines.

In addition to understanding the fluid dynamical principles of turbomachinery, it is important for a turbomachinery design engineer to learn other allied fields. The main ones are material selection, shaft and disk vibration, stress analysis of disks and blades, and topics covering bearings and seals. Finally, understanding control theory is important for optimum use of any machine.

In recent years, the world has awoken to the fact that fossil fuels are finite and that renewable energy sources will not be sufficient to provide for the entire world the material conditions that Western countries now enjoy. Hence, it is important that the machines that make use of these resources be well designed so that the remaining fuels are used with consideration, recognizing their finiteness and their value in providing for some of the vital needs of humanity.

1.2 HISTORICAL SURVEY

This section gives a short historical review of turbomachines. Turbines are power-producing machines and include water and wind turbines from early history. Gas and steam turbines date from the beginning of the last century. Rotary pumps have been in use for 200 years. Compressors developed as advances were made in aircraft propulsion during the last century.

1.2.1 Water power

The origin of turbomachinery can be traced to the use of flowing water as a source of energy. Indeed, waterwheels, lowered into a river, were already known to the Greeks. The early design moved to the rest of Europe and became known as the *norse mill* because the archeological evidence first surfaced in northern Europe. This machine consists of a set of radial paddles fixed to a shaft. As the shaft was vertical, or somewhat inclined, its efficiency of energy extraction could be increased by directing the flow of water against the blades with the aid of a *mill race and a chute*. Such a waterwheel could provide only about one-half horsepower (0.5 hp), but owing to the simplicity of its construction, it survived in use until 1500 and can still be found in some primitive parts of the world.

By placing the axis horizontally and lowering the waterwheel into a river, a better design is obtained. In this *undershot waterwheel*, dating from Roman times, water flows through the lower part of the wheel. Such a wheel was first described by the Roman architect and engineer Marcus Vitruvius Pollio during the first century BCE.

Overshot waterwheel came into use in the hilly regions of Rome during the second century CE. By directing water from a chute above the wheel into the blades increases the power delivered because now, in addition to the kinetic energy of the water, also part of the potential energy can be converted to mechanical energy. Power of overshot waterwheels increased from 3 hp to about 50 hp during the Middle Ages. These improved overshot waterwheels were partly responsible for the technical revolution in the twelfth–thirteenth century. In the William the Conqueror’s *Domesday Book* of 1086, the number of watermills in England is said to have been 5684. By 1700, about 100000 mills were powered by flowing water in France [12].

The genius of Leonardo da Vinci (1452–1519) is well recorded in history, and his notebooks show him to have been an exceptional observer of nature and technology around him. Although he is best known for his artistic achievements, most of his life was spent in the art of engineering. Illustrations of fluid machinery are found in da Vinci’s notebooks, in *De Re Metallica*, published in 1556 by Agricola [1], and in a tome by Ramelli published in 1588. From these, a good understanding of the construction methods can be gained and of the scale of the technology then in use. In Ramelli’s book, there is an illustration of a mill in which a grinding wheel, located upstairs, is connected to a shaft, the lower end of which has an enclosed impact wheel that is powered by water. There are also illustrations that show windmills to have been in wide use for grinding grain.

Important progress to improve waterwheels came in the hands of the Frenchman Jean Victor Poncelet (1788–1867), who curved the blades of the undershot waterwheel so that water would enter tangentially to the blades. This improved its efficiency. In 1826, he came up with a design for a wheel and with radial inward flow. A water turbine of this design was built a few years later in New York by Samuel B. Howd and then improved by James Bicheno Francis (1815–1892). Improved versions of Francis turbines are in common use today.

About the same time in France, an outward flow turbine was designed by Claude Burdin (1788–1878) and his student Benoît Fourneyron (1802–1867). They benefited greatly from the work of Jean-Charles de Borda (1733–1799) on hydraulics. Their machine had a set of guide vanes to direct the flow tangentially to the blades. In 1835, Fourneyron designed a turbine that operated from a head of 108 m with a flow rate of 20 liters per second (L/s), rotating at 2300 rpm, delivering 40 hp as output power at 80% efficiency.

In the 1880s, in the California gold fields, an impact wheel known as a *Pelton wheel*, after Lester Allen Pelton (1829–1918) of Vermillion, Ohio, came into wide use.

An axial-flow turbine was developed by Carl Anton Henschel (1780–1861) in 1837 and by Feu Jonval in 1843. Modern turbines are improvements of Henschel's and Jonval's designs. A propeller type of turbine was developed by the Austrian engineer Victor Kaplan (1876–1934) in 1913. In 1926, a 11000-hp Kaplan turbine was placed into service in Sweden. It weighed 62.5 tons, had a rotor diameter of 5.8 m, and operated at 62.5 rpm with a water head of 6.5 m. Modern water turbines in large hydroelectric power plants are either of the Kaplan type or variations of this design.

1.2.2 Wind turbines

Humans have drawn energy from wind and water since ancient times. The first recorded account of a windmill is from the Persian-Afghan border region in 644 CE, where these vertical axis windmills were still in use in recent times [39]. They operate on the principle of drag in the same way as square sails do when ships sail downwind.

In Europe, windmills were in use by the twelfth century, and historical research suggests that they originated from waterwheels, for their axis was horizontal, and the masters of the late Middle Ages had already developed gog-and-ring gears to transfer energy from a horizontal shaft into a vertical one. This then turned a wheel to grind grain [82]. An early improvement was to turn the entire windmill toward the wind. This was done by centering a round platform on a large diameter *vertical post* and securing the structure of the windmill on this platform. The platform was free to rotate, but the force needed to turn the entire mill limited the size of the early *post-mills*. This restriction was removed in a *tower mill* in which only the platform, affixed to the top of the mill, was free to rotate. The blades were connected to a wind shaft, which leaned about 15° from the horizontal so that the blades would clear the structure. The shaft was supported by a wooden main bearing at the *blade end* and a thrust bearing at the *tail end*. A band brake was used to limit the rotational speed at high wind speeds. The power dissipated by frictional forces in the brake rendered the arrangement susceptible to fire.

Over the next 500 years, to the beginning of the industrial revolution, progress was made in windmill technology, particularly in Great Britain. By accumulated experience, designers learned to move the position of the spar supporting a blade from mid-cord to quarter-cord position and to introduce a nonlinear twist and leading edge camber to the blade [82]. The blades were positioned at a steep angle to the wind and made use of the lift



Figure 1.4 A traditional windmill (a) and an American farm windmill (b) for pumping water.

force, rather than drag. It is hard not to speculate that the use of lift had not been learned from sailing vessels using *lanteen sails* to tack.

A towermill is shown in Figure 1.4a. It is seen to be many meters tall, and each of the four quarter-cord blades is about 1 m in width. The blades of such mills were covered with either fabric or wooden slats. By an arrangement such as is found in window shutters today, the angle of attack of the blades could be changed at will, providing also a braking action at high winds.

The American windmill is shown in Figure 1.4b. It is a small multibladed wind turbine with a vertical vane to keep it oriented toward the wind. Some models had downwind orientation and did not need to be controlled in this way. The first commercially successful wind turbine was introduced by Halladay in 1859 to pump water for irrigation in the Plains States. It was about 5 m in diameter and generated about 1 kW at windspeed of 7 m/s [82]. The windmill shown in the figure is an 18-steel-bladed model by Aermotor Company of Chicago, a company whose marketing and manufacturing success made it the prime supplier of this technology during the period 1900–1925.

New wind turbines with a vertical axis were invented during the 1920s in France by G. Darrieus and in Finland by S. Savonius [80]. They offer the advantage of working without regard to wind direction, but their disadvantages include fluctuating torque over each revolution and difficulty of starting. For these reasons, they have not achieved wide use.

1.2.3 Steam turbines

Although the history of steam to produce rotation of a wheel can be traced to Hero of Alexandria in the year 100 CE, his invention is only a curiosity, for it did not arise out of a historical necessity, such as was imposed by the world's increasing population at the beginning of the industrial revolution. Another minor use to rotate a roasting spit was suggested in 1629 Giovanni de Branca. The technology to make shafts and overcome friction was too primitive at that time to put his ideas to more important uses. The age of steam began with the steam engine, which ushered in the industrial revolution in Great Britain. During the eighteenth century, steam engines gained in efficiency, particularly when James Watt in 1765 reasoned that better performance could be achieved if the boiler and the condenser were separate units. Steam engines are, of course, positive-displacement machines.

Sir Charles Parsons (1854–1931) is credited with the development of the first *steam turbine* in 1884. His design used multiple turbine wheels, about 8 cm in diameter each,

to drop the pressure in *stages*, and this way to reduce the angular velocities. The first of Parson's turbines generated 7.5 kW using steam at inlet pressure of 550 kPa and rotating at 17000 rpm. It took some 15 years before Parsons' efforts received their proper recognition.

An impulse turbine was developed in 1883 by the Swedish engineer Carl Gustav Patrik de Laval (1845–1913) for use in a cream separator. To generate the large steam velocities, he also invented the supersonic nozzle and exhibited it in 1894 at the Columbian World's Fair in Chicago. From such humble beginnings arose rocketry and supersonic flight. Laval's turbines rotated at 26000 rpm, and the largest of the rotors had a tip speed of 400 m/s. He used flexible shafts to alleviate vibration problems in the machinery.

In addition to the efforts in Great Britain and Sweden, the Swiss Federal Institute of Technology in Zurich (Eidgenössische Technische Hochschule [ETH]) had become an important center of research in early steam turbine theory through the efforts of Aurel Stodola (1859–1942). His textbook *Steam and Gas Turbines* became the standard reference on the subject for the first half of last century [89]. A similar effort was led by William J. Kearton (1893–1978) at the University of Liverpool in Great Britain.

1.2.4 Jet propulsion

The first patent for gas turbine development was issued to John Barber (1734–c. 1800) in England in 1791, but again, technology was not yet sufficiently advanced to build a machine on the basis of the proposed design. Eighty years later in 1872, Franz Stolze (1836–1910) received a patent for a design of a gas turbine power plant consisting of a multistage axial-flow compressor and turbine on the same shaft, together with a combustion chamber and a heat exchanger. The first US patent was issued to Charles Gordon Curtis (1860–1953) in 1895.

Starting in 1935, Hans J. P. von Ohain (1911–1998) directed efforts to design gas turbine power plants for the Heinkel aircraft in Germany. The model He178 was a fully operational jet aircraft, and in August 1939, it was first such aircraft to fly successfully.

During the same time frame, Sir Frank Whittle (1907–1996) in Great Britain was developing gas turbine power plants for aircraft based on a centrifugal compressor and a turbojet design. In 1930, he filed for a patent for a single-shaft engine with a two-stage axial compressor followed by a radial compressor from which the compressed air flowed into a straight-through burner. The burned gases then flowed through a two-stage axial turbine on a single disk. This design became the basis for the development of jet engines in Great Britain and later in the United States.

Others, such as Alan Arnold Griffith (1893–1963) and Hayne Constant (1904–1968), worked in 1931 on the design and testing of axial-flow compressors for use in gas turbine power plants. Already in 1926, Griffith had developed an aerodynamic theory of turbine design based on flow past airfoils.

In Figure 1.5 is the De Havilland Goblin engine designed by Frank Halford in 1941. The design was based on the original work of Sir Frank Whittle. It is a turbojet engine with single-stage centrifugal compressor and with can combustors exhausting the burned combustion gases into a turbine that drives the compressor. The remaining kinetic energy leaving the turbine goes to propulsive thrust.

Since the 1950s, there has been continuous progress in the development of gas turbine technology for aircraft power plants. Rolls Royce in Great Britain brought to the market its Olympus twin-spool engine, its Dart single-spool engine for low-speed aircraft, and in 1967 the Trent, which was the first three-shaft turbofan engine. The Olympus was also used in stationary power plants and in marine propulsion.

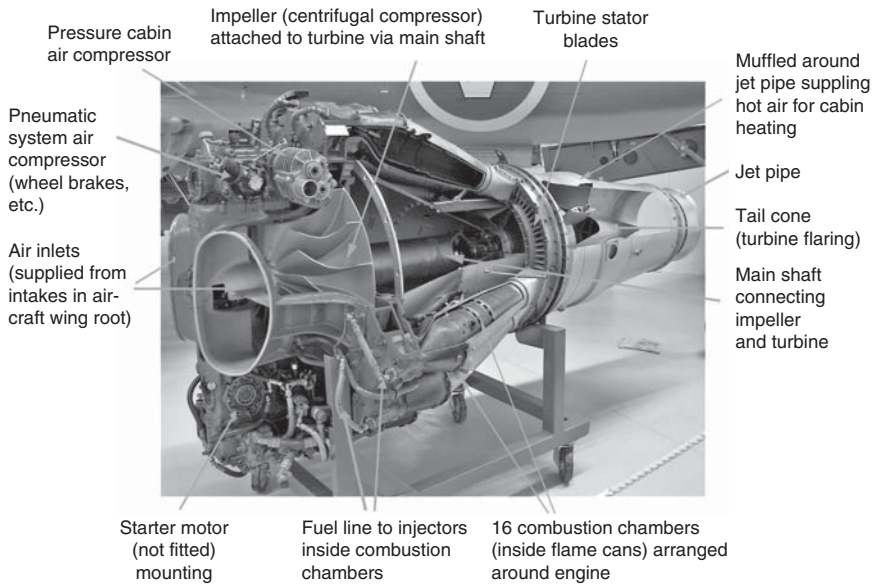


Figure 1.5 De Havilland Goblin turbojet engine.

General Electric in the United States has also a long history in gas turbine development. Its I-14, I-16, I-20, and I-40 models were developed in the 1940s. The I-14 and I-16 powered the Bell P-59A aircraft, which was the first American turbojet. It had a single centrifugal compressor and a single-stage axial turbine. Allison Engines, then a division of General Motors, took over the manufacture and improvement of model I-40. Allison also began the manufacture of General Electric's TG series of engines.

Many new engines were developed during the latter half of the twentieth century, not only by Rolls Royce and General Electric but also by Pratt and Whitney in the United States and Canada, Rateau in France, and by companies in Soviet Union, Sweden, Belgium, Australia, and Argentina. The modern engines that power the flight of today's large commercial aircraft by Boeing and by Airbus are based on the Trent design of Rolls Royce or on General Electric's GE90 [7].

1.2.5 Industrial turbines

Brown Boveri in Switzerland developed a 4000-kW turbine power plant in 1939 to Neuchatel for standby operation for electric power production. On the basis of this design, an oil-burning closed-cycle gas turbine plant with a rating of 2 MW was built the following year.

Industrial turbine production at Ruston and Hornsby Ltd. of Great Britain began by establishment of a design group in 1946. The first unit produced by them was sold to Kuwait Oil Company in 1952 to power pumps in oil fields. It was still operational in 1991 having completed 170000 operating hours. Industrial turbines are in use today as turbocompressors and in electric power production.

1.2.6 Pumps and compressors

The centrifugal pump was invented by Denis Papin (1647–1710) in 1698 in France. To be sure, a suggestion to use centrifugal force to effect pumping action had also been made by

Leonardo da Vinci, but neither his nor Papin's invention could be built, owing to the lack of sufficiently advanced shop methods. Leonhard Euler (1707–1783) gave a mathematical theory of the operation of a pump in 1751. This date coincides with the early part of the industrial revolution, and the advances made in manufacturing during the ensuing 100 years brought centrifugal pumps to wide use by 1850. The Massachusetts pump, built in 1818, was the first practical centrifugal pump manufactured. W. D. Andrews improved its performance in 1846 by introducing double-shrouding. At the same time in Great Britain, engineers such as John Appold (1800–1865) and Henry Bessemer (1813–1898) were working on improved designs. Appold's pump operated at 788 rpm with an efficiency of 68% and delivered 78 L/s and a head of 5.9 m.

The same companies that built steam turbines in Europe in 1900 also built centrifugal blowers and compressors. The first applications were for providing ventilation in mines and for the steel industry. Compressors have been used in chemical industries since 1916, in the petrochemical industries since 1930, and in the transmission of natural gas since 1947. The period 1945–1950 saw a large increase in the use of centrifugal compressors in American industry. Since 1956, they have been integrated into gas turbine power plants and have replaced reciprocating compressors in other applications.

The efficiencies of single-stage centrifugal compressors increased from 70% to over 80% over the period 1935–1960 as a result of work done in companies such as Rateau, Moss-GE, Birmann-DeLaval, and Whittle in Europe and General Electric and Pratt & Whitney in the United States. The pressure ratios increased from 1.2 : 1 to 7 : 1. This development owes much to the progress that had been made in gas turbine design [29].

For large flow rates, multistage axial compressors are used. Figure 1.6 shows such a compressor, manufactured by MAN Diesel & Turbo SE in Germany. It has 14 axial stages followed by a centrifugal compressor stage. The rotor blades are seen in the exposed rotor. The stator blades are fixed to the casing, the lower half of which is shown. The flow is from right to left. The flow area decreases toward the exit, for in order to keep the axial velocity constant, as is commonly done, the increase in density on compression is accommodated by a decrease in the flow area.

1.2.7 Note on units

The *Système International* (d'Unités) (SI) system of units is used in this text. It is still customary in some industries to use the English Engineering system of units, and if other

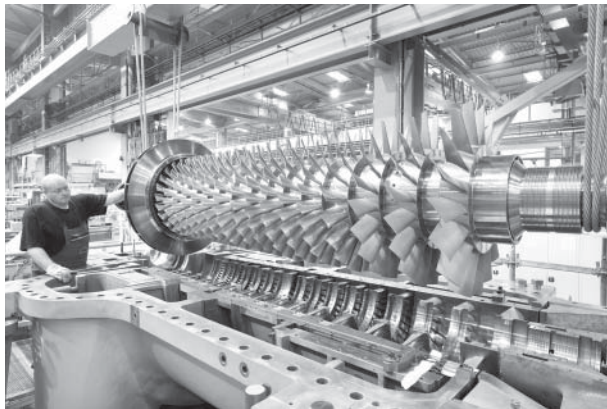


Figure 1.6 Multistage compressor. Source: Courtesy MAN Diesel & Turbo SE.

reference books are consulted, in some of them, one finds this system used too. In this set of units, mass is expressed as pound (lbm), and foot is the unit of length. The British gravitational system of units has *slug* as the unit of mass, and the unit of force is pound force (lbf), obtained from Newton's law, as it represents a force needed to accelerate a mass of one slug at the rate of 1 ft/s^2 . The use of slug for mass makes the traditional British gravitational system of units analogous to the SI units. When pound (lbm) is used for mass, it ought to be first converted to slugs ($1 \text{ slug} = 32.174 \text{ lbm}$), for then calculations follow as in the SI units. The unit of temperature is Fahrenheit or Rankine. Thermal energy in this set of units is reported in British thermal units (Btu)'s for short. As it is a unit for energy, it can be converted to one encountered in mechanics by remembering that $1 \text{ Btu} = 778.17 \text{ ft lbf}$. The conversion factor to SI units is $1 \text{ Btu} = 1055 \text{ J}$. Conversion of power from units of horsepower to kilowatts is $1 \text{ hp} = 0.7457 \text{ kW}$. The flow rate in pumps is often given in gallons per minute (gpm). The conversion to standard units is carried out by recalling that $1 \text{ gal} = 231 \text{ in}^3$. World energy consumption is often given in quads. The conversion to SI units is $1 \text{ quad} = 1.055 \text{ EJ}$, where EJ is exajoule equal to 10^{18} J .

CHAPTER 2

PRINCIPLES OF THERMODYNAMICS AND FLUID FLOW

This chapter begins with a review of the conservation principle for mass for steady uniform flow. After this follows the first and second laws of thermodynamics, also for steady uniform flow. Next, thermodynamic properties of gases and liquids are reviewed. These pave the way to a discussion of various turbine and compressor efficiencies and thermodynamic losses. The final section is on the momentum balance in fluid flow.

2.1 MASS CONSERVATION PRINCIPLE

Mass flow rate \dot{m} in a *uniform flow* is related to the density ρ and the velocity V of a fluid, as well as the cross-sectional area of the flow channel A by

$$\dot{m} = \rho V_n A$$

When this equation is used in the analysis of steam flows, specific volume, which is the reciprocal of density, is commonly used. The subscript n denotes the direction *normal* to the flow area. The product $V_n A$ arises from the scalar product $\mathbf{V} \cdot \mathbf{n} = V \cos \theta$, in which \mathbf{n} is a unit normal vector on the surface A and θ is the angle between the normal and the direction of the velocity vector. Consequently, the scalar product can be written in the two alternative forms

$$\mathbf{V} \cdot \mathbf{n} A = V A \cos \theta = V_n A = V A_n$$

in which A_n is the area normal to the flow. The principle of conservation of mass for a uniform steady flow through a control volume with one inlet and one exit takes the form

$$\rho_1 V_1 A_{n1} = \rho_2 V_2 A_{n2}$$

Turbomachinery flows are steady only in a time-averaged sense; that is, the flow is periodic, with a period equal to the time taken for a blade to move a distance equal to the spacing between adjacent blades. Despite the unsteadiness, in elementary analysis, all variables are assumed to have steady values.

If the flow has more than one inlet and exit, then, in steady uniform flow, conservation of mass requires that

$$\sum_i \rho_i V_i A_{ni} = \sum_e \rho_e V_e A_{ne} \quad (2.1)$$

in which the sums are over all the inlets and exits.

■ EXAMPLE 2.1

Steam flows at the rate $\dot{m} = 0.20 \text{ kg/s}$ through each nozzle in the bank of nozzles shown in Figure 2.1. Steam conditions are such that at the inlet, specific volume is $0.80 \text{ m}^3/\text{kg}$ and at the outlet, it is $1.00 \text{ m}^3/\text{kg}$. Spacing of the nozzles is $s = 5.0 \text{ cm}$, wall thickness at the inlet is $t_1 = 2.5 \text{ mm}$, and at the outlet it is $t_2 = 2.0 \text{ mm}$. Blade height is $b = 3.0 \text{ cm}$. Nozzle angle is $\alpha_2 = 70^\circ$. Find the steam velocity at the inlet and at the outlet.

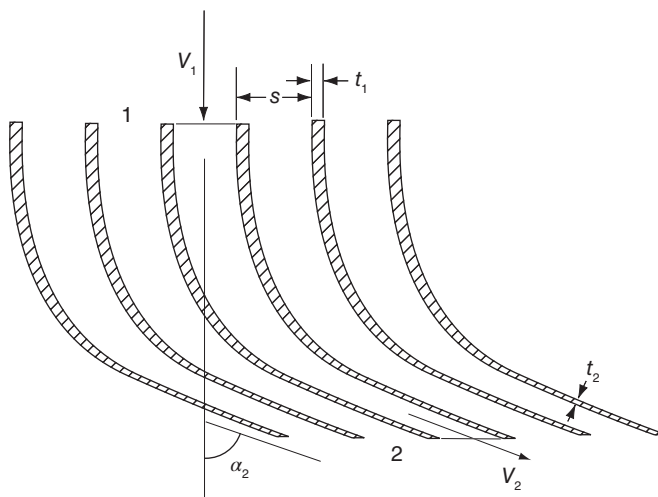


Figure 2.1 Turning of flow by steam nozzles.

Solution: The area at the inlet is

$$A_1 = b(s - t_1) = 3(5 - 0.25) = 14.25 \text{ cm}^2$$

Velocity at the inlet is solved from the mass balance

$$\dot{m} = \rho_1 V_1 A_1 = \frac{V_1 A_1}{v_1}$$

which gives

$$V_1 = \frac{\dot{m}v_1}{A_1} = \frac{0.20 \cdot 0.80 \cdot 100^2}{14.25} = 112.3 \text{ m/s}$$

At the exit, the flow area is

$$A_{2n} = b(s \cos \alpha_2 - t_2) = 3(5 \cos(70^\circ) - 0.20) = 4.53 \text{ cm}^2$$

Hence, the velocity is

$$V_2 = \frac{\dot{m}v_2}{A_{2n}} = \frac{0.2 \cdot 1.00 \cdot 100^2}{4.53} = 441.5 \text{ m/s}$$

■

2.2 FIRST LAW OF THERMODYNAMICS

For a uniform steady flow in a channel, the first law of thermodynamics has the form

$$\dot{m} \left(u_1 + p_1 v_1 + \frac{1}{2} V_1^2 + g z_1 \right) + \dot{Q} = \dot{m} \left(u_2 + p_2 v_2 + \frac{1}{2} V_2^2 + g z_2 \right) + \dot{W} \quad (2.2)$$

The sum of specific internal energy u , kinetic energy $V^2/2$, and potential energy gz is the specific energy $e = u + \frac{1}{2}V^2 + gz$ of the fluid. In the potential energy, term g is the acceleration of gravity and z is a height. The term $p_1 v_1$, in which p is the pressure, represents the work done by the fluid in the flow channel just upstream of the inlet to move the fluid ahead of it into the control volume, and it thus represents energy flow into the control volume. This work is called *flow work*. Similarly, $p_2 v_2$ is the flow work done by the fluid inside the control volume to move the fluid ahead of it out of the control volume. It represents energy transfer as work leaving the control volume. The sum of internal energy and flow work is defined as enthalpy $h = u + pv$. The heat transfer rate into the control volume is denoted as \dot{Q} , and the rate at which work is delivered is \dot{W} . Equation (2.2) can be extended to multiple inlets and outlets in the same manner as was done in Eq. (2.1).

Dividing both sides by \dot{m} gives the first law of thermodynamics the form

$$h_1 + \frac{1}{2} V_1^2 + g z_1 + q = h_2 + \frac{1}{2} V_2^2 + g z_2 + w$$

in which $q = \dot{Q}/\dot{m}$ and $w = \dot{W}/\dot{m}$ denote the heat transfer and work done per unit mass. By convention, heat transfer *into* the thermodynamic system is taken to be a positive quantity, as is *work done by the system* on the surroundings.

The sum of enthalpy, kinetic energy, and potential energy is called the *stagnation enthalpy*

$$h_0 = h + \frac{1}{2} V^2 + g z$$

and thus, the first law can also be written as

$$h_{01} + q = h_{02} + w$$

In the flow of gases, the potential energy terms are small and can be neglected. Similarly, for a control volume around a pump the changes in elevation are small and the potential

energy difference is negligible. For pumps and water turbines when the suction and discharge conduits are included into the control volume, the potential energy terms need to be retained. When the change in potential energy is neglected, the first law reduces to

$$h_1 + \frac{1}{2}V_1^2 + q = h_2 + \frac{1}{2}V_2^2 + w$$

In addition, even if velocity is large, the difference in kinetic energy between the inlet and exit may be small. In such a case, first law is simply

$$h_1 + q = h_2 + w$$

Turbomachinery flows are nearly adiabatic, so q can be dropped. Then work delivered by a turbine is given as

$$w_t = h_{01} - h_{02}$$

and the work done on the fluid in a compressor or a pump is

$$w_c = h_{02} - h_{01}$$

The compressor work has been written in a form that gives the work done a positive value. Hence, the convention of thermodynamics of denoting *work out* from a system as positive and *work in* as negative is ignored, and the equations are written in a form that gives a positive value for work, for both a turbine and a compressor.

■ EXAMPLE 2.2

Steam flows adiabatically at a rate $\dot{m} = 0.01$ kg/s through a diffuser, shown in Figure 2.2, with inlet diameter $D_1 = 1.0$ cm. Specific volume at the inlet $v_1 = 2.40$ m³/kg. Exit diameter is $D_2 = 2.5$ cm, with specific volume at the outlet $v_2 = 3.80$ m³/kg. Find the change in enthalpy neglecting any change in the potential energy.

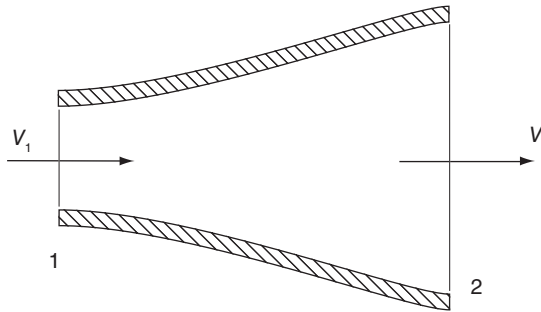


Figure 2.2 Flow through a diffuser.

Solution: The areas at the inlet and outlet are

$$A_1 = \frac{\pi D_1^2}{4} = \frac{\pi (0.01)^2}{4} = 7.85 \cdot 10^{-5} \text{ m}^2$$

$$A_2 = \frac{\pi D_2^2}{4} = \frac{\pi (0.025)^2}{4} = 4.91 \cdot 10^{-4} \text{ m}^2$$

The velocity at the inlet is

$$V_1 = \frac{\dot{m}v_1}{A_1} = \frac{0.01 \cdot 2.4}{7.85 \cdot 10^{-5}} = 305.6 \text{ m/s}$$

and at the outlet it is

$$V_2 = \frac{\dot{m}v_2}{A_2} = \frac{0.01 \cdot 3.8}{4.91 \cdot 10^{-4}} = 77.4 \text{ m/s}$$

Since no work is done and the flow is adiabatic, the stagnation enthalpy remains constant $h_{01} = h_{02}$. With negligible change in potential energy, this equation reduces to

$$h_2 - h_1 = \frac{1}{2}V_1^2 - \frac{1}{2}V_2^2 = \frac{1}{2}(305.6^2 - 77.4^2) = 43.7 \text{ kJ/kg}$$

■

2.3 SECOND LAW OF THERMODYNAMICS

For a uniform steady flow in a channel, the second law of thermodynamics takes the form

$$\dot{m}(s_2 - s_1) = \int_{\ell_1}^{\ell_2} \frac{\dot{Q}'}{T} d\ell + \int_{\ell_1}^{\ell_2} \dot{S}'_p d\ell \quad (2.3)$$

in which s is the entropy. On the right-hand side (RHS) \dot{Q}' is the rate at which heat is transferred from the walls of the flow channel into the fluid per unit length of the channel. The incremental length of the channel is $d\ell$, and the channel extends from location ℓ_1 to ℓ_2 . The absolute temperature T in this expression may vary along the channel. The term \dot{S}'_p on the RHS is the rate of entropy production per unit length of the flow channel. If the heat transfer is internally reversible, entropy production is the result of internal friction and mixing in the flow. In order for the heat transfer to be reversible, the temperature difference between the walls and the fluid has to be small. In addition, the temperature gradient in the flow direction must be small. This requires the flow to move rapidly so that energy transfer by bulk motion far exceeds the transfer by conduction and radiation in the flow direction.

As Eq. (2.3) shows, when heat is transferred into the fluid, its contribution is to increase the entropy in the downstream direction. If, on the other hand, heat is transferred from the fluid to the surroundings, its contribution is to reduce the entropy. Entropy production \dot{S}'_p is always positive, and its contribution is to increase the entropy in the flow direction. For the ideal case of an *internally reversible process*, entropy production vanishes.

2.3.1 Tds-equations

The first law of thermodynamics for a *closed system* relates the work and heat interactions to a change in internal energy U . For infinitesimal work and heat interactions, the first law can be written as

$$dU = \delta Q - \delta W$$

For a simple compressible substance, defined to be one for which the only relevant work is compression or expansion, reversible work is given by

$$\delta W_s = p dV$$

This expression shows that when a fluid is compressed so that its volume decreases, work is negative, meaning that work is done on the system. For an internally reversible process, the second law of thermodynamics relates heat transfer to a change in entropy by

$$\delta Q_s = T dS$$

in which it must be remembered that T is the absolute temperature. Hence, for an internally reversible process, the first law takes the differential form

$$dU = T dS - p dV$$

Dividing by the mass of the system converts this to the expression

$$du = Tds - p dv$$

between specific properties. Although derived for reversible processes, this is a *relationship between intensive properties*, and for this reason, it is valid for all processes: reversible, or irreversible. It shows that $u = u(s, v)$ and is usually written as

$$Tds = du + p dv \quad (2.4)$$

and is called the first *Gibbs equation*.

Writing $u = h - pv$ and differentiating gives $du = dh - p dv - v dp$. Substituting this into the first Gibbs equation gives

$$Tds = dh - v dp \quad (2.5)$$

which is the second *Gibbs equation* and it shows that $h = h(s, p)$.

2.4 EQUATIONS OF STATE

The *state principle* of thermodynamics guarantees that a thermodynamic state for a simple compressible substance is completely determined by specifying two independent thermodynamic properties. Such functional relations are called *equations of state* and the two fundamental ones are $u = u(s, v)$ and $h = h(s, p)$.

In this section, the equations of state for steam and those of ideal gases are reviewed. In addition, ideal gas mixtures are considered as they arise in combustion of hydrocarbon fuels. Combustion gases flow through the gas turbines of a jet engine and through industrial turbines burning natural gas. Preliminary calculations can be carried out using properties of air since air is 78% of nitrogen by volume, which, although contributing to formation of nitric oxides, is otherwise largely inert during combustion. Later in the chapter, a better model for combustion gases is discussed, but for accurate calculations, the actual composition is to be taken into account. Also in many applications, such as in oil and gas production, mixtures rich in complex molecules flow through compressors and expanders. Their equations of state may be very complicated, particularly at high pressures.

2.4.1 Properties of steam

It has been found that a useful way to present properties of steam is to construct a chart, such as is shown in Figure 2.3, with entropy on the abscissa and temperature on the ordinate. On the heavy line, water exists as a saturated liquid on the descending part on the left and as saturated vapor on the right. Away from this *vapor dome*, on the right, water is superheated vapor, that is to say *steam*; and to the left, water exists as a compressed liquid. The state at the top of the vapor dome is called a *critical state*, with pressure $p_c = 220.9$ bar and temperature $T_c = 374.14$ °C. At this condition, entropy is $s_c = 4.4298$ kJ/(kg K) and enthalpy is $h_c = 2099.6$ kJ/kg. Below the vapor dome, water exists as a two-phase mixture of saturated vapor and saturated liquid. Such a state may exist in the last stages of a steam turbine where the saturated steam is laden with water droplets.

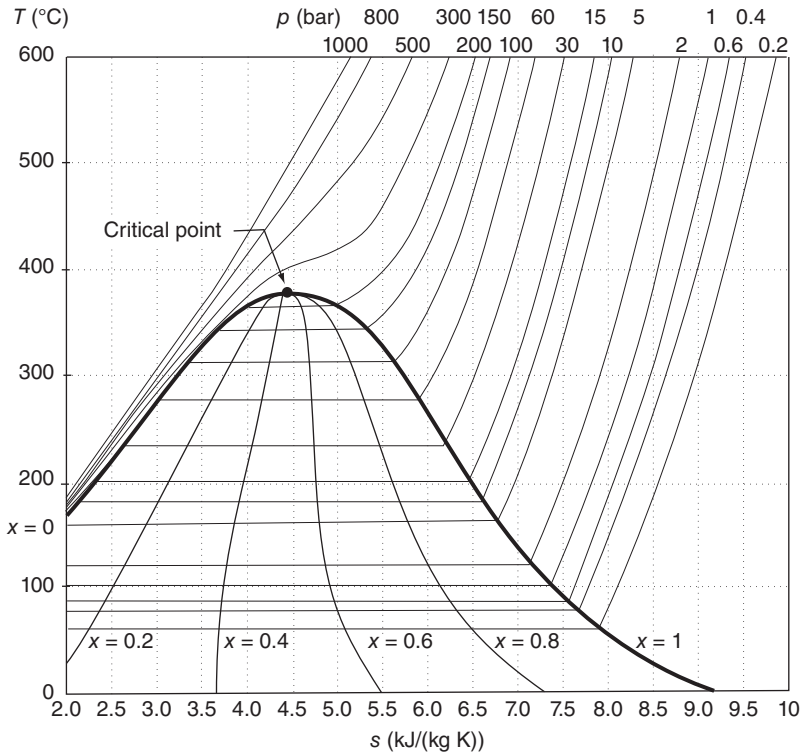


Figure 2.3 Ts -diagram for water.

The lines of constant pressure are also shown in Figure 2.3. As they intersect the vapor dome, their slopes become horizontal across the two-phase region. Thus they are parallel to lines of constant temperature, and this indicates that temperature and pressure are *not independent* properties in the two-phase region. To specify the thermodynamic state in this region, quality denoted by x is used. It is defined as the mass of vapor divided by the mass of the mixture. In terms of quality, thermodynamic properties of a two-phase mixture are calculated as a weighted average of the saturation properties. Thus, for example

$$h = (1 - x)h_f + xh_g$$

or

$$h = h_f + xh_{fg}$$

in which h_f denotes the enthalpy of saturated liquid, h_g that of saturated vapor, and their difference is denoted by $h_{fg} = h_g - h_f$. Similarly, entropy of the two-phase mixture is

$$s = s_f + xs_{fg}$$

and its specific volume is

$$v = v_f + xv_{fg}$$

Integrating the second Gibbs equation $Tds = dh - vdp$ between the saturated vapor and liquid states at constant pressure gives

$$h_{fg} = Ts_{fg}$$

The first law of thermodynamics shows that the amount of heat transferred to a fluid flowing at constant pressure when it is evaporated from its saturated liquid state to saturated vapor state is

$$q = h_g - h_f = h_{fg}$$

and this is therefore also

$$q = T(s_g - s_f) = Ts_{fg}$$

States with pressure above the critical pressure have the peculiar property that if water at such pressures is heated at constant pressure, it converts from a liquid state to a vapor state without ever forming a two-phase mixture. Thus, neither liquid droplets nor vapor bubbles can be discerned in the water during the transformation. This region is of interest because in a typical supercritical steam power plant built today water is heated at supercritical pressure of 262 bar to temperature 566 °C, and in ultra-supercritical power plants steam generator pressures of 600 bar are in use. Steam at these pressures and temperatures then enters a high-pressure (HP) steam turbine, which must be designed with these conditions in mind.

Steam tables, starting with those prepared by H. L. Callendar in 1900, and Keenan and Kays in 1936, although still in use, are being replaced by computer programs today. Steam tables, found in Appendix B, were generated by the software EES, a product of the company F-chart Software, in Madison, Wisconsin. It was also used to prepare Figures 2.3 and 2.4. The mathematical software MATLAB has also a tool for calculating the properties of steam. It was written by Magnus Holmgren and called XSteam.¹ Its use is demonstrated in the following example. This can also be executed without any changes with GNU/OCTAVE software.

■ EXAMPLE 2.3

Steam at $p_1 = 6000$ kPa and $T_1 = 400$ °C expands reversibly and adiabatically through a steam turbine to pressure $p_2 = 60$ kPa. (a) Find the exit quality and (b) the work delivered if the change in kinetic energy is neglected.

¹<https://www.mathworks.com/matlabcentral/profile/authors/870351-magnus-holmgren>

Solution: (a) The thermodynamic properties at the inlet to the turbine are first found from the steam tables, or calculated using computer software. Either way shows that $h_1 = 3178.2$ kJ/kg and $s_1 = 6.5431$ kJ/(kg K). Since the process is reversible and adiabatic, it takes place at constant entropy and $s_2 = s_1$. The exit state is in the two-phase region, and steam quality is calculated from

$$x_2 = \frac{s_2 - s_f}{s_g - s_f} = \frac{6.5431 - 1.1452}{7.5311 - 1.1452} = 0.8453$$

in which $s_f = 1.1452$ kJ/(kg K) and $s_g = 7.5311$ kJ/(kg K) are the values of entropy for saturated liquid and saturated vapor at $p_2 = 60$ kPa. Exit enthalpy is then obtained from

$$h_2 = h_f + x_2 h_{fg} = 359.84 + 0.8453 \cdot 2293.0 = 2298.1 \text{ kJ/kg}$$

(b) Work delivered is

$$w_s = h_1 - h_2 = 3178.2 - 2298.1 = 880.1 \text{ kJ/kg}$$

The calculations have been carried out using the MATLAB script shown below.

```
%Example 2.3
clear all
%State 1
p1=60; T1=400; %pressure in units of bar
h1=XSteam('h_pT',p1,T1)
s1=XSteam('s_pT',p1,T1)
%State 2
p2=0.6;
s2=s1;
sf2=XSteam('sL_p',p2)
sg2=XSteam('sV_p',p2)
x2=(s2-sf2)/(sg2-sf2)
hf2=XSteam('hL_p',p2)
hg2=XSteam('hV_p',p2)
h2=(1-x2)*hf2+x2*hg2
%Performance Calculations
ws=h1-h2;
```

The results are

| | |
|---------------------------|---------------------------|
| $h_1 = 3178.2$ kJ/kg | $h_2 = 2298.1$ kJ/kg |
| $h_{f2} = 359.84$ kJ/kg | $h_{g2} = 2652.9$ kJ/kg |
| $p_1 = 6000$ kPa | $p_2 = 60$ kPa |
| $s_1 = 6.5431$ kJ/kg-K | $s_2 = 6.5431$ kJ/kg-K |
| $s_{f2} = 1.1452$ kJ/kg-K | $s_{g2} = 7.5311$ kJ/kg-K |
| $T_1 = 400$ C | $x_2 = 0.8453$ |
| | $w_s = 880.1$ kJ/kg |

Calculation of enthalpy and steam quality at state 2 could have been shortened by simply writing

```

p2=60    % pressure in units of bar
x2=XSteam('x_ps',p2,s2)
h2=XSteam('h_px',p2,x2)    % or    h2=XSteam('h_ps',p2,s2)

```

The Ts -diagram is a convenient representation of the properties of steam, for lines of constant temperature on this chart are horizontal in the two-phase region, as are the lines of constant pressure. Isentropic processes pass through points along vertical lines. Adiabatic irreversible processes veer to the right of vertical lines, as entropy must increase. These make various processes easy to visualize.

An even more useful representation is one in which entropy is on the abscissa and enthalpy is on the ordinate. A diagram of this kind was developed by R. Mollier in 1906. A Mollier diagram, with accurate steam properties calculated using EES, is shown in Figure 2.4. The enthalpy drop used in the calculation of the work delivered by a steam turbine is now represented as a vertical distance between the end states.

If the exit state is inside the vapor dome, there is a practical limit beyond which exit steam quality cannot be reduced. In a *condensing steam turbine* a complicating factor in the

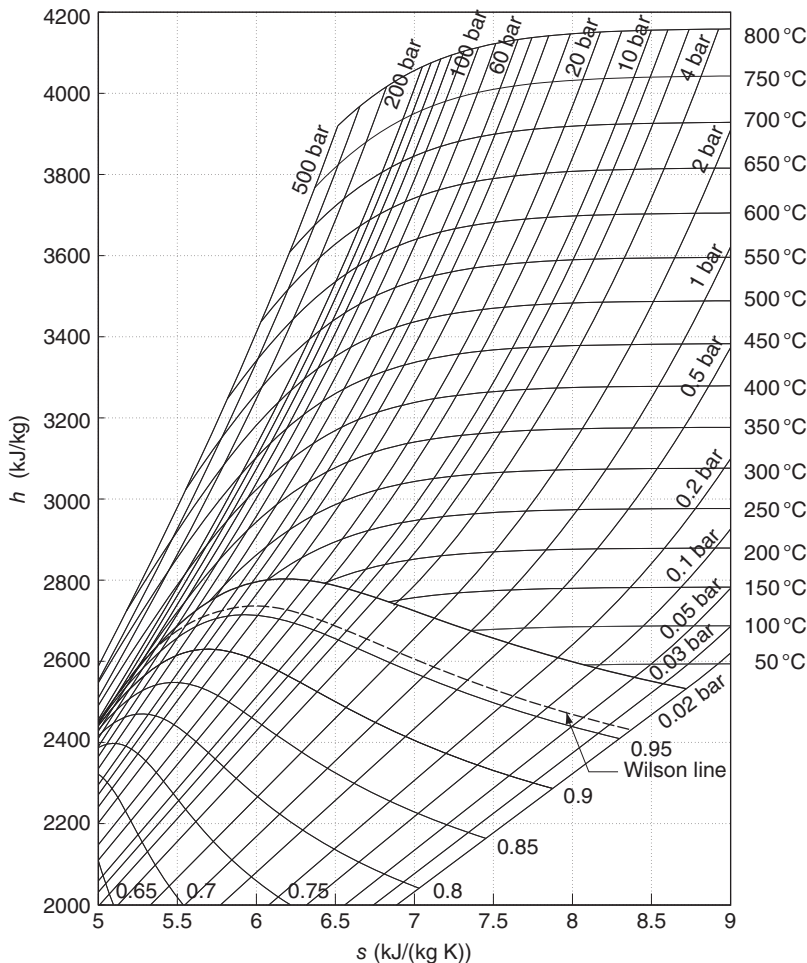


Figure 2.4 Mollier diagram for steam.

analysis is the lack of thermodynamic equilibrium as steam crosses into the vapor dome. Water droplets take a finite time to form, and if the steam is clean and free of nucleation sites, their formation is delayed. Also, if the quality is not too low, by the time droplets form, steam may have left the turbine.

The line below which droplet formation is likely to occur is called the *Wilson line*. It is about 115 kJ/kg below the saturated vapor line, with a steam quality 0.96 at low pressures of about 0.1 bar. The quality decreases to 0.95 along the Wilson line as pressure increases to 14 bar. Steam inside the vapor dome is *supersaturated* above the Wilson line, a term that arises from water existing as vapor at conditions at which condensation should be taking place.

■ EXAMPLE 2.4

Steam from a steam chest of a single-stage turbine at $p_1 = 3$ bar and $T_1 = 440^\circ\text{C}$ expands reversibly and adiabatically through a nozzle to pressure of $p_2 = 1$ bar. Find the velocity of the steam at the exit of the nozzle.

Solution: Since the process is isentropic, the states move down along a vertical line on the Mollier chart. From the chart, steam tables, or using XSteam, enthalpy of steam in the reservoir is determined to be $h_1 = 3359.2$ kJ/kg, and its entropy is $s_1 = 8.155$ kJ/(kg K). For an isentropic process, the exit state is specified by $p_2 = 100$ kPa and $s_2 = 8.155$ kJ/(kg K). Enthalpy, obtained by interpolating in the tables, is $h_2 = 3039.7$ kJ/kg.

Assuming that the velocity in the steam chest is negligible, the exit velocity is obtained from

$$h_1 = h_2 + \frac{1}{2}V_2^2$$

or

$$V_2 = \sqrt{2(h_1 - h_2)} = \sqrt{2(3359.2 - 3039.7) 1000} = 799.3 \text{ m/s}$$

A MATLAB or GNU/OCTAVE script used to solve this example is shown below.

```
%Example 2.4
clear all
p1=3; T1=440;
h1=XSteam('h_pT',p1,T1);
s1=XSteam('s_pt',p1,T1);
p2=1;
s2=s1;
h2=XSteam('h_ps',p2,s2);
p1=p1*100; p2=p2*100;
V2=sqrt(2*(h1-h2)*1000);
```

The results are

| | |
|-----------------------|-----------------------|
| $h_1 = 3359.2$ kJ/kg | $h_2 = 3039.7$ kJ/kg |
| $s_1 = 8.155$ kJ/kg-K | $s_2 = 8.155$ kJ/kg-K |
| $p_1 = 300.00$ kPa | $p_2 = 100.00$ kPa |
| $T_1 = 440$ C | $V_2 = 799.3$ m/s |



To the left of the saturated liquid line, water exists as a *compressed liquid*. Since specific volume and internal energy do not change appreciably as a result of water being compressed, their values may be approximated as

$$v(T, p) \approx v_f(T)$$

$$u(T, p) \approx u_f(T)$$

Enthalpy can then be obtained from

$$h(p, T) \approx u_f(T) + pv_f(T)$$

which can also be written as

$$h(p, T) = u_f(T) + p_f(T)v_f(T) + (p - p_f(T))v_f(T)$$

or as

$$h = h_f + v_f(p - p_f) \quad (2.6)$$

in which explicit dependence on temperature has been dropped and it is understood that all the properties are given at the saturation temperature.

Consider next the calculation of a change in enthalpy along an isentropic path from the saturated liquid state to a compressed liquid state at higher pressure. Integration of

$$Tds = dh - v dp$$

along an isentropic path, assuming v to be constant, gives

$$h = h_f + v_f(p - p_f) \quad (2.7)$$

This equation is identical to Eq. (2.6). Both approximations use the value of specific volume at the saturation state.

■ EXAMPLE 2.5

Water as saturated liquid at $p_1 = 6$ kPa is pumped to pressure $p_2 = 3400$ kPa. Find the specific work done by assuming the process to be reversible and adiabatic, and assuming that the difference in kinetic energy between inlet and exit is small and can be neglected. Also calculate the enthalpy of water at the state with temperature $T_2 = 36.16$ °C and pressure $p_2 = 3400$ kPa.

Solution: Since at the inlet to the pump, water exists as saturated liquid, its temperature is $T_1 = 36.16$ °C, specific volume is $v_1 = v_f = 0.0010064$ m³/kg, and entropy is $s_1 = s_f = 0.5209$ kJ/(kg K). At this state its enthalpy $h_1 = h_f = 151.494$ kJ/kg.

Along the isentropic path from state 1 to state 2s, Eq. (2.7), gives the value of enthalpy $h_{2sa} = 154.910$ kJ/kg. On the other hand, the value using XSteam at $p_{2s} = 3400$ kPa and $s_{2s} = 0.5209$ kJ/(kg K) is $h_{2s} = 154.894$ kJ/kg, which for practical purposes is the same as the approximate value. Hence, the work done is

$$w_s = h_{2s} - h_1 = 154.89 - 151.49 = 3.40 \text{ kJ/kg}$$

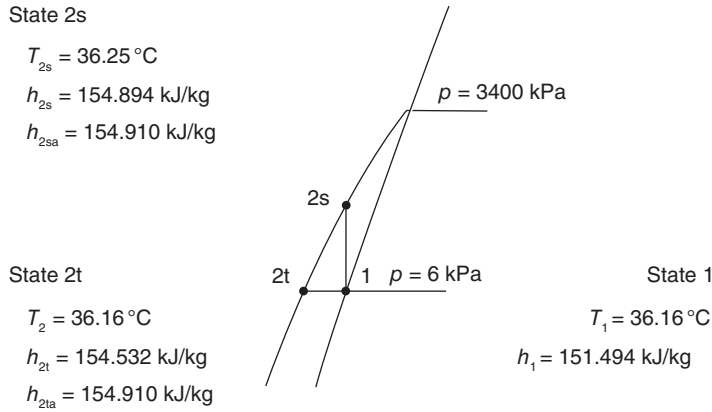


Figure 2.5 Actual and approximate values for the enthalpy of compressed liquid.

From Eq. (2.6) at pressure 3400 kPa an approximate value for enthalpy becomes

$$h_{2ta} = 151.494 + (3400 - 6) \cdot 0.0010064 = 154.910 \text{ kJ/kg}$$

whereas an accurate value obtained by XSteam for compressed liquid is 154.532 kJ/kg. These values are shown at points 1 and 2t in Figure 2.5. ■

2.4.2 Ideal gases

An ideal gas model assumes that internal energy is only a function of temperature $u = u(T)$ and the *equation of state* relates pressure and specific volume to temperature by

$$pv = RT \quad \text{or} \quad p = \rho RT \quad (2.8)$$

in which R is an ideal gas constant. It is equal to the universal gas constant, $\bar{R} = 8.314 \text{ kJ}/(\text{kmol K})$, divided by the molecular mass \mathcal{M} of the gas and is thus calculated according to $R = \bar{R}/\mathcal{M}$. The ideal gas model has been shown to be valid for various gases at low pressures. From Eq. (2.8), it follows that enthalpy for an ideal gas can be written in the form $h = u + RT$, and this shows that enthalpy is also a function of temperature only.

Specific heats for an ideal gas at constant volume and constant pressure simplify to

$$c_v(T) = \left(\frac{\partial u}{\partial T} \right)_v = \frac{du}{dT} \quad \text{so that} \quad du = c_v(T) dT$$

and

$$c_p(T) = \left(\frac{\partial h}{\partial T} \right)_p = \frac{dh}{dT} \quad \text{so that} \quad dh = c_p(T) dT$$

Differentiating next, $h = u + RT$ gives

$$dh = du + R dT \quad \text{or} \quad c_p(T) dT = c_v(T) dT + R dT$$

from which it follows that

$$c_p(T) = c_v(T) + R$$

Thus even if specific heats depend on temperature, their difference does not. Henceforth, the explicit dependence on temperature is not displayed. With $\gamma = c_p/c_v$ denoting the ratio of specific heats, the relations

$$c_v = \frac{R}{\gamma - 1} \quad c_p = \frac{\gamma R}{\gamma - 1} \quad (2.9)$$

follow directly. The values of c_v , c_p , and γ are shown for air in Figure 2.6.

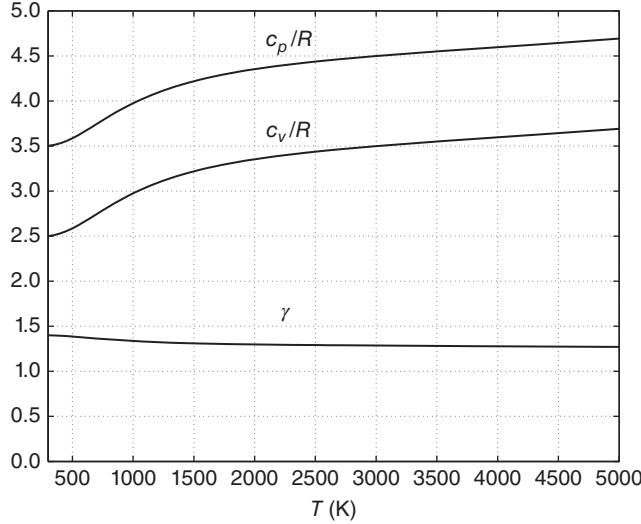


Figure 2.6 Specific heats for air and their ratio.

An approximate value for the ratio of specific heats is obtained from the *equipartition of energy principle* of kinetic theory of gases. It states that each degree of freedom of a molecule contributes $\frac{1}{2}R$ to the specific heat at constant volume. For a monatomic gas, there are three translational degrees of freedom: one for each of the three orthogonal coordinate directions. This means that for monatomic gases

$$c_v = \frac{3}{2}R \quad c_p = \frac{5}{2}R \quad \gamma = \frac{5}{3} = 1.67$$

If a molecule of a diatomic gas is regarded as a dumbbell, the rotational degrees of freedom about the two axes giving the largest moments of inertia contribute each one degree of freedom and the third is neglected. The vibrational degrees of freedom are not excited at relatively low temperatures. Hence, for diatomic gases the specific heats, and their ratio, are

$$c_v = \frac{5}{2}R \quad c_p = \frac{7}{2}R \quad \gamma = \frac{7}{5} = 1.40$$

Since air is made up mainly of the diatomic N_2 and O_2 , Figure 2.6 shows that the equipartition principle explains the low-temperature behavior of specific heats very well. Activation of greater number of vibrational modes takes place as temperature is increased.

Products of combustion flowing through a gas turbine consist of complex molecules, and the reasoning above suggests that the ratio of specific heats for them is closer to unity

than for diatomic molecules, since all three rotational and low-level vibrational modes are excited. For combustion gases, the value $\gamma = 1.333$ is appropriate. For superheated steam at low pressures, the value $\gamma = 1.3$ is acceptable, and for steam that is just below the saturated vapor line, Zeuner's empirical equation $\gamma = 1.035 + 0.1x$ is often used, with x as the steam quality. At saturation condition $x = 1$, and this gives $\gamma = 1.135$ for saturated steam.

2.4.3 Air tables and isentropic relations

In this section, the influence of temperature variation of specific heats on the thermodynamic properties of air are considered. Entropy for ideal gases can be determined by first writing

$$Tds = dh - v dp$$

in the form

$$ds = c_p \frac{dT}{T} - R \frac{dp}{p}$$

and integrating. This gives

$$s(T_2, p_2) - s(T_1, p_1) = s^0(T_2) - s^0(T_1) - R \ln \frac{p_2}{p_1} \quad (2.10)$$

in which s^0 is defined as

$$s^0(T) = \int_{T_{\text{ref}}}^T c_p(T) \frac{dT}{T}$$

Entropy is assigned the value zero at the reference state, $T_{\text{ref}} = 0 \text{ K}$ and $p_{\text{ref}} = 1 \text{ atm}$. The value of entropy at temperature T and pressure p is then calculated from

$$s(T, p) = s^0(T) - R \ln \frac{p}{p_{\text{ref}}}$$

For a reversible process $s_2 = s_1$, and Eq. (2.10) shows that

$$\frac{p_2}{p_1} = \exp \left[\frac{s^0(T_2) - s^0(T_1)}{R} \right]$$

which can be also be written as

$$\frac{p_2}{p_1} = \frac{\exp[s_2^0(T_2)/R]}{\exp[s_1^0(T_1)/R]}$$

Defining a relative pressure as

$$p_r(T) = \exp[s^0(T)/R]$$

it is seen that p_r is only a function of temperature. The ratio of pressures at the endpoints of a reversible process can now be expressed as

$$\frac{p_2}{p_1} = \frac{p_{r2}}{p_{r1}}$$

By using the ideal gas relation, the pressure ratio can be recast into the form

$$\frac{p_2}{p_1} = \frac{RT_2}{v_2} \frac{v_1}{RT_1} = \frac{p_{r2}}{p_{r1}}$$

Solving for the specific volume ratio yields

$$\frac{v_2}{v_1} = \left[\frac{RT_2}{p_r(T_2)} \right] \left[\frac{p_r(T_1)}{RT_1} \right]$$

Now defining $v_r(T) = RT/p_r(T)$ allows the specific volume ratio to be written as

$$\frac{v_2}{v_1} = \frac{v_{r2}}{v_{r1}}$$

The values of $s^0(T)$, $p_r(T)$, and $v_r(T)$ are listed in the air Table B.4. An alternative to the tables is to calculate the thermodynamic properties by a computer program. Such a function is listed in Table B.7.

■ EXAMPLE 2.6

Air enters a compressor at $p_1 = 100$ kPa and $T_1 = 300$ K. It is compressed isentropically to $p_2 = 1200$ kPa. Assuming that there is no change in the kinetic energy between the inlet and the exit, find the work done by the compressor using the air tables.

Solution: Reversible work done is

$$w_s = h_{2s} - h_1$$

At $T_1 = 300$ K, $p_{r1} = 1.386$, and $h_1 = 300.19$ kJ/kg. For an isentropic process,

$$p_{r2} = \frac{p_2}{p_1} p_{r1} = \frac{1200}{100} 1.386 = 16.632$$

Temperature corresponding to this value of p_{r2} is $T_{2s} = 603.5$ K and $h_{2s} = 610.64$ kJ/kg. Hence

$$w_s = h_{2s} - h_1 = 610.64 - 300.19 = 310.45 \text{ kJ/kg}$$

Carrying out the calculations with YAir from Table B.7 gives

```
%Example 2.6
clear all
Rbar=8.31447; M=28.943; R=Rbar/M;
%State 1
p1=100; T1=300;
p2=1200; R=0.287;
[T1,h1,u1,s01,pr1,vr1]=YAir('T',T1);
%State 2
pr2=p2*pr1/p1;
```



```
[T2s,h2s,u2s,s02,pr2,vr2]=YAir('pr',pr2);
%Work
ws=h2s-h1;
```

The results are

```
p1 = 100 kPa    T1 = 300.0 K    h1 = 300.19 kJ/kg-K    pr1 = 1.386
p2 = 1200 kPa   T2s = 603.7 K    h2s = 611.01 kJ/kg-K    pr2 = 16.654
ws = 310.82 kJ/kg
```

■

The function `YAir` was written in such a way that with one call, all the important variables are returned. The variables are listed in a certain logical order, namely temperature is first, enthalpy and internal energy are next followed by the temperature dependent part of entropy. Internal energy is seldom needed in turbomachinery analysis, but it is listed next to enthalpy as it is closely related to it. The last two entries are the relative pressure and volume.

When specific heats are assumed to be constant, integrating the Tds equations gives

$$s_2 - s_1 = c_v \ln \frac{T_2}{T_1} + R \ln \frac{v_2}{v_1}$$

or

$$s_2 - s_1 = c_p \ln \frac{T_2}{T_1} - R \ln \frac{p_2}{p_1}$$

For an isentropic process, the first of these gives

$$\frac{v_2}{v_1} = \left(\frac{T_2}{T_1} \right)^{-1/(\gamma-1)}$$

and the second one can be written as

$$\frac{p_2}{p_1} = \left(\frac{T_2}{T_1} \right)^{\gamma/(\gamma-1)}$$

Eliminating the temperature ratios gives

$$\frac{p_2}{p_1} = \left(\frac{v_1}{v_2} \right)^{\gamma} = \left(\frac{\rho_2}{\rho_1} \right)^{\gamma}$$

The next example illustrates, the use of these equations for the same conditions as in the previous example.

■ EXAMPLE 2.7

Air enters a compressor at $p_1 = 100$ kPa and $T_1 = 300$ K. It is compressed isentropically to $p_2 = 1200$ kPa. Find the work done by the compressor assuming constant specific heats with $\gamma = 1.4$ and using variable specific heats with `YAir`.

Solution: Work done is

$$w_s = c_p(T_{2s} - T_1)$$

Temperature T_{2s} is found from

$$T_{2s} = T_1 \left(\frac{p_2}{p_1} \right)^{(\gamma-1)/\gamma} = 300 \cdot 12^{0.4/1.4} = 610.18 \text{ K}$$

Hence,

$$w_s = c_p(T_{2s} - T_1) = 1.0045(610.18 - 300) = 311.58 \text{ kJ/kg}$$

The calculations with MATLAB or GNU/OCTAVE are the same as in the previous example but for the sake of illustration, the final state is found by calculating the temperature-dependent part of entropy and using it as input to function YAir.

```
%Example 2.7
clear all
Rbar=8.31447; M=28.943; R=Rbar/M;
p1=100; T1=300; p2=1200;
%State 1
[T1,h1,u1,s01,pr1,vr1]=YAir('T',T1);
%State 2
s02=s01+R*log(p2/p1);
[T2s,h2s,u2s,s02,pr2,vr2]=YAir('s0',s02);
%Work
ws=h2s-h1;
```

The results are

```
p1 = 100 kPa   T1 = 300.0 K   h1 = 300.19 kJ/kg-K   pr1 = 1.386
p2 = 1200 kPa  T2s = 603.7 K  h2s = 611.01 kJ/kg-K   pr2 = 16.654
ws = 310.82 kJ/kg
```

Owing to the relatively small temperature range, the error made in assuming constant specific heats is quite small. The difference between the computer calculation and using the air tables arises from interpolation and it is insignificant. ■

2.4.4 Ideal gas mixtures

Kinetic theory of ideal gas mixtures originates from the intuitive notion that the pressure on the walls of a vessel containing a gas is caused by the momentum of colliding molecules. This suggests that at relatively low densities, each molecular species may be assumed to act independently.

Dalton's model is based on such a consideration, and it states that the mixture pressure is equal to the sum of the component pressures p_i , which each of the molecular species in the mixture would exert if it were to exist alone at the mixture temperature and volume. Expressed algebraically, this is

$$p = p_1 + p_2 + \cdots + p_n$$

When ideal gas behavior may be assumed, the component pressure p_i can be represented by

$$p_i = \frac{N_i \bar{R}T}{V}$$

in which N_i is the number of moles of the i th component, T is the mixture temperature, and V is the mixture volume. For the mixture, the ideal gas law is

$$p = \frac{N \bar{R}T}{V}$$

and N is the number of moles in the mixture. Dividing the last two equations by each other gives

$$p_i = \frac{N_i}{N} p = y_i p$$

and here y_i is the mole fraction and p_i is the *partial pressure* of the i th component. It is equal to the component pressure only for ideal gases.

Other properties of an ideal gas mixture can be obtained by a generalization of Dalton's rule, called the *Gibbs–Dalton* rule. Thus internal energy of a mixture is given by

$$U = U_1 + U_2 + \cdots + U_n$$

Since the internal energy of the i th component can be written as

$$U_i = N_i \bar{u}_i$$

in which \bar{u}_i is the internal energy per mole of the i th species, the internal energy of the mixture may be expressed as

$$U = N_1 \bar{u}_1 + N_2 \bar{u}_2 + \cdots + N_n \bar{u}_n$$

Dividing this by the total number of moles gives

$$\bar{u} = y_1 \bar{u}_1 + y_2 \bar{u}_2 + \cdots + y_n \bar{u}_n$$

On a mass basis internal energy may be written as

$$U = m_1 u_1 + m_2 u_2 + \cdots + m_n u_n$$

in which m_i is the mass of the i th component. Dividing this by the mass of the mixture gives

$$u = x_1 u_1 + x_2 u_2 + \cdots + x_n u_n$$

and here $x_i = m_i/m$ is the mass fraction of the i th component. Similar equations hold for enthalpy:

$$\bar{h} = y_1 \bar{h}_1 + y_2 \bar{h}_2 + \cdots + y_n \bar{h}_n$$

$$h = x_1 h_1 + x_2 h_2 + \cdots + x_n h_n$$

Using the Gibbs–Dalton rule, entropy of the i th component in an ideal gas mixture behaves as if it existed alone at the mixture temperature and its own partial pressure. Thus

$$S = N_1 \bar{s}_1(T, p_1) + N_2 \bar{s}_2(T, p_2) + \cdots + N_n \bar{s}_n(T, p_n)$$

or

$$S = m_1 s_1(T, p_1) + m_2 s_2(T, p_2) + \cdots + m_n s_n(T, p_n)$$

On a molar basis the specific entropy is

$$\bar{s} = y_1 \bar{s}_1(T, p_1) + y_2 \bar{s}_2(T, p_2) + \cdots + y_n \bar{s}_n(T, p_n)$$

and on a mass basis it is

$$s = x_1 s_1(T, p_1) + x_2 s_2(T, p_2) + \cdots + x_n s_n(T, p_n)$$

Gibbs equation for the i th component can be written as

$$T ds_i = dh_i - v_i dp_i$$

in which $v_i = V/m_i$ is the specific volume of the i th component. Using the ideal gas relation $p_i v_i = R_i T$ puts the Gibbs equation into the form

$$ds_i = c_{p,i} \frac{dT}{T} - R_i \frac{dp_i}{p_i}$$

By assuming the specific heat to be constant, integrating this gives

$$\Delta s_i = c_{p,i} \ln \frac{T_2}{T_1} - R_i \ln \frac{p_{i,2}}{p_{i,1}}$$

or on a molar basis

$$\Delta \bar{s}_i = \bar{c}_{p,i} \ln \frac{T_2}{T_1} - \bar{R} \ln \frac{p_{i,2}}{p_{i,1}}$$

The pressure term on the right is used in the definition of *entropy of mixing*. In combustion reactions, once the combustion is complete, the mixture of combustion products may be considered a pure substance, just as is done for atmospheric air. Expansion through a turbine then takes place at a constant mixture composition and the entropy of mixing vanishes. If the specific heats are assumed to be constant, then, in order to carry out the calculations, it only remains to determine the specific heat and molecular mass of the mixture.

The molecular mass of the mixture is obtained from

$$\begin{aligned} \mathcal{M} &= \frac{m_1 + m_2 + \cdots + m_n}{N} = \frac{N_1 \mathcal{M}_1 + N_2 \mathcal{M}_2 + \cdots + N_n \mathcal{M}_n}{N} \\ &= y_1 \mathcal{M}_1 + y_2 \mathcal{M}_2 + \cdots + y_n \mathcal{M}_n \end{aligned}$$

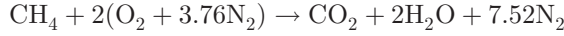
or

$$\mathcal{M} = \sum_{i=1}^n y_i \mathcal{M}_i$$

The constant pressure specific heat of the mixture is

$$\bar{c}_p = \sum_{i=1}^n y_i \bar{c}_{pi} \quad \text{and} \quad c_p = \frac{\bar{c}_p}{\mathcal{M}}$$

From earlier studies of combustion, it may be recalled that combustion of methane with a stoichiometric amount of theoretical air leads to the chemical equation



Assuming that the water in the products remains as vapor, the total number of moles in the gaseous products is 10.52. If the amount of theoretical air is 125% of the stoichiometric amount, then the previous chemical equation becomes



and the number of moles of gaseous products is 12.90. The next example illustrates the calculation of the mixture specific heat.

■ EXAMPLE 2.8

Consider the combustion of methane with 125% of theoretical air. Find the molecular mass of the mixture and the specific heat at constant pressure.

Solution: The number of moles of each species has been calculated above and are as follows: $N_{\text{CO}_2} = 1$, $N_{\text{H}_2\text{O}} = 2$, $N_{\text{O}_2} = 0.5$, and $N_{\text{N}_2} = 9.4$. Hence the total number of moles is $N = 12.9$ and the mole fractions are $y_{\text{CO}_2} = 0.0775$, $y_{\text{H}_2\text{O}} = 0.1550$, $y_{\text{O}_2} = 0.0388$, and $y_{\text{N}_2} = 0.7287$. The specific heats of common gases are listed in the Table B.5. The molecular mass of the mixture is given by

$$\begin{aligned} \mathcal{M} &= y_{\text{CO}_2} \mathcal{M}_{\text{CO}_2} + y_{\text{H}_2\text{O}} \mathcal{M}_{\text{H}_2\text{O}} + y_{\text{O}_2} \mathcal{M}_{\text{O}_2} + y_{\text{N}_2} \mathcal{M}_{\text{N}_2} \\ &= 0.0775 \cdot 44.0 + 0.1550 \cdot 18.0 + 0.0388 \cdot 32.0 + 0.7287 \cdot 28.0 \\ &= 27.845 \text{ kg/kmol} \end{aligned}$$

The molar specific heat at constant pressure is then

$$\begin{aligned} \bar{c}_p &= y_{\text{CO}_2} \bar{c}_{p, \text{CO}_2} + y_{\text{H}_2\text{O}} \bar{c}_{p, \text{H}_2\text{O}} + y_{\text{O}_2} \bar{c}_{p, \text{O}_2} + y_{\text{N}_2} \bar{c}_{p, \text{N}_2} \\ &= 0.0775 \cdot 37.3292 + 0.1550 \cdot 33.5702 + 0.0388 \cdot 29.3683 + 0.7287 \cdot 29.1533 \\ &= 30.480 \text{ kJ/(kmol K)} \end{aligned}$$

The mixture specific heat is

$$c_p = \frac{\bar{c}_p}{\mathcal{M}} = 1.0946 \text{ kJ/(kg K)}$$

As pointed out by Cohen et al. [15], it has been found that for combustion products of jet fuel, it is sufficiently accurate to use the values

$$c_p = 1148 \text{ J/(kg K)} \quad R = 287 \text{ J/(kg K)} \quad \gamma = \frac{4}{3}$$

As inspection of Figure 2.6 shows that the value of γ decreases and that of c_p increases as temperature increases. Hence, if the actual mean temperature during a process is lower than that for which these values apply, then the value of γ is too large in the calculation in which it is used to determine the temperature change, and therefore this leads to an excessively large change in the temperature. But then the value of c_p is too low and the product $c_p \Delta T$ to determine the enthalpy change during the process is nearly correct, as it involves compensating errors. By a similar argument, the constant values for air are

$$c_p = 1004.5 \text{ J/(kg K)} \quad R = 287 \text{ J/(kg K)} \quad \gamma = 1.4$$

2.4.5 Incompressibility

The important distinction between an *incompressible fluid* and *incompressible flow* is introduced next. Incompressibility may, on the one hand, mean that specific volume does not change with pressure, but it is allowed to change with temperature. A stricter model is to have the specific volume remain absolutely constant. In liquid water even large changes in pressure lead to only small changes in the specific volume, and by this definition it is nearly incompressible, even if its specific volume changes appreciably with temperature. In the flow of gases at low speeds, pressure changes are mild and the *flow is considered incompressible*, even if the fluid is clearly compressible.

With these distinctions in mind, consider a strictly incompressible fluid. With v constant, the first Gibbs equation reduces to

$$du = Tds$$

This shows that internal energy changes only if the entropy changes. If the flow is adiabatic, entropy increases only as a result of irreversibilities, and hence, this can be the only cause of an increase in internal energy. Similarly, if the flow is reversible and adiabatic, then internal energy must remain constant. As a consequence, the first law of thermodynamics in such a flow takes the form

$$\frac{p_1}{\rho} + \frac{1}{2}V_1^2 + gz_1 = \frac{p_2}{\rho} + \frac{1}{2}V_2^2 + gz_2 + w_s \quad (2.11)$$

Thermal energy terms are completely absent, and this equation involves only mechanical energy. When no work is done, it reduces to

$$\frac{p_1}{\rho} + \frac{1}{2}V_1^2 + gz_1 = \frac{p_2}{\rho} + \frac{1}{2}V_2^2 + gz_2 \quad (2.12)$$

This equation was developed for a flow through a control volume with properties that are uniform at its inlet and exit. By taking a control surface to coincide with a stream-tube of infinitesimal cross section, this requirement is automatically Satisfied, and this equation goes by the name Bernoulli equation, valid between any two point on the same streamline. The sum of the three terms is thus constant and when written as

$$p + \frac{1}{2}\rho V^2 + \rho gz = p_0$$

the constant p_0 is called the *Bernoulli constant*, or more commonly the stagnation pressure in an incompressible flow, as discussed in the next section.

2.4.6 Stagnation state

Stagnation state is defined by the equations

$$\begin{aligned} h_0 &= h + \frac{1}{2}V^2 + gz \\ s_0 &= s \end{aligned} \quad (2.13)$$

It is a *reference state* that may not correspond to any actual state in the flow. As was pointed out earlier, enthalpy h_0 is called the *stagnation enthalpy* and h is now called the *static enthalpy*. Other properties, such as pressure, temperature, specific volume, or density are designated similarly. This definition fixes to each static state in the flow a corresponding unique stagnation state. The stagnation state is arrived at by a *thought experiment* in which the flow is decelerated isentropically to zero velocity, while it descends or ascends to a reference elevation.

From the definition of a stagnation state, integrating $Tds = dh - v dp$ from a static state to its stagnation state gives the following equation, since $ds = 0$,

$$h_0 - h = \int_p^{p_0} v dp = \int_p^{p_0} \frac{dp}{\rho}$$

For an *incompressible fluid* this reduces to

$$h_0 - h = \frac{p_0}{\rho} - \frac{p}{\rho}$$

Substituting for h_0 from Eq. (2.13) into this gives

$$p_0 = p + \frac{1}{2}\rho V^2 + \rho gz \quad (2.14)$$

which, as mentioned above, defines the stagnation pressure for an incompressible fluid. This expression can also be used in low-speed compressible flow as an approximation to the true stagnation pressure.

2.5 EFFICIENCY

In this section, various measures of efficiency for turbomachinery flows and their relationship to thermodynamic losses are discussed.

2.5.1 Efficiency measures

Work delivered by a turbine is given as the difference between inlet and exit stagnation enthalpy. A greater amount of work would be delivered during an expansion along a reversible path to the same exit pressure. With w the actual work and w_s the isentropic work, their ratio

$$\eta_{tt} = \frac{w}{w_s} = \frac{h_{01} - h_{03}}{h_{01} - h_{03s}} \quad (2.15)$$

is called a *total-to-total* efficiency. In the analysis of a turbine stage, inlet to a stator (nozzle) is given label 1 and 3 is the exit state from the rotor. Label 2 is reserved to

two equations

$$s_3 - s_1 = c_p \ln \frac{T_3}{T_{3s}} \quad s_3 - s_1 = \ln \frac{T_{03}}{T_{03s}}$$

from which

$$\frac{T_3}{T_{3s}} = \frac{T_{03}}{T_{03s}} \quad \text{or} \quad \frac{T_{03}}{T_3} = \frac{T_{03s}}{T_{3s}}$$

From the definition of a stagnation state the following two equations are obtained

$$\frac{T_{03}}{T_3} = 1 + \frac{V_3^2}{2c_p T_3} \quad \frac{T_{03s}}{T_{3s}} = 1 + \frac{V_{3s}^2}{2c_p T_{3s}}$$

and the equality of the temperature ratios on the left-hand sides (LHSs) of these equations shows that

$$\frac{V_3}{V_{3s}} = \sqrt{\frac{T_3}{T_{3s}}}$$

so that $V_3 > V_{3s}$. Without a great loss of accuracy, the temperature ratio is often replaced by unity, and then V_{3s} is replaced by V_3 .

If a stage is designed such that $V_1 = V_3$, then the kinetic energy terms in the numerator of Eq. (2.17) cancel. If next the approximation $V_3 = V_{3s}$ is used, then Eq. (2.15) for total-to-total efficiency reduces to

$$\eta_t = \frac{h_1 - h_3}{h_1 - h_{3s}}$$

This is the familiar definition of turbine efficiency from the study in the first course of thermodynamics. In a multistage turbine, the exit state would need a different label. It will be denoted by label e when the distinction needs to be made.

■ EXAMPLE 2.9

Steam enters an adiabatic multistage turbine at static pressure of 80 bar, static temperature 520 °C, and velocity 50 m/s. It leaves the turbine at pressure 0.35 bar, temperature 80 °C, and velocity 200 m/s. Find the stagnation enthalpy and pressure at the inlet, stagnation enthalpy and pressure at the exit, total-to-total efficiency, total-to-static efficiency, and the specific work done.

Solution: Using steam tables static enthalpy and entropy of steam at the inlet and exit are

$$\begin{aligned} h_1 &= 3448.6 \text{ kJ/kg} & s_1 &= 6.7893 \text{ kJ/(kg K)} \\ h_e &= 2645.2 \text{ kJ/kg} & s_e &= 7.7561 \text{ kJ/(kg K)} \end{aligned}$$

Stagnation enthalpies are

$$\begin{aligned} h_{01} &= h_1 + \frac{1}{2} V_1^2 = 3448.6 + \frac{50^2}{2 \cdot 1000} = 3449.9 \text{ kJ/kg} \\ h_{0e} &= h_e + \frac{1}{2} V_e^2 = 2645.2 + \frac{200^2}{2 \cdot 1000} = 2665.2 \text{ kJ/kg} \end{aligned}$$

Had the flow been isentropic, the exit state would have corresponded to $p_e = 0.35$ bar and $s_{es} = s_1$. This is inside the vapor dome at quality

$$x_{es} = \frac{s_{es} - s_f}{s_g - s_f} = \frac{6.7893 - 0.9876}{7.7146 - 0.9876} = 0.8624$$

and the enthalpy at this state is

$$h_{es} = h_f + x_{es}(h_g - h_f) = 304.25 + 0.8624 \cdot (2630.7 - 304.25) = 2310.7 \text{ kJ/kg}$$

Assuming that $V_{es} = V_e$ then gives

$$h_{0es} = h_{es} + \frac{1}{2} V_e^2 = 2310.7 + \frac{200^2}{2 \cdot 1000} = 2330.7 \text{ kJ/kg}$$

and the total-to-total efficiency is

$$\eta_{tt} = \frac{h_{01} - h_{0e}}{h_{01} - h_{0es}} = \frac{3449.9 - 2665.2}{3449.1 - 2329.9} = 0.7011$$

The total-to-static efficiency is

$$\eta_{ts} = \frac{h_{01} - h_{0e}}{h_{01} - h_{es}} = \frac{3449.9 - 2665.2}{3449.9 - 2310.7} = 0.6888$$

and the definition of efficiency when kinetic energy changes are neglected is

$$\eta_t = \frac{h_1 - h_e}{h_1 - h_{es}} = \frac{3448.6 - 2645.2}{3448.6 - 2310.7} = 0.7061$$

The specific work delivered is

$$w = h_{01} - h_{0e} = 3449.9 - 2665.2 = 784.7 \text{ kJ/kg}$$

■

Consider next a single-stage centrifugal compressor. The flow leaving the impeller enters a *diffuser section*, and then a *volute*. These stationary parts of the machine are designed to decelerate the flow so that at the exit velocity is well matched with the desired flow velocity in the discharge pipe. Since kinetic energy from the impeller is utilized in this way, it is again appropriate to define the efficiency as the total-to-total efficiency. It is given by

$$\eta_{tt} = \frac{w_s}{w} = \frac{h_{03s} - h_{01}}{h_{03} - h_{01}} \quad (2.18)$$

The process lines between the stagnation states and the corresponding static states are shown in Figure 2.8. Now, as for the turbine, the state 03s is assumed to be on the constant-pressure line p_{03} , and the sketch reflects this. Had the same amount of compression work been done reversibly the exit stagnation pressure would have been p_{03i} , which is also shown in the figure.

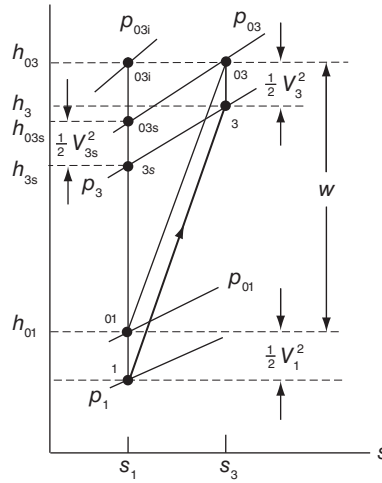


Figure 2.8 Thermodynamic states used to define a compressor efficiency.

In ventilating blowers, no use is made of the exit kinetic energy, and in such applications, the total-to-static efficiency is used. In these cases efficiency is defined as

$$\eta_{ts} = \frac{h_{3s} - h_{01}}{h_{03} - h_{01}}$$

Since h_{3s} is smaller than h_{03s} , the efficiency is likewise smaller, and the difference accounts for the wasted kinetic energy. To be sure, in ventilating a space, high velocity may be needed to blow off light particulate matter sitting on the floors or attached to walls. In this case, a blower may be placed upstream of the ventilated space and *forced draft* used to remove the particles. In *induced draft* contaminated air is drawn from the ventilated space into a blower and the kinetic energy in the exhaust stream is lost to the surroundings.

■ EXAMPLE 2.10

Air is drawn into a fan of diameter $D = 95.4$ cm from atmosphere at pressure 101.3 kPa and temperature 288.0 K. The volumetric flow rate is $Q = 4.72$ m³/s of standard air, and the power to the fan is $\dot{W} = 2.52$ kW. The total-to-total efficiency of the fan is 0.8. (a) Find the total-to-static efficiency. (b) Find the stagnation pressure rise across the fan.

Solution: (a) As air is drawn from the atmosphere at standard temperature and pressure. It then undergoes a reversible adiabatic acceleration to the inlet of the blower. The inlet stagnation pressure is therefore $p_{01} = 101.3$ kPa, and the stagnation temperature is $T_{01} = 288.0$ K. The stagnation density of standard air is given by

$$\rho_{01} = \frac{p_{01}}{RT_{01}} = \frac{101300}{287 \cdot 288.0} = 1.225 \text{ kg/m}^3$$

The mass flow rate is therefore

$$\dot{m} = \rho_{01} Q = 1.225 \cdot 4.72 = 5.78 \text{ kg/s}$$

The fan flow area and velocity, assuming $A_1 = A_3$, are

$$A = \frac{1}{4} \pi D^2 = 0.715 \text{ m}^2 \quad V_1 = V_3 = \frac{Q}{A} = \frac{4.72}{0.715} = 6.6 \text{ m/s}$$

Velocity is quite low and the flow can be considered incompressible with constant density. The specific work is

$$w = \frac{\dot{W}}{\dot{m}} = \frac{2520}{5.78} = 435.8 \text{ J/kg}$$

and the isentropic work is

$$w_s = \eta_{tt} w = 0.8 \cdot 435.8 = 348.7 \text{ J/kg}$$

Assuming that $V_{3s} = V_3$, the total-to-static efficiency may be written as

$$\eta_{ts} = \frac{T_{3s} - T_{01}}{T_{03} - T_{01}} = \frac{T_{03s} - T_{01} - V_3^2 / (2c_p)}{T_{03} - T_{01}} = \eta_{tt} - \frac{V_3^2}{2w} = 0.8 - \frac{6.6^2}{2 \cdot 435.8} = 0.75$$

(b) The stagnation pressure rise can be calculated from

$$p_{03} - p_{01} = \rho w_s = 1.225 \cdot 348.7 = 427 \text{ Pa} = 43.6 \text{ mm H}_2\text{O}$$

The exit states were labeled with subscript 3 even though this machine does not have anything that functions as a stator. ■

In a multistage compressor with large pressure and temperature differences, the variability of specific heats with temperature needs to be factored in to obtain an accurate result. This is illustrated in the next example.

■ EXAMPLE 2.11

Air from the atmosphere flows into a multistage compressor at pressure 1 bar and temperature 300 K. The ratio of stagnation pressures across the compressor is 30, and its total-to-total efficiency is 0.82. (a) Find the loss of stagnation pressure during this compression process, assuming specific heats to be constant. (b) Find also the loss in stagnation pressure assuming specific heats to vary with temperature.

Solution: (a) The inlet to the compressor is labeled as state 1, and its exit is denoted as e. The isentropic compression gives the stagnation temperature

$$T_{0es} = T_{01} \left(\frac{p_{0e}}{p_{01}} \right)^{(\gamma-1)/\gamma} = 300 \cdot 30^{1/3.5} = 792.8 \text{ K}$$

From the definition of efficiency

$$\eta_{tt} = \frac{T_{0es} - T_{01}}{T_{0e} - T_{01}}$$

the exit temperature is

$$T_{0e} = T_{01} + \frac{1}{\eta_{tt}}(T_{0es} - T_{01}) = 300 + \frac{1}{0.82}(792.8 - 300) = 901.0 \text{ K}$$

If the same amount of work had been done isentropically, the pressure ratio would have been

$$\frac{p_{0ei}}{p_{01}} = \left(\frac{T_{0e}}{T_{01}} \right)^{\gamma/(\gamma-1)} = \left(\frac{901}{300} \right)^{3.5} = 46.94$$

Hence, $p_{0ei} = 46.94$ bar and the loss of stagnation pressure is $\Delta p_{0L} = p_{0ei} - p_{0e} = 46.94 - 30 = 16.94$ bar.

(b) For variable specific heats, at $T_{01} = 300$ K and (with the script YAir) $p_{r1} = 1.386$ and $h_{01} = 300.19$ kJ/kg. Hence

$$p_{re} = p_{r1} \frac{p_{0e}}{p_{01}} = 1.386 \cdot 30 = 41.58$$

Thus $T_{0es} = 771.80$ K and $h_{0es} = 791.27$ kJ/kg. Using the definition of total-to-total efficiency

$$\eta_{tt} = \frac{h_{0es} - h_{01}}{h_{0e} - h_{01}}$$

gives for the exit enthalpy the value

$$h_{0e} = h_{01} + \frac{h_{0es} - h_{01}}{\eta_{tt}} = 300.19 + \frac{791.27 - 300.19}{0.82} = 899.07 \text{ kJ/kg}$$

From the air tables for this value $p_{rei} = 65.85$. It then follows that

$$\frac{p_{0ei}}{p_{01}} = \frac{p_{rei}}{p_{r1}} = \frac{65.85}{1.386} = 47.51$$

and $p_{0ei} = 47.51$ bar. Hence the loss of stagnation pressure is $\Delta p_{0L} = p_{0ei} - p_{0e} = 47.51 - 30.0 = 17.51$ bar. There is now a small difference in the calculated results because the temperature range between inlet and exit states is large. ■

2.5.2 Thermodynamic losses

The effect of thermodynamic losses is illustrated by considering an increment on either a turbine or a compressor process line, as shown in Figure 2.9. From the Gibbs equation

$$Tds = dh - v dp$$

the slope of the constant-pressure line is

$$\left(\frac{\partial h}{\partial s} \right)_p = T$$

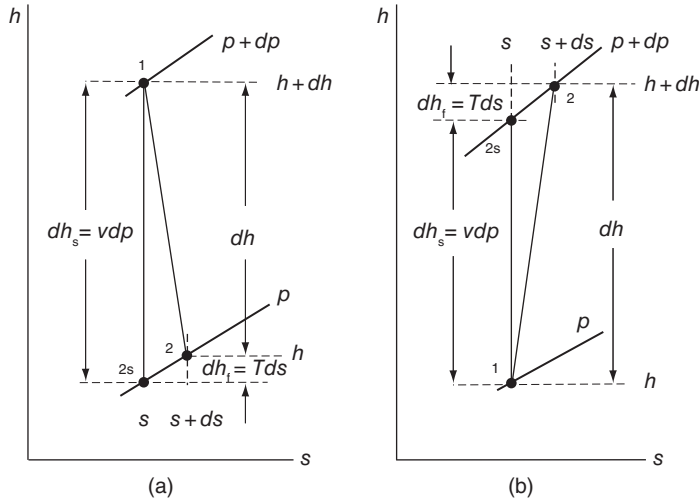


Figure 2.9 (a) An infinitesimal irreversible process in a turbine and (b) an infinitesimal irreversible process in a compressor.

which shows that this slope is equal to the absolute temperature on an enthalpy–entropy (h - s) diagram. The enthalpy change between the end states may be considered to be made up of two parts. The irreversible change in enthalpy is $dh_f = T ds$, and the isentropic change is obtained by setting $ds = 0$, which gives $dh_s = v dp$. Substituting these back into the $T ds$ equation shows that in this notation

$$dh = dh_s + dh_f$$

For a compressor, all three terms are positive. For a turbine, dh_f is positive, but dh and dh_s have negative values. The irreversible process associated with dh_f is called *reheating*, or *internal heating*. Although the former term is in general use to describe this, the latter is better for it reflects what is happening physically. In other words, the irreversibilities cause an increase in temperature.

The nature of the irreversibilities may be further illustrated by considering a flow channel that extends from an inlet at location ℓ_1 to some general location ℓ . The first law of thermodynamics for this control volume is

$$\dot{Q} + \dot{m} \left(u_1 + p_1 v_1 + \frac{1}{2} V_1^2 + g z_1 \right) = \dot{m} \left(u + p v + \frac{1}{2} V^2 + g z \right) + \dot{W}$$

Differentiating this with respect to ℓ and rearranging gives

$$\dot{m} \frac{du}{d\ell} = \dot{Q}' - \dot{m} \left[\frac{d(pv)}{d\ell} + \frac{1}{2} \frac{dV^2}{d\ell} + g \frac{dz}{d\ell} \right] - \dot{W}' \quad (2.19)$$

in which the rate of heat transfer and work interaction per unit length along the element $d\ell$ have been defined as

$$\dot{Q}' = \frac{d\dot{Q}}{d\ell} \quad \dot{W}' = \frac{d\dot{W}}{d\ell}$$

Clearly, in those parts of the flow in which there are no heat interactions $\dot{Q}' = 0$ and similarly $\dot{W}' = 0$ in those parts where there are no work interactions.

Differentiating the second law of thermodynamics

$$\dot{m}(s - s_1) = \int_{\ell_1}^{\ell} \frac{\dot{Q}'}{T} d\ell + \int_{\ell_1}^{\ell} \dot{S}'_p d\ell$$

with respect to ℓ gives

$$\dot{m} \frac{ds}{d\ell} = \frac{\dot{Q}'}{T} + \dot{S}'_p \quad (2.20)$$

2.5.3 Incompressible fluid

For an incompressible fluid, density and its reciprocal specific volume are constant. For this kind of fluid, the first Gibbs equation reduces to

$$T \frac{ds}{d\ell} = \frac{du}{d\ell}$$

Combining this with the second law in Eq. (2.20) gives

$$\dot{m} \frac{du}{d\ell} = \dot{Q}' + T \dot{S}'_p \quad (2.21)$$

As was remarked earlier, the second term on the right shows that internal energy in incompressible flow *always increases* as a result of irreversibilities. The first term on the right side shows that internal energy increases by heat transfer into the fluid, but decreases when heat is lost to the surroundings. Integrating Eq. (2.21) gives

$$u_2 - u_1 = q + \frac{1}{\dot{m}} \int_{\ell_1}^{\ell_2} T \dot{S}'_p d\ell \quad (2.22)$$

Substituting Eq. (2.21) into Eq. (2.19) puts the latter into the form

$$\dot{m} \left(\frac{d(pv)}{d\ell} + \frac{1}{2} \frac{dV^2}{d\ell} + g \frac{dz}{d\ell} \right) + \dot{W}' = -T \dot{S}'_p$$

Integrating this gives

$$p_2 v + \frac{1}{2} V_2^2 + g z_2 = p_1 v + \frac{1}{2} V_1^2 + g z_1 - w - \int_{\ell_1}^{\ell_2} T s'_p d\ell \quad (2.23)$$

The specific entropy production per unit length of the flow channel, s'_p , has been introduced via $s'_p = \dot{S}'_p / \dot{m}$ to simplify the notation. In Eqs. (2.21) and (2.23) absolute temperature T multiplies the specific entropy production per unit length, and it is the product $T s'_p$, having the dimensions of specific energy per unit length of the channel, which represents a thermodynamic energy loss.

In the first law of thermodynamics, flow work, kinetic and potential energy, and external work are all associated with *mechanical energy*. On the other hand, internal energy and heat interactions are *thermal energy* terms. Viewed from this perspective Eq. (2.22) may be

said to be a *thermal energy balance* and Eq. (2.23) a *mechanical energy balance*. The term associated with entropy production represents an *irreversible conversion of mechanical energy into internal energy* and is the reason why it is also called a *thermodynamic energy loss*. In contrast to a conservation principle in which there are no terms that would represent conversion of one form of energy to another, in a balance equation such a conversion term may be present. Further examination shows that heat transfer to, or from, an incompressible fluid changes only the internal energy and not the pressure, velocity, or elevation. These quantities change only as a result of work done or extracted, and they decrease as a result of irreversibilities in the flow. It is customary not to make a distinction between conservation and balance principles in practice, and often the principle of conservation of mass, for example is called simply the *mass balance*. This practice will also be followed in this text.

For an *incompressible fluid* stagnation pressure has been shown to be given by

$$p_0 = p + \frac{1}{2}\rho V^2 + \rho gz$$

Making use of this relationship Eq. (2.23) takes the form

$$p_{02} = p_{01} - \rho w - \frac{\rho}{\dot{m}} \int_{\ell_1}^{\ell_2} T \dot{s}'_p d\ell \quad (2.24)$$

This shows that stagnation pressure changes because of a work interaction with the surroundings and it drops because of irreversibilities in the flow.

2.5.4 Compressible flows

For compressible flows, the first law of thermodynamics is written for a flow extending from location ℓ_1 to an arbitrary location ℓ , as

$$\dot{Q} + \dot{m} \left(h_1 + \frac{1}{2}V_1^2 + gz_1 \right) = \dot{W} + \dot{m} \left(h + \frac{1}{2}V^2 + gz \right)$$

or in terms of stagnation enthalpies as

$$\dot{Q} + \dot{m}h_{01} = \dot{W} + \dot{m}h_0$$

Differentiating gives

$$\dot{Q}' - \dot{W}' = \dot{m} \frac{dh_0}{d\ell} \quad (2.25)$$

The second law of thermodynamics in the differential form has been shown to have the form

$$\dot{m} \frac{ds}{d\ell} = \frac{\dot{Q}'}{T} + \dot{S}'_p$$

Writing next the second Tds equation between stagnation states as

$$T_0 \frac{ds}{d\ell} = \frac{dh_0}{d\ell} - v_0 \frac{dp_0}{d\ell}$$

and substituting $ds/d\ell$ from this into the second law leads to

$$\dot{m} \frac{dh_0}{d\ell} - \dot{m} v_0 \frac{dp_0}{d\ell} = \frac{T_0}{T} \dot{Q}' + T_0 \dot{S}'_p$$

Using Eq. (2.25) to eliminate $dh_0/d\ell$ yields the equation

$$\dot{m} v_0 \frac{dp_0}{d\ell} = \left(\frac{T_0}{T} - 1 \right) \dot{Q}' - T_0 \dot{S}'_p - \dot{W}' \quad (2.26)$$

Turbomachinery flows are adiabatic so the heat transfer term may be dropped.

In an adiabatic flow integrating Eq. (2.26) gives

$$\int_{p_{01}}^{p_{02}} v_0 dp_0 + w = - \int_{\ell_1}^{\ell_2} T_0 s'_p d\ell \quad (2.27)$$

If the same amount of work had been done reversibly, then the exit stagnation pressure would have been different. Because the work done is the same, the pressure p_{02i} lies along the constant h_{02} line. A process line for this is shown in Figure 2.7, except that in that figure the exit enthalpy h_{03} corresponds to the enthalpy h_{02} .

Integrating next Eq. (2.26) for a reversible adiabatic process gives

$$\int_{p_{01}}^{p_{02i}} v_0 dp_0 + w_s = 0 \quad (2.28)$$

Thus, since it has been stipulated that $w = w_s$, subtracting Eq. (2.27) from Eq. (2.28) gives

$$\int_{p_{02}}^{p_{02i}} v_0 dp_0 = \int_{\ell_1}^{\ell_2} T_0 s'_p d\ell$$

Integration of this along the constant h_{02} line means that $T_0 = T_{02}$ remains constant and factors out after the substitution $v_0 = RT_0/p_0$. Then, carrying out the integration gives

$$R \ln \frac{p_{02i}}{p_{02}} = \int_{\ell_1}^{\ell_2} s'_p d\ell$$

But in an adiabatic flow $ds = s'_p d\ell$, and this equation reduces to

$$s_2 - s_1 = s_p = R \ln \frac{p_{02i}}{p_{02}}$$

This relates the entropy increase to a loss in stagnation pressure.

■ EXAMPLE 2.12

The inlet stagnation temperature to a multistage turbine is 1400 K, and the inlet stagnation pressure is 1000 kPa. The stagnation pressure ratio is $p_{01}/p_{0e} = 10$, and the total-to-total efficiency of the turbine is $\eta_{tt} = 0.89$. Assuming that gases flowing through the turbine have $\gamma = \frac{4}{3}$ and $R = 287 \text{ J/(kg K)}$, find the specific entropy production during the expansion assuming constant specific heats.

Solution: In this multistage turbine, the inlet state is denoted by 1 and the exit by e. Assuming constant specific heats, the definition of total-to-total efficiency reduces to

$$\eta_{tt} = \frac{T_{01} - T_{0e}}{T_{01} - T_{0es}} \quad \text{or} \quad \eta_{tt} = \frac{1 - T_{0e}/T_{01}}{1 - T_{0es}/T_{01}}$$

from which

$$\frac{T_{0e}}{T_{01}} = 1 - \eta_{tt} \left(1 - \frac{T_{0es}}{T_{01}} \right)$$

The isentropic temperature ratio is

$$\frac{T_{0es}}{T_{01}} = \left(\frac{p_{0e}}{p_{01}} \right)^{(\gamma-1)/\gamma} = \frac{1}{10^{1/4}} = 0.5623$$

so that

$$T_{0es} = 1400 \cdot 0.5623 = 787.3 \text{ K}$$

and

$$T_{0e} = 1400 [1 - 0.89(1 - 0.5623)] = 854.7 \text{ K}$$

Since the amount of work done is proportional to the difference between the stagnation temperatures, if this work had been done reversibly, the exit pressure would reach the value p_{0ei} which is higher than before. It can be calculated from

$$\frac{p_{0ei}}{p_{01}} = \left(\frac{T_{0e}}{T_{01}} \right)^{\gamma/(\gamma-1)} = \left(\frac{854.7}{1400} \right)^4 = 0.1389$$

Hence, $p_{0ei} = 1000 \cdot 0.1389 = 138.9 \text{ kPa}$. Since the pressure ratio is 10, the exit stagnation pressure is $p_{0e} = 100 \text{ kPa}$, and the stagnation pressure loss is

$$p_{0ei} - p_{0e} = 138.9 - 100 = 38.9 \text{ kPa}$$

This represents 4.3% of the overall pressure difference $p_{01} - p_{02} = 900 \text{ kPa}$. The entropy production is calculated to be

$$s_p = R \ln \frac{p_{0ei}}{p_{0e}} = 287 \ln \frac{138.9}{100.0} = 94.3 \text{ J/(kg K)}$$

■

2.6 MOMENTUM BALANCE

In this section, use of the momentum balance is illustrated in applications of interest in turbomachinery. In uniform steady flow in a channel, the momentum balance reduces to

$$\dot{m}(\mathbf{V}_2 - \mathbf{V}_1) = \mathbf{F}_p + \mathbf{F}_v + \mathbf{F}_m \quad (2.29)$$

in which \mathbf{F}_p is a pressure force and \mathbf{F}_v is a viscous force. The force \mathbf{F}_m is present if the control volume cuts across the solid parts of the machine. If the control volume contains only fluid, this term is absent. Weights of the fluid and hardware have been omitted with the understanding that when stress analysis is carried out, they will be taken into account. The first illustration on the use of the momentum equation is to calculate the force that a deflection of a jet causes on a fixed vane.

EXAMPLE 2.13

Consider a jet of water that flows into a vane at an angle α_1 . The vane is *equiangular* with $\alpha_2 = -\alpha_1$, and it turns the flow so that it leaves at a negative angle α_2 , as shown in Figure 2.10. Positive angles are measured in the counterclockwise direction from the x -axis. The jet velocity at the inlet is V , and pressure surrounding the jet and the vane is atmospheric. Find the y component of the force on the vane.

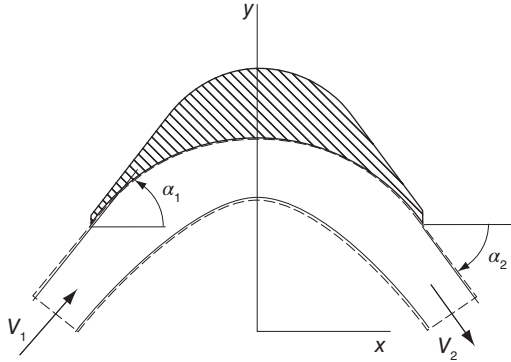


Figure 2.10 Turning of a flow by a vane.

Solution: The inlet to the vane is denoted as station 1, and the exit as station 2. Since both at the inlet and at the exit the streamlines are straight, pressure at both of these locations is equal to the atmospheric pressure p_a across the jet. Then, with gravity neglected, Bernoulli equation shows that velocity at the exit is the same as at the inlet so that $V_1 = V_2 = V$.

Momentum equation in the y direction gives

$$\dot{m}(V_{2y} - V_{1y}) = F_{py}$$

in which the force F_{py} is the y component of the pressure force exerted by the vane on the fluid. An equal and opposite force acts on the vane and it is denoted by R_y . At the inlet $V_{1y} = V \sin \alpha_1$ and at the exit $V_{2y} = V \sin \alpha_2$, and for a negative value of α_2 this velocity component points in the minus y direction. The force on the blade is therefore

$$R_y = \dot{m}V(\sin \alpha_1 - \sin \alpha_2)$$

The mass flow rate is $\dot{m} = \rho VA$. Since the blade is equiangular, $\alpha_2 = -\alpha_1$. Substituting gives the force as

$$R_y = 2\rho AV^2 \sin \alpha_1$$

The force is largest when $\alpha_1 = 90^\circ$ and the flow is turned 180° . ■

Consider again the flow shown in Figure 2.10, but now let the blade move in the y direction with velocity \mathbf{U} , as shown in Figure 2.11. It is known that Newton's second law is valid in all coordinate systems that move at constant speed. Thus the momentum balance given by Eq. (2.29) is also valid for a control volume that moves with a uniform velocity \mathbf{U} , if all

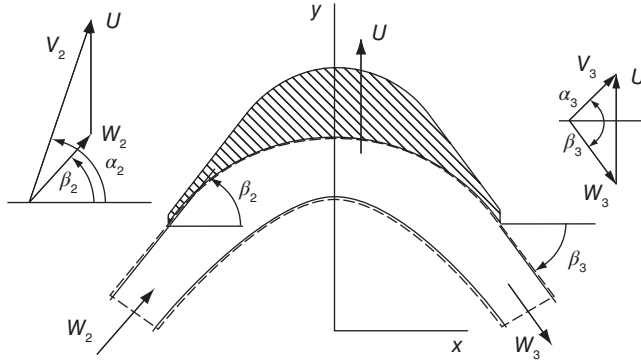


Figure 2.11 A water jet impinging on a moving blade.

velocities are replaced by relative velocities. In fact, noting that the relationship between the absolute velocity \mathbf{V} and relative velocity \mathbf{W} is given by

$$\mathbf{V} = \mathbf{W} + \mathbf{U}$$

and substituting this into Eq. (2.29) gives

$$\dot{m}(\mathbf{W}_2 + \mathbf{U} - \mathbf{W}_1 - \mathbf{U}) = \mathbf{F}_p + \mathbf{F}_v + \mathbf{F}_m$$

or

$$\dot{m}(\mathbf{W}_2 - \mathbf{W}_1) = \mathbf{F}_p + \mathbf{F}_v + \mathbf{F}_m \quad (2.30)$$

In the next example, the momentum balance is used to analyze the force on a moving blade.

■ EXAMPLE 2.14

Consider a waterjet directed at a blade that moves with speed U . The angle α_2 of the jet is such that the relative velocity meets the blade smoothly at the angle β_2 . The blade is shaped such that it deflects the flow backward at an angle $\beta_3 = -\beta_2$, as is shown in Figure 2.11. (a) Find the work done on the blade per unit mass of the flow and the blade speed for maximum work by carrying out the analysis in a set of fixed coordinates. (b) Carry out the same analysis in a set of moving coordinates, and find the y component of the force on the blade.

Solution: (a) The analysis is carried out first in fixed coordinates. Station 1 is now the inlet to a nozzle (not shown) that issues the water to station 2 at velocity V_2 and angle α_2 . Station 2 is also the inlet to the moving blade, and its exit is station 3. The force that the blade exerts on the fluid is

$$F_{py} = \dot{m}(V_3 \sin \alpha_3 - V_2 \sin \alpha_2)$$

and with $R_y = -F_{py}$ the force on the blade is

$$R_y = \dot{m}(V_2 \sin \alpha_2 - V_3 \sin \alpha_3)$$

Assuming that there are no losses so that $w = w_s$, and applying the first law to the control volume shown gives

$$\frac{p_a}{\rho} + \frac{1}{2}V_2^2 = \frac{p_a}{\rho} + \frac{1}{2}V_3^2 + w_s \quad (2.31)$$

and since the rate at which work is delivered to the blade is $\dot{W} = R_y U$, then

$$w_s = U(V_2 \sin \alpha_2 - V_3 \sin \alpha_3) \quad (2.32)$$

Substituting this into Eq. (2.31) gives

$$\frac{1}{2}V_2^2 = \frac{1}{2}V_3^2 + U(V_2 \sin \alpha_2 - V_3 \sin \alpha_3) \quad (2.33)$$

As is shown in the vector diagrams for the velocities in Figure 2.11, the x and y velocity components of absolute and relative velocity are related by

$$W_2 \cos \beta_2 = V_2 \cos \alpha_2 \quad W_2 \sin \beta_2 = V_2 \sin \alpha_2 - U \quad (2.34)$$

Squaring each equation and adding them yields

$$W_2^2 = V_2^2 + U^2 - 2V_2 U \sin \alpha_2$$

A similar equation is obtained at the exit, namely

$$\begin{aligned} W_3 \cos \beta_3 &= V_3 \cos \alpha_3 & W_3 \sin \beta_3 &= V_3 \sin \alpha_3 - U \\ W_3^2 &= V_3^2 + U^2 - 2V_3 U \sin \alpha_3 \end{aligned} \quad (2.35)$$

Solving for $V_2 \sin \alpha_2$ and $V_3 \sin \alpha_3$ from the squared equations and substituting them into Eq. (2.33) reduces it to

$$W_2^2 = W_3^2$$

so that $W_2 = W_3$. Thus the relative velocity at the exit is the same as at the inlet. This means that an observer in moving coordinates sees that the blade changes only the direction of the flow, but not its magnitude.

Substituting from Eqs. (2.34) and (2.35) into Eq. (2.32) gives

$$w_s = U[V_2 \sin \alpha_2 - (W_3 \sin \beta_3 + U)] = U(V_2 \sin \alpha_2 + W_2 \sin \beta_2 - U)$$

since $\beta_3 = -\beta_2$ and $W_3 = W_2$. Also $W_2 \sin \beta_2 = V_2 \sin \alpha_2 - U$, so that

$$w_s = 2U(V_2 \sin \alpha_2 - U)$$

From this equation, it is seen that $w_s = 0$ when $U = 0$, or $U = V_2 \sin \alpha_2$. In the former case, the load on the blade is too large to move the blade. In the latter case, the load is too light, and the blade is *free-wheeling*. The condition for maximum power to the blade is obtained by differentiating w_s with respect to U and setting it to zero. This gives

$$\frac{dw_s}{dU} = V_2 \sin \alpha_2 - 2U = 0 \quad \text{or} \quad \frac{U}{V_2} = \frac{1}{2} \sin \alpha_2$$

For $\alpha_2 = 90^\circ$ the maximum work is done by the jet on the blade when the blade moves at half the jet speed.

(b) If the moving coordinates are used, then

$$R_y = \dot{m}(W_2 \sin \beta_2 - W_3 \sin \beta_3)$$

Substituting $W_3 = W_2$ and $\beta_3 = -\beta_2$ gives

$$R_y = 2\dot{m}W_2 \sin \beta_2 = 2\dot{m}(V_2 \sin \alpha_2 - U)$$

and with the rate of work done $\dot{W} = R_y U$, the specific work becomes

$$w_s = 2U(V_2 \sin \alpha_2 - U)$$

as before. ■

Next, the momentum equation is applied to situations in which the results may be used to quantify thermodynamic losses.

■ EXAMPLE 2.15

Water with density $\rho = 1000 \text{ kg/m}^3$ and velocity $V_1 = 20 \text{ m/s}$ flows into a sudden expansion as shown in Figure 2.12. The supply pipe has a diameter $D_1 = 7 \text{ cm}$, and the pipe downstream has a diameter $D_2 = 14 \text{ cm}$. Find the increase in pressure $p_2 - p_1$.

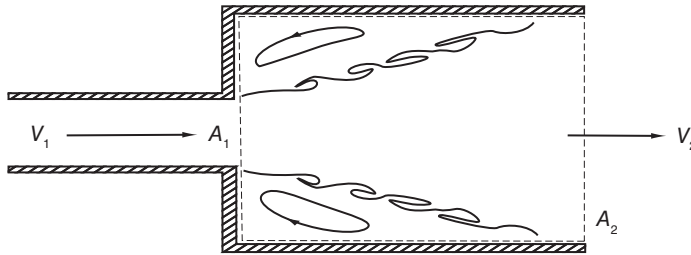


Figure 2.12 Flow in a channel with a sudden expansion.

Solution: Mass balance gives

$$A_1 V_1 = A_2 V_2$$

Thus

$$V_2 = V_1 \frac{D_1^2}{D_2^2} = 20 \left(\frac{7}{14} \right)^2 = 5.0 \text{ m/s}$$

As the water enters a sudden expansion, it detaches from the boundaries and moves into the larger space as a *jet*. Regions of recirculating flow develop at the upstream corners. Flow speed in these corners is sufficiently low to make the pressure uniform.

The pressure across the jet at the exit plane is therefore equal to that in the recirculating regions. The stream velocity rises from small backflow in the recirculating regions to a large forward velocity in the jet. This leads to appreciable viscous forces in the *free shear layers* forming the jet boundary. Such free shear layers are unstable to small disturbances and roll up into vortices. These cause mixing of the low velocity fluid in the recirculating zone with the fast flow in the jet. As a consequence, the jet spreads and fills the channel. In the mixing zone, the shear forces along the walls influence pressure much less than the mixing, and therefore, they may be neglected.

Applying the momentum balance in the x direction leads to

$$\rho A_2 V_2 (V_2 - V_1) = (p_1 - p_2) A_2$$

in which the mass balance, $\dot{m} = \rho V_2 A_2$ was used. Thus

$$p_2 - p_1 = \rho V_2 (V_1 - V_2)$$

and the numerical value for the pressure increase is

$$p_2 - p_1 = 1000 \cdot 5.0(20 - 5.0) = 75 \text{ kPa}$$

As the area A_2 , is increased, the exit velocity is reduced, and finally becomes zero. In that case $p_2 = p_1$. This is the situation of a jet discharging to an atmosphere and then the exit pressure is equal to the atmospheric pressure.

The loss in stagnation pressure in a sudden expansion is

$$p_{01} - p_{02} = p_1 + \frac{1}{2}\rho V_1^2 - p_2 - \frac{1}{2}\rho V_2^2 = \frac{1}{2}\rho V_1^2 - \rho V_1 V_2 + \frac{1}{2}\rho V_2^2 = \frac{1}{2}\rho(V_1 - V_2)^2$$

or

$$p_{01} - p_{02} = \frac{1}{2} 1000 (20 - 5)^2 = 112.5 \text{ kPa}$$

If the flow were to diffuse to the exit pipe without irreversibilities, there would be no loss of stagnation pressure and the exit pressure could be calculated from the Bernoulli equation. It would have the value

$$p_{2i} - p_1 = \frac{1}{2}\rho(V_1^2 - V_2^2) = \frac{1}{2}1000(20^2 - 5^2) = 187.5 \text{ kPa}$$

above the inlet pressure. Contrasting this to the value 75 kPa calculated in the actual case shows that not all pressure is *recovered*, and the irreversibility can be regarded as a loss in pressure.

This underscores the importance of a well-designed diffuser to recover as much of the pressure as possible. The reduction of kinetic energy in diffusion goes into flow work on the fluid particles ahead, causing pressure to increase. If part of the kinetic energy is dissipated by viscous action in mixing, less is available for increasing the pressure. This is clearly true if the sudden expansion takes place into a vast reservoir, for then all the kinetic energy leaving the pipe will be dissipated in the reservoir and none is recovered. ■

As a third example on the application of the momentum balance, consider how mixing of a stream in a constant-area duct changes the pressure. This requires the use of the balance equations in their integral forms.

■ EXAMPLE 2.16

An incompressible fluid flows in channel of cross-sectional area A , as shown in Figure 2.13. The flow is in the z direction with a nonuniform velocity profile $V_1 = V(1 + f(x, y))$ at station 1 with the nonuniformity such that V is the average velocity. As a result of mixing, the flow enters station 2 with a uniform profile. Find the pressure change between stations 1 and 2. Work out the solution when the inlet velocity consists of two adjacent streams, one moving with velocity $V(1 + f_a)$ and the other with velocity $V(1 + f_b)$. Note that, since V is the average velocity, f_b must have a negative value.

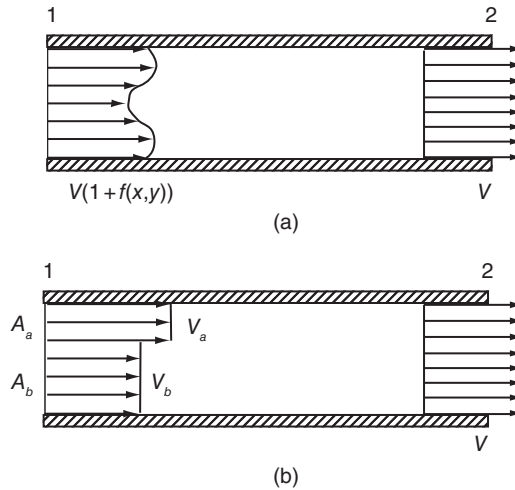


Figure 2.13 (a) The upper sketch shows mixing in a constant area channel with an arbitrary inlet velocity profile. (b) The lower sketch shows mixing with stepwise constant inlet velocity profile

Solution: Integral form of the mass balance

$$\dot{m} = \int_{A_1} \rho V_1 dA = \int_{A_2} \rho V_2 dA$$

applied to a control volume between stations 1 and 2, with $A = A_1 = A_2$ and $V_2 = V$, yields an expression that may be written as

$$\int_A V(1 + f(x, y)) dA = VA$$

Since V is the constant average velocity, this gives the condition

$$\int_A f(x, y) dA = 0$$

The x component of the momentum equation applied to this control volume gives

$$\int_{A_2} \rho V_2^2 dA - \int_{A_1} \rho V_1^2 dA = (p_1 - p_2)A$$

Again, since at the exit velocity $V_2 = V$ is uniform, this can be written as

$$-\rho V^2 A + \rho \int_A V^2 (1 + f(x, y))^2 dA = (p_2 - p_1)A$$

Wall shear has been neglected under the assumption that mixing influences the pressure change much more than does wall shear.

Expanding the integral leads to

$$\int_A (1 + f(x, y))^2 dA = \int_A (1 + 2f(x, y) + f^2(x, y)) dA = A + \int_A f^2(x, y) dA$$

for, as shown above, the middle term is zero. Denoting

$$\bar{f}^2 = \frac{1}{A} \int_A f^2(x, y) dA$$

the pressure increase is seen to be

$$p_2 - p_1 = \rho V^2 \bar{f}^2$$

With the velocities as shown on the bottom half of the figure, mass balance gives

$$A_a V_a + A_b V_b = AV$$

and since $A = A_a + A_b$, this reduces to

$$V = \frac{V_a A_a + V_b A_b}{A_a + A_b}$$

Writing

$$V_a = V(1 + f_a) \quad \text{and} \quad V_b = V(1 + f_b)$$

and solving for f_a and f_b gives

$$f_a = \frac{V_a}{V} - 1 = \frac{(V_a - V_b)A_b}{V_a A_a + V_b A_b}$$

and

$$f_b = \frac{V_b}{V} - 1 = \frac{(V_b - V_a)A_a}{V_a A_a + V_b A_b}$$

The value of \bar{f}^2 is the area-weighted average

$$\bar{f}^2 = \frac{f_a^2 A_a + f_b^2 A_b}{A_a + A_b} = \frac{(V_a - V_b)^2 A_a A_b}{(V_a A_a + V_b A_b)^2}$$

Hence the pressure increase is

$$p_2 - p_1 = \rho(V_a - V_b)^2 \frac{A_a A_b}{(A_a + A_b)^2}$$

As a special case, consider the situation in which $V_b = 0$. Then

$$V = \frac{V_a A_a}{A_a + A_b} \quad \text{and} \quad V_a - V = \frac{V_a A_b}{A_a + A_b}$$

and

$$p_2 - p_1 = \rho V(V_a - V) \quad (2.36)$$

This is the same result that was developed in Example 2.15. ■

In these examples, the momentum equation could be used to obtain information about the downstream pressure. This was possible because the viscous forces could be neglected. Such a situation also characterizes many turbomachinery flows in which the important force balance is between the inertia of the flow and pressure forces.

EXERCISES

2.1 Steam flows through a bank of nozzles shown in Figure 2.1 with wall thickness $t_2 = 2$ mm, spacing $s = 4$ cm, blade height $b = 2.5$ cm, and exit angle $\alpha_2 = 68^\circ$. The exit velocity $V_2 = 400$ m/s, pressure is $p_2 = 1.5$ bar, and temperature is $T_2 = 200^\circ\text{C}$. Find the mass flow rate. [Ans: 0.09 kg/s]

2.2 Air enters a compressor from atmosphere at pressure 102 kPa and temperature 42°C . Assuming that its density remains constant, determine the specific compression work required to raise its pressure to 140 kPa in a reversible adiabatic process, given an exit velocity of 50 m/s. [Ans: 34.95 kJ/kg]

2.3 Steam flows through a turbine at the rate of $\dot{m} = 9000$ kg/h. The rate at which power is delivered by the turbine is $\dot{W} = 440$ hp. The inlet stagnation pressure is $p_{01} = 70$ bar, and stagnation temperature is $T_{01} = 420^\circ\text{C}$. For a reversible and adiabatic process, find the stagnation pressure and temperature leaving the turbine. [Ans: 43.59 bar, 348.3°C]

2.4 Water enters a pump as saturated liquid at stagnation pressure of $p_{01} = 0.08$ bar and leaves it at $p_{02} = 30$ bar. The mass flow rate is $\dot{m} = 10000$ kg/h and assuming that the process takes place reversibly and adiabatically, determine the power required. [Ans: 8.11 kW]

2.5 Liquid water at 700 kPa and temperature 20°C flows at velocity 15 m/s. Find the stagnation temperature and stagnation pressure. [Ans: 20.027°C , 812.5 kPa]

2.6 Water at temperature $T_1 = 20^\circ\text{C}$ flows through a turbine with inlet velocity $V_1 = 3$ m/s, static pressure $p_1 = 780$ kPa, and elevation $z_1 = 2$ m. At the exit, the conditions are $V_2 = 6$ m/s, $p_2 = 100$ kPa, and $z_2 = 1.2$ m. Find the specific work delivered by the turbine assuming it to be reversible. [Ans: 674.35 J/kg]

2.7 Air at static pressure 2 bar and static temperature 300 K flows with velocity 60 m/s. Find stagnation temperature and pressure assuming constant specific heats. [Ans: 301.8 K, 204.2 kPa]

2.8 Air at static temperature 300 K and static pressure 140 kPa flows with velocity 60 m/s. (a) Evaluate the stagnation temperature and stagnation pressure of air. (b) Repeat the calculation assuming that the airspeed is 300 m/s assuming constant specific heats. [Ans: (a) 301.8 K, 142.9 kPa, (b) 344.8 °C, 227.9 kPa]

2.9 Air undergoes an increase of 1.75 kPa in stagnation pressure through a blower. The inlet stagnation pressure is one atmosphere, and the inlet stagnation temperature is 21 °C. (a) Evaluate the exit stagnation temperature assuming that the process is reversible adiabatic. (b) Evaluate the specific energy added to the air. [Ans: (a) 22.4 °C (b) 1.46 kJ/kg]

2.10 Air enters a blower from the atmosphere where pressure is 101.3 kPa and temperature is 27 °C. Its velocity at the inlet is 46 m/s. At the exit, the stagnation temperature is 28 °C and the velocity is 123 m/s. Assuming that the flow is reversible and adiabatic, determine (a) the change in stagnation pressure in millimeters of water and (b) the change in static pressure, also in millimeters of water. [Ans: (a) 120 mm of water, (b) -639 mm of water]

2.11 The stagnation pressure, static pressure, and the stagnation temperature of air at a certain point in a flow are 700 kPa, 350 kPa, and 450 K, respectively. Find the velocity at that point. [Ans: 403 m/s]

2.12 Air has static pressure 2 bar and static temperature 300 K while flowing at speed 1000 m/s. (a) Assuming that air obeys the ideal gas law with constant specific heats, determine its stagnation temperature and stagnation pressure. (b) Repeat part (a) using the air tables or YAir. [Ans: (a) 61.33 bar, (b) 62.56 bar]

2.13 At a certain location, the velocity of air flowing in a duct is 321.5 m/s. At that location, the stagnation pressure is 700 kPa and stagnation temperature is 450 K. What is the static density at this location? [Ans: 4.00 kg/m³]

2.14 Air flows in a circular duct of diameter 4 cm at the rate of 0.5 kg/s. The flow is adiabatic with stagnation temperature 288 K. At a certain location, the static pressure is 110 kPa. Find the velocity at this location. [Ans: 263.2 m/s]

2.15 Saturated steam enters a nozzle at static pressure 14 bar at velocity 52 m/s. It expands isentropically to pressure 8.2 bar. Mass flow rate is $\dot{m} = 0.7$ kg/s. Find the exit area, assuming that (a) steam behaves as an ideal gas with $\gamma = 1.135$, and $c_p = 2731$ J/(kg K); (b) the end state is calculated with properties obtained from the steam tables. [Ans: (a) 3.82 cm², (b) 3.47 cm²]

2.16 A fluid enters a turbine with stagnation temperature of 330 K and stagnation pressure of 700 kPa. The outlet stagnation pressure is 100 kPa, and assume that the expansion process through the turbine is isentropic. Evaluate (a) the work per unit mass flow assuming that the fluid is incompressible with a density 1000 kg/m³, (b) and assuming that the fluid is air. [Ans: (a) 0.6 kJ/kg, (b) 141.4 kJ/kg]

2.17 Air flows through a turbine that has a stagnation pressure ratio 5 to 1. The total-to-total efficiency is 80%, and the flow rate is 1.5 kg/s. The desired output power is to be 250 hp (186.4 kW). Determine (a) the inlet stagnation temperature, (b) the outlet stagnation temperature, (c) the outlet static temperature given an exit velocity 90 m/s. (d) Then draw the process on a Ts -diagram and determine the total-to-static efficiency of the turbine. [Ans: (a) 419.5 K, (b) 295.8 K, (c) 291.8 K, 0.78]

2.18 A blower has a change in stagnation enthalpy of 6000 J/kg, an inlet stagnation temperature 288 K, and an inlet stagnation pressure 101.3 kPa. Find (a) the exit stagnation temperature assuming that the working fluid is air, (b) the stagnation pressure ratio across the machine, given a total-to-total efficiency of 75%. (c) If the working fluid is water, find the pressure ratio. [Ans: (a) 294 K, (b) 1.056, (c) 45.4 multi-stage pump]

2.19 A multistage turbine has a stagnation pressure ratio of 2.5 across each of the four stages. The inlet stagnation temperature is $T_{01} = 1200$ K and the total-to-total efficiency of each stage is 0.87. Evaluate the overall total-to-total efficiency of the turbine by assuming that steam is flowing through it. Steam can be assumed to behave as a perfect gas with $\gamma = 1.3$. Why is the overall efficiency higher than the stage efficiency? [Ans: 0.904]

2.20 Gases from a combustion chamber enter a gas turbine at a stagnation pressure of 700 kPa and a stagnation temperature of 1100 K. The stagnation pressure and stagnation temperature at the exit of the turbine are 140 kPa and 780 K. Assuming that $\gamma = \frac{4}{3}$ is used for the mixture of combustion gases, which has a molecular mass of 28.97 kg/kmol, find the total-to-total efficiency and the total-to-static efficiency of the turbine, for an exit velocity of 210 m/s. [Ans: 0.878, 0.834]

2.21 Air enters a compressor from atmosphere at 101.3 kPa, 288 K. It is compressed to a static pressure of 420 kPa, and at the exit its velocity is 300 m/s. Assume that air behaves as an ideal gas with constant specific heats and that the compressor total-to-total efficiency is 0.82. (a) Find the exit static temperature by assuming that $V_{2s} = V_2$. (b) Find the exit static temperature, without making the assumption that V_{2s} is equal to V_2 . [Ans: (a) 473.9 K, (b) 469.6 K]

2.22 Steam enters a turbine with the speed 190 m/s at static pressure 50 bar and static temperature 560 °C. It expands to 0.07 bar and 120 °C and leaves with speed 220 m/s. Find (a) the total-to-total efficiency, (b) total-to-static efficiency, and (c) static-to-static efficiency. Carry out the calculations using the function XSteam. [Ans: (a) 0.826, (b) 0.807, (c) 0.821].

2.23 Air enters a multistage compressor at static pressure of 1 bar and 300 K. The inlet velocity is velocity 50 m/s. The overall pressure ratio across the compressor is 25. The total-to-total efficiency is 0.86. If the exit velocity is 300 m/s, find (a) its total-to-static efficiency and (b) its static-to-static efficiency. Assume that the air is an ideal gas with constant specific heats. (c) Repeat the calculation assuming air to be an ideal gas with variable specific heats. [Ans: (a) 0.7622, (b) 0.8453, (c) 0.7619, 0.8452].

2.24 If CO_2 is taken into account in the composition of air, then the mole fractions of air are: Nitrogen $y_{\text{N}_2} = 0.7808$, oxygen $y_{\text{O}_2} = 0.2095$, Argon $y_{\text{Ar}} = 0.0093$, and carbon dioxide $y_{\text{CO}_2} = 0.0004$. (a) Find the molecular mass and the gas constant for this mixture. (b) Find the specific heat at constant pressure. (c) Find the specific heat at constant volume. (d) Find the ratio of specific heats. [Ans: (a) 28.966, (b) 1.0054 kJ/kg K, (c) 0.7184 kJ/kg K, (d) 1.3995].

2.25 Steam as saturated liquid flows through a throttling valve, in which pressure drops from 40 to 1 bar. (a) Find the steam density downstream of the valve. Assume that the exit is designed such that the inlet and exit velocities are the same. (b) What is the ratio of the exit area to the inlet area? [Ans: (a) 1.986 kg/m³, (b) 402].

2.26 Steam enters a throttling valve as a two phase mixture at pressure of 20 bar and at velocity 15 m/s. It leaves the valve at pressure 1 bar and temperature 120 °C. (a) Find the quality of the incoming steam. (b) Find the exit velocity. [Ans:(a) 0.9769 (b) 274.6 m/s]

2.27 A jet of diameter D strikes a plate with a small orifice. Most of the jet leaves in directions parallel to the plane of the plate, but part flows through the orifice. The diameter of the jet emerging from the orifice is d . Find the force the jet exerts on the plate. [Ans: $F_d = \frac{\pi}{4}\rho V^2(D^2 - d^2)$]

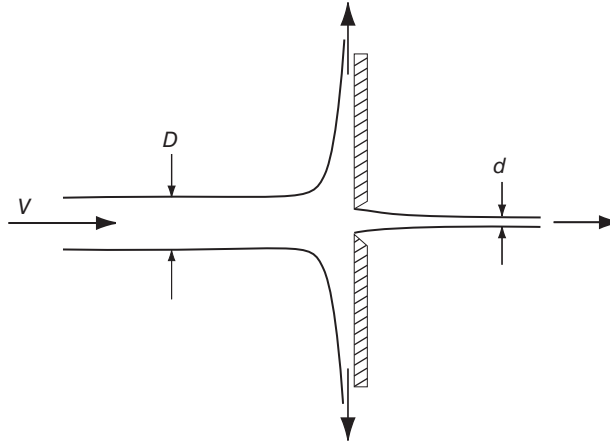


Figure 2.14 A jet and orifice.

2.28 A long blade is tested in a water channel, as shown in Figure 2.15, with upstream velocity V . The speed is fast enough that behind the blade a vapor cavity is formed. Velocity in this vapor cavity can be assumed to be zero and pressure uniform and equal to the vapor pressure, p_v , at the temperature of the surroundings. The width of the channel is a and that of the vapor cavity is b . (a) Find how the upstream pressure is related to the vapor pressure p_v , the channel width a , the cavity width b , and the upstream velocity V . (b) Find the drag on the blade per unit length to the plane of the paper in terms of ρ , a , b , and V . [Ans: $F_d = \frac{1}{2}\rho a \left(\frac{a}{a-b}\right)^2 V^2$].

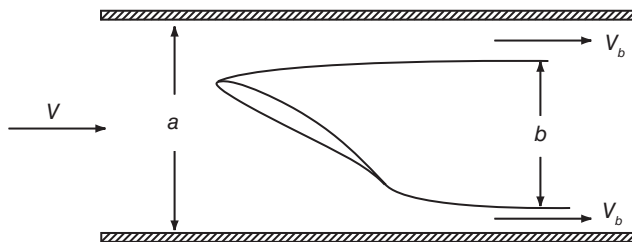


Figure 2.15 A blade test

2.29 Air flows upstream velocity V across a circular cylinder located in a channel of width $2h$ as shown in Figure 2.16a. The velocity in the wake behind the cylinder rises from zero at the centerline linearly to V_m at the wall. If the pressure difference is $p_1 - p_2 = \frac{3}{4}\rho V^2$, find the drag force. [Ans: $F_d = \frac{5}{12}\rho V^2$.]

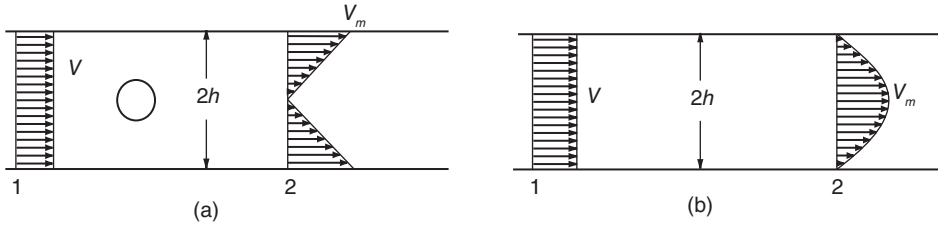


Figure 2.16 (a) Triangular wake and (b) developing flow.

2.30 Water flows in a channel of width $2h$ as shown in Figure 2.16b. At the inlet, its velocity has the uniform value V . Downstream it has the velocity profile $u = V_m(1 - y^2/h^2)$. Find the pressure drop between the upstream and downstream stations, assuming the wall shear can be neglected. [Ans: $\frac{1}{5}\rho V^2$]

2.31 A jet pump is shown in Figure 2.17. Water at high speed V_a issues from the nozzle of area A_a , that is centrally located in the discharge tube of area A . Secondary stream at the nozzle exit has a velocity V_b and it mixes with the jet so that downstream the velocity is uniform. Show that the pressure increase in the flow is given by

$$p_2 - p_1 = \rho(V_a - V_b)^2 \frac{A_a A_b}{(A_a + A_b)^2}$$

where $A_b = A - A_a$.

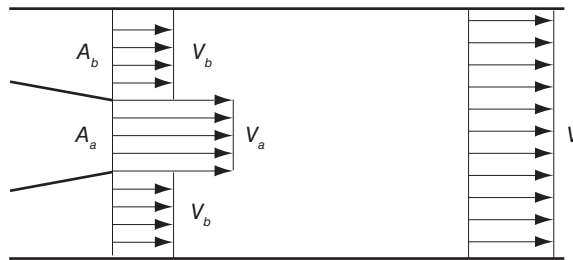


Figure 2.17 A jet pump.

2.32 Rework the previous exercise by the method used in Example 2.16.

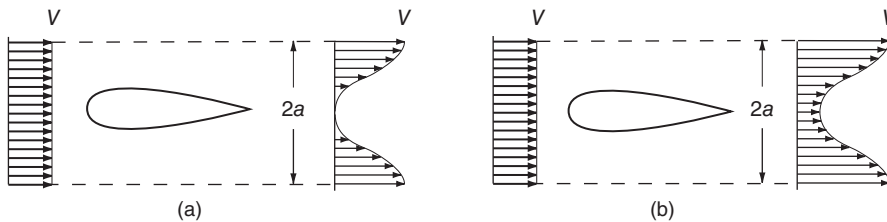


Figure 2.18 (a) Wake profile with a strong velocity defect. (b) Wake profile with a weak velocity defect.

2.33 Air flows upstream with velocity V across an airfoil as shown in Figure 2.18a. The velocity in the wake behind the airfoil rises from zero at the centerline as $u(y) = \frac{1}{2}V(1 - \cos \frac{\pi y}{a})$ and beyond the distance a it has reached the free stream velocity V . Find the drag force on the airfoil. [Ans: $F_d = \frac{1}{4}\rho a V^2$]

2.34 Air flows upstream with velocity V across an airfoil as shown in Figure 2.18b. The velocity profile in the wake behind the airfoil is given by $u(y) = V - u_d[1 + \cos(\pi y/a)]$ and beyond the distance a , it has reached the free stream velocity V . Find the drag force on the airfoil. [Ans: $F_d = \rho a u_d(2V - 3u_d)$]

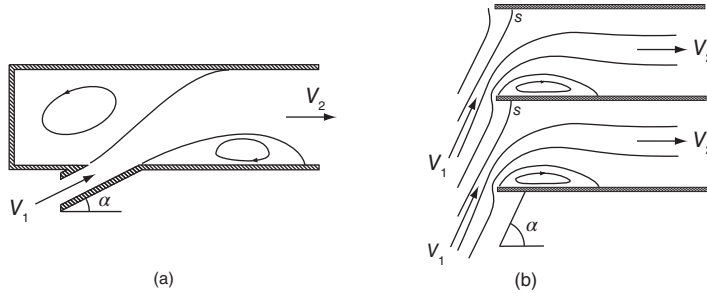


Figure 2.19 (a) Flow from a side pipe to the main. (b) Flow into a blade row.

2.35 Liquid water flows at velocity V_1 from a side pipe of area A_1 welded at angle α to the main, as shown in Figure 2.19a. The area of the main pipe is A_2 . Using the mass and momentum balance, (a) find the downstream velocity V_2 , (b) find the pressure increase in the flow, (c) Introduce into the energy balance a loss term $KV_1^2/2$ and find the loss coefficient in terms of α and the area ratios of the two streams. [Ans: $K = \left(\frac{A_1}{A_2}\right)^2 - 2\frac{A_1}{A_2} \cos \alpha + 1$]

2.36 Consider the flow into a cascade, shown in Figure 2.19b. The flow separates at the leading edge and forms a recirculation region. The point s identifies a stagnation point in the flow. Show that the kinetic energy lost in the flow as it moves to the downstream section can be associated with the transverse component of the velocity, $V_t = V_1 \sin \alpha$. *Hint:* Choose a control volume with inlet and outlet far enough upstream and downstream that the streamlines are straight and pressures are uniform.

CHAPTER 3

COMPRESSIBLE FLOW

In this chapter, the dynamics and thermodynamics of compressible fluid flow are discussed. First, the isentropic relations are developed and applied to a converging nozzle, and then, friction is considered. To account for friction, various loss coefficients are introduced. The next topic is the flow in converging–diverging nozzles and where normal shocks may develop. The last section is on oblique shocks and the Prandtl–Meyer expansion.

3.1 MACH NUMBER AND THE SPEED OF SOUND

Consider a stationary fluid in which a weak *pressure wave* travels to the right at velocity c , as is shown in Figure 3.1a. Pressure and other thermodynamic properties change across the *wave front*. Ahead of the front the fluid is stagnant so that its velocity $V = 0$. Its pressure has the value p and its density is ρ . After the front has passed through a given location, let the velocity there be ΔV and pressure and density be $p + \Delta p$ and $\rho + \Delta \rho$, respectively. It is advantageous to shift to a frame of reference that moves to the right with speed c , for in that frame, the front is stationary. Hence, the balance principles in their steady form can be applied to a stationary control volume containing the front as shown in Figure 3.1b. In this frame, fluid approaches the control volume with speed c from the right. Mass balance then gives

$$\rho c A = (\rho + \Delta \rho)(c - \Delta V)A \quad (3.1)$$

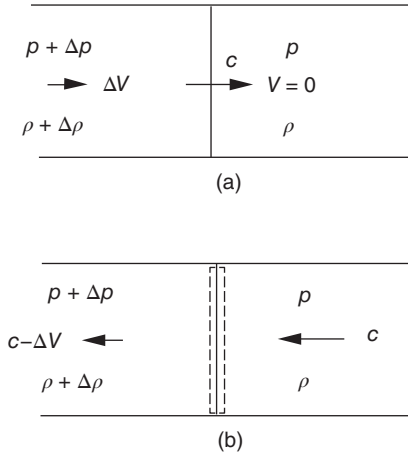


Figure 3.1 Sketch illustrating a weak pressure wave. (a) Stationary frame and (b) moving frame.

Carrying out the multiplications on the right-hand side (RHS) and assuming that the pressure wave is weak so that $\Delta V \Delta \rho$ can be neglected reduces this equation to

$$\Delta V = \frac{c \Delta \rho}{\rho} \quad (3.2)$$

With the positive x direction pointing to the right, the x component of momentum equation, obtained from Eq. (2.29) and applied to this control volume, gives

$$\rho c A [c - (c - \Delta V)] = (p + \Delta p) A - p A$$

which reduces to

$$\rho c \Delta V = \Delta p$$

Substituting the expression for ΔV from Eq. (3.2) into this gives

$$c^2 = \frac{\Delta p}{\Delta \rho}$$

Since the pressure wave is assumed to be weak, the entire process may be assumed to be isentropic. In that case, the speed of the wave is given by

$$c = \sqrt{\left(\frac{\partial p}{\partial \rho} \right)_s} \quad (3.3)$$

This quantity is called the *speed of sound* because sound waves are weak pressure waves. For an ideal gas, for which $p\rho^{-\gamma}$ is constant in an isentropic process, taking logarithms and differentiating gives

$$\ln p - \gamma \ln \rho = \text{constant} \quad \frac{dp}{p} - \gamma \frac{d\rho}{\rho} = 0$$

from which can be formed the partial derivative

$$\left(\frac{\partial p}{\partial \rho}\right)_s = \gamma \frac{p}{\rho} = \gamma RT$$

Speed of sound c for an ideal gas is therefore given by

$$c = \sqrt{\gamma RT} = \sqrt{\gamma \bar{R}T/\mathcal{M}}$$

For air, with $R = \bar{R}/\mathcal{M} = 8314/28.97 = 287 \text{ J}/(\text{kg K})$ and $\gamma = 1.4$, the speed of sound at $T = 300 \text{ K}$ is $c = 347 \text{ m/s}$. For combustion gases, with $\gamma = \frac{4}{3}$ and $R = 287 \text{ J}/(\text{kg K})$, at $T = 1200 \text{ K}$, it is $c = 677.6 \text{ m/s}$. For gases of large molecular mass, the speed of sound is small and the opposite is true for gases of low molecular mass. For example, the refrigerant R134a, or tetrafluoroethane, with a chemical formula CH_2FCF_3 , has a molecular mass of $\mathcal{M} = 102.0 \text{ kg/kmol}$. Its ratio of specific heats is $\gamma = 1.14$. Hence, at $T = 300 \text{ K}$, the speed of sound in R134a is only $c = 167 \text{ m/s}$. For helium at the same temperature, speed of sound is $c = 1019 \text{ m/s}$.

Mach number is defined to be the ratio of the local fluid velocity to the local sound speed

$$M = \frac{V}{c}$$

Subsonic flows have $M < 1$, *supersonic* ones $M > 1$, and for *hypersonic* flows, $M \gg 1$. Flows for which $M \sim 1$ are called *transonic*.

3.1.1 Mach number relations

In an ideal gas with constant specific heats, the definition of stagnation enthalpy

$$h_0 = h + \frac{1}{2}V^2$$

can be recast as

$$T_0 = T + \frac{V^2}{2c_p} = T + \frac{(\gamma - 1)}{2\gamma R}V^2 = T \left(1 + \frac{\gamma - 1}{2}M^2\right)$$

from which

$$\frac{T_0}{T} = 1 + \frac{\gamma - 1}{2}M^2$$

From the definition of a stagnation state, it follows that

$$\frac{p_0}{p} = \left(\frac{T_0}{T}\right)^{\gamma/(\gamma-1)} \quad \frac{\rho_0}{\rho} = \left(\frac{T_0}{T}\right)^{1/(\gamma-1)}$$

These can be written in terms of Mach number as

$$\frac{p_0}{p} = \left(1 + \frac{\gamma - 1}{2}M^2\right)^{\gamma/(\gamma-1)} \quad (3.4)$$

and

$$\frac{\rho_0}{\rho} = \left(1 + \frac{\gamma - 1}{2} M^2\right)^{1/(\gamma - 1)} \quad (3.5)$$

These equations are in dimensionless form, and they represent the most economical way to show the functional dependence of the variables on the flow velocity.

Equation (3.4) for pressure can be expanded by the binomial theorem¹ for small values of Mach number. This leads to

$$\frac{p_0}{p} = 1 + \frac{\gamma}{2} M^2 + \frac{\gamma}{8} M^4 - \frac{\gamma(\gamma - 2)}{48} M^6 + \dots = 1 + \frac{\gamma}{2} M^2 \left(1 + \frac{1}{4} M^2 + \dots\right)$$

which, when only the first two terms are retained, can be rearranged as

$$\frac{p_0}{p} = 1 + \frac{\gamma V^2}{2\gamma RT} = 1 + \frac{\rho}{2p} V^2$$

so that

$$p_0 = p + \frac{1}{2} \rho V^2$$

For incompressible fluids, this was taken to be the definition of stagnation pressure. In fact, it is seen to be approximately valid also for flows of compressible fluids when $M \ll 1$. In practice, this approximation is quite accurate if $M < 0.3$.

■ EXAMPLE 3.1

At a certain location in a flow of air, static pressure has been measured to be $p = 2.4$ bar and stagnation pressure, $p_0 = 3$ bar. Measurement of the total temperature shows it to be $T_0 = 468$ K. Find the Mach number and flow rate per unit area.

Solution: Static temperature can be determined from

$$T = T_0 \left(\frac{p}{p_0}\right)^{(\gamma - 1)/\gamma} = 468 \left(\frac{2.4}{3}\right)^{1/3.5} = 439.1 \text{ K}$$

Then, solving

$$\frac{T_0}{T} = 1 + \frac{\gamma - 1}{2} M^2$$

for Mach number, gives $M = 0.574$. With Mach number known, velocity can be determined from $V = Mc$. Speed of sound at this temperature is

$$c = \sqrt{\gamma RT} = \sqrt{1.4 \cdot 287 \cdot 439.1} = 420.0 \text{ m/s}$$

so that the velocity is

$$V = Mc = 241 \text{ m/s}$$

¹Binomial theorem gives the expansion $(1 + a)^n = 1 + na + \frac{n(n-1)}{2!}a^2 + \frac{n(n-1)(n-2)}{3!}a^3 + \dots$

Static density is given by

$$\rho = \frac{p}{RT} = \frac{240000}{287 \cdot 439.1} = 1.904 \text{ kg/m}^3$$

Hence, the mass flow rate per unit area is

$$\frac{\dot{m}}{A} = \rho V = 1.904 \cdot 241 = 458.9 \text{ kg/(s m}^2\text{)}$$

■

3.2 ISENTROPIC FLOW WITH AREA CHANGE

Consider a one-dimensional isentropic gas flow in a converging–diverging nozzle as shown in Figure 3.2. Since the mass flow rate is

$$\dot{m} = \rho V A$$

and \dot{m} is constant, taking logarithms and then differentiating yields

$$\frac{d\rho}{\rho} + \frac{dA}{A} + \frac{dV}{V} = 0$$

Since in adiabatic flow h_0 is constant, differentiating

$$h_0 = h + \frac{1}{2}V^2$$

gives

$$dh = -V dV$$

From the Gibbs equation, $T ds = dh - dp/\rho$ for isentropic flow, the relation

$$dh = \frac{1}{\rho} dp$$

is obtained. Equating the last two expressions for enthalpy change gives

$$-V dV = \frac{1}{\rho} dp = \frac{1}{\rho} \left(\frac{\partial p}{\partial \rho} \right)_s d\rho = c^2 \frac{d\rho}{\rho}$$

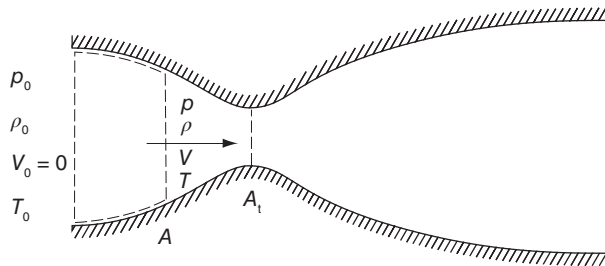


Figure 3.2 A converging–diverging nozzle.

Using this to eliminate density from the mass balance and simplifying it gives

$$(M^2 - 1) \frac{dV}{V} = \frac{dA}{A} \quad (3.6)$$

From this, it is seen that for subsonic flow, with $M < 1$, an increase in area decreases the flow velocity. Thus, walls of a subsonic *diffuser diverge* in the downstream direction. For supersonic flow with $M > 1$, a *decrease in area leads to diffusion*. Since a *nozzle* increases the velocity of a flow, in a subsonic nozzle flow, area decreases, and in supersonic flow, it increases in the flow direction.

In a continuously accelerating flow $dV > 0$, and Eq. (3.6) shows that at the *throat*, where $dA = 0$, the flow is *sonic* with $M = 1$. If the flow continues its acceleration to a supersonic speed, the area must diverge after the throat. Such a converging–diverging nozzle, shown in Figure 3.2, is called *de Laval nozzle*. The assumptions made in arriving at these results are that the flow is steady and one-dimensional and that it is reversible and adiabatic. It has not been assumed that the fluid obeys the ideal gas relation.

It was shown in the previous chapter that Mach number is a convenient parameter for expressing the relationship between the static and stagnation properties. By assuming ideal gas behavior and constant specific heats, the expressions

$$\begin{aligned} \frac{T_0}{T} &= 1 + \frac{\gamma - 1}{2} M^2 \\ \frac{p_0}{p} &= \left(1 + \frac{\gamma - 1}{2} M^2 \right)^{\gamma/(\gamma-1)} \\ \frac{\rho_0}{\rho} &= \left(1 + \frac{\gamma - 1}{2} M^2 \right)^{1/(\gamma-1)} \end{aligned}$$

were obtained. Inverses of these ratios for a gas with $\gamma = 1.4$ are shown in Figure 3.3.

At the *sonic condition*, denoted by the symbol (*) and for which $M = 1$, they reduce to

$$\frac{T^*}{T_0} = \frac{2}{\gamma + 1} = 0.8333$$

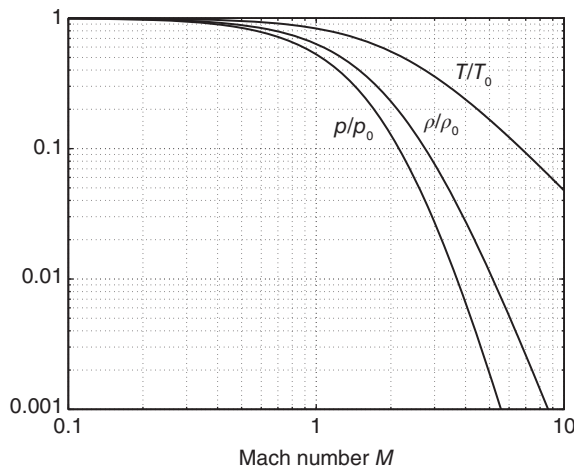


Figure 3.3 Pressure, density, and temperature ratios as functions of Mach number.

$$\frac{p^*}{p_0} = \left(\frac{2}{\gamma + 1} \right)^{\gamma/(\gamma-1)} = 0.5283$$

$$\frac{\rho^*}{\rho_0} = \left(\frac{2}{\gamma + 1} \right)^{1/(\gamma-1)} = 0.6339$$

The numerical values correspond to $\gamma = 1.4$.

Mass balance for a compressible flow, which obeys the ideal gas model, may be written as

$$\dot{m} = \rho V A = \frac{p A M}{R T} \sqrt{\gamma R T} = p A M \sqrt{\frac{\gamma}{R T}}$$

Multiplying and dividing the RHS by stagnation pressure and the square root of stagnation temperature, and expressing p/p_0 ratio in terms of temperature ratio T/T_0 gives

$$\dot{m} = \frac{p_0 A M \gamma}{\sqrt{c_p (\gamma - 1) T_0}} \left(\frac{T_0}{T} \right)^{1/2 - \gamma/(\gamma-1)}$$

which can be recast as

$$F = \frac{\dot{m} \sqrt{c_p T_0}}{A p_0} = \frac{\gamma M}{\sqrt{\gamma - 1}} \left(1 + \frac{\gamma - 1}{2} M^2 \right)^{-(\gamma+1)/2(\gamma-1)} \quad (3.7)$$

The symbol F is called a *flow function*. Denoting the area at which the flow would reach $M = 1$ by A^* , the previous equation at this state gives

$$\frac{\dot{m} \sqrt{c_p T_0}}{A^* p_0} = \frac{\gamma}{\sqrt{\gamma - 1}} \left(\frac{\gamma + 1}{2} \right)^{-(\gamma+1)/2(\gamma-1)} \quad (3.8)$$

The ratio of the last two equations is

$$\frac{A}{A^*} = \frac{1}{M} \left(\frac{2}{\gamma + 1} + \frac{\gamma - 1}{\gamma + 1} M^2 \right)^{(\gamma+1)/2(\gamma-1)} \quad (3.9)$$

In the usual case, area A^* is the throat area in a supersonic flow through a converging-diverging nozzle. But this equation is useful also when there is no location in the actual flow, where $M = 1$ is reached. Then, A^* can be regarded as a reference area. In the same manner in which stagnation properties are reached in a thought experiment in an isentropic deceleration of the flow to a rest state, so can the area A^* in a thought experiment be taken to be an area at which the sonic condition is reached in a hypothetical extension of a properly designed and operated variable area duct. If the velocity V^* denotes the velocity at the location where $M = 1$, it can be used as a reference velocity, and a velocity ratio can be written as

$$\frac{V}{V^*} = M \sqrt{\frac{T}{T^*}} = M \left(\frac{2}{\gamma + 1} + \frac{\gamma - 1}{\gamma + 1} M^2 \right)^{-1/2} \quad (3.10)$$

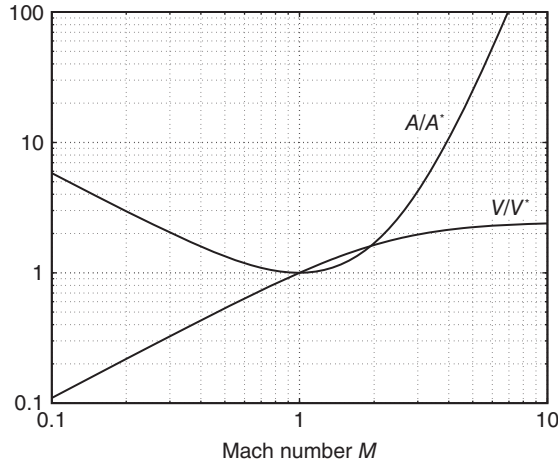


Figure 3.4 Area and velocity ratios as functions of Mach number.

This and the area ratio are shown in Figure 3.4. Maximum flow rate per unit area takes place at the throat where $M = 1$. It is given by Eq. (3.8) as

$$\frac{\dot{m}}{A^*} = \frac{\gamma p_0}{\sqrt{c_p(\gamma - 1)T_0}} \left(\frac{2}{\gamma + 1} \right)^{(\gamma+1)/2(\gamma-1)} \quad (3.11)$$

■ EXAMPLE 3.2

Air flows through a circular duct of diameter $D = 10$ cm at the rate of $\dot{m} = 1.5$ kg/s. At a certain location, static pressure is $p = 120$ kPa and stagnation temperature is $T_0 = 318$ K. At this location, find the values for Mach number, velocity, and static density.

Solution: Since the mass flow rate and diameter of the duct are known, mass balance

$$\dot{m} = \rho V A$$

can be recast into a form in which the known quantities of area, pressure, and stagnation temperature appear, and Mach number is the only unknown. Thus,

$$\dot{m} = \frac{p}{RT} M \sqrt{\gamma RT} A = p M A \sqrt{\frac{T_0}{T}} \sqrt{\frac{\gamma}{RT_0}}$$

or

$$\frac{\dot{m}}{pA} \sqrt{\frac{RT_0}{\gamma}} = M \left(1 + \frac{\gamma - 1}{2} M^2 \right)^{1/2}$$

Squaring both sides leads to a quadratic equation for M^2 , which may be simplified and cast into the standard form:

$$M^4 + \frac{2}{\gamma - 1} M^2 - \frac{2}{\gamma - 1} \left(\frac{\dot{m}}{pA} \right)^2 \frac{RT_0}{\gamma} = 0$$

For the data given, this reduces to

$$M^4 + 5M^2 - 0.826 = 0,$$

and solving it gives $M = 0.40$. Static temperature is then

$$T = \frac{T_0}{1 + \frac{\gamma-1}{2}M^2} = \frac{318}{1.032} = 308.1 \text{ K},$$

and the velocity and density are

$$V = M\sqrt{\gamma RT} = 140.8 \text{ m/s} \quad \rho = \frac{p}{RT} = \frac{120}{0.287 \cdot 308.1} = 1.357 \text{ kg/m}^3$$

■

3.2.1 Converging nozzle

A converging nozzle is shown in Figure 3.5. Consider a flow that develops from upstream stagnation state and in which the back pressure p_b is controlled by a throttling valve located downstream of the nozzle. When the valve is closed, there is no flow. With a slight opening of the valve, pressure in the nozzle follows the line marked 1, and the flow leaves the nozzle with the exit pressure $p_e = p_{b1}$. The mass flow rate corresponds to condition labeled 1 in the bottom right part of the figure. As the back pressure is reduced to p_{b2} , pressure in the nozzle drops along the curve 2, and the mass flow rate has increased to a value indicated by the label 2. A further decrease in the back pressure increases the flow rate until the back pressure is reduced to a critical value $p_b = p^*$, at which point Mach number reaches unity at the exit plane. Further reduction of the exit pressure has no effect on the flow upstream, for the disturbances caused by further opening of the valve cannot propagate upstream of the throat when the velocity there has reached the sonic speed. The flow at this condition is said to be *choked*, and its mass flow rate can no longer be increased. How the flow adjusts from this exit pressure to the value of back pressure cannot be analyzed by one-dimensional methods.

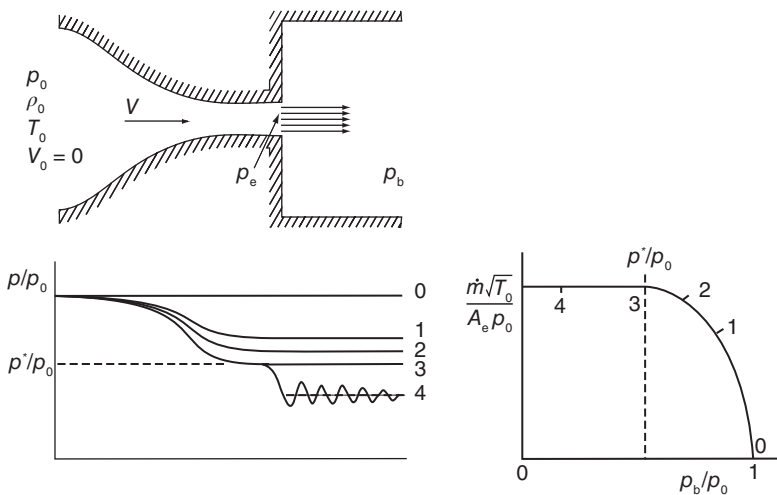


Figure 3.5 Flow through a converging nozzle.

Flow rate through the nozzle can be determined at the choked condition if, in addition to the stagnation pressure and stagnation temperature, the throat area is known. This is illustrated in the next example.

■ EXAMPLE 3.3

Air at stagnation temperature $T_0 = 540$ K and stagnation pressure $p_0 = 200$ kPa flows isentropically in a converging nozzle, with exit area $A_t = 10$ cm². (a) If the flow is choked, what are the exit pressure and the mass flow rate? (b) Assuming that the back pressure is $p_b = 160$ kPa, find the flow rate.

Solution: (a) With the flow choked, the pressure ratio is

$$\frac{p_e}{p_0} = 0.5283$$

from which the exit pressure is determined to be $p_e = 105.7$ kPa. The flow rate can be obtained by first calculating the flow function

$$F^* = \frac{\gamma}{\sqrt{\gamma-1}} \left(\frac{2}{\gamma+1} \right)^{(\gamma+1)/2(\gamma-1)}$$

which has the numerical value

$$F^* = \frac{1.4}{\sqrt{0.4}} \left(\frac{2}{2.4} \right)^3 = 1.281$$

Then, the mass flow rate per unit area can be determined to be

$$\frac{\dot{m}}{A_t} = \frac{F^* p_0}{\sqrt{c_p T_0}} = \frac{1.281 \cdot 200,000}{\sqrt{1004.5 \cdot 540}} = 347.9 \text{ kg/(s m}^2\text{)}$$

so the flow rate is $\dot{m} = 0.348$ kg/s.

(b) The second part of the example asks for the flow rate when back pressure is $p_b = 160$ kPa. Since this pressure is larger than the critical value 105.7 kPa, the flow is no longer choked and $p_e = p_b$. The exit Mach number is obtained from

$$\frac{p_0}{p_e} = \left(1 + \frac{\gamma-1}{2} M_e^2 \right)^{\gamma/(\gamma-1)}$$

Solving for M_e gives

$$M_e = \sqrt{\frac{2}{\gamma-1} \left[\left(\frac{p_0}{p_e} \right)^{(\gamma-1)/\gamma} - 1 \right]} = \sqrt{5(1.25^{1/3.5} - 1)} = 0.574$$

The flow function at this Mach number is

$$F_e = \frac{\gamma M_e}{\sqrt{\gamma-1}} \left(1 + \frac{\gamma-1}{2} M_e^2 \right)^{-(\gamma+1)/2(\gamma-1)},$$

and its numerical value is

$$F_e = \frac{1.4 \cdot 0.574}{\sqrt{0.4}} (1 + 0.2 \cdot 0.574^2)^{-3} = 1.049$$

The mass flow rate can then be determined from

$$\dot{m} = \frac{F p_0 A_t}{\sqrt{c_p T_0}} = \frac{1.049 \cdot 200000 \cdot 10}{\sqrt{1004.5 \cdot 540 \cdot 100^2}} = 0.285 \text{ kg/s}$$

■

3.3 INFLUENCE OF FRICTION ON FLOW THROUGH NOZZLES

There are various ways in which the irreversibilities caused by friction have been taken into account in studies of nozzle flow. These are discussed in this section. First, a polytropic efficiency is introduced, and it is then related to a static enthalpy loss coefficient, which, in turn, is related to a loss of stagnation pressure. Next, nozzle efficiency and the velocity coefficient are discussed. After this, the equations for compressible flow in a variable-area duct with wall friction are given. In the discussion that follows, the flow is adiabatic, and no work is done. Therefore, the stagnation temperature remains constant, and assuming constant specific heats and ideal gas behavior, the relation

$$\frac{T_0}{T} = 1 + \frac{\gamma - 1}{2} M^2 \quad (3.12)$$

remains valid for adiabatic flow even when friction is present.

3.3.1 Polytropic efficiency

The concept of polytropic efficiency follows from examining the Tds equation

$$T ds = dh - v dp$$

for an isentropic process,

$$dh_s = v dp \quad (3.13)$$

and a nonisentropic one. A *polytropic efficiency* of an incremental expansion process is defined as

$$\eta_p = \frac{dh}{dh_s}$$

so that $dh = \eta_p dh_s$. The process is shown in Figure 2.9a. Substituting this into Eq. (3.13) and making use of the ideal gas relation gives

$$dh = c_p dT = \eta_p v dp = \eta_p \frac{RT}{p} dp$$

From this follows the relation

$$\frac{dT}{T} = \frac{\eta_p (\gamma - 1)}{\gamma} \frac{dp}{p} \quad (3.14)$$

A polytropic index n is now introduced via the equation

$$\frac{n-1}{n} = \frac{\eta_p(\gamma-1)}{\gamma} \quad \text{so that} \quad \eta_p = \left(\frac{n-1}{n} \right) \left(\frac{\gamma}{\gamma-1} \right), \quad (3.15)$$

and Eq. (3.15) can also be written as

$$n = \frac{\gamma}{\eta_p + \gamma(1 - \eta_p)} \quad (3.16)$$

Assuming that η_p and hence also n remain constant along the entire expansion path, integrating Eq. (3.14) yields

$$\frac{T_2}{T_1} = \left(\frac{p_2}{p_1} \right)^{(n-1)/n} \quad (3.17)$$

Rewriting this as

$$\frac{n-1}{n} = \frac{\ln T_2/T_1}{\ln p_2/p_1}$$

gives an equation from which the polytropic exponent may be calculated, if the inlet and exit pressures and temperatures have been determined experimentally. Real gas effects have been incorporated into the theory by Shultz [83], Mallen and Saville [62], and Huntington [49].

If the inlet state is a stagnation state, then, writing Eq. (3.17) as

$$\frac{T_{01}}{T_2} = \left(\frac{p_{01}}{p_2} \right)^{(n-1)/n} \quad (3.18)$$

and making use of the ideal gas relation in Eq. (3.18) it follows that

$$\frac{\rho_{01}}{\rho_2} = \left(\frac{T_{01}}{T_2} \right)^{1/(n-1)} \quad \frac{p_{01}}{p_2} = \left(\frac{\rho_{01}}{\rho} \right)^n$$

Finally, using Eq. (3.12), the pressure and density ratios may be written as

$$\frac{p_{01}}{p_2} = \left(1 + \frac{\gamma-1}{2} M_2^2 \right)^{n/(n-1)} \quad \frac{\rho_{01}}{\rho_2} = \left(1 + \frac{\gamma-1}{2} M_2^2 \right)^{1/(n-1)}$$

The flow velocity is

$$V = M \sqrt{\gamma R T} = M \sqrt{\gamma R T_0} \left(1 + \frac{\gamma-1}{2} M^2 \right)^{-(1/2)},$$

which can be used to express the mass flow rate per unit area at the throat in the form

$$\frac{\dot{m} \sqrt{c_p T_{01}}}{p_{01} A_2} = \frac{\gamma}{\sqrt{\gamma-1}} M_2 \left(1 + \frac{\gamma-1}{2} M_2^2 \right)^{-(n+1)/2(n-1)} \quad (3.19)$$

With the conditions at the inlet fixed, M_2 is the only variable in this equation. Differentiating with respect to M_2 gives that value of Mach number at the throat for which the maximum flow rate per unit area is achieved. This operation leads to

$$1 + \frac{\gamma-1}{2} M_2^2 - \frac{(n+1)(\gamma-1)}{2(n-1)} M_2^2 = 0,$$

which when simplified and solved for M_t , gives

$$M_t = \sqrt{\frac{n-1}{\gamma-1}} \quad (3.20)$$

in which the subscript has been changed to indicate that this is the Mach number at the throat at a choked condition. Two alternative forms are

$$M_t = \sqrt{\frac{\eta_p}{\eta_p + \gamma(1 - \eta_p)}} \quad M_t = \sqrt{1 - (1 - \eta_p)n} \quad (3.21)$$

It is seen that Mach number at the throat is slightly less than one. Making use of this value of Mach number, the critical pressure ratio becomes

$$\frac{p_t}{p_{01}} = \left(\frac{2}{n+1} \right)^{n/(n-1)} \quad (3.22)$$

This has the same form as the expression for isentropic flow when γ replaced by n . Substituting M_t from Eq. (3.21) into Eq. (3.19) gives

$$\left(\frac{\dot{m}}{A_t} \right)_{\max} = \sqrt{2\eta_p n p_{01} \rho_{01} \left(\frac{2}{n+1} \right)^{(n+1)/(n-1)}} \quad (3.23)$$

Velocity at the throat at this condition is

$$V_t = \sqrt{2c_p(T_{01} - T_t)} = \sqrt{\frac{2\gamma}{\gamma-1} R T_t \left(\frac{T_{01}}{T_t} - 1 \right)} = \sqrt{\eta_p n R T_t}$$

in which the relation $T_{01}/T_t = (n+1)/2$ was used. Alternatively, velocity at the throat may be determined from $V_t = M_t \sqrt{\gamma R T_t}$.

■ EXAMPLE 3.4

Air in a reservoir, with temperature 540 K and pressure 200 kPa, flows into a converging nozzle with a polytropic efficiency $\eta_p = 0.98$. The throat area is $A_t = 10 \text{ cm}^2$. (a) If the flow is choked, what are the exit pressure and the mass flow rate? (b) Given that the back pressure is $p_b = 160 \text{ kPa}$, find the mass flow rate.

Solution: (a) The polytropic exponent is

$$n = \frac{\gamma}{\eta_p + \gamma(1 - \eta_p)} = \frac{1.4}{0.98 + 1.4 \cdot 0.02} = 1.389,$$

and the throat Mach number can then be determined to be

$$M_t = \sqrt{\frac{n-1}{\gamma-1}} = \sqrt{\frac{1.389-1}{1.4-1}} = 0.986$$

With the flow choked, pressure and temperature at the throat are

$$p_t = p_{01} \left(\frac{2}{n+1} \right)^{n/(n-1)} = 200 \left(\frac{2}{1.389+1} \right)^{1.389/0.389} = 106 \text{ kPa}$$

$$T_t = \frac{2T_{01}}{n+1} = \frac{2 \cdot 540}{1.389+1} = 450.0 \text{ K}$$

Mass flux at the throat at choked condition is

$$\frac{\dot{m}}{A_t} = p_{01} \sqrt{\frac{\gamma}{RT_{01}}} M_2 \left(\frac{n+1}{2} \right)^{-(n+1)/2(n-1)} = 343.42 \text{ kg/(s m}^2\text{)},$$

and with $A_t = 10 \text{ cm}^2$, flow rate is

$$\dot{m} = 0.343 \text{ kg/s}$$

(b) For $p_b = 160 \text{ kPa}$, the flow is not choked. Hence, M_t is calculated from

$$M_t = \sqrt{\frac{2}{\gamma-1} \left[\left(\frac{p_{01}}{p_b} \right)^{(n-1)/n} - 1 \right]} = 0.5678,$$

and the mass flux at the throat is obtained from

$$\frac{\dot{m}}{A_t} = \rho_t V_t = p_{01} \sqrt{\frac{\gamma}{RT_{01}}} M_t \left(1 + \frac{\gamma-1}{2} M_t^2 \right)^{-(n+1)/2(n-1)} = 281.7 \text{ kg/(s m}^2\text{)}$$

Hence, the mass flow rate is

$$\dot{m} = 0.282 \text{ kg/s}$$

By comparing this to the calculation in Example 3.3 for an isentropic flow, the mass flow rate is seen to be slightly smaller for the polytropic process. ■

Since the sonic state does not appear anywhere in the actual flow, it serves as a reference state. At the sonic state, the static properties may be calculated from the stagnation state upstream by using the following equations:

$$\frac{T^*}{T_{01}} = \frac{2}{\gamma+1} \quad \frac{p^*}{p_{01}} = \left(\frac{2}{\gamma+1} \right)^{n/(n-1)} \quad \frac{\rho^*}{\rho_{01}} = \left(\frac{2}{\gamma+1} \right)^{1/(n-1)}$$

Since T_{01} remains constant, the relationship between the static temperature at the sonic state, and its value at the inlet is

$$\frac{T^*}{T_1} = \frac{T^*}{T_{01}} \frac{T_{01}}{T_1} = \left(\frac{2}{\gamma+1} \right) \left(1 + \frac{\gamma-1}{2} M_1^2 \right)$$

or

$$\frac{T^*}{T_1} = \frac{2}{\gamma+1} + \frac{\gamma-1}{\gamma+1} M_1^2$$

The pressure ratio is clearly

$$\frac{p^*}{p_1} = \left(\frac{2}{\gamma + 1} + \frac{\gamma - 1}{\gamma + 1} M_1^2 \right)^{\gamma/(\gamma - 1)},$$

and the density ratio is

$$\frac{\rho^*}{\rho_1} = \left(\frac{2}{\gamma + 1} + \frac{\gamma - 1}{\gamma + 1} M_1^2 \right)^{1/(\gamma - 1)}$$

3.3.2 Loss coefficients

In addition to the polytropic efficiency, there are other measures of irreversibility in nozzle flow. The first of these is the loss coefficient for static enthalpy, defined as

$$\zeta = \frac{h_2 - h_{2s}}{h_{02} - h_2} = \frac{h_2 - h_{2s}}{\frac{1}{2} V_2^2} \quad (3.24)$$

where the end states are as shown in Figure 3.6. The numerator is the change in enthalpy owing to internal heating.

This may also be written as

$$\zeta = \frac{h_{02} - h_{2s} - (h_{02} - h_2)}{h_{02} - h_2} = \frac{V_{2s}^2 - V_2^2}{V_2^2} = \frac{1}{c_v^2} - 1$$

in which $c_v = V_2/V_{2s}$ is called a *velocity coefficient*. For the given inlet conditions and exit pressure, the static enthalpy loss coefficient may be related to the polytropic efficiency, as the next example illustrates.

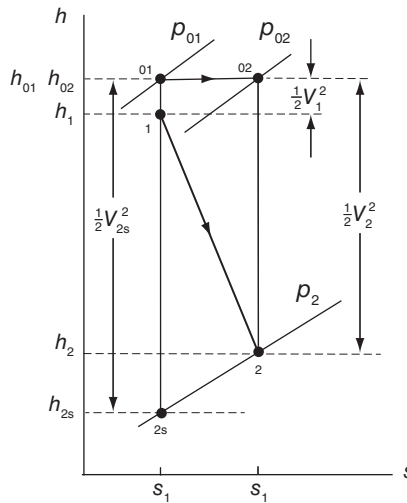


Figure 3.6 The thermodynamic states for a flow through a nozzle with friction.

EXAMPLE 3.5

Air in a reservoir, with temperature 540 K and pressure 200 kPa, flows into a converging nozzle with a polytropic efficiency $\eta_p = 0.98$. (a) Find the static enthalpy loss coefficient, given an exit pressure of $p_2 = 160$ kPa. (b) Find the velocity coefficient. (c) Find the loss in stagnation pressure.

Solution: (a) As in the previous example, the polytropic exponent is

$$n = \frac{\gamma}{\eta_p + \gamma(1 - \eta_p)} = \frac{1.4}{0.98 + 1.4 \cdot 0.02} = 1.389$$

The exit temperature is therefore

$$T_2 = T_{01} \left(\frac{p_2}{p_{01}} \right)^{(n-1)/n} = 540 \left(\frac{160}{200} \right)^{1.389/0.389} = 507.29 \text{ K},$$

and the Mach number at the exit is

$$M_2 = \sqrt{\frac{2}{\gamma - 1} \left(\frac{T_{01}}{T_2} - 1 \right)} = \sqrt{\frac{2}{0.4} \left(\frac{540}{507.29} - 1 \right)} = 0.5678$$

The exit velocity is therefore

$$V_2 = M_2 \sqrt{\gamma R T_2} = 0.5678 \sqrt{1.4 \cdot 287 \cdot 507.3} = 256.34 \text{ m/s}$$

The temperature T_{2s} is obtained from the expression for isentropic expansion

$$T_{2s} = T_{01} \left(\frac{p_2}{p_{01}} \right)^{(k-1)/k} = 540 \left(\frac{160}{200} \right)^{1/3.5} = 506.65 \text{ K}$$

Hence, the static enthalpy loss coefficient is

$$\zeta = \frac{2c_p(T_2 - T_{2s})}{V_2^2} = \frac{2 \cdot 1004.5 \cdot (507.29 - 506.65)}{256.34^2} = 0.01976$$

(b) The velocity coefficient is then

$$c_v = \frac{1}{\sqrt{1 + \zeta}} = 0.9903$$

(c) The loss of stagnation pressure is obtained by noting that

$$\frac{p_{02}}{p_{01}} = \frac{p_{02}}{p_2} \frac{p_2}{p_{01}} = \left(\frac{T_{02}}{T_2} \right)^{\gamma/(\gamma-1)} \left(\frac{T_{2s}}{T_{02}} \right)^{\gamma/(\gamma-1)} = \left(\frac{T_{2s}}{T_2} \right)^{\gamma/(\gamma-1)}$$

Hence,

$$p_{02} = p_{01} \left(\frac{T_{2s}}{T_2} \right)^{\gamma/(\gamma-1)} = 200 \left(\frac{506.65}{507.29} \right)^{3.5} = 199.11 \text{ kPa}$$

The loss in stagnation pressure is $\Delta p_0 = p_{01} - p_{02} = 890$ Pa. Because the values of p_{01} and p_{02} are nearly equal, on subtracting one from the other, a number of significant figures are lost. If the value of the static enthalpy loss coefficient is known, then the polytropic efficiency may be calculated by reversing the steps in this example. ■

The ratio of stagnation pressures p_{02}/p_{01} may also be developed by integrating the Gibbs equation

$$T ds = dh - v dp$$

along the constant p_2 line. This gives

$$s_2 - s_1 = c_p \ln \frac{T_2}{T_{2s}}$$

Similarly, integrating it between states 01 and 02 along the constant h_0 line leads to

$$s_2 - s_1 = R \ln \frac{p_{01}}{p_{02}}$$

Hence,

$$\frac{p_{02}}{p_{01}} = \left(\frac{T_{2s}}{T_2} \right)^{\gamma/(\gamma-1)} \quad (3.25)$$

This may also be written as

$$\frac{T_{2s}}{T_2} = \left(\frac{p_{02}}{p_{01}} \right)^{(\gamma-1)/\gamma} = \left(\frac{p_{01} - \Delta p_0}{p_{01}} \right)^{(\gamma-1)/\gamma} = \left(1 - \frac{\Delta p_0}{p_{01}} \right)^{(\gamma-1)/\gamma}$$

in which $\Delta p_0 = p_{01} - p_{02}$. Assuming that $\Delta p_0/p_{01} \ll 1$ and making use of the binomial theorem, the following approximation can be used

$$\frac{T_{2s}}{T_2} = 1 - \frac{\gamma-1}{\gamma} \frac{\Delta p_0}{p_{01}}$$

which may be also recast as

$$\frac{T_2 - T_{2s}}{T_2} = \frac{\gamma-1}{\gamma} \frac{\Delta p_0}{p_{01}},$$

and from which

$$h_2 - h_{2s} = \frac{RT_2 \Delta p_0}{p_{01}} = \frac{\Delta p_0 / \rho_{01}}{1 + \frac{\gamma-1}{2} M_2^2}$$

so that the static enthalpy loss coefficient is

$$\zeta = \frac{\Delta p_0 / \rho_{01}}{\frac{1}{2} V_2^2 \left(1 + \frac{\gamma-1}{2} M_2^2 \right)}$$

For small values of exit Mach number, this reduces to

$$\zeta = \frac{\Delta p_0 / \rho_{01}}{\frac{1}{2} V_2^2},$$

and this is often called a *stagnation pressure loss coefficient*.

Another measure of the loss of stagnation pressure is given by

$$Y_p = \frac{p_{01} - p_{02}}{p_{02} - p_2}$$

which may be written as

$$Y_p = \frac{p_{01}/p_{02} - 1}{1 - p_2/p_{02}}$$

The pressure ratios in this expression are

$$\frac{p_2}{p_{02}} = \left(\frac{T_2}{T_{02}} \right)^{\gamma/(\gamma-1)}$$

and

$$\frac{p_{02}}{p_{01}} = \left(\frac{T_{2s}}{T_2} \right)^{\gamma/(\gamma-1)}$$

Using the definition of static enthalpy loss coefficient, Eq. (3.24) can be rewritten as

$$\frac{T_{2s}}{T_2} = 1 - \zeta \left(\frac{T_{02}}{T_2} - 1 \right)$$

Substituting these into the expression for Y_p gives it the form

$$Y_p = \frac{\left[1 - \zeta \left(\frac{T_{02}}{T_2} - 1 \right) \right]^{-\gamma/(\gamma-1)} - 1}{1 - \left(\frac{T_{02}}{T_2} \right)^{-\gamma/(\gamma-1)}}$$

or

$$Y_p = \frac{\left(1 - \zeta \frac{\gamma-1}{2} M_2^2 \right)^{-\gamma/(\gamma-1)} - 1}{1 - \left(1 + \frac{\gamma-1}{2} M_2^2 \right)^{-\gamma/(\gamma-1)}}$$

For small M_2 , this reduces to $Y_p = \zeta$. The development indicates that the value of ζ is not dependent on Mach number, but the loss of stagnation pressure is, and therefore also the value of Y_p . For this reason, ζ ought to be favored over other measures of irreversibility [18]. However, it is worthwhile to be familiar with the various loss coefficients, as they have been and still are in use in the analysis of turbine nozzles.

3.3.3 Nozzle efficiency

The nozzle efficiency is defined as

$$\eta_N = \frac{h_1 - h_2}{h_1 - h_{2s}},$$

or since the stagnation enthalpy remains constant so that $h_1 + V_1^2/2 = h_2 + V_2^2/2$, this relation can be rewritten as

$$\eta_N = \frac{V_2^2 - V_1^2}{2(h_1 - h_{2s})}$$

Similarly, when $h_1 + V_1^2/2 = h_{2s} + V_{2s}^2/2$ is used to rewrite the isentropic enthalpy change in the denominator in terms of kinetic energy differences, nozzle efficiency takes the alternative form

$$\eta_N = \frac{V_2^2 - V_1^2}{V_{2s}^2 - V_1^2}$$

If the fluid enters the nozzle from a large reservoir where $V_1 = 0$, nozzle efficiency becomes

$$\eta_N = \frac{V_2^2}{2(h_{01} - h_{2s})} = \frac{V_2^2}{V_{2s}^2} = c_v^2$$

Thus, nozzle efficiency can be interpreted as a ratio of the actual increase in kinetic energy of the flow to that in reversible adiabatic flow. Nozzle efficiency takes into account the losses in the entire nozzle, from its inlet to its exit. If the nozzle is a converging–diverging type, and the flow is subsonic, then most of the losses take place in the diverging part in which the flow diffuses to a low velocity. Nozzle efficiency of a converging nozzle has a value very close to unity.

For a flow that starts from the stagnation state nozzle efficiency

$$\eta_N = \frac{V_2^2}{2c_p(T_{01} - T_{2s})}$$

may be further manipulated into the form

$$\eta_N = \frac{\gamma - 1}{2} \frac{M_2^2}{\left(1 - \frac{T_{2s}}{T_{01}}\right)} \frac{T_2}{T_{01}}$$

Expressing the isentropic temperature ratio T_{2s}/T_{01} and T_{01}/T_2 as

$$\frac{T_{2s}}{T_{01}} = \left(\frac{p_2}{p_{01}}\right)^{(\gamma-1)/\gamma} \quad \frac{T_{01}}{T_2} = 1 + \frac{\gamma - 1}{2} M_2^2$$

and solving the resulting equation for the pressure ratio gives

$$\frac{p_2}{p_{01}} = \left[1 - \frac{(\gamma - 1)M_2^2}{\eta_N(2 + (\gamma - 1)M_2^2)}\right]^{\gamma/(\gamma-1)} \quad (3.26)$$

The following development of an expression for mass flow rate through a converging nozzle makes use of this equation. In such a nozzle, the exit area A_2 is equal to the throat area A_t , and the mass flux, which is the mass flow rate per unit area, at the throat is given by

$$\frac{\dot{m}}{A_t} = \rho_t V_t = p_t M_t \sqrt{\frac{\gamma}{RT_{01}}} \sqrt{\frac{T_{01}}{T_t}}$$

or

$$\frac{\dot{m}}{A_t} = p_{01} \sqrt{\frac{\gamma}{RT_{01}}} \frac{p_t}{p_{01}} M_t \sqrt{1 + \frac{\gamma - 1}{2} M_t^2}$$

Substituting the pressure ratio from Eq. (3.26) into this gives

$$\frac{\dot{m}}{A_t} = p_{01} \sqrt{\frac{\gamma}{RT_{01}}} \left[1 - \frac{(\gamma - 1)M_t^2}{\eta_N(2 + (\gamma - 1)M_t^2)} \right]^{\gamma/(\gamma-1)} \left[M_t^2 \left(1 + \frac{\gamma - 1}{2} M_t^2 \right) \right]^{1/2} \quad (3.27)$$

In this equation, square of Mach number appears, and therefore, differentiating this equation with respect to M_t^2 and setting the result to zero gives the value of M_t for maximum mass flux at the throat. Carrying out the differentiation gives the equation

$$(\gamma - 1)^2(1 - \eta_N)M_t^4 - [(\gamma - 1)3\eta_N - 2\gamma]M_t^2 - 2\eta_N = 0$$

From this, the throat Mach number at the condition of maximum mass flux is obtained as

$$M_t = \left[\frac{(\gamma - 1)(3\eta_N - 1) - 2\gamma + \sqrt{[(\gamma - 1)(3\eta_N - 1) - 2\gamma]^2 + 8\eta_N(1 - \eta_N)(\gamma - 1)^2}}{2(\gamma - 1)^2(1 - \eta_N)} \right]^{1/2} \quad (3.28)$$

If the nozzle efficiency is known, then, polytropic efficiency can be calculated by equating the Mach number obtained from Eq. (3.28) to $M_t = \sqrt{(n - 1)/(\gamma - 1)}$. For $\gamma = 1.4$ and $\eta_N = 0.98$, the polytropic exponent becomes $n = 1.3868$.

Neither the polytropic efficiency nor the overall nozzle efficiency reveals how the length of the nozzle influences the magnitude of irreversibilities in the flow. This issue is discussed in the next section.

3.3.4 Combined Fanno flow and area change

Compressible flow with friction in constant-area ducts goes by the name *Fanno flow*, and for this flow, the momentum equation is used to relate pressure and velocity changes to wall friction. There are two closely related friction factors in use. The *Fanning friction factor* is defined as

$$\bar{f} = \frac{\tau_w}{\frac{1}{2}\rho V^2}$$

The *Darcy friction factor* is four times the Fanning value, $f = 4\bar{f}$. Care must be exercised that the right one is used. The Darcy friction factor can be calculated for turbulent flow from the *Colebrook* formula

$$\frac{1}{\sqrt{f}} = -2\log_{10} \left(\frac{\varepsilon/D_h}{3.7} + \frac{2.51}{Re\sqrt{f}} \right) \quad (3.29)$$

in which ε is a root-mean-square (RMS) roughness of the walls and D_h is a hydraulic diameter, equal to $D_h = 4A/C$. Here, A is a cross-sectional area, and C is a wetted perimeter.

Since this equation is nonlinear, the value of f for given Re has to be determined iteratively; that is, an initial guess can be obtained by assuming Reynolds number Re to be so large that the second term in the parentheses may be neglected. The value of f obtained from this calculation is then substituted on the RHS. In this way, a new value of f is then found, and it is sufficiently accurate that the iterations can be stopped. In the equations that follow, the Fanning friction factor is used, but the equations are left in a form in which $4\bar{f}$ appears explicitly.

To analyze the combined effects of friction and area change, equation of continuity and energy are used together with the momentum equation. The x -component of the momentum balance for the control volume, shown in Figure 3.7, gives

$$\rho AV(V + dV - V) = pA - p dA - (p + dp)(A - dA) - \tau_w C \cos \alpha dL$$

Since in the sketch the flow area decreases, the downstream area is written as $A - dA$. In order to draw the vector $p dA$ in the correct direction for a converging channel, the area change must be assumed to have the sign that is consistent with the sketch.

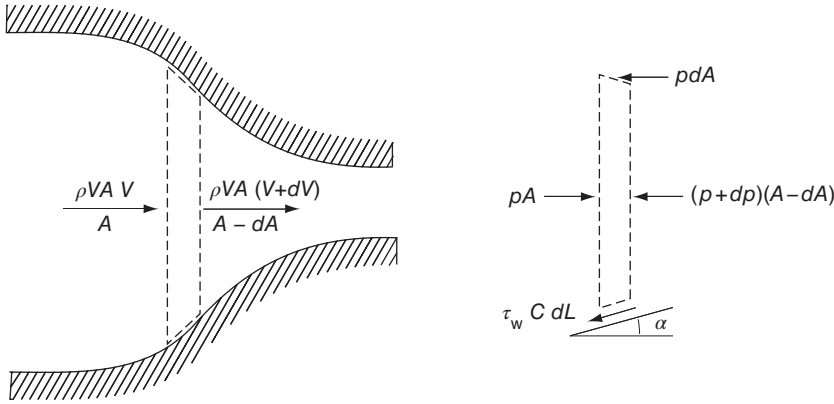


Figure 3.7 A converging nozzle with friction.

Making use of the relations $C = 4A/D_h$ and $\cos \alpha dL = dx$ in this equation and neglecting the small term $dp dA$, reduces it to the form

$$\rho V dV = -dp - \frac{4\tau_w}{D_h} dx$$

Introduction of the Fanning friction factor puts it into the form

$$\rho V dV = -dp - \frac{4\bar{f}}{D_h} \frac{1}{2} \rho V^2 dx$$

Using the ideal gas relation and definition of Mach number to establish the equality $\rho V^2 = \gamma p M^2$ gives, after each term has been divided by p , the equation

$$\frac{dp}{p} + \frac{\gamma M^2}{2} \frac{dV^2}{V^2} + \frac{\gamma M^2}{2} 4\bar{f} \frac{dx}{D_h} = 0 \quad (3.30)$$

To see the effect of area ratio and friction on the flow, this equation is next recasted into a form in which the first two terms are expressed in terms of area ratio and Mach number. The second term is considered first. Since $V^2 = M^2 \gamma R T$, taking logarithms and differentiating this gives

$$\frac{dV^2}{V^2} = \frac{dM^2}{M^2} + \frac{dT}{T}$$

Next, since in adiabatic flow T_0 is constant, taking logarithms and differentiating the adiabatic relation $T_0 = T(1 + \frac{\gamma-1}{2}M^2)$ gives

$$\frac{dT}{T} = - \frac{\frac{\gamma-1}{2}M^2}{1 + \frac{\gamma-1}{2}M^2} \frac{dM^2}{M^2} \quad (3.31)$$

and eliminating dT/T between the last two equations gives

$$\frac{dV^2}{V^2} = \frac{1}{1 + \frac{\gamma-1}{2}M^2} \frac{dM^2}{M^2} \quad (3.32)$$

Next, an equation between Mach number, area ratio, and friction factor is obtained by taking logarithms and differentiating the mass balance $\dot{m} = \rho A V$. This gives

$$\frac{d\rho}{\rho} + \frac{dA}{A} + \frac{dV}{V} = 0$$

A similar operation on the ideal gas relation $p = \rho R T$ leads to

$$\frac{dp}{p} = \frac{d\rho}{\rho} + \frac{dT}{T}$$

Eliminating the term involving density between these two equations gives

$$\frac{dp}{p} = -\frac{dA}{A} - \frac{1}{2} \frac{dV^2}{V^2} + \frac{dT}{T}$$

Substituting this expression for dp/p into Eq. (3.30) gives

$$-\frac{dA}{A} - \frac{1}{2}(1 - \gamma M^2) \frac{dV^2}{V^2} + \frac{dT}{T} + \frac{\gamma M^2}{2} 4\bar{f} \frac{dx}{D} = 0$$

Substituting Eqs. (3.31) and (3.32) into this yields the form

$$\frac{1 - M^2}{2 + (\gamma - 1)M^2} \frac{dM^2}{M^2} = -\frac{dA}{A} + \frac{\gamma M^2}{2} 4\bar{f} \frac{dx}{D} \quad (3.33)$$

from which the qualitative behavior of the flow can be seen. For sufficiently low back pressure, this equation shows that in a converging duct with $dA/A < 0$ both terms on the right are positive. Hence, in a flow that begins from a stagnation state, the Mach number increases in the flow direction, as was also true in isentropic flow. If the nozzle has a throat with $dA = 0$, the right side is still positive, and the Mach number must still increase as it

passes through the throat. This means that the Mach number is less than unity at the throat. In a supersonic nozzle, the flow may reach $M = 1$ in the diverging part, with $dA/A > 0$, when the terms on the RHS exactly cancel. Stagnation pressure may be calculated by solving

$$\frac{dp_0}{p_0} = -\frac{\gamma}{2} M^2 4\bar{f} \frac{dx}{D_h} \quad (3.34)$$

which shows that it drops only because of friction.

In steam turbines high-pressure steam is admitted into the turbine from a *steam chest*, to which it has entered via a regulated valve system. From the steam chest it flows first through a nozzle row arranged as shown in Figure 3.8. After leaving the nozzles it enters an interblade gap and then a set of rotor blades. Steam enters the nozzles in the axial direction, and the nozzles turn it into the general direction of the wheel velocity. Curvature of the nozzle passage does not introduce new complications into the analysis of frictional flow except, of course, at the initial stage when the geometry is laid out. Sidestepping such complications the calculation in the next example are for a flow channel for which the areas can be calculated from a simple equation.

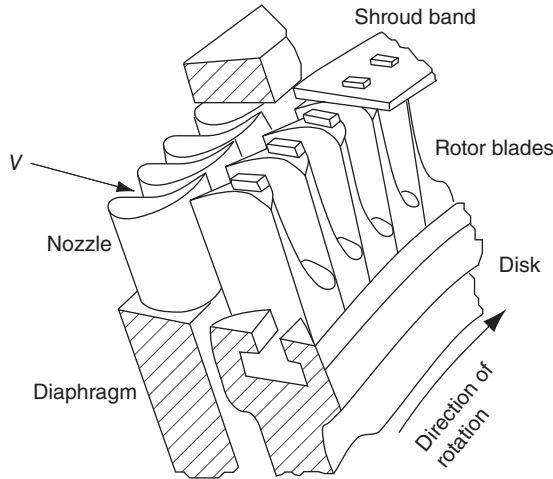


Figure 3.8 Steam turbine nozzles and blades. Source: Adapted from Keenan [54].

■ EXAMPLE 3.6

Consider steam flow through a rectangular nozzle of width 1cm and height is given by the equation

$$y = 2 + 5 \exp(-0.4x) + 2.5 \exp(0.1x)$$

It extends from $0 < x < 10$ cm. At the inlet, steam is superheated with pressure $p_1 = 1000$ kPa and temperature $T_1 = 640$ K and $M_1 = 0.2$. The friction factor is assumed to be $4\bar{f} = 0.04$. Plot the Mach number and $p(x)/p_1$ along the nozzle, assuming that it remains superheated as an ideal gas with $\gamma = 1.3$.

Solution: The areas at the inlet and outlet are

$$A_i = 9.5 \text{ cm}^2 \quad A_e = 8.887 \text{ cm}^2$$

First consider the isentropic flow. With $M_1 = 0.2$ at the inlet, the area at the sonic state can be determined from

$$\begin{aligned}\frac{A_i}{A^*} &= \frac{1}{M_1} \left(\frac{2 + (\gamma - 1)M_1^2}{\gamma + 1} \right)^{(\gamma+1)/2(\gamma-1)} \\ &= \frac{1}{0.2} \left(\frac{2 + 0.3 \cdot 0.2^2}{2.3} \right)^{3.833} = 2.994\end{aligned}$$

Hence, $A^* = 3.173$ cm. The exit Mach number can be found by the usual procedure of finding the M_e satisfying the equation

$$\frac{8.887}{3.173} = 2.801 = \frac{1}{M_e} \left(\frac{2 + (\gamma - 1)M_e^2}{\gamma + 1} \right)^{(\gamma+1)/2(\gamma-1)}$$

It is $M_e = 0.2145$, and the normalized pressure is $p_e/p_1 = 0.9961$.

The numerical solution is carried out by using the Runge–Kutta method ode45 found in MATLAB or GNU/OCTAVE, and the important lines of the code are

```
xspan=[0:0.01:10]; f=0.01; k=1.3; w=1; M1=0.2;
mx1=M1^2;
[x,mx] = ode45(@(x,mx) odefun(x,mx,f,k,w),xspan,mx1);
M=sqrt(mx);

function dmdx = odefun(x,mx,f,k,w)
A=2+5*exp(-0.4*x)+2.5*exp(0.1*x);
dAdx=-2*exp(-0.4*x)+0.25*exp(0.1*x);
D=2*A/(A+w);
dmdx=-(2*mx+(k-1)*mx*mx)/(1-mx)*(dAdx/A) ...
      +k*mx*(2+(k-1)*mx)/(1-mx)*4*f/D;
end
```

The numerical calculation of the isentropic flow is carried out by setting $\bar{f} = 0$. This also serves as a check to partially confirm that there are no errors in the computer program, as the calculation must yield the exit Mach number $M_e = 0.2145$.

Plots of Mach number and normalized pressure for isentropic and frictional flow are shown in Figure 3.9. Friction is seen to increase the Mach number and cause the pressure to be always lower than in the isentropic case. ■

In the foregoing example, length of the nozzle was taken into account explicitly. Since the irreversibilities are clearly a function of both the surface roughness and the length of the flow passage, this is an improvement over assigning a polytropic exponent to the process, or by estimating the nozzle efficiency by past experience. However, an objection may be raised in the use of friction factors, obtained experimentally from flow of incompressible fluids in pipes, to *compressible flow with large area change*.

Today, it is possible to carry out *computational fluid dynamics* CFD simulations to take account of frictional effects better than the one-dimensional analysis discussed here yields. Nevertheless, it is still worthwhile to carry out a one-dimensional analysis by hand and by the use of effective software, for such methods increase intuition, which is difficult to gain by CFD alone.

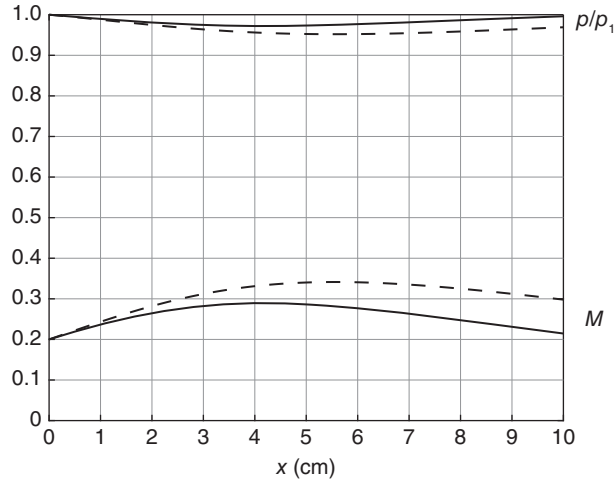


Figure 3.9 Mach numbers and normalized pressure for a steam flow through a nozzle. At the inlet $M_1 = 0.2$ and the dashed lines correspond to frictional flow whereas solid lines to isentropic flow.

3.4 SUPERSONIC NOZZLE

In this section, compressible flow in a converging–diverging nozzle is considered, and in the next section the theory of normal shocks is developed. In addition to friction, shocks cause additional irreversibilities in the flow. Ignoring friction and shocks, the flow in a converging–diverging nozzle can be considered isentropic, particularly if the flow is accelerating to supersonic speeds after the throat of the nozzle.

Consider the operation of a converging–diverging nozzle in the same manner as was described for the converging one. The flow rate is adjusted by a regulating valve downstream of the nozzle. With the valve closed, there is no flow, and the pressure throughout equals the stagnation pressure. As the valve is opened slightly, flow is accelerated in the converging part of the nozzle, and its pressure drops. It is then decelerated after the throat with rising pressure such that the exit plane pressure p_e reaches the back pressure p_b . This corresponds to case 1 shown in Figure 3.10. Further opening of the valve drops the back pressure, and the flow rate increases until the valve is so far open that the Mach number has the value of unity at the throat, and the pressure at the throat is equal to the critical pressure p^* . After the throat, the flow diffuses and pressure rises until the exit plane is reached. The pressure variation is shown as condition 2 in the figure. If the valve is opened further, acoustic waves to signal what has happened downstream cannot propagate past the throat once the flow speed there is equal to the sound speed. The flow is now *choked*, and no further adjustment in the mass flow rate is possible.

The adjustment to the back pressure now takes place through a *normal shock* and diffusion after it in the diverging part of the nozzle. This situation is shown as condition 3 in Figure 3.10. Flows with normal shocks are discussed in the next section. A weak normal shock appears just downstream of the throat for back pressures slightly lower than that at which the flow becomes choked, and as the back pressure is further reduced, the position of the shock moves further downstream until it reaches the exit plane, which is shown as condition 4 in the figure. After this, any decrease in the back pressure cannot cause any change in the exit plane pressure. Condition 5 corresponds to an *overexpanded*

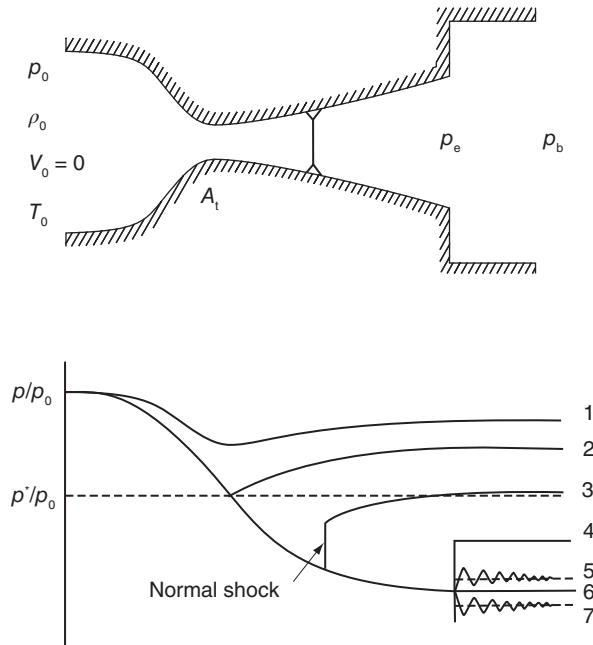


Figure 3.10 Supersonic nozzle with a shock in the diverging part of the nozzle.

flow because the exit pressure has dropped below the back pressure, and the adjustment to the back pressure takes place after the nozzle through a series of *oblique shock waves* and *expansion fans*.

There is one value of back pressure for which the flow is isentropic and supersonic all the way to the exit plane, and at this condition, the exit plane pressure reaches the value of the back pressure. This corresponds to one of the two solutions in the area ratio graph of Figure 3.4. It is also shown by line 6 in Figure 3.10. For back pressures below this value, the flow is said to be *underexpanded* as its pressure remains above the back pressure. The flow adjusts to the back pressure by expanding through a series of *oblique expansion waves* and *shock waves* as schematically shown by line 7 in the figure. The next example illustrates the conditions for isentropic supersonic flow.

■ EXAMPLE 3.7

Air flows isentropically in a converging–diverging nozzle, with a throat area of 10 cm^2 , such that at the exit $M_e = 2$. The supply pressure and temperature at the inlet are 2 bar and 540 K, respectively, and the inlet velocity is negligibly small. (a) Find the fluid properties at the throat, (b) the exit area, pressure, and temperature, and (c) the flow rate.

Solution: (a) At the stagnation state, density is

$$\rho_0 = \frac{p_0}{RT_0} = \frac{200}{0.287 \cdot 540} = 1.2905 \text{ kg/m}^3$$

Since the flow is supersonic downstream of the throat, it is sonic at the throat. Hence,

$$\begin{aligned} p^* &= 0.5283 p_0 = 0.5283 \cdot 2 = 1.056 \text{ bar} \\ T^* &= 0.8333 T_0 = 0.8333 \cdot 540 = 450.0 \text{ K} \\ \rho^* &= 0.6339 \rho_0 = 0.6339 \cdot 1.32905 = 0.8181 \text{ kg/m}^3 \\ V^* &= \sqrt{\gamma R T^*} = \sqrt{1.4 \cdot 287 \cdot 450.0} = 425.2 \text{ m/s} \end{aligned}$$

(b) At the exit plane, where $M_e = 2$, temperature is

$$T_e = \frac{T_0}{1 + \frac{\gamma - 1}{2} M_e^2} = \frac{540}{1 + 0.2 \cdot 4} = 300 \text{ K},$$

and pressure and density are

$$\begin{aligned} p_e &= p_0 \left(\frac{T_e}{T_0} \right)^{\gamma/(\gamma-1)} = 2 \left(\frac{300}{540} \right)^{3.5} = 25.56 \text{ kPa} \\ \rho_e &= \rho_0 \left(\frac{T_e}{T_0} \right)^{1/(\gamma-1)} = 1.2905 \left(\frac{300}{540} \right)^{2.5} = 0.2969 \text{ kg/m}^3 \end{aligned}$$

Since the throat area is $A^* = 10 \text{ cm}^2$, exit area is obtained by first calculating the area ratio

$$\frac{A_e}{A^*} = \frac{1}{M_e} \left(\frac{2}{\gamma + 1} + \frac{\gamma - 1}{\gamma + 1} M_e^2 \right)^{(\gamma+1)/2(\gamma-1)} = \frac{1.5^3}{2} = 1.6875$$

from which the exit area is $A_e = 16.875 \text{ cm}^2$.

(c) The mass flow rate is obtained from

$$\dot{m} = \rho^* A^* V^* = 0.8181 \cdot 0.001 \cdot 425.2 = 0.348 \text{ kg/s}$$

■

Examination of Figure 3.4 shows that for a given area ratio A/A^* , the Mach number can be supersonic or subsonic. The supersonic solution requires a low exit pressure, and this was examined in the previous example. To find the subsonic solution, Eq. (3.9) needs to be solved for Mach number when the area ratio is given. This can be carried out with MATLAB'S or GNU/OCTAVE'S `fzero` function. Its syntax is

$$x = \text{fzero}(@(\mathbf{x}) F(\mathbf{x}), [\mathbf{x}_1, \mathbf{x}_2]);$$

This finds the value of x that satisfies $F(x) = 0$, with the zero in the range $[x_1, x_2]$.

To obtain the subsonic solution, in the following MATLAB script, Mach number is bracketed to the range $[0.05, 1.0]$. The variable k is used for γ , and a is the area ratio.

```
clear all;
a=1.6875; k=1.4;
M = fzero(@(M) farea(M,a,k), [0.05,1.0])
```

The function farea is defined as

```
function f = farea(M,a,k)
f = a-(1/M)*((2/(k+1))*(1+0.5*(k-1)*M^2))^(0.5*(k+1)/(k-1));
```

The result is:

```
M=0.3722
```

In the MATLAB and GNU/OCTAVE, the *function body* is placed *after the main program* in the same file as the main program, and then, it must be terminated with the command `end`. A separate function is not needed if this is written as:

```
a=1.6875; k=1.4;
M = fzero(@(M) a-(1/M)*((2/(k+1))* ...
    (1+0.5*(k-1)*M^2))^(0.5*(k+1)/(k-1)), [0.05,1.0])
```

3.5 NORMAL SHOCKS

In a converging–diverging duct two *isentropic* solutions can be found for a certain range of back pressures. If the back pressure is reduced slightly from that corresponding to the subsonic branch of the flow, a *normal shock* develops just downstream of the throat where the flow is now supersonic. It will be seen that the flow after the shock is subsonic, and there is a jump in pressure across the shock. After the shock, the flow diffuses to the back pressure. A Schlieren photograph of a normal shock is shown in Figure 3.11. To understand the details of what is happening in the flow has to wait until the theory of oblique shocks and their interaction with the boundary layers along the walls are well understood. For now, it is sufficient to know that the central section of the shock corresponds to the normal shock. After the shock, the boundary layer interaction influences the flow across the entire channel. Still, one-dimensional analysis gives good results even in this part of the flow.

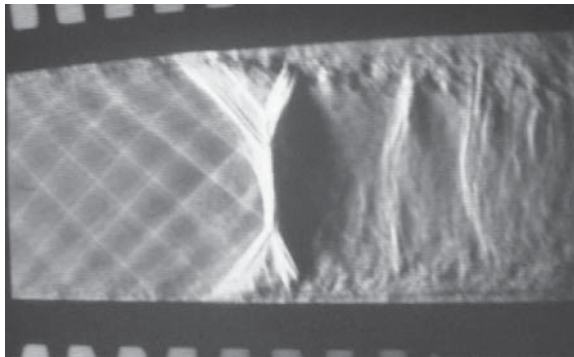


Figure 3.11 Interaction between a normal shock and wall boundary layers. Source: Photograph courtesy Professor D. Papamoschou.

The flow through a shock can be analyzed by considering a control volume around the shock. Since the flow is adiabatic, the energy equation reduces to

$$h_1 + \frac{1}{2}V_1^2 = h_2 + \frac{1}{2}V_2^2 \quad (3.35)$$

where the subscript 1 denotes the upstream state and subscript 2 the downstream state. Mass balance for this control volume yields

$$\frac{\dot{m}}{A} = \rho_1 V_1 = \rho_2 V_2 \quad (3.36)$$

and A is the area at the location of the shock. The momentum equation becomes

$$\dot{m}(V_2 - V_1) = (p_1 - p_2)A \quad (3.37)$$

since the wall friction can be neglected. Pressure increase across the shock is thus

$$p_2 - p_1 = \frac{\dot{m}}{A}(V_1 - V_2) \quad (3.38)$$

Making use of the mass balance, this equation takes the form

$$p_1 + \rho_1 V_1^2 = p_2 + \rho_2 V_2^2 \quad (3.39)$$

Since the flow is adiabatic, the energy equation, if ideal gas behavior is assumed, may be written as

$$c_p T_1 + \frac{1}{2}V_1^2 = c_p T_2 + \frac{1}{2}V_2^2 \quad (3.40)$$

or as

$$T_{01} = T_{02} \quad (3.41)$$

From the definition of stagnation state, the expression

$$\frac{T_{01}}{T_1} = 1 + \frac{\gamma - 1}{2} M_1^2$$

is obtained, and a similar equation holds on the downstream side. Hence, their ratio yields

$$\frac{T_2}{T_1} = \frac{1 + \frac{\gamma - 1}{2} M_1^2}{1 + \frac{\gamma - 1}{2} M_2^2} \quad (3.42)$$

Making use of the ideal gas relation $p = \rho RT$ and the mass balance $\rho_1 V_1 = \rho_2 V_2$ in this equation gives

$$\frac{T_2}{T_1} = \frac{p_2 \rho_1}{p_1 \rho_2} = \frac{p_2 V_2}{p_1 V_1} \quad (3.43)$$

and, using $V = Mc$ to eliminate the velocities, leads to

$$\frac{T_2}{T_1} = \frac{p_2 M_2 c_2}{p_1 M_1 c_1} = \frac{p_2 M_2}{p_1 M_1} \sqrt{\frac{T_2}{T_1}}$$

from which

$$\frac{T_2}{T_1} = \left(\frac{p_2}{p_1}\right)^2 \left(\frac{M_2}{M_1}\right)^2 \quad (3.44)$$

Combining this with Eq. (3.42) gives

$$\frac{p_2}{p_1} = \frac{M_1}{M_2} \frac{\sqrt{1 + \frac{\gamma-1}{2} M_1^2}}{\sqrt{1 + \frac{\gamma-1}{2} M_2^2}} \quad (3.45)$$

For an ideal gas, $\rho_1 V_1^2 = \gamma p_1 M_1^2$ and $\rho_2 V_2^2 = \gamma p_2 M_2^2$. Substituting these into Eq. (3.39) gives

$$\frac{p_2}{p_1} = \frac{1 + \gamma M_1^2}{1 + \gamma M_2^2} \quad (3.46)$$

The velocity ratio across the shock is next related to the pressure ratio and Mach number ratio by equating Eq. (3.43) to Eq. (3.44). It gives

$$\frac{V_2}{V_1} = \frac{p_2}{p_1} \left(\frac{M_2}{M_1}\right)^2 \quad (3.47)$$

Equating next two expressions, Eqs. (3.45) and (3.46), for pressure gives

$$\frac{M_1 \sqrt{1 + \frac{\gamma-1}{2} M_1^2}}{1 + \gamma M_1^2} = \frac{M_2 \sqrt{1 + \frac{\gamma-1}{2} M_2^2}}{1 + \gamma M_2^2}$$

This is clearly satisfied if $M_1 = M_2$, but in this case, nothing interesting happens, and the flow moves through the control volume undisturbed. Squaring both sides yields a quadratic equation in M_2^2 . Solving it gives the result

$$M_2^2 = \frac{2 + (\gamma - 1)M_1^2}{2\gamma M_1^2 - (\gamma - 1)} \quad (3.48)$$

This equation relates the upstream and downstream Mach numbers across a shock, and the expression is plotted in Figure 3.12. It shows that upstream states have $M_1 > 1$, and those downstream have $M_2 < 1$. As will be shown in the following, only in this situation will entropy increase across the shock, as it must.

Pressure before and after the shock is obtained by substituting Eq. (3.48) into Eq. (3.46), giving the result

$$\frac{p_2}{p_1} = \frac{2\gamma}{\gamma + 1} M_1^2 - \frac{\gamma - 1}{\gamma + 1} \quad (3.49)$$

This shows that if $M_1 = 1$, there is no pressure jump. Defining the fractional increase in pressure as measure of the strength of the shock, the strength is defined as

$$\frac{p_2}{p_1} - 1 = \frac{2\gamma}{\gamma + 1} (M_1^2 - 1) \quad (3.50)$$

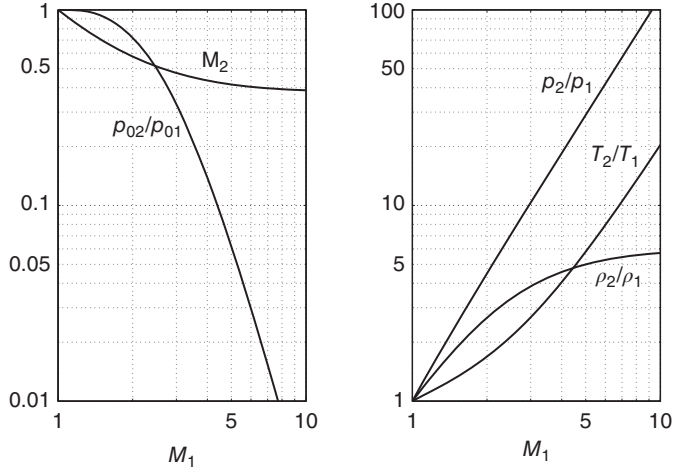


Figure 3.12 Normal shock relations for $\gamma = 1.4$.

Since across the shock, $\rho_1 V_1 = \rho_2 V_2$, the velocity ratio and inverse of density ratio are reduced to

$$\frac{V_1}{V_2} = \frac{\rho_2}{\rho_1} = \frac{(\gamma + 1)M_1^2}{2 + (\gamma - 1)M_1^2} \quad (3.51)$$

The temperature ratio across a shock could now be obtained by substituting the value of M_2^2 from Eq. (3.48) into Eq. (3.42). The result is

$$\frac{T_2}{T_1} = \frac{[2\gamma M_1^2 - (\gamma - 1)][2 + (\gamma - 1)M_1^2]}{(\gamma + 1)^2 M_1^2} \quad (3.52)$$

Usually, however, the pressure and density ratios are calculated first, and the temperature ratio is obtained from

$$\frac{T_2}{T_1} = \frac{p_2}{p_1} \frac{\rho_1}{\rho_2}$$

which is formed by using the ideal gas relation on both sides of the shock.

Since $T_{01} = T_{02}$, Eq. (3.11) shows that

$$\frac{p_{02}}{p_{01}} = \frac{A_1^*}{A_2^*} \quad (3.53)$$

This equation is useful for finding the area at which a shock is located when the upstream Mach number is known.

The ratio of stagnation pressures across a shock is obtained from

$$\frac{p_{02}}{p_{01}} = \frac{p_{02}}{p_2} \frac{p_2}{p_1} \frac{p_1}{p_{01}} \quad (3.54)$$

which takes the form

$$\frac{p_{02}}{p_{01}} = \left(\frac{(\gamma + 1)M_1^2}{2 + (\gamma - 1)M_1^2} \right)^{\gamma/\gamma-1} \left(\frac{\gamma + 1}{2\gamma M_1^2 - (\gamma - 1)} \right)^{1/(\gamma-1)} \quad (3.55)$$

This ratio and others are shown in Figure 3.12. The stagnation pressure ratio curve has zero for its slope at $M_1 = 1$, and the ratio decreases mildly when the Mach number increases to values only slightly greater than one. At $M_1 = 2$, it has decreased to 0.7209 for a gas with $\gamma = 1.4$. At this Mach number, the pressure ratio has increased to 4.5, and the temperature ratio is 3.11. They keep increasing as the Mach is increased. However, both the Mach number downstream of the shock and the density ratio reach asymptotic values as $M_1 \rightarrow \infty$. Their asymptotic values are $M_2 = \sqrt{(\gamma - 1)/2\gamma} = 0.3781$ and $\rho_2/\rho_1 = (\gamma + 1)/(\gamma - 1) = 6$.

■ EXAMPLE 3.8

Air flows isentropically in a diverging supersonic nozzle. Consider a section of this supersonic nozzle, with an inlet area A_i . The static pressure at the inlet is $p_i = 80$ kPa, the static temperature is $T_i = 250$ K, and the Mach number is $M_i = 1.2$. The exit area is 2.5 times the inlet area. What should the back pressure be for a shock to form at the location where the area is 1.5 times the inlet area?

Solution: The stagnation temperature and pressure are first calculated from

$$\frac{T_{0i}}{T_i} = 1 + \frac{\gamma - 1}{2} M_i^2 = 1 + 0.2 \cdot 1.2^2 = 1.288$$

$$\frac{p_{0i}}{p_i} = \left(\frac{T_{0i}}{T_i} \right)^{\gamma/(\gamma-1)} = 1.288^{3.5} = 2.425$$

so that $T_{0i} = 322$ K and $p_{0i} = 194$ kPa.

Since the flow is supersonic and the conditions at the inlet are known, imagine the extension of the nozzle upstream to a location where the flow is sonic. At that location, the area can be calculated from

$$\frac{A_i}{A_1^*} = \frac{1}{M_i} \left(\frac{2}{\gamma + 1} + \frac{\gamma - 1}{\gamma + 1} M_i^2 \right)^{(\gamma+1)/2(\gamma-1)}$$

which gives

$$\frac{A_i}{A_1^*} = \frac{1}{1.2} \left(\frac{2}{2.4} + \frac{0.4}{2.4} 1.2^2 \right)^3 = 1.0304$$

One may assign a convenient value for the inlet area, say $A_i = 1$ cm². Then, $A_1^* = 0.970$ cm². With this area known, the Mach number ahead of the shock can be determined by solving the equation

$$\frac{A_1}{A_1^*} = \frac{1}{M_1} \left(\frac{2}{\gamma + 1} + \frac{\gamma - 1}{\gamma + 1} M_1^2 \right)^{(\gamma+1)/2(\gamma-1)}$$

The left side is known since $A_1 = 1.5 \cdot A_i = 1.5$ cm. The solution is best done with MATLAB or GNU/OCTAVE, and the way it is done was demonstrated in the discussion

after Example 3.4. This calculation gives $M_1 = 1.892$. With the Mach number ahead of the shock known, the stagnation pressure ratio is

$$\begin{aligned} \frac{p_{02}}{p_{01}} &= \left(\frac{(\gamma + 1)M_1^2}{2 + (\gamma - 1)M_1^2} \right)^{\gamma/(\gamma-1)} \left(\frac{\gamma + 1}{2\gamma M_1^2 - (\gamma - 1)} \right)^{1/(\gamma-1)} \\ &= \left(\frac{2.4 \cdot 1.892^2}{2 + 0.4 \cdot 1.892^2} \right)^{3.5} \left(\frac{2.4}{2 \cdot 1.4 \cdot 1.892^2 - 0.4} \right)^{2.5} = 0.771 \end{aligned}$$

so that $p_{02} = 149.56$ kPa.

From Eq.(3.53), the area at the hypothetical sonic condition downstream of the shock can be calculated to be

$$A_2^* = A_1^* \frac{p_{01}}{p_{02}} = \frac{0.970}{0.771} = 1.259$$

The exit Mach number, M_e , can now be determined from

$$\frac{A_e}{A_2^*} = \frac{1}{M_e} \left(\frac{2}{\gamma + 1} + \frac{\gamma - 1}{\gamma + 1} M_e^2 \right)^{(\gamma+1)/2(\gamma-1)}$$

Since the exit area is 2.5 times the inlet value, and inlet area was chosen to be 1 cm^2 , the left-hand side of this equation is $A_e/A_2^* = 2.5/1.259 = 1.986$. The `fzero` function in MATLAB or GNU/OCTAVE now gives $M_e = 0.308$. The pressure at the exit is therefore

$$p_e = p_{02} \left(1 + \frac{\gamma - 1}{2} M_e^2 \right)^{\gamma/(\gamma-1)} = 149.56(1 + 0.2 \cdot 0.308^2)^{3.5} = 140.0 \text{ kPa}$$

■

3.5.1 Rankine–Hugoniot relations

A relationship between the pressure and density ratio across the shock can be obtained from the momentum equation

$$p_2 - p_1 = \rho_1 V_1^2 - \rho_2 V_2^2 = \rho_1 V_1^2 \left(1 - \frac{\rho_1}{\rho_2} \right),$$

which when solved for upstream velocity, gives

$$V_1 = \left[\frac{(p_2 - p_1)\rho_2}{(\rho_2 - \rho_1)\rho_1} \right]^{1/2} \quad (3.56)$$

A similar expression is obtained downstream of the shock:

$$V_2 = \left[\frac{(p_2 - p_1)\rho_1}{(\rho_2 - \rho_1)\rho_2} \right]^{1/2}$$

The energy equation across the shock is

$$h_1 + \frac{1}{2}V_1^2 = h_2 + \frac{1}{2}V_2^2$$

Since

$$h_1 - h_2 = c_p(T_1 - T_2) = \frac{\gamma}{\gamma - 1} \left(\frac{p_1}{\rho_1} - \frac{p_2}{\rho_2} \right), \quad (3.57)$$

the energy equation can be written as

$$\frac{\gamma}{\gamma - 1} \frac{p_1}{\rho_1} + \frac{p_2 - p_1}{2(\rho_2 - \rho_1)} \frac{\rho_2}{\rho_1} = \frac{\gamma}{\gamma - 1} \frac{p_2}{\rho_2} + \frac{p_2 - p_1}{2(\rho_2 - \rho_1)} \frac{\rho_1}{\rho_2}$$

from which

$$\frac{p_2}{p_1} = \frac{\frac{\gamma + 1}{\gamma - 1} \frac{\rho_2}{\rho_1} - 1}{\frac{\gamma + 1}{\gamma - 1} - \frac{\rho_2}{\rho_1}} \quad (3.58)$$

Solving this for the density ratio gives

$$\frac{\rho_2}{\rho_1} = \frac{\frac{\gamma + 1}{\gamma - 1} \frac{p_2}{p_1} + 1}{\frac{\gamma + 1}{\gamma - 1} + \frac{p_2}{p_1}} \quad (3.59)$$

Equations (3.58) and (3.59) are known as Rankine–Hugoniot relations [46, 74].

The strength of the shock is obtained from the first of the Rankine–Hugoniot equations. It is

$$\frac{p_2}{p_1} - 1 = \frac{\frac{2\gamma}{\gamma - 1} \left(\frac{\rho_2}{\rho_1} - 1 \right)}{\frac{2}{\gamma - 1} - \left(\frac{\rho_2}{\rho_1} - 1 \right)} \quad (3.60)$$

and the density ratio in terms of the strength of the shock is

$$\frac{\rho_2}{\rho_1} = \frac{1 + \frac{\gamma + 1}{2\gamma} \left(\frac{p_2}{p_1} - 1 \right)}{1 + \frac{\gamma - 1}{2\gamma} \left(\frac{p_2}{p_1} - 1 \right)} \quad (3.61)$$

Entropy change across a shock is given by integrating

$$Tds = du + p dv$$

across the shock. This gives

$$s_2 - s_1 = c_v \ln \frac{T_2}{T_1} + R \ln \frac{v_2}{v_1} = c_v \ln \left(\frac{T_2}{T_1} \right) \left(\frac{v_2}{v_1} \right)^{\gamma-1}$$

The temperature ratio is

$$\frac{T_2}{T_1} = \frac{p_2}{p_1} \frac{v_2}{v_1} = \frac{p_2}{p_1} \frac{\rho_1}{\rho_2}$$

so that the entropy change can also be written as

$$s_2 - s_1 = c_v \ln \left(\frac{p_2}{p_1} \right) \left(\frac{\rho_1}{\rho_2} \right)^\gamma$$

Substituting the expression for ρ_2/ρ_1 from Eq. (3.61) to this gives

$$\frac{s_2 - s_1}{c_v} = \ln \left(\frac{p_2}{p_1} \right) - \gamma \ln \left[1 + \frac{\gamma + 1}{2\gamma} \left(\frac{p_2}{p_1} - 1 \right) \right] + \gamma \ln \left[1 + \frac{\gamma - 1}{2\gamma} \left(\frac{p_2}{p_1} - 1 \right) \right]$$

For weak shocks, p_2/p_1 is just slightly greater than one. For this reason, let $p_2/p_1 = 1 + \varepsilon$, and on substituting this into the previous equation and expanding in Taylor series for small value of ε leads to²

$$\frac{s_2 - s_1}{c_v} = \frac{\gamma^2 - 1}{12\gamma^2} \left(\frac{p_2}{p_1} - 1 \right)^3 - \frac{\gamma^2 - 1}{8\gamma^2} \left(\frac{p_2}{p_1} - 1 \right)^4 + \dots$$

or after using $c_v = R/(\gamma - 1)$

$$\frac{s_2 - s_1}{R} = \frac{\gamma + 1}{12\gamma^2} \left(\frac{p_2}{p_1} - 1 \right)^3 - \frac{\gamma + 1}{8\gamma^2} \left(\frac{p_2}{p_1} - 1 \right)^4 + \dots$$

Using Eq. (3.50) to express the shock strength in terms of Mach number gives

$$\frac{s_2 - s_1}{R} = \frac{2}{3} \frac{\gamma}{(\gamma + 1)^2} (M_1^2 - 1)^3 - \frac{2\gamma^2}{(\gamma + 1)^3} (M_1^2 - 1)^4 + \dots \quad (3.62)$$

This shows that were $M_1 < 1$, entropy would decrease across the shock. Thus shocks are possible only for $M_1 > 1$. Furthermore, entropy increases only slightly across weak shocks.

The stagnation pressure change across weak shocks can also be developed by writing $M_1^2 = 1 + \varepsilon$ in

$$\frac{p_{02}}{p_{01}} = \left(\frac{(\gamma + 1)M_1^2}{2 + (\gamma - 1)M_1^2} \right)^{\gamma/\gamma-1} \left(\frac{\gamma + 1}{2\gamma M_1^2 - (\gamma - 1)} \right)^{1/(\gamma-1)}$$

and expanding the resulting expression for small values of ε . The result, when written in terms of $M_1^2 - 1$, is

$$\frac{p_{02}}{p_{01}} = 1 - \frac{2}{3} \frac{\gamma}{(\gamma + 1)^2} (M_1^2 - 1)^3 + \frac{2\gamma^2}{(\gamma + 1)^3} (M_1^2 - 1)^4 + \dots \quad (3.63)$$

This is an important result as it shows that flows through weak shocks experience only a small loss in stagnation pressure. In fact, the first two terms of Eq. (3.63) may be shown to be accurate to 1% for $M_1 < 1.2$, and for $M_1 = 1.2$, it gives $p_{02}/p_{01} = 0.986$ or a stagnation pressure drop of less than 2%. The significance of this result for turbomachinery design is that in transonic flows with shocks, stagnation pressure losses are relatively small.

²For small values of ε series expansion yields $\ln(1 + \varepsilon) = \varepsilon - \varepsilon^2/2 + \varepsilon^3/3 - \varepsilon^4/4 + \dots$.

3.6 MOVING SHOCKS

In situations in which a shock moves through still air, it is of interest to calculate the velocity after the shock and the changes in the stagnation properties. By choosing a reference frame that moves with the shock, for the observer in this reference frame, the shock appears stationary, and the situation is reduced to the one already considered. The static properties are the same in the fixed and moving frames. But the stagnation properties are not. The absolute velocity \mathbf{V} is the sum of the velocity of the frame \mathbf{U} and the relative velocity \mathbf{W}

$$\mathbf{V} = \mathbf{U} + \mathbf{W}$$

How this transformation is used to analyze moving shocks is illustrated by an example.

■ EXAMPLE 3.9

A normal shock, as shown in Figure 3.13, is moving at a speed 800 m/s to the left through still air at atmospheric conditions with temperature 300 K and pressure 100 kPa. Find the air velocity and show by calculations that the entropy change both in fixed and in the moving coordinates is the same.

Solution: In Figure 3.13a is shown the shock that moves with velocity $-U$, since the x -axis points to the right. The velocities before and after the shock are $V_1 = 0$ and V_2 in the stationary frame. The assumed direction of the unknown V_2 is in the positive x -direction, even though it is expected to be moving to the left. Hence, the analysis should give it a negative value.

The relative velocity approaching the shock is $W_1 = V_1 - (-U) = U$, and after the shock, it is $W_2 = V_2 - (-U) = V_2 + U$. As mentioned, the static properties are the same in stationary and moving coordinates, but stagnation properties are different. Hence, $T_1 = 300$ K and $p_1 = 100$ kPa, and since the air is stagnant $T_{01} = 300$ K and $p_{01} = 100$ kPa. The speed of sound and the relative Mach number before the shock are

$$c_1 = \sqrt{\gamma RT_1} = \sqrt{1.4 \cdot 287 \cdot 300} = 347.2 \text{ m/s} \quad M_{1R} = \frac{W_1}{c_1} = \frac{800}{347.2} = 2.304$$

The relative Mach number after the shock is obtained from the standard formula

$$M_{2R} = \sqrt{\frac{2 + (\gamma - 1)M_{1R}^2}{2\gamma M_{1R}^2 - (\gamma - 1)}} = \sqrt{\frac{2 + 0.4 \cdot 2.304^2}{2 \cdot 1.4 \cdot 2.304^2 - 0.4}} = 0.534$$

The density ratio can be determined from

$$\frac{\rho_2}{\rho_1} = \frac{(\gamma + 1)M_{1R}^2}{2 + (\gamma - 1)M_{1R}^2} = \frac{2.4 \cdot 0.534^2}{2 + 0.4 \cdot 0.534^2} = 3.090$$

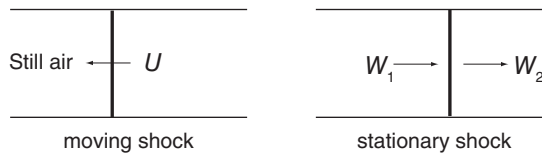


Figure 3.13 Shock moving to still air.

and the pressure ratio from

$$\frac{p_2}{p_1} = \frac{2\gamma}{\gamma+1} M_{1R}^2 - \frac{\gamma-1}{\gamma+1} = \frac{2 \cdot 1.4 \cdot 2.304^2 - 0.4}{2.4} = 6.0277$$

The value of pressure after the shock is $p_2 = 6.0277 \cdot 100 = 602.77$ kPa.

The temperature T_2 is then

$$T_2 = T_1 \frac{p_2}{p_1} \frac{\rho_1}{\rho_2} = 300 \frac{6.0277}{3.090} = 585.2 \text{ K}$$

The relative stagnation temperature is

$$T_{01R} = T_1 \left(1 + \frac{\gamma-1}{2} M_{1R}^2 \right) = 300(1 + 0.2 \cdot 2.304^2) = 618.57 \text{ K},$$

and the relative stagnation pressure is

$$p_{01R} = p_1 \left(\frac{T_{01R}}{T_1} \right)^{\gamma/(\gamma-1)} = 100 \cdot \left(\frac{618.57}{300} \right)^{3.5} = 1258.7 \text{ kPa}$$

Since $T_{01R} = T_{02R}$, the relative stagnation pressure after the shock is

$$p_{02R} = p_2 \left(\frac{T_{02R}}{T_2} \right)^{\gamma/(\gamma-1)} = 602.8 \cdot \left(\frac{618.57}{585.2} \right)^{3.5} = 731.9 \text{ kPa}$$

The relative velocity after the shock is

$$W_2 = c_2 M_{2R} = \sqrt{\gamma R T_2} M_{2R} = \sqrt{1.4 \cdot 287 \cdot 585.2} \cdot 0.534 = 258.9 \text{ m/s}$$

hence, the absolute velocity after the shock is

$$V_2 = W_2 + (-U) = 258.9 - 800 = -541.1 \text{ m/s}$$

and it is moving to the left in the fixed frame, as expected. Mach number after the shock is $M_2 = |V_2|/\sqrt{\gamma R T_2} = 1.1159$.

The stagnation temperature is

$$T_{02} = T_2 \left(1 + \frac{\gamma-1}{2} M_2^2 \right) = 585.2(1 + 0.2 \cdot 1.1159^2) = 730.9 \text{ K},$$

and the stagnation pressure is

$$p_{02} = p_2 \left(\frac{T_{02}}{T_2} \right)^{\gamma/(\gamma-1)} = 602.8 \left(\frac{730.9}{585.2} \right)^{3.5} = 1312.7 \text{ kPa}$$

The entropy change can be calculated in two ways. In the moving coordinates, since $T_{01R} = T_{02R}$, the entropy change is simply

$$s_2 - s_1 = -R \ln \left(\frac{p_{02R}}{p_{01R}} \right) = -287 \ln \left(\frac{731.86}{1258.72} \right) = 155.6 \text{ J/(kg K)}$$

and in fixed frame, it is calculated from

$$s_2 - s_1 = R \ln \left[\left(\frac{T_{02}}{T_{01}} \right)^{\frac{\gamma}{\gamma-1}} \frac{p_{01}}{p_{02}} \right] = 287 \ln \left[\left(\frac{730.9}{300} \right)^{3.5} \frac{100}{1312.7} \right] = 155.6 \text{ kJ}/(\text{kg K})$$

Since entropy is a static property, its change is independent of the frame. ■

3.7 OBLIQUE SHOCKS AND EXPANSION FANS

Oblique shocks occur in supersonic flows more commonly than normal shocks. They appear when the boundary surface has a sharp concave corner. If the corner is convex, a rarefaction wave is formed. This, so called *expansion fan*, is centered at the corner. Both oblique shocks and expansion fans appear in transonic compressors in which the desire to achieve a high flow rate in a small machine leads to velocity being higher than sound speed, at least in part of the flow. The aim of this section is to develop the theoretical background for understanding such flows, in order to carry out calculations of flow fields in simple settings and to use the knowledge so gained to interpret those theoretical studies that are carried out today mainly by CFD software.

3.7.1 Mach waves

Consider a source of small disturbances that moves with supersonic speed to the left, as shown in Figure 3.14. The source produces spherical acoustic waves that propagate outward with speed c . Next, consider five instances of time, the present time and four preceding instances of time, separated by equal time increments. At time $-4\Delta t$, the source was at location $4V\Delta t$ to the right of the present location, and the wavefront which formed at time $-4\Delta t$ has moved a distance $4c\Delta t$ from the source. Similar reasoning applies to disturbances formed at $-3\Delta t$, $-2\Delta t$, and $-\Delta t$. The spherical wavefronts generated at these times are shown in the figure. Examination of the figure reveals that a *region of influence* of the disturbances is inside a cone with cone angle μ given by

$$\sin \mu = \frac{c}{V} = \frac{1}{M} \quad (3.64)$$

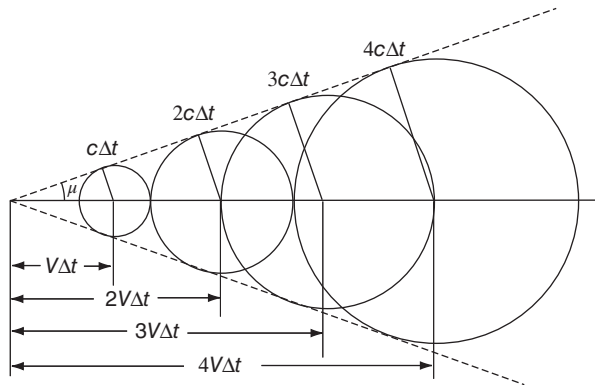


Figure 3.14 Illustration of the formation of Mach cone.

If a fluid moves to the right at speed V and meets a body at rest, then, the acoustic signal from the body is again a spherical wave. It travels upstream with the absolute velocity $c - V$ and downstream with velocity $c + V$. In supersonic flow, $c - V$ is negative, and the disturbance cannot influence the flow outside a cone with cone angle μ given by Eq. (3.64). This is called a *Mach cone*.

In a two-dimensional flow in which the source of small disturbances is a line perpendicular to the plane of the paper, the cone becomes a wedge. The region inside the cone, or the wedge, is called a *zone of action*, that outside is a *zone of silence*. The dividing surface between these zones is called a *Mach wave* or *Mach line*. When viewed in the downstream direction, the upper Mach wave in Figure 3.14 is said to be *left-running* and the lower one *right-running* wave, or line.

3.7.2 Oblique shocks

The normal shock introduced earlier can be considered to be a special case of a compression shock for which the shock front is *normal* to the approaching flow. For *oblique shocks*, as their name implies, the shock front forms an angle with the approaching flow. Again, when viewed in the downstream direction, oblique shocks form two families, one of which is left-running and the other right-running. Oblique shocks develop, when, for example, a supersonic flow along a straight wall meets an interior (concave) corner. They may also occur in flows over wedges for which the symmetry plane could clearly be replaced by a wall in an inviscid flow. When a supersonic flow encounters an exterior (convex) corner, an *expansion fan*, centered at the corner, is formed. Both oblique shocks and expansion fans were mentioned briefly when the *underexpanded* and *overexpanded* flows at the exit of a supersonic nozzle were discussed.

Consider the flow along the wall shown in Figure 3.15, with a concave (interior) corner of angle θ . The straight oblique shock that develops in this flow emanates from this corner and is inclined at angle β . After the shock, the flow direction has changed by θ , as the flow is forced to move in the direction of the downstream wall. To analyze what happens to the flow as it crosses the shock, the incoming velocity vector is resolved into one component normal to the shock and the other aligned with the shock front.

Mass balance for a control volume surrounding the shock gives

$$\rho_1 V_{n1} = \rho_2 V_{n2} \quad (3.65)$$

The momentum equation is resolved to a component normal to the shock and one tangential to it. The tangential component gives

$$\rho_1 V_{n1} V_{t1} = \rho_2 V_{n2} V_{t2}, \quad (3.66)$$

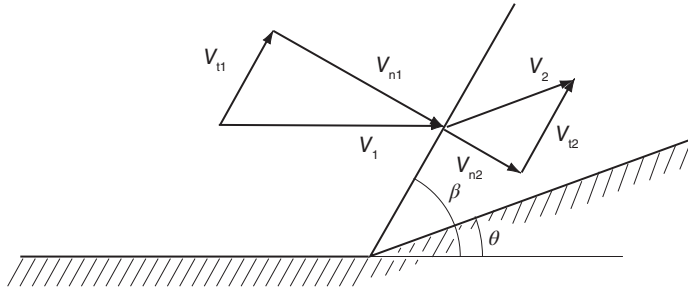


Figure 3.15 An oblique shock.

and making use of the continuity equation gives $V_{t1} = V_{t2}$. That is, the tangential component does not change in magnitude.

The normal component of the momentum equation gives

$$p_1 - p_2 = \rho_2 V_{n2}^2 - \rho_1 V_{n1}^2 \quad (3.67)$$

The energy equation takes the form

$$h_1 + \frac{1}{2}(V_{n1}^2 + V_{t1}^2) = h_2 + \frac{1}{2}(V_{n2}^2 + V_{t2}^2) \quad (3.68)$$

and after canceling, since $V_{t1} = V_{t2}$, it reduces to

$$h_1 + \frac{1}{2}V_{n1}^2 = h_2 + \frac{1}{2}V_{n2}^2 \quad (3.69)$$

These normal component equations are identical to the normal shock equations. Hence, one may conclude that oblique shocks may occur in the flow when the upstream Mach number based on the normal component of the velocity is larger than one. The next example helps fix these ideas to mind.

■ EXAMPLE 3.10

Air with static temperature $T_1 = 280$ K, static pressure $p_1 = 35$ kPa and $M_1 = 2$ approaches a corner of magnitude θ on a wall. The angle of the oblique shock is observed to be $\beta = 40^\circ$. Find the air speed downstream of the shock and the angle θ .

Solution: The velocity upstream is

$$V_1 = M_1 \sqrt{\gamma R T_1} = 2 \sqrt{1.4 \cdot 287 \cdot 280} = 670.8 \text{ m/s}$$

The stagnation temperature is obtained from

$$T_0 = T_1 \left(1 + \frac{\gamma - 1}{2} M_1^2 \right) = 280(1 + 0.2 \cdot 2^2) = 504 \text{ K}$$

The normal component of velocity is $V_{n1} = V_1 \sin \beta = 670.8 \sin(40^\circ) = 431.2$ m/s, and Mach number based on this velocity is $M_{n1} = M_1 \sin \beta = 2 \sin(40^\circ) = 1.286$. The pressure ratio across the shock is therefore

$$\frac{p_2}{p_1} = \frac{2\gamma M_{n1}^2 - (\gamma - 1)}{\gamma + 1} = \frac{2.8 \cdot 1.286^2 - 0.4}{2.4} = 1.762,$$

and the temperature ratio is

$$\begin{aligned} \frac{T_2}{T_1} &= \frac{[2\gamma M_{n1}^2 - (\gamma - 1)][2 + (\gamma - 1)M_{n1}^2]}{(\gamma + 1)^2 M_{n1}^2} \\ &= \frac{(2.8 \cdot 1.286^2 - 0.4)(2 + 0.4 \cdot 1.286^2)}{(2.4 \cdot 1.286)^2} = 1.182 \end{aligned}$$

The Mach number after the shock is

$$M_2 = \sqrt{\left(\frac{2}{\gamma - 1}\right) \left(\frac{T_0}{T_2} - 1\right)} = \sqrt{\frac{2}{0.4} \left(\frac{504}{331} - 1\right)} = 1.617$$

The normal component of M_2 is

$$M_{n2} = \sqrt{\frac{2 + (\gamma - 1)M_{n1}^2}{2\gamma M_{n1}^2 - (\gamma - 1)}} = \sqrt{\frac{2 + 0.4 \cdot 1.286^2}{2.8 \cdot 1.286^2 - 0.4}} = 0.793$$

From Figure 3.15, it is seen that

$$\sin(\beta - \theta) = \frac{V_{n2}}{V_2} = \frac{M_{n2}}{M_2} = \frac{0.793}{1.617} = 0.4906$$

Hence, $\beta - \theta = \sin^{-1}(0.4906) = 29.4^\circ$ and $\theta = 40 - 29.4 = 10.6^\circ$. ■

The foregoing example demonstrates that for given Mach number and shock angle β , the value of the flow angle θ can be determined quite directly. It is not equally straightforward to determine the shock angle if the wall angle and Mach number are specified, or for given wall and shock angles, the Mach number is sought. A general equation is developed next that may be used in these situations.

Since the tangential component of velocity does not change across the shock

$$V_1 \cos \beta = V_2 \cos(\beta - \theta) \quad (3.70)$$

The mass balance gives the further relation

$$\rho_1 V_1 \sin \beta = \rho_2 V_2 \sin(\beta - \theta) \quad (3.71)$$

From these two equations, the density ratio is as follows

$$\frac{\rho_2}{\rho_1} = \frac{\tan \beta}{\tan(\beta - \theta)} \quad (3.72)$$

The density ratio can also be formed by using the ideal gas relations and the pressure and temperature ratios given by

$$\frac{p_2}{p_1} = \frac{2\gamma M_{n1}^2 - (\gamma - 1)}{\gamma + 1} \quad (3.73)$$

and

$$\frac{T_2}{T_1} = \frac{[2\gamma M_{n1}^2 - (\gamma - 1)][2 + (\gamma - 1)M_{n1}^2]}{(\gamma + 1)^2 M_{n1}^2}$$

These give

$$\frac{\rho_2}{\rho_1} = \frac{(\gamma + 1)M_{n1}^2}{2 + (\gamma - 1)M_{n1}^2} = \frac{(\gamma + 1)M_1^2 \sin^2 \beta}{2 + (\gamma - 1)M_1^2 \sin^2 \beta} \quad (3.74)$$

Dropping the subscript from the upstream Mach number and equating the density ratios in Eqs. (3.72) and (3.74), the following equation is obtained

$$\frac{\tan \beta}{\tan(\beta - \theta)} = \frac{(\gamma + 1)M^2 \sin^2 \beta}{2 + (\gamma - 1)M^2 \sin^2 \beta} \quad (3.75)$$

or after substituting for $\tan(\beta - \theta)$, the trigonometric identity

$$\tan(\beta - \theta) = \frac{\tan \beta - \tan \theta}{1 + \tan \beta \tan \theta}, \quad (3.76)$$

and solving the equation so obtained for $\tan \theta$ gives

$$\tan \theta = \frac{2(M^2 \sin^2 \beta - 1) \tan \beta}{(\gamma + 1)M^2 \sin^2 \beta + [2 + (\gamma - 1)M^2 \sin^2 \beta] \tan^2 \beta} \quad (3.77)$$

Dividing the numerator and denominator on the RHS by $\tan^2 \beta$ and simplifying gives

$$\tan \theta = 2 \cot \beta \frac{M^2 \sin^2 \beta - 1}{(\gamma + 1)M^2 \cos^2 \beta + 2 + (\gamma - 1)M^2 \sin^2 \beta}$$

After using the trigonometric identity $\cos^2 \beta = 1 - \sin^2 \beta$ and simplifying, this can be written as

$$\tan \theta = 2 \cot \beta \frac{M^2 \sin^2 \beta - 1}{M^2(\gamma + 1 - 2 \sin^2 \beta) + 2} \quad (3.78)$$

or as

$$\tan \theta = 2 \cot \beta \frac{M^2 \sin^2 \beta - 1}{M^2(\gamma + \cos 2\beta) + 2} \quad (3.79)$$

For a given γ , the value of θ can be found from this equation for various values of M and β . The functional relation between these parameters is shown graphically for $\gamma = 1.4$ in Figure 3.16. The separate graphs are labeled by the value of the corresponding Mach number, with a line extending to the maximum value of θ for each value of M . Since the graphs of M are concave down, for a given M and θ , there are two possible values of β . The solution for the larger value of β is called a *strong shock* and for the smaller one a *weak shock*. The Mach number after a strong shock is always less than one, and for a weak shock, it is generally less than one. Strong *attached* shocks are not observed in nature. Thus, this solution can be ignored for now.

Each graph of constant M shows that there is a maximum value of θ for which these two solutions exit. For values of $\theta \geq \theta_{\max}$, there is no solution. It is left as an exercise to show that this occurs at the value of β given by

$$\sin^2 \beta = \frac{1}{\gamma M^2} \left[\frac{(\gamma + 1)M^2}{4} - 1 + \sqrt{(\gamma + 1) \left[\frac{(\gamma + 1)M^4}{16} + \frac{(\gamma - 1)M^2}{2} + 1 \right]} \right] \quad (3.80)$$

The locus of points for the maxima for various values of M is given by the dashed line on the right.

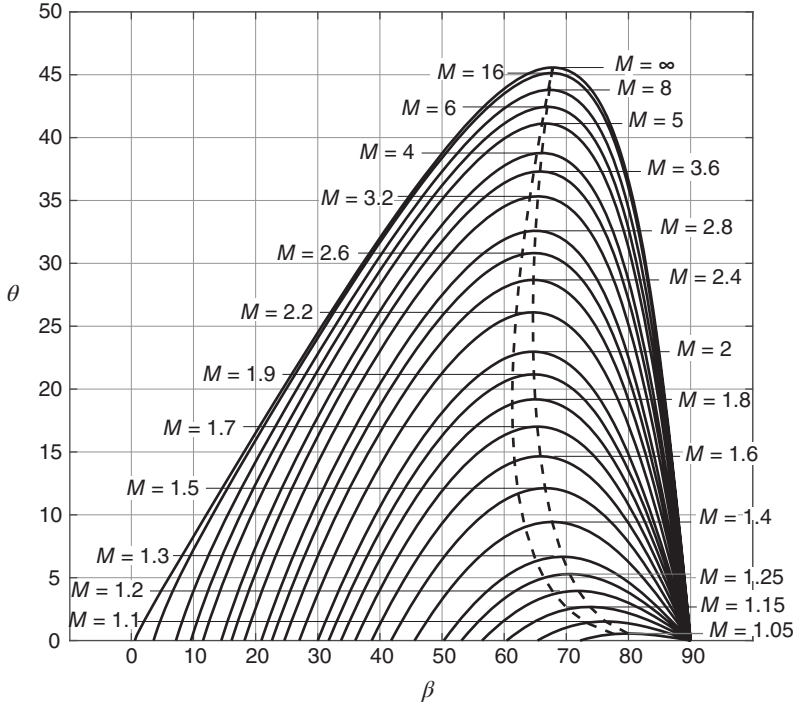


Figure 3.16 Oblique shock angles.

The value of θ_{\max} increases as the Mach number of the incoming flow increases, and in the limit as $M \rightarrow \infty$, the value of θ_{\max} takes place at $\sin \beta = \sqrt{(\gamma + 1)/2\gamma}$. Its value is given by

$$\tan \theta_{\max} = \frac{1}{\sqrt{\gamma^2 - 1}},$$

and for $\gamma = 1.4$, it is $\theta_{\max} = 45.58^\circ$.

The dashed line on the left in Figure 3.16 is a locus of points for which the $M_2 = 1$ after the shock. It is given by

$$\sin^2 \beta = \frac{(\gamma + 1)M^2 + (\gamma - 3) + \sqrt{[(\gamma + 1)M^2 + (\gamma - 3)]^2 + 16\gamma}}{4\gamma M^2} \quad (3.81)$$

For values of β larger than what are obtained from this equation, the flow after the shock is subsonic, and below this value, it is supersonic. Hence, the flow after an *attached oblique shock* is generally supersonic.

The pressure rise across an oblique shock is given by Eq. (3.73), which can be written as

$$\frac{p_2}{p_1} = \frac{2\gamma M^2 \sin^2 \beta - (\gamma - 1)}{\gamma + 1} \quad (3.82)$$

Solving this for $\sin \beta$ gives

$$\sin \beta = \sqrt{\frac{\gamma - 1}{2\gamma M^2} + \frac{\gamma + 1}{2\gamma M^2} \frac{p_2}{p_1}}$$

The expression for $\cos \beta$ is

$$\cos \beta = \sqrt{\frac{2\gamma M^2 - (\gamma - 1)}{2\gamma M^2} - \frac{\gamma + 1}{2\gamma M^2} \frac{p_2}{p_1}}$$

Hence,

$$\cot \beta = \left[\frac{\frac{2\gamma(M^2 - 1)}{\gamma + 1} - \left(\frac{p_2}{p_1} - 1\right)}{\frac{p_2}{p_1} + \frac{\gamma - 1}{\gamma + 1}} \right]^{1/2} \quad (3.83)$$

In addition, since $\cos 2\beta = \cos^2 \beta - \sin^2 \beta$,

$$\cos 2\beta = \frac{\gamma M^2 - (\gamma - 1)}{\gamma M^2} - \frac{\gamma + 1}{\gamma M^2} \frac{p_2}{p_1} \quad (3.84)$$

Substituting Eqs. (3.83) and (3.84) into Eq. (3.79) gives

$$\tan \theta = \frac{\frac{p_2}{p_1} - 1}{\gamma M^2 - \left(\frac{p_1}{p_1} - 1\right)} \left[\frac{\frac{2\gamma}{\gamma + 1}(M^2 - 1) - \left(\frac{p_2}{p_1} - 1\right)}{\frac{p_2}{p_1} + \frac{\gamma - 1}{\gamma + 1}} \right]^{1/2} \quad (3.85)$$

Squaring and multiplying out the terms shows that this is a third-order polynomial equation for the pressure ratio. Thus, it has three roots. Its graph is shown in Figure 3.17. The strong shock solution, as its name implies, corresponds to the largest pressure ratio. The solution with a pressure ratio less than unity is not a physically realizable. The weak solution is the one sought for attached oblique shocks. The graph also shows that for a given Mach number, no straight shock exists if the value of θ is too large. That is the dashed vertical line may not cross the graph at all except at the location for which the pressure ratio is less than unity and which does not represent a valid solution.

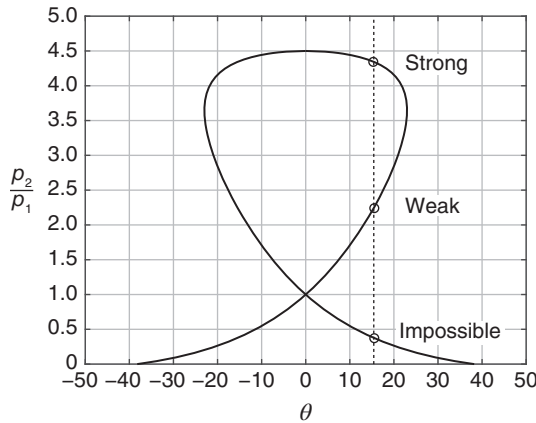


Figure 3.17 Pressure ratio for an oblique shock.

3.7.3 Supersonic flow over a rounded concave corner

Consider a supersonic flow along a wall in which there is a rounded interior (concave) corner, such as shown in Figure 3.18b. Next, as shown in Figure 3.18a, approximate the boundary curve by a set of short line segments with lengths chosen such that the angle between successive ones is equal to ϕ . Since the line segments are short, the angle ϕ is small, and weak oblique shocks emanate from each break in the segmented curve. The task now is to develop an approximate formula for the pressure ratio and entropy increase across the weak oblique shocks.

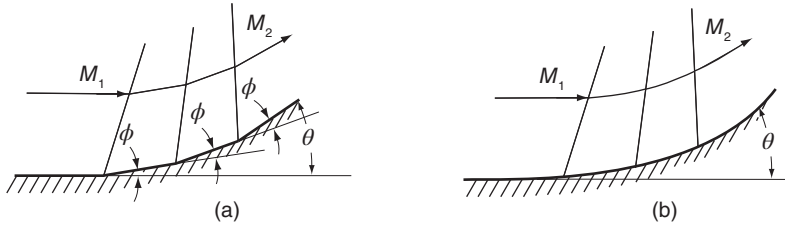


Figure 3.18 Compression shocks in a segmented and a smooth corner.

Equation (3.75) may be rearranged as

$$\frac{1}{M^2 \sin^2 \beta} = \frac{\gamma + 1}{2} \frac{\tan(\beta - \phi)}{\tan \beta} - \frac{\gamma - 1}{2}$$

and using again Eq. (3.76), this becomes

$$\frac{1}{M^2 \sin^2 \beta} = \frac{(\gamma + 1)(\tan \beta - \tan \phi) - (\gamma - 1)(\tan \beta + \tan^2 \beta) \tan \phi}{2 \tan \beta (1 + \tan \beta \tan \phi)}$$

Inverting this and simplifying yields then

$$M^2 \sin^2 \beta = \frac{2 \tan \beta (1 + \tan \beta \tan \phi)}{2 \tan \beta - [(\gamma - 1) \tan^2 \beta + (\gamma + 1)] \tan \phi}$$

Subtracting unity from both sides and simplifying gives finally

$$M^2 \sin^2 \beta - 1 = \frac{(\gamma + 1)(1 + \tan^2 \beta) \tan \phi}{2 \tan \beta - [(\gamma - 1) \tan^2 \beta + (\gamma + 1)] \tan \phi} \quad (3.86)$$

For small values of ϕ , the second term in the denominator can be dropped, and making use of the approximation $\tan \phi \approx \phi$ in the numerator gives

$$M^2 \sin^2 \beta - 1 = \frac{(\gamma + 1)(\tan^2 \beta + 1) \phi}{2 \tan \beta} = \frac{\gamma + 1}{2} \frac{\phi}{\sin \beta \cos \beta} \quad (3.87)$$

The general expression for the pressure ratio across an oblique shock is

$$\frac{p_2}{p_1} = \frac{2\gamma M^2 \sin^2 \beta - (\gamma - 1)}{\gamma + 1}$$

Subtracting unity from both sides, the strength of the weak shock emanating from the j th corner is obtained, after Eq. (3.87) is used. It is

$$\frac{p_{j+1}}{p_j} - 1 = \frac{\gamma\phi}{\sin\beta \cos\beta}$$

For weak waves, the shock angle β is the Mach angle μ . Since

$$\sin\mu = \frac{1}{M} \quad \cos\mu = \frac{\sqrt{M^2 - 1}}{M},$$

and the final expression for the pressure ratio becomes

$$\frac{p_{j+1}}{p_j} - 1 = \frac{\gamma M^2}{\sqrt{M^2 - 1}} \phi \quad (3.88)$$

The previously derived Eq. (3.62) gives the entropy change across a weak shock. For the j th line segment, the entropy increase becomes

$$\frac{s_{j+1} - s_j}{R} = \frac{\gamma + 1}{12\gamma^2} \left(\frac{p_{j+1}}{p_j} - 1 \right)^3 \quad \text{or} \quad \frac{s_{j+1} - s_j}{R} = \frac{\gamma(\gamma + 1)}{12} \frac{M^6}{(M^2 - 1)^{3/2}} \phi^3$$

As shown, for example by Rotty [78], summing up the contributions from the n line segments gives, with $\theta = n\phi$, the overall pressure ratio across the set of weak waves. It leads to

$$\frac{s_2 - s_1}{R} = \frac{\gamma(\gamma + 1)}{12} \frac{M^6}{(M^2 - 1)^{3/2}} n\phi^3 = \frac{\gamma(\gamma + 1)}{12} \frac{M^6}{(M^2 - 1)^{3/2}} \frac{\theta^3}{n^2} \quad (3.89)$$

Now taking the limit $n \rightarrow \infty$ gives $s_2 - s_1 \rightarrow 0$. Hence, compression over a rounded corner is *isentropic*.

3.7.4 Reflected shocks and shock interactions

Consider a flow channel with a concave corner of angle θ . An oblique shock is formed at this corner at an angle β_1 . Here, the shock is left-running, and the flow after the shock bends toward the shock in such a way that it flows in the direction of the lower wall; that is its flow direction is θ . When this shock impinges on the upper wall of the channel, a reflected right-running shock is formed. The reason that a reflected shock must form is that the flow must again turn so that the flow after this reflected shock is parallel to the upper wall. This is illustrated in Figure 3.19, and its analysis is carried out in the next example.

■ EXAMPLE 3.11

Air at $M_1 = 3.0$ flows in a channel with a sharp corner as shown in Figure 3.19. The angle $\theta = 15^\circ$. The pressure of the incoming stream is $p = 80$ kPa, and its temperature is $T_1 = 280$ K. Find the Mach number after the reflected shock and the pressure and temperature in this region.

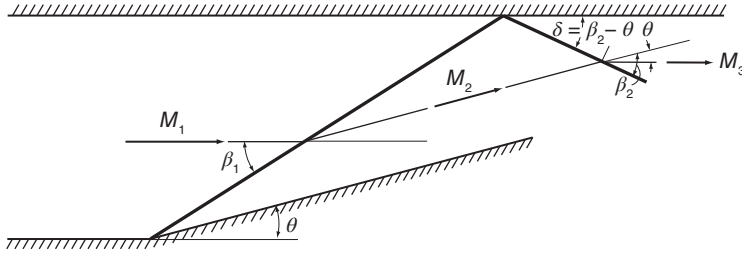


Figure 3.19 Reflection of a shock from a wall.

Solution: The shock angle β_1 is obtained with the function GNU/OCTAVE or MATLAB call

```
k=1.4; theta=15*pi/180; M1=3.0;
beta1=fzero(@(beta1) tan(theta)- ...
2*cot(beta1)*(M1^2*sin(beta1)^2-1)/ (M1^2*(k+cos(2*beta1))+2),0.4)
```

The shock angle is determined to be $\beta_1 = 32.24^\circ$. The normal component of M_1 is $M_{n12} = M_1 \sin \beta_1 = 3.0 \sin(32.24) = 1.60$, and the normal component of M_2 is

$$M_{n21} = \sqrt{\frac{2 + (\gamma - 1)M_{n12}^2}{2\gamma M_{n12}^2 + (\gamma - 1)}} = \sqrt{\frac{2 + 0.4 \cdot 1.60^2}{2.8 \cdot 1.60^2 + 0.4}} = 0.668$$

Examination of the figure shows

$$M_2 = \frac{M_{n21}}{\sin(\beta_1 - \theta)} = \frac{0.668}{\sin(32.24^\circ - 15^\circ)} = 2.255$$

The angle β_2 is obtained by the GNU/OCTAVE or MATLAB script above with β_1 replaced by β_2 and M_1 replaced by M_2 . This gives $\beta_2 = 40.35^\circ$. From the construction, the shock angle with the horizontal direction is seen to be $\delta = \beta_2 - \theta = 40.35^\circ - 15.0^\circ = 25.35^\circ$. The Mach number component upstream and normal to the reflected shock is

$$M_{n23} = M_2 \sin \beta_2 = 2.255 \sin(40.35^\circ) = 1.46$$

Hence, the normal component of the Mach number after the reflected shock is

$$M_{n32} = \sqrt{\frac{2 + (\gamma - 1)M_{n23}^2}{2\gamma M_{n23}^2 + (\gamma - 1)}} = \sqrt{\frac{2 + 0.4 \cdot 1.46^2}{2.8 \cdot 1.46^2 + 0.4}} = 0.716,$$

and the Mach number after the reflected shock is

$$M_3 = \frac{M_{n32}}{\sin(\beta_2 - \theta)} = \frac{0.716}{\sin(40.35^\circ - 15^\circ)} = 1.672$$

The pressure ratio is calculated from the shock relation

$$p_r = \frac{2\gamma M_n^2 - (\gamma - 1)}{\gamma + 1}$$

and replacing in turn M_n by M_{n12} and M_{n23} yields

$$p_{r1} = 2.822 \quad p_{r2} = 2.320$$

The reflected shock is seen to be weaker than the original one, as these pressure ratios show. The pressures are $p_2 = p_{r1}p_1 = 2.822 \cdot 80 = 225.7$ kPa and $p_3 = p_{r2}p_2 = 2.320 \cdot 225.7 = 523.7$ kPa. The temperature ratio for shock is

$$T_r = \frac{[2\gamma M_n^2 - (\gamma - 1)][(2 + (\gamma - 1)M_n^2)]}{(\gamma + 1)^2 M_n^2}$$

so that

$$T_{r1} = 1.388 \quad T_{r2} = 1.294,$$

and thus, $T_2 = T_{r1}T_1 = 1.388 \cdot 280 = 388.7$ K and $T_3 = T_{r2}T_2 = 1.294 \cdot 388.7 = 502.9$ K. ■

3.7.5 Mach reflection

When the value of the angle θ is increased, a condition is reached in which the flow passing through the reflected shock cannot turn enough to be parallel to the upper wall. This value is obtained from Eq. (3.80) in which the value of Mach number is that before the reflected shock. In this situation, the original shock terminates before it reaches the upper wall, and a new shock extends from the terminal location to the wall. This shock, called a *Mach stem*, is shown in Figure 3.20. The Mach stem is curved in such a way that it ends normal to the wall. Since the flow after a normal shock is subsonic, the flow after the Mach stem does not have straight streamlines, as it does after a regular reflection. In addition, a *slip line* develops from the point where Mach stem and the incident and reflected shocks meet. Across this slip line, pressure is continuous, but other properties are not. It is possible to determine the values of θ and β as functions of the incoming Mach number [66] that mark the conditions between a regular and a Mach reflection. These curves are shown in Figure 3.21.

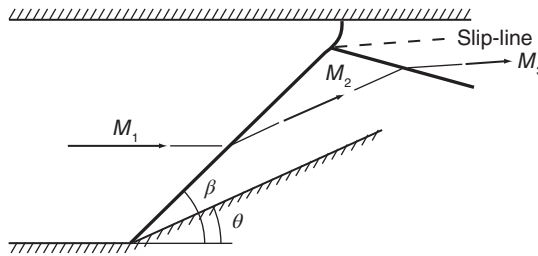


Figure 3.20 A Mach reflection.

3.7.6 Detached oblique shocks

For values of θ that are too large for a straight oblique shock to form at a sharp concave corner or at an apex of a wedge, a detached curved shock forms ahead of a corner or a wedge. These are shown in Figure 3.22.

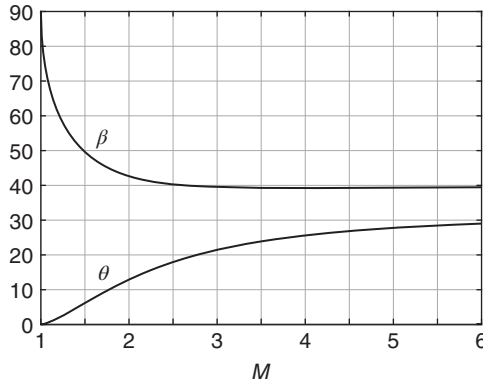


Figure 3.21 Limits of flow and corner angles for attached straight shocks.

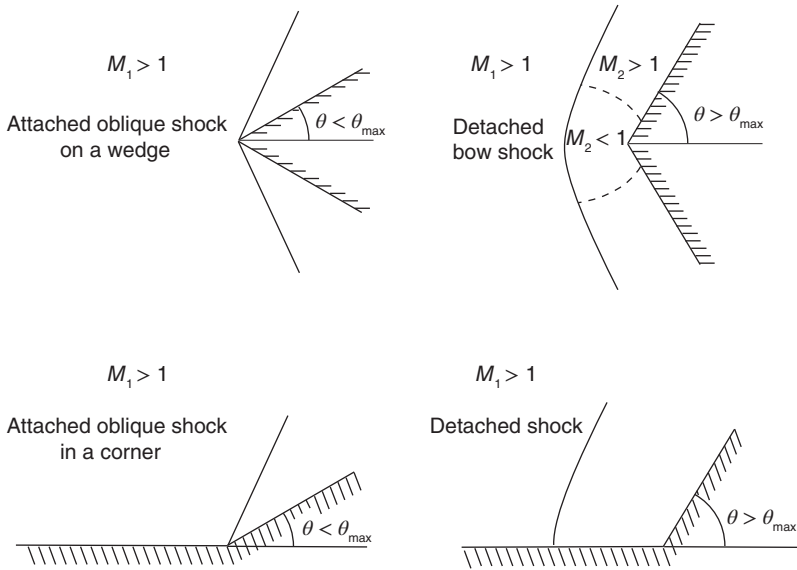


Figure 3.22 Attached and detached oblique shocks.

These detached shocks correspond to strong solutions. At the symmetry plane of a wedge, this shock is normal to the flow. Similarly, since a wall may be substituted for the plane of symmetry, this kind of a *bow shock* also appears ahead of a corner on a plane wall.

For the flow over a wedge, consider a particular value of the free stream Mach number, say $M = 2.4$. At the right bottom corner in Figure 3.16, the curve $M = 2.4$ (as all the others) has $\theta = 0$ and $\beta = 90^\circ$. This condition corresponds to a *locally normal shock* situated some distance ahead of the vertex of the wedge. This distance is called the *shock detachment distance*. The flow is subsonic after the shock. Moving along the bow shock away from this point, the shock remains on the strong shock branch, and the flow remains subsonic after the shock. The angle β has decreased somewhat, and the angle θ has increased. Further along the shock, the conditions pass from the strong shock to the weak solution branch. For $M = 2.4$, this takes place when $\beta = 62.7^\circ$ and $\theta = 28.7^\circ$. A short distance down along the weak shock branch, a point is reached at which the flow after the

shock is sonic. The angles β and θ for this condition may be calculated from Eq. (3.81). For $M = 2.4$, these are $\beta = 62.4^\circ$ and $\theta = 28.5^\circ$. The dashed line in Figure 3.22 shows the sonic line, which separates the supersonic and subsonic regions downstream of the shock. The weak shock branch terminates at condition $\theta = 0$ at which $\beta = \mu$ and $\sin \mu = 1/M$. For $M = 2.4$, the angle is $\mu = 24.6^\circ$.

Figure 3.23 shows a supersonic airflow over a double wedge airfoil. With an angle of attack of 5° , the flow structure is asymmetrical with a stronger oblique shock below the leading edge than on the upper side. At the convex corners in the middle of the airfoil, expansion fans in the flow. At the trailing edge, the flow bends toward the free stream direction, and thus, a stronger oblique shock develops on the upper side. The strength of these shocks is seen qualitatively by the sharper change in the gray color. The flow features illustrated in this figure are qualitatively the same as those that may be found in a transonic compressor, with the exception that a bow shock is expected to develop at the leading edge, for the compressor blades have a rounded leading edge, even if the blades are quite thin.

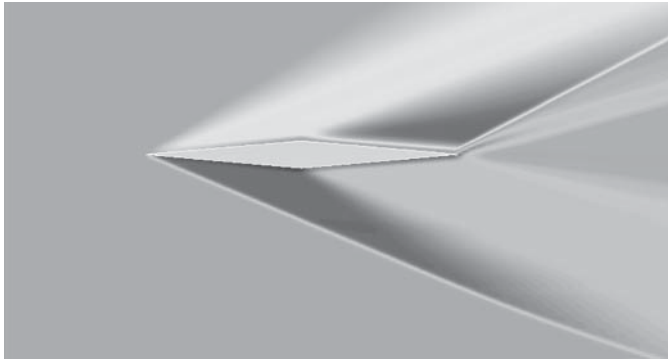


Figure 3.23 Transonic flow over a supersonic airfoil, $M = 3$ angle of attach 5° . Source: From Prasad et al. [72].

In a blade cascade, an oblique shock that develops below the leading edge of one blade impinges on the next one, and a reflected shock is formed. The pressure rise across the shock may cause a separation of the boundary layer on that blade. This is shown schematically in Figure 3.24.

3.7.7 Prandtl–Meyer theory

In a supersonic flow over an exterior corner, shown in Figure 3.25a, as the flow turns, Mach waves emanating from the sharp corner form an *expansion fan*. Since the flow is supersonic and moves to a larger area, its Mach number increases and pressure drops.

The expansion fan is located in the region between the Mach waves oriented at angles $\sin \mu_1 = c_1/V_1 = 1/M_1$ and $\sin \mu_2 = c_2/V_2 = 1/M_2$, with μ_2 defining the terminal Mach wave at which V is parallel to the downstream wall. Such an expansion fan is said to be *centered* about the corner. Upstream of the leading Mach wave, pressure is uniform, and the incremental pressure drop across a given Mach wave is the same regardless of where the flow crosses it. If the expansion fan is considered to consist of a discrete number of Mach waves, then, the wedges between successive Mach waves are regions of constant thermodynamic properties.

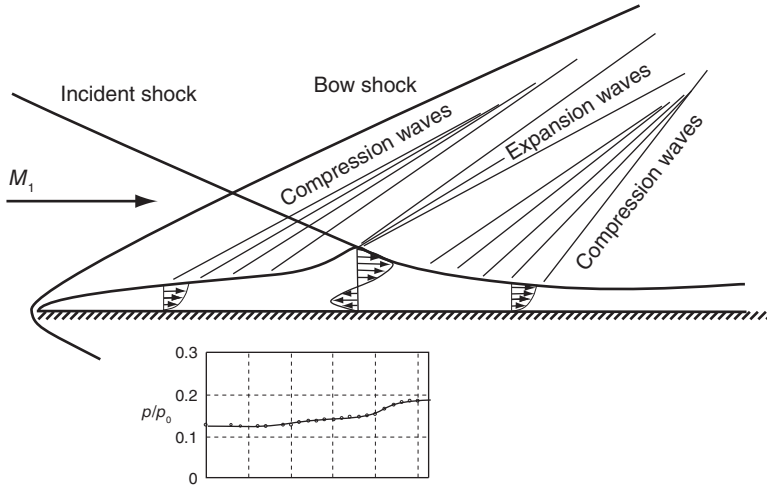


Figure 3.24 Shock and boundary layer interaction.

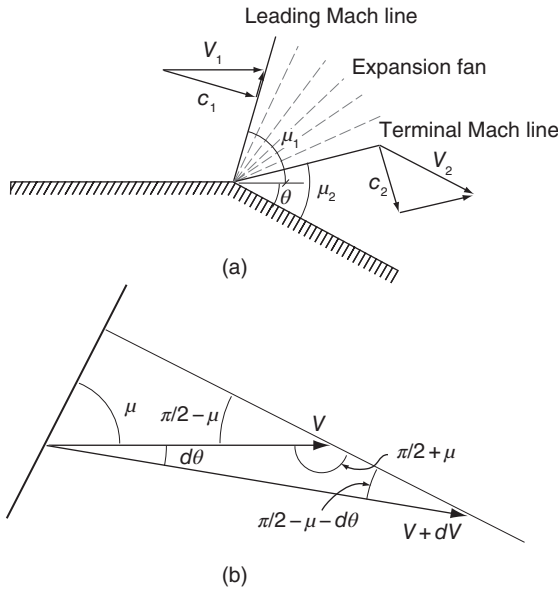


Figure 3.25 (a) Supersonic expansion of a compressible flow over a convex corner. (b) Diagram to illustrate the notation of angles.

Turning of the flow across one Mach wave is shown in Figure 3.25b. From the law of sines

$$\frac{V + dV}{V} = \frac{\sin(\pi/2 + \mu)}{\sin(\pi/2 - \mu - d\theta)}$$

or

$$1 + \frac{dV}{V} = \frac{\cos \mu}{\cos \mu \cos d\theta - \sin \mu \sin d\theta}$$

The angle $d\theta$ is small and is assumed to *increase in the clockwise* direction so that the previous equation can be written as

$$1 + \frac{dV}{V} = \frac{\cos \mu}{\cos \mu - d\theta \sin \mu} = \frac{1}{1 - d\theta \tan \mu}$$

Again making use of the smallness of $d\theta$, this can be expanded by binomial theorem, and the following equation is obtained:

$$\frac{dV}{V} = d\theta \tan \mu$$

Since $\tan \mu = c/\sqrt{V^2 + c^2} = 1/\sqrt{M^2 - 1}$, this can be written as

$$d\theta = \sqrt{M^2 - 1} \frac{dV}{V} \quad (3.90)$$

Taking logarithms and differentiating $V = M\sqrt{\gamma RT}$ gives

$$\frac{dV}{V} = \frac{dM}{M} + \frac{1}{2} \frac{dT}{T} = \frac{1}{2} \frac{dM^2}{M^2} + \frac{1}{2} \frac{dT}{T}$$

The same operations on $T_0 = T[1 + (\gamma - 1)M^2/2]$ give

$$-\frac{dT}{T} = \frac{\frac{\gamma - 1}{2} M^2}{1 + \frac{\gamma - 1}{2} M^2} \frac{dM^2}{M^2}$$

Using this to eliminate dT/T from the previous equation leads to

$$\frac{dV}{V} = \frac{1}{2 \left(1 + \frac{\gamma - 1}{2} M^2 \right)} \frac{dM^2}{M^2}$$

This can now be substituted into Eq. (3.90), which is then written as

$$d\theta = \frac{\sqrt{M^2 - 1}}{2 \left(1 + \frac{\gamma - 1}{2} M^2 \right)} \frac{dM^2}{M^2}$$

Next defining,

$$\nu(M) = \int_1^M \frac{\sqrt{M^2 - 1}}{2 \left(1 + \frac{\gamma - 1}{2} M^2 \right)} \frac{dM^2}{M^2}$$

and integrating gives

$$\nu(M) = \sqrt{\frac{\gamma + 1}{\gamma - 1}} \tan^{-1} \sqrt{\frac{\gamma - 1}{\gamma + 1} (M^2 - 1)} - \tan^{-1} \sqrt{M^2 - 1}, \quad (3.91)$$

so that a flow that expands to a state at which the Mach number is M_2 turns by an amount

$$\theta_2 - \theta_1 = \nu_2 - \nu_1$$

and the *fan angle* is $\nu_2 - \nu_1 + \mu_1 - \mu_2$. If the coordinates are aligned such that $\theta_1 = 0$, then,

$$\nu_2 = \nu_1 + \theta_2$$

Two common situations are encountered. First, the wall along which the flow moves has a convex corner of known magnitude. Hence, the angle θ_2 is known; the angle ν_2 can be determined, and then, the M_2 calculated from Eq. (3.91). The second situation is one in which the flow leaves as a jet from a nozzle to a space in which the back pressure is known. The next example illustrates the flow over a known convex corner.

■ EXAMPLE 3.12

Consider a supersonic air flow over a convex corner, as shown in Figure 3.25, with angle $\theta_2 = 10^\circ$, when the inflow moves in the direction of $\theta_1 = 0^\circ$. The Mach number of the flow upstream of the corner is $M_1 = 1.46$, pressure is $p_1 = 575.0$ kPa, and temperature is $T_1 = 360.0$ K. Find the Mach number, temperature, and pressure after the expansion is complete.

Solution: Mach number is obtained by the following script.

```
M1=1.46; k=1.4; thetadeg=10; theta=thetadeg*pi/180;
nu1=atan(1/(sqrt(M1^2-1)))*180/pi;
nu1=sqrt((k+1)/(k-1))*atan(sqrt((k-1)*(M1^2-1)/(k+1))) ...
    -atan(sqrt(M1^2-1));
nu2=nu1+theta;
M2 = fzero(@(M2) nu2-sqrt((k+1)/(k-1))* ...
    atan(sqrt((k-1)*(M2^2-1)/(k+1))) ...
    +atan(sqrt(M2^2-1)), [1.4,4]);
Result:
M2=1.800
```

The angle of the leading Mach wave is $\mu_1 = 43.23^\circ$. After that, the upstream Prandtl–Meyer function is calculated, and when converted to degrees, it is $\nu_1 = 10.73^\circ$. The Prandtl–Meyer function for complete turning is obtained as

$$\nu_2 = \nu_1 + \theta_2 = 10.73^\circ + 10^\circ = 20.73^\circ \quad \nu_2 = 0.3618 \text{ radian}$$

Since the Prandtl–Meyer function is implicit in the downstream Mach number, its value is obtained by invoking MATLAB'S or GNU/OCTAVE'S `fzero` function. An assumed range of downstream Mach numbers is given as $[1.4, 4]$, or something similar. The value of Mach number after the expansion is $M_2 = 1.80$.

The temperature and pressure after expansion are obtained by the usual method. With

$$\frac{T_0}{T_1} = 1 + \frac{\gamma - 1}{2} M_1^2 = 1 + 0.2 \cdot 1.46^2 = 1.426 \quad T_0 = 513.48 \text{ K},$$

the downstream temperature is

$$\frac{T_0}{T_2} = 1 + \frac{\gamma - 1}{2} M_2^2 \quad \text{so that} \quad T_2 = 311.55 \text{ K},$$

and the downstream pressure is therefore

$$p_2 = p_1 \left(\frac{T_2}{T_1} \right)^{\gamma/(\gamma-1)} = 575.0 \left(\frac{311.55}{360.00} \right)^{3.5} = 346.7 \text{ kPa}$$

■

The second application of Prandtl–Meyer theory is from Kearton [53], who considers a steam nozzle such as that shown in Figure 3.26. Assuming isentropic and choked flow, the Mach number at the throat is unity. Hence, the speed of sound and the velocity are equal, and the Mach waves are perpendicular to the flow, and therefore aligned with the exit cross-section of the nozzle. In addition, $\nu(M_1) = 0$. Next, an angle ϕ is defined to be that between the leading Mach wave and a Mach wave at any location in the expansion fan. Hence

$$\phi = \frac{\pi}{2} - \mu + \theta$$

in which θ is the angle by which the flow has turned at this location. Since $\nu(M) = \nu(M_1) + \theta$, then

$$\phi = \nu(M) + \frac{\pi}{2} - \tan^{-1} \frac{1}{\sqrt{M^2 - 1}}$$

or

$$\phi = \sqrt{\frac{\gamma + 1}{\gamma - 1}} \tan^{-1} \sqrt{\frac{\gamma - 1}{\gamma + 1} (M^2 - 1)} + \frac{\pi}{2} - \tan^{-1} \sqrt{M^2 - 1} - \tan^{-1} \frac{1}{\sqrt{M^2 - 1}}$$

But from a right triangle, it is seen that

$$\tan^{-1} \sqrt{M^2 - 1} + \tan^{-1} \frac{1}{\sqrt{M^2 - 1}} = \frac{\pi}{2};$$

therefore, the expression for ϕ reduces to

$$\phi \sqrt{\frac{\gamma - 1}{\gamma + 1}} = \tan^{-1} \sqrt{\frac{\gamma - 1}{\gamma + 1} (M^2 - 1)} \quad (3.92)$$

The term inside the square root on the RHS of Eq. (3.92) may be replaced by a pressure ratio, for

$$\frac{p_0}{p} = \left(1 + \frac{\gamma - 1}{2} M^2 \right)^{\gamma/(\gamma-1)},$$

and therefore,

$$\frac{\gamma - 1}{\gamma + 1} (M^2 - 1) = \frac{2}{\gamma + 1} \left[\left(\frac{p_0}{p} \right)^{(\gamma-1)/\gamma} - 1 \right]$$

Substitution yields

$$\phi \sqrt{\frac{\gamma-1}{\gamma+1}} = \tan^{-1} \sqrt{\frac{2}{\gamma+1} \left[\left(\frac{p_0}{p} \right)^{(\gamma-1)/\gamma} - 1 \right]} \quad (3.93)$$

Denoting

$$\delta = \phi \sqrt{\frac{\gamma-1}{\gamma+1}}$$

it follows that

$$\tan \delta = \sqrt{\frac{2}{\gamma+1} \left[\left(\frac{p_0}{p} \right)^{(\gamma-1)/\gamma} - 1 \right]},$$

and therefore

$$\cos^2 \delta = \frac{\gamma+1}{2} \left(\frac{p}{p_0} \right)^{(\gamma-1)/\gamma} \quad (3.94)$$

This can be reduced further using the identity $2\cos^2 x = 1 + \cos 2x$. Hence,

$$1 + \cos(2\delta) = (\gamma+1) \left(\frac{p}{p_0} \right)^{(\gamma-1)/\gamma}$$

Rewriting this in terms of ϕ gives

$$1 + \cos \left(2\sqrt{\frac{\gamma-1}{\gamma+1}} \phi \right) = (\gamma+1) \left(\frac{p}{p_0} \right)^{(\gamma-1)/\gamma}, \quad (3.95)$$

which can be solved for the pressure ratio. The final form is

$$\frac{p}{p_0} = \left[\frac{1 + \cos \left(2\sqrt{\frac{\gamma-1}{\gamma+1}} \phi \right)}{\gamma+1} \right]^{\gamma/(\gamma-1)}$$

Streamlines can be calculated by considering a control volume of a wedge-shaped region with an inlet at the throat and exit coinciding with an arbitrary Mach wave in the expansion fan. The lateral boundary is taken to be a streamline across which there is no flow. Since the component of velocity perpendicular to a Mach wave is the local sonic velocity, it is this component that carries the flow through the inflow and outflow boundaries of the chosen control volume. For this reason, the continuity equation reduces to

$$\rho_1 A_1 c_1 = \rho A c$$

Since the nozzle is rectangular, $A = rb$, in which b is the nozzle height, and r is the distance from the corner to the chosen streamline. At the throat, the area is $A_1 = r_1 b$, and r_1 is the distance from the corner to the same streamline. Hence

$$\frac{r}{r_1} = \frac{\rho_1 c_1}{\rho c} = \frac{p_1}{p} \sqrt{\frac{T}{T_1}}$$

In isentropic flow, $T/T_1 = (p/p_1)^{(\gamma-1)/\gamma}$, and this equation reduces to

$$\frac{r}{r_1} = \frac{p_1}{p} \left(\frac{p}{p_1} \right)^{(\gamma-1)/2\gamma} = \left(\frac{p}{p_1} \right)^{-(\gamma+1)/2\gamma}$$

From Eq. (3.94), the expression

$$\cos \delta = \left(\frac{\gamma+1}{2} \right)^{1/2} \left(\frac{p}{p_0} \right)^{(\gamma-1)/2\gamma} \quad (3.96)$$

is obtained. With sonic conditions at station 1, the pressure ratio there is

$$\frac{p_0}{p_1} = \left(\frac{\gamma+1}{2} \right)^{\gamma/(\gamma-1)} \quad \text{so that} \quad \left(\frac{\gamma+1}{2} \right)^{1/2} = \left(\frac{p_0}{p_1} \right)^{(\gamma-1)/2\gamma},$$

and Eq. (3.96) can be recast as

$$\frac{p}{p_1} = \left[\cos \left(\sqrt{\frac{\gamma-1}{\gamma+1}} \phi \right) \right]^{2\gamma/(\gamma-1)}$$

Hence, the distance from the corner to the streamline bounding the control volume is

$$\frac{r}{r_1} = \frac{1}{\left(\cos \sqrt{\frac{\gamma-1}{\gamma+1}} \phi \right)^{(\gamma+1)/(\gamma-1)}} \quad (3.97)$$

Some streamlines have been plotted to Figure 3.26. The uppermost streamline in the figure corresponds to r_1 , which is the width of the nozzle at the throat. This streamline leaves the nozzle before the slanted nozzle exit. If the nozzle shape were to coincide with the contour of this streamline, the Prandtl–Meyer flow would be an exact solution of the equations for

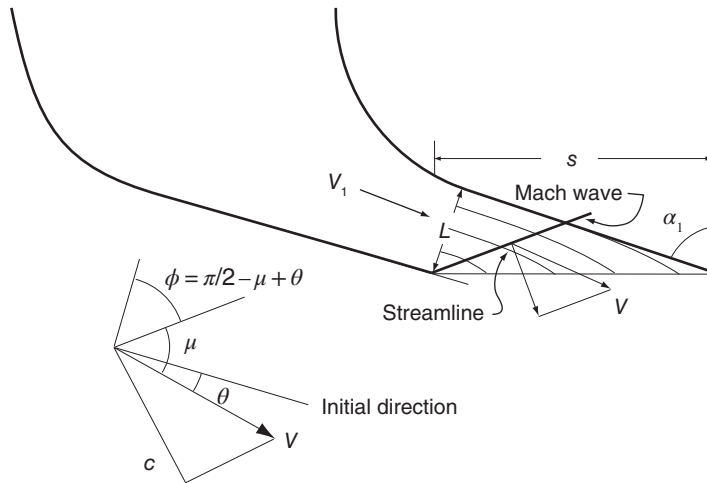


Figure 3.26 Expansion of steam from a choked nozzle.

inviscid compressible flow through a nozzle of this shape. Since the nozzle wall is straight, the solution presented is an *approximation* to the actual situation.

Equation (3.92) may be recast into the form

$$\tan \left(\sqrt{\frac{\gamma-1}{\gamma+1}} \phi \right) = \sqrt{\frac{\gamma-1}{\gamma+1}} \sqrt{M^2 - 1},$$

and since $1/\sqrt{M^2 - 1} = \tan \mu$, the following relation is obtained

$$\tan \mu = \sqrt{\frac{\gamma-1}{\gamma+1}} \cot \sqrt{\frac{\gamma-1}{\gamma+1}} \phi \quad (3.98)$$

For a given exit pressure lower than the critical one, the angle ϕ can be found from either Eq. (3.93) or from Eq. (3.95), and Eq. (3.98) is then used to determine the angle of the terminal Mach wave. After that the amount of turning of the flow is obtained from

$$\theta_2 = \phi - \frac{\pi}{2} + \mu_2$$

The flow direction is given by $\alpha_2 = \alpha_1 - \theta_2$.

■ EXAMPLE 3.13

Consider steam flow from a low-pressure nozzle, such as shown in Figure 3.26, with nozzle angle $\alpha = 65^\circ$. At the inlet of the nozzle, steam is saturated vapor with stagnation pressure $p_0 = 20$ kPa. Steam exhausts into the interblade space where the pressure is 8 kPa. Find the angle θ_5 by which the flow turns on leaving the nozzle, the far downstream velocity, and its direction.

Solution: Since at the inlet, steam is saturated, its adiabatic index, according to Zeuner's equation, is $\gamma = 1.135$, and its temperature is $T_0 = 333.2$ K. Denoting station 1 to be the throat and station 2 the exit where the back pressure is $p_2 = 8$ kPa, the ratio of back pressure to stagnation pressure is $p_2/p_0 = 8/20 = 0.4$, and therefore, the flow is choked. The Mach number after the expansion is

$$M_2 = \sqrt{\frac{2}{\gamma-1} \left[\left(\frac{p_0}{p_2} \right)^{(\gamma-1)/\gamma} - 1 \right]} = 1.306$$

With this value of Mach number, the temperature at the exit is

$$T_2 = T_0 \left(\frac{p_2}{p_0} \right)^{(\gamma-1)/\gamma} = 333.2 \left(\frac{8}{20} \right)^{0.135/1.135} = 298.8 \text{ K}$$

The sonic speed at the exit is

$$c_2 = \sqrt{\gamma R T_2} = \sqrt{1.135 \cdot 8314 \cdot 298.8/18} = 395.8 \text{ m/s}$$

Hence, $V_2 = M_2 c_2 = 516.9$ m/s. Angle ϕ_2 can be calculated using Eq. (3.92), with the result that $\phi_2 = 47.44^\circ$. The Mach angle at the exit is

$$\mu_2 = \sin^{-1} \left(\frac{1}{M_2} \right) = \tan^{-1} \frac{1}{\sqrt{M_2^2 - 1}} = 49.97^\circ$$

Hence, the amount of turning is

$$\theta_2 = \phi_2 + \mu_2 - \frac{\pi}{2} = 47.44^\circ + 49.96^\circ - 90^\circ = 7.40^\circ$$

The flow angle after turning is complete is

$$\alpha_2 = \alpha_1 - \theta_2 = 65^\circ - 7.40^\circ = 57.60^\circ$$

The extent of the jet after it has reached the back pressure is

$$\frac{r}{r_1} = \frac{1}{\left(\cos \sqrt{\frac{\gamma-1}{\gamma+1}} \phi \right)^{(\gamma+1)/(\gamma-1)}} = 1.412$$

■

There is a limit on the extent to which the flow can turn. This limit is reached when the axial component of velocity of the jet reaches sonic speed. The condition may be analyzed by writing the mass flow rate in terms of the flow function $F(M)$. This results in the equations

$$\dot{m} \sqrt{c_p T_0} = F(M_1) A_1 p_{01} = F(M_2) A_2 p_{02}$$

so that

$$F(M_2) = F(M_1) \frac{A_1 p_{01}}{A_2 p_{02}}$$

For a nozzle of constant height,

$$\frac{A_1}{A_2} = \frac{L_1}{L_2} = \frac{s \cos \alpha_1}{s \cos \alpha_2} = \frac{\cos \alpha_1}{\cos \alpha_2}$$

The axial component of velocity at sonic speed can be written as

$$V_{x2} = V_2 \cos \alpha_2 = M_2 \sqrt{\gamma R T_2} \cos \alpha_2 = \sqrt{\gamma R T_2}$$

so that $\cos \alpha_2 = 1/M_2$.

Substituting and simplifying gives

$$\frac{\gamma}{\sqrt{\gamma-1}} \left(1 + \frac{\gamma-1}{2} M_2^2 \right)^{-(\gamma+1)/2(\gamma-1)} = F(M_1) \frac{p_{01}}{p_{02}} \cos \alpha_1$$

from which M_2 may be determined.

■ EXAMPLE 3.14

Steam with $\gamma = 1.3$ flows from a low-pressure nozzle shown in Figure 3.26, with nozzle angle $\alpha = 65^\circ$. The throat at the exit plane is choked. Find the limiting Mach number and the value of α_2 for the flow.

Solution: With flow choked at the throat, $M_1 = 1$, and

$$F^* = \frac{\gamma}{\sqrt{\gamma-1}} \left(\frac{\gamma+1}{2} \right)^{-(\gamma+1)/2(\gamma-1)} = \frac{1.3}{\sqrt{0.3}} (0.5 \cdot 2.3)^{-2.3/0.6} = 1.389$$

Since $\cos \alpha_2 = 1/M_2$, assuming no losses so that $p_{02} = p_{01}$, the relation

$$F(M_2) \cos \alpha_2 p_{02} = F^* \cos \alpha_1 p_{01}$$

can be written as

$$\frac{\gamma}{\sqrt{\gamma-1}} \left(1 + \frac{\gamma-1}{2} M_2^2 \right)^{-(\gamma+1)/2(\gamma-1)} = F^* \cos \alpha_1$$

With $\alpha_1 = 65^\circ$, solving this for M_2^2 gives

$$M_2^2 = \frac{2}{\gamma-1} \left[\left(\frac{\gamma}{\sqrt{\gamma-1}} \frac{1}{F^* \cos \alpha_1} \right)^{2(\gamma-1)/(\gamma+1)} - 1 \right] = 2.9314$$

so that $M_2 = 1.712$. Therefore,

$$\alpha_2 = \cos^{-1} \left(\frac{1}{M_2} \right) = \cos^{-1} \left(\frac{1}{1.712} \right) = 54.26^\circ$$

■

The turbine nozzle may also be designed such that the throat is upstream of the exit plane, in which case the flow may become supersonic at the exit plane. Then, in an *underexpanded* expansion, the flow adjusts to the back pressure through a set of oblique shocks emanating from the trailing edge. For transonic flows, as has been seen in the examples in this chapter, the stagnation pressure losses are small.

As the final example, consider the intersection of two shocks of the same family. In the analysis, both the oblique shock and Prandtl–Meyer theory are used.

■ EXAMPLE 3.15

Air at pressure $p_1 = 101.3$ kPa, temperature $T_1 = 288$ K, and Mach number $M_1 = 2.4$ encounters a concave corner of angle $\theta_1 = 8^\circ$. After the corner, a second corner changes the flow direction by another $\theta_2 = 5^\circ$. The oblique shocks emanating from these corners intersect and form another oblique shock starting from their point of intersection, as shown in Figure 3.27. Find the pressure, the angle of the slip line, the Mach numbers M_4 and M_5 , and the change in entropy in the regions across the slip line.

Solution: With M_1 and θ_1 known, the value of β_1 can be obtained from the implicit equation

$$\tan \theta_1 = 2 \cot \beta_1 \frac{M_1^2 \sin^2 \beta_1 - 1}{M_1^2 (\gamma + \cos 2\beta_1) + 2}$$

Its value is $\beta_1 = 31.15^\circ$. The Mach number normal to the first oblique shock is

$$M_{n12} = M_1 \sin \beta_1 = 2.4 \cdot \sin(31.15^\circ) = 1.24$$

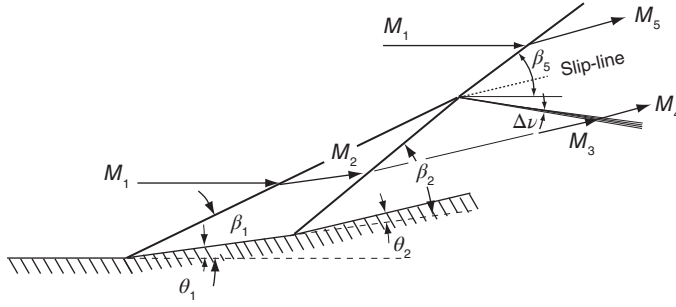


Figure 3.27 Interaction of two oblique shocks of the same family.

The normal component of the Mach number after this shock is

$$M_{n21} = \sqrt{\frac{2 + (\gamma - 1)M_{n12}^2}{2\gamma M_{n12}^2 - (\gamma - 1)}} = \sqrt{\frac{2 + 0.4 \cdot 1.24^2}{2.8 \cdot 1.24^2 - 0.4}} = 0.817$$

The Mach number after the first shock is thus

$$M_2 = \frac{M_{n21}}{\sin(\beta_1 - \theta_1)} = \frac{0.817}{\sin(31.15^\circ - 8^\circ)} = 2.08$$

The ratio of the stagnation temperature to the static temperature before this shock is

$$\frac{T_{01}}{T_1} = 1 + \frac{\gamma - 1}{2} M_1^2 = 1 + 0.2 \cdot 2.4^2 = 2.152,$$

and the corresponding pressure ratio is

$$\frac{p_{01}}{p_1} = \left(\frac{T_{01}}{T_1} \right)^{\gamma/(\gamma-1)} = 2.152^{3.5} = 14.62$$

Hence,

$$T_{01} = 2.152 \cdot 288 = 619.78 \text{ K} \quad p_{01} = 14.620 \cdot 101.3 = 1481.0 \text{ kPa}$$

The pressure after the shock is

$$\frac{p_2}{p_1} = \frac{2\gamma M_{n12}^2 - (\gamma - 1)}{\gamma + 1} = \frac{2.8 \cdot 1.24^2 - 0.4}{2.4} = 1.631 \quad p_2 = 165.26 \text{ kPa}$$

The stagnation temperature remains constant so that the static temperature after this shock is obtained from

$$\frac{T_{02}}{T_2} = 1 + \frac{\gamma - 1}{2} M_2^2 = 1 + 0.2 \cdot 2.08^2 = 1.865 \quad T_2 = \frac{619.78}{1.865} = 332.35 \text{ K}$$

It then follows that

$$\frac{p_{02}}{p_2} = \left(\frac{T_{02}}{T_2} \right)^{\gamma/(\gamma-1)} = 1.865^{3.5} = 8.856 \quad p_{02} = 8.856 \cdot 165.26 = 1463.5 \text{ kPa}$$

The velocity after the first shock is

$$V_2 = M_2 \sqrt{\gamma R T_2} = 2.08 \sqrt{1.4 \cdot 287 \cdot 332.35} = 759.9 \text{ m/s}$$

The properties after the second shock are calculated similarly. The shock angle β_2 is obtained from

$$\tan \theta_2 = 2 \cot \beta_2 \frac{M_2^2 \sin^2 \beta_2 - 1}{M_2^2 (\gamma + \cos 2\beta_2) + 2}$$

It has the value $\beta_2 = 32.94^\circ$. Next, the normal component of Mach number before the second shock is

$$M_{n23} = M_2 \sin \beta_2 = 2.08 \cdot \sin(32.94^\circ) = 1.13,$$

and the normal component of the Mach number after this shock is

$$M_{n32} = \sqrt{\frac{2 + (\gamma - 1) M_{n23}^2}{2\gamma M_{n23}^2 - (\gamma - 1)}} = \sqrt{\frac{2 + 0.4 \cdot 1.13^2}{2.8 \cdot 1.13^2 - 0.4}} = 0.889$$

The Mach number after the second shock is therefore

$$M_3 = \frac{M_{n32}}{\sin(\beta_2 - \theta_2)} = \frac{0.889}{\sin(32.94^\circ - 5^\circ)} = 1.90$$

The pressure ratio across the second shock is

$$\frac{p_3}{p_2} = \frac{2\gamma M_{n23}^2 - (\gamma - 1)}{\gamma + 1} = \frac{2.8 \cdot 1.13^2 - 0.4}{2.4} = 1.325$$

and the pressure is

$$p_3 = 1.325 \cdot 165.26 = 218.9 \text{ kPa}$$

Since $T_{03} = T_{02} = T_{01}$, the static temperature after the shock is

$$\frac{T_{03}}{T_3} = 1 + \frac{\gamma - 1}{2} M_3^2 = 1 + 0.2 \cdot 1.90^2 = 1.720 \quad T_3 = \frac{619.78}{1.720} = 360.39 \text{ K},$$

and the stagnation pressure is

$$\frac{p_{03}}{p_3} = \left(\frac{T_{03}}{T_3} \right)^{\gamma/(\gamma-1)} = 1.720^{3.5} \quad p_{03} = 218.92 \cdot 1.720^{3.5} = 1460.2 \text{ kPa}$$

The velocity after this shock is

$$V_3 = M_3 \sqrt{\gamma R T_3} = 1.8970 \sqrt{1.4 \cdot 287 \cdot 360.39} = 721.88 \text{ m/s}$$

Next, it is tempting to assume that the flow after the second shock is parallel to the wall after the second corner and that the flow after the detached shock is also in this direction. Then, that the slip line that forms from the intersection of the two attached shocks is also parallel to this direction. It turns out that carrying out the rest of the

calculations this way does not make the pressures equal across the slip line. The difference is small, but this needs to be taken into an account. To make the pressures equal, an expansion fan forms at the point of intersection. Across this fan, the flow is turned in such a way that it can be made parallel to the flow after the detached shock, and the pressures become equal. This calculation requires an iterative solution.

With $M_3 = 1.897$, the Prandtl–Meyer function may be calculated. Its value is $\nu_3 = 23.5^\circ$. The rest of the calculation is carried out by iteration. The flow direction after the detached shock is assumed, and the pressure after it is calculated. Similarly, the Mach number after the expansion fan (or isentropic compression, as the case might be) is calculated with this assumed direction, and the value of ν_3 and the pressure can be determined since the Mach number is known. The difference in the pressures calculated this way is used to guess the new flow direction, and the process is repeated until the pressure difference is below an acceptable level. The iterations, shown in Table 3.1, were carried out with the *secant* method. The starting values for θ_5 can be taken near the value of $\theta_3 = 13^\circ$, and the range $11^\circ < \theta_5 < 15^\circ$ was chosen.

Table 3.1 Secant iteration.

| deg | deg | kPa | kPa | |
|------------------------|--------------------|-----------------------|-----------------|----------------|
| $\theta_5 = 11.000000$ | $\beta_5 = 34.001$ | $\Delta p = +47.8634$ | $p_4 = 243.854$ | $M_4 = 1.8270$ |
| $\theta_5 = 15.000000$ | $\beta_5 = 38.214$ | $\Delta p = -47.5664$ | $p_4 = 196.041$ | $M_4 = 1.9683$ |
| $\theta_5 = 13.006225$ | $\beta_5 = 36.050$ | $\Delta p = -0.03052$ | $p_4 = 218.844$ | $M_4 = 1.8973$ |
| $\theta_5 = 13.004945$ | $\beta_5 = 36.049$ | $\Delta p = -0.00001$ | $p_4 = 218.859$ | $M_4 = 1.8972$ |
| $\theta_5 = 13.004944$ | $\beta_5 = 36.049$ | $\Delta p = +0.00000$ | $p_4 = 218.859$ | $M_4 = 1.8972$ |

The final pressures and angles are

$$p_4 = p_5 = 218.86 \text{ kPa} \quad \beta_5 = 36.05^\circ \quad \theta_5 = 13.005^\circ$$

This shows that the *expansion fan* is very weak, for the value of θ_5 differs only slightly from $\theta_3 = 13^\circ$. The entropy changes from region 1 to 4 and from region 1 to 5 are:

$$\Delta s_{14} = 4.0635 \text{ J}/(\text{kg} \cdot \text{K}) \quad \Delta s_{15} = 13.1963 \text{ J}/(\text{kg} \cdot \text{K})$$

and the Mach numbers across the slip line have the values: $M_4 = 1.8972$ and $M_5 = 1.8766$. ■

EXERCISES

3.1 Conditions in an air reservoir are 680 kPa and 560 K. From there, the air flows isentropically through a convergent nozzle to a back pressure of 101.3 kPa. Find the velocity at the exit plane of the nozzle. [Ans: 433 m/s]

3.2 Air flows in a converging duct at the rate $\dot{m} = 0.25 \text{ kg/s}$. At the location where the area is $A_1 = 6.5 \text{ cm}^2$, air pressure is $p_1 = 140 \text{ kPa}$, and Mach number is $M_1 = 0.6$.

(a) Find the stagnation temperature. (b) When the flow is choked, what is the size of the throat area? (c) Give the percent reduction in area from station 1 to the throat. (d) Find the pressure at the throat. [Ans: (a) 249.4 K, (b) 5.47 cm^2 , (c) 15.8 %, (d) 94.3 kPa]

3.3 Air flows in a convergent nozzle. At a certain location, where the area is $A_1 = 5 \text{ cm}^2$, pressure is $p_1 = 240 \text{ kPa}$ and temperature is $T_1 = 360 \text{ K}$. Mach number at this location is $M_1 = 0.4$. Find the mass flow rate. [Ans: 0.177 kg/s]

3.4 The area of a throat in a circular nozzle is $A_t = 1 \text{ cm}^2$. (a) For a choked flow of air, find the diameter at the location where $M_1 = 0.5$. (b) Determine the Mach number at the location where the diameter is $D_2 = 1.941 \text{ cm}$. Assume the flow to be isentropic and $\gamma = 1.4$. [Ans: (a) 1.306 cm , (b) 0.200]

3.5 At the location where the area is $A_1 = 4 \text{ cm}^2$, Mach number for air has the value $M_1 = 0.2$. Find the diameter at the location where $M = 0.6$. [Ans: 1.43 cm]

3.6 Air flows through a circular duct 15 cm in diameter with a flow rate 2.25 kg/s . The total temperature and static pressure at a certain location in the duct are 30°C and 106 kPa , respectively. Find (a) the flow velocity, (b) the static temperature, (c) the stagnation pressure, and (d) the density at this location. [Ans: (a) 102.7 m/s , (b) 297.9 K , (c) 112.7 kPa , and (d) 1.24 kg/m^3]

3.7 (a) Show that for one-dimensional isentropic with area change flow, the relationship

$$\frac{dA}{A} = \frac{(M^2 - 1)}{1 + \frac{\gamma-1}{2}M^2} \frac{dM}{M}$$

holds between the changes in area and Mach number. (b) Conclude that Mach number has the value unity at the minimum. Determine d^2A/dx^2 , and show that this is positive as $M \rightarrow 1$, so that the area is indeed minimum.

3.8 Show that in compressible flow, the velocity can be written as

$$V = \sqrt{\frac{2\gamma RT_0}{\gamma - 1}} \left[1 - \left(\frac{p}{p_0} \right)^{(\gamma-1)/\gamma} \right]^{1/2}$$

3.9 Air flows subsonically in a converging nozzle. At a downstream location where the Mach number is $M_2 = 0.5$, the flow area is A_2 . What is the Mach number at an upstream location where $A_1 = 2A_2$. [Ans: 0.222]

3.10 Air flows into a supersonic nozzle from an air reservoir where its pressure is 500 kPa and temperature is 470 K , the ratio of the exit area to the throat area is 2.3 . The nozzle efficiency is $\eta = 0.91$, but the flow may be assumed to be isentropic to the throat and free of shocks thereafter. (a) Find the exit pressure, (b) the exit temperature, and (c) the exit Mach number. [Ans: (a) 36.85 kPa , (b) 245.3 K , (c) 2.14]

3.11 Conditions in an air reservoir are 380 kPa and 460 K . From there, the air flows through a convergent nozzle to a back pressure of 101.3 kPa . The polytropic efficiency of the nozzle is $\eta_p = 0.98$. Find (a) exit plane pressure, (b) exit plane temperature, (c) Mach number at the exit, and (d) the velocity at the exit plane of the nozzle. [Ans: (a) 198.1 kPa , (b) 383.3 K , (c) 0.986 , and (d) 387 m/s]

3.12 Air issues from a reservoir at conditions 260 kPa and 540 K into a converging nozzle. The nozzle efficiency is estimated to be $\eta_N = 0.986$. The back pressure is $p_b = 101.3 \text{ kPa}$. Find, (a) exit Mach number, (b) exit plane temperature, (c) exit plane pressure, and (d) exit velocity. [Ans: (a) 0.9883 , (b) 450 K , (c) 135.9 kPa , and (d) 420.2 m/s]

3.13 At the inlet to a nozzle, the conditions are $M_1 = 0.3$, $p_{01} = 320$ kPa and $T_{01} = 430$ K. The flow is irreversible with polytropic exponent $n = 1.396$. Show that

$$\frac{T_{02}}{T_2} = \left(\frac{p_{01}}{p_1}\right)^{\gamma/(\gamma-1)} \left(\frac{p_1}{p_2}\right)^{(n-1)/n}$$

Find the Mach number at a location where $p_2 = 210$ kPa. [Ans: 0.80]

3.14 Air from a reservoir with $p_{01} = 260$ kPa and $T_{01} = 530$ K flows through a nozzle. It is estimated that the static enthalpy loss coefficient is $\zeta = 0.020$. The exit pressure is $p_2 = 180$ kPa. (a) Find the exit Mach number. (b) Find the polytropic efficiency of the nozzle. [Ans: (a) 0.736, (b) 0.979]

3.15 A two-dimensional nozzle has a symmetrical shape, the upper part of which is given by

$$\hat{y} = \frac{4}{5} + \frac{\hat{x}(\hat{x} - 1)}{2(\hat{x} + 2)}$$

and $\hat{x} = x/a$ and the \hat{y}/a are dimensionless coordinates for which the reference length $a = 0.1$ m. The nozzle extends from $0 < x < 8$ cm. (a) As a preliminary step, write the GNU/OCTAVE script to calculate the results in Example 3.6. (b) Find the location of the throat. (c) Assuming that the flow is isentropic, find the Mach number at the throat. (d) Assuming that the friction factor is $4f = 0.02$, write a MATLAB or GNU/OCTAVE script and solve for the Mach number along the duct, as well as the pressure ratio $p(x)/p_1$. Plot them as functions of x . Do this by using the ode45 code in the software. (e) Carry out the calculation also by setting $f = 0$ and check that the Mach number at the throat is the same as that you calculated in part (a). [Ans: (b) 0.48 cm, (c) 0.5498]

3.16 Air, as shown in Figure 3.28a, flows from a reservoir at pressure $p_{01} = 280$ kPa and temperature $T_{01} = 1000$ K into a duct with an area $A_3 = 2.5$ cm² and pressure $p_3 = 170$ kPa. The nozzle area is $A_1 = 1$ cm. (a) Find the Mach number M_3 in the flow that has been fully mixed. (b) Find the mass flow rate of air. (c) Find the pressure p_2 . [Ans: (a) 0.376, (b) 0.0358 kg/s, (c) 102.74 kPa]

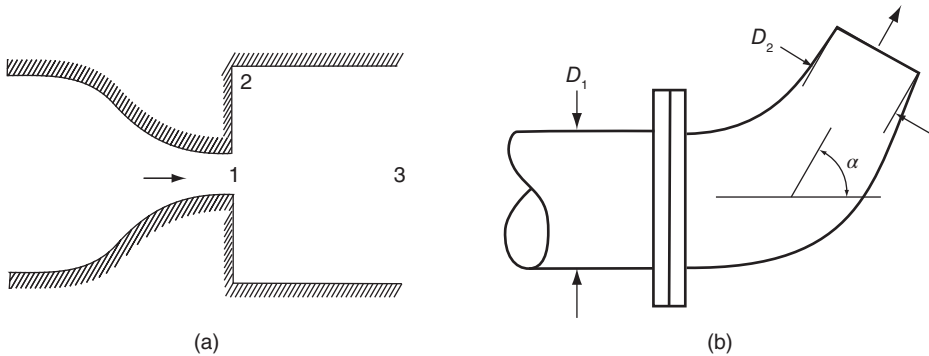


Figure 3.28 (a) Expansion of air into a large duct. (b) Exhaust of air through an offset nozzle.

3.17 Air exhausts through an offset nozzle shown in Figure 3.28b, into the atmosphere, where temperature is 20°C , and pressure is 101.3 kPa . The absolute pressure at the flange is $p_1 = 530\text{ kPa}$, and temperature there is $T_1 = 700\text{ K}$. The diameter is $D_1 = 15\text{ cm}$. The exit diameter of the nozzle is $D_2 = 10\text{ cm}$. Find (a) the velocity V_1 , (b) the exit velocity V_2 , and (c) the x -component of the force the fluid exerts on the flange. The flow leaves at 60° as shown. [Ans: (a) 142.4 m/s , (b) 487.6 m/s , and (c) 6.14 kN]

3.18 Show that for a normal shock

$$h_1 - h_2 = -\frac{1}{2}(p_2 - p_1)(v_1 + v_2)$$

3.19 Air enters a section in the diverging part of a supersonic nozzle with $M_i = 4$. The flow is slowed down by a shock such that at the exit of the nozzle, where $A_e = 2A_i$, Mach number is $M_e = 0.3$. (a) Find the Mach number M_1 just upstream of the shock. (b) Find the pressure ratio across the shock. [Ans: (a) 4.46 and (b) 23.0]

3.20 A shock wave moves into still air at temperature 300 K and pressure 101.3 kPa . This results in the air behind the shock moving at velocity 400 m/s . (a) Find the velocity at which the shock moves. (b) Find the pressure behind the shock. [Ans: (a) 662.1 m/s and (b) 413 kPa]

3.21 A shock moving into still air. Show that the shock speed is given by

$$U = c_1 \sqrt{\frac{\gamma - 1}{2\gamma} + \frac{\gamma + 1}{2\gamma} \frac{p_2}{p_1}}$$

3.22 A shock moves into still air. Show that the velocity after the shock is given by

$$V_2 = \frac{c_1}{\gamma} \left(\frac{p_2}{p_1} - 1 \right) \left(\frac{\frac{2\gamma}{\gamma+1}}{\frac{p_2}{p_1} + \frac{\gamma-1}{\gamma+1}} \right)^{1/2}$$

3.23 Consider a supersonic air flow over a convex corner with angle $\theta_1 = 5^\circ$. The upstream Mach number is $M_1 = 1.1$, pressure is $p_1 = 130\text{ kPa}$, and $T_1 = 310\text{ K}$. Find (a) Mach number, (b) temperature, (c) pressure, and (d) the fan angle after the expansion is complete. [Ans: (a) 1.306 , (b) 287.1 K , (c) 99.4 kPa , and (d) 20.4°]

3.24 Consider a supersonic air flow over a convex corner with angle $\theta_1 = 10^\circ$. The upstream Mach number is $M_1 = 1.8$, pressure is $p_1 = 130\text{ kPa}$, and $T_1 = 310\text{ K}$. After the first corner, the air flows over another convex corner, also $\theta_2 = 10^\circ$. Find (a) Mach number, (b) temperature, and (c) pressure after the expansion is complete. [Ans: (a) 2.57 , (b) 220.1 K , and (c) 39.2 kPa]

3.25 An oblique shock, as shown in Figure 3.29, is incident on a wall at the location where the wall has a convex corner of angle θ . If the Mach number of the incoming air flow is $M_1 = 2.0$, and the angle of the incident oblique shock is $\phi = 31^\circ$, find the angle θ such that there will not be a reflected wave. [Ans: 9.09°]

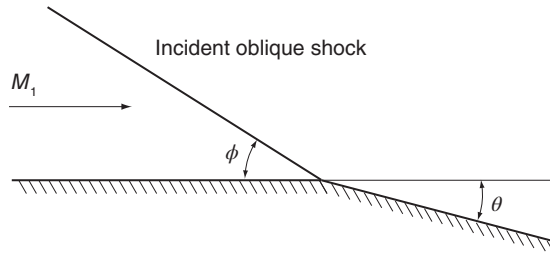


Figure 3.29 An oblique shock incident on a corner.

3.26 Consider the steam flow from a low-pressure nozzle at an angle $\alpha_1 = 65^\circ$, as shown in Figure 3.26. At the inlet of the nozzle, steam is saturated vapor with $\gamma = 1.135$ and at pressure $p_0 = 18$ kPa. Steam exhausts into the interblade space, where pressure is 7 kPa. Find (a) the angle θ by which the flow turns on leaving the nozzle, (b) the far downstream velocity, and (c) its direction α_2 . [Ans: (a) 8.11° , (b) 522.6 m/s, and (c) 56.89°]

3.27 Consider the steam flow from a low-pressure nozzle at angle $\alpha_1 = 65^\circ$. At the inlet of the nozzle, steam is saturated vapor at pressure $p_0 = 18$ kPa. Steam exhausts to the interblade space, where pressure is $p_2 = 7$ kPa. Using the continuity equation, and with the aid of Figure 3.30, find (a) the angle θ by which the flow turns on leaving the nozzle, (b) the far downstream velocity, and (c) its direction α_2 . [Ans: (a) 2.68° , (b) 522.6 m/s, and (c) 62.32°]

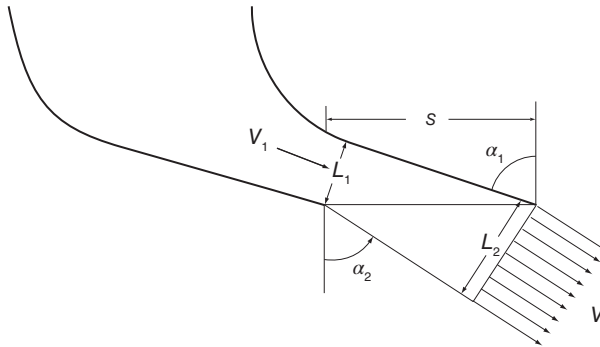


Figure 3.30 Steam nozzle.

3.28 Flat plate is oriented at angle of attack $\alpha_1 = 5^\circ$ to the incoming supersonic stream, as shown in Figure 3.31. The upstream air pressure and temperature are $p_1 = 101.3$ kPa and $T_1 = 288$ K, and the Mach number is $M_1 = 2.9$. (a) Find the pressure above and below the plate. (b) Assuming that the flow after the plate is in the direction of the incoming stream, find the pressure after the plate for the air that flows over the plate and for that which flows under the plate. (Here it is assumed that no slip line forms). [Ans: (a) 68.45 and 145.7 kPa, (b) 101.26 and 101.31 kPa]

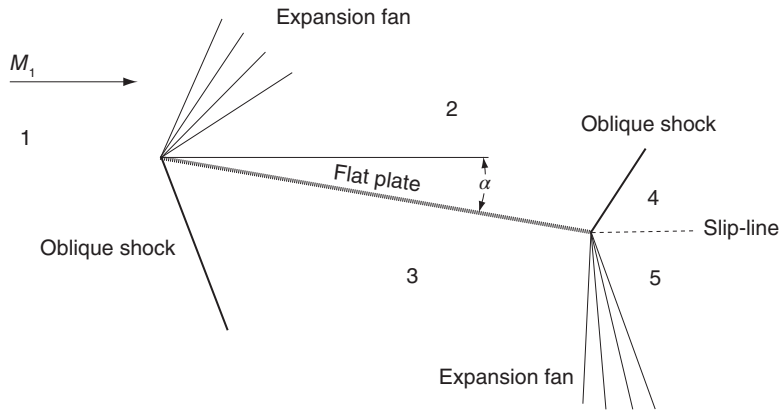


Figure 3.31 Flat plate in a supersonic stream.

3.29 Flat plate is oriented at angle of attack $\alpha_1 = 5^\circ$ to the incoming supersonic stream. The upstream pressure and temperature are $p_1 = 101.3$ kPa and $T_1 = 288$ K, and the Mach number is $M_1 = 2.9$. (a) Find the pressure above and below the plate. (b) Find direction of the slip line after the plate and the entropy change of the air that flows over the plate and the same for that flows under the plate. [Ans: (a) 68.45 and 145.7 kPa, (b) 0.0033° and $\Delta s_{14} = 1.756$ J/(kg K) and $\Delta s_{15} = 1.404$ J/(kg K)]

3.30 Two shocks of different families intersect as shown in Figure 3.32. The wall angles are $\theta_2 = 20^\circ$ and $\theta_3 = 10^\circ$. The incoming air flow has $M_1 = 4.1$, pressure $p_1 = 103$ kPa, and temperature $T_1 = 288$ K. Find the angle ϕ of the slip line, and the entropy differences Δs_{14} and Δs_{15} across it. [Ans: $\phi = 9.54^\circ$, $\Delta s_{14} = 138.1$ J/(kg K), $\Delta s_{15} = 102.9$ J/(kg K)]

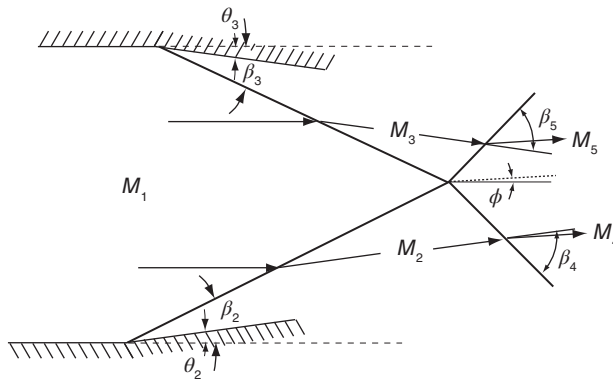


Figure 3.32 Interaction of two shocks of different family.

CHAPTER 4

GAS DYNAMICS OF WET STEAM

The compressible flow equations developed in the previous chapter apply to one-dimensional flow of pure gases or their mixtures, such as superheated steam and dry air. How these equations need to be modified for a wet steam flow is the subject of this chapter. The theory developed below is relevant to understanding the flow of steam in the latter stages of low-pressure steam turbines. There, the flow passage in a blade row is similar to converging–diverging nozzle, but with the important difference that they are not straight. As discussed in the previous chapter, oblique shocks and expansion fans are likely to develop in such flows.

Owing to the specialized topic, readers who wish to move directly to the analysis of turbomachinery may wish to omit this chapter at their first reading and return to it at a later time.

The study of wet steam flows in nozzles and low pressure turbine stages has been under study since the seminal work by Gyarmathy [37] in 1962. Subsequent advances were made by Marble [63] and by Jackson and Davidson [50]. The theory has been examined by Young and coworkers [102–104], by Kirillov and Yablonik [56], and by Wróblewski et al. [102]. As computational fluid dynamics (CFD) calculations have matured, the calculation of wet steam flow was taken up among others, by Starzmann et al. [88]. Nucleation simulations in a nozzle flow were undertaken by Zhang et al. [107], and turbulence models were investigated by Patel et al. [68] in a turbine cascade. Many more studies could be added to this list.

This chapter follows closely the work of Young and Guha [105] for the reason that they handle the topic systematically and completely. They not only formulated and solved the equations for the various relaxation zones that develop after a shock, but Guha [34] also gave the jump conditions across shocks in wet steam. He considered, in addition, condensation shocks and gave exact solutions for them when a particular set of upstream and downstream properties are known. Subsequently, Guha [35] extended the theory to include a carrier gas and in a review article [36] summarized the results, as well as extended them to particle laden flows of dry gases. The aim of the chapter is to review the theoretical development of the flow of wet steam, with the hope that its understanding is useful, even if the practical calculations are carried out with the aid of commercial computer codes.

4.1 COMPRESSIBLE FLOW OF WET STEAM

In compressible one-dimensional flow with area change, the gas is assumed to flow isentropically except across shocks. A new complicating feature in the flow of wet steam is the presence of liquid water in the form of small droplets. In this section, the fundamental theory that takes them into account is reviewed.

4.1.1 Clausius–Clapeyron equation

The specific thermodynamic properties of a two-phase equilibrium mixture of saturated liquid water and its vapor are usually written with the steam quality, x , as the independent variable, since saturation pressure, $p(T_s)$, is a function of temperature alone. As discussed in Chapter 2, in terms of x , the mixture properties for enthalpy, entropy, and specific volume may be written as

$$h = h_f + xh_{fg} \quad s = s_f + xs_{fg} \quad v = v_f + xv_{fg} \quad (4.1)$$

in which h_f stands for the enthalpy of saturated liquid, h_v is the enthalpy for saturated vapor, and the corresponding properties for specific entropy and specific volume are similarly defined. The conventional double subscript “fg” in a term such as $h_{fg} = h_v - h_f$ is retained. When these equations are written in terms of *degree of wetness*, $y = 1 - x$, they are

$$h = yh_f + (1 - y)h_v \quad s = ys_f + (1 - y)s_v \quad v = yv_f + (1 - y)v_v$$

For low-pressure steam, the specific volume of liquid water is much less than that of saturated vapor (at $p = 0.4$ bar about 4000 times less), and if the degree of wetness is, say $y = 0.1$ or smaller, the specific volume may be well approximated by $v = (1 - y)v_v$. Under these conditions, the density of vapor is related to the density of the mixture by the equation

$$\rho_v = (1 - y)\rho \quad (4.2)$$

The symbols without subscripts refer to the properties of the two-phase mixture, except for c_p , which wherever it appears represents the specific heat of vapor.

With these basic definitions understood, the Clausius–Clapeyron equation encountered in the study of thermodynamics is discussed next. Consider therefore a process in which water changes from the saturated liquid state to saturated vapor state at the same pressure.

Integrating the Gibbs equation

$$Tds = dh - vdp \quad (4.3)$$

for this process gives

$$T(s_v - s_f) = h_v - h_f, \quad (4.4)$$

which may also be written as

$$h_v - T_s s_v = h_f - T_s s_f, \quad (4.5)$$

and here, T_s denotes a saturation temperature.

Gibbs function is defined as $g = h - Ts$. Hence, the previous equation shows that the Gibbs function is the same for the two phases at equilibrium. Another name for the Gibbs function is chemical potential, denoted by the symbol μ . It is the fundamental property in the study of phase equilibria. The differential of $\mu = h - Ts$ is

$$d\mu = dh - Tds - sdT$$

Using the second Gibbs equation, $Tds = dh - vdp$, changes this into

$$d\mu = vdp - sdT$$

When this is written for states along the saturated vapor line and the corresponding states on the saturated liquid line, and the two are then subtracted, it leads to

$$d(\mu_v - \mu_f) = v_{fg} dp - s_{fg} dT_s$$

The *saturation pressure* is written without a subscript, but it is functionally related to saturation temperature by $p = p(T_s)$, as was already mentioned.

Since the difference of the chemical potentials is zero as long as the end states are saturation states, it follows that

$$\frac{dp}{dT_s} = \frac{s_{fg}}{v_{fg}} = \frac{h_{fg}}{T_s v_{fg}} \quad (4.6)$$

This is the Clausius–Clapeyron equation. Replacing next v_{fg} by v_v and using the ideal gas relation $pv_v = R_v T_s$ at the saturation state, puts the Clausius–Clapeyron equation into the form

$$\frac{dp}{p} = \frac{h_{fg}}{R_v T_s} \frac{dT_s}{T_s} \quad (4.7)$$

4.1.2 Adiabatic exponent

It is possible to develop an expression for an equivalent adiabatic exponent, γ_e , that reduces the compressible flow equations to the same form as those for pure gases or their mixtures. It is developed next.

For wet steam, the differential of enthalpy is given by

$$dh = (1 - y)dh_v + ydh_f - (h_v - h_f)dy$$

or

$$dh = (1 - y)c_p dT_s + yc_f dT_s - h_{fg} dy$$

With a modified specific heat denoted as

$$c = c_p + \frac{y}{1-y} c_f,$$

this equation becomes

$$dh = (1-y)cdT_s - h_{fg}dy \quad (4.8)$$

For isentropic flow $dh = dp/\rho$ and Eq. (4.8) can be written as

$$\frac{dp}{\rho} - (1-y)cdT_s = -h_{fg}dy \quad (4.9)$$

Differentiating next the ideal gas relation for the vapor

$$p = \rho_v R_v T$$

logarithmically gives

$$\frac{dp}{p} = \frac{d\rho_v}{\rho_v} + \frac{dT}{T}$$

This is, of course, true for superheated steam, and the absence of subscript “s” on T signifies this. However, it is also a good approximation for low-pressure saturated vapor, and at that state, the subscript must be attached to temperature. This is how temperature appears in the equations that follow.

Logarithmic differentiation of Eq. (4.2) leads to

$$\frac{d\rho_v}{\rho_v} = \frac{d\rho}{\rho} - \frac{dy}{1-y}$$

and adding the last two equations gives

$$\frac{dp}{p} - \frac{d\rho}{\rho} - \frac{dT_s}{T_s} = -\frac{dy}{1-y}$$

Eliminating dy between this and Eq. (4.9) gives then

$$\frac{1}{h_{fg}} \frac{dp}{\rho} - \frac{(1-y)cT_s}{h_{fg}} \frac{dT_s}{T_s} = (1-y) \left(\frac{dp}{p} - \frac{d\rho}{\rho} - \frac{dT_s}{T_s} \right)$$

Replacing the density in the first term on the left by $\rho = \rho_v/(1-y)$ and then using the ideal gas relation gives the equation

$$\frac{R_v T_s}{h_{fg}} \frac{dp}{p} - \frac{cT_s}{h_{fg}} \frac{dT_s}{T_s} = \frac{dp}{p} - \frac{d\rho}{\rho} - \frac{dT_s}{T_s}$$

The temperature ratios are now converted to pressure ratios by the Clausius–Clapeyron equation. This gives

$$\left(1 - \frac{2R_v T_s}{h_{fg}} + \frac{cT_s}{h_{fg}} \frac{R_v T_s}{h_{fg}} \right) \frac{dp}{p} = \frac{d\rho}{\rho}$$

By defining the equivalent adiabatic index as

$$\gamma_e = \frac{1}{1 - \frac{2R_v T_s}{h_{fg}} + \frac{c T_s}{h_{fg}} \frac{R_v T_s}{h_{fg}}} \quad (4.10)$$

gives the relation

$$\frac{dp}{p} = \gamma_e \frac{d\rho}{\rho} \quad (4.11)$$

With γ_e replaced by γ , this is the familiar form for isentropic flow in the absence of water droplets. Calculation of γ_e by Eq. (4.10) shows it not to vary greatly, making this a useful approximation for the adiabatic index. In addition, it gives a basis for defining the speed of sound in a two-phase mixture namely, $c_e = \sqrt{\gamma_e p / \rho} = \sqrt{\gamma_e (1 - y) R_v T_s}$.

The values of γ_e are plotted in Figure 4.1. An approximate straight line for $p = 1$ bar is $\gamma_e = 1.144 - 0.275y$. The Zeuner equation, $\gamma_e = 1.135 - 0.1y$, is also plotted. It is seen that the approximate form of the adiabatic exponent represents this experimentally obtained formula reasonably well, although the slope in Zeuner's equation is milder. In order to obtain accurate values for c_p and c_f , the calls

`cpv=XSteam('CpV_p',p)`

`cf=XSteam('CpL_p',p)`

to the function XSteam were used.

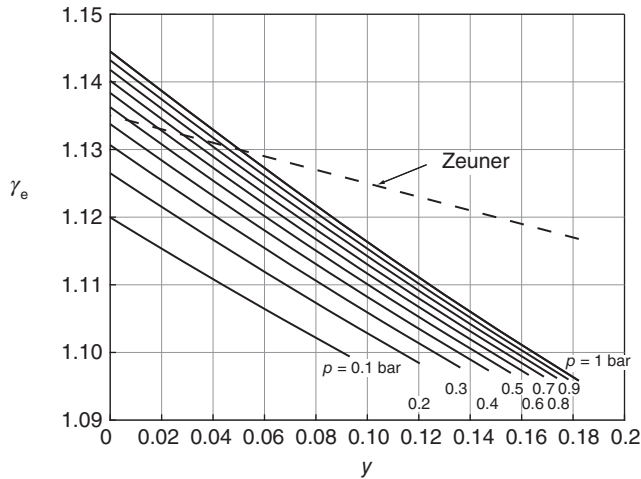


Figure 4.1 Equivalent adiabatic exponent for wet steam for different values of pressure.

■ EXAMPLE 4.1

Wet steam flows isentropically in a diffuser at a rate of $\dot{m} = 0.2$ kg/s, and at the location where the diffuser diameter is $d_1 = 4$ cm, its pressure is $p_1 = 1.0$ bar, and its quality is $x_1 = 0.9$. (a) Find the Mach number at this location. (b) Find the quality of the steam at the location where the pressure of the steam is $p_2 = 1.1$ bar. (c) Find the diameter of the diffuser at this location. (d) Find the Mach number at this location. Assume phase equilibrium between the liquid and vapor during the process.

Solution: (a) To find the Mach number, the flow velocity and speed of sound need to be determined. The velocity is given by

$$V_1 = \frac{\dot{m}}{\rho_1 A_1}$$

The flow area is

$$A_1 = \frac{1}{4}\pi D_1^2 = \frac{1}{4} \cdot \pi \cdot 0.04^2 = 0.001257 \text{ m}^2$$

The saturation specific volume of the vapor is $v_v = 1.694 \text{ m}^3/\text{kg}$, and therefore, the mixture specific volume and density are

$$v_1 = x_1 v_v = 0.9 \cdot 1.694 = 1.5246 \text{ m}^3/\text{kg} \quad \rho_1 = \frac{1}{v_1} = 0.6559 \text{ kg/m}^3$$

The entropy is calculated from

$$s_1 = s_f + x_1 s_{fg} = 1.3026 + 0.9 \cdot 6.0562 = 6.7532 \text{ kJ}/(\text{kg K})$$

The velocity becomes

$$V_1 = \frac{\dot{m}}{\rho_1 A_1} = \frac{0.2}{0.6559 \cdot 0.001257} = 242.6 \text{ m/s}$$

The adiabatic index is calculated from Eq. (4.10). The latent heat of vaporization and specific heats of vapor and liquid at the saturation temperature $T_s = 99.61^\circ \text{C}$ are

$$h_{fg} = 2257 \text{ kJ/kg} \quad c_p = 2.076 \text{ kJ}/(\text{kg K}) \quad c_f = 4.216 \text{ kJ}/(\text{kg K})$$

so that

$$c = c_p + \frac{y_1}{1 - y_1} c_f = 2.067 + \frac{0.1}{0.9} 4.216 = 2.544 \text{ kJ}/(\text{kg K})$$

and therefore

$$\gamma_e = \left(1 - \frac{2 \cdot 0.461 \cdot 372.8}{2257} + \frac{2.544 \cdot 372.8}{2257} \cdot \frac{0.461 \cdot 372.8}{2257} \right)^{-1} = 1.137,$$

and the speed of sound is

$$c_1 = \sqrt{\gamma_e p_1 / \rho_1} = \sqrt{1.137 \cdot 100000 / 0.656} = 416.3 \text{ m/s}$$

Hence, the Mach number is $M_1 = V_1 / c_1 = 242.6 / 416.3 = 0.583$. The flow is subsonic, and thus, no shocks are formed.

(b) With $p_2 = 1.1 \text{ bar}$, and the flow assumed isentropic, so that $s_2 = s_1$, the quality at this state is

$$x_2 = \frac{s_2 - s_f}{s_{fg}} = \frac{6.7532 - 1.3328}{7.3268 - 1.3328} = 0.9043$$

(c) The area A_2 can be determined using the mass balance, once V_2 and ρ_2 are known. Density is given by

$$\rho_2 = \frac{\rho_{v2}}{x_2} = \frac{0.6453}{0.9043} = 0.7136 \text{ kg/m}^3$$

Velocity, V_2 , is obtained by first calculating h_0 and h_2 . They are

$$h_0 = h_1 + \frac{1}{2}V_1^2 = 2449.2 + \frac{242.6^2}{2 \cdot 1000} = 2478.6 \text{ kJ/kg}$$

and

$$h_2 = h_f + x_2 h_{fg} = 428.8 + 0.9043 \cdot (2679.2 - 428.8) = 2463.8 \text{ kJ/kg}$$

so that

$$V_2 = \sqrt{2(h_0 - h_2)} = \sqrt{2(2478.6 - 2463.8)1000} = 172.2 \text{ m/s}$$

Therefore,

$$A_2 = A_1 \frac{\rho_1 V_1}{\rho_2 V_2} = 0.001257 \frac{0.6559 \cdot 242.6}{0.7136 \cdot 172.2} = 0.001628 \text{ m}^2$$

and

$$D_2 = \sqrt{\frac{4A_2}{\pi}} = \sqrt{\frac{4 \cdot 0.001628}{\pi}} = 4.55 \text{ cm}$$

(d) The speed of sound and Mach number at this state are

$$c_2 = \sqrt{\frac{\gamma_e p_2}{\rho_2}} = \sqrt{\frac{1.137 \cdot 110000}{0.7136}} = 418.6 \text{ m/s} \quad M_2 = \frac{V_2}{c_2} = \frac{172.3}{418.6} = 0.411$$

The calculations illustrated in this example work as long as the flow remains in the two-phase region and need to be modified when all the liquid evaporates during the process. Such a modification is needed in one of the exercises.

4.2 CONSERVATION EQUATIONS FOR WET STEAM

The applications of interest in this chapter involve wet steam with $0 < y < 0.2$, and the simplest model assumes that all the droplets are *monodisperse*, i.e. of equal size. The droplets are further assumed neither to break up nor to coagulate to form larger droplets. For this reason, the number of droplets in a given volume remains constant. The number of droplets is obtained by integrating the number of droplets per unit volume over the given volume. Thus, the number of droplets is

$$N = \int_V \frac{n \rho_v}{1 - y} dV$$

In the integrand, n is the *number of droplets per unit mass of the mixture* and $\rho_v/(1-y)$ is the mixture density. Hence, their product is the number of droplets per unit volume. This number remains constant for a control volume that moves with the fluid. Hence

$$\frac{D}{Dt} \int_V \frac{n\rho_v}{1-y} dV = 0$$

The time derivative is the total derivative, or *derivative following the motion*, denoted by capital D . Using the Reynolds transport theorem, encountered in the first course in fluid dynamics, this equation can be cast into the form

$$\int_V \frac{\partial}{\partial t} \left(\frac{n\rho_v}{1-y} \right) dV + \int_A \frac{n\rho_v}{1-y} V_i dA = 0$$

in which V_i is the droplet velocity, and since the droplets are monodisperse, each droplet is assumed to have the same velocity. In steady flow, the unsteady term drops out. Thus, for steady one-dimensional flow in a *constant area duct*, this equation shows that the integrand is independent of the location in the duct, so that

$$\frac{d}{dx} \left(\frac{n\rho_v V_i}{1-y} \right) = 0 \quad (4.12)$$

When shocks appear in variable area ducts, it may be still permissible to cancel the areas, in the balance equations across the shock, if the shock thickness is not unduly large. In contrast to the thin aerodynamic shocks discussed in the previous chapter, it turns out that shocks in wet steam are thicker and to be able to cancel the areas in shock relations would require a constant area duct or a slowly diverging one. The general equations for variable area ducts will be discussed later.

The term in the parenthesis in the aforementioned equation represents the *flux* of droplets. That is the rate at which the droplets flow per unit area and time. As mentioned, the physical meaning of this equation is that the number of droplets remains constant in the flow.

The mass balance leads to a similar expression. If the mass of a single droplet is denoted by symbol m , then $y = nm$ is the mass of liquid water per unit mass of the mixture. The mass flow rate consists of vapor flow and liquid flow. The vapor flux is $\rho_v V_v$, in which V_v is the vapor velocity. The liquid flux is $mn\rho_v V_i/(1-y)$ or $y\rho_v V_i/(1-y)$, and the mass conservation requires that their sum remains constant. Thus

$$\frac{d}{dx} \left(\rho_v V_v + \frac{y\rho_v V_i}{1-y} \right) = 0 \quad (4.13)$$

The momentum balance

$$\frac{d}{dx} \left(p + \rho_v V_v^2 + \frac{y\rho_v V_i^2}{1-y} \right) = 0 \quad (4.14)$$

is obtained similarly. This equation shows that the sum of pressure and the momentum fluxes of the vapor and liquid remain constant.

With heat transfer absent, the energy equation reduces to

$$\frac{d}{dx} \left[\rho_v V_v \left(h_v + \frac{1}{2} V_v^2 \right) + \frac{y\rho_v V_i}{1-y} \left(h_i + \frac{1}{2} V_i^2 \right) \right] = 0 \quad (4.15)$$

The ideal gas relation for the vapor and the Clausius–Clapeyron equation are two additional equations to determine the unknowns.

4.2.1 Relaxation times

When a shock forms in wet steam flow, the vapor properties change across the shock similarly to those in a pure gas; but the droplet temperature lags the vapor temperature, and since the velocity of the vapor decreases after a shock, whereas the velocity of the droplets are not immediately affected, it takes some time to reduce their velocity to that of the vapor. In addition, the hotter vapor causes evaporation of the droplets, but this takes even longer. The times to adjust to the equilibrium values are called relaxation times. Expressions for these relaxation times are developed in this section.

Consider a small spherical liquid droplet of mass m , evaporating at the rate M to the vapor. Its mass decreases at this rate, so that

$$\frac{Dm}{Dt} = -M \quad (4.16)$$

If the droplets move with velocity \mathbf{V}_i , then, this derivative, for a general property Φ , has the form

$$\frac{D\Phi}{Dt} = \frac{\partial\Phi}{\partial t} + \mathbf{V}_i \cdot \nabla\Phi$$

or in one-dimensional flow in the x -direction

$$\frac{D\Phi}{Dt} = \frac{\partial\Phi}{\partial t} + V_i \frac{\partial\Phi}{\partial x}$$

For steady flow, Eq. (4.16) can thus be replaced by

$$V_i \frac{dm}{dx} = -M \quad (4.17)$$

In order to integrate this, the dependence of V_i and M as functions of x would need to be known.

Inertial relaxation. Consider now the drag on a liquid drop as it moves with velocity V_i through vapor that itself moves with velocity V_v . For sufficiently small droplets, the drag force obeys the Stokes law $F = 6\pi a\mu(V_v - V_i)$, in which μ is the viscosity of the vapor and a is the radius of the droplet. Thus, if the droplet and the vapor move in the positive x -direction with vapor velocity larger than that of the droplet, then, the drag force is in the positive direction, and Newton's second law reduces to

$$m \frac{DV_i}{Dt} = F \quad (4.18)$$

In this form of Newton's second law, the mass m has been assumed to be constant, even if it decreases by evaporation. This kind of *quasi-steady* assumption is often used in order to keep the resulting equations simple enough that an analytical solution is possible. The validity of the assumption can be checked against numerical computer calculations of the more general equations.

For steady one-dimensional flow, this becomes

$$V_i \frac{dV_i}{dx} + \frac{9\mu}{2a^2\rho_i} (V_i - V_v) = 0 \quad (4.19)$$

in which the mass of the droplet has been written as $m = \rho_i \frac{4}{3}\pi a^3$. The coefficient of the second term has the dimensions of inverse time. By generalizing it, a time constant is defined by

$$\tau_i = \frac{2a^2\rho_i}{9\mu} [\phi(Re) + 4.5Kn] \quad (4.20)$$

Now Eq. (4.19) takes the form

$$\frac{dV_i}{dx} + \frac{V_i - V_v}{V_i\tau_i} = 0 \quad (4.21)$$

The expression for the time constant extends the validity of the Stokes drag law to somewhat larger Reynolds numbers and to small enough droplets that the Knudsen number, Kn , is no longer small. Reynolds number and Knudsen number are defined by the expressions

$$Re = \frac{2a\rho_v|V_v - V_i|}{\mu} \quad Kn = \frac{\lambda}{2a}$$

Here, λ is the mean free path [92], and it can be calculated from

$$\lambda = \frac{\mu}{p} \sqrt{\frac{\pi R_v T_v}{2}} \quad (4.22)$$

The Reynolds number dependence is given by

$$\phi(Re) = \frac{1}{1 + 0.15Re^{0.687}}$$

Droplet temperature relaxation. To determine the relaxation time for droplet temperature equilibration, the energy equation for a droplet is written as

$$mV_i \frac{dh_i}{dx} = -(h_v - h_i)M - Q \quad (4.23)$$

The increase in the droplet temperature is caused by both M and Q , both of which are negative, as seen below. The first term represents the net rate at which energy is transferred to the droplet as a result of phase change, for the energy of the condensing molecules is larger than that of the evaporating ones. If the approximation $h_v - h_i = h_{fg}$ is used, then, this denotes the energy of the phase change. The second term, Q , is the heat transfer given by

$$Q = \frac{4\pi a k_v}{1 + 4.5Kn/Pr} (T_i - T_v) \quad (4.24)$$

in which $Pr = \mu_v/k_v c_p$ is the Prandtl number. The numerator is obtained by considering conduction from vapor at the temperature T_v to a droplet at temperature T_i . Since $T_v > T_i$, this term is negative. It would be more accurate to use the saturation temperature, T_s , rather than T_i as the surface temperature, but this would lead to more complicated equations.

The expression for the evaporation is derived from the kinetic theory of gases. It is given by

$$M = 4\pi a^2 \frac{2q}{2-q} \left[\frac{p_s(T_i)}{\sqrt{2\pi R_v T_i}} - \frac{p}{\sqrt{2\pi R_v T'}} \right] \quad (4.25)$$

This expression contains the surface area of a droplet of radius a and a factor involving q that accounts for the fact that not all the molecules incident to the droplets get stuck to the surface. The first term in the square brackets represents the rate at which molecules leave the droplet, emanating from temperature T_i , and the second term accounts for the incoming molecules originating from the effective temperature T' . This temperature is defined by

$$\frac{T' - T_v}{T_i - T_v} = \frac{1}{1 + 4.5Kn/Pr}$$

In the continuum case, when $Kn \rightarrow 0$, then $T' \rightarrow T_i$. For highly rarefied vapor, $Kn \rightarrow \infty$ and $T' \rightarrow T_v$. When evaporation is larger than condensation, the term in the brackets is positive, and Eq. (4.17) shows that the mass of the droplet decreases.

In order to cast Eq. (4.17) to a form from which the relaxation phenomena is apparent, Eq. (4.25) needs to be linearized. Denoting first

$$\alpha = \frac{1}{1 + 4.5Kn/Pr} \quad \text{from which} \quad 4Kn = \frac{8}{9} \left(\frac{1-\alpha}{\alpha} \right) Pr \quad (4.26)$$

so that

$$T' = T_v + \alpha(T_i - T_v) = T_i - (1 - \alpha)(T_i - T_v)$$

Now assuming that $(T_i - T_v)/T_i \ll 1$ and expanding $1/\sqrt{T'}$ by the binomial theorem gives

$$\frac{1}{\sqrt{T'}} = \frac{1}{\sqrt{T_i}} \left[1 + \frac{1}{2}(1 - \alpha) \frac{T_i - T_v}{T_i} \right] \dots$$

Furthermore,

$$p = p_s(T_i) + \left(\frac{dp}{dT} \right)_{T=T_i} (T_s - T_i) + \dots,$$

and using the Clausius–Clapeyron equation, this becomes

$$p = p_s(T_i) + \frac{h_{fg}}{R_v T_i} \frac{(T_v - T_i)}{T_i} p_s(T_i) + \dots$$

Substituting this and the expansion for $1/\sqrt{T'}$ into Eq. (4.25) gives

$$M = -4\pi a^2 \frac{2q}{2-q} \frac{p(T_i)}{\sqrt{2\pi R_v T_i}} \left[\frac{h_{fg}}{R_v T_i} \frac{(T_s - T_i)}{T_i} + \frac{1}{2}(1 - \alpha) \frac{(T_i - T_v)}{T_i} \right] + \dots$$

Finally, replacing T_i by T_s in the denominators in this equation leads to the approximate form

$$M = -4\pi a^2 \frac{2q}{2-q} \frac{p(T_i)}{\sqrt{2\pi R_v T_s}} \left[\frac{h_{fg}}{R_v T_s} \frac{(T_s - T_i)}{T_s} + \frac{1}{2}(1 - \alpha) \frac{(T_i - T_v)}{T_s} \right] \quad (4.27)$$

The far downstream temperature is obtained by noting that for large value of x , the left-hand side of Eq. (4.23) tends to zero, and after Eq. (4.22) is expressed in terms of Knudsen number, the right-hand side reduces to

$$\frac{h_{fg}}{c_p T_s} \frac{Pr}{4Kn} \left(\frac{2q}{2-q} \right) \left[\frac{h_{fg}}{R_v T_s} \left(\frac{T_s - T_{i\infty}}{T_s} \right) + \frac{1}{2}(1-\alpha) \left(\frac{T_{i\infty} - T_v}{T_s} \right) \right] = \alpha(T_{i\infty} - T_v)$$

in which $T_{i\infty}$ represents the droplet temperature at the end of the relaxation zone. It is assumed that T_v remains constant during this process. Expressing the Knudsen number in terms of α and introducing the parameters

$$\beta = \frac{h_{fg}}{c_p T_s} \frac{9}{8(1-\alpha)} \left(\frac{2q}{2-q} \right) \quad \text{and} \quad H = \frac{h_{fg}}{R_v T_s},$$

this equation reduces to

$$\beta \left[H(1 - \bar{T}_{i\infty}) + \frac{1}{2}(1-\alpha)(\bar{T}_{i\infty} - \bar{T}_v) \right] = \bar{T}_{i\infty} - \bar{T}_v$$

into which the definitions $\bar{T}_v = T_v/T_s$ and $\bar{T}_{i\infty} = T_{i\infty}/T_s$ have been introduced. Now letting

$$A = \frac{1-\alpha}{2H} - \frac{1}{\beta H} \quad (4.28)$$

and solving for $T_{i\infty}$ gives

$$T_{i\infty} = T_s - \frac{A}{1-A}(T_v - T_s) \quad (4.29)$$

In the relaxation zone, Eq. (4.23) can be written as

$$\bar{c} V_i \frac{dT_i}{dx} = \left[\beta \left(\frac{1-\alpha}{2} \right) - 1 - \beta H \right] (T_i - 1) + \left[\beta \left(\frac{1-\alpha}{2} \right) - 1 \right] \frac{A-1}{A} (T_{i\infty} - 1)$$

in which

$$\bar{c} = \frac{\rho_1 c_1 a^2}{3\alpha k}$$

The RHS can be simplified, and this equation can be written as

$$\bar{c} V_i \frac{dT_i}{dx} = -(1-A)H\beta(\bar{T}_i - \bar{T}_{i\infty})$$

Rearranging Eq. (4.28) to express β in terms of A , gives $\beta = 2/(1-\alpha-2AH)$, and substituting this to the last equation gives

$$V_i \frac{dT_i}{dx} + \frac{2(1-A)H}{(1-\alpha-2AH)\bar{c}} (T_i - T_{i\infty}) = 0 \quad (4.30)$$

If the time scale is defined as

$$\tau_D = \frac{\bar{c}(1-\alpha-2AH)}{2(1-A)H},$$

Then, this equation has the form

$$\frac{dT_i}{dx} + \frac{(T_i - T_{i\infty})}{V_i \tau_D} = 0 \quad (4.31)$$

The time constant can be reworked into the form

$$\tau_D = \frac{1}{1 - A} \left(\frac{2 - q}{2q} \right) \left(\frac{R_v T_s}{h_{fg}} \right)^2 \frac{\rho_i c_i a}{3R_v} \frac{\sqrt{2\pi R_v T_s}}{p} \quad (4.32)$$

Usually, the choice $q = 1$ is made.

Vapor relaxation. Combining Eqs. (4.17) and (4.23) gives

$$(h_v - h_i) V_i \frac{dm}{dx} = m V_i \frac{dh_i}{dx} + Q$$

Since $y = nm$, multiplying both sides by y/mV_i gives

$$(h_v - h_i) \frac{y}{m} \frac{dm}{dx} = y \frac{dh_i}{dx} + \frac{yQ}{mV_i}$$

Substituting Eq. (4.24) into this gives

$$(h_v - h_i) \frac{y}{m} \frac{dm}{dx} = y c_i \frac{dT_i}{dx} + \frac{3y k_v (T_i - T_v)}{\rho_i a^2 V_i} \left(1 + 4.5 \frac{Kn}{Pr} \right)$$

Using Eq. (4.31) and defining the time constant

$$\tau_T = \frac{(1 - y)}{y} \frac{\rho_i c_p a^2}{3k_v} \left(1 + 4.5 \frac{Kn}{Pr} \right) \quad (4.33)$$

gives finally the equation

$$(h_v - h_i) \frac{y}{m} \frac{dm}{dx} = \frac{y c_i (T_s - T_i)}{V_i \tau_D} + \frac{(1 - y) c_p (T_s - T_v)}{V_i \tau_T} \quad (4.34)$$

In the first term on the right, the droplet temperature, $T_{i\infty}$ after the relaxation is complete has been replaced by the saturation temperature T_s , without introducing, but a small error. In the second term, similarly T_i has been replaced by T_s , and this substitution will be seen in the subsequent results to be justified. The equation now shows that, as both the droplet and vapor temperature approach the saturation temperature, the right-hand side approaches zero, and the mass of the droplet remains constant.

The magnitudes of the scales are such that

$$\tau_D \ll \tau_I \ll \tau_T,$$

and their values for a range of droplet radii are seen from Figure 4.2. This means that the droplet temperature relaxation takes place first, followed by the inertial relaxation, and the vapor relaxation is the slowest.

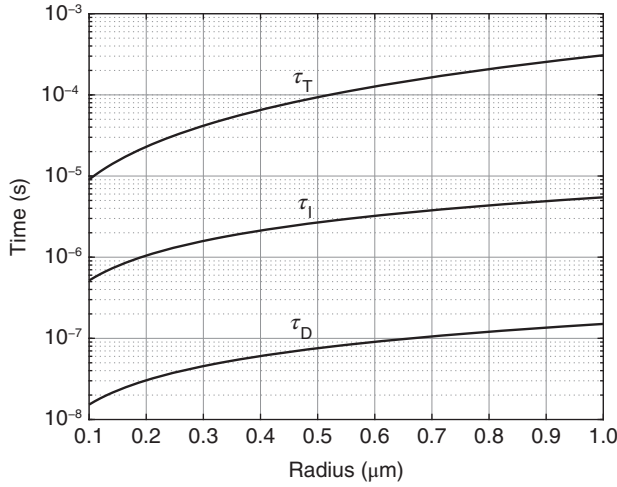


Figure 4.2 Time constants for $p = 0.5$ bar, $y = 0.1$, $\gamma = 1.32$, $V_i = 496$ m/s, and $V_v = 511$ m/s.

4.2.2 Conservation equations in their working form

Sound propagates at different speeds in different relaxation zones. In this section, the conservation equations are written in forms from which the different sound speeds are more readily determined.

Equation (4.13) can be written as

$$\frac{d}{dx} \left(\rho_v V_v + \frac{y \rho_v V_i}{1 - y} \right) = 0 \quad (4.35)$$

Expanding Eq. (4.12) for the number flux of droplets as

$$\frac{d}{dx} \left(\frac{n \rho_v V_i}{1 - y} \right) = \frac{\rho_v V_i}{1 - y} \frac{dn}{dx} + n \frac{d}{dx} \left(\frac{\rho_v V_i}{1 - y} \right) = 0$$

and multiplying this by m leads to

$$\frac{m \rho_v V_i}{1 - y} \frac{dn}{dx} + y \frac{d}{dx} \left(\frac{\rho_v V_i}{1 - y} \right) = 0$$

Expanding next Eq. (4.35) gives

$$\frac{d}{dx} (\rho_v V_v) + y \frac{d}{dx} \left(\frac{\rho_v V_i}{1 - y} \right) + \frac{\rho_v V_i}{1 - y} \frac{dy}{dx} = 0 \quad (4.36)$$

and combining this with the previous equation gives

$$\frac{d}{dx} (\rho_v V_v) - \frac{m \rho_v V_i}{1 - y} \frac{dn}{dx} + \frac{\rho_v V_i}{1 - y} \frac{dy}{dx} = 0$$

Substituting $y = nm$ into the third term, expanding it and then cancelling, leads to

$$\frac{d}{dx} (\rho_v V_v) + \frac{y \rho_v V_i}{1 - y} \frac{1}{m} \frac{dm}{dx} = 0 \quad (4.37)$$

After expanding the first term in this equation and dividing through by $\rho_v V_v$, yields

$$\frac{1}{V_v} \frac{dV_v}{dx} + \frac{1}{\rho_v} \frac{d\rho_v}{dx} + \frac{yV_i}{V_v(1-y)} \frac{1}{m} \frac{dm}{dx} = 0$$

Logarithmic differentiation of the ideal gas relation gives

$$\frac{1}{p} \frac{dp}{dx} = \frac{1}{\rho_v} \frac{d\rho_v}{dx} + \frac{1}{T_v} \frac{dT_v}{dx},$$

and eliminating the term $d\rho_v/dx$ between the previous two equations leads to

$$\frac{1}{p} \frac{dp}{dx} - \frac{1}{T_v} \frac{dT_v}{dx} + \frac{1}{V_v} \frac{dV_v}{dx} + \frac{V_i}{V_v} \frac{y}{1-y} \frac{1}{m} \frac{dm}{dx} = 0 \quad (4.38)$$

The momentum balance, Eq. (4.14)

$$\frac{dp}{dx} + \frac{d}{dx}(\rho_v V_v^2) + \frac{d}{dx} \left(\frac{y\rho_v V_i^2}{1-y} \right) = 0$$

when expanded out gives

$$\frac{dp}{dx} + V_v \frac{d}{dx}(\rho_v V_v) + \rho_v V_v \frac{dV_v}{dx} + V_i \frac{d}{dx} \left(\frac{y\rho_v V_i}{1-y} \right) + \frac{y\rho_v V_i}{1-y} \frac{dV_i}{dx} = 0$$

Using Eq. (4.35), the fourth term can be replaced by a term that can be combined with the second. This leads to equation

$$\frac{dp}{dx} + (V_v - V_i) \frac{d}{dx}(\rho_v V_v) + \rho_v V_v \frac{dV_v}{dx} + \frac{y\rho_v V_i}{1-y} \frac{dV_i}{dx} = 0$$

Equation (4.35) is next used to rewrite the second term in this equation, after which the entire equation is divided by $p = \rho_v R_v T_v$. This results in

$$\frac{1}{p} \frac{dp}{dx} + \frac{V_v^2}{R_v T_v} \left[\frac{1}{V_v} \frac{dV_v}{dx} + \frac{yV_i}{(1-y)V_v^2} \frac{dV_i}{dx} + \frac{V_i - V_v}{V_v^2} \frac{yV_i}{(1-y)} \frac{1}{m} \frac{dm}{dx} \right] = 0 \quad (4.39)$$

Energy balance, Eq. (4.15) can also be recasted. Differentiating gives

$$\begin{aligned} \left(h_v + \frac{1}{2} V_v^2 \right) \frac{d(\rho_v V_v)}{dx} + \rho_v V_v \frac{d}{dx} \left(h_v + \frac{1}{2} V_v^2 \right) + \left(h_i + \frac{1}{2} V_i^2 \right) \frac{d}{dx} \left(\frac{y\rho_v V_i}{1-y} \right) \\ + \frac{y\rho_v V_i}{1-y} \frac{d}{dx} \left(h_i + \frac{1}{2} V_i^2 \right) = 0 \end{aligned}$$

Making use of Eqs. (4.35) and (4.37), puts this equation into the form

$$\begin{aligned} \rho_v V_v c_p \frac{dT_v}{dx} + \rho_v V_v \frac{dV_v}{dx} + (h_i - h_v) \frac{y\rho_v V_i}{1-y} \frac{1}{m} \frac{dm}{dx} + \frac{1}{2} (V_i^2 - V_v^2) \frac{y\rho_v V_i}{1-y} \frac{1}{m} \frac{dm}{dx} \\ + \frac{y\rho_v V_i c_i}{1-y} \frac{dT_i}{dx} + \frac{y\rho_v V_i^2}{1-y} \frac{dV_i}{dx} = 0 \end{aligned}$$

and this can be further simplified to

$$\begin{aligned} & \frac{1}{T_v} \frac{dT_v}{dx} + \frac{y}{1-y} \frac{V_i}{V_v} \frac{c_i}{c_p} \frac{1}{T_v} \frac{dT_i}{dx} + \frac{V_v^2}{c_p T_v} \\ & \times \left[\frac{1}{V_v} \frac{dV_v}{dx} + \frac{y}{1-y} \left(\frac{V_i}{V_v} \right)^2 \frac{1}{V_v} \frac{dV_i}{dx} - \frac{(h_v - h_i + \frac{1}{2}V_v^2 - \frac{1}{2}V_i^2)}{c_p T_v} \frac{V_i}{V_v} \frac{y}{1-y} \frac{1}{m} \frac{dm}{dx} \right] \\ & = 0 \end{aligned} \quad (4.40)$$

When Eq. (4.34) is substituted for dm/dx in Eqs. (4.39) and (4.40), this substitution gives terms that are proportional to $\Delta T_i \cdot \Delta V_v$ and $\Delta T_v \cdot \Delta V_v$. These terms are small, being products of small differences. These second-order terms are dropped in the following, and the working form of the conservation equations can be written as

$$\frac{1}{p} \frac{dp}{dx} - \frac{1}{T_v} \frac{dT_v}{dx} + \frac{1}{V_v} \frac{dV_v}{dx} + \frac{V_i}{V_v} \frac{y}{1-y} \frac{1}{m} \frac{dm}{dx} = 0 \quad (4.41)$$

$$\frac{1}{p} \frac{dp}{dx} + \frac{V_v^2}{R_v T_v} \left[\frac{1}{V_v} \frac{dV_v}{dx} + \frac{y V_i}{(1-y) V_v^2} \frac{dV_i}{dx} \right] = 0 \quad (4.42)$$

$$\begin{aligned} & \frac{1}{T_v} \frac{dT_v}{dx} + \frac{y}{1-y} \frac{V_i}{V_v} \frac{c_i}{c_p} \frac{1}{T_v} \frac{dT_i}{dx} + \frac{V_v^2}{c_p T_v} \left[\frac{1}{V_v} \frac{dV_v}{dx} + \frac{y}{1-y} \left(\frac{V_i}{V_v} \right)^2 \frac{1}{V_v} \frac{dV_i}{dx} \right] \\ & - \frac{(h_v - h_i)}{c_p T_v} \frac{V_i}{V_v} \frac{y}{1-y} \frac{1}{m} \frac{dm}{dx} = 0 \end{aligned} \quad (4.43)$$

4.2.3 Sound speeds

In this section, the sound speeds in different relaxation zones are discussed. The three differences

$$\Delta T_i = T_s - T_i \quad \Delta V_i = V_v - V_i \quad \Delta T = T_i - T_v \quad (4.44)$$

are defined, and it is expected that these tend toward zero during the relaxation process. In the first definition, T_s has been substituted for $T_{i\infty}$, for these are close to the same after the droplet temperature relaxation is complete. The three relaxation equations are

$$\frac{dT_i}{dx} - \frac{\Delta T_i}{V_i \tau_D} = 0 \quad (4.45)$$

$$\frac{dV_i}{dx} - \frac{\Delta V_i}{V_i \tau_I} = 0 \quad (4.46)$$

$$(h_v - h_i) \frac{y}{m} \frac{dm}{dx} = \frac{(1-y)c_p \Delta T}{V_i \tau_T} + \frac{y c_i \Delta T_i}{V_i \tau_D} \quad (4.47)$$

As was seen previously, the time constants are such that the *droplet relaxation* takes place in the shortest zone, followed by *inertial relaxation*, and then *vapor relaxation* requires the longest zone for completion. To separate these zones clearly, four model conditions are assumed.

First, none of the variables are assumed to have relaxed to their equilibrium values. This is achieved by assuming that the time constants all tend to be infinitely large. That is $\tau_D \rightarrow \infty$, $\tau_I \rightarrow \infty$, and $\tau_T \rightarrow \infty$.

Second case has only the droplet temperature in equilibrium. Intuitively, this means that the droplet temperature $T_i \rightarrow T_{i\infty}$, or as already been mentioned, this condition can be approximated by $T_i \rightarrow T_s$. Mathematically, this limit is obtained by letting $\tau_D \rightarrow 0$ and $\Delta T_i \rightarrow 0$ in such a way that their ratio remains finite. Neither inertial nor vapor relaxation has taken place, and this is assured by the conditions $\tau_I \rightarrow \infty$ and $\tau_T \rightarrow \infty$.

Third case consists of both the droplet temperature and inertial relaxation being complete, but the vapor relaxation has not yet taken place. Again, the limits $\tau_D \rightarrow 0$ and $\Delta T_i \rightarrow 0$ in such a way that their ratio remains finite, fulfills the condition that droplet temperature relaxation is complete, and the limits $\tau_I \rightarrow 0$ and $\Delta V_i \rightarrow 0$ with their ratio remaining finite leads to complete inertial relaxation. Since vapor relaxation has not taken place, the condition $\tau_T \rightarrow \infty$ reflects this.

Fourth and final case consist of vapor equilibration. The appropriate limits are now that $\tau_D \rightarrow 0$ and $\Delta T_i \rightarrow 0$ with their ratio remaining finite and $\tau_I \rightarrow 0$ and $\Delta V_i \rightarrow 0$ with their ratio remaining finite. Finally, the limits $\tau_T \rightarrow 0$ and $\Delta T \rightarrow 0$, and with a finite value for their ratio, gives the condition for vapor relaxation.

To illustrate the development of the expression for the sound speed, consider the second case. The droplet temperature relaxation is complete, but the inertial and vapor relaxation have not taken place. Since $\Delta T_i \rightarrow 0$, when $\tau_D \rightarrow 0$, with their ratio remaining constant, then, $T_i = T_s$ and $dT_i/dx = dT_s/dx$. In addition, with $\tau_I \rightarrow \infty$, Eq. (4.46) shows that

$$\frac{dV_i}{dx} = 0$$

Furthermore, the condition $\tau_T \rightarrow \infty$ reduces Eq. (4.47) to the form

$$\frac{1}{m} \frac{dm}{dx} = \frac{c_i T_s}{h_{fg}} \frac{1}{T_s} \frac{dT_s}{dx}$$

Mass, momentum, and energy conservation equations can now be written as

$$\frac{1}{p} \frac{dp}{dx} - \frac{1}{T_v} \frac{dT_v}{dx} + \frac{1}{V_v} \frac{dV_v}{dx} + \frac{y}{1-y} \frac{V_i}{V_v} \frac{c_i T_s}{h_{fg}} \frac{1}{T_s} \frac{dT_s}{dx} = 0 \quad (4.48)$$

$$\frac{1}{p} \frac{dp}{dx} + \frac{V_v^2}{R_v T_v} \frac{1}{V_v} \frac{dV_v}{dx} = 0 \quad (4.49)$$

$$\frac{1}{T_v} \frac{dT_v}{dx} + \frac{c_i}{c_p} \frac{y}{1-y} \frac{V_i}{V_v} \frac{1}{T_s} \frac{dT_s}{dx} + \frac{V_v^2}{c_p T_v} \frac{1}{V_v} \frac{dV_v}{dx} - \frac{c_i}{c_p} \frac{y}{1-y} \frac{V_i}{V_v} \frac{1}{T_s} \frac{dT_s}{dx} = 0 \quad (4.50)$$

The second and fourth term cancel in this equation, and comparing the reduced equation to Eq. (4.49) shows that

$$\frac{1}{T_v} \frac{dT_v}{dx} = \frac{R_v}{c_p} \frac{1}{p} \frac{dp}{dx}$$

Substituting this into Eq. (4.48) and making use of the Clausius–Clapeyron gives

$$\left(1 - \frac{R_v}{c_p} - \frac{R_v T_v}{V_v^2} + \frac{y}{1-y} \frac{V_i}{V_v} \frac{c_i T_s}{h_{fg}} \frac{R_v T_s}{h_{fg}} \right) \frac{dp}{dx} = 0$$

The coefficient of dp/dx must therefore be zero. Introducing $c_p = \gamma R_v/(\gamma - 1)$ gives

$$\frac{\gamma R_v T_v}{V_v^2} = 1 + \frac{y}{1-y} \frac{V_i}{V_v} \frac{\gamma c_i}{R_v} \left(\frac{R_v T_s}{h_{fg}} \right)^2$$

Assuming that all the variable changes are small, then $V_v = c_{e1}$ and the ratio $V_i/V_v \approx 1$, so that the speed of sound is given by

$$c_{e1}^2 = \frac{\gamma R_v T_v}{1 + \frac{y}{1-y} \frac{\gamma c_i}{R_v} \left(\frac{R_v T_s}{h_{fg}} \right)^2} \quad (4.51)$$

Having established this speed of sound, consider next the situation in which all the relaxation processes are complete. In this case, the limits $\Delta T_i \rightarrow 0$, when $\tau_D \rightarrow 0$ leads to $T_i = T_s$, and the limit $\Delta V_i \rightarrow 0$, when $\tau_i \rightarrow 0$ results in $V_i = V_v$. Equation (4.34) can be written as

$$(h_v - h_i) \frac{y}{m} \frac{dm}{dx} = \frac{y c_i \Delta T_i}{V_i \tau_D} + \frac{(1-y) c_p \Delta T}{V_i \tau_T} \quad (4.52)$$

The vapor relaxation requires that in the limit $\tau_T \rightarrow 0$ also $\Delta T \rightarrow 0$, so that their ratio remains constant. Therefore, $T_v = T_s$. This condition is sufficient to cast the conservation equations into a form from which the sound speed can be determined.

Thus, Eqs. (4.41)–(4.43) can be written as

$$\frac{1}{p} \frac{dp}{dx} - \frac{1}{T_s} \frac{dT_s}{dx} + \frac{1}{V_v} \frac{dV_v}{dx} + \frac{y}{1-y} \frac{1}{m} \frac{dm}{dx} = 0 \quad (4.53)$$

$$\frac{1}{p} \frac{dp}{dx} + \frac{V_v^2}{R_v T_v (1-y)} \frac{1}{V_v} \frac{dV_v}{dx} = 0 \quad (4.54)$$

$$\frac{1}{T_s} \frac{dT_s}{dx} + \frac{c_i}{c_p} \frac{y}{1-y} \frac{1}{T_s} \frac{dT_s}{dx} + \frac{V_v^2}{c_p T_v (1-y)} \frac{1}{V_v} \frac{dV_v}{dx} - \frac{h_{fg}}{c_p T_s} \frac{y}{1-y} \frac{1}{m} \frac{dm}{dx} = 0 \quad (4.55)$$

Solving Eq. (4.53) for $(1/m)(dm/dx)$ and substituting it to Eq. (4.55) and using the Clausius–Clapeyron equation, these equations take the forms

$$\left(1 - \frac{R_v T_s}{h_{fg}} \right) \frac{1}{p} \frac{dp}{dx} + \frac{1}{V_v} \frac{dV_v}{dx} + \frac{y}{1-y} \frac{1}{m} \frac{dm}{dx} = 0 \quad (4.56)$$

$$\frac{1}{p} \frac{dp}{dx} + \frac{V_v^2}{R_v T_v (1-y)} \frac{1}{V_v} \frac{dV_v}{dx} = 0 \quad (4.57)$$

$$\frac{c}{c_p} \frac{R_v T_s}{h_{fg}} \frac{1}{p} \frac{dp}{dx} + \frac{V_v^2}{c_p T_v (1-y)} \frac{1}{V_v} \frac{dV_v}{dx} + \frac{h_{fg}}{c_p T_s} \left[\left(1 - \frac{R_v T_s}{h_{fg}} \right) \frac{1}{p} \frac{dp}{dx} + \frac{1}{V_v} \frac{dV_v}{dx} \right] = 0 \quad (4.58)$$

Solving Eq. (4.57) for $(1/V_v)(dV_v/dx)$ and substituting into this gives

$$\left[1 - 2 \frac{R_v T_s}{h_{fg}} + \frac{c T_s}{h_{fg}} \frac{R_v T_s}{h_{fg}} - \frac{(1-y) R_v T_v}{V_v^2} \right] \frac{1}{p} \frac{dp}{dx} = 0$$

Since dp/dx is not zero, the coefficient vanishes and leads to an expression for the sound speed, i.e. $c_{ec} = V_v$. It is given by

$$c_{ec}^2 = \frac{(1-y)R_v T_v}{1 - 2 \frac{R_v T_s}{h_{fg}} + \frac{c T_s}{h_{fg}} \frac{R_v T_s}{h_{fg}}} \quad (4.59)$$

The derivations of the other two sound speeds are left as exercises. In summary, the four sound speeds are given by

$$c_{fz}^2 = \gamma R_v T_v \quad (4.60)$$

$$c_{e1}^2 = \frac{\gamma R_v T_v}{1 + \frac{y}{1-y} \frac{\gamma c_i}{R_v} \left(\frac{R_v T_s}{h_{fg}} \right)^2} \quad (4.61)$$

$$c_{e2}^2 = \frac{(1-y)\gamma R_v T_v}{1 + \frac{y}{1-y} \frac{\gamma c_i}{R_v} \left(\frac{R_v T_s}{h_{fg}} \right)^2} \quad (4.62)$$

$$c_{ec}^2 = \frac{(1-y)R_v T_v}{1 - 2 \frac{R_v T_s}{h_{fg}} + \frac{c T_s}{h_{fg}} \frac{R_v T_s}{h_{fg}}} \quad (4.63)$$

and for saturated steam at $p = 0.5$ bar, their ratios scale as

$$c_{fz} : c_{e1} : c_{e2} : c_{ec} = 1 : 0.998 : 0.947 : 0.878$$

4.3 RELAXATION ZONES

In the previous section, it was shown that there exists four sound speeds, of which the frozen speed c_{fz} is the largest, and the complete equilibrium speed c_{ec} is the smallest. If the upstream flow velocity is lower than c_{ec} , then no waves form. Also, if the upstream velocity is greater than the frozen sound speed c_{fz} , then, a discontinuous shock forms after which the flow relaxes into an equilibrium state. This kind of shock is called *partly dispersed*. If the velocity is larger than the complete equilibrium speed and smaller than the frozen sound speed, then, the waves that form are called *fully dispersed*. Young and Guha [105] classify the situation according to the following schema.

Type I wave corresponds to $c_{ecu} < V_{vu} < c_{e2u}$

Type II wave corresponds to $c_{e2u} < V_{vu} < c_{e1u}$

Type III wave corresponds to $c_{e1u} < V_{vu} < c_{fzu}$

where the subscript “u” denotes the upstream state.

4.3.1 Type I wave

For the Type I wave, the droplet and inertial relaxations can be assumed to be complete. In such a case $T_i = T_s$ and $V_i = V_v$. Under this condition,

$$\frac{1}{m} \frac{dm}{dx} = \frac{1-y}{y} \frac{c_p T_v}{h_{fg}} \frac{\Delta T}{T_v V_v \tau_T} + \frac{c_i T_s}{h_{fg}} \frac{1}{T_s} \frac{dT_s}{dx} \quad (4.64)$$

and the working equations, Eqs. (4.41)–(4.43) can be written as

$$\frac{1}{p} \frac{dp}{dx} - \frac{1}{T_v} \frac{dT_v}{dx} + \frac{1}{V_v} \frac{dV_v}{dx} + \frac{y}{1-y} \frac{c_i T_s}{h_{fg} T_s} \frac{1}{T_s} \frac{dT_s}{dx} + \frac{c_p T}{h_{fg} T_v V_v \tau_T} \frac{\Delta T}{dx} = 0 \quad (4.65)$$

$$\frac{1}{p} \frac{dp}{dx} + \frac{V_v^2}{(1-y)R_v T_v} \frac{1}{V_v} \frac{dV_v}{dx} = 0 \quad (4.66)$$

$$\frac{1}{T_v} \frac{dT_v}{dx} + \frac{R_v V_v^2}{c_p (1-y) R_v T_v} \frac{1}{V_v} \frac{dV_v}{dx} - \frac{\Delta T}{T_v V_v \tau_T} = 0 \quad (4.67)$$

In Eq. (4.65), making the substitution $dT_v/dx = dT_s/dx - d\Delta T/dx$ and then using the Clausius–Clapeyron equation gives

$$\left[1 + \frac{y}{1-y} \frac{c_i}{R_v} \left(\frac{R_v T_s}{h_{fg}} \right)^2 - \frac{T_s R_v T_s}{T_v h_{fg}} \right] \frac{1}{p} \frac{dp}{dx} + \frac{1}{V_v} \frac{dV_v}{dx} + \frac{1}{T_v} \frac{dT_s}{dx} + \frac{c_p T_v}{h_{fg} T_v V_v \tau_T} \frac{\Delta T}{dx} = 0$$

Using Eq. (4.66) to eliminate the pressure gives

$$\begin{aligned} & \left[1 - \left(1 + \frac{y}{1-y} \frac{c_i}{R_v} \left(\frac{R_v T_s}{h_{fg}} \right)^2 - \frac{T_s R_v T_s}{T_v h_{fg}} \right) \frac{V_v^2}{(1-y)R_v T_v} \right] \frac{1}{V_v} \frac{dV_v}{dx} \\ & + \frac{1}{T_v} \frac{dT_s}{dx} + \frac{c_p T_v}{h_{fg} T_v V_v \tau_T} \frac{\Delta T}{dx} = 0 \end{aligned} \quad (4.68)$$

By similar steps, making the substitution $dT_v/dx = dT_s/dx - d\Delta T/dx$ in Eq. (4.67) and then using the Clausius–Clapeyron equation gives

$$\frac{T_s R_v T_s}{T_v h_{fg}} \frac{dp}{dx} + \frac{R_v}{c_p} \left[\frac{V_v^2}{(1-y)R_v T_v} \right] \frac{1}{V_v} \frac{dV_v}{dx} - \frac{1}{T_v} \frac{dT_s}{dx} - \frac{\Delta T}{T_v V_v \tau_T} = 0$$

Eliminating pressure by using Eq. (4.66) gives

$$\left(\frac{R_v}{c_p} - \frac{T_s R_v T_s}{T_v h_{fg}} \right) \frac{V_v^2}{(1-y)R_v T_v} \frac{1}{V_v} \frac{dV_v}{dx} - \frac{1}{T_v} \frac{dT_s}{dx} - \frac{\Delta T}{T_v V_v \tau_T} = 0 \quad (4.69)$$

Adding Eqs. (4.68) and (4.69) gives

$$\left\{ 1 - \left[1 + \frac{y}{1-y} \frac{\gamma c_i}{R_v} \left(\frac{R_v T_s}{h_{fg}} \right)^2 \right] \frac{V_v^2}{(1-y)\gamma R_v T_v} \right\} \frac{1}{V_v} \frac{dV_v}{dx} - \left(1 - \frac{c_p T_v}{h_{fg}} \right) \frac{\Delta T}{T_v V_v \tau_T} = 0$$

Introducing the sound speed c_{e2} into this gives

$$\left(1 - \frac{V_v^2}{c_{e2}^2} \right) \frac{1}{V_v} \frac{dV_v}{dx} - \left(1 - \frac{c_p T_v}{h_{fg}} \right) \frac{\Delta T}{T_v V_v \tau_T} = 0 \quad (4.70)$$

Next multiplying Eq. (4.69) by $c_p T_v/h_{fg}$ and adding it and Eq. (4.70) gives

$$\begin{aligned} & \left\{ 1 - \left[1 + \frac{y}{1-y} \frac{c_i T_s}{h_{fg}} \left(\frac{R_v T_s}{h_{fg}} \right)^2 - \frac{2T_s R_v T_s}{T_v h_{fg}} \right] \frac{V_v^2}{(1-y)R_v T_v} \right\} \frac{1}{V_v} \frac{dV_v}{dx} \\ & + \left(1 + \frac{c_p T_v}{h_{fg}} \right) \frac{1}{T_v} \frac{dT_s}{dx} = 0 \end{aligned}$$

Setting the ratio $T_s/T_v = 1$ in this and introducing the sound speed c_{ec} gives

$$\left(1 - \frac{V_v^2}{c_{ec}^2}\right) \frac{1}{V_v} \frac{dV_v}{dx} + \left(1 - \frac{c_p T_v}{h_{fg}}\right) \frac{d\Delta T}{dx} = 0 \quad (4.71)$$

Combining Eqs. (4.70) and (4.71) gives

$$\frac{d\Delta T}{dx} + \left[\frac{1 - M_{ec}^2}{1 - M_{e2}^2} \right] \frac{\Delta T}{V_v \tau_T} = 0 \quad (4.72)$$

This equation shows that these waves, indeed, fall into the Type I wave category. That is $c_{ecu} < V_v < c_{e2u}$, so that upstream the quantity in the brackets is negative. Were the bracketed term assumed *constant*, $-\Delta T$ would grow exponentially toward plus infinity.

Equation (4.70) shows that the velocity is governed by

$$\frac{dV_v}{dx} = \left[\frac{1 - \frac{c_p T_v}{h_{fg}}}{1 - M_{e2}^2} \right] \Theta V_v \quad (4.73)$$

in which

$$\Theta = \frac{\Delta T}{T_v V_v \tau_T}$$

and Eq. (4.66) can be solved for the pressure gradient, giving

$$\frac{dp}{dx} = - \left[\frac{\gamma}{1 - y} \frac{V_v^2}{c_{tz}^2} \frac{1 - \frac{c_p T_v}{h_{fg}}}{1 - M_{e2}^2} \right] \Theta p \quad (4.74)$$

Next, the equation for the temperature gradient is obtained from Eq. (4.67)

$$\frac{dT_v}{dx} = \left[1 - \frac{\gamma - 1}{1 - y} \frac{V_v^2}{c_{tz}^2} \frac{1 - \frac{c_p T_v}{h_{fg}}}{1 - M_{e2}^2} \right] \Theta T_v \quad (4.75)$$

The equation for the mass of the droplet, Eq. (4.64) can be cast as

$$\frac{dm}{dx} = \left[\frac{1 - y}{y} \frac{c_p T_v}{h_{fg}} - \frac{c_i}{R_v} \left(\frac{R_v T_s}{h_{fg}} \right)^2 \frac{\gamma}{1 - y} \frac{V_v^2}{c_{tz}^2} \frac{1 - \frac{c_p T_v}{h_{fg}}}{1 - M_{e2}^2} \right] \Theta m \quad (4.76)$$

and the degree of wetness as

$$\frac{dy}{dx} = \left[\frac{1 - y}{y} \frac{c_p T_v}{h_{fg}} - \frac{c_i}{R_v} \left(\frac{R_v T_s}{h_{fg}} \right)^2 \frac{\gamma}{1 - y} \frac{V_v^2}{c_{tz}^2} \frac{1 - \frac{c_p T_v}{h_{fg}}}{1 - M_{e2}^2} \right] \Theta y \quad (4.77)$$

Equations (4.72)–(4.77) can now be solved by any of the numerical methods given in MATLAB or GNU/OCTAVE. The fourth-order Runge–Kutta method is a good choice, but even the Euler method would work well, since the small time step required is not an impediment as computers are very fast today.

The evolution of the variables is shown in Figure 4.3. The low value of upstream $|\Delta T|$ is manifested in its initially slow growth. But, since the growth is exponential, its value increases rapidly until the velocity has dropped to c_{ec} . At that point, the derivative of ΔT vanishes, and $|\Delta T|$ reaches its maximum value and then begins to decrease. The saturation temperature increases as the pressure increases. The degree of wetness decreases so that the steam becomes drier as the states across this fully dispersed wave move to higher values of entropy and thus closer to the saturated vapor line. At $x = 500$ mm, the relaxation is nearly complete.

The results were calculated for upstream velocity of $V_{vu} = 1.05 c_{ec}$ that falls into the range $c_{ec} < V_v < c_{e2}$. The degree of wetness was $y_u = 0.1$, the pressure $p_u = 0.5$ bar,

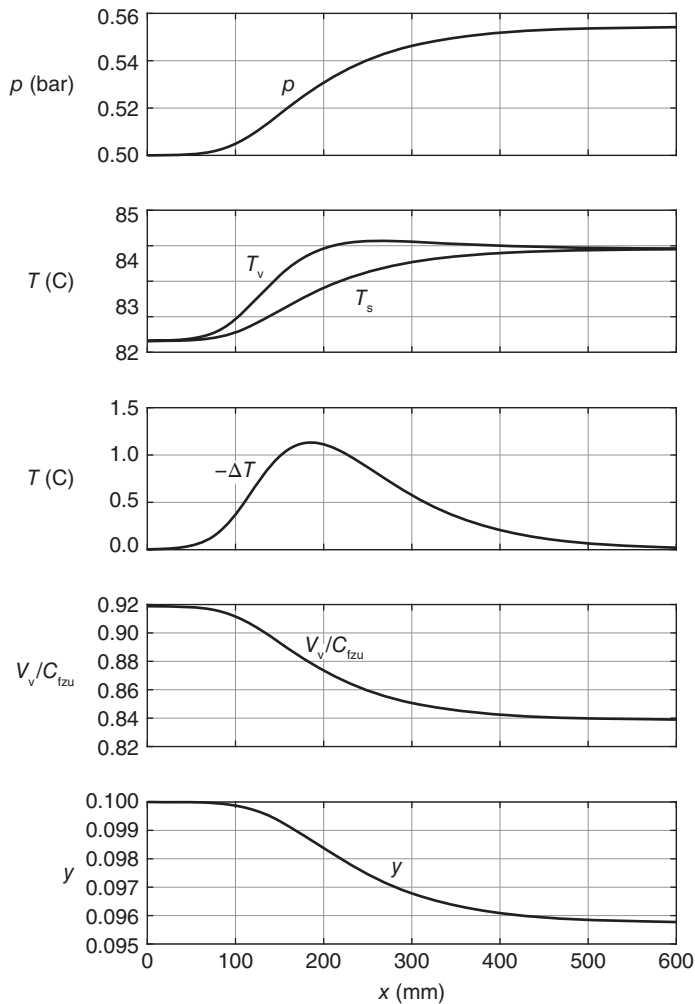


Figure 4.3 Relaxation of the fluid properties for a Type I wave.

and the vapor temperature was $T_{vu} = T_{su} + 0.003^\circ\text{C}$, so that $\Delta T = -0.003^\circ\text{C}$. The initial droplet radius was chosen to be $a_u = 0.5\ \mu\text{m}$, which gives the initial droplet mass $m_u = 5.08 \cdot 10^{-16}\ \text{kg}$. The script to carry out the calculations is given below.

```
%Relaxation for Type I waves
clear all,
Runiv=8314; M=18.02; Rv=Runiv/M; gamma=1.32; cp=Rv*gamma/(gamma-1);
cf=4181.3; y=0.1; c=cp+y*cf/(1-y); a=0.5e-6;
pbar=0.5; p=pbar*1e5;
Ts=XSteam('Tsat_p',pbar); TsK=Ts+273.15; TvK=TsK+0.003; Tv=TvK-273.15;
hf=XSteam('hL_T',Ts); hg=XSteam('hV_T',Ts); hfg=(hg-hf)*1000;
rhof=XSteam('rhoL_p',pbar);
cfz=sqrt(gamma*Rv*TvK);
cec=sqrt((1-y)*Rv*TvK/(1-(Rv*TsK/hfg)*(2-c*TsK/hfg)));
Mec=1.05; Vv=Mec*cec;
DeltaT=Ts-Tv; m=rhof*4*pi*a^3/3;
%
z0=[DeltaT;Vv;p;TvK;y;m;a];
x0=0; xf=0.5; xspan=[x0 xf];
[x,z] = ode45(@relaxwaveI,xspan,z0);
%
subplot(5,1,1); plot(x,z(:,3)/1.e5); grid
subplot(5,1,2); plot(x,z(:,4),x,z(:,4)+z(:,1)); grid;
subplot(5,1,3); plot(x,-z(:,1)); grid;
subplot(5,1,4); plot(x,z(:,2)/cfz); grid;
subplot(5,1,5); plot(x,z(:,5)); grid;
%
function zprime = relaxwaveI(x,z)
    DeltaT = z(1); Vv=z(2); p=z(3); TvK=z(4); y=z(5); m=z(6); a=z(7);
    Runiv=8314; M=18.02; Rv=Runiv/M; gamma=1.32; cp=Rv*gamma/(gamma-1);
    cf=4181.3; c=cp+y*cf/(1-y); a=0.5e-6; Tv=TvK-273.15;
    pbar=p*1e-5; rhof=XSteam('rhoL_p',pbar);
    c=cp+y*cf/(1-y); rhof=XSteam('rhoL_p',pbar);
    Ts=XSteam('Tsat_p',pbar); TsK=Ts+273.15;
    hf=XSteam('hL_T',Ts); hg=XSteam('hV_T',Ts); hfg=(hg-hf)*1000;
    cfz=sqrt(gamma*Rv*TvK);
    ce1=cfz/sqrt(1+y/(1-y)*(gamma*cf/Rv)*(Rv*TsK/hfg)^2);
    ce2=ce1*sqrt(1-y);
    ce=sqrt((1-y)*Rv*TsK/(1-(Rv*TsK/hfg)*(2-c*TsK/hfg)));
    mu=XSteam('my_pT',pbar,Ts+1); k=XSteam('tcV_p',pbar);
    lambda=mu/p*sqrt(pi*Rv*TsK/2); Kn=0.5*lambda/a; Pr=mu*cp/k;
    tauT=((1-y)*cp*a^2*rhof/(3*k*y))*(1+4.5*Kn/Pr);
    DeltaT=TsK-TvK; Theta=DeltaT/(TvK*Vv*tauT);
    CP=(1-cp*TvK/hfg);
    zdot(1)=-(1-(Vv/ce)^2)/(1-(Vv/ce2)^2)*Theta*TvK;
    zdot(2) = CP*Theta*Vv/(1-(Vv/ce2)^2);
    zdot(3)=-gamma/(1-y)*(Vv/cfz)^2*CP/(1-(Vv/ce2)^2)*Theta*p;
    zdot(4)=(1-(gamma-1)/(1-y)*(Vv/cfz)^2*CP/(1-(Vv/ce2)^2))*Theta*TvK;
    zdot(5)=((1/y-1)*(cp*TvK/hfg)-(cf/Rv)*(Rv*TsK/hfg)^2* ...
        gamma/(1-y)*(Vv/cfz)^2*CP/(1-(Vv/ce2)^2))*y*Theta;
    zdot(6)=((1/y-1)*(cp*TvK/hfg)-(cf/Rv)*(Rv*TsK/hfg)^2* ...
        gamma/(1-y)*(Vv/cfz)^2*CP/(1-(Vv/ce2)^2))*y*Theta;
    zdot(7)=3*((1/y-1)*(cp*TvK/hfg)-(cf/Rv)*(Rv*TsK/hfg)^2* ...
```

```

gamma/(1-y)*(Vv/cfz)^2*CP/(1-(Vv/ce2)^2))*a*Theta;
zprime=[zdot(1);zdot(2);zdot(3);zdot(4);zdot(5);zdot(6);zdot(7)];
end

```

As the disperse wave develops, its velocity drops, and after reaching the value c_{ec} , the bracketed term becomes positive, and the solution begins to decay. If the starting condition for velocity is just below the value c_{e2} , then, the denominator in the coefficient of Eq. (4.72) is small, and $|\Delta T|$ would appear to increase rapidly until the velocity has dropped, which makes the denominator grow. However, for this condition, the value of ΔT remains small, so that its derivative does not increase to a large value. The time to reach equilibrium does increase. It is a simple matter to change the conditions in the computer program to explore how the solution behaves as the initial conditions are changed.

4.3.2 Type II wave

For waves of Type II, the velocity upstream satisfies the condition $c_{e2u} < V_{vu} < c_{e1u}$. For this wave, the droplet temperature relaxation is assumed complete, so that $T_i = T_s$, and with $\tau_T \rightarrow \infty$, no vapor relaxation takes place. Hence, the aim here is to give a detailed view of how the velocity relaxation proceeds.

First the working equations, (4.41)–(4.43) under this condition become

$$\frac{1}{p} \frac{dp}{dx} - \frac{1}{T_v} \frac{dT_v}{dx} + \frac{1}{V_v} \frac{dV_v}{dx} + \frac{V_i}{V_v} \frac{y}{1-y} \frac{1}{m} \frac{dm}{dx} = 0 \quad (4.78)$$

$$\frac{1}{p} \frac{dp}{dx} + \frac{V_v^2}{R_v T_v} \left[\frac{1}{V_v} \frac{dV_v}{dx} + \frac{y V_i}{(1-y) V_v^2} \frac{dV_i}{dx} \right] = 0 \quad (4.79)$$

$$\begin{aligned} \frac{1}{T_v} \frac{dT_v}{dx} + \frac{y}{1-y} \frac{V_i}{V_v} \frac{c_i}{c_p} \frac{1}{T_v} \frac{dT_s}{dx} + \frac{V_v^2}{c_p T_v} \left[\frac{1}{V_v} \frac{dV_v}{dx} + \frac{y}{1-y} \left(\frac{V_i}{V_v} \right)^2 \frac{1}{V_v} \frac{dV_i}{dx} \right] \\ - \frac{(h_v - h_i)}{c_p T_v} \frac{V_i}{V_v} \frac{y}{1-y} \frac{1}{m} \frac{dm}{dx} = 0 \end{aligned} \quad (4.80)$$

and, after the Clausius–Clapeyron equation has been used, the derivative of the mass of the droplet is given by

$$\frac{1}{m} \frac{dm}{dx} = \frac{c_i T_s}{h_{fg}} \frac{1}{T_s} \frac{dT_i}{dx} = \frac{c_i}{R_v} \left(\frac{R_v T_s}{h_{fg}} \right)^2 \frac{1}{p} \frac{dp}{dx} \quad (4.81)$$

Substituting this into Eqs. (4.53) and (4.55) leads to

$$\left[1 + \frac{y}{1-y} \frac{V_i}{V_v} \frac{c_i}{R_v} \left(\frac{R_v T_s}{h_{fg}} \right)^2 \right] \frac{1}{p} \frac{dp}{dx} - \frac{1}{T_v} \frac{dT_v}{dx} + \frac{1}{V_v} \frac{dV_v}{dx} = 0 \quad (4.82)$$

$$\frac{1}{p} \frac{dp}{dx} + \frac{V_v^2}{R_v T_v} \left(\frac{1}{V_v} \frac{dV_v}{dx} + \Pi \right) = 0 \quad (4.83)$$

and

$$\frac{1}{T_v} \frac{dT_v}{dx} + \frac{V_v^2}{c_p T_v} \left(\frac{1}{V_v} \frac{dV_v}{dx} + \Pi \right) = 0 \quad (4.84)$$

In this last equation, the term V_i/V_v originally appears in front of the factor Π , but it is replaced by unity, as was done when the sound speed c_{e1} was derived. The factor Π is defined by

$$\Pi = \frac{y}{1-y} \frac{\Delta V_i}{V_v^2 \tau_i} \quad (4.85)$$

Now adding Eqs. (4.82) and (4.84), eliminates the temperature and results in

$$\frac{1}{V_v} \frac{dV_v}{dx} + \frac{V_v^2}{c_p T_v} \left(\frac{1}{V_v} \frac{dV_v}{dx} + \Pi \right) + \left[1 + \frac{y}{1-y} \frac{c_i}{R_v} \left(\frac{R_v T_s}{h_{fg}} \right)^2 \right] \frac{1}{p} \frac{dp}{dx} = 0 \quad (4.86)$$

Finally, solving Eq. (4.83) for the pressure and substituting it to the last equation gives after simplification

$$\frac{1}{V_v} \frac{dV_v}{dx} - \left(\frac{1}{V_v} \frac{dV_v}{dx} + \Pi \right) \frac{V_v^2}{\gamma R_v T_v} \left[1 + \frac{y}{1-y} \frac{\gamma c_i}{R_v} \left(\frac{R_v T_s}{h_{fg}} \right)^2 \right] = 0 \quad (4.87)$$

The last part of the second term is identified as V_v^2/c_{e1}^2 so that this can be written as

$$\left(1 - \frac{V_v^2}{c_{e1}^2} \right) \frac{1}{V_v} \frac{dV_v}{dx} - \frac{V_v^2}{c_{e1}^2} \Pi = 0 \quad (4.88)$$

and Eqs. (4.83) and (4.84) reduce to

$$\left(1 - \frac{V_v^2}{c_{e1}^2} \right) \frac{1}{p} \frac{dp}{dx} + \frac{V_v^2}{R_v T_v} \Pi = 0 \quad (4.89)$$

$$\left(1 - \frac{V_v^2}{c_{e1}^2} \right) \frac{1}{T_v} \frac{dT_v}{dx} + \frac{V_v^2}{c_p T_v} \Pi = 0 \quad (4.90)$$

Equation (4.85) takes the form

$$\left(1 - \frac{V_v^2}{c_{e1}^2} \right) \frac{1}{m} \frac{dm}{dx} + \frac{\gamma c_i}{R_v} \left(\frac{R_v T_s}{h_{fg}} \right)^2 \frac{V_v^2}{\gamma R_v T_v} \Pi = 0 \quad (4.91)$$

By setting $V_v/V_i = 1$, the droplet velocity is given by

$$\frac{1}{V_i} \frac{dV_i}{dx} - \frac{1-y}{y} \Pi = 0 \quad (4.92)$$

The remaining unknown is the degree of wetness, y . There are two ways to handle this. Since the number of droplets remains fixed,

$$\frac{d}{dx} \left(\frac{y}{1-y} \frac{p V_i}{R_v T_v m} \right) = 0$$

so that

$$\frac{y}{1-y} \frac{p V_i}{R_v T_v m} = \frac{y_u}{1-y_u} \frac{p_u V_{iu}}{R_v T_{vu} m_u}$$

and this is solved for y at each location in the dispersive wave. The second method is to differentiate this expression logarithmically, leading to

$$\frac{y}{y(1-y)} \frac{dy}{dx} + \frac{1}{p} \frac{dp}{dx} + \frac{1}{V_i} \frac{dV_i}{dx} - \frac{1}{T_v} \frac{dT_v}{dx} - \frac{1}{m} \frac{dm}{dx} = 0 \quad (4.93)$$

Substituting the various derivatives into this and simplifying the result gives

$$\left(1 - \frac{V_v^2}{c_{e1}^2}\right) \frac{1}{y} \frac{dy}{dx} + \left[(1-y) \left(1 - \frac{V_v^2}{c_{e1}^2}\right) - y \frac{V_v^2}{c_{fz}^2}\right] \Pi = 0 \quad (4.94)$$

With a computer program similar to the one aforementioned, these equations can be integrated. The results are shown in Figure 4.4. The velocity differences remain small throughout the relaxation zone. The vapor temperature rises and remains about three degrees above the saturation temperature because in this form of the equations, the vapor relaxation was not allowed to take place.

For the Type II waves, it is of interest also to develop the equations for which the droplet temperature relaxation is complete, but both the inertial relaxation and vapor relaxation are taking place. This falls under the heading of combined relaxation. The study of this kind

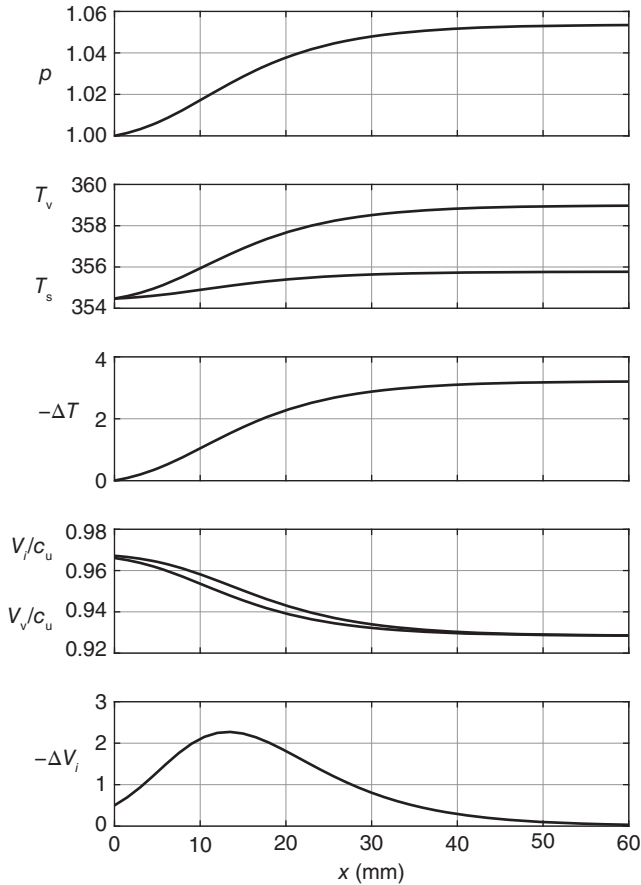


Figure 4.4 Relaxation of the fluid properties for a Type II wave.

of combined relaxation is left as an exercise. The general case of combined relaxation is discussed after the Type III waves are briefly mentioned.

4.3.3 Type III wave

The Type III waves occur when the upstream velocity is larger than c_{e1} but smaller than the frozen speed c_{fz} . But since a typical value of the ratio $c_{e1}/c_{fz} = 0.997$, they are rare. If, however, the upstream velocity were to fall into this range, a set of equations can be obtained, which show how the droplet temperature relaxes while the inertial and vapor relaxation have not yet started. That is assuming that $\tau_I \rightarrow \infty$ and $\tau_T \rightarrow \infty$, while $\tau_D \rightarrow 0$ and $\Delta T_i \rightarrow 0$, with their ratio constant. Because these waves are quite unimportant, the equations that govern them are not listed here.

4.3.4 Combined relaxation

The equation that govern the variables in the relaxation zone when all three relaxation mechanisms are taken into account are developed next. After making the substitution

$$\frac{y}{1-y} \frac{1}{m} \frac{dm}{dx} = \frac{c_p}{h_{fg}} \frac{\Delta T}{V_i \tau_T} + \frac{y}{1-y} \frac{c_i}{h_{fg}} \frac{\Delta T_i}{V_i \tau_D}$$

and

$$\frac{dT_i}{dx} = \frac{\Delta T_i}{V_i \tau_D} \quad \frac{dV_i}{dx} = \frac{\Delta V_i}{V_i \tau_I}$$

into Eqs. (4.41)–(4.43), they become

$$\frac{1}{p} \frac{dp}{dx} - \frac{1}{T_v} \frac{dT_v}{dx} + \frac{1}{V_v} \frac{dV_v}{dx} + \frac{c_p T_v}{h_{fg}} \Theta + \frac{c_i T_s}{h_{fg}} \sigma = 0 \quad (4.95)$$

$$\frac{1}{p} \frac{dp}{dx} + \frac{V_v^2}{R_v T_v} \left(\frac{1}{V_v} \frac{dV_v}{dx} + \Pi \right) = 0 \quad (4.96)$$

$$\frac{1}{T_v} \frac{dT_v}{dx} + \frac{V_v^2}{c_p T_v} \left(\frac{1}{V_v} \frac{dV_v}{dx} + \frac{V_i}{V_v} \Pi \right) - \Theta = 0 \quad (4.97)$$

where the parameters

$$\Theta = \frac{\Delta T}{V_v T_v \tau_T} \quad \Pi = \frac{y}{1-y} \frac{\Delta V_i}{V_v^2 \tau_I} \quad \sigma = \frac{y}{1-y} \frac{\Delta T_i}{V_v T_s \tau_D} \quad (4.98)$$

have been introduced.

To cast these equations into the standard form, as has been done previously, add the energy equation and the mass balance together. This eliminates dT_v/dx . Next, subtract the momentum equation from the resulting equation to eliminate dp/dx . This leaves an equation in which only the derivative of velocity appears. Carrying this out gives

$$(1 - M_f^2) \frac{1}{V_v} \frac{dV_v}{dx} = \left(1 - \frac{c_p T_v}{h_{fg}} \right) \Theta - \frac{c_i T_s}{h_{fg}} \sigma + M_f^2 \frac{V_i}{V_v} \Pi$$

Substituting dV_v/dx from this equation into the momentum equation and energy equation in turn gives

$$(1 - M_f^2) \frac{1}{p} \frac{dp}{dx} = \frac{V_v^2}{c_p T_v} \left[- \left(1 - \frac{c_p T_v}{h_{fg}} \right) \Theta + \frac{c_i T_s}{h_{fg}} \sigma - \Pi \right]$$

$$(1 - M_f^2) \frac{1}{T_v} \frac{dT_v}{dx} = \left[1 - \frac{V_v^2}{R_v T_v} \left(1 - \frac{R_v T_v}{h_{fg}} \right) \right] \Theta + \frac{V_v^2}{c_p T_v} \frac{c_i T_s}{h_{fg}} \sigma - \frac{V_v^2}{c_p T_v} \frac{V_i}{V_v} \Pi$$

To this set are added the equations

$$\frac{1}{m} \frac{dm}{dx} = \frac{1 - y}{y} \frac{c_p T_v}{h_{fg}} \frac{V_v}{V_i} \Theta + \frac{1 - y}{y} \frac{c_i T_s}{h_{fg}} \frac{V_v}{V_i} \sigma$$

and

$$\frac{1}{V_i} \frac{dV_i}{dx} = \frac{1 - y}{y} \left(\frac{V_v}{V_i} \right)^2 \Pi \quad \frac{1}{T_i} \frac{dT_i}{dx} = \frac{1 - y}{y} \frac{T_s}{T_i} \frac{V_v}{V_i} \sigma$$

Since the number of droplets remains constant, the degree of wetness is obtained by noting that

$$\frac{d}{dx} \left(\frac{y}{1 - y} \frac{p V_i}{R_v T_v m} \right) = 0 \quad \text{so that} \quad \frac{y}{1 - y} \frac{p V_i}{R_v T_v m} = K$$

and K is a constant. Differentiating this logarithmically gives

$$\frac{1 - M_f^2}{y(1 - y)} \frac{dy}{dx} = (1 - M_f^2) \left(\frac{1}{T_v} \frac{dT_v}{dx} + \frac{1}{m} \frac{dm}{dx} - \frac{1}{p} \frac{dp}{dx} - \frac{1}{V_i} \frac{dV_i}{dx} \right) \quad (4.99)$$

Substituting the aforementioned expressions and carrying out the algebra gives the equation

$$\frac{1 - M_f^2}{1 - y} \frac{dy}{dx} = y \Theta + \left[(1 - y)(1 - M_f^2) \left(\frac{V_v}{V_i} \right) - y M_f^2 \right] \left(\frac{c_p T_v}{h_{fg}} \Theta + \frac{c_i T_s}{h_{fg}} \sigma \right)$$

$$- \left[(1 - y)(1 - M_f^2) \left(\frac{V_v}{V_i} \right)^3 - y M_f^2 \right] \frac{V_i}{V_v} \Pi \quad (4.100)$$

The terms $(V_i/V_v - 1)$ that appear during the manipulations are set to zero; but other velocity ratios are kept. It turns out that the results displayed in Figure 4.5 are somewhat sensitive to these factors. The parameters for the sample calculation are an upstream Mach number $M_{fu} = 1.5$ and pressure $p_u = 0.35$ bar. The saturation temperature for this pressure is 345.83 K. The initial droplet radius is $a_u = 0.1 \mu\text{m}$, and the degree of wetness is $y_u = 0.1$. The graphs in Figure 4.5 show that the length of droplet relaxation zone is indeed very short, as the time scale τ_D is about one-twentieth of τ_1 and four hundred times smaller than τ_T . Since the flow is supersonic ahead of the shock, an aerodynamic shock forms, and the droplet temperature and velocity right after the shock are equal to their upstream values. They then adjust to their equilibrium values in their respective relaxation zones. Thus, the scaled droplet temperature T_i/T_{iu} increases from unity to a value 1.065 in a region of width on the order of about a millimeter. In this region, the droplet radius also increases from 0.10 to 0.13 μm and then begins to drop.

The inertial relaxation takes about 70 mm to complete, and the vapor equilibrium is achieved in a zone of about 400 mm. As the pressure increases across all the relaxation zones, so does the saturation temperature and the vapor temperature, after an initial rise, begins to drop toward the value of the saturation temperature.

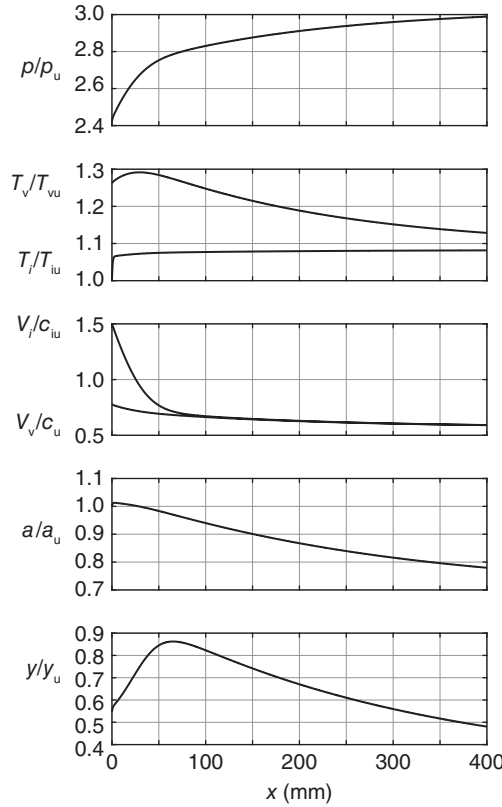


Figure 4.5 Variation of the variables through the droplet, inertial, and vapor relaxation regions. $y_u = 0.1$, $a_u = 0.1 \mu\text{m}$, $p_u = 0.35$ and with an upstream Mach number $M_{fu} = 1.5$.

4.3.5 Flow in a variable area nozzle

The equations governing wet steam flow in channels of variable area are obtained from the general balance equations that are of the form

$$\frac{d}{dx}(A\rho_v V_v) + \frac{d}{dx}\left(A\frac{y\rho_v V_i}{1-y}\right) = 0 \quad (4.101)$$

The momentum balance

$$\frac{d}{dx}(A\rho_v V_v^2) + \frac{d}{dx}\left(A\frac{y\rho_v V_i^2}{1-y}\right) + A\frac{dp}{dx} = 0 \quad (4.102)$$

is the same as before, except the extra term that accounts for the additional unbalanced pressure force.

The energy equation is

$$\frac{d}{dx}\left[A\rho_v V_v\left(h_v + \frac{1}{2}V_v^2\right)\right] + \frac{d}{dx}\left[A\frac{y\rho_v V_i}{1-y}\left(h_i + \frac{1}{2}V_i^2\right)\right] = 0 \quad (4.103)$$

That the number of droplets remains constant is described by the equation

$$\frac{d}{dx} \left(\frac{Ay}{1-y} \frac{\rho_v V_i}{m} \right) = 0 \quad (4.104)$$

which can be simplified and rearranged as

$$\frac{y\rho_v V_i}{1-y} \left(\frac{1}{A} \frac{dA}{dx} - \frac{1}{m} \frac{dm}{dx} \right) + \frac{d}{dx} \left(\frac{y\rho_v V_i}{1-y} \right) = 0 \quad (4.105)$$

Differentiating out the terms in the Eq. (4.101) and making use of Eq. (4.105) reduces it to

$$\frac{1}{A} \frac{dA}{dx} + \frac{1}{V_v} \frac{dV_v}{dx} + \frac{1}{p} \frac{dp}{dx} - \frac{1}{T_v} \frac{dT_v}{dx} + \frac{y}{1-y} \frac{V_i}{V_v} \frac{1}{m} \frac{dm}{dx} = 0 \quad (4.106)$$

Equation (4.102) is next expanded and combined with Eq. (4.105), and then from the resulting equation, the term dm/dx is eliminated with Eq. (4.106). This operation yields

$$\frac{1}{p} \frac{dp}{dx} + \frac{V_v^2}{R_v T_v} \left[\frac{1}{V_v} \frac{dV_v}{dx} + \frac{y}{1-y} \left(\frac{V_i}{V_v} \right)^2 \frac{1}{V_i} \frac{dV_i}{dx} \right] = 0 \quad (4.107)$$

To arrive at this equation, certain intermediate terms cancel when the approximation $V_i = V_v$ is used.

The energy Eq. (4.103) can be reduced to

$$\begin{aligned} \frac{1}{T_v} \frac{dT_v}{dx} + \frac{V_v^2}{c_p T_v} \frac{1}{V_v} \frac{dV_v}{dx} + \frac{y}{1-y} \frac{V_i}{V_v} \frac{c_i T_s}{c_p T_v} \frac{1}{T_s} \frac{dT_i}{dx} + \frac{V_v^2}{c_p T_v} \frac{y}{1-y} \left(\frac{V_i}{V_v} \right)^3 \frac{1}{V_i} \frac{dV_i}{dx} \\ - \frac{h_v - h_i}{c_p T_v} \frac{y}{1-y} \left(\frac{V_i}{V_v} \right) \frac{1}{m} \frac{dm}{dx} = 0 \end{aligned} \quad (4.108)$$

To arrive at this form, the kinetic energy terms, as before, are of higher order and can be neglected.

Using the parameters as defined in Eqs. (4.98), the derivative of the mass of the droplet can be written as

$$\frac{1}{m} \frac{dm}{dx} = \frac{1-y}{y} \frac{c_p T_v}{h_{fg}} \left(\frac{V_v}{V_i} \right) \Theta + \frac{1-y}{y} \frac{c_i T_s}{h_{fg}} \left(\frac{V_v}{V_i} \right) \sigma \quad (4.109)$$

and the equations for velocity and droplet relaxation become

$$\frac{1}{V_i} \frac{dV_i}{dx} = \frac{\Delta V_i}{V_i^2 \tau_i} = \frac{1-y}{y} \left(\frac{V_v}{V_i} \right)^2 \Pi \quad \frac{1}{T_i} \frac{dT_i}{dx} = \frac{\Delta T_i}{T_i V_i \tau_D} = \frac{1-y}{y} \left(\frac{V_v}{V_i} \right) \left(\frac{T_s}{T_i} \right) \sigma$$

The rest of the development is as before, with temperature eliminated by adding Eq. (4.108) and Eq. (4.106), and then Eq. (4.107) is solved for the pressure gradient, and it is substituted in the resulting equation. This leads to

$$(1 - M_f^2) \frac{1}{V_v} \frac{dV_v}{dx} = -\frac{1}{A} \frac{dA}{dx} + \left(1 - \frac{c_p T_v}{h_{fg}} \right) \Theta + M_f^2 \Pi - \frac{c_i T_s}{h_{fg}} \sigma \quad (4.110)$$

Similarly, Eq. (4.107) can be recast as

$$(1 - M_f^2) \frac{1}{p} \frac{dp}{dx} = \gamma M_f^2 \left[\frac{1}{A} \frac{dA}{dx} - \left(1 - \frac{c_p T_v}{h_{fg}} \right) \Theta - \Pi + \frac{c_i T_s}{h_{fg}} \sigma \right] \quad (4.111)$$

and Eq. (4.108) becomes

$$(1 - M_f^2) \frac{1}{T_v} \frac{dT_v}{dx} = (\gamma - 1) M_f^2 \left[\frac{1}{A} \frac{dA}{dx} - \Pi + \frac{c_i T_s}{h_{fg}} \sigma - \frac{\gamma}{\gamma - 1} \left(1 - \frac{R_v T_v}{h_{fg}} \right) \Theta \right] + \Theta \quad (4.112)$$

With $A = A(x)$ given, these equations can be solved by the Runge–Kutta methods used previously.

4.4 SHOCKS IN WET STEAM

To recapitulate what has been discussed in this chapter, when wet steam flows in a nozzle or in the flow passage between the blades of a low pressure turbine, shocks can occur if the velocities are sufficiently high and the back pressure low. When the steam is laden with liquid droplets, across such a shock, the droplet temperature lags the temperature of the vapor owing to its thermal inertia. After the shock, owing to the heat capacity of liquid droplets, heat is transferred from the vapor to the droplets. This heat transfer goes into evaporating some of the liquid into vapor. The pressure after the shock is higher than before, and thus, the saturation temperature has also increased. A complicating feature in the analysis is that during the time before equilibrium is reached, the droplets have moved some distance downstream. In the previous subsection, the equations have been developed that point to a way to calculate the evolution of the flow through the relaxation zones for a channel with a changing area.

In addition to these thermal effects, owing to the inertia of the droplets, the droplets experience a drag force by the vapor and accelerate. Again, by the time they have reached the vapor velocity, they have moved further downstream. A shock can now be modeled as consisting of an aerodynamic shock followed by a relaxation zone. Such a shock is called *partially dispersed*. Through the aerodynamic shock, the fluid behaves as if the droplets were completely absent, and this model has the name *frozen flow*. The aerodynamic shock is sufficiently thin that there is no time for any of the transport processes to influence the droplets as they flow through the shock.

Consider now a shock wave moving into steam that is stationary. In the previous chapter, moving shocks were discussed, and the shock speed was shown to be given by

$$M_{fu} = \frac{U^2}{c_{fz}^2} = \frac{\gamma + 1}{2\gamma} \frac{p_f}{p_1} + \frac{\gamma - 1}{2\gamma}$$

The approximate theory for the equilibrium flow gives instead

$$M_{ec} = \frac{U^2}{c_{ec}^2} = \frac{\gamma_e + 1}{2\gamma_e} \frac{p_2}{p_1} + \frac{\gamma_e - 1}{2\gamma_e}$$

in which the frozen and equilibrium sound speeds are given by $c_{fz} = \sqrt{\gamma R_v T}$ and $c_{ec} = \sqrt{\gamma_e R_v T}$, respectively. Solving the second equation for U and substituting it to the previous one, allows p_f to be determined. Since the calculations and Figure 4.1 show that

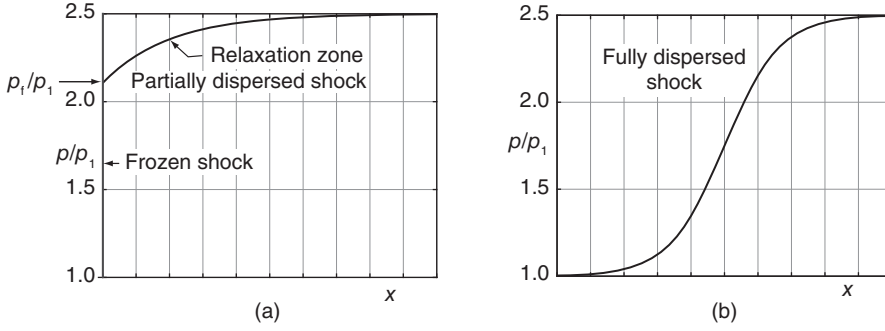


Figure 4.6 Schematic of (a) partially dispersed shock, (b) fully dispersed shock, for $\gamma = 1.32$, $p_1 = 0.3$ bar, $y_1 = 0.08$, and $p_2/p_1 = 2.5$.

$\gamma_e < \gamma$, it follows that $M_{ec} > M_f$. This means that $p_f < p_2$ and the pressure continues to increase across the relaxation zone. The pressure rise is shown schematically in Figure 4.6.

For wet steam, the mass, momentum, and energy balances across a shock are

$$\begin{aligned}\rho_1 V_1 &= \rho_2 V_2 \\ p_1 + \rho_1 V_1^2 &= p_2 + \rho_2 V_2^2 \\ h_1 + \frac{1}{2} V_1^2 &= h_2 + \frac{1}{2} V_2^2\end{aligned}$$

For weak shocks, the entropy change is small, and Eq. (4.3) is reduced to

$$dh = \frac{dp}{\rho} \quad (4.113)$$

By use of the chain rule and the definition of the speed of sound, Eq. (4.11), this can be written as

$$dh = \frac{\gamma_e}{\gamma_e - 1} d\left(\frac{p}{\rho}\right) \quad (4.114)$$

Assuming γ_e to be constant, this can be integrated and

$$h_2 - h_1 = \frac{\gamma_e}{\gamma_e - 1} \left(\frac{p_2}{\rho_2} - \frac{p_1}{\rho_1} \right)$$

follows. Substituting this to the energy equation gives

$$\frac{\gamma_e}{\gamma_e - 1} \frac{p_1}{\rho_1} + \frac{1}{2} V_1^2 = \frac{\gamma_e}{\gamma_e - 1} \frac{p_2}{\rho_2} + \frac{1}{2} V_2^2$$

Equation (4.11) is

$$\frac{dp}{d\rho} = \gamma_e \frac{p}{\rho}$$

and, the equilibrium speed of sound can be written as $c_e = \sqrt{\gamma_e p / \rho}$. This also means that the pressure to density ratio can be written as $p/\rho = V^2 / \gamma_e M_e^2$ when the equilibrium Mach number is introduced.

Writing the velocities in terms of Mach numbers puts the energy equation to the form

$$\frac{p_1}{\rho_1} \left(\frac{1}{\gamma_e - 1} + \frac{1}{2} M_{e1}^2 \right) = \frac{p_2}{\rho_2} \left(\frac{1}{\gamma_e - 1} + \frac{1}{2} M_{e2}^2 \right) \quad (4.115)$$

and this can be recasted as

$$\frac{p_1}{p_2} \frac{\rho_2}{\rho_1} = \frac{2 + (\gamma_e - 1) M_{e2}^2}{2 + (\gamma_e - 1) M_{e1}^2}$$

or using the just mentioned pressure to density ratio, as

$$\frac{M_{e2}^2}{M_{e1}^2} \frac{V_1^2}{V_2^2} = \frac{2 + (\gamma_e - 1) M_{e2}^2}{2 + (\gamma_e - 1) M_{e1}^2}$$

According to the mass balance, the velocity ratio is $V_1/V_2 = \rho_2/\rho_1$, so that the previous equation takes the form

$$\frac{\rho_2}{\rho_1} = \frac{M_{e1}}{M_{e2}} \frac{\sqrt{2 + (\gamma_e - 1) M_{e2}^2}}{\sqrt{2 + (\gamma_e - 1) M_{e1}^2}}$$

Substituting this back to Eq. (4.115) gives finally

$$\frac{p_1}{p_2} = \frac{M_{e2}}{M_{e1}} \frac{\sqrt{2 + (\gamma_e - 1) M_{e2}^2}}{\sqrt{2 + (\gamma_e - 1) M_{e1}^2}}$$

Factoring out the pressure in the momentum equation and using the definitions of speed of sound and Mach number results in

$$\frac{p_1}{p_2} = \frac{1 + \gamma_e M_{e1}^2}{1 + \gamma_e M_{e2}^2}$$

Finally, equating the two expressions for the pressure ratios gives

$$\frac{M_{e1} \sqrt{2 + (\gamma_e - 1) M_{e1}^2}}{1 + \gamma_e M_{e1}^2} = \frac{M_{e2} \sqrt{2 + (\gamma_e - 1) M_{e2}^2}}{1 + \gamma_e M_{e2}^2}$$

This is the same expression as was developed in the last chapter, and when solved for M_{e2}^2 , it gives

$$M_{e2}^2 = \frac{2 + (\gamma_e - 1) M_{e1}^2}{2\gamma_e M_{e1}^2 - (\gamma_e - 1)}$$

Therefore, the pressure rise across the shock is

$$\frac{p_2}{p_1} = \frac{2\gamma_e}{\gamma_e + 1} M_{e1}^2 - \frac{\gamma_e - 1}{\gamma_e + 1}$$

and the density and velocity ratios are

$$\frac{\rho_2}{\rho_1} = \frac{V_1}{V_2} = \frac{(\gamma_e + 1) M_{e1}^2}{2 + (\gamma_e - 1) M_{e1}^2}$$

Calculations can now be carried out exactly as for pure gases or mixtures of gases, provided that the steam remains wet on both sides of the shock. Only a reasonable value for γ_e first needs to be calculated from Eq. (4.10).

Temperature after the shock is determined by the Clausius–Clapeyron equation

$$\frac{dp}{p} = \frac{h_{fg}}{R_v T_s} \frac{dT_s}{T_s} \quad (4.116)$$

By assuming that the factor multiplying the fractional change in temperature is constant, integration gives

$$\frac{p_2}{p_1} = \left(\frac{T_{s2}}{T_{s1}} \right)^{h_{fg}/R_v T_s}$$

in which T_s may be taken to be T_{s1} and after T_{s2} is calculated this way, a new value can be calculated using $T_s = \frac{1}{2}(T_{s1} + T_{s2})$.

The second method is to assume that h_{fg} is constant, so that

$$\ln \frac{p_2}{p_1} = \frac{h_{fg}}{R_v T_{s1}} \left(\frac{1}{T_{s1}} - \frac{1}{T_{s2}} \right)$$

The third method is to assume that $h_{fg} = a - bT$. The constants are $a = 3.193 \cdot 10^6$ and $b = 2.51 \cdot 10^3$ [56]. Substituting this form of h_{fg} into the Clausius–Clapeyron equation and integrating yields

$$\ln \frac{p_2}{p_1} = \frac{a}{R_v} \left(\frac{1}{T_{s1}} - \frac{1}{T_{s2}} \right) - b \ln \frac{T_{s2}}{T_{s1}}$$

To determine T_2 by this third method still requires the solution of this nonlinear algebraic equation for T_{s2} , but it can be done easily by various numerical methods. The approximate method discussed in this section yields good results for low Mach numbers. Its advantage is that the conditions upstream of the shock can be specified, and the state after the shock can then be determined.

4.4.1 Evaporation in the flow after the shock

If the degree of wetness is low, then, since temperature increases across a shock, in the relaxation zone, the steam tends to become drier, or completely dry. For steam that is completely dry after the shock, $y_2 = 0$. Then, if the temperature, pressure, and degree of wetness are known before the shock, and the pressure ratio across the shock is known as well, the balance equations can be combined in such a way that the temperature after the shock can be calculated together with the minimum value of degree wetness, which will cause the steam to just dry up as it passes through the shock. These will now be discussed.

Enthalpy, from Eq. (4.1), ahead of the shock can be written as

$$h_1 = h_{v1} - y_1 h_{fg1}$$

and, with the steam after the shock dry, the energy balance takes the form

$$c_p T_{s1} - y_1 h_{fg1} + \frac{1}{2} V_1^2 = c_p T_2 + \frac{1}{2} V_2^2$$

Using the ideal gas relation and expressing the specific heat at constant pressure in terms of the gas constant and the ratio of specific heats, this equation becomes

$$\frac{\gamma}{\gamma-1} \frac{p_2}{\rho_2} - \frac{\gamma R_v}{\gamma-1} T_{s1} = \frac{1}{2} (V_1^2 - V_2^2) - y_1 h_{fg1}$$

The ratio of the specific heats is the actual one for steam with $\gamma = 1.3$ the accepted value, (or more accurately $\gamma = 1.32$).

Using the mass and momentum balances, velocities can be expressed by the Hugoniot relations as,

$$V_1^2 = \left(\frac{p_2 - p_1}{\rho_2 - \rho_1} \right) \frac{\rho_2}{\rho_1} \quad V_2^2 = \left(\frac{p_2 - p_1}{\rho_2 - \rho_1} \right) \frac{\rho_1}{\rho_2}$$

When these are substituted into the previous form of the energy equation, and after it has been multiplied through by $(\gamma - 1)/\gamma$ and the first term on the right has been simplified, the energy balance becomes

$$\frac{p_2}{\rho_2} - R_v T_{s1} = \frac{\gamma - 1}{2\gamma} (p_2 - p_1) \left(\frac{1}{\rho_2} + \frac{1}{\rho_1} \right) - y_1 h_{fg1} \frac{\gamma - 1}{\gamma}$$

Expanding the first term on the right-hand side and collecting factors involving ρ_2 to the left gives

$$\begin{aligned} \frac{1}{\rho_2} \left[p_2 \left(1 - \frac{\gamma - 1}{2\gamma} \right) + p_1 \left(\frac{\gamma - 1}{2\gamma} \right) \right] &= R_v T_{s1} + \frac{p_2}{\rho_1} \left(\frac{\gamma - 1}{2\gamma} \right) \\ &\quad - \frac{p_1}{\rho_1} \left(\frac{\gamma - 1}{2\gamma} \right) - y_1 h_{fg1} \frac{\gamma - 1}{\gamma} \end{aligned}$$

Finally, using the ideal gas relations $\rho_2 = p_2/R_v T_2$ and $\rho_1 = p_1/R_v T_{s1}(1 - y_1)$ and collecting terms gives

$$\frac{T_2}{T_{s1}} = \frac{\left[1 + \frac{\gamma - 1}{2\gamma} \left(\frac{p_2}{p_1} - 1 \right) \right] - y_1 \left[\frac{h_{fg1}}{c_p T_{s1}} + \frac{\gamma - 1}{2\gamma} \left(\frac{p_2}{p_1} - 1 \right) \right]}{1 - \frac{\gamma - 1}{2\gamma} \left(1 - \frac{p_1}{p_2} \right)} \quad (4.117)$$

It is seen that the temperature T_2 after the shock decreases linearly with y_1 . When there is no liquid present, the kinetic energy ahead of the shock becomes converted to internal energy and expended as flow work, the former being $1/(\gamma - 1)$ times the latter. With liquid droplets present, some of the internal energy goes to vaporize the droplets, and therefore, the temperature is lower as the degree of wetness is increased. The drop in temperature, as y_1 increases toward $y_{1\text{lim}}$, is shown in Figure 4.7.

The velocity before the shock can now be determined by calculating the density from $\rho_2 = p_2/R_v T_2$ and then the velocity V_1 from

$$V_1^2 = \frac{(p_2 - p_1)}{(\rho_2 - \rho_1)} \frac{\rho_2}{\rho_1}$$

From this, the frozen Mach number, $M_f = V_1/c_{fz}$, can be calculated, by noting that the speed of sound $c_{fz} = \sqrt{\gamma R_v T_{s1}}$, and not forgetting that upstream of the shock, the steam

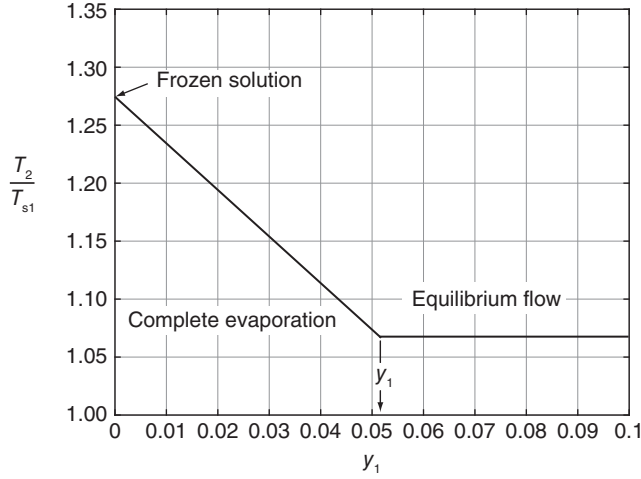


Figure 4.7 Temperature ratio as a function of degree wetness before and after complete evaporation for $\gamma = 1.32$, $p_1 = 0.3$ bar, and $p_2/p_1 = 2.5$.

exists as a two-phase mixture, with its density approximated by $\rho_1 = \rho_{v1}/(1 - y_1)$. The reduction in the frozen Mach number and thus the velocity is shown in Figure 4.8.

The curves on the left-hand sides in Figures 4.7 and 4.8 hold for degree of wetness $y_1 < y_{1\text{lim}}$. The value of $y_{1\text{lim}}$ is obtained from Eq. (4.117) by setting T_2 equal to T_{s2} . This limit is therefore

$$y_{\text{lim}} = \frac{1 + \frac{\gamma - 1}{2\gamma} \left(\frac{p_2}{p_1} - 1 \right) - \frac{T_{s2}}{T_{s1}} \left[1 - \frac{\gamma - 1}{2\gamma} \left(1 - \frac{p_2}{p_1} \right) \right]}{\frac{h_{fg1}}{c_p T_{s1}} + \frac{\gamma - 1}{2\gamma} \left(\frac{p_2}{p_1} - 1 \right)} \quad (4.118)$$

This is shown in Figure 4.9

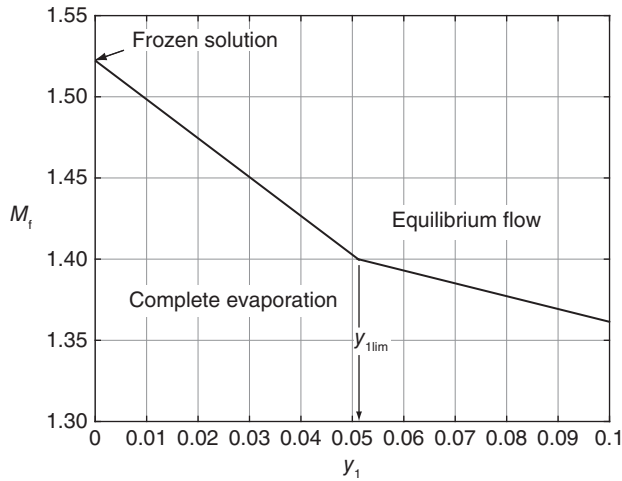


Figure 4.8 Frozen Mach number as a function of degree wetness before and after complete evaporation for $\gamma = 1.32$, $p_1 = 0.3$ bar, and $p_2/p_1 = 2.5$.

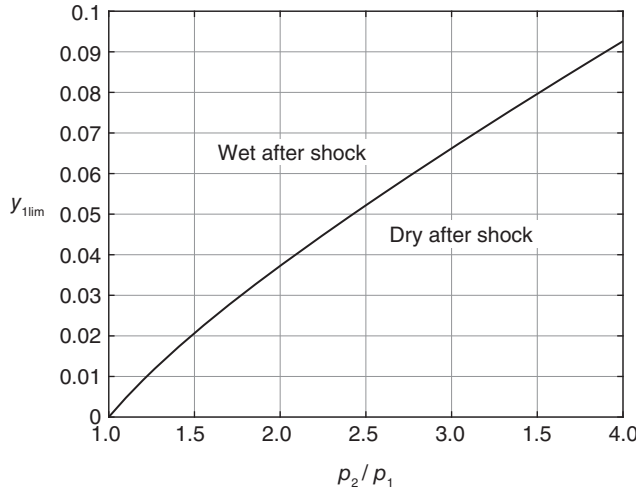


Figure 4.9 Boundary between wet and dry steam after a shock.

If the steam is wetter than that given by the minimum value of y_1 , then, not only all the liquid will have evaporated and the temperature after the shock no longer changes, but the amount of liquid water, y_2 , also does. The development of the expression for y_2 follows closely the steps used to arrive at Eq. (4.117) and is left as an exercise. The result is

$$y_2 = \frac{\frac{2\gamma}{\gamma-1} \left(\frac{T_{s2}}{T_{s1}} - 1 \right) + \frac{2y_1 h_{fg1}}{R_v T_{s1}} - (1 - y_1) \left(\frac{p_2}{p_1} - 1 \right) - \frac{T_{s2}}{T_{s1}} \left(1 - \frac{p_1}{p_2} \right)}{\frac{T_{s2}}{T_{s1}} \left[\frac{2h_{fg2}}{R_v T_{s2}} - \left(1 - \frac{p_1}{p_2} \right) \right]} \quad (4.119)$$

The expression for the velocity ahead of the shock becomes

$$V_1^2 = \frac{(p_2 - p_1)/\rho_1}{1 - \rho_1(1 - y_2)R_v T_{s2}/p_2}$$

from which the frozen Mach number can be formed. These results are shown also in Figures 4.7 and 4.8.

4.5 CONDENSATION SHOCKS

Condensation shocks differ from aerodynamic shocks in a crucial detail; namely, the location of an aerodynamic shock is determined by the back pressure, whereas a condensation shock forms when temperature drops sufficiently to cause rapid condensation.

To understand what happens, consider steam flow through a nozzle. Upstream in the steam chest, the thermodynamic state corresponds to the stagnation state. As usual, the flow through the nozzle can be taken to be isentropic, except across shocks that may be present. If the flow were to progress through states of thermodynamic equilibrium, some of the steam would begin to condense into small droplets as soon as the process crosses the saturated vapor line. The droplet formation is delayed however, for the reason that the formation of droplets takes time, and their growth involves growth kinetics and transport phenomena, both nonequilibrium effects.

The incipient formation of droplets is called *nucleation*. It may begin at the crevices along the nozzle walls, in which case it is called *heterogeneous nucleation*, or it may also form at dust particles or ions in the bulk steam, and this phenomena is called *homogeneous nucleation*. Some put nucleation from dust particles into the category of heterogeneous nucleation since the dust particles may not be dispersed homogeneously in the vapor phase. The word *nucleation* suggests that droplets start from molecular processes in which water molecules with low kinetic energy become attached to the walls, or at dust particles and then subsequently grow as more and more molecules accumulate at such sites.

As the steam in nozzle flow expands further, its temperature drops still more, and thus, the average kinetic energy of the molecules is now lower, and they are more likely to condense into the molecular clusters that grow into small droplets. The finite time for this process makes it possible for the steam to remain in this *supersaturated* state until it is so cold that the droplet growth becomes very rapid. Steam at this nonequilibrium state is also said to be *undercooled* or *subcooled*.

Experimental observations have shown that the degree of undercooling or supersaturation usually does not exceed the point where the steam quality is approximately $x = 0.96$. The line $x = 0.96$ in the Mollier chart is called the Wilson line, and when the steam pressure reaches the Wilson line, condensation front appears in the flow. To be sure, the value of undercooling depends on the expansion rate and the number of nucleation sites; that is to say, the cleanliness of the nozzle and the presence or absence of foreign matter in the steam. Typical amount of undercooling in low pressure steam is 20°C , the exact amount depending where the steam crosses the Wilson line.

The mixture after the condensation shock is not in phase equilibrium but tends toward it as it moves downstream. The adjustment to equilibrium conditions takes place in the relaxation zone, the extent of which is determined by rate of heat and mass transfer between the droplets and the vapor. Binnie and Woods [8] measured the pressure change across such a condensation shock, and their results are shown in Figure 4.10. A discussion of their work is in Kearton [53]. At a somewhat earlier date, Yellott alone and Yellott and Holland (cited by J.H. Keenan [54]) also carried out experiments on condensation shocks. Their work is also discussed by Kearton.

For purposes of calculation, the Wilson line will be assumed to correspond to constant quality of $x = 0.96$. By this measure, the Wilson line is reached by isentropic expansion

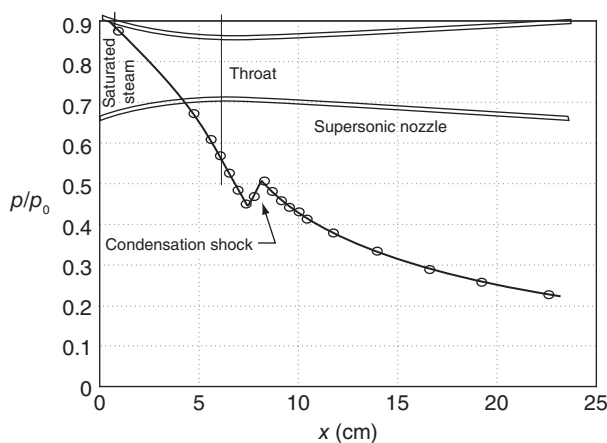


Figure 4.10 Illustration of a condensation shock from Binnie and Woods [8].

when enthalpy is about 130 kJ/kg below the saturation line. Supersaturated steam above $x = 0.96$ can be assumed to behave as an ideal gas with $\gamma = 1.3$. Thus, steam at stagnation conditions with temperature T_0 and pressure p_0 , when it expands isentropically to pressure p_1 , reaches a temperature

$$T_1 = T_0 \left(\frac{p_1}{p_0} \right)^{(\gamma-1)/\gamma}$$

The saturation pressure corresponding to temperature T_1 is denoted by p_{ss} , and the ratio of the pressure p_1 to which the expansion takes place and p_{ss} is called the *degree of supersaturation*. It is given by

$$S = \frac{p_1}{p_{ss}} \quad (4.120)$$

The saturation temperature T_{s1} corresponding to pressure p_1 is larger than T_2 , and the amount of undercooling is given by $\Delta T = T_{s1} - T_1$.

■ EXAMPLE 4.2

Steam expands from stagnation state $p_0 = 10$ bar and $T_0 = 200^\circ\text{C}$ isentropically through a nozzle to pressure $p_1 = 3.60$ bar. Find the degree of supersaturation and the amount of undercooling, assuming superheated steam behaves as an ideal gas with $\gamma = 1.3$ even when it is supersaturated.

Solution: At the inlet condition, the entropy of steam is $s_0 = 6.695$ kJ/(kg K). At pressure $p_1 = 3.60$ bar and entropy $s_1 = 6.695$ kJ/(kg K), the steam quality is $x_1 = 0.9547$. Thus, the quality is close to the Wilson line. Assuming that the steam is supersaturated, its temperature is

$$T_1 = T_0 \left(\frac{p_1}{p_0} \right)^{(\gamma-1)/\gamma} = 473.15 \left(\frac{3.60}{10} \right)^{0.3/1.3} = 373.8 \text{ K}$$

Saturation pressure corresponding to this temperature is $p_{ss} = 1.037$ bar. Hence, the degree of supersaturation is

$$S = \frac{p_1}{p_{ss}} = \frac{3.600}{1.037} = 3.472$$

The saturation temperature corresponding to $p_1 = 3.6$ bar is $T_{s1} = 413.0$ K, and the amount of undercooling is $\Delta T = T_{s1} - T_1 = 413.0 - 373.8 = 39.2$ K. ■

4.5.1 Jump conditions across a condensation shock

Assuming a thin condensation shock, the mass balance can be written as

$$\rho_1 V_1 = \rho_2 V_2$$

in which the density of the two-phase mixture after the shock is related to the vapor density by

$$\rho_{v2} = (1 - y_2)\rho_2 \quad (4.121)$$

The momentum balance is

$$p_1 + \rho_1 V_1^2 = p_2 + \rho_2 V_2^2$$

Since steam after the shock is a two-phase mixture, the pressure $p_2 = p_s(T_2)$ is the saturation pressure at temperature T_2 . The mass and momentum balance can be used to express the velocities before and after the shock as

$$V_1 = \left[\frac{(p_1 - p_2) \rho_2}{(\rho_1 - \rho_2) \rho_1} \right]^{1/2} \quad V_2 = \left[\frac{(p_1 - p_2) \rho_1}{(\rho_1 - \rho_2) \rho_2} \right]^{1/2} \quad (4.122)$$

The energy balance is given by

$$h_1 + \frac{1}{2} V_1^2 = h_2 + \frac{1}{2} V_2^2$$

Since the thermodynamic state of steam after the shock is in the two-phase region, its enthalpy is given by

$$h_2 = h_{v2} - y_2 h_{fg2} = h_{v2} + (1 - y_2) h_{fg2} - h_{fg2}$$

in which in the second form, the term h_{fg2} has been added and subtracted on the right-hand side. The energy equation can be now written as

$$2c_p(T_1 - T_2) - 2(1 - y_2)h_{fg2} + 2h_{fg2} = V_2^2 - V_1^2$$

Substituting the velocities from Eq. (4.122) into this and simplifying gives

$$2c_p(T_1 - T_2) - 2(1 - y_2)h_{fg2} + 2h_{fg2} = \left(\frac{1}{\rho_1} + \frac{1}{\rho_2} \right) (p_1 - p_2)$$

Finally, substituting the mixture density from Eq. (4.121) into this gives

$$2c_p(T_1 - T_2) - 2(1 - y_2)h_{fg2} + 2h_{fg2} = \frac{1}{\rho_1} (p_1 - p_2) + \frac{1 - y_2}{\rho_{v2}} (p_1 - p_2)$$

Solving this for $1 - y_2$ gives

$$1 - y_2 = \frac{2h_{fg2} + 2c_p(T_1 - T_2) + \left(1 - \frac{p_1}{p_2}\right)}{2h_{fg2} - \left(1 - \frac{p_1}{p_2}\right) R_v T_2}$$

If T_2 is known, then the quality $x_2 = 1 - y_2$ can be calculated from this expression. After that the velocity before the shock is calculated from Eq. (4.122), in which $\rho_2 = \rho_{v2}/(1 - y_2)$ and ρ_{v2} is obtained from $\rho_{v2} = p_2/R_v T_2$. The upstream Mach number can now be calculated from

$$M_1 = \frac{V_1}{c_1} \quad \text{where} \quad c_1 = \sqrt{\gamma R_v T_1}$$

This Mach number can now be compared to the one calculated from the known upstream properties. It is given by

$$M_1 = \sqrt{\frac{2}{\gamma - 1} \left[\left(\frac{p_0}{p_1} \right)^{(\gamma-1)/\gamma} - 1 \right]}$$

That value of T_2 is chosen for which the Mach numbers agree. This constitutes an iteration scheme for T_2 . To set up a robust iteration scheme requires the knowledge of the allowable temperatures after the shock. The allowable range requires further investigation.

Consider the expansion of steam through a supersonic nozzle from the stagnation state $p_0 = 1.0$ bar and $T_0 = 120$ °C. The first task is to find the pressure ahead of the shock. Examination of the Mollier chart shows that the pressure is about half away between 0.2 and 0.5 bar. The following statements find the pressure:

```
p0=1.0
T0=120;
T0K=T0+273.15;
s0=XSteam('s_pT',p0,T0);
xw=0.96;
p1=fzero(@(p1) xw-XSteam('x_ps',p1,s0), [0.2,0.5])
```

Alternatively, a call to the function `wilsonline`, shown below (and a much less sophisticated piece of code than `fzero`) accomplishes the same thing. Although the function `fzero` is designed to be robust, it is a *black box* to the user. The function `wilsonline` that uses the bisection method to find the pressure is robust and takes only 11 bisections to reach a 5 significant figure accuracy and executes in about 2 ms on a 2017 vintage computer.

```
function [pc, xc]=wilsonline(s0)
xw=0.96;
%Bisection for finding p where xw=0.96;
pl=0.2; pr=0.5; tol=0.00001;
n=1; nmax=30;
while n < nmax
    pc=0.5*(pl+pr);
    xl=XSteam('x_ps',pl,s0);
    xr=XSteam('x_ps',pr,s0);
    xc=XSteam('x_ps',pc,s0);
    if abs(xc-xw) < tol
        break
    end
    if (xc-xw)*(xr-xw) > 0
        pr = pc;
        xr = xc;
    else
        pl = pc;
        xl = xc;
    end
    n=n+1;
end
xc=0.5*(xr+xl);
pc=0.5*(pr+pl);
end
```

The pressure ahead of the shock is $p_1 = 0.3265$ bar, and the Mach number is $M_1 = 1.402$. In Figure 4.11, two solution branches are shown. On the left is an expansion

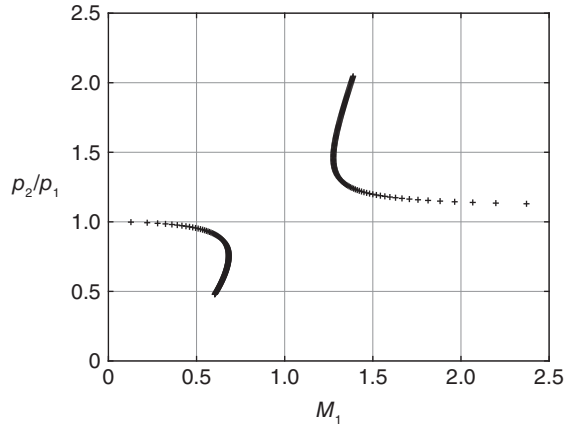


Figure 4.11 Two solution branches for a condensation shock.

wave with $p_2 < p_1$. The maximum Mach number on this branch is $M_1 = 0.6824$, and the temperature at this condition is 64.7°C . On the right, a compression shock, with the minimum Mach number $M_1 = 1.2754$ and $T_2 = 80.1^\circ\text{C}$. Between these two Mach numbers, there are no real solutions, for the velocity becomes a complex number. Both waves can also be split into two parts, the upper part for the expansion being a weak expansion and the lower part a strong expansion. Similarly, the upper part of the compression shock on the right is a strong compression and the lower part a weak compression. The temperature range for real solutions and with $y_2 > 0$ and $\Delta s > 0$ was found by trial to be between 54.8 and 71.09°C for the expansion waves, and for the compression shocks, it was from 73.5 to 90.8°C . The upper value was chosen such that it is just below the value at which the line of constant entropy crosses the saturation line. It turns out that this is slightly too high since the entropy increase across the shock takes the solution to the superheated steam region. By trial, the value $T_2 = 88.7^\circ\text{C}$ keeps the solution under the vapor dome. Hence, this was taken to be another constraint on the range of possible values of T_2 .

Another way to represent the results is shown in Figure 4.12. For weak compressions, the equilibrium Mach number $M_{e2} > 1$ after the shock. Temperature was changed in

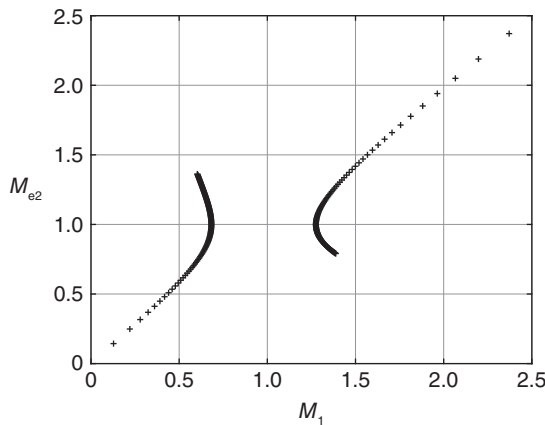


Figure 4.12 Two branches of the solution in the M_1, M_{e2} plane.

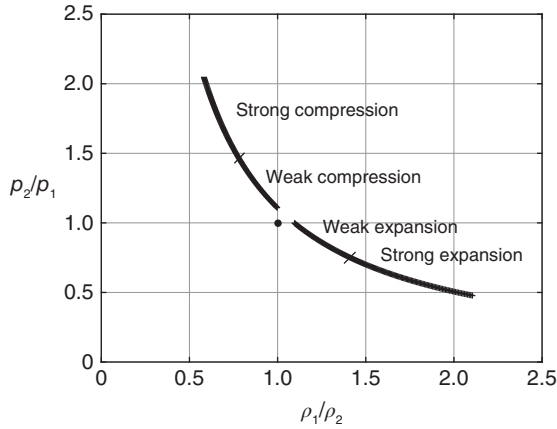


Figure 4.13 Identification of the structure of condensation expansions and compressions.

increments of 0.1°C , and the distance between the points is larger along the strong compression and strong expansion segments.

In Figure 4.13 are shown the same solution branches in a plot of ρ_1/ρ_2 on the abscissa and p_2/p_1 on the ordinate. The gap in which no solution is possible corresponds to previously mentioned situation in which the velocity after the shock becomes a complex number. Again, only the solutions in which y_2 is positive and there is an increase in entropy are plotted. Thus, for strong expansions as the upstream Mach number is lowered, the entropy change becomes negative, as seen from Figure 4.14. This solution branch is rejected as not being physically meaningful. Weak expansions are also ruled out in an expanding supersonic flow. Strong compressions have not been seen in laboratory experiments, but weak compressions have. In fact, weak shocks are the most likely outcome in a supersonic nozzle flow.

The entropy change across a condensation shock can be calculated by noting that $s_1 = s_0$, and thus,

$$s_2 - s_1 = s_{f2} + (1 - y_2)s_{fg2} - s_0$$

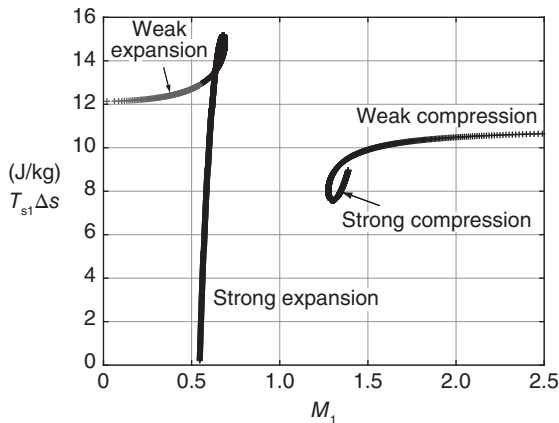


Figure 4.14 Entropy increase across a condensation front.

with saturation values calculated at the saturation pressure p_2 . The entropy increase across the condensation fronts is plotted in Figure 4.14.

The properties of the supersaturated state before the shock, and the equilibrium state with $x_2 = 0.974$ after it are:

$$\begin{array}{llllll} M_1 = 1.402 & p_1 = 0.326 \text{ bar} & T_1 = 30.5^\circ\text{C} & V_1 = 598 \text{ m/s} & s_1 = 7.468 \text{ kJ}/(\text{kg K}) \\ M_{e2} = 1.290 & p_2 = 0.402 \text{ bar} & T_2 = 76.0^\circ\text{C} & V_2 = 544 \text{ m/s} & s_2 = 7.495 \text{ kJ}/(\text{kg K}) \end{array}$$

EXERCISES

4.1 Find the equivalent adiabatic index for saturated steam at pressure $p = 0.6$ bar and degree of wetness $y = 0.1$. [Ans: 1.132]

4.2 Using the conservation and relaxation equations, show that for a completely frozen flow the speed of sound is given by $c_{fz}^2 = \gamma R_v T_v$.

4.3 Using the conservation and relaxation equations, show that after the droplet temperature relaxation are complete, but complete thermal relaxation has not taken place; in this zone, the speed of sound is given by

$$c_{e1}^2 = \frac{(1-y)\gamma R_v T_v}{1 + \frac{y}{1-y} \frac{\gamma c_i}{R_v} \left(\frac{R_v T_s}{h_{fg}} \right)^2}$$

4.4 For waves of Type II, for which $c_{e2u} < V_{vu} < V_{e1u}$, show that

$$\frac{d\Delta V}{dx} + \left[\frac{1 - M_{e2}^2}{1 - M_{e1}^2} \right] \frac{\Delta V}{V_v \tau_1} = 0$$

4.5 For waves of Type III, for which $c_{e1u} < V_{vu} < V_{fzu}$, show that

$$\frac{d\Delta T_i}{dx} + \left[\frac{1 - M_{e1}^2}{1 - M_f^2} \right] \frac{\Delta T_i}{V_v \tau_D} = 0$$

4.6 Steam flow through a diffuser at the rate of $\dot{m} = 0.17$ kg/s. At a location where diameter $D_1 = 3$ cm, pressure is measured to be $p_1 = 1$ bar, and quality is $x_1 = 0.9$. (a) Find the Mach number at this location. (b) Find the velocity at a location where the pressure is $p_2 = 1.3$ bar, by assuming that the diffuser efficiency is $\eta = (h_{2s} - h_1)/(h_2 - h_1) = 0.97$. (c) Find the Mach number M_{e2} and (d) the diameter D_2 . Assume that the liquid and vapor remain at phase equilibrium during the process. [Ans: (a) 0.881, (b) 225.2 m/s, (c) 0.533, (d) 3.41 cm]

4.7 Steam flows through a supersonic at the rate of $\dot{m} = 0.08$ kg/s. At a location where diameter $D_1 = 2.5$ cm, pressure is measured to be $p_1 = 0.9$ bar, and quality is $x_1 = 0.92$, (a) find the Mach number at this location. (b) Find the velocity at a location where the quality has reached pressure $x_2 = 0.85$, by assuming isentropic flow. (c) Find the Mach number M_{e2} and (d) the diameter D_2 . Assume that the liquid and vapor remain at phase equilibrium during the process. [Ans: (a) 0.668, (b) 752.8 m/s, (c) 1.971, (d) 3.30 cm].

4.8 Steam flows isentropically at a rate $\dot{m} = 0.04$ kg/s through a diffuser from the inlet state at diameter $d_1 = 7.8$ cm, $p_1 = 0.03$ bar, and $x_1 = 0.985$ and exits at the pressure $p_2 = 0.047$ bar. (a) Determine the value for the effective adiabatic index. (b) Find the pressure at which all the liquid has evaporated from the stream. (c) Find the velocity at the exit V_2 . (d) Find the Mach number at the exit. (e) Find the exit diameter of the diffuser. [Ans: (a) 1.1096, (b) 0.0423 bar, (c) 132.6 m/s, (d) 0.333, and (e) 10.8 cm]

4.9 A shock develops in wet steam flow with a pressure ratio is $p_2/p_1 = 2.5$. The pressure ahead of the shock is $p_1 = 0.35$ bar, and the degree of wetness is $y_1 = 0.08$. (a) Find the approximate degree of wetness after the shock by calculating the effective adiabatic index and using the normal shock relations. (b) Find the degree of wetness after the shock by the method discussed in the text, with $\gamma = 1.32$, and compare it to that calculated in the previous part. [Ans: (a) $y_2 = 0.0257$, (b) $y_2 = 0.0312$]

4.10 Develop the Eq. (4.119) in the text.

4.11 Steam enters a nozzle from a steam chest at saturated vapor state at pressure $p_0 = 0.8$ bar. It expands isentropically, with $\gamma = 1.32$ through a steam nozzle. Find the degree of supersaturation when it crosses the Wilson line at $x = 0.96$. [Ans: 7.46.]

4.12 Steam with $\gamma = 1.3$ flows in a nozzle from the stagnation state in a steam chest at $p_0 = 1.5$ bar and $T_0 = 125$ °C. Write a MATLAB or GNU/OCTAVE function that calculates the quality of steam when it has been undercooled by 15, 20, and 25 °C. [Ans: 0.9560, 0.9415, and 0.9271]

CHAPTER 5

PRINCIPLES OF TURBOMACHINE ANALYSIS

In this chapter, the fundamental equation for turbomachinery analysis is developed from the moment of momentum balance. It leads to an expression for the shaft torque in terms of the difference at which the rate of angular momentum of the working fluid leaves and enters a properly chosen control volume. Power delivered (or absorbed) by a turbomachine is then simply the product of the torque and the angular speed of the shaft. This equation is called the *Euler equation of turbomachinery*.

In the earlier chapters, power transferred to, or from, a turbomachine was expressed as the product of mass flow rate and a change in stagnation enthalpy. By equating the expression for work from the Euler equation of turbomachinery to the change in stagnation enthalpy, concepts from fluid mechanics become linked to thermodynamics. This link is central in turbomachinery performance analysis.

In applying the momentum of momentum balance to a *stationary control volume*, angular momentum is usually expressed in terms of absolute velocity of the fluid. In the analysis of the rotating blades, velocity relative to the rotor is also needed. From it, together with the absolute velocity and the blade velocity, one can construct a velocity triangle. These velocity triangles are discussed first in this chapter. They are followed by the development of the Euler equation for turbomachinery. After that, the work delivered, or absorbed, is recast in an alternative form, and a concept of degree of reaction is developed. One measure of the effectiveness at which work transfer takes place in a turbomachine is called *utilization*. Although this concept is not extensively used today, it is introduced, and its relationship to energy transfer and reaction is developed. The final section is on the

theory of scaling and similitude, both of which are useful in determining the performance of one turbomachine from the known performance of a similar one.

5.1 VELOCITY TRIANGLES

The velocity vector of a fluid particle that flows through a turbomachine is expressed most conveniently by its components in cylindrical coordinates, with the z -coordinate as the axis of rotation of the machine. These components are shown in Figure 5.1.

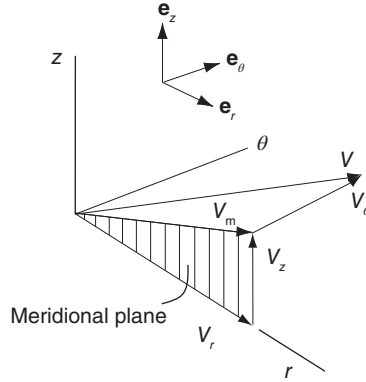


Figure 5.1 Meridional and tangential components of absolute velocity.

The vector sum of radial and axial components

$$\mathbf{V}_m = V_r \mathbf{e}_r + V_z \mathbf{e}_z \quad (5.1)$$

is called the *meridional velocity*, for it lies on the meridional plane, which is a radial plane containing the axis of rotation. For axial machines, the radial component of velocity is small and can be ignored, making the meridional velocity equal to the axial velocity. Similarly, at the outlet of a centrifugal compressor, or a radial pump, the axial velocity vanishes, and the meridional velocity then equals the radial velocity.

The *absolute velocity* \mathbf{V} is the sum of the *relative velocity* \mathbf{W} and the velocity of the frame, or *blade velocity* \mathbf{U} . They are related by the vector equation

$$\mathbf{V} = \mathbf{W} + \mathbf{U} \quad (5.2)$$

By the usual construction, this gives a *velocity triangle*, shown in Figure 5.2.

The angle that the absolute velocity makes with the meridional direction is denoted by α , and the angle that the relative velocity makes with this direction is β . These are called the *absolute* and *relative flow angles*. Since the flow tends to follow the blade, the relative velocity leaving the rotor is at the angle β , which is close to the actual blade angle designated by the symbol χ .

From Eq. (5.2) and Figure 5.2, it is seen that the meridional components give

$$V_m = W_m \quad (5.3)$$

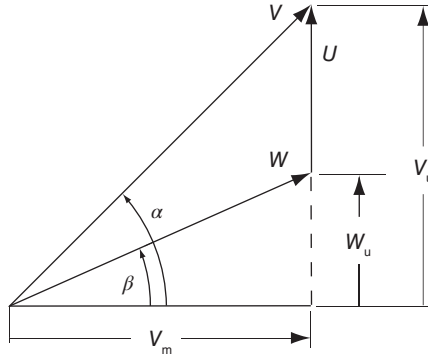


Figure 5.2 A typical velocity triangle.

and the tangential components yield the equation

$$V_u = W_u + U \quad (5.4)$$

These tangential components are related to the meridional velocity by

$$V_u = V_m \tan \alpha \quad W_u = W_m \tan \beta \quad (5.5)$$

It is convenient to denote the tangential component by the subscript u and to take it positive when it is in the direction of the blade motion. The meridional components are associated with the rate at which fluid flows through the machine; the tangential components with the blade forces.

The tangential and meridional velocity components can be also written as

$$V \sin \alpha = U + W \sin \beta \quad (5.6)$$

$$V \cos \alpha = W \cos \beta \quad (5.7)$$

Squaring each of these and adding gives

$$V^2 = U^2 + W^2 + 2UW \sin \beta \quad (5.8)$$

This is the law of cosines in a slightly disguised form. The purpose to carry out this kind of manipulation was to eliminate the angle α from the final equation.

Eliminating next the velocity V by multiplying Eq. (5.6) by $\cos \alpha$ and Eq. (5.7) by $\sin \alpha$ and subtracting them gives

$$U \cos \alpha = W \sin(\alpha - \beta) \quad \text{or} \quad \frac{\cos \alpha}{W} = \frac{\sin(\alpha - \beta)}{U} \quad (5.9)$$

This is essentially the law of sines.

■ EXAMPLE 5.1

Consider the velocity diagram for an axial flow machine, shown in Figure 5.3. The magnitude of the absolute velocity is $V_1 = 240$ m/s, and the flow angle is

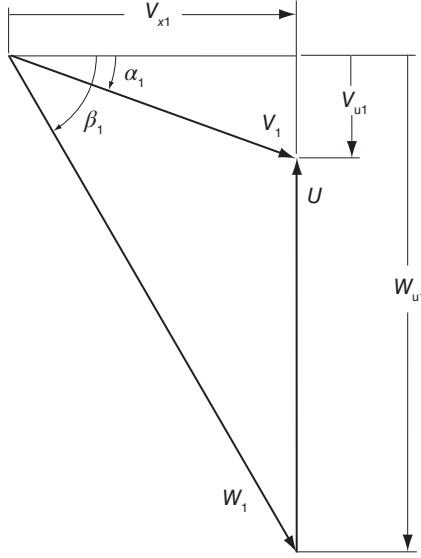


Figure 5.3 A velocity diagram illustrating negative flow angles.

$\alpha_1 = -20^\circ$. The blade speed is $U = 300$ m/s. Find the magnitude of the relative velocity and its flow angle.

Solution: The axial velocity is given by

$$V_{x1} = V_1 \cos \alpha_1 = 240 \cos(-20^\circ) = 225.5 \text{ m/s}$$

and $W_{x1} = V_{x1}$. The tangential components of the absolute and relative velocities are calculated as

$$V_{u1} = V_1 \sin \alpha_1 = 240 \sin(-20^\circ) = -82.1 \text{ m/s}$$

$$W_{u1} = V_{u1} - U = -82.1 - 300 = -382.1 \text{ m/s}$$

Hence, the magnitude of the relative velocity is

$$W_1 = \sqrt{W_{x1}^2 + W_{u1}^2} = \sqrt{225.5^2 + 382.2^2} = 443.7 \text{ m/s}$$

and the flow angle of the relative velocity becomes

$$\beta_1 = \tan^{-1} \left(\frac{W_{u1}}{W_{x1}} \right) = \tan^{-1} \left(-\frac{382.1}{225.5} \right) = -59.4^\circ$$

■

The foregoing example illustrates the sign convention for angles. Positive angles are measured from the meridional direction, and they increase in counterclockwise direction. Negative angles become more negative in the clockwise direction. This book will strictly adhere to this convention and doing so makes computer calculations easy to implement.

5.2 MOMENT OF MOMENTUM BALANCE

Consider a flow through a pump, shown in the schematic diagram in Figure 5.4. To apply the moment of momentum equation, a control volume is chosen to include both the pump impeller and the fluid. The velocity vector is written in cylindrical coordinates as

$$\mathbf{V} = V_r \mathbf{e}_r + V_\theta \mathbf{e}_\theta + V_z \mathbf{e}_z \quad (5.10)$$

in terms of the unit vectors \mathbf{e}_r , \mathbf{e}_θ , and \mathbf{e}_z . A working equation for the angular momentum balance for a uniform steady flow is

$$\dot{m}(\mathbf{r}_2 \times \mathbf{V}_2 - \mathbf{r}_1 \times \mathbf{V}_1) = \mathbf{T}_m + \mathbf{T}_f \quad (5.11)$$

On the right side, \mathbf{T}_m is the torque the shaft exerts on the impeller, and \mathbf{T}_f is a contribution from fluid pressure and viscous stresses. The z component of this equation is obtained by taking its scalar product with \mathbf{e}_z . Thus,

$$\dot{m} \mathbf{e}_z \cdot (\mathbf{r}_2 \times \mathbf{V}_2 - \mathbf{r}_1 \times \mathbf{V}_1) = \mathbf{e}_z \cdot \mathbf{T}_m = T$$

Owing to symmetry about the axis of rotation, pressure forces do not contribute to the axial torque, as they have radial and axial components only. Viscous forces act in the direction opposite to rotation and increase the required torque in a shaft of a compressor and decrease it in a turbine. These are neglected, or T is taken to be the net torque after they have been subtracted, or added. Rotation is taken to be clockwise when the pump is viewed in the flow direction. Hence, the rotation vector is $\boldsymbol{\Omega} = \Omega \mathbf{e}_z$. In order for the shaft to rotate the pump impeller in this direction, torque must be given by $\mathbf{T}_m = \mathbf{e}_z T$, and thus $\mathbf{e}_z \cdot \mathbf{T}_m = T$.

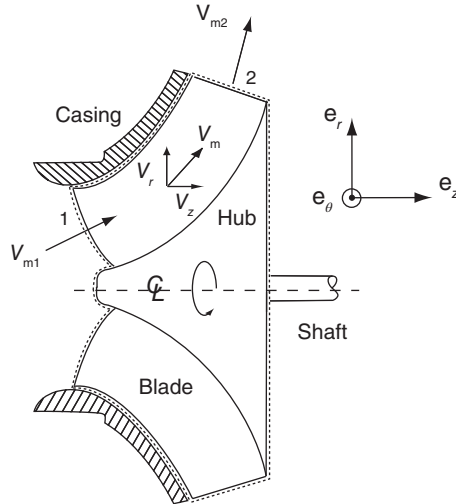


Figure 5.4 A schematic of a pump and a flow through it.

In cylindrical coordinates, the radius vector is $\mathbf{r} = r\mathbf{e}_r + z\mathbf{e}_z$, so that

$$\mathbf{r} \times \mathbf{V} = \begin{vmatrix} \mathbf{e}_r & \mathbf{e}_\theta & \mathbf{e}_z \\ r & 0 & z \\ V_r & V_\theta & V_z \end{vmatrix} = -\mathbf{e}_r z V_\theta - \mathbf{e}_\theta (r V_z - z V_r) + \mathbf{e}_z r V_\theta$$

and

$$\mathbf{e}_z \cdot (\mathbf{r} \times \mathbf{V}) = r V_\theta$$

Hence, the angular momentum equation becomes

$$T = \dot{m}(r_2 V_{\theta 2} - r_1 V_{\theta 1})$$

5.3 ENERGY TRANSFER IN TURBOMACHINES

The power delivered *to a turbomachine* is given by

$$\dot{W} = \mathbf{T} \cdot \boldsymbol{\Omega} = T\Omega = \dot{m}\Omega(r_2 V_{\theta 2} - r_1 V_{\theta 1})$$

The blade speeds are $U_1 = r_1\Omega$ and $U_2 = r_2\Omega$, and r_1 and r_2 are the mean radii at the inlet and outlet. Dividing this equation by the mass flow rate gives an expression for the work done per unit of mass, i.e. *specific work*

$$w = U_2 V_{\theta 2} - U_1 V_{\theta 1} \quad (5.12)$$

This is the *Euler equation for turbomachinery*.

As was already done in Figure 5.2, it is common to relabel the various terms and call the axial component of velocity V_x and denote the component of the velocity in the direction of the blade motion, as V_u . In this notation, there is no need to keep track of whether the rotor moves in clockwise or counterclockwise direction. The sense of rotation, of course, depends also on whether a rotor is viewed from the upstream or downstream direction. With these changes in notation, the Euler equation for turbomachinery may be written as

$$w = U_2 V_{u2} - U_1 V_{u1} \quad (5.13)$$

This gives the work done by the shaft on the rotor, and it is thus applicable to a compressor and a pump. For turbines, however, power is delivered by the machine, and the sign of the work would need to be changed. Since it is generally known whether the machine is power-absorbing or power-producing, work transfer will be taken as positive, and the Euler turbine equation is written as

$$w = U_2 V_{u2} - U_3 V_{u3} \quad (5.14)$$

For turbines, since a stage consists of a stator followed by a rotor, the inlet to the stator is designated as location 1, the inlet to the rotor is location 2, and the exit from the rotor is location 3.

For an axial turbomachine, $U_2 = U_3 = U$. Work delivered by a turbine stage is then given by

$$w = U(V_{u2} - V_{u3})$$

EXAMPLE 5.2

The shaft of small turbine turns at 20000 rpm, and the blade speed is $U = 250$ m/s. The axial velocity leaving the stator is $V_{x2} = 175$ m/s. The angle at which the absolute velocity leaves the stator blades is $\alpha_2 = 67^\circ$, the flow angle of the relative velocity leaving the rotor is $\beta_3 = -60^\circ$, and the absolute velocity leaves the rotor at the angle $\alpha_3 = -20^\circ$. These are shown in Figure 5.5. Find (a) the mean radius of the blades, (b) the angle of the relative velocity entering the rotor, (c) the magnitude of the axial velocity leaving the rotor, (d) the magnitude of the absolute velocity leaving the stator, and (e) the specific work delivered by the stage.

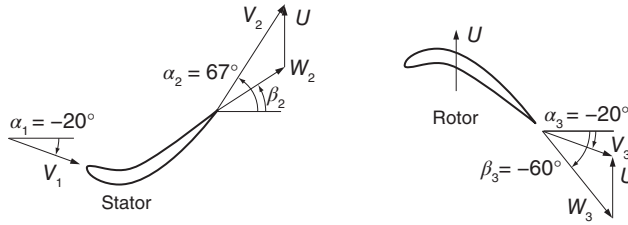


Figure 5.5 An axial turbine stage.

Solution: (a) The mean radius of the rotor is

$$r = \frac{U}{\Omega} = \frac{250 \cdot 60}{20000 \cdot 2\pi} = 11.94 \text{ cm}$$

(b) With the axial velocity and flow angle known, the tangential component of the velocity is

$$V_{u2} = V_{x2} \tan \alpha_2 = 175 \tan(67^\circ) = 412.3 \text{ m/s}$$

and therefore,

$$W_{u2} = V_{u2} - U = 412.3 - 250 = 162.3 \text{ m/s}$$

Since $W_{x2} = V_{x2}$,

$$\beta_2 = \tan^{-1} \left(\frac{W_{u2}}{W_{x2}} \right) = \tan^{-1} \left(\frac{162.3}{175} \right) = 42.8^\circ$$

(c) At the exit of the rotor,

$$V_{u3} = W_{u3} + U \quad V_{x3} \tan \alpha_3 = V_{x3} \tan \beta_3 + U$$

so that

$$V_{x3} = \frac{U}{\tan \alpha_3 - \tan \beta_3} = \frac{250}{\tan(-20^\circ) - \tan(-60^\circ)} = 182.7 \text{ m/s}$$

The absolute velocity is obtained by first calculating the tangential component

$$V_{u3} = V_{x3} \tan \alpha_3 = 182.7 \tan(-20^\circ) = -66.5 \text{ m/s}$$

and then,

$$V_3 = \sqrt{V_{x3}^2 + V_{u3}^2} = \sqrt{182.7^2 + 66.5^2} = 194.4 \text{ m/s}$$

(d) Specific work done is $w = U(V_{u2} - V_{u3}) = 250(412.3 + 66.5) = 119.7 \text{ kJ/kg}$. ■

In this example, the axial velocity increased slightly across the stage. As the flow expands through the turbine, its density decreases. Hence, the cross-sectional area would need to be adjusted to account for the increase in velocity and a decrease in density.

Usually, axial turbines are designed such that the axial velocity is constant and furthermore that the inlet velocity is equal to the velocity at the exit of the stage. Such a stage is called a *normal stage*. For a *repeating stage*, in addition, the inlet and exit angles of the absolute velocity for the stage are equal. Such a design allows for the blade shapes to be similar. However, for a normal stage α_1 need not be equal to α_3 , as long as $V_1 = V_3$. This assumption simplifies the subsequent theory. For a single-stage turbine, the inlet is likely to be axial, but as the previous example showed, neither the angle α_1 nor the velocity V_1 were used in the analysis. They are needed if the cross-sectional area at the inlet to the stage is to be determined.

The work done by a stage is

$$w = U(V_{u2} - V_{u3}) = UV_x(\tan \alpha_2 - \tan \alpha_3)$$

when the axial velocity is constant. Dividing by U^2 gives

$$\frac{w}{U^2} = \frac{V_x}{U}(\tan \alpha_2 - \tan \alpha_3)$$

Defining the *blade-loading coefficient* and *flow coefficient* as

$$\psi = \frac{w}{U^2} \quad \phi = \frac{V_x}{U} \quad (5.15)$$

gives a nondimensional version of this equation:

$$\psi = \phi(\tan \alpha_2 - \tan \alpha_3)$$

The blade-loading coefficient is an appropriate term for ψ because it is the blade force times the blade velocity that gives the rate at which work is delivered. Also, the flow coefficient ϕ is a ratio of the axial velocity to blade velocity and is thus a measure of the flow rate through the machine. Much use will be made of these nondimensional parameters, for they are independent of the size of machine, and their values for best designs have been established over many years of practice.

As another example in which the Euler equation for turbomachinery is used, an analysis of a centrifugal pump is considered next.

■ EXAMPLE 5.3

Water at 20 °C leaves a pump impeller with an absolute velocity of 13.94 m/s at the angle 72.1°. The blade speed at the exit is 25.17 m/s, and the shaft speed is 3450 rpm. The absolute velocity is axial at the inlet. The flow rate is 18.0 L/s.

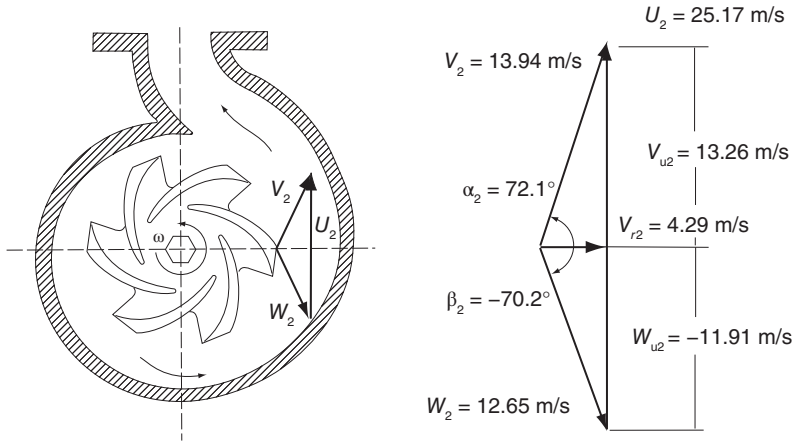


Figure 5.6 Pump exit and its velocity diagram.

Find (a) the magnitude of the relative velocity and its flow angle β_2 , (b) the power required, and (c) the outlet blade radius and the blade height assuming that the open area at the periphery is 93% of the total area. The pump is shown in Figure 5.6.

Solution: (a) The tangential component of the absolute velocity at the exit is given by

$$V_{u2} = V_2 \sin \alpha_2 = 13.94 \sin(72.1^\circ) = 13.26 \text{ m/s}$$

and its meridional component, which is radial here, is

$$V_{r2} = V_2 \cos \alpha_2 = 13.94 \cos(72.1^\circ) = 4.29 \text{ m/s}$$

The tangential component of the relative velocity is determined as

$$W_{u2} = V_{u2} - U_2 = 13.26 - 25.17 = -11.91 \text{ m/s}$$

Since the radial component of the relative velocity is $W_{r2} = V_{r2} = 4.29 \text{ m/s}$, the angle of the relative flow can be calculated as

$$\beta_2 = \tan^{-1} \left(\frac{W_{u2}}{W_{r2}} \right) = \tan^{-1} \left(-\frac{11.91}{4.29} \right) = -70.2^\circ$$

The magnitude of the relative velocity is then

$$W_2 = \sqrt{W_{r2}^2 + W_{u2}^2} = \sqrt{4.29^2 + 11.91^2} = 12.65 \text{ m/s}$$

A velocity triangle can now be completed. The flow angle of the relative velocity is approximately equal to the blade angle χ , and in this pump, the impeller blades curve backward; that is they are curved in the direction opposite to blade rotation.

(b) Since the flow is axial at the inlet, $V_{u1} = 0$, and the work done is

$$w = U_2 V_{u2} = 25.17 \cdot 13.26 = 333.88 \text{ J/kg}$$

With density of water is close to $\rho = 1000 \text{ kg/m}^3$, the mass flow rate is

$$\dot{m} = \rho Q = 1000 \cdot 0.018 = 18.0 \text{ kg/s}$$

and the power required is $\dot{W} = \dot{m}w = 18.0 \cdot 333.88 = 6.0 \text{ kW}$.

(c) The outlet radius is

$$r_2 = \frac{U_2}{\Omega} = \frac{25.17 \cdot 30}{3450 \cdot \pi} = 6.97 \text{ cm}$$

With the flow rate $Q = 0.018 \text{ m}^3/\text{s}$, the outlet area is

$$A_2 = \frac{Q}{V_{r2}} = \frac{0.018}{4.29} = 42.0 \text{ cm}^2$$

The blade height is then

$$b_2 = \frac{A_2}{0.93 \cdot 2\pi \cdot r_2} = \frac{42.0}{0.93 \cdot 2\pi \cdot 6.97} = 1.03 \text{ cm}$$

The blade-loading coefficient and flow coefficient are defined in terms of the tip speed of the blade at the exit:

$$\psi = \frac{w}{U_2^2} = \frac{333.88}{25.17^2} = 0.527 \quad \phi = \frac{V_{r2}}{U_2} = \frac{4.29}{25.17} = 0.170$$

■

5.3.1 Trothalpy and specific work in terms of velocities

Since no work is done in the stator, total enthalpy remains constant across it. In this section, an analogous quantity to the total enthalpy is developed for the rotor. Specifically, consider a mixed-flow compressor in which the meridional velocity at the inlet is not completely axial and at the exit from the blades not completely radial. The work done by the rotor blades is

$$w = h_{02} - h_{01} = U_2 V_{u2} - U_1 V_{u1} \quad (5.16)$$

When this equation is written as

$$h_{01} - U_1 V_{u1} = h_{02} - U_2 V_{u2}$$

the quantity

$$I = h_0 - UV_u$$

is seen to be constant across the impeller. It can also be written as

$$I = h + \frac{1}{2}V^2 - UV_u = h + \frac{1}{2}V_m^2 + \frac{1}{2}V_u^2 - UV_u$$

Adding and subtracting $U^2/2$ to complete the square gives

$$I = h + \frac{1}{2}V_m^2 + \frac{1}{2}(V_u - U)^2 - \frac{1}{2}U^2 = h + \frac{1}{2}V_m^2 + \frac{1}{2}W_u^2 - \frac{1}{2}U^2$$

or since $V_m = W_m$, and $W^2 = W_m^2 + W_u^2$, it follows that

$$I = h_1 + \frac{1}{2}W_1^2 - \frac{1}{2}U_1^2 = h_2 + \frac{1}{2}W_2^2 - \frac{1}{2}U_2^2 \quad (5.17)$$

is constant across the impeller. The quantity I is called *trothalpy*.¹

Solving Eq. (5.17) for h_1 and h_2 and substituting them into the equation for work

$$w = h_{02} - h_{01} = h_2 + \frac{1}{2}V_2^2 - h_1 - \frac{1}{2}V_1^2 \quad (5.18)$$

gives, after I has been canceled, the following equation:

$$w = \frac{1}{2}V_2^2 - \frac{1}{2}W_2^2 + \frac{1}{2}U_2^2 - \left(\frac{1}{2}V_1^2 - \frac{1}{2}W_1^2 + \frac{1}{2}U_1^2 \right)$$

Rearranging gives the form

$$w = \frac{1}{2}(V_2^2 - V_1^2) + \frac{1}{2}(U_2^2 - U_1^2) + \frac{1}{2}(W_1^2 - W_2^2) \quad (5.19)$$

Equating this and Eq. (5.18) leads to

$$h_2 - h_1 = \frac{1}{2}(U_2^2 - U_1^2) + \frac{1}{2}(W_1^2 - W_2^2) \quad (5.20)$$

From Eq. (5.18), it is seen that the work done in a centrifugal pump increases the kinetic energy and the static enthalpy. Equation (5.20) shows first that the static enthalpy increase involves moving the fluid to a larger radius, resulting in increased pressure. The second term causes an increase in pressure when the relative velocity is reduced; that is diffusion with $W_2 < W_1$ leads to pressure recovery. Pressure is increased further in the volute of a centrifugal pump where diffusion of the absolute velocity takes place. Since this diffusion is against an adverse pressure gradient, the kinetic energy at the exit of the impeller cannot be so large that its deceleration through the volute causes separation of boundary layers and a great increase in irreversibility. The use of these concepts is illustrated in the next example.

■ EXAMPLE 5.4

A small centrifugal pump with an impeller radius $r_2 = 4.5$ cm operates at 3450 rpm. Blades at the exit are curved back at an angle $\beta_2 = -65^\circ$. Radial velocity at the exit is $V_{r2} = W_{r2} = 3.0$ m/s. Flow at the inlet is axial with velocity $V_1 = 4.13$ m/s. The mean radius of the impeller at the inlet is $r_1 = 2.8$ cm. (a) Find the work done using Eq. (5.16). (b) Calculate the kinetic energy change of the relative velocity, absolute velocity, and that associated with the change in the blade speed, and calculate work done using Eq. (5.19). Confirm that the two methods give the same answer.

¹This quantity is commonly called *rothalpy*, a compound word combining the terms *rotation* and *enthalpy*. Its construction does not conform to the established rules for formation of new words in the English language, namely, that the roots of the new word originate from the same language. The word *trothalpy* satisfies this requirement as *trohos* is the Greek root for *wheel* and *enthalpy* is to put heat in, whereas *rotation* is derived from Latin *rotare*.

Solution: (a) Blade speed at the exit is

$$U_2 = r_2 \Omega = \frac{0.045 \cdot 3450 \cdot 2\pi}{60} = 16.26 \text{ m/s}$$

Since $W_{r2} = V_{r2}$, the tangential component of the relative velocity is

$$W_{u2} = V_{r2} \tan \beta_2 = 3.0 \tan(-65^\circ) = -6.43 \text{ m/s}$$

Tangential component of the absolute velocity is then

$$V_{u2} = U_2 + W_{u2} = 16.26 - 6.43 = 9.83 \text{ m/s}$$

Since the flow at the inlet is axial $V_{u1} = 0$, the inlet does not contribute to the work done as calculated by the Euler equation for turbomachinery, which reduces to

$$w = U_2 V_{u2} = 16.26 \cdot 9.83 = 159.7 \text{ J/kg}$$

(b) Magnitudes of the relative and absolute velocities at the exit are given by

$$W_2 = \sqrt{W_{u2}^2 + W_{r2}^2} = \sqrt{6.43^2 + 3.0^2} = 7.10 \text{ m/s}$$

$$V_2 = \sqrt{V_{u2}^2 + V_{r2}^2} = \sqrt{9.83^2 + 3.0^2} = 10.27 \text{ m/s}$$

Since the flow is axial at the inlet. $V_{x1} = V_1 = 4.13 \text{ m/s}$. The blade speed at the inlet is

$$U_1 = r_1 \Omega = \frac{0.028 \cdot 3450 \pi}{30} = 10.11 \text{ m/s}$$

The tangential component of the relative velocity at the inlet is given by

$$W_{u1} = V_{u1} - U_1 = 0 - 10.11 = -10.11 \text{ m/s}$$

and therefore, the magnitude of the relative velocity is

$$W_1 = \sqrt{W_{u1}^2 + W_{r1}^2} = \sqrt{10.11^2 + 4.13^2} = 10.92 \text{ m/s}$$

The kinetic energy changes are

$$\frac{1}{2}(V_2^2 - V_1^2) = \frac{1}{2}(10.27^2 - 4.13^2) = 44.21 \text{ m}^2/\text{s}^2 = 44.21 \text{ J/kg}$$

$$\frac{1}{2}(U_2^2 - U_1^2) = \frac{1}{2}(16.26^2 - 10.11^2) = 80.99 \text{ m}^2/\text{s}^2 = 80.99 \text{ J/kg}$$

$$\frac{1}{2}(W_1^2 - W_2^2) = \frac{1}{2}(10.92^2 - 7.10^2) = 34.51 \text{ m}^2/\text{s}^2 = 34.51 \text{ J/kg}$$

Their sum checks with the direct calculation of the work done. ■

Since in the previous example there was no swirl at the inlet, $V_{u1} = 0$, the work done is independent of the inlet conditions. This means that when work is represented in terms of kinetic energy changes, terms involving inlet velocities must cancel. Velocity triangle at

the inlet is a right triangle with W_1 as its hypotenuse, so that $V_1^2 + U_1^2 = W_1^2$. Hence, in this case,

$$w = \frac{1}{2}(V_2^2 + U_2^2 - W_2^2)$$

and using the law of cosines gives $w = U_2 V_{u2}$, as it should.

When the analysis in this subsection is carried out for a turbine, the results are

$$w = \frac{1}{2}(V_2^2 - V_3^2) + \frac{1}{2}(U_2^2 - U_3^2) + \frac{1}{2}(W_3^2 - W_2^2) \quad (5.21)$$

and

$$h_2 - h_3 = \frac{1}{2}(U_2^2 - U_3^2) + \frac{1}{2}(W_3^2 - W_2^2) \quad (5.22)$$

These are similar to Eqs. (5.19) and (5.20) and differ only by subscript 3 replacing 1.

5.3.2 Degree of reaction

Degree of reaction, or *reaction* for short, is defined as the change in static enthalpy across the rotor divided by the static enthalpy change across the entire stage. For a turbine, this is given as

$$R = \frac{h_2 - h_3}{h_1 - h_3}$$

Work delivered by a rotor in a turbine is

$$w = h_{02} - h_{03} = h_2 + \frac{1}{2}V_2^2 - h_3 - \frac{1}{2}V_3^2$$

Since for nozzles (or stator) $h_{01} = h_{02}$, work can also be written as

$$w = h_1 - h_3 + \frac{1}{2}(V_1^2 - V_3^2)$$

Solving the last two equations for static enthalpy differences and substituting them into the definition of reaction gives

$$R = \frac{\frac{1}{2}(V_3^2 - V_2^2) + w}{\frac{1}{2}(V_3^2 - V_1^2) + w} \quad (5.23)$$

The work delivered by a turbine is given in Eq. (5.21). Substituting it to Eq. (5.23) and simplifying leads to

$$R = \frac{U_2^2 - U_3^2 + W_3^2 - W_2^2}{V_2^2 - V_1^2 + U_2^2 - U_3^2 + W_3^2 - W_2^2} \quad \text{turbine} \quad (5.24)$$

In a flow in which $V_1 = V_2$, reaction $R = 1$. A lawn sprinkler is such a pure reaction machine, for all the pressure drop takes place in the sprinkler arms. They turn as a *reaction* to the momentum leaving them.

The steam turbine shown in Figure 3.8 is an axial machine in which $U_2 = U_3$, and its reaction is zero when $W_2 = W_3$. For the rotor buckets shown, the blade angles are equal but opposite in sign and by adjustment of the flow area to account for the increase in specific volume, the magnitude of the relative velocity can be made constant across the rotor. Since the trothalpy is also constant across the rotor, enthalpy change across it vanishes, giving $R = 0$.

■ EXAMPLE 5.5

Consider an axial turbine stage with blade speed $U = 350$ m/s and axial velocity $V_x = 280$ m/s. Flow enters the rotor at angle $\alpha_2 = 60^\circ$. It leaves the rotor at angle $\alpha_3 = -30^\circ$. Assume a stage for which $\alpha_1 = \alpha_3$ and a constant axial velocity. Find the velocities and the degree of reaction.

Solution: Since axial velocity is constant and the flow angles are equal at both the entrance and exit of the stage, the velocity diagrams at the inlet of the stator and the exit of the rotor are identical. From a velocity triangle, such as shown in Figure 5.2, the tangential velocities are:

$$V_{u2} = V_x \tan \alpha_2 = 280.0 \tan(60^\circ) = 484.97 \text{ m/s}$$

$$V_{u3} = V_x \tan \alpha_1 = 280.0 \tan(-30^\circ) = -161.66 \text{ m/s}$$

and work done is

$$w = U(V_{u2} - V_{u3}) = 350(484.97 + 161.66) = 226.32 \text{ kJ/kg}$$

Tangential components of the relative velocities are

$$W_{u2} = V_{u2} - U = 484.97 - 350.00 = 134.97 \text{ m/s}$$

$$W_{u3} = V_{u3} - U = -161.66 - 350.00 = -511.66 \text{ m/s}$$

Hence,

$$V_2 = \sqrt{V_{u2}^2 + V_x^2} = \sqrt{484.97^2 + 280.0^2} = 560.00 \text{ m/s}$$

$$V_3 = \sqrt{V_{u3}^2 + V_x^2} = \sqrt{161.66^2 + 280.0^2} = 323.32 \text{ m/s}$$

$$W_2 = \sqrt{W_{u2}^2 + W_x^2} = \sqrt{134.97^2 + 280.0^2} = 310.83 \text{ m/s}$$

$$W_3 = \sqrt{W_{u3}^2 + W_x^2} = \sqrt{511.66^2 + 280.0^2} = 583.26 \text{ m/s}$$

Since $U_2 = U_3$, the expression for reaction is

$$R = \frac{W_3^2 - W_2^2}{2w} = \frac{583.26^2 - 310.83^2}{2 \cdot 226320} = 0.538$$

A reaction ratio close to one-half is often used to make the enthalpy drop, and thus also the pressure drop, in the stator and the rotor nearly equal. ■

The analysis of a compressor follows similar lines, and the resulting equation for the reaction is

$$R = \frac{h_2 - h_1}{h_3 - h_1}$$

which can be cast into the form

$$R = \frac{U_2^2 - U_1^2 + W_1^2 - W_2^2}{V_2^2 - V_3^2 + U_2^2 - U_1^2 + W_1^2 - W_2^2} \quad \text{compressor} \quad (5.25)$$

Since an enthalpy change is proportional to a pressure change, the degree of reaction can be viewed in terms of pressure changes. In compressors, pressure increases downstream, and in order to keep the adverse pressure gradient small to prevent boundary layer separation, the value of reaction cannot be very large.

5.4 UTILIZATION

A measure of how effectively a turbine rotor converts the available kinetic energy at its inlet to work is called *utilization*, and a *utilization factor* is defined as the ratio

$$\varepsilon = \frac{w}{w + \frac{1}{2}V_3^2} \quad (5.26)$$

The denominator is the available energy consisting of what is converted to work and the kinetic energy that leaves the turbine. This expression for utilization equals unity if the exit kinetic energy is negligible. But the exit kinetic energy cannot vanish completely because the flow has to leave the turbine. Hence, utilization factor is always less than one. Maximum utilization is reached by turning the flow so much that the swirl component vanishes; i.e. for the best utilization, the exit velocity vector should lie on the meridional plane.

For a turbine, when Eq. (5.21) is substituted into Eq. (5.26), the expression for utilization, in terms of velocities alone, becomes

$$\varepsilon = \frac{V_2^2 - V_3^2 + U_2^2 - U_3^2 + W_3^2 - W_2^2}{V_2^2 + U_2^2 - U_3^2 + W_3^2 - W_2^2} \quad (5.27)$$

Next, from Eq. (5.23), it is easy to see that the work delivered is also

$$w = -\frac{V_3^2}{2} + \frac{1}{2} \left(\frac{V_2^2 - RV_1^2}{1 - R} \right) \quad (5.28)$$

Substituting this into Eq. (5.26) gives

$$\varepsilon = \frac{V_2^2 - RV_1^2 - (1 - R)V_3^2}{V_2^2 - RV_1^2} \quad (5.29)$$

In the situation in which $R = 1$ and therefore also $V_2 = V_1$, this expression becomes indeterminate. It is valid for other values of R .

In a usual design of a multistage axial turbine, the exit velocity triangle is identical to the velocity triangle at the inlet of a stage. Under this condition, $V_1 = V_3$ and $\alpha_1 = \alpha_3$, and the utilization factor simplifies to

$$\varepsilon = \frac{V_2^2 - V_3^2}{V_2^2 - RV_3^2} \quad (5.30)$$

The expression for work reduces to

$$w = \frac{V_2^2 - V_3^2}{2(1 - R)} \quad (5.31)$$

With velocities expressed in terms of their tangential and axial components, this becomes

$$w = \frac{V_{x2}^2 + V_{u2}^2 - (V_{x3}^2 + V_{u3}^2)}{2(1 - R)}$$

or

$$w = \frac{V_2^2 \sin^2 \alpha_2 + V_{x2}^2 - (V_3^2 \sin^2 \alpha_3 + V_{x3}^2)}{2(1 - R)} \quad (5.32)$$

At maximum utilization, $\alpha_3 = 0$, and the work is $w = UV_{u2}$. Equating this to the work given in Eq. (5.32) leads to the equality

$$UV_2 \sin \alpha_2 = \frac{V_2^2 \sin^2 \alpha_2 + V_{x2}^2 - V_{x3}^2}{2(1 - R)}$$

from which follows the relation

$$\frac{U}{V_2} = \frac{(V_{x2}^2 - V_{x3}^2)/V_2^2 + \sin^2 \alpha_2}{2(1 - R) \sin \alpha_2} \quad (5.33)$$

The left-hand side (LHS) is a speed ratio. It is denoted by $\lambda = U/V_2$. Since $V_{x2}/V_2 = \cos \alpha_2$, this reduces to

$$\lambda = \frac{1 - V_{x3}^2/V_2^2}{2(1 - R) \sin \alpha_2} \quad (5.34)$$

from which the ratio

$$\frac{V_{x3}^2}{V_2^2} = 1 - 2(1 - R)\lambda \sin \alpha_2 \quad (5.35)$$

is obtained. For maximum utilization, $V_3 = V_{x3}$, and solving Eq. (5.30) for this ratio gives

$$\frac{V_{x3}^2}{V_2^2} = \frac{1 - \varepsilon_m}{1 - \varepsilon_m R}$$

Here, the subscript m designates the condition of maximum utilization. Equating the last two expressions and solving for ε_m gives

$$\varepsilon_m = \frac{2\lambda \sin \alpha_2}{1 + 2R\lambda \sin \alpha_2} \quad (5.36)$$

If a stage is designed such that $V_{x3} = V_{x2}$, then the speed ratio in Eq. (5.34) may be written as follows:

$$\lambda = \frac{1 - V_{x2}^2/V_2^2}{2(1 - R) \sin \alpha_2} = \frac{\sin \alpha_2}{2(1 - R)} \quad (5.37)$$

Substituting this into Eq. (5.36) and simplifying gives

$$\varepsilon_m = \frac{\sin^2 \alpha_2}{1 - R \cos^2 \alpha_2} \quad (5.38)$$

This is shown in Figure 5.7.

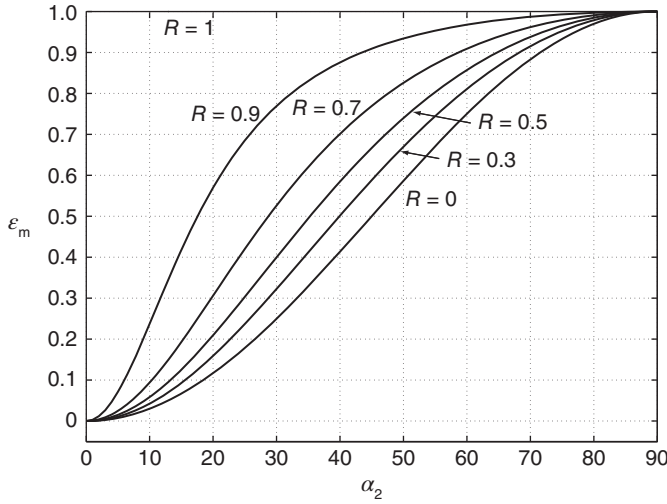


Figure 5.7 Maximum utilization factor for various degrees of reaction as a function of the nozzle angle.

It was mentioned earlier that a rotary lawn sprinkler is a pure reaction machine with $R = 1$. Its utilization is therefore unity for all nozzle angles. Inspection of Figure 5.7, as well as Eq. (5.38), shows that maximum utilization factor increases from zero to unity, when the nozzle angle α_2 increases from zero to 90° . Hence, large nozzle angles give high utilization factors. Typically, the first stage of a steam turbine has $R = 0$, with a nozzle angle in the range from 65° to 78° .

Many turbines are designed with a 50% stage reaction. For a *normal stage* with $R = 1/2$, it turns out that $\beta_3 = -\alpha_2$ and $\alpha_3 = -\beta_2$ and also that $V_3^2 = W_2^2$ (see Exercise 5.5). Work delivered by a 50% reaction stage is

$$w = U(V_{u2} - V_{u3}) = U(V_{u2} - V_x \tan \alpha_3) = U(V_{u2} + V_x \tan \beta_2)$$

or

$$w = U(V_{u2} + W_{u2}) = U(V_{u2} + V_{u2} - U) = U(2V_2 \sin \alpha_2 - U)$$

The quantity $w + V_3^2/2$ becomes

$$w + \frac{1}{2}V_3^2 = w + \frac{1}{2}W_2^2 = w + \frac{1}{2}(V_x^2 + (V_{u2} - U)^2)$$

Hence,

$$w + \frac{1}{2}V_3^2 = w + \frac{1}{2}(V_2^2 - 2UV_2 \sin \alpha_2 + U^2)$$

and the utilization factor from Eq. (5.26) is given as

$$\varepsilon = \frac{2U(2V_2 \sin \alpha_2 - U)}{2U(V_2 \sin \alpha_2 - U) + V_2^2 + U^2}$$

In nondimensional form, this is

$$\varepsilon = \frac{2\lambda(2 \sin \alpha_2 - \lambda)}{2\lambda(\sin \alpha_2 - \lambda) + 1 + \lambda^2} \quad (5.39)$$

Figure 5.8 gives a graphical representation of this relation. For high inflow angles, the curves are quite flat near the maximum, but there are two values of λ that give the same utilization. This means that the absolute value of the exit velocity is the same, but the exit angles are equal but of opposite sign. The positive value of α_3 has a larger blade speed, and thus, the smaller value of λ .

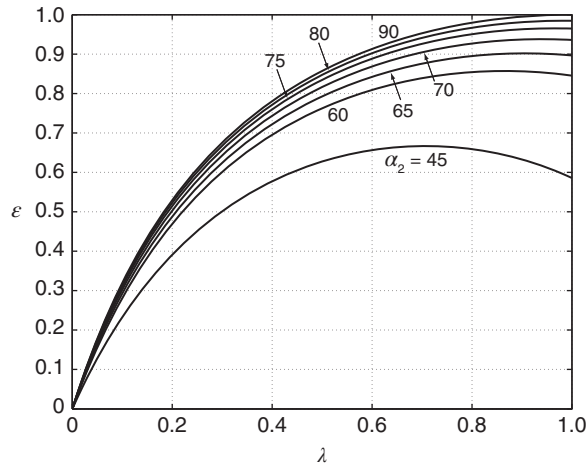


Figure 5.8 Utilization factor for an axial turbine with a 50% reaction stage.

By differentiating this with respect to λ shows that the maximum utilization factor is at $\lambda = \sin \alpha_2$, and the maximum utilization is given by

$$\varepsilon_m = \frac{2 \sin^2 \alpha_2}{1 + \sin^2 \alpha_2}$$

which is consistent with Eq. (5.38).

■ EXAMPLE 5.6

Combustion gases flow from a stator of an axial turbine with absolute speed $V_2 = 500$ m/s at angle $\alpha_2 = 67^\circ$. The relative velocity is at an angle $\beta_2 = 30^\circ$ as it enters the rotor and at $\beta_3 = -65^\circ$ as it leaves the rotor. (a) Find the utilization factor and (b) the reaction. Assume the axial velocity to be constant.

Solution: (a) The axial and tangential velocity components at the exit of the nozzle are

$$V_x = V_2 \cos \alpha_2 = 500 \cos(67^\circ) = 195.37 \text{ m/s}$$

$$V_{u2} = V_2 \sin \alpha_2 = 500 \sin(67^\circ) = 460.25 \text{ m/s}$$

Since $W_x = V_x$, the tangential component of the relative velocity is

$$W_{u2} = W_x \tan \beta_2 = 195.37 \tan(30^\circ) = 112.80 \text{ m/s}$$

so that

$$W_2 = \sqrt{W_x^2 + W_{u2}^2} = \sqrt{195.37^2 + 112.80^2} = 225.59 \text{ m/s}$$

Next, the blade speed is obtained as

$$U = V_{u2} - W_{u2} = 460.25 - 112.80 = 347.46 \text{ m/s}$$

Since the axial velocity remains constant, at the rotor exit, the tangential component of the relative velocity is obtained as

$$W_{u3} = W_x \tan \beta_3 = 195.37 \tan(-65^\circ) = -418.96 \text{ m/s}$$

so that

$$W_3 = \sqrt{W_x^2 + W_{u3}^2} = \sqrt{195.37^2 + 418.96^2} = 462.27 \text{ m/s}$$

Tangential component of the exit velocity is then obtained as

$$V_{u3} = W_{u3} + U = -418.96 + 347.46 = -71.50 \text{ m/s}$$

At the exit,

$$\tan \alpha_3 = \frac{V_{u3}}{V_x} = -\frac{71.50}{195.37} = -0.366 \quad \text{so that} \quad \alpha_3 = -20.1^\circ$$

and the absolute velocity at the exit is

$$V_3 = \sqrt{V_x^2 + V_{u3}^2} = \sqrt{195.37^2 + 71.50^2} = 208.04 \text{ m/s}$$

To calculate the utilization factor using its definition Eq. (5.26), work is first determined to be

$$w = U(V_{u2} - V_{u3}) = 347.46 \cdot (460.25 + 71.50) = 184763 \text{ J/kg}$$

the utilization factor then becomes

$$\varepsilon = \frac{w}{w + \frac{1}{2}V_3^2} = \frac{184763}{184763 + 0.5 \cdot 208.04^2} = 0.895$$

(b) Reaction is obtained from

$$R = \frac{W_3^2 - W_2^2}{2w} = \frac{462.27^2 - 225.59^2}{2 \cdot 184763} = 0.44$$

■

As a second example, consider an axial turbine stage in which both utilization factor and reaction are given, together with the nozzle angle and efflux velocity from the nozzle.

■ EXAMPLE 5.7

An axial turbine operates at reaction $R = 0.48$ with utilization factor $\varepsilon = 0.82$. Superheated steam leaves the nozzles at speed $V_2 = 430$ m/s in the direction $\alpha_2 = 60.6^\circ$. Find the (a) work delivered by the stage and (b) relative flow angles at the inlet and exit of the rotor. Assume the axial velocity to be constant through the stage.

Solution: Since the axial velocity is constant, the expression for the utilization factor may be written as

$$\varepsilon = \frac{V_2^2 - V_3^2}{V_2^2 - RV_3^2} = \frac{1 - \cos^2\alpha_2/\cos^2\alpha_3}{1 - R\cos^2\alpha_2/\cos^2\alpha_3}$$

Solving for the ratio of cosines gives

$$\frac{\cos\alpha_2}{\cos\alpha_3} = \sqrt{\frac{1 - \varepsilon}{1 - R\varepsilon}} = \sqrt{\frac{1 - 0.82}{1 - 0.48 \cdot 0.82}} = 0.5448$$

Thus,

$$\cos\alpha_3 = \frac{\cos(60.6^\circ)}{0.5448} = 0.901 \quad \text{and} \quad \alpha_3 = \pm 25.7^\circ$$

There are two solutions. Which to choose? Inspection of Figure 5.8 shows that the curves of constant nozzle angle are concave downward so that for given utilization factor, there are two speed ratios that satisfy the flow conditions. It is clear, however, that the speed ratio must be less than one, for blades cannot move faster than the flow. The correct choice for the sign can be determined after calculations have been carried out for both angles. Turbine blades typically turn the flow over 80° , and on this basis, the negative angle may be tentatively chosen as being the correct one.

Next, the velocity components at the inlet to the blades are calculated as follows:

$$V_x = V_2 \cos\alpha_2 = 430 \cos(60.6^\circ) = 211.1 \text{ m/s}$$

$$V_{u2} = V_2 \sin\alpha_2 = 430 \sin(60.6^\circ) = 374.6 \text{ m/s}$$

With the axial velocity constant, the tangential component at the exit is

$$V_{u3} = V_x \tan\alpha_3 = 211.1 \tan(-25.7^\circ) = -101.6 \text{ m/s}$$

The magnitude of the absolute velocity at the exit is thus

$$V_3 = \sqrt{V_x^2 + V_{u3}^2} = 234.3 \text{ m/s}$$

(a) Work delivered by the turbine may now be calculated from

$$\varepsilon = \frac{w}{w + \frac{1}{2}V_3^2} \quad \text{or} \quad w = \frac{\varepsilon V_3^2}{2(1 - \varepsilon)} = \frac{0.82 \cdot 234.3^2}{2(1 - 0.82)} = 125.015 \text{ kJ/kg}$$

(b) The blade speed is obtained from the expression

$$w = U(V_{u2} - V_{u3}) \quad U = \frac{w}{V_{u2} - V_{u3}} = \frac{125015}{374.6 + 101.6} = 262.5 \text{ m/s}$$

Thus, $\lambda = U/V_2 = 262.5/430 = 0.61$, and since this number is less than one, the negative angle gives the correct solution.

It is worthwhile also to calculate the extent by which the blades turn the relative velocity. Tangential components of the relative velocity at the inlet and exit of the blade row are

$$W_{u2} = V_{u2} - U = 374.6 - 262.5 = 112.1 \text{ m/s}$$

$$W_{u3} = V_{u3} - U = -101.6 - 262.5 = -364.1 \text{ m/s}$$

The flow angles of the relative velocity are finally

$$\beta_2 = \tan^{-1} \left(\frac{W_{u2}}{W_x} \right) = \tan^{-1} \left(\frac{112.1}{211.1} \right) = 28.0^\circ$$

$$\beta_3 = \tan^{-1} \left(\frac{W_{u3}}{W_x} \right) = \tan^{-1} \left(-\frac{364.1}{211.1} \right) = -59.9^\circ$$

and the amount of turning is $28^\circ + 59.9^\circ = 87.9^\circ$.

For the positive exit flow angle, $\alpha_3 = 25.7^\circ$, and the tangential velocity becomes

$$V_{u3} = V_x \tan \alpha_3 = 211.1 \tan(25.7^\circ) = 101.6 \text{ m/s}$$

and therefore, the magnitude of V_3 is the same as before; so is the work delivered since the utilization factor is the same. The blade speed, however, is changed, as it is now calculated to be

$$U = \frac{w}{V_{u2} - V_{u3}} = \frac{125015}{374.6 - 101.6} = 457.9 \text{ m/s}$$

Consequently, the blade speed ratio is $\lambda = U/V_2 = 457.9/430 = 1.06$, a value greater than one. Therefore, this angle is the incorrect one. Proceeding with the calculation, the tangential velocities of the relative motion are as follows:

$$W_{u2} = V_{u2} - U = 374.6 - 457.9 = -83.3 \text{ m/s}$$

$$W_{u3} = V_{u3} - U = 101.6 - 457.9 = -356.3 \text{ m/s}$$

Calculating the flow angles of the relative velocity gives

$$\beta_2 = \tan^{-1} \left(\frac{W_{u2}}{W_x} \right) = \tan^{-1} \left(-\frac{83.3}{211.1} \right) = -21.6^\circ$$

$$\beta_3 = \tan^{-1} \left(\frac{W_{u3}}{W_x} \right) = \tan^{-1} \left(-\frac{356.3}{211.1} \right) = -59.3^\circ$$

Now, the flow turns only $-21.6^\circ + 59.3^\circ = 37.7^\circ$. This small amount of turning is typical of compressors, but not of turbines. Another way is to check the value of blade-loading coefficient. It is $\psi = w/U^2 = 1.82$ for the negative angle. Blade-loading coefficients for turbines in the range $1 < \psi < 2.5$ give good designs.

The data may be such that both exit angles are reasonable, which simply means that with the magnitude of the exit velocity fixed, the same utilization is obtained if the tangential component leaves at a positive or negative angle of equal size. ■

The examples in this chapter have illustrated the principles of turbomachinery analysis. Some of the thermodynamic properties that appear in the examples are extensive, and some are intensive. Few are nondimensional, and of these, the ones encountered so far include the blade-loading coefficient, flow coefficient or speed ratio, reaction, utilization factor, and Mach number. In addition, flow angles of the absolute and relative velocities are nondimensional quantities. Once the nondimensional parameters, including the flow angles, have been chosen, a choice is made for the magnitude of the exit velocity from the nozzles or the value of the axial velocity. The blade speed can then be calculated. In order to complete the aerothermodynamic analysis, thermodynamic losses need to be estimated. After this, all the intensive parameters will be known.

For this much of the analysis, there was no need to introduce any extensive variables. But, for example, a rate at which a liquid needs to be pumped, or a power delivered by a turbine, are typical design specifications. The size of the machine depends on these extensive variables. Thus, the cross-sectional flow areas are calculated with these specifications in mind together with the size of rotor or impeller. Their diameter and the blade speed determine the rotational speed of the shaft. In large machines, rotational speeds are low; in small machines, they are high. Undoubtedly, a design iteration needs to be carried out so that the machine conforms to a class of successful past designs. This includes also a stress analysis and vibrational characteristics of the blades, disks, and shafts. The next section introduces other aspects in the use of nondimensional variables.

5.5 SCALING AND SIMILITUDE

The aim of scaling analysis is to compare the performance of two turbomachines of similar design. Thus, it is also used to relate the performance of a model turbomachine to its prototype. Both tasks are carried out in terms of proper nondimensional variables. In this section, the conventional nondimensional groups for turbomachinery are introduced, scaling analysis of a model and a prototype is reviewed, and performance characteristics of a compressor and a turbine are presented.

5.5.1 Similitude

Similitude broadly refers to similarity in geometry and flow in two turbomachines. More precisely, *dynamic similarity* is obtained if the ratios of force components at corresponding points in the flow through these machines are equal. A necessary condition for dynamic similarity is *kinematic similarity*, which means that streamline patterns in two machines are the same. To achieve this, the two machines must be *geometrically similar*. This means that they differ only in scale. Proportionality of viscous force components implies that the Reynolds number is the same for the two machines. To obtain full dynamic similarity, the two flows must have similar density distributions, for then inertial forces are proportional at two corresponding points in kinematically similar flows. This is trivially satisfied for an incompressible fluid of uniform density, but for compressible fluids, Mach numbers must be the same at two corresponding points in the flow. The definition of Mach number involves temperature, which together with pressure determine the value of density. Thus, in compressible flows in which Reynolds numbers and also Mach numbers match, forces at corresponding points in kinematically similar flows are proportional to each other, and the flows are said to be dynamically similar.

In courses on fluid dynamics, systematic methods are presented for finding dimensionless groups. They consist of deciding first what the important variables are and grouping

them in categories of *geometric parameters*, *fluid properties*, *operational variables*, and *performance variables*.

The most obvious geometric variable is the diameter D of the rotor. Density ρ and viscosity μ are the two most common fluid properties encountered in turbomachinery flows, and since the fluid particles move along *curved paths* through the machine, the flow is dominated by *inertial effects*. This means that pressure force is in balance with inertial force, and viscous forces are small when compared to these. Since the inertial term is proportional to density, in turbomachinery flows, density is a more important fluid property than viscosity.

The rotational speed Ω of the rotor is the most important operational variable. It is conventionally given in revolutions per minute, and in many performance plots, it is *not converted* to the standard form of radians per second. The performance variables include the volumetric flow rate Q and the work done per unit mass w and quantities such as the power \dot{W} , related to them.

5.5.2 Incompressible flow

The meridional velocity in a turbomachine accounts for the rate at which fluid flows through a machine. Thus, the ratio V_m/U is a measure of the flow rate. As has been seen already, this ratio is used in theoretical analysis, but in testing, it is converted and expressed in terms of more readily measurable quantities. The meridional velocity times the flow area equals the volumetric flow rate, and the blade speed is equal to radius times the rotational speed. Then, with V_m proportional to Q/D^2 and blade speed proportional to ΩD , the combination

$$\phi_d = \frac{Q}{\Omega D^3} \quad (5.40)$$

is dimensionless. It is called a *flow coefficient*.

A nondimensional variable that includes the fluid viscosity μ will lead to some form of Reynolds number, such as $Re = \rho V_m D / \mu$, for example. The usual form, however, is

$$Re = \frac{\rho \Omega D^2}{\mu} = \frac{\Omega D^2}{\nu}$$

in which ν is the kinematic viscosity and the blade speed, proportional to ΩD , is used in place of the meridional velocity. If the boundary layers on the flow passage do not separate, viscous forces remain important only near the walls. Thus, as the machine size increases, boundary-layer regions become a smaller part of the flow. One contributing factor to losses in turbulent boundary layers is the size of wall roughness, which depends on manufacturing methods used. Hence, for example the casing and the impeller of two pumps of different size but manufactured the same way may have about equal roughness. Since much of the flow through the larger pump does not contact the walls of the flow channel, this part of the flow does not experience as great a viscous loss as does the flow through the boundary layer. This concept goes by the name *scale effect*, and it makes the performance variables quite independent of Reynolds number, provided the machine is sufficiently large. It is for this reason that in large machines, efficiency increases with machine size, and viscous effects are ignored in preliminary design. This discussion of the influence of Reynolds number applies at a design condition. However, when turbomachines are operated at off-design conditions, boundary layers may separate. In worst cases, such operation can be catastrophic. Thus, the Reynolds number enters the theory of turbomachines indirectly through its influence on the behavior of boundary layers.

The most important performance variable is the work done on the fluid, or delivered by the machine. Its nondimensional form is the *work coefficient*

$$\psi_d = \frac{w_s}{\Omega^2 D^2}$$

in which w_s is the isentropic work, and the product ΩD in the denominator is proportional to the blade speed, so that the denominator has the units of energy per unit mass, as does isentropic work.

In the Bernoulli equation,

$$p_1 + \frac{1}{2}\rho V_1^2 + \rho g z_1 = p_2 + \frac{1}{2}\rho V_2^2 + \rho g z_2$$

the kinetic energy term shows that in this form, the dimensions of each term are energy per unit volume, since density has replaced mass. Furthermore, weight equals mass times gravitational acceleration, and specific weight of a fluid is defined as ρg . Dividing each term by ρg gives

$$\frac{p_1}{\rho g} + \frac{1}{2g} V_1^2 + z_1 = \frac{p_2}{\rho g} + \frac{1}{2g} V_2^2 + z_2$$

and each term has the dimensions of energy per unit weight of the fluid, which can be reduced to a length, as the potential energy term shows. From hydraulic practice, it is common to call the first term in this equation a *pressure head*. The second term has the name *kinetic energy* or *dynamic head*, and the third term is an *elevation head*. The sum is called the *total head*.

The first law of thermodynamics applied to a flow through a pump gives

$$\frac{p_1}{\rho} + \frac{1}{2} V_1^2 + g z_1 + w_s = \frac{p_2}{\rho} + \frac{1}{2} V_2^2 + g z_2$$

which can also be written as

$$w_s = gH$$

and here, H is the *change* in the total head across the pump. Pump manufacturers report the performance of pumps in terms of their head, making the values independent of the fluid being pumped. They also report a value for efficiency, so that actual work may be determined as $w = w_s/\eta$.

From the definition of total pressure, isentropic work for an incompressible fluid can also be calculated from

$$w_s = \frac{p_{02} - p_{01}}{\rho} \quad (5.41)$$

which shows that if the total pressure change across the pump is reported, then, to obtain the work done, density of the fluid being pumped needs to be known.

Also from the hydraulic practice comes the custom of expressing pressure as a height of a mercury, or a water column, particularly in fans and blowers in which the pressure rise is small. The conversion is carried out by the manometer formula

$$\Delta p = \rho_m g d \quad (5.42)$$

in which ρ_m is the density of the manometer fluid and d is the manometer deflection. As a consequence of the earlier discussion, for a pump, the work coefficient may be written as

$$\psi_d = \frac{gH}{\Omega^2 D^2}$$

Power coefficient may be introduced as

$$\hat{P}_d = \frac{\dot{W}}{\rho \Omega^3 D^5}$$

Here, \dot{W} is the actual rate at which work is done. Hence, multiplying the denominator of ψ_d by the mass flow rate and dividing it by a quantity with dimensions of mass flow rate, namely, by $\rho \Omega D D^2$, gives this form, except that efficiency of the machine must also be taken into account. It is easy to see that the power coefficients for a turbine with efficiency η_t and compressor with efficiency η_c are

$$\hat{P}_d = \eta_t \psi_d \phi_d \quad \hat{P}_d = \frac{\psi_d \phi_d}{\eta_c} \quad (5.43)$$

respectively.

For dynamically similar situations, two machines have the same values of the nondimensional parameters ψ_d and ϕ_d . They are also expected to have the same efficiency if the scale effect is neglected. This means that for machines 1 and 2, the following relationships are true:

$$\left(\frac{w_s}{\Omega^2 D^2} \right)_1 = \left(\frac{w_s}{\Omega^2 D^2} \right)_2 \quad \left(\frac{Q}{\Omega D^3} \right)_1 = \left(\frac{Q}{\Omega D^3} \right)_2$$

■ EXAMPLE 5.8

Water with density $\rho = 1000 \text{ kg/m}^3$ flows through a pump, with a rotor diameter of 30 cm at a rate of $163 \text{ m}^3/\text{h}$. The pump operates at 1600 rpm, and its efficiency is $\eta_p = 0.78$. The pump work is 410.5 J/kg . If a second pump in the same series has a diameter of 20 cm and operates at 3200 rpm, at the condition of same efficiency, find (a) the mass flow rate, (b) the total pressure increase across it, and (c) the input power.

Solution: (a) Since the pumps are geometrically similar and their efficiencies are the same, dynamic similarity may be assumed. Thus,

$$\frac{Q_1}{\Omega_1 D_1^3} = \frac{Q_2}{\Omega_2 D_2^3} \quad Q_2 = Q_1 \frac{\Omega_2 D_2^3}{\Omega_1 D_1^3} = 163 \frac{3200 \cdot 20^3}{1600 \cdot 30^3} = 96.6 \text{ m}^3/\text{h}$$

and the mass flow rate is

$$\dot{m}_2 = \rho Q_2 = \frac{1000 \cdot 96.6}{3600} = 26.8 \text{ kg/s}$$

(b) With equal work coefficient and efficiency, it follows that

$$\frac{w_{s1}}{\Omega_1^2 D_1^2} = \frac{w_{s2}}{\Omega_2^2 D_2^2} \quad w_2 = w_1 \frac{\Omega_2^2 D_2^2}{\Omega_1^2 D_1^2} = 410.5 \frac{3200^2 \cdot 20^2}{1600^2 \cdot 30^2} = 730 \text{ J/kg}$$

The total pressure rise is given by

$$\Delta p_{02} = \rho \eta w_2 \quad \text{so that} \quad \Delta p_{02} = 1000 \cdot 0.78 \cdot 730 = 569.2 \text{ kPa}$$

(c) Pumping power is

$$\dot{W}_2 = \dot{m}_2 w_2 = 26.86 \cdot 730 = 19.6 \text{ kW}$$

Since the ratio of rotational speeds and flow rates are used in the calculations, there was no need to convert them to standard units. ■

5.5.3 Shape parameter or specific speed and specific diameter

Flow coefficient and work coefficient can be combined in such a way that the diameter is eliminated. Raising the result to a power such that it becomes *directly proportional to the rotational speed* gives a parameter that is called the *specific speed*, and it is given by

$$\Omega_s = \left(\frac{Q}{\Omega D^3} \right)^{1/2} \left(\frac{\Omega^2 D^2}{gH} \right)^{3/4} = \frac{\Omega Q^{1/2}}{(gH)^{3/4}} \quad (5.44)$$

This equation shows that machines with low flow rates and large change in a head have low Ω_s . In centrifugal machines, the inlet area, which is close to the shaft, is relatively small, and to keep the inlet velocity within a desirable range, the flow rate is relatively low. The centrifugal action causes a large pressure rise in such machines. Both make the specific speed low. In axial pumps and turbines, a large flow rate is possible, as the annular flow area is far from the axis and is therefore large. This leads to a high specific speed. The shape of the machines thus changes from a radial to an axial type as the specific speed increases. Thus, a better name for Ω_s would be a *shape parameter*. Shapes for pumps are shown in Figure 5.9. Other turbomachines, such as hydraulic turbines, have similar shapes in corresponding ranges of the specific speed.

The figure shows that large machines have higher efficiencies owing to the scale effect discussed previously. To see how to develop a formula to account for this, consider a turbulent flow in a pipe. The wall friction depends on the pipe Reynolds number, $Re = V_m D_h / \nu$ and the relative roughness of the pipe $\epsilon_{\text{rms}} / D_h$. Here, V_m is the meridional component of the velocity, and $D_h = 4A/C$ is the hydraulic diameter, with A the cross-sectional area and C the length of the wetted perimeter. The quantity ϵ_{rms} is the root-mean-square-roughness of the wall. The wall friction, expressed as a dimensionless friction factor, is given by the Colebrook–White formula, which may also be written as

$$\frac{1}{\sqrt{f}} = 1.14 - 2 \log \frac{\epsilon_{\text{rms}}}{D_h} - 2 \log \left(1 + 9.35 \frac{D_h / \epsilon_{\text{rms}}}{Re \sqrt{f}} \right) \quad (5.45)$$

Here, \log is the logarithm of base 10. The Moody chart for frictional flow in a pipe is based on this formula. For large Reynolds number, the last term can be neglected, and the friction factor is seen to depend only on the relative roughness. The resulting equation can be put into a different form, by calculating the value of friction factor for various values of relative roughness and fitting the results into the form

$$f = a \left(\frac{\epsilon_{\text{rms}}}{D_h} \right)^n \quad (5.46)$$

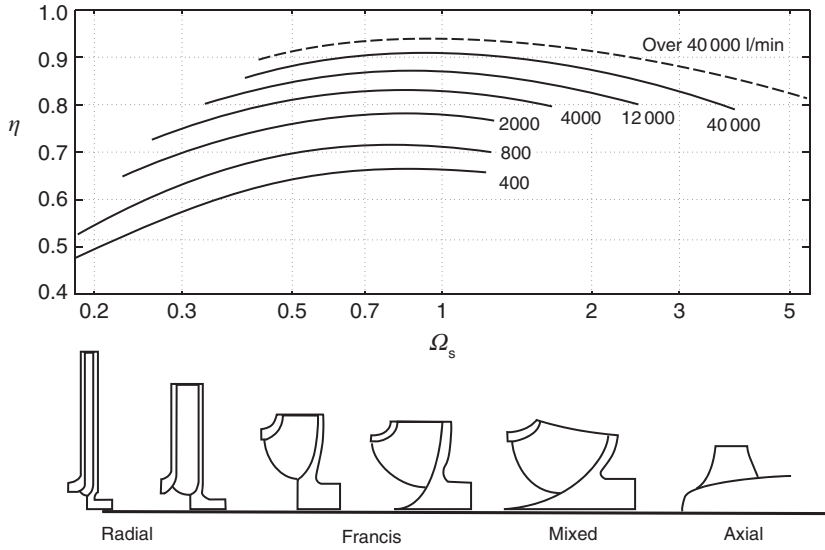


Figure 5.9 Shapes of pumps with increasing specific speed. Source: Modified from a graph in Wislicenus [100, p. 68].

For the range $0.00001 < \epsilon_{rms}/D_h < 0.001$, the coefficient is $a = 0.072$, and the exponent is $n = 0.193$, and for the range $0.001 < \epsilon_{rms}/D_h < 0.02$, the coefficient is $a = 0.159$, and the power is $n = 0.309$. The similarity relationship can now be written as

$$\frac{f_p}{f_m} = \left(\frac{\epsilon_p D_m}{\epsilon_m D_p} \right)^n \quad (5.47)$$

The hydraulic efficiency of a pump can be expressed as

$$1 - \eta = 1 - \frac{w_s}{w} = \frac{w - w_s}{w} = \frac{w_L}{w}$$

where w_L is the loss. Using the pipe flow loss expression for the flow passage through a pump gives

$$w_L = f \frac{L_h}{D_h} \frac{W^2}{2}$$

The hydraulic efficiency can now be written as

$$1 - \eta = f \frac{L_h}{D_h} \frac{W^2}{2w} = f \frac{L_h}{D_h} \frac{W^2}{U^2} \frac{1}{2\psi} \quad (5.48)$$

Owing to geometric similarity, L_h/D_h is the same for a prototype and its model. Similarly, dynamic similarity requires that the velocity ratio W/U and ψ are the same. Making use of Eq. (5.47), this leads to the similarity equation

$$\frac{1 - \eta_p}{1 - \eta_m} = \left(\frac{\epsilon_p D_m}{\epsilon_m D_p} \right)^n \quad (5.49)$$

Assuming finally that the surface roughness to be the same for the model and the prototype, this reduces to

$$\frac{1 - \eta_p}{1 - \eta_m} = \left(\frac{D_m}{D_p} \right)^n \quad (5.50)$$

This is a form first suggested by Moody [64, Sec. 26, p. 48], with the power $n = 0.2$, in agreement with the correlation for fairly smooth pipes.

Equation (5.48) only accounts for the wall friction. But the flow experiences other fluid dynamic losses, such as gap losses. To account for them, Ackeret [70, p. 280] suggested inclusion of factor V that represents the fraction from the wall friction. Hence, $1 - V$ represents other losses. Hutton [64, Sec. 26, p. 48] gave a similar form for hydraulic turbines. On the basis of their reasoning, the similarity relation can be written as

$$\frac{1 - \eta_p}{1 - \eta_m} = (1 - V) + V \left(\frac{D_m}{D_p} \right)^n$$

Pfleiderer and Petermann [70, p. 281] suggest that V be in the range from 0.5 to 0.7.

In addition to Figure 5.9, Wislicenus also provides a plot of efficiency as a function of flow rate, for two values of specific speed, and they can be used to develop the correlation

$$\eta = 0.95 - \frac{5.056}{\Omega_s^{0.5145} [\ln(Q/3.7854)]^2} \quad (5.51)$$

Here, the volumetric flow rate Q is given liters per minute, as in Figure 5.9. The validity of this correlations is for the centrifugal pumps in the range $0.4 < \Omega_s < 0.7$ and flow rates in the range $800 \text{ l/min} < Q < 40000 \text{ l/min}$.

Another important parameter is the *specific diameter* obtained by combining the work coefficient and the flow coefficient in such a way that the rotational speed does not appear. It is given by

$$D_s = \frac{D(gH_e)^{1/4}}{\sqrt{Q}} \quad (5.52)$$

A useful compilation of data from a large variety of turbomachines was carried out by Cordier² at conditions of best efficiency, and the revised diagram is shown in Figure 5.10. The left graph is for turbines, and the right one for pumps and compressors. It also includes the range of specific speed for a given type of machine.

The lines of constant flow coefficient, ϕ_d and constant work coefficient ψ_d are also shown in this figure. The relationships between these and the specific speed and specific diameter are

$$\Omega_s = \frac{\sqrt{\phi_d}}{\psi_d^{3/4}} \quad D_s = \frac{\psi_d^{1/4}}{\sqrt{\phi_d}} \quad (5.53)$$

■ EXAMPLE 5.9

Water flows through a pump, with an impeller diameter of 30 cm at a rate of $163 \text{ m}^3/\text{h}$. The pump operates at 1600 rpm, near its optimal efficiency point. Find the power required.

²The Cordier diagram appears in the book by Csanady [17, p. 21]; in Pfleiderer and Petermann [70, p. 273], it is called the Cordier diagram after its originator. A revised version can be found in the article *Strömungsmaschinen*, by Dibelius and Stoff, in *Dubbel Taschenbuch für den Maschinenbau*, [22, p. R18].

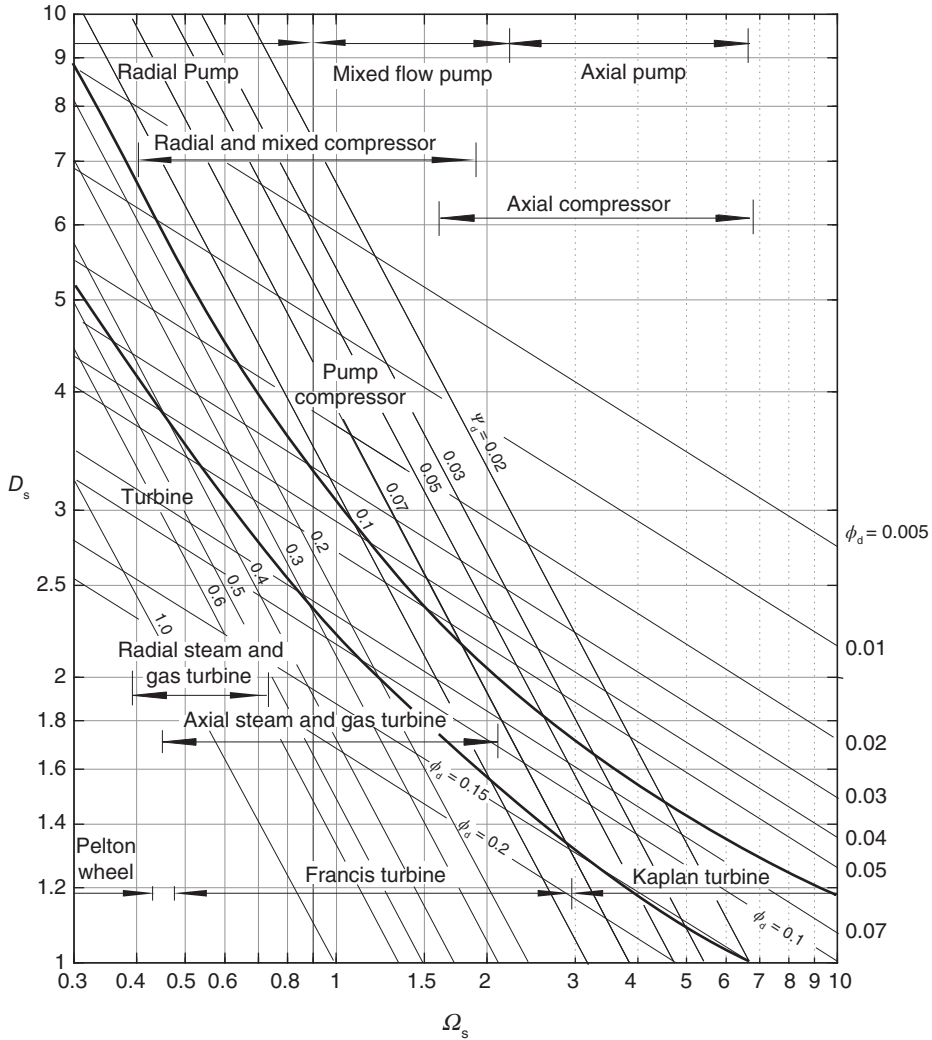


Figure 5.10 Cordier Diagram. Source: Adapted from the diagram by Dibelius and Stoff, in Dubbel Taschenbuch für den Maschinenbau, [22, p. R18].

Solution: Fewer pieces of data are given than in the previous example, but the additional information is that the pump operates at its optimal operating point. Also, the flow coefficient can be calculated. It is

$$\phi_d = \frac{Q}{\Omega D^3} = \frac{163}{3600} \frac{30}{1600 \cdot \pi} \left(\frac{1}{0.3} \right)^3 = 0.01$$

Since the reversible work is not given, the equations need to be combined in such a way that it is eliminated from them. Thus, solving the second of Eqs. (5.53) for $\psi_d^{1/4}$ gives

$$\psi_d^{1/4} = D_s \sqrt{\phi_d}$$

and substituting the cube of this into the first of Eqs. (5.53) gives

$$\Omega_s = \frac{1}{D_s^3 \phi_d}$$

Following the line $\phi_d = 0.01$ line on the Cordier diagram to the pump line, gives $D_s = 6.0$, and substituting this into the previous equation gives

$$\Omega_s = \frac{1}{6^3 \cdot 0.1} = 0.463$$

The work coefficient is then

$$\psi_d = D_s^4 \phi_d^2 = 6.0^4 \cdot 0.01^2 = 0.13$$

This is in agreement with the reading from the Cordier diagram. The reversible work is

$$w_s = \psi_d \Omega^2 D^2 = 0.13 \left(\frac{1600 \cdot \pi}{30} \right)^2 0.3^2 = 328.0 \text{ J/kg}$$

To calculate the power required, the flow rate is first converted to liters per minute $Q = 163 \text{ m}^3/\text{h} = 2717 \text{ l/min}$, and the correlation Eq. (5.51) gives $\eta = 0.78$. The efficiency curves are quite flat over a fairly wide range of specific speeds near the maximum efficiency, and the flow rate influences the efficiency more than the specific speed. The work is

$$w = \frac{w_s}{\eta} = \frac{328.0}{0.78} = 420.53 \text{ J/kg}$$

and the power can now be calculated to be

$$\dot{W} = \rho Q w = 1000 \cdot \frac{163}{3600} \cdot 420.53 = 19.04 \text{ kW}$$

■

5.5.4 Compressible flow analysis

For compressible flows, temperature must be listed among the fundamental dimensions. It appears in the Mach number, $M = V/c$, through the speed of sound for an ideal gas, $c = \sqrt{\gamma R T}$. It is also seen that the ratio of specific heats appears as an additional parameter.

Flows with Mach numbers less than 0.3 can be approximated as incompressible. Hence, in low-Mach-number flows, the influence of Mach number will be slight. Testing of centrifugal compressors with refrigerants as working fluids also shows that their performance depends only weakly on the ratio of specific heats [17]. This is useful to notice, for then performance maps generated for air are not expected to lead to large errors when they are used for other gases.

In compressible flows, the volumetric flow rate is replaced by the mass flow rate, as only the latter is constant through a machine. Conventional practice is to replace the volumetric flow rate with \dot{m}/ρ_{01} , where ρ_{01} is the inlet stagnation density. The other parameters include a modified blade Mach number $\Omega D/c_{01}$, Reynolds number $\rho_{01} \Omega D^2/\mu$, and the ratio of specific heats. In the definition of c_{01} , the inlet stagnation temperature is used.

The functional relationship between the reversible work and these parameters can be expressed as

$$\frac{\Delta h_{0s}}{\Omega^2 D^2} = f \left(\frac{\dot{m}}{\rho_{01} \Omega D^3}, \frac{\Omega D}{c_{01}}, \frac{\rho_{01} \Omega D^2}{\mu}, \gamma \right) \quad (5.54)$$

For an ideal gas, it was shown in Chapter 2 that

$$\frac{\Delta h_{0s}}{c_{01}^2} = \frac{1}{\gamma - 1} \left[\left(\frac{p_{02}}{p_{01}} \right)^{(\gamma-1)/\gamma} - 1 \right]$$

which may be recast as

$$\frac{\Delta h_{0s}}{\Omega^2 D^2} = \frac{c_{01}^2}{\Omega^2 D^2} \frac{1}{\gamma - 1} \left[\left(\frac{p_{02}}{p_{01}} \right)^{(\gamma-1)/\gamma} - 1 \right]$$

Since the blade Mach number and the ratio of specific heats are already taken as independent parameters, the ideal work coefficient can be replaced by a *stagnation pressure ratio*. This is done, regardless of whether the gas is ideal or not.

The flow coefficient may be written as

$$\frac{\dot{m}}{\rho_{01} \Omega D^3} = \frac{\dot{m}}{\rho_{01} c_{01} D^2} \frac{c_{01}}{\Omega D} = \frac{c_{01}}{\Omega D} \frac{\dot{m} \sqrt{RT_{01}}}{p_{01} \sqrt{\gamma} D^2}$$

Again, since the blade Mach number and γ are already counted as independent parameters, inspection of the right side shows that the flow coefficient may be modified to

$$\phi_d = \frac{\dot{m} \sqrt{RT_{01}}}{p_{01} D^2}$$

The power coefficient is manipulated into the form

$$\frac{\dot{W}}{\rho_{01} \Omega^3 D^5} = \frac{\dot{m} c_p \Delta T_0}{\rho_{01} \Omega^3 D^5} = \frac{\dot{m}}{\rho_{01} \Omega D^3} \frac{1}{\gamma - 1} \frac{c_{01}^2}{\Omega^2 D^2} \frac{\Delta T_0}{T_{01}}$$

The first factor on the right is the original flow coefficient. It is multiplied by a factor dependent only on γ and the reciprocal of the blade Mach number squared. Since all these factors have been taken into account separately, the power coefficient may be replaced by $\Delta T_0/T_{01}$. Hence,

$$\frac{p_{02}}{p_{01}} = f_1 \left(\frac{\dot{m} \sqrt{RT_{01}}}{p_{01} D^2}, \frac{\Omega D}{\sqrt{\gamma RT_{01}}}, \frac{\rho_{01} \Omega D^2}{\mu}, \gamma \right) \quad (5.55)$$

and

$$\frac{\Delta T_0}{T_{01}} = f_2 \left(\frac{\dot{m} \sqrt{RT_{01}}}{p_{01} D^2}, \frac{\Omega D}{\sqrt{\gamma RT_{01}}}, \frac{\rho_{01} \Omega D^2}{\mu}, \gamma \right) \quad (5.56)$$

Efficiency is another performance variable, and it is functionally related to the parameters listed on the right in the aforementioned equations. For an ideal gas undergoing

compression, it can be calculated from

$$\eta = \frac{T_{02s} - T_{01}}{T_{02} - T_{01}} = \frac{T_{01}}{\Delta T_0} \left[\left(\frac{p_{02}}{p_{01}} - 1 \right)^{(\gamma-1)/\gamma} \right]$$

For a particular design and fluid, the geometric parameters and γ are fixed. This allows the flow coefficient and the blade Mach number to be replaced by

$$\phi_m = \frac{\dot{m} \sqrt{T_{01}}}{p_{01}} \quad \Omega_m = \frac{\Omega}{\sqrt{T_{01}}} \quad (5.57)$$

These are *not dimensionless*. Alternatively, the *corrected* mass flow rate and the rotational speed

$$\dot{m}_c = \frac{\dot{m} \sqrt{T_{01}/T_{0r}}}{p_{01}/p_{0r}} \quad \Omega_c = \frac{\Omega}{\sqrt{T_{01}/T_{0r}}} \quad (5.58)$$

are used, in which subscript “r” refers to a reference condition.

5.6 PERFORMANCE CHARACTERISTICS

The use of a performance map is illustrated in this section by representative compressor and turbine maps for an automotive turbocharger. A turbocharger is used to precompress air before it is inducted to an internal combustion engine, thereby allowing a larger mass flow rate than is possible in a naturally aspirated engine. A turbocharger is shown in Figure 5.11. It consists of a centrifugal compressor and a radial inflow turbine. The exhaust gases from the engine drive the turbine. Shaft speeds vary from 60000 to 200000 rpm in automotive applications.

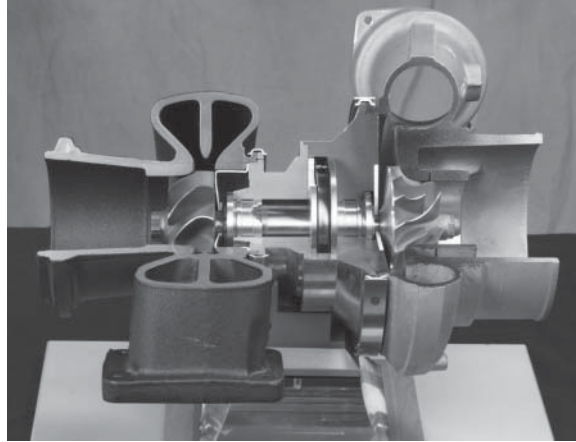


Figure 5.11 A turbocharger. Source: Photo courtesy NASA.

5.6.1 Compressor performance map

To characterize the performance of a compressor, the pressure ratio is typically plotted as a function of the flow coefficient, as is shown in Figure 5.12. Here, the flow rate and the

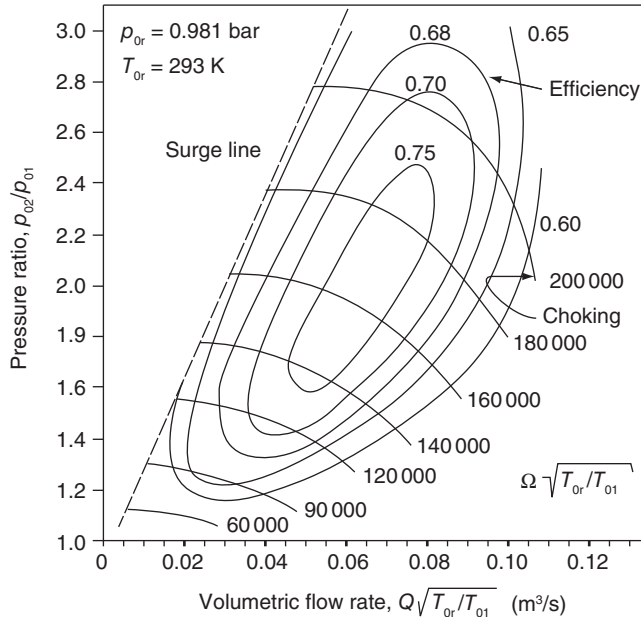


Figure 5.12 Characteristics of a centrifugal compressor. Source: Courtesy BorgWarner Turbo Systems.

rotational speed are modified to a corrected flow rate and a corrected shaft speed

$$Q_c = Q \sqrt{\frac{T_{0r}}{T_{01}}} \quad \Omega_c = \Omega \sqrt{\frac{T_{0r}}{T_{01}}}$$

This particular *compressor map* is for a centrifugal compressor of an automotive turbocharger manufactured by BorgWarner Turbo Systems, similar to that shown in Figure 5.11. Air is drawn in from stagnant atmosphere with reference pressure $p_{0r} = 0.981$ bar and reference temperature $T_{0r} = 293$ K. These are the nominal inlet stagnation properties.

Efficiency curves are superimposed on this plot on a family of curves at constant corrected speed, given in rpm. The constant speed curves terminate at a line called a *surge line*. If the flow rate decreases beyond this, the blades will stall. Severe stall leads to a condition known as *surge*. Under surge conditions, the flow may actually *reverse* in direction, leading to a possible *flameout* in a jet engine.

In an automotive application, the operating speed of the turbomachine follows the engine speed of the internal combustion engine. When the shaft speed is increased, the operating condition moves *across* the constant speed curves in the general direction parallel to the surge line to lower efficiency. At large flow rates, the flow in the blade passages will *choke*, and this is indicated by the sharp drop in the constant-speed curves.

5.6.2 Turbine performance map

A sample plot of turbine characteristics is shown in Figure 5.13 for the radial inflow turbine of the same BorgWarner turbocharger. Inlet to the turbine is identified by the label 3, and

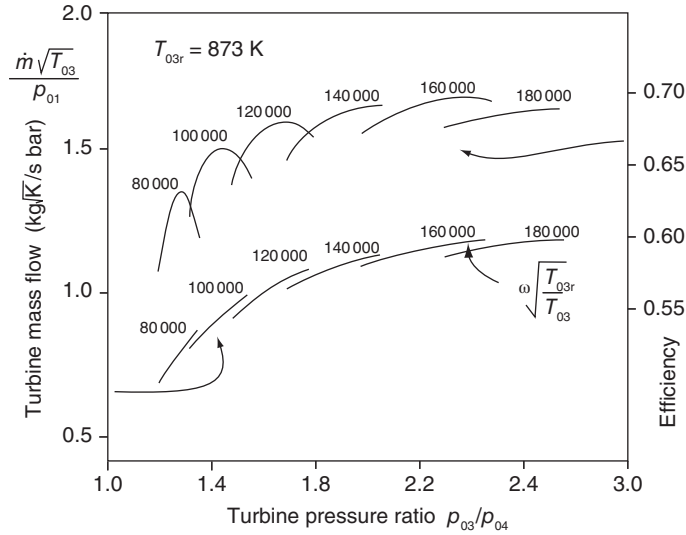


Figure 5.13 Characteristics of a radial inflow turbine. Source: Courtesy BorgWarner Turbo Systems.

its exit is a state 4. Pressure ratio is given as the ratio of stagnation pressures at states 3 and 4. Inlet *reference* temperature has a value $T_{03r} = 873$ K. The rotational speed of the shaft is corrected by the square root of the ratio of the reference temperature to its actual value at the inlet. This arises from the square root dependence of speed of sound on temperature.

Since the exit pressure from the turbine is close to the atmospheric value, the pressure ratio is determined by the inlet pressure to the turbine, which in turn is related to engine pressure. A high pressure ratio leads to choking of the turbine. Thus, an increase in the pressure ratio no longer increases the flow rate, and the lines of constant speed remain flat, as seen in Figure 5.13.

Efficiency curves are also flat near choking conditions, for the aerodynamic design is optimized for these conditions. This is in contrast to the small *envelope* of high efficiency at low pressure ratios when the turbine can still accommodate a large change in the mass flow rate as the pressure ratio is increased.

Although it would be desirable to have a consistent representation of the dimensionless parameters, this is not yet a common practice. Hence, the dimensions and units in each of the parameters need to be examined for each performance map encountered.

EXERCISES

5.1 (a) By eliminating the angle β between Eqs. (5.6) and (5.7), derive the law of cosines in the form

$$W^2 = U^2 + V^2 - 2UV \sin \alpha \quad (5.59)$$

(b) By eliminating W between these equations develop a form of the law of sines

$$\frac{\sin(\alpha - \beta)}{U} = \frac{\cos \beta}{V} \quad (5.60)$$

5.2 In a velocity diagram at the inlet of a turbine, the angle of the absolute velocity is 60° and the flow angle of the relative velocity is -51.74° . Draw the velocity diagram, and find the value of U/V and V_x/U . [Ans: $U/V = 1.5$, $V_x/U = 1/3$]

5.3 Following the method described in the text, carry out the steps to develop the Eqs. (5.21) and (5.22).

5.4 For an axial turbine stage, with $R = 0$, show that the blade speed is equal to the average of the tangential velocities before and after the rotor. Find the work done by the rotor if the exit angle $\alpha_3 = 0$. [Ans: $w = 2U^2$]

5.5 Determine the relationship between α_2 and β_3 for an axial turbine stage with reaction equal to 0.5 and constant axial velocity. Find the work done if the exit angle $\alpha_3 = 0$. [Ans: $w = U^2$]

5.6 Steam enters a rotor of an axial turbine with an absolute velocity $V_2 = 320$ m/s at an angle $\alpha_2 = 73^\circ$. The axial velocity remains constant. The blade speed is $U = 165$ m/s. The rotor blades are equiangular so that $\beta_3 = -\beta_2$, and the magnitude of the relative velocity remains constant across the rotor. Draw the velocity triangles. Find (a) the relative flow angle β_2 , (b) the axial velocity V_x assumed constant across the stage, and (c) the flow angle α_3 that V_3 makes with the axial direction. [Ans: (a) 56.4° , (b) 96.6 m/s, (c) 14.38°]

5.7 An axial turbine has a reaction ratio $R = 1/2$. Air enters the rotor with relative velocity at an angle $\beta_2 = 15^\circ$, and the axial velocity is constant for the stage. The blade speed is $U = 300$ m/s, and the tangential velocity change across the rotor is $V_{u2} - V_{u3} = 320$ m/s. (a) Find the axial velocity. (b) Find the angle at which the absolute velocity enters the rotor. [Ans: (a) 37.3 m/s, (b) 83.1°]

5.8 The axial component of airflow leaving a stator in an axial-flow turbine is $V_{x2} = 175$ m/s, and its flow angle is 64° . The axial velocity is constant, the reaction of the stage is $R = 0.5$, and the blade speed is $U = 140$ m/s. Find the flow angle of the absolute velocity entering the stator. [Ans: -51.3°]

5.9 The exit flow angle of stator in an axial steam turbine is 68° . The flow angle of the relative velocity leaving the rotor is -67° . Steam leaves the stator at $V_2 = 120$ m/s, and the axial velocity is $V_{x2} = 0.41U$. At the exit of the rotor blades, the axial steam velocity is $V_{x3} = 0.42U$. The mass flow rate is $\dot{m} = 2.2$ kg/s. Find (a) the flow angle entering the stator, assuming it to be the same as the absolute flow angle leaving the rotor; (b) the flow angle of the relative velocity entering the rotor; (c) the reaction; and (d) the power delivered by the stage. [Ans: (a) 1.44° , (b) 2.07° , (c) 0.491 , (d) 26.6 kW]

5.10 The speed of airflow leaving the rotor of an axial-flow turbine is $V_{x3} = 140$ m/s, and its flow angle is 0° . The axial velocity is constant and equal to the blade speed. The inlet flow angle to the rotor is $\alpha_2 = 60^\circ$. Find the reaction. [Ans: 0.134]

5.11 Water with density 1000 kg/m³ flows in a centrifugal pump at the rate of 22 L/s. The impeller radius is $r_2 = 7.7$ cm, and the blade width at the impeller exit is $b_2 = 0.8$ cm. If the flow angles at the impeller exit are $\alpha_2 = 67^\circ$ and $\beta_2 = -40^\circ$, what is the rotational speed of the shaft in rpm? [Ans: 2252 rpm]

5.12 A small axial-flow turbine has an output power of 37 kW when handling 1 kg of air per second with an inlet total temperature of 335 K. The total-to-total efficiency of the turbine is 80% . The rotor operates at 50000 rpm, and the mean blade diameter is 10 cm.

Evaluate (a) the average driving force on the turbine blades, (b) the change in the tangential component of the absolute velocity across the rotor, and (c) the required total pressure ratio across the turbine. [Ans: (a) 141.3 N, (b) 141.3 m/s, (c) 1.68]

5.13 Consider a normal, zero reaction, $R = 0$, axial turbine stage with $V_{x1} = V_{x2} = V_{x3}$. Show that the utilization is given by the expression $\varepsilon = 4\lambda(\sin \alpha_2 - \lambda)$, where $\lambda = U/V_2$ is the speed ratio. Show that the maximum utilization takes place at the speed ratio

$$\lambda = \frac{1}{2} \sin \alpha_2 \quad \text{and} \quad \varepsilon_m = \sin^2 \alpha_2$$

5.14 (a). Carry out the analysis to show that for a normal stage with reaction $R = 0.5$, the maximum utilization is at $\lambda = \sin \alpha_2$ and the maximum utilization is then

$$\varepsilon_m = \frac{2\sin^2 \alpha_2}{1 + \sin^2 \alpha_2}$$

(b) Plot the results with utilization on the ordinate and the speed ratio on the abscissa, for values of α_2 in the range $10^\circ - 90^\circ$. (c) Show that work at maximum utilization is $w = U^2$.

5.15 For a normal stage with reaction $R = 1$, show that the utilization is given by the expression

$$\varepsilon = \frac{4\lambda \sin \alpha_2}{4\lambda \sin \alpha_2 + 1}$$

Plot the utilization on the ordinate and the speed ratio on the abscissa for values α_2 in the range $10^\circ - 90^\circ$. To find the maximum utilization, differentiate the expression for ε and interpret the result.

5.16 Gas, at the speed of 500 m/s and flow angle 60° , enters the rotor a normal axial turbine stage, that is designed to have constant axial velocity. The reaction ratio is 0.4, and the utilization is 0.8. (a) Find the value of the absolute exit velocity. (b) Find the flow coefficient $\phi = V_x/U$. (c) Find the blade-loading coefficient $\psi = w/U^2$. (d) Find the angle at which the relative velocity leaves the stage. [Ans: (a) 271.2 m/s, (b) 0.915, (c) 1.97, (d) -56.5°]

5.17 Show that work from an axial turbine at maximum utilization is given by $w = 2U^2(1 - R)$.

5.18 Gas enters the rotor of an axial turbine stage at the speed 520 m/s at the flow angle of 65° . The blade speed is 300 m/s. The reaction is 0.46, and utilization is 0.82. Do not assume that the axial velocity is constant. (a) Find the magnitude of the exit velocity. (b) Find the work done by the stage. (c) Find the angle at which the relative velocity leaves the stage. [Ans: (a) 279.6 m/s, (b) 178.0 kJ/kg, (c) -61.5°]

5.19 Gas enters the rotor of an axial turbine stage at the speed 520 m/s at the flow angle of 65° . If flow angle of the relative velocity leaving the stage is -55° , then the reaction is 0.46 and utilization is 0.82. Do not assume that the axial velocity is constant. (a) Find the magnitude of the exit velocity. (b) Find the work done by the stage. (c) Find the blade speed and the exit angle of the absolute velocity. (d). At what blade speed is the exit angle of the absolute velocity zero. Hint: work the previous exercise first and then consider solving this by trial and error. [Ans: (a) $V_3 = 279.6$ m/s, (b) $w = 178$ kJ/kg, (c) $U = 340.1$ m/s or $U = 468.8$ m/s, (d) $U = 377.7$ m/s]

5.20 The flow enters the rotor of a normal axial turbine stage with 50% reaction with absolute velocity 200 m/s and angle 65° . The relative velocity at the inlet of the rotor is at angle 35° , and at the exit from the rotor, the angle of the relative velocity is -60° . Do not assume that the axial velocity is constant. (a) Find the magnitude of the exit velocity. (b) Find the work done by the stage. (c) Find the utilization. [Ans: (a) 109.5 m/s, (b) 28.0 kJ/kg, and (c) 0.824]

5.21 Air flows at the rate of 500 L/s through a fan when operating at 1800 rpm. (a) What is the flow rate if the fan speed is increased to 3600 rpm? (b) What is the percentage increase in total pressure rise? (c) What is the power input required at 3600 rpm relative to that at 1800 rpm? [Ans: (a) 1000 L/s, (b) 300%, (c) eight times]

5.22 An axial-flow pump having a rotor diameter of 20 cm handles water at the rate of 60 L/s when operating at 3550 rpm. The corresponding increase in total enthalpy of the water is 120 J/kg, and the total-to-total efficiency is 75%. Suppose that a second pump in the same series is to be designed to handle water having a rotor diameter of 30 cm and operating at 1750 rpm. For this second pump, what will be the predicted values for (a) the flow rate, (b) the change in the total pressure of water, and (c) the input power? [Ans: (a) 99.8 L/s, (b) 49.2 kPa, (c) 6.55 kW]

5.23 A small centrifugal pump handles water at the rate of 6 L/s with input power of 5 hp and total-to-total efficiency of 70%. Suppose that the fluid being handled is changed to gasoline having specific gravity 0.70. What are the predicted values for (a) flow rate, (b) input power, and (c) total pressure rise of the gasoline? [Ans: (b) 3.5 hp, (c) 304.5 kPa]

5.24 A blower handling air at the rate of 240 L/s at the inlet conditions of 103.1 kPa for total pressure and 288 K for total temperature. It produces a pressure rise of air equal to 250 mm of water. If the blower is operated at the same rotational speed, but with an inlet total pressure and total temperature of 20 kPa and 253 K. What are (a) the predicted value for the mass flow rate and (b) the total pressure rise? [Ans: (a) 0.066 kg/s and (b) 56.2 mm of water]

5.25 Consider a fan with a flow rate of 1500 cfm, (ft^3/min), and a shaft speed of 3600 rpm. If a similar fan one half its size is to have the same tip speed, what will the flow rate be at a dynamically similar operating condition? What is the ratio of power consumption of the second fan compared to the first one? [Ans: 1/4]

5.26 A fan operating at 1750 rpm at a volumetric flow of $4.25 \text{ m}^3/\text{s}$ develops a head of 153 mm of water. It is required to build a larger, geometrically similar fan that will deliver the same head at the same efficiency as the existing fan, but at the rotational speed of 1440 rpm. (a) Determine the volume flow rate of the larger fan. (b) If the diameter of the original fan is 40 cm, what is the diameter of the larger fan? (c) What are the specific speeds of these fans? [Ans: 6.28 m^3/s , (b) 48.6 cm, (c) 1.8]

5.27 The impeller of a centrifugal pump, with an outlet radius $r_2 = 8.75 \text{ cm}$ and a blade width $b_2 = 0.7 \text{ cm}$, operates at 3550 rpm and produces a pressure rise of 522 kPa at a flow rate of 1450 l/min. Assume that the inlet flow is axial, and that the pump efficiency is 0.63. (a) Find the specific speed. (b) Estimate the efficiency. (c) Show that Eq. (5.19) for work reduces to $w = (V_{u2}^2 + U_2^2 - W_{u2}^2)/2$, and calculate the work two ways and confirm that they are equal. [Ans: (a) 0.529, (b) 0.752, (c) 694.4 J/kg]

5.28 A centrifugal pump handles water at the rate of $Q = 150 \text{ L/s}$. The impeller diameter is $D_2 = 50 \text{ cm}$, and the blade height at the exit is $b_2 = 5 \text{ cm}$. The velocity at the inlet is axial. (a) Calculate the efficiency by the formula given in the text. (b) Find the work done by the impeller if it rotates at 700 rpm. What is the angle of the relative velocity at the outlet. [Ans: 0.825, 297.3 J/kg, -47.8°]

5.29 A centrifugal pump is to be designed with an impeller diameter equal to $D_2 = 43 \text{ cm}$ rotating at 960 rpm and with capacity of $Q = 0.1 \text{ m}^3/\text{s}$. Using the Cordier diagram, determine the ideal head developed by the pump.

5.30 A centrifugal pump with capacity $Q = 0.15 \text{ m}^3/\text{s}$ has a tip speed $U_2 = 8 \text{ m/s}$ and an impeller diameter $D_2 = 0.5 \text{ m}$. The width of the blade at the outlet $b_2 = 0.1D_2$. If the blade makes an angle $\beta_2 = -35^\circ$ at the outlet and the flow enters the pump without swirl, find how many horsepower this pump requires at this operating condition. Estimate the efficiency first to calculate the specific speed. [Ans: 10.72 hp]

CHAPTER 6

STEAM TURBINES

6.1 INTRODUCTION

The prime mover in a steam power plant is a steam turbine that converts part of the thermal energy of steam at high pressure and temperature to shaft power. Other components of the plant are a steam generator, a condenser, and feedwater pumps and heaters. The plants operate on various modifications of the Rankine cycle. The basic Rankine cycle, operating between 40 and 565 °C, has a Carnot efficiency of 37%. Modifications, including superheating, reheating, and feedwater heating, increase the efficiency by approximately an additional 10%.

Most large power plants have two reheats and three or more turbines. The turbines are said to be *compounded* when steam passes through each of them in series. The high-pressure (HP) turbine receives steam from the steam generator. After leaving this turbine, the steam is reheated and then enters an intermediate-pressure (IP) turbine, also called a *reheat turbine*, through which it expands to an intermediate pressure. After the second reheat, the rest of the expansion takes place through a low-pressure (LP) turbine, from which the steam flows into a condenser at a pressure below the atmospheric value.

A turbine in which the steam leaves at quality near 90% is called a *condensing turbine*. An *extraction* turbine has ports from which steam is extracted for feedwater heating. An *induction* turbine receives steam at intermediate pressures for additional power generation.

In a *noncondensing or backpressure* turbine, steam leaves at superheated conditions, and the thermal energy in the exhaust steam is used in various industrial processes. A well-designed *combined heat and power* plant generates appropriate amount of power

to drop the steam temperature and pressure to values that meet the process heating needs. District heating is an application in which steam is used at even lower temperatures than in many industrial processes. An important consideration in providing the heating needs of an economy is to match the source to the application. Combined heat and power plants are designed with this in mind.

In modern coal-burning power plants, axial steam turbines are typically housed in three, four, or five casings. Many LP turbines are *double-flow* type, and their single casing accommodates a pair of turbines in which steam flows in opposite directions to balance axial forces on the turbine shaft. When two or more turbines are connected to a common shaft, they are said to operate in *tandem*, and the plant is said to be of a tandem compound type. If the steam is directed to a set of turbines on different shafts, then the system is said to be *cross-compounded*. For example, a 1000-MW power plant could have an HP turbine and an IP turbine on a single shaft and three LP turbines on a different shaft. Rotational speeds are typically either 3600 or 1800 rpm; the lower speed for the LP turbines that have larger rotors in order to accommodate the larger volumetric flow rate of steam at low pressure. The large volumetric flow rate at the low pressure end requires very long blades. As an example, a General Electric/Toshiba LP steam turbine running at 3600 rpm has blades 1016 mm in length and a flow area 8.2 m^2 in the last stage. When this is designed to run at 3000 rpm for generating electricity at 50 Hz, the blades of the last stage are designed to be 1220 mm long, with a corresponding flow area 11.9 m^2 . For a 26-stage steam turbine, the hub-to-casing radius ratio for the last stage may have a value 0.42, whereas for the first stage, a typical value is 0.96.

Outlet pressures from the boiler vary from a subcritical 10 MPa to a supercritical 30 MPa, or more. The condenser pressure is below the atmospheric pressure, typically about 8 kPa, which corresponds to a saturation temperature of 41°C . This makes the overall pressure ratio equal to 1250 for a conventional plant and three times this for supercritical plants. In a 400-MW power plant, the HP turbine provides about 100 MW of power, and about an equal rate is delivered by the IP turbine. A double-flow LP turbine delivers the remaining 200 MW. The pressure ratios are 4.5 for the HP turbine and 3 for the IP turbine. The LP turbine has ports for extracting steam to feedwater heaters at pressure ratios ranging from 1.5 to 4.5.

Owing to the large inlet pressure, design of the HP turbine differs from that of the others. The first stage is designed for low reaction, so that most of the pressure drop takes place at the nozzles feeding this stage. This brings the steam to a very high velocity as it enters the first rotor. However, the pressure is now sufficiently low that leakage flow through seals is tolerable. Later stages are designed for higher reaction, and in IP and LP turbines, the reaction is close to 50%.

Table 6.1 lists some typical designs and rated power outputs for coal-burning steam power plants. Designations such as 1SF and 3DF refer to one single-flow and three double-flow turbines [25]. At the preliminary design stage, steam inlet pressure to the HP turbine is specified. Intermediate pressures at which reheating takes place are then calculated according to how much moisture is allowed at the exit of the HP and IP turbines. A similar decision is made for the reheat (RH) turbine to determine the appropriate pressure at the inlet of the LP turbines.

The steam turbine industry is very large. The year 2017 worldwide electricity generation from steam plants is 48.7 EJ (exajoules) equal to 1.55 TW (terawatts) of generated power. This means that on the order of 12000 steam turbines are in use. The major manufacturers include GE power systems in the United States, Siemens, Alstom, and Ansaldo Energia in Western Europe, and Mitsubishi Heavy Industries, Hitachi, and Toshiba in Japan. Many

Table 6.1 Fossil steam power turbine arrangements.

| Output (MW) | Reheats | Steam pressure (MPa) | HP | IP | RH | LP |
|----------------|---------|-------------------------|-----|-----|-----|-----|
| 50–150 | 0 or 1 | 10.1 | 1SF | — | — | 1SF |
| 150–200 | 1 | 12.5 | 1SF | 1SF | — | 1DF |
| 250–450 | 1 | 16.6 | 1SF | 1SF | — | 1DF |
| 450–600 | 1 | 16.6 | 1SF | 1SF | — | 2DF |
| 450–600 | 1 | 24.2 | 1SF | 1SF | — | 2DF |
| 600–850 | 1 | 16.6 | 1DF | 1DF | — | 2DF |
| 600–850 | 1 or 2 | 24.2 | 1SF | 1SF | 1DF | 2DF |
| 850–1100 | 1 | 16.6 | 1DF | 1DF | — | 3DF |
| 850–1100 | 1 or 2 | 24.2 | 1SF | 1SF | 1DF | 3DF |

of the steam turbines in Eastern and Central Europe are supplied by LMZ in Russia and Skoda in the Czech Republic.

Worldwide production of electricity during the year 2017 was 26000 billion kWh. In standard units, this is 93.6 EJ. In *thermal plants*, electricity generation is fueled by coal, natural gas, oil, and uranium. Coal provides 36 EJ; natural gas, 22 EJ; and oil, 3 EJ, of the generated electricity. Nuclear fuels provide 10 EJ. The remainder comes from renewable sources, with 15 EJ from hydropower, 4 EJ from wind, 1 EJ from solar, and the rest from biomass. In coal, fuel oil, and nuclear power plants, the working fluid is water, and these *steam plants* provide 51% of the generated electricity. The other 49% comes from hydropower, wind, and solar and from gas turbine power plants fueled by natural gas and some by oil [91]. Since these figures relate to production of electricity, they do not take into account the energy value of coal, gas, and uranium that needs to be mined. A rough value for thermal efficiency of fossil fuel plants is 38%, and therefore, the energy content of the fuels delivered to the plants is a factor of 2.6 larger. Ordinarily, the energy requirement for mining and transporting the fuel needed by power stations is not factored into the energy evaluation, as it should be.

6.2 IMPULSE TURBINES

This section begins with a discussion of impulse turbines and how a single-stage turbine is compounded to multiple stages by two methods. These are called *pressure compounding*, or Rateau staging, and *velocity compounding*, or Curtis staging. Both are used to reduce the shaft speed, which in a single-stage impulse turbine may be intolerably high.

6.2.1 Single-stage impulse turbine

Carl Gustaf Patrik de Laval (1845–1913) of Sweden in 1883 developed an impulse turbine consisting of a set of nozzles and a row of blades, as shown in Figure 6.1. This turbine is designed to undergo the entire pressure drop in the nozzles and none across the rotor. For sufficiently low exit pressure, *converging–diverging* nozzles accelerate the steam to a supersonic speed. The angle of the relative velocity approaching the rotor blades is β_2 , and the exit angle has a negative value β_3 . For *equiangular* blades, $\beta_3 = -\beta_2$. This gives the blades a *bucket* shape because at the design condition, the actual metal angles of the blades are close to the flow angles of the relative velocity.

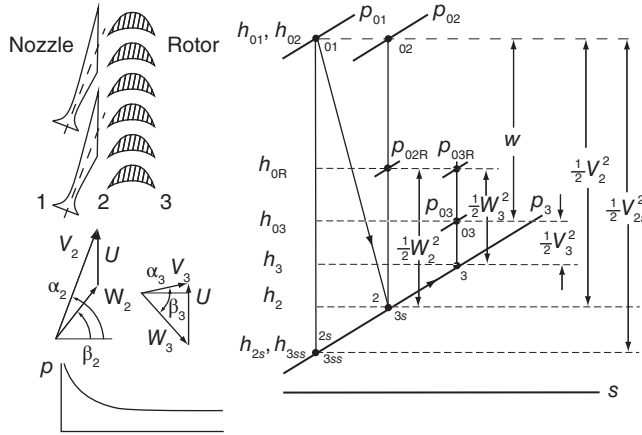


Figure 6.1 Single-stage impulse turbine and its Mollier chart.

The blades change the direction of the momentum of the flow, and this gives an *impulsive force* to the blades. This is the origin of the name for this turbine, for it appears as if the fluid particles were executing trajectories similar to a ball striking a wall and caused to bounce back by an impulsive force. But if the surface forces on the blades are examined, it is clear that the difference between the high pressure on the concave side of the blade and the low pressure on the convex side is the actual cause of the blade force. A combination of a nozzle row and a rotor row make up a *stage*. For this reason, the de Laval turbine is also called a *single-stage impulse turbine*.

Work done on the blades is given by

$$w = h_{02} - h_{03} = U(V_{u2} - V_{u3})$$

and since the relative stagnation enthalpy is constant across the rotor

$$h_2 + \frac{1}{2}W_2^2 = h_3 + \frac{1}{2}W_3^2 \quad (6.1)$$

As seen from the h - s diagram in Figure 6.1, irreversibilities cause the static enthalpy to increase from h_2 to h_3 , and then Eq. (6.1) shows that W_3 is less than W_2 . For equiangular blades, this means that the tangential and axial components of the relative velocity must decrease in the same proportion.

It is assumed that steam flows into the nozzles from a steam chest in which velocity is negligibly small. The nozzle efficiency, as shown in the previous chapter, is given by

$$\eta_N = \frac{h_{01} - h_2}{h_{01} - h_{2s}} = \frac{h_{02} - h_2}{h_{02} - h_{2s}}$$

and the second expression follows since $h_{01} = h_{02}$. This can also be written in the form

$$\eta_N = \frac{V_2^2}{V_{2s}^2} = c_N^2$$

in which the velocity coefficient for the nozzle has been defined as $c_N = V_2/V_{2s}$. The loss of stagnation pressure across the nozzles is $\Delta p_{0LN} = p_{01} - p_{02}$. Examination of Figure 6.1

shows that the velocity coefficient is defined such that it represents the loss of kinetic energy in the nozzles.

For the rotor $c_R = W_3/W_{3s}$, but since the state 3s is the same as state 2, the velocity coefficient for the rotor is also $c_R = W_3/W_2$. The loss of stagnation pressure is given by $\Delta p_{0LR} = p_{02R} - p_{03R}$. The constant pressure lines p_{02R} and p_{03R} are shown in Figure 6.1. The velocity coefficient c_R has been defined such that the decrease in kinetic energy of the relative velocities represents a thermodynamic loss. The sum of the separate stagnation pressure losses across the nozzles and the rotor gives a different and correct value for the total loss than what was calculated in Chapter 2, where this loss in stagnation pressure was determined for the entire stage.

The efficiency of the rotor is defined as

$$\eta_R = \frac{h_{02} - h_{03}}{h_{02} - h_{3s}}$$

because the kinetic energy leaving the rotor is assumed to be wasted. Since $h_2 = h_{3s}$, this can also be written as

$$\eta_R = \frac{w}{\frac{1}{2} V_2^2}$$

The product

$$\eta_{ts} = \eta_N \eta_R$$

can be written as

$$\eta_{ts} = \frac{h_{02} - h_2}{h_{02} - h_{2s}} \frac{h_{02} - h_{03}}{h_{02} - h_{3s}} = \frac{h_{01} - h_{03}}{h_{01} - h_{3ss}}$$

since $h_2 = h_{3s}$ and $h_{2s} = h_{3ss}$ and the standard definition of the total-to-static efficiency is recovered. With this introduction, the principles learned in Chapter 3 are next applied to a single-stage impulse steam turbine.

■ EXAMPLE 6.1

Steam flows from nozzles at the rate 0.2 kg/s and speed 900 m/s. It then enters the rotor of single-stage impulse turbine with equiangular blades. The flow leaves the nozzles at an angle of 70° , the mean radius of the blades is 120 mm, and the rotor speed is 18000 rpm. The frictional loss in the rotor blades is 15% of the relative kinetic energy entering the rotor. (a) Draw the velocity diagrams at the inlet and outlet of the rotor with properly calculated values of the inlet and outlet flow angles for the relative and absolute velocities. (b) Find the power delivered by the turbine. (c) Find the rotor efficiency.

Solution: (a) The blade speed is

$$U = r \Omega = \frac{0.12 \cdot 18000 \cdot 2\pi}{60} = 226.2 \text{ m/s}$$

and the axial velocity is

$$V_{x2} = V_2 \cos \alpha_2 = 900 \cos(70^\circ) = 307.8 \text{ m/s}$$

and the tangential component of the absolute velocity at the inlet to the rotor is

$$V_{u2} = V_2 \sin \alpha_2 = 900 \sin(70^\circ) = 845.7 \text{ m/s}$$

The tangential component of the relative velocity entering the rotor is therefore

$$W_{u2} = V_{u2} - U = 845.7 - 226.2 = 619.5 \text{ m/s}$$

so that the relative flow speed, since $W_{x2} = V_{x2}$, comes out to be

$$W_2 = \sqrt{W_{x2}^2 + W_{u2}^2} = \sqrt{307.8^2 + 619.5^2} = 691.8 \text{ m/s}$$

The inlet angle of the relative velocity is then

$$\beta_2 = \tan^{-1} \left(\frac{W_{u2}}{W_{x2}} \right) = \tan^{-1} \left(\frac{619.5}{307.8} \right) = 63.6^\circ$$

Since 15% of the kinetic energy of the relative motion is lost, at the exit, the kinetic energy of the relative flow is

$$\frac{1}{2} W_3^2 = \frac{1}{2} (1 - 0.15) W_2^2 \quad \text{and} \quad W_3 = \sqrt{0.85 \cdot 691.8^2} = 637.8 \text{ m/s}$$

For equiangular blades, $\beta_3 = -\beta_2$, and the axial velocity leaving the rotor is

$$W_{x3} = W_3 \cos \beta_3 = 637.8 \cos(-63.6^\circ) = 283.8 \text{ m/s}$$

and the tangential component of the relative velocity is

$$W_{u3} = W_3 \sin \beta_3 = 637.8 \sin(-63.6^\circ) = -571.2 \text{ m/s}$$

The tangential component of the absolute velocity becomes

$$V_{u3} = U + W_{u3} = 226.2 - 571.2 = -345.0 \text{ m/s}$$

Hence, with $V_{x3} = W_{x3}$, the flow angle at the exit is

$$\alpha_3 = \tan^{-1} \left(\frac{V_{u3}}{V_{x3}} \right) = \tan^{-1} \left(-\frac{345.0}{283.8} \right) = -50.6^\circ$$

and the velocity leaving the rotor is

$$V_3 = \sqrt{V_{x3}^2 + V_{u3}^2} = \sqrt{283.8^2 + 345^2} = 446.7 \text{ m/s}$$

The velocity triangles at the inlet and outlet are shown in Figure 6.2.

(b) The specific work done on the blades is obtained as

$$w = U(V_{u2} - V_{u3}) = 226.2(845.7 + 345.0) = 269.3 \text{ kJ/kg}$$

and the power delivered is

$$\dot{W} = \dot{m}w = 0.2 \cdot 269.3 = 53.87 \text{ kW}$$

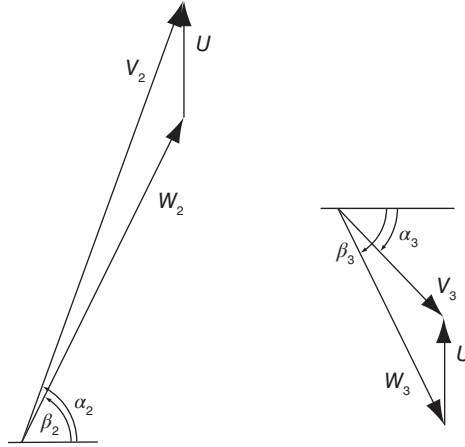


Figure 6.2 Velocity diagrams for a single-stage impulse turbine.

(c) The kinetic energy leaving the nozzle is

$$\frac{1}{2}V_2^2 = \frac{1}{2}900^2 = 405.0 \text{ kJ/kg}$$

and the rotor efficiency therefore becomes

$$\eta_R = \frac{w}{V_2^2/2} = \frac{269.3}{405.0} = 0.665 \quad \text{or} \quad 66.5\%$$

Of the difference $1 - \eta_R$, a fraction is lost as irreversibilities, and the rest is the kinetic energy leaving the rotor. The latter is obtained by calculating the ratio $V_3^2/2$ to $V_2^2/2$, which is $(446.7/900)^2 = 0.246$. Hence, losses from irreversibilities are $1 - 0.665 - 0.246 = 0.089$, or about 9%. It turns out that the blade speed in this example is too low for optimum performance, as will be shown next. ■

As the theory of turbomachinery advanced, measures more general than the velocity coefficients to account for irreversibility replaced them. A useful measure is the increase in the static enthalpy by internal heating. The loss coefficients ζ_N and ζ_R are defined by the equations

$$h_2 - h_{2s} = \frac{1}{2}\zeta_N V_2^2 \quad h_3 - h_{3s} = \frac{1}{2}\zeta_R W_3^2 \quad (6.2)$$

with the thermodynamic states as shown in Figure 6.1. Since the stagnation enthalpy is constant for the flow through the nozzle, it follows that

$$h_{2s} + \frac{1}{2}V_{2s}^2 = h_2 + \frac{1}{2}V_2^2$$

which is rearranged to the form

$$h_2 - h_{2s} = \frac{1}{2}\zeta_N V_2^2 = \frac{1}{2}V_{2s}^2 - \frac{1}{2}V_2^2$$

With $V_{2s} = V_2/c_N$, this equation can be expressed as

$$c_N = \frac{V_2}{V_{2s}} = \frac{1}{\sqrt{1 + \zeta_N}} \quad (6.3)$$

Similarly, the relative stagnation enthalpy is constant for the rotor,

$$h_{3s} + \frac{1}{2}W_2^2 = h_3 + \frac{1}{2}W_3^2$$

and this equation can be rewritten in the form

$$h_3 - h_{3s} = \frac{1}{2}\zeta_R W_3^2 = \frac{1}{2}W_2^2 - \frac{1}{2}W_3^2$$

from which

$$c_R = \frac{W_3}{W_2} = \frac{1}{\sqrt{1 + \zeta_R}} \quad (6.4)$$

The stagnation pressure loss across the nozzles is $\Delta p_{0LN} = p_{01} - p_{02}$, and the stagnation pressure loss across the rotor is $\Delta p_{0LR} = p_{02R} - p_{03R}$. The relative stagnation pressures are determined by first calculating the relative stagnation temperatures, which are obtained from

$$T_{02R} = T_2 + \frac{W_2^2}{2c_p} \quad T_{03R} = T_3 + \frac{W_3^2}{2c_p}$$

and then relative stagnation pressures are determined from

$$\frac{p_{02R}}{p_2} = \left(\frac{T_{02R}}{T_2} \right)^{\gamma/(\gamma-1)} \quad \frac{p_{03R}}{p_3} = \left(\frac{T_{03R}}{T_3} \right)^{\gamma/(\gamma-1)}$$

To calculate the total-to-static efficiency from $\eta_{ts} = \eta_N \eta_R$, the nozzle efficiency is first determined from

$$\eta_N = c_N^2 = \frac{1}{1 + \zeta_N} \quad (6.5)$$

and then the rotor efficiency needs to be found. This is done by manipulating its definition into the form

$$\frac{1}{\eta_R} - 1 = \frac{h_{03} - h_{3s}}{h_{02} - h_{03}} = \frac{\frac{1}{2}V_3^2 + (h_3 - h_{3s})}{w}$$

which can be recast as

$$\frac{1}{\eta_R} - 1 = \frac{V_3^2 + \zeta_R W_3^2}{2w} \quad (6.6)$$

Then, using

$$V_{u2} = U + W_{u2} \quad V_{u3} = U + W_{u3}$$

the work done on the blades may be written as

$$w = U(V_{u2} - V_{u3}) = U(W_{u2} - W_{u3}) = U(W_2 \sin \beta_2 - W_3 \sin \beta_3)$$

For equiangular blades, $\beta_3 = -\beta_2$, and making use of the relationship $W_3 = W_2/\sqrt{1 + \zeta_R}$, this equation takes the form

$$w = UW_2 \left(1 + \frac{1}{\sqrt{1 + \zeta_R}} \right) \sin \beta_2$$

or with further substitution of $W_2 \sin \beta_2 = V_2 \sin \alpha_2 - U$, it is

$$w = U \frac{(1 + \sqrt{1 + \zeta_R})}{\sqrt{1 + \zeta_R}} (V_2 \sin \alpha_2 - U) \quad (6.7)$$

The numerator of Eq. (6.6) still needs to be expressed in terms of V_2 and α_2 , as was done for work. After the component equations for the velocities

$$W_3 \cos \beta_3 = V_3 \cos \alpha_3 \quad W_3 \sin \beta_3 + U = V_3 \sin \alpha_3$$

are squared and added, the relationship

$$W_3^2 + 2UW_3 \sin \beta_3 + U^2 = V_3^2$$

is obtained. Making use of Eq. (6.4), the term $V_3 + \zeta_R W_3^2$ can be written as

$$V_3^2 + \zeta_R W_3^2 = \frac{W_2^2}{1 + \zeta_R} - \frac{2UW_2 \sin \beta_2}{\sqrt{1 + \zeta_R}} + U^2 + \frac{\zeta_R W_2^2}{1 + \zeta_R}$$

or as

$$V_3^2 + \zeta_R W_3^2 = W_2^2 - \frac{2UW_2 \sin \beta_2}{\sqrt{1 + \zeta_R}} + U^2$$

The relative velocity W_2 is next expressed in terms of V_2 and α_2 . Again, the component equations for the definition of relative velocity give

$$W_2 \cos \beta_2 = V_2 \cos \alpha_2 \quad W_2 \sin \beta_2 = V_2 \sin \alpha_2 - U$$

which, when squared and added, leads to

$$W_2^2 = V_2^2 - 2UV_2 \sin \alpha_2 + U^2$$

Hence, the expression for $V_3^2 + \zeta_R W_3^2$ takes the final form

$$V_3^2 + \zeta_R W_3^2 = \frac{(V_2^2 - 2UV_2 \sin \alpha_2 + U^2)(1 + \zeta_R) - 2U(V_2 \sin \alpha_2 - U)\sqrt{1 + \zeta_R}}{1 + \zeta_R}$$

The equation for the efficiency can now be written as

$$\frac{1}{\eta_R} - 1 = \frac{(V_2^2 - 2UV_2 \sin \alpha_2 + U^2)(1 + \zeta_R) - 2U(V_2 \sin \alpha_2 - U)\sqrt{1 + \zeta_R}}{2U(1 + \zeta_R + \sqrt{1 + \zeta_R})(V_2 \sin \alpha_2 - U)}$$

Introducing the speed ratio $\lambda = U/V_2$ into this gives

$$\frac{1}{\eta_R} - 1 = \frac{(1 - 2\lambda \sin \alpha_2 + 2\lambda^2)(1 + \zeta_R) - 2\lambda(\sin \alpha_2 - \lambda)\sqrt{1 + \zeta_R}}{2\lambda(1 + \zeta_R + \sqrt{1 + \zeta_R})(\sin \alpha_2 - \lambda)}$$

The rotor efficiency now can be expressed as

$$\eta_R = \frac{2\lambda(1 + \zeta_R + \sqrt{1 + \zeta_R})(\sin \alpha_2 - \lambda)}{1 + \zeta_R} \quad (6.8)$$

and the stage efficiency as

$$\eta_{ts} = \eta_N \eta_R = \frac{2\lambda(1 + \zeta_R + \sqrt{1 + \zeta_R})(\sin \alpha_2 - \lambda)}{(1 + \zeta_N)(1 + \zeta_R)} \quad (6.9)$$

By making use of Eqs. (6.3) and (6.4), this can also be written as

$$\eta_{ts} = 2\lambda c_N^2 (1 + c_R)(\sin \alpha_2 - \lambda) \quad (6.10)$$

The blade speed at which the stage efficiency reaches its maximum value is obtained by differentiating this with respect to λ and setting the result to zero. This gives

$$\frac{d\eta_{ts}}{d\lambda} = 2c_N^2(1 + c_R)(\sin \alpha_2 - 2\lambda) = 0$$

and the maximum efficiency is obtained when the speed ratio is

$$\lambda = \frac{U}{V_2} = \frac{1}{2} \sin \alpha_2$$

This equation is independent of the velocity coefficients. For typical nozzle angles, in the range from 65° to 75° , the speed ratio $\lambda = U/V_2$ is about 0.47, so that the blade speed at this optimum condition is about one-half of the exit velocity from the nozzles. The turbine efficiency at this value of U/V_2 is

$$\eta_{ts_{opt}} = \frac{1}{2} c_N^2 (1 + c_R) \sin^2 \alpha_2$$

so that for $c_N = 0.979$, $c_R = 0.940$, and $\alpha_2 = 70^\circ$, the stage efficiency at the optimal condition is $\eta_{ts_{opt}} = 0.821$. Figure 6.3 shows the stage efficiency for these parameters and for an ideal case, with $c_N = 1$ and $c_R = 1$.

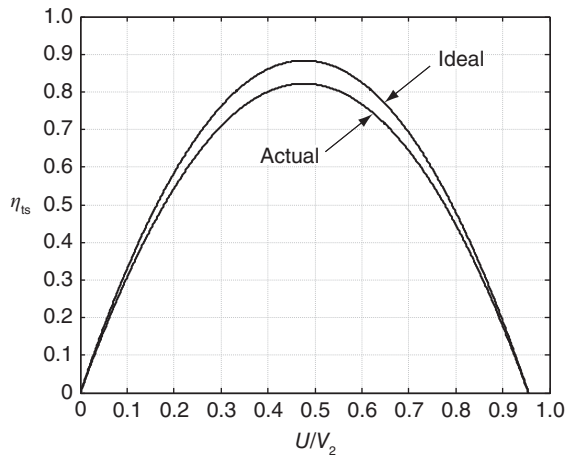


Figure 6.3 Efficiency of a single-stage impulse turbine: ideal and actual with $c_N = 0.979$, $c_R = 0.940$, and $\alpha_2 = 70^\circ$.

EXAMPLE 6.2

Steam leaves the nozzles of a single-stage impulse turbine at the speed 900 m/s. Even though the blades are not equiangular, the blade speed is set at the optimum for equiangular blades when the nozzles are at the angle 68° . The velocity coefficient of the nozzles is $c_N = 0.97$, and for the rotor blades, it is $c_R = 0.95$. The absolute value of the relative flow angle at the exit of the rotor is 3° greater than the corresponding inlet flow angle. Find (a) the total-to-static efficiency, and (b) find again the total-to-static efficiency of the turbine, assuming that it operates at the same conditions, but has equiangular blades. If one efficiency is higher than the other, then, explain the reason; if they are the same, then, give an explanation for this as well.

Solution: (a) With the optimum operating blade speed determined from

$$U = \frac{1}{2} V_2 \sin \alpha_2 = \frac{1}{2} 900 \sin(68^\circ) = 417.2 \text{ m/s}$$

the velocity components at the exit from the nozzles are

$$V_{x2} = V_2 \cos \alpha_2 = 900 \cos(68^\circ) = 337.2 \text{ m/s}$$

$$V_{u2} = V_2 \sin \alpha_2 = 900 \sin(68^\circ) = 834.5 \text{ m/s}$$

the velocity components of the relative velocity are

$$W_{x2} = V_{x2} = 337.2 \text{ m/s} \quad W_{u2} = V_{u2} - U = 834.5 - 417.2 = 417.3 \text{ m/s}$$

The magnitude of the relative velocity is

$$W_2 = \sqrt{W_{x2}^2 + W_{u2}^2} = \sqrt{337.2^2 + 417.3^2} = 536.4 \text{ m/s}$$

The angle at which the relative velocity enters the rotor row is

$$\beta_2 = \tan^{-1} \left(\frac{W_{u2}}{W_{x2}} \right) = \tan^{-1} \left(\frac{417.3}{337.2} \right) = 51.06^\circ$$

and the exit angle is $\beta_3 = -51.06^\circ - 3^\circ = -54.06^\circ$, and the magnitude of the relative velocity is $W_3 = c_R W_2 = 0.95 \cdot 536.4 = 509.6 \text{ m/s}$. Work delivered by the rotor is

$$w = U(W_{u2} - W_{u3}) = U(1 + c_R C)W_2 \sin \beta_2$$

in which $C = \sin |\beta_3| / \sin \beta_2 = 1.041$ and $c_R = 0.95$. Therefore, the work delivered is $w = 346.23 \text{ kJ/kg}$. Since the exit kinetic energy is wasted, its value is needed. The exit velocity components are

$$V_{x3} = W_{x3} = W_3 \cos \beta_3 = 509.6 \cos(-54.06^\circ) = 299.1 \text{ m/s}$$

$$V_{u3} = W_3 \sin \beta_3 + U = 509.6 \sin(-54.06^\circ) + 417.2 = 4.6 \text{ m/s}$$

Hence,

$$V_3 = \sqrt{V_{x3}^2 + V_{u3}^2} = \sqrt{299.1^2 + 4.6^2} = 299.1 \text{ m/s}$$

In the calculation of rotor efficiency, the rotor loss coefficient is $\zeta_R = 1/c_R^2 - 1 = 0.108$, so that

$$\eta_R = \frac{2w}{2w + V_3^2 + \zeta_R W_3^2} = \frac{2 \cdot 346230}{2 \cdot 346230 + 299.1^2 + 0.108 \cdot 509.6^2} = 0.875$$

and since $\eta_N = c_N^2 = 0.97^2 = 0.941$, the total-to-static efficiency becomes

$$\eta_{ts} = \eta_N \eta_R = 0.941 \cdot 0.875 = 0.823$$

(b) If the blades were equiangular and the turbine were to operate at its optimal condition, then, the total-to-static efficiency would be

$$\eta_{ts} = \frac{1}{2} c_N^2 (1 + c_R) \sin^2 \alpha_2 = 0.789$$

The loss of efficiency for equiangular blades is caused by the exit kinetic energy now being larger than before. When the blades are not equiangular, even when the turbine is not operated at its optimum blade speed, it has a high efficiency because the exit velocity is nearly axial, and the turbine has a high utilization. For equiangular blades, the exit flow angle is slightly larger, and therefore, the flow is faster, with more of the kinetic energy leaving the stage. ■

6.2.2 Pressure compounding

The optimum blade speed for a single-stage impulse turbine is about one-half the exit velocity from the nozzles. Such a high blade speed requires a high shaft speed, which may lead to large blade stresses. To reduce the shaft speed, two or more single-stage impulse turbines are arranged in series, and the steam is then expanded partially in each of the set of nozzles. This decreases the velocity from the nozzles, and thus the blade speed for optimal performance. This arrangement, shown in Figure 6.4, is called *pressure compounding*, or *Rateau staging*, after Auguste Camille Edmond Rateau (1863–1930) of France. Between any two rotors, there is a nozzle row. The pressure drop takes place in the nozzles and none across the rotor. As the steam expands, its specific volume increases, and a larger flow area is needed in order to keep the increase in velocity moderate. One approach is to keep the mean radius of the wheel constant and to increase the blade height. When this is done, the blade speed at the mean radius remains the same for all stages, and the velocities leaving and entering a stage can be made equal. Such a stage is called a *normal stage*, or a *repeating stage* if, in addition, the exit flow angle is equal to that at the inlet to the stage.

Consider a multistage pressure-compounded impulse turbine with repeating stages. Unlike in the single-stage turbine, the flow now enters the second set of nozzles at a velocity equal to the exit velocity from the preceding stage, and the function of the nozzle is to increase it. The process lines are shown in Figure 6.5. The stagnation states 03, 03s, and 03ss are reached from the static states 3, 3s, and 3ss, which are on the constant pressure line p_3 . As was discussed earlier, it does not necessarily follow that the states 03s and 03ss are on the constant-pressure line p_{03} since the magnitudes of the velocities V_{3s} and V_{3ss} in

$$h_{03s} = h_{3s} + \frac{1}{2} V_{3s}^2 \quad h_{03ss} = h_{3ss} + \frac{1}{2} V_{3ss}^2$$

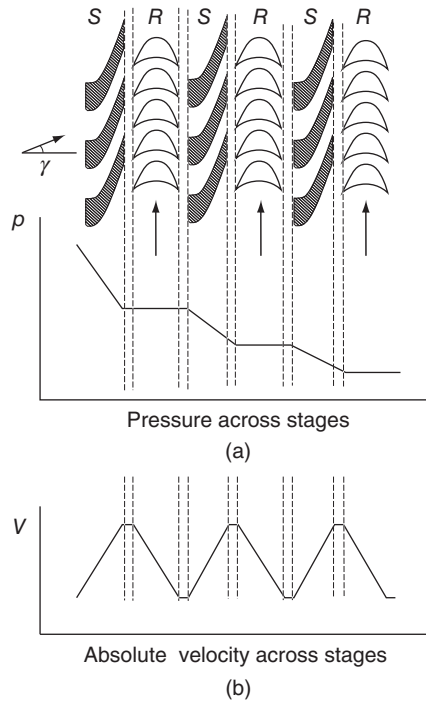


Figure 6.4 Sketch of a multistage pressure-compounded impulse turbine (a) and the pressure drop and velocity variation across each stage (b).

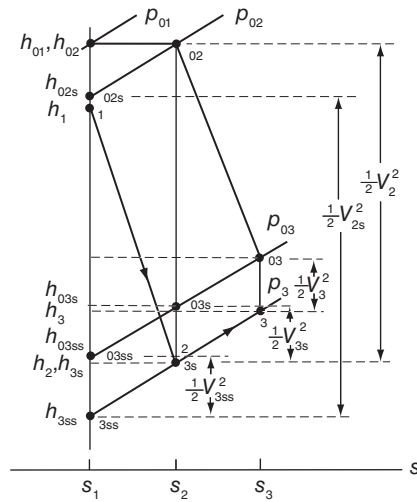


Figure 6.5 The process lines for a pressure-compounded impulse stage.

are not known. However, a consistent theory can be developed if it is *assumed* that the stagnation states 03s and 03ss are on the constant pressure line p_{03} , and their thermodynamic states are then fixed by the known value of pressure and entropy. The previous equations then fix the magnitudes of V_{3s} and V_{3ss} to definite values.

With this assumption, the Gibbs equation

$$Tds = dh - v dp \quad ds = c_p \frac{dT}{T} - R \frac{dp}{p}$$

when integrated between states 03s and 03 and then between states 03ss and 03s along the constant pressure line p_{03} and similarly along the corresponding states along the constant pressure line p_3 give

$$s_2 - s_1 = c_p \ln \frac{T_{03s}}{T_{03ss}} \quad s_3 - s_2 = c_p \ln \frac{T_{03}}{T_{03s}}$$

and

$$s_2 - s_1 = c_p \ln \frac{T_{3s}}{T_{3ss}} \quad s_3 - s_2 = c_p \ln \frac{T_3}{T_{3s}}$$

from which

$$\frac{T_{03}}{T_{03s}} = \frac{T_3}{T_{3s}} \quad \text{and} \quad \frac{T_{03s}}{T_{03ss}} = \frac{T_{3s}}{T_{3ss}} \quad (6.11)$$

and from these, it follows that

$$\frac{T_{03}}{T_3} = \frac{T_{03s}}{T_{3s}} = \frac{T_{03ss}}{T_{3ss}}$$

Expressing these temperature ratios in terms of Mach numbers yields

$$\frac{T_{03}}{T_3} = 1 + \frac{\gamma - 1}{2} M_3^2 \quad \frac{T_{03s}}{T_{3s}} = 1 + \frac{\gamma - 1}{2} M_{3s}^2 \quad \frac{T_{03ss}}{T_{3ss}} = 1 + \frac{\gamma - 1}{2} M_{3ss}^2 \quad (6.12)$$

so that $M_3 = M_{3s} = M_{3ss}$.

The stage efficiency for a pressure-compounded stage is the total-to-total efficiency

$$\eta_{tt} = \frac{h_{01} - h_{03}}{h_{01} - h_{03ss}}$$

which can be recast into the form

$$\frac{1}{\eta_{tt}} - 1 = \frac{h_{03} - h_{03ss}}{h_{01} - h_{03}} = \frac{h_{03} - h_{03s} + h_{03s} - h_{03ss}}{h_{01} - h_{03}} \quad (6.13)$$

Subtracting one from each side of both Eqs. (6.11), multiplying by c_p , and rearranging gives

$$h_{03} - h_{03s} = \frac{T_{03s}}{T_{3s}} (h_3 - h_{3s}) \quad h_{03s} - h_{03ss} = \frac{T_{03ss}}{T_{3ss}} (h_{3s} - h_{3ss})$$

Substituting these into Eq. (6.13) leads to

$$\frac{1}{\eta_{tt}} - 1 = \frac{\frac{T_{03s}}{T_{3s}} (h_3 - h_{3s}) + \frac{T_{03ss}}{T_{3ss}} (h_{3s} - h_{3ss})}{w} \quad (6.14)$$

or, since the temperature ratios are the same, according to Eq. (6.12), this expression for efficiency becomes

$$\frac{1}{\eta_{tt}} - 1 = \frac{\left(1 + \frac{\gamma - 1}{2} M_3^2\right) (h_3 - h_{3s} + h_2 - h_{2s})}{w} \quad (6.15)$$

The Mach number at the exit of the rotor is quite low and is often set to zero. It is, of course, easily determined once the work, and exit velocity have been calculated. Then,

$$T_{03} = T_{01} - \frac{w}{c_p} \quad T_3 = T_{03} - \frac{V_3^2}{2c_p} \quad \text{and} \quad M_3 = \frac{V_3}{\sqrt{\gamma R T_3}}$$

Ignoring the Mach number and introducing the static enthalpy loss coefficients gives

$$\frac{1}{\eta_{tt}} - 1 = \frac{\zeta_R W_3^2 + \zeta_N V_2^2}{2w} \quad (6.16)$$

The relationship $W_3^2 = c_R^2 W_2^2$ may be substituted into this, giving

$$\frac{1}{\eta_{tt}} - 1 = \frac{\zeta_R c_R^2 W_2^2 + \zeta_N V_2^2}{2w}$$

or

$$\eta_{tt} = \frac{2w}{\zeta_R c_R^2 W_2^2 + \zeta_N V_2^2 + 2w} \quad (6.17)$$

The relative velocity W_2 can be written as

$$W_2^2 = V_2^2 - 2V_2 U \sin \alpha_2 + U^2$$

so that

$$\frac{1}{\eta_{tt}} - 1 = \frac{\zeta_R c_R^2 (V_2^2 - 2V_2 U \sin \alpha_2 + U^2) + \zeta_N V_2^2}{2w}$$

The work delivered by the stage is

$$w = U(V_{u2} - V_{03}) = U(W_{u2} - W_{u3}) = U(1 + c_R)W_{u2} = U(1 + c_R)(V_2 \sin \alpha_2 - U)$$

Substituting $\lambda = U/V_2$ into the previous expression for the stage efficiency gives it the form

$$\frac{1}{\eta_{tt}} - 1 = \frac{\zeta_R c_R^2 (1 - 2\lambda \sin \alpha_2 + \lambda^2) + \zeta_N}{2\lambda(1 + c_R)(\sin \alpha_2 - \lambda)}$$

Defining the quantity f_L as

$$f_L = \frac{\zeta_R (\lambda^2 - 2\lambda \sin \alpha_2 + 1) + \zeta_N (1 + \zeta_R)}{2(1 + \zeta_R + \sqrt{1 + \zeta_R})(\lambda \sin \alpha_2 - \lambda^2)}$$

in which the relation $c_R = 1/\sqrt{1 + \zeta_R}$ has been used, the stage efficiency can now be written as

$$\eta_{tt} = \frac{1}{1 + f_L}$$

from which it is clear that f_L is a measure of the losses. The maximum value for the efficiency of a pressure-compounded stage is obtained by minimizing f_L . Thus, differentiating it with respect to λ and setting the result to zero gives

$$\lambda^2 - \frac{2(\zeta_R + \zeta_N(1 + \zeta_R))}{\zeta_R \sin \alpha_2} \lambda + \frac{\zeta_R + \zeta_N(1 + \zeta_R)}{\zeta_R} = 0$$

Of the two roots

$$\lambda_{\text{opt}} = \frac{U}{V_2} = \frac{\zeta_R + \zeta_N(1 + \zeta_R) + \sqrt{(\zeta_R + \zeta_N(1 + \zeta_R))(\zeta_R + \zeta_N(1 + \zeta_R) + \zeta_R \sin^2 \alpha_2)}}{\zeta_R \sin \alpha_2}$$

is the correct one, as the second root leads to U/V_2 ratio greater than unity. This would mean that the wheel moves faster than the approaching steam. The stage efficiency now can be written as

$$\eta_{\text{tt}} = \frac{2\lambda(1 + c_R)(\sin \alpha_2 - \lambda)}{2\lambda(1 + c_R)(\sin \alpha_2 - \lambda) + \zeta_R c_R^2 (\lambda^2 - 2\lambda \sin \alpha_2 + 1) + \zeta_N} \quad (6.18)$$

The stage efficiencies for various nozzle angles are shown in Figure 6.6 for both a pressure-compounded stage and for a single-stage impulse turbine with exit kinetic energy wasted. The efficiency curves for the pressure-compounded stage are quite flat at the top and naturally higher as the exit kinetic energy is used at the inlet of the next stage.

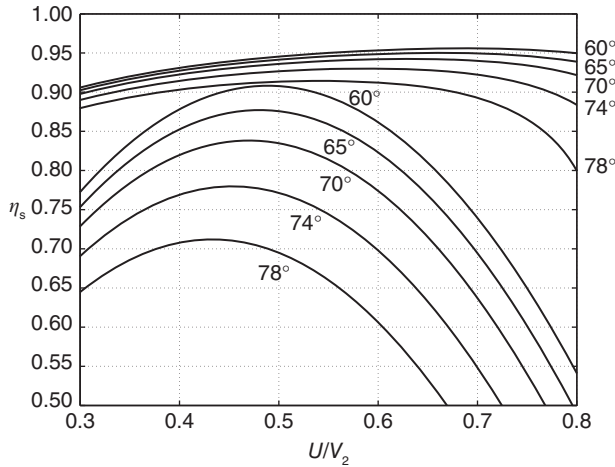


Figure 6.6 Stage efficiencies of single-stage impulse turbines with nozzle angles in the range from 60° to 78° with $\zeta_N = 0.02$ and $\zeta_R = 0.14$; the exit kinetic energy is wasted for the set of graphs with lower efficiency, and the family of graphs of higher efficiency are total-to-total efficiencies applicable to a pressure-compounded turbine stage.

6.2.3 Blade shapes

Some details of the construction of impulse blades are considered next. The equiangular blades are shown in the sketch Figure 6.7. The concave side of the blade is circular, drawn

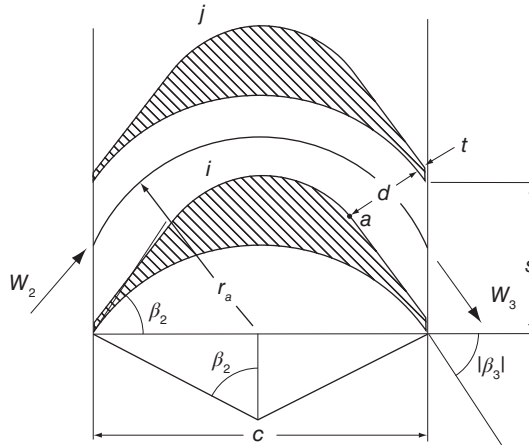


Figure 6.7 Equiangular bucket blade shape. Source: Modified from Kearton [53].

with its center a distance $c \cot \beta_2 / 2$ below the mid-cord point. Here, c is the length of the cord, and the radius of the circular arc is given by

$$r = \frac{c}{2 \sin \beta_2}$$

To establish the geometric dimensions of the blade, Brilling's rule may be followed, which establishes the interblade spacing as $d = r_a / 2$, and r_a is the radius of a circular arc that divides the gap between the blades in half. A line segment of length equal to the interblade spacing is marked off from the center along the line of symmetry. This point becomes the center of the circular arc of the concave side of blade j . The convex side of the blade i consists of a circular arc that is drawn from the same origin, and its extent is such that a straight-line segment in the direction of the blade angle meets the exit at a location that gives the correct spacing to the blades; that is the radius of the arc is chosen such that this line segment is tangent to the arc at point a . This point is chosen at the location of the intersection of a perpendicular from the trailing edge of blade j to this line segment. The blade at the inlet is made quite sharp, and at the outlet, the blade may also have a straight segment extending past the conventional exit plane. In a multistage turbine, the extent of the straight segment controls the spacing between the exit of the rotor and the inlet to the next set of nozzles. These nozzles are usually designed to have an axial entry. If the turbine operates at the design condition, and the absolute velocity at the exit is axial, then the steam flows smoothly into these nozzles. At off-design conditions, the flow angle at the entry will not match the metal angle of the nozzles, leading to increased *losses in the nozzles*, particularly for blades with sharp edges. In order to improve steam turbine's operation at a fractional flow rate, absolute values of the flow angles, at both inlet and exit, are made larger by 2° or 3° , and in a multistage turbine, for the blades next to the last stage, this may be 4° or 5° . For the last stage, the range from 5° to 10° is used [53].

Impulse blading is designed to ensure equal pressures at the inlet and exit of the rotor. However, owing to irreversibilities, temperature increases across the rotor, and this causes the specific volume to increase. Since mass flow rate is constant, mass balance gives

$$\dot{m} = \frac{A_2 W_2 \cos \beta_2}{v_2} = \frac{A_3 W_3 \cos \beta_3}{v_3}$$

in which $V_{x2} = W_2 \cos \beta_2$ and $V_{x3} = W_3 \cos \beta_3$ have been used. Since $\beta_3 = -\beta_2$ and $W_3 < W_2$, then with $v_3 > v_2$, the flow area has to be increased. This is done by increasing the height of the blade. However, it is also possible to alter the exit angle as previously mentioned.

For blades that are not equiangular, the absolute value of the outlet blade angle in most impulse turbines is larger than the inlet angle. For them, the radius of the concave surface of the blade is given by

$$r = \frac{c}{\sin \beta_2 + \sin |\beta_3|}$$

The offset between the leading and trailing edges in this case is

$$x = r(\cos \beta_2 - \cos |\beta_3|)$$

With $|\beta_3| = \beta_2 + 3^\circ$, the bisector of the blade profile will lean to the right, as shown in Figure 6.8. The channel width at the exit is given by $d = b(s \cos |\beta_3| - t)$, in which t is the trailing edge blade thickness. For a flow with mass flow rate \dot{m} and specific volume v_3 mass balance gives

$$\dot{m}v_3 = W_3 Z b(s \cos |\beta_3| - t) \quad (6.19)$$

in which Z is the number of blades in the rotor. For a given spacing of the blades, their thickness and number, and for a specified mass flow rate and exit specific volume, this equation shows that only two of the three parameters: blade height b , relative velocity W_3 , and flow angle $|\beta_3|$, may be chosen independently. If it is possible to accommodate the increase in specific volume in the downstream direction by an increase in the blade height, then this equation shows that increasing $|\beta_3|$ decreases the channel width d , and this leads to an increase in the relative velocity W_3 . Equation (6.1) then shows that since the trothalpy is constant, the static enthalpy decreases. A drop in static enthalpy along the

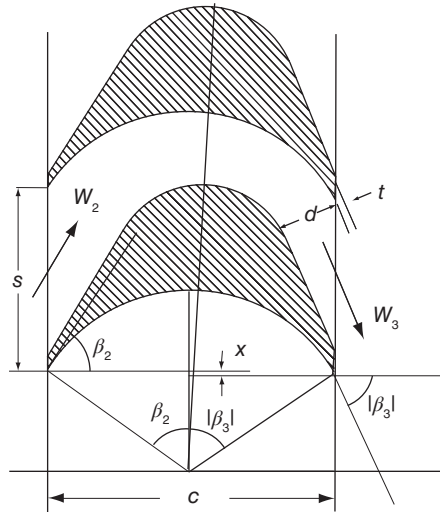


Figure 6.8 Bucket construction details for unequal blade angles. Source: Modified from Kearton [53].

flow is associated with a drop of pressure, as process lines on a Mollier diagram show. The acceleration of the flow increases the force on the blade, for by the momentum principle

$$F_u = \dot{m}(V_{u2} - V_{u3}) = \dot{m}(W_{u2} - W_{u3})$$

and since W_{u3} is negative, an increase in its magnitude increases the force component F_u . It has become conventional to call this additional force a *reaction force* in analogy to the thrust force given to a rocket being a reaction to the exit momentum leaving the rocket nozzle. Reaction turbines are discussed more fully in the next chapter.

6.2.4 Velocity compounding

A second way of *compounding* a turbine was developed by the American Charles Gordon Curtis (1860–1953). In his design, steam first enters an impulse stage, and as it leaves this stage, it enters a stator row of equiangular vanes. They redirect it to the second rotor row of equiangular blades, but of course with a different magnitude for their angles than that in the first row. All the pressure drop takes place in the upstream nozzles, and thus, no further reduction of pressure takes place as the steam moves through the downstream stages. There are practical reasons for not fitting the turbine by more than four stages. Namely, work done by later stages drops rapidly. In this kind of Curtis staging, velocity is said to be compounded from one stage to the next.

Consider an n -stage Curtis turbine with equal velocity coefficients c_v for each blade row. Analysis of the first stage is the same as for a single-stage impulse turbine. Work delivered is

$$w_{1n} = U(V_{u2} - V_{u3}) = U(W_{u2} - W_{u3})$$

As was shown previously for equiangular blades, $W_{u3} = -c_v W_{u2}$, and work delivered by the first stage may be written as

$$w_{1n} = U(1 + c_v)W_{u2}$$

In the same way, work delivered by the second and third stages are

$$w_{2n} = U(1 + c_v)W_{u4}$$

and

$$w_{3n} = U(1 + c_v)W_{u6}$$

If the relative velocity W_{u4} is related to W_{u2} , and W_{u6} is related to W_{u4} , then, work from each stage can be expressed in terms of W_{u2} . With $V_{u4} = -c_v V_{u3}$ for equiangular stator blades, W_{u4} can be written as

$$W_{u4} = V_{u4} - U = -c_v V_{u3} - U = -c_v(W_{u3} + U) - U = -c_v(-c_v W_{u2} + U) - U$$

in which $W_{u3} = -c_v W_{u2}$ has been used. Hence, the final result is

$$W_{u4} = c_v^2 W_{u2} - (1 + c_v)U$$

Similarly,

$$W_{u6} = c_v^2 W_{u4} - (1 + c_v)U$$

Substituting W_{u4} from the previous expression into this gives

$$W_{u6} = c_v^4 W_{u2} - (1 + c_v)(1 + c_v^2)U$$

Work delivered by each of the three rotors is then

$$\begin{aligned} w_{1n} &= U(1 + c_v)(V_2 \sin \alpha_2 - U) \\ w_{2n} &= U(1 + c_v)c_v^2(V_2 \sin \alpha_2 - U) - (1 + c_v)(1 + c_v)U^2 \\ w_{3n} &= U(1 + c_v)c_v^4(V_2 \sin \alpha_2 - U) - (1 + c_v)(1 + c_v + c_v^2 + c_v^3)U^2 \end{aligned}$$

Work delivered by the next stage is easily shown to be

$$w_{4n} = U(1 + c_v)c_v^6(V_2 \sin \alpha_2 - U) - (1 + c_v)(1 + c_v + c_v^2 + c_v^3 + c_v^4 + c_v^5)U^2$$

Inspection of these shows that work delivered by the n th stage is¹

$$w_{nn} = U(1 + c_v)c_v^{2n-2}(V_2 \sin \alpha_2 - U) - (1 + c_v) \sum_{i=1}^{2n-2} c_v^{i-1} U^2$$

which can also be written as

$$w_{nn} = U(1 + c_v)c_v^{2n-2}(V_2 \sin \alpha_2 - U) - \left(\frac{1 + c_v}{1 - c_v} \right) (1 - c_v^{2n-2})U^2 \quad (6.20)$$

Optimum operating conditions are now developed for turbines with different number of wheels. Work delivered by the single wheel of single-stage turbine is given by

$$w_1 = U(1 + c_v)(V_2 \sin \alpha_2 - U)$$

and the optimum blade speed was shown in the beginning of this chapter to be

$$\frac{U}{V_2} = \frac{1}{2} \sin \alpha_2$$

At the optimum speed, work from a single-stage turbine is

$$w_1 = \frac{1 + c_v}{4} V_2^2 \sin^2 \alpha_2$$

and if $c_v = 1$, this is

$$w_1 = \frac{1}{2} V_2^2 \sin^2 \alpha_2$$

Work delivered by a two-wheel Curtis turbine is $w_2 = w_{12} + w_{22}$, or

$$w_2 = U(1 + c_v)(1 + c_v^2)(V_2 \sin \alpha_2 - U) - (1 + c_v)(1 + c_v)U^2$$

¹That this conjecture is true can be shown by first proving by mathematical induction the three-term recurrence relationship $w_{i+2,n} - (1 + c_v^2)w_{i+1,n} + c_v^2 w_{i,n} = 0$ between the stages and solving this difference equation.

and when this is differentiated with respect to U and the result is set to zero, the optimum blade speed is found to be

$$\frac{U}{V_2} = \frac{(1 + c_v^2) \sin \alpha_2}{2(2 + c_v + c_v^2)}$$

For $c_v = 1$, this reduces to

$$\frac{U}{V_2} = \frac{1}{4} \sin \alpha_2$$

Hence, a two-wheel Curtis turbine can be operated at *about one-half* the shaft speed of a single-stage impulse turbine. At the optimum speed, work delivered by a two-wheel turbine is as follows:

$$w_2 = \frac{(1 + c_v)(1 + c_v^2)^2}{4(2 + c_v + c_v^2)} V_2^2 \sin^2 \alpha_2$$

For $c_v = 1$, this reduces to

$$w_2 = \frac{1}{2} V_2^2 \sin^2 \alpha_2$$

which is *exactly the same* as in a single-stage turbine. For a three-wheel Curtis turbine, work delivered is $w_3 = w_{13} + w_{23} + w_{33}$, and the expression for the work, when written in full, is

$$\begin{aligned} w_3 = & U(1 + c_v)(1 + c_v^2 + c_v^4)(V_2 \sin \alpha_2 - U) \\ & - (1 + c_v)(1 + c_v + c_v^2 + c_v^3)U^2 - (1 + c_v)(1 + c_v)U^2 \end{aligned}$$

Differentiating this to determine the value of blade speed for which work is maximum gives

$$\frac{U}{V_2} = \frac{(1 + c_v^2 + c_v^4) \sin \alpha_2}{2[(1 + c_v^2 + c_v^4) + (1 + c_v + c_v^2 + c_v^3) + (1 + c_v)]}$$

and for $c_v = 1$, this reduces to

$$\frac{U}{V_2} = \frac{1}{6} \sin \alpha_2$$

and the work delivered at this speed is

$$w_3 = \frac{(1 + c_v)(1 + c_v^2 + c_v^4)^2}{4(3 + 2c_v + 2c_v^2 + c_v^3 + c_v^4)} V_2^2 \sin^2 \alpha_2$$

Finally, the optimum blade speed for a four-wheel turbine is

$$\frac{U}{V_2} = \frac{(1 + c_v^2 + c_v^4 + c_v^6) \sin \alpha_2}{2[(1 + c_v^2 + c_v^4 + c_v^6) + (1 + c_v + c_v^2 + c_v^3 + c_v^4 + c_v^5) + (1 + c_v + c_v^2 + c_v^3) + (1 + c_v)]}$$

and work delivered at this speed is

$$w_4 = \frac{(1 + c_v)(1 + c_v^2 + c_v^4 + c_v^6)^2}{4(4 + 3c_v + 3c_v^2 + 2c_v^3 + 2c_v^4 + c_v^5 + c_v^6)} V_2^2 \sin^2 \alpha_2$$

Although velocity compounding with four wheels have been built in the past, they are no longer in use.

If $c_v = 1$ for a two wheel turbine, then, the ratio of the work done is 3 : 1 between the first and second stage. If further stages are included, the work ratios become 5 : 3 : 1 and 7 : 5 : 3 : 1 for three- and four-stage turbines, respectively, and the optimum blade speeds drop to $U = \sin \alpha_2 V_2/6$ and $U = \sin \alpha_2 V_2/8$. As has been shown, addition of successive stages does not increase the amount of work delivered by the turbine in the ideal case, and its advantage lies entirely in the reduction of the shaft speed. When irreversibilities are taken into account, turbines with multiple stages deliver less work than does a single-stage impulse turbine.

■ EXAMPLE 6.3

Consider a velocity-compounded two-stage steam turbine. The velocity at the inlet to the nozzle is axial, and it leaves the nozzle with speed $V_2 = 850$ m/s at angle $\alpha_2 = 67^\circ$. The blade speed is $U = 195.6$ m/s. The velocity coefficient for the nozzle is $c_N = 0.967$, and for the rotors, they are $c_{R1} = 0.939$ and $c_{R2} = 0.971$. For the stator between the rotors, it is $c_S = 0.954$. The rotors and the stator are equiangular. Find the efficiency of the turbine.

Solution: The axial and tangential velocity components are

$$V_{x2} = V_2 \cos \alpha_2 = 850 \cos(67^\circ) = 332.1 \text{ m/s}$$

$$V_{u2} = V_2 \sin \alpha_2 = 850 \sin(67^\circ) = 782.4 \text{ m/s}$$

The relative velocity components are $W_{x2} = V_{x2} = 332.1$ m/s and

$$W_{u2} = V_{u2} - U = 782.4 - 195.6 = 586.8 \text{ m/s}$$

so that

$$W_2 = \sqrt{W_{x2}^2 + W_{u2}^2} = \sqrt{332.1^2 + 586.8^2} = 674.3 \text{ m/s}$$

and the flow angle becomes

$$\beta_2 = \tan^{-1} \left(\frac{W_{u2}}{W_{x2}} \right) = \tan^{-1} \left(\frac{586.8}{332.1} \right) = 60.49^\circ$$

The flow angle of the relative velocity leaving the first rotor is $\beta_3 = -60.49^\circ$, and its relative velocity is

$$W_3 = c_{R1} W_2 = 0.939 \cdot 674.3 = 633.2 \text{ m/s}$$

so that its components are

$$W_{x3} = W_3 \cos \beta_3 = 633.2 \cos(-60.49^\circ) = 311.9 \text{ m/s}$$

$$W_{u3} = W_3 \sin \beta_3 = 633.2 \sin(-60.49^\circ) = -551.0 \text{ m/s}$$

The axial component of the absolute velocity entering the stator is $V_{x3} = W_{x3} = 311.9$ m/s, and its tangential component is

$$V_{u3} = W_{u3} + U = -551.0 + 195.6 = -355.4 \text{ m/s}$$

Therefore,

$$V_3 = \sqrt{V_{x3}^2 + V_{u3}^2} = \sqrt{311.9^2 + 355.4^2} = 472.9 \text{ m/s}$$

and the flow angle is

$$\alpha_3 = \tan^{-1} \left(\frac{V_{u3}}{V_{x3}} \right) = \tan^{-1} \left(-\frac{355.4}{311.9} \right) = -48.74^\circ$$

The flow angle leaving the stator is $\alpha_4 = -\alpha_3 = 48.74^\circ$ and the magnitude of the velocity is

$$V_4 = c_s V_3 = 0.954 \cdot 472.9 = 451.1 \text{ m/s}$$

The components are

$$V_{x4} = V_4 \cos \alpha_4 = 451.1 \cos(48.74^\circ) = 297.5 \text{ m/s}$$

$$V_{u4} = V_4 \sin \alpha_4 = 451.1 \sin(48.74^\circ) = 339.1 \text{ m/s}$$

The axial component of the relative velocity is $W_{x4} = V_{x4} = 297.5 \text{ m/s}$, and its tangential component is

$$W_{u4} = V_{u4} - U = 339.1 - 195.6 = 143.5 \text{ m/s}$$

so that

$$W_4 = \sqrt{W_{x4}^2 + W_{u4}^2} = \sqrt{297.5^2 + 143.5^2} = 330.3 \text{ m/s}$$

and the flow angle is

$$\beta_4 = \tan^{-1} \left(\frac{W_{u4}}{W_{x4}} \right) = \tan^{-1} \left(\frac{143.5}{297.5} \right) = 25.75^\circ$$

At the inlet of the second rotor, relative velocity is at the angle $\beta_5 = -\beta_4 = -25.75^\circ$, and its relative velocity is

$$W_5 = c_{R2} W_4 = 0.971 \cdot 330.3 = 320.7 \text{ m/s}$$

so that its components are

$$W_{x5} = W_5 \cos \beta_5 = 320.7 \cos(-25.75^\circ) = 288.9 \text{ m/s}$$

$$W_{u5} = W_5 \sin \beta_5 = 320.7 \sin(-25.75^\circ) = -139.3 \text{ m/s}$$

The axial component of the absolute velocity leaving the second rotor is $V_{x5} = W_{x5} = 288.89 \text{ m/s}$, and its tangential component is

$$V_{u5} = W_{u5} + U = -139.3 + 195.6 = 56.3 \text{ m/s}$$

For the exit velocity, this gives the value

$$V_5 = \sqrt{V_{x5}^2 + V_{u5}^2} = \sqrt{288.9^2 + 56.3^2} = 294.3 \text{ m/s}$$

and the flow angle is

$$\alpha_5 = \tan^{-1} \left(\frac{V_{u5}}{V_{x5}} \right) = \tan^{-1} \left(\frac{56.3}{288.9} \right) = 11.03^\circ$$

Work delivered by the two stages are

$$w_{12} = U(V_{u2} - V_{u3}) = 195.6(782.4 + 355.4) = 222.6 \text{ kJ/kg}$$

$$w_{22} = U(V_{u4} - V_{u5}) = 195.6(339.1 - 56.3) = 55.3 \text{ kJ/kg}$$

Therefore, the total work is

$$w_2 = w_{12} + w_{22} = 222.6 + 55.3 = 277.9 \text{ kJ/kg}$$

If all the velocity coefficients had been equal to $c_v = 0.96$, then, the work would have been

$$w_2 = \frac{(1 + c_v)(1 + c_v^2)^2}{4(2 + c_v + c_v^2)} V_2^2 \sin^2 \alpha_2 = 285.4 \text{ kJ/kg}$$

The total-to-total efficiency is

$$\frac{1}{\eta_{tt}} - 1 = \frac{V_5^2 + \zeta_{R2} W_5^2 + \zeta_S V_4^2 + \zeta_{R1} W_3^2 + \zeta_N V_2^2}{2w_2}$$

With

$$\zeta_N = \frac{1}{c_N^2} - 1 = \frac{1}{0.967^2} - 1 = 0.0694 \quad \zeta_S = \frac{1}{c_S^2} - 1 = \frac{1}{0.954^2} - 1 = 0.0988$$

and

$$\zeta_{R1} = \frac{1}{c_{R1}^2} - 1 = \frac{1}{0.939^2} - 1 = 0.1341 \quad \zeta_{R2} = \frac{1}{c_{R2}^2} - 1 = \frac{1}{0.971^2} - 1 = 0.0606$$

the reciprocal of efficiency is

$$\begin{aligned} \frac{1}{\eta_{tt}} &= 1 + \frac{294.3^2 + 0.0606 \cdot 320.7^2 + 0.0988 \cdot 451.1^2 + 0.1341 \cdot 633.2^2 + 0.0694 \cdot 850^2}{2 \cdot 277890} \\ &= 1.390 \end{aligned}$$

so that $\eta_{tt} = 0.719$. ■

6.3 STAGE WITH ZERO REACTION

A stage design that is closely related to the impulse stage is one with zero reaction. As Eq. (5.24) shows, for such a stage $W_3 = W_2$, and since trothalpy does not change across the rotor, neither does the static enthalpy. If the axial velocity is constant, then the blades need to be equiangular with $\beta_3 = -\beta_2$. The process lines are shown in

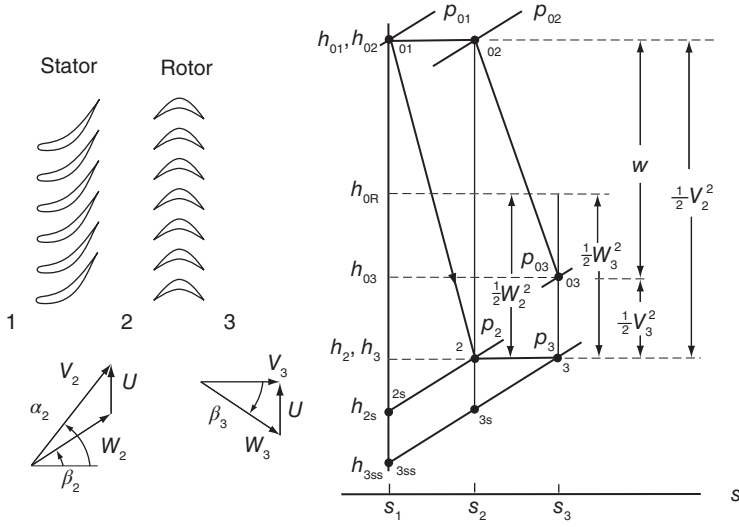


Figure 6.9 Process lines for a turbine with 0% reaction.

Figure 6.9. If the exit kinetic energy is wasted, the stage efficiency is the total-to-static efficiency:

$$\eta_{ts} = \frac{h_{01} - h_{03}}{h_{01} - h_{3ss}}$$

This is now rewritten in the form

$$\frac{1}{\eta_{ts}} - 1 = \frac{h_{03} - h_{3ss}}{h_{01} - h_{03}} = \frac{\frac{1}{2}V_3^2 + h_3 - h_{3ss}}{h_{01} - h_{03}}$$

which can be recast further as

$$\frac{1}{\eta_{ts}} - 1 = \frac{\frac{1}{2}V_3^2 + h_3 - h_{3s} + h_{3s} - h_{3ss}}{h_{01} - h_{03}} = \frac{V_3^2 + \zeta_R W_3^2 + \zeta_N V_2^2}{2w}$$

The work delivered by the stage is

$$w = U(V_{u2} - V_{u3}) = U(W_{u2} - W_{u3}) = 2UW_{u2} = 2U(V_2 \sin \alpha_2 - U)$$

As before, the component equations for velocities are

$$W_3 \cos \beta_3 = V_3 \cos \alpha_3 \quad W_3 \sin \beta_3 + U = V_3 \sin \alpha_2$$

and squaring and adding them gives

$$V_3^2 = W_3^2 + 2UW_3 \sin \beta_3 + U^2$$

Since $W_3 = W_2$ and $\beta_3 = -\beta_2$, this can be written as

$$V_3^2 = W_2^2 - 2UW_2 \sin \beta_2 + U^2$$

Similarly,

$$W_2 \cos \beta_2 = V_2 \cos \alpha_2 \quad W_2 \sin \beta_2 = V_2 \sin \alpha_2 - U$$

which when squared and added give

$$W_2^2 = V_2^2 - 2UV_2 \sin \alpha_2 + U^2$$

When these are included in the expression for efficiency, it takes the form

$$\frac{1}{\eta_{ts}} - 1 = \frac{V_2^2 - 4UV_2 \sin \alpha_2 + 4U^2 + \zeta_R(V_2^2 - 2UV_2 \sin \alpha_2 + U^2) + \zeta_N V_2^2}{4U(V_2 \sin \alpha - U)}$$

This can be written as

$$\eta_{ts} = \frac{1}{1 + f_L}$$

in which, after the substitution $\lambda = U/V_2$ has been made, f_L is given by

$$f_L = \frac{1 - 4\lambda \sin \alpha_2 + 4\lambda^2 + \zeta_R(1 - 2\lambda \sin \alpha_2 + \lambda^2) + \zeta_N}{4\lambda(\sin \alpha_2 - \lambda)}$$

The maximum efficiency is obtained by minimizing the loss f_L . Thus, differentiating f_L with respect to λ and setting it to zero yields

$$\lambda^2 - \frac{2(1 + \zeta_R + \zeta_N)}{\zeta_R \sin \alpha_2} \lambda + \frac{1 + \zeta_R + \zeta_N}{\zeta_R} = 0$$

and the maximum efficiency is at the speed ratio

$$\lambda = \frac{1 + \zeta_R + \zeta_N - \sqrt{(1 + \zeta_R + \zeta_N)(1 + \zeta_R + \zeta_N - \zeta_R \sin^2 \alpha_2)}}{\zeta_R \sin \alpha_2}$$

The efficiency may be written as

$$\eta_{ts} = \frac{4\lambda(\sin \alpha_2 - \lambda)}{1 + \zeta_R(\lambda^2 - 2\lambda \sin \alpha_2 + 1) + \zeta_N}$$

These results are shown as the lower set of curves in Figure 6.10. The efficiencies of a zero reaction stage for various nozzle angles are slightly lower than those for the pressure-compounded impulse stage shown in Figure 6.6. The graphs for a 0% *repeating stage* are also shown. Both are denoted by η_s , which needs to be interpreted appropriately, either as repeating stage or as single stage with kinetic energy wasted.

The efficiency of a repeating stage is obtained from

$$\eta_{tt} = \frac{4\lambda(\sin \alpha_2 - \lambda)}{(\zeta_R - 4)\lambda^2 + (4 - 2\zeta_R)\lambda \sin \alpha_2 + \zeta_R + \zeta_N}$$

with maxima at speed ratios

$$\lambda = \frac{\zeta_R + \zeta_N - \sqrt{(\zeta_R + \zeta_N)(\zeta_R + \zeta_S - \zeta_R \sin^2 \alpha_2)}}{\zeta_R \sin \alpha_2}$$

These are left to be worked out as an exercise.

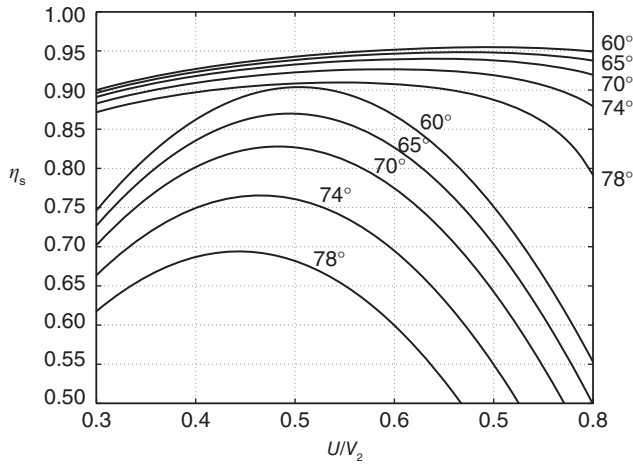


Figure 6.10 Stage efficiencies of single-stage and pressure-compounded zero-reaction turbines with nozzle angles in the range from 60° to 78° with $\zeta_N = 0.02$ and $\zeta_R = 0.14$; the exit kinetic energy is wasted for the set of graphs with lower efficiency, and the family of graphs of higher efficiency are total-to-total efficiencies applicable to a pressure-compounded turbine stage.

6.4 LOSS COEFFICIENTS

A simple correlation for the loss coefficients was developed by Soderberg [86]. In the definition

$$h - h_s = \frac{1}{2} \zeta V^2$$

V replaced by V_2 for the stator and by W_3 for the rotor. The loss coefficients are calculated from

$$\zeta = 0.04 + 0.06 \left(\frac{\varepsilon}{100} \right)^2$$

in which ε is the amount of turning of the flow. For the nozzles, the amount of turning is $\varepsilon_N = \alpha_2 - \alpha_3$, and for the rotor, it is $\varepsilon_R = \beta_2 - \beta_3$. In both expressions, the angles are in degrees. Soderberg's correlation is based on steam turbine designs, which commonly have axial entry into the nozzles, but it gives good results for the flow through the rotor as well, for the loss appears to depend mainly on the deflection of the flow.

■ EXAMPLE 6.4

Steam enters the nozzles of single-stage impulse turbine axially and leaves from the nozzles with speed $V_2 = 555$ m/s at angle $\alpha_2 = 74^\circ$. The blade speed is $U = 260$ m/s. The exit flow angle of the relative velocity from the rotor is $\beta_3 = -65^\circ$. What is the efficiency of the stage if the exit kinetic energy is wasted?

Solution: The tangential and axial velocities at the exit of the nozzles are

$$V_{u2} = V_2 \sin \alpha_2 = 555 \cdot \sin(74^\circ) = 533.5 \text{ m/s}$$

$$V_{x2} = V_2 \cos \alpha_2 = 555 \cdot \cos(74^\circ) = 153.0 \text{ m/s}$$

The components of the relative velocity at this location are

$$W_{u2} = V_{u2} - U = 533.5 - 260 = 273.5 \text{ m/s} \quad W_{x2} = V_{x2} = 153.0 \text{ m/s}$$

Hence,

$$W_2 = \sqrt{W_{x2}^2 + W_{u2}^2} = \sqrt{153.0^2 + 273.5^2} = 313.4 \text{ m/s}$$

and the flow angle of the relative velocity is

$$\beta_2 = \tan^{-1} \left(\frac{W_{u2}}{W_{x2}} \right) = \tan^{-1} \left(\frac{273.5}{153.0} \right) = 60.78^\circ$$

The amount of turning by the nozzles and by the rotor blades are

$$\varepsilon_N = \alpha_2 - \alpha_1 = 74^\circ \quad \varepsilon_R = \beta_2 - \beta_3 = 60.78^\circ + 65^\circ = 125.78^\circ$$

The static enthalpy loss coefficients are

$$\zeta_N = 0.04 + 0.06 \left(\frac{74}{100} \right)^2 = 0.07286 \quad \zeta_R = 0.04 + 0.06 \left(\frac{125.78}{100} \right)^2 = 0.1349$$

and the velocity coefficients are therefore

$$c_N = \frac{1}{\sqrt{1 + \zeta_N}} = 0.9654 \quad c_R = \frac{1}{\sqrt{1 + \zeta_R}} = 0.9387$$

At the exit of the rotor, the relative velocity has the magnitude

$$W_3 = c_R W_2 = 0.9387 \cdot 313.4 = 294.2 \text{ m/s}$$

and its components are

$$W_{u3} = W_3 \sin \beta_3 = 294.2 \sin(-65^\circ) = -266.6 \text{ m/s}$$

$$W_{x3} = W_3 \cos \beta_3 = 294.2 \cos(-65^\circ) = 124.3 \text{ m/s}$$

The components of the absolute velocity at the exit are

$$V_{u3} = U + W_{u3} = 260 - 266.6 = -6.6 \text{ m/s} \quad V_{x3} = W_{x3} = 124.5 \text{ m/s}$$

Hence,

$$V_3 = \sqrt{V_{x3}^2 + V_{u3}^2} = \sqrt{124.3^2 + 6.6^2} = 124.5 \text{ m/s}$$

and the flow angle is

$$\alpha_3 = \tan^{-1} \left(\frac{V_{u3}}{V_{x3}} \right) = \tan^{-1} \left(-\frac{6.6}{124.3} \right) = -3.04^\circ$$

The work delivered by the turbine is

$$w = U(V_{u2} - V_{u3}) = 260(533.5 + 6.60) = 140430 \text{ J/kg}$$

The nozzle efficiency is

$$\eta_N = c_N^2 = 0.9654^2 = 0.9321$$

and the rotor efficiency is

$$\eta_R = \frac{2w}{2w + V_3^2 + \zeta_R W_3^2} = \frac{2 \cdot 140426}{2 \cdot 140426 + 124.5^2 + 0.1349 \cdot 294.2^2} = 0.9118$$

The turbine efficiency is therefore

$$\eta_{ts} = \eta_N \eta_R = 0.9321 \cdot 0.9118 = 0.850$$



EXERCISES

6.1 Steam leaves the nozzle of a turbine with the velocity $V_2 = 1000$ m/s. The flow angle from the nozzle is $\alpha_2 = 70^\circ$, the blade velocity is $U = 360$ m/s, and the mass flow rate is 800 kg/h. The rotor velocity coefficient is $c_R = 0.8$, and the rotor blades are equiangular. Draw the velocity diagrams and determine (a) the flow angle of the relative velocity leaving the rotor, (b) the relative velocity of the steam leaving the rotor blade row, (c) the magnitude of the tangential force on the blades, (d) the magnitude of the axial thrust on the blades, (e) the power developed, and (f) the rotor efficiency. [Ans: (a) 59.46° , (b) 538.5 m/s, (c) 231.9 N, (d) 15.2 N, (e) 83.5 kW, (f) 0.751]

6.2 The diameter of a wheel of a single-stage impulse turbine is 1060 mm and shaft speed, 3000 rpm. The nozzle angle is 72° , and the ratio of the blade speed to the speed at which steam issues from the nozzles is 0.42. The ratio of the relative velocity leaving the blades is 0.84 of that entering the blades. The outlet flow angle of the relative velocity is 3° more than the inlet flow angle. The mass flow rate of steam is 7.23 kg/s. Draw the velocity diagram for the blades and determine (a) the magnitude of the axial thrust on the blades, (b) the magnitude of the tangential force on the blades, (c) power developed by the blade row, and (d) rotor efficiency. [Ans: (a) 209.7 N, (b) 2838 N, (c) 472.5 kW, (d) 0.8317]

6.3 The wheel diameter of a single-stage impulse steam turbine is 400 mm, and the shaft speed is 3000 rpm. The steam issues from nozzles at velocity 275 m/s at the nozzle angle of 70° . The rotor blades are equiangular, and friction reduces the relative velocity as the steam flows through the blade row to 0.86 times the entering velocity. Find the power developed by the wheel when the axial thrust is $F_x = 120$ N. [Ans: 208.3 kW]

6.4 Steam issues from the nozzles of a single-stage impulse turbine with the velocity 400 m/s. The nozzle angle is at 74° . The absolute velocity at the exit is 94 m/s, and its direction is -8.2° . Assuming that the blades are equiangular, find (a) the power developed by the blade row when the steam flow rate is 7.3 kg/s and (b) the rate of irreversible energy conversion per kilogram of steam flowing through the rotor. [Ans: (a) 490 kW, (b) 61.7 kW]

6.5 Carry out the steps in the development of the expression for ratio of the optimum blade speed to the steam velocity for a single-stage impulse turbine with equiangular blades. Note that this expression is independent of the velocity coefficient. Carry out the algebra to obtain the expression for the rotor efficiency at this condition. (a) Find the

numerical value for the velocity ratio when the nozzle angle is 76° . (b) Find the rotor efficiency at this condition, assuming that $c_R = 0.9$. (c) Find the flow angle of the relative velocity entering the blades at the optimum condition. [Ans: (a) 0.485, (b) 0.894, (c) 63.5°]

6.6 Steam flows from a set of nozzles of a single-stage impulse turbine at $\alpha_2 = 78^\circ$ with the velocity $V_2 = 305$ m/s. The blade speed is $U = 146$ m/s. The outlet flow angle of the relative velocity is 3° greater than its inlet angle, and the velocity coefficient is $c_R = 0.84$. The nozzle velocity coefficient is $c_N = 1$. The power delivered by the wheel is 1000 kW. Draw the velocity diagrams at the inlet and outlet of the blades. (a) Find the angle at which the relative velocity leaves the rotor. (b) Calculate the mass flow rate of steam. [Ans: (a) -70.4° , (b) 24.2 kg/s]

6.7 Steam flows from a set of nozzles of a single-stage impulse turbine at an angle $\alpha_2 = 70^\circ$. (a). Find the maximum total-to-static efficiency given velocity coefficients $c_R = 0.83$ and $c_N = 0.98$. (b) If the rotor efficiency is 90% of its maximum value, what are the possible outlet flow angles for the relative velocity. [Ans: (a) 0.808, (b) 43.21° and 61.06°]

6.8 The nozzles of a single-stage impulse turbine have a wall thickness $t = 0.3$ cm and height $b = 15$ cm. The mean diameter of the wheel is 1160 mm, and the nozzle angle is $\alpha_2 = 72^\circ$. The number of nozzles in a ring is 72. The specific volume of steam at the exit of the nozzles is 15.3 m³/kg, and the velocity there is $V_2 = 366$ m/s and the shaft turns at 3000 rpm. (a) Find the mass flow rate of steam through the steam nozzle ring. (b) Find the power developed by the blades of an impulse wheel of equiangular blades, given that the velocity coefficient is $c_R = 0.86$ and $c_N = 1.0$. [Ans: (a) 3.27 kg/s, (b) 183.6 kW]

6.9 The isentropic static enthalpy change across a stage of a single-stage impulse turbine is $\Delta h_s = 22$ kJ/kg. The nozzle exit angle is $\alpha_2 = 74^\circ$. The mean diameter of the wheel is 148 cm, and the shaft turns at 1500 rpm. The blades are equiangular with a velocity coefficient of $c_R = 0.87$. The nozzle velocity coefficient is $c_N = 0.98$. (a) Find the steam velocity at the exit of the nozzles. (b) Find the relative velocity and its flow angle at the exit of the rotor. (c) Find the overall efficiency of the stage. [Ans: (a) 215 m/s, (b) 94.0 m/s and -56.76° , (c) 0.817]

6.10 An impulse turbine has a nozzle angle $\alpha_2 = 72^\circ$ and steam velocity $V_2 = 244$ m/s. The velocity coefficient for the rotor blades is $c_R = 0.85$, and the nozzle efficiency is $\eta_N = 0.92$. The output power generated by the wheel is $\dot{W} = 562$ kW when the mass flow rate is $\dot{m} = 23$ kg/s. Find the total-to-static efficiency of the turbine. [Ans: 0.755]

6.11 A two-row velocity-compounded impulse wheel is part of a steam turbine. The steam velocity from the nozzles is $V_2 = 580$ m/s, and the mean speed of the blades is $U = 116$ m/s. The flow angle leaving the nozzle is $\alpha_2 = 74^\circ$, and the flow angle of the relative velocity leaving the first set of rotor blades is $\beta_3 = -72^\circ$. The absolute velocity of the flow as it leaves the stator vanes between the two rotors is $\alpha_4 = 68^\circ$, and the outlet angle of the relative velocity leaving the second rotor is $\beta_5 = -54^\circ$. The steam flow rate is $\dot{m} = 2.4$ kg/s. The velocity coefficient is $c_v = 0.84$ for both the stator and the rotor row. (a) Find the magnitude of the axial thrust from each wheel. (b) Find the magnitude tangential force on each wheel. (c) Find the total-to-static efficiency of the rotors defined as the work out divided by the kinetic energy available from the nozzles. [Ans: (a) 91.1 and 50.4 N, (b) 1960 and 485 N, (c) 0.703]

6.12 A velocity-compounded impulse wheel has two rows of moving blades with a mean diameter of $D = 72$ cm. The shaft rotates at 3000 rpm. Steam issues from the nozzles at angle $\alpha_2 = 74^\circ$ with velocity $V_2 = 555$ m/s. The mass flow rate is $\dot{m} = 5.1$ kg/s. The energy loss through each of the moving blades is 24% of the kinetic energy entering the blades, based on the relative velocity. Steam leaves the first set of moving blades at $\beta_3 = -72^\circ$, the guide vanes between the rows at $\alpha_4 = 68^\circ$, and the second set of moving blades at $\beta_5 = -52^\circ$. (a) Draw the velocity diagrams, and find the flow angles at the blade inlets both for absolute and relative velocities. (b) Find the power developed by each row of blades. (c) Find the rotor efficiency as a whole. [Ans: (a) $\beta_2 = -70.0^\circ$, $\beta_4 = 51.5^\circ$, $\alpha_3 = -64.9^\circ$, $\alpha_5 = 7.44^\circ$, (b) 456.4 kW and 126.6 kW, (c) 0.742]

6.13 A two wheel velocity compounded steam turbine has the nozzle angle $\alpha_2 = 67^\circ$, and the blade speed is $U = 195$ m/s. The velocity coefficient for the rotors and stator is $c_R = 0.94$. If the exit velocity from the second wheel is axial, what is the inlet velocity to the first wheel. Assume equiangular blades. [Ans: 932 m/s]

6.14 Steam at the state of dry saturated vapor at 8 bar enters from a steam chest, a set of nozzles from which it leaves at angle $\alpha_2 = 74^\circ$ and pressure 0.5 bar. The nozzle coefficient is $c_N = 0.94$, and the blade speed is $U = 470$ m/s. It then flows through an impulse stage with equiangular blades and with the rotor blade coefficient $c_R = 0.90$. (a) Find the specific work delivered by the turbine and the rotor efficiency. Find the (b) the rotor efficiency and the total-to-static stage efficiency. [Ans: (a) $w = 364.3$ kJ/kg, (b) $\eta_R = 0.855$, (c) $\eta_{ts} = 0.804$]

6.15 Consider a repeating 0% reaction stage. By neglecting the temperature factor, show that the approximate form of the total-to-total efficiency is

$$\eta_{tt} = \frac{4\lambda(\sin \alpha_2 - \lambda)}{(\zeta_R - 4)\lambda^2 + (4 - 2\zeta_R)\lambda \sin \alpha_2 + \zeta_R + \zeta_N}$$

and its maximum value is at the condition $\lambda = U/V_2$ given by

$$\lambda = \frac{\zeta_R + \zeta_N - \sqrt{(\zeta_R + \zeta_N)(\zeta_R + \zeta_N - \zeta_R \sin^2 \alpha_2)}}{\zeta_R \sin \alpha_2}$$

6.16 Steam flows from the nozzles of a 0% repeating stage at an angle $\alpha_2 = 69^\circ$ and speed $V_2 = 450$ m/s and enters the rotor with blade speed moving at $U = 200$ m/s. Find (a) its efficiency when the loss coefficients are calculated from Soderberg's correlation and (b) the work delivered by the stage. [Ans: (a) 0.889, (b) 85.82 kJ/kg]

CHAPTER 7

AXIAL TURBINES

In the previous chapter, the impulse stages of steam turbines were analyzed. This chapter extends the development of axial turbine theory to reaction turbines. These include gas turbines and all except the leading stages of steam turbines. The extent of the global steam turbine industry was mentioned in the last chapter. Gas turbine industry is even larger, owing to the use of gas turbine in a jet engine. Gas turbines are also used for electric power generation in central station power plants. In addition, they drive the large pipeline compressors that transmit natural gas across continents and provide power on oil-drilling platforms.

The chapter begins with the development of the working equations for the reaction stages. These relate the flow angles of the absolute and relative velocities to the degree of reaction, flow coefficient, and the blade-loading coefficient. Three-dimensional aspects of the flow are considered next. Then, semiempirical theories are introduced to calculate the static enthalpy rise caused by internal heating, which is then used to develop an expression for the stage efficiency. After this, the equations used to calculate the stagnation pressure losses across the stator and the rotor are developed.

7.1 INTRODUCTION

Two adjacent blades of an axial reaction turbine are shown in Figure 7.1. Their spacing along the periphery of the disk is called the *pitch*. The pitch increases in the radial direction from the *hub* of the rotor to its *casing*. The nominal value of the pitch is at the mean radius.

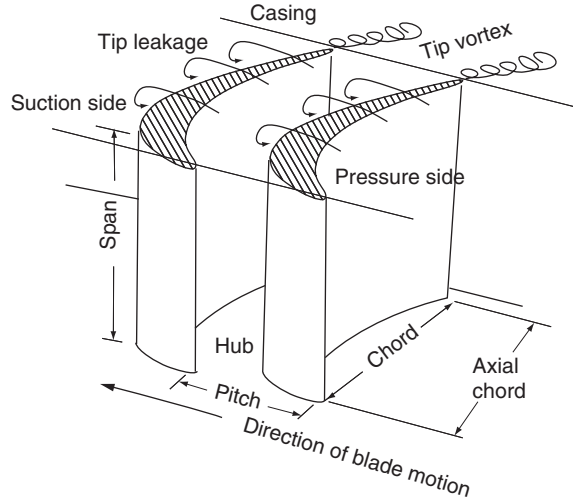


Figure 7.1 Flow channel between two adjacent turbine blades.

The lateral boundaries of the flow channel are along the *pressure* and *suction* sides of the blades and the *endwalls* along the hub and the casing.

The flow is from front to back in Figure 7.1. The blade *chord* is the straight distance from the leading edge of the blade to its trailing edge. Its projection in the axial direction is the *axial chord*. The path of a fluid particle, as it passes through the *blade passage*, is curved and thus, longer than the chord.

The annular region formed from the blade passage areas is called the *flow annulus*. The annulus area is calculated as

$$A = 2\pi r_m(r_c - r_h) = \pi(r_c^2 - r_h^2)$$

if the mean radius r_m is taken as the arithmetic average

$$r_m = \frac{1}{2}(r_c + r_h)$$

of the casing radius r_c and the hub radius r_h . The blade height, or span, is $b = r_c - r_h$ and $2\pi r_m = Zs$, in which Z is the number of blades, and s is the mean pitch or spacing of the blades. Therefore, the annulus area is also $A = Zsb$.

An alternative is to define a mean radius such that the flow area from it to the hub and to the casing are equal. This definition leads to the equality

$$\pi(\bar{r}_m^2 - r_h^2) = \pi(r_c^2 - \bar{r}_m^2)$$

which, when solved for \bar{r}_m , gives

$$\bar{r}_m = \sqrt{\frac{r_c^2 + r_h^2}{2}}$$

In using this root-mean-square (RMS) value of the radius, the annulus area is clearly

$$A = \pi(r_c^2 - r_h^2) = 2\pi(\bar{r}_m^2 - r_h^2) = 2\pi(r_c^2 - \bar{r}_m^2)$$

The distance between the tip of the rotor blade and the casing is called a *tip clearance*. This is kept small in order to prevent *tip leakage flow* in the rotor. Because the tip clearance is small, the distinction between the casing radius and tip radius is usually ignored in the following discussion. The stator blades, as shown in Figure 7.2, are fixed to the casing, and their tips are near the hub of the rotor blades. In many designs, their tips are fastened to a diaphragm that extends inward. At the end of the diaphragm, a labyrinth seal separates it from the rotating shaft. The seal prevents the leakage flow that is caused by the pressure difference across the stator. Since the seal is located close to the shaft, the flow area for the possible leakage flow is small.

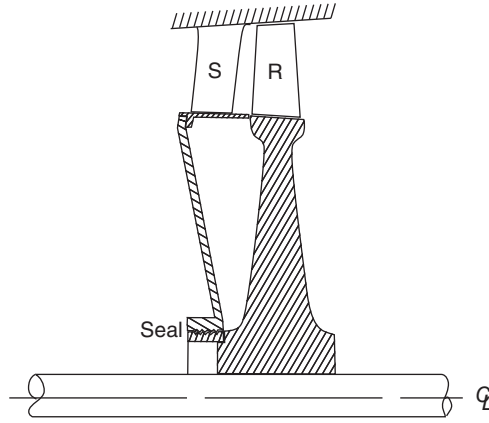


Figure 7.2 A stage of an axial turbine.

Axial turbines are commonly designed such that the axial velocity remains constant, or nearly so. Therefore, as the gas expands through the turbine, the annulus area must increase from stage to stage. This flaring of the annulus is accomplished by changing the hub radius, the casing radius, or both. If both are changed, the mean radius can be kept constant.

7.2 TURBINE STAGE ANALYSIS

Consider a turbine stage as shown schematically in Figure 7.3. It consists of a *stator followed by a rotor*. As in the previous chapter on steam turbines, the inlet to the stage is station 1, and the outlet from the stator is station 2, which is also the inlet to the rotor. The outlet from the rotor, and hence the stage, is station 3. For a *normal stage* in a multistage machine, the magnitude of the velocity at the outlet of the rotor is the same as that at the inlet to the stator. If the flow angles are also the same, the stage is called a *repeating stage*. Pressure, temperature, and density naturally change from stage to stage.

Work delivered by a turbine stage is given by the Euler equation for turbomachinery

$$w = U(V_{u2} - V_{u3}) = U(W_{u2} - W_{u3}) \quad (7.1)$$

For the situation shown in Figure 7.3, the inlet flow angle of the absolute velocity is negative as the flow enters the stator. For the rotor, a *deflection* is the difference in the swirl velocities $V_{u2} - V_{u3} = W_{u2} - W_{u3}$. It is also measured by the amount of turning, $\beta_2 - \beta_3$. The amount of turning across the stator is given by $\alpha_2 - \alpha_1$. Clearly, if a stage is

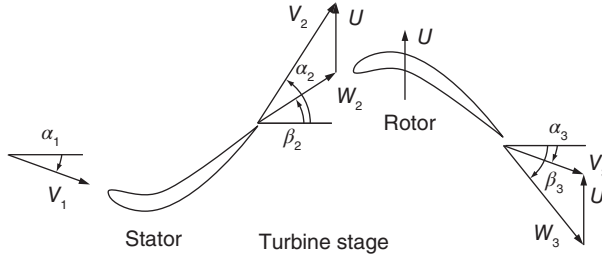


Figure 7.3 Velocity triangles for a turbine stage.

to deliver a large amount of the work, for a given blade velocity, turning across the rotor must be large. A typical value is 70° , and it rarely exceeds 90° . A large deflection also means that the average pressure difference between the pressure and suction sides of a blade must be large. Such blades are said to be *heavily loaded*.

In order to achieve a large amount of turning in the rotor, the stator must also turn the flow, but in the opposite direction. The velocity diagrams in Figure 7.3 show that, as the stator deflects the flow toward the direction of rotation, the stream velocity increases. Since the stagnation enthalpy remains constant across the stator, it follows that

$$h_1 + \frac{1}{2}V_1^2 = h_2 + \frac{1}{2}V_2^2 \quad h_1 - h_2 = \frac{1}{2}(V_2^2 - V_1^2)$$

and the increase in kinetic energy leads to a drop in the static enthalpy. This expression may be written as

$$(u_1 - u_2) + p_1 v_1 - p_2 v_2 = \frac{1}{2}(V_2^2 - V_1^2)$$

It shows that the increase in kinetic energy comes from conversion of internal energy and from the difference in the flow work done in pushing the fluid into and out of the flow passage. This may also be written in a differential form. By considering station 2 to be an arbitrary location, and differentiating, yields

$$-\frac{du}{d\ell} - \frac{d(pv)}{d\ell} = \frac{1}{2} \frac{dV^2}{d\ell} = V \frac{dV}{d\ell}$$

in which $d\ell$ is an element of length along the flow path. This shows that a drop in the internal energy increases the kinetic energy of the flow, as does the net pv work term in this small section of the channel. That both terms have the same sign is clear for an ideal gas, for then $du = c_v dT$ and $d(pv) = R dT$, and since internal energy drops in the flow direction, so does temperature and pv . The ratio of these contributions is

$$\frac{du}{d(pv)} = \frac{1}{\gamma - 1} = 3$$

with the numerical value corresponding to $\gamma = \frac{4}{3}$. Thus, the conversion of internal energy contributes more to the increase in kinetic energy than the flow work.

As the gas passes through the rotor, it is directed back toward the axis, reducing its kinetic energy. The work delivered by the stage is given by

$$w = h_{02} - h_{03} = h_2 - h_3 + \frac{1}{2}(V_2^2 - V_3^2) \quad (7.2)$$

With the reaction defined as the static enthalpy drop across the rotor divided by the static enthalpy drop across the stage, for positive stage reaction, $h_2 > h_3$. An exception to this is an expansion at constant pressure in impulse blades. Equation (7.2) may be written as

$$w = u_2 - u_3 + p_2 v_2 - p_3 v_3 + \frac{1}{2}(V_2^2 - V_3^2) \quad (7.3)$$

and, since each term is expected to be positive, each contributes to the work delivered by the turbine. This is illustrated in the following example.

■ EXAMPLE 7.1

Consider the flow of combustion gases through a repeating turbine stage. The flow angle entering the stator is $\alpha_1 = -14.4^\circ$, and since this is a repeating stage, the flow leaves the rotor at the angle $\alpha_3 = -14.4^\circ$. The ratio of specific heats for the gases is $\gamma = \frac{4}{3}$, and their gas constant is $R = 287 \text{ J/(kg K)}$. The inlet stagnation temperature is $T_{01} = 1200 \text{ K}$. The axial velocity is constant $V_x = 280 \text{ m/s}$, and the flow leaves the stator at angle $\alpha_2 = 57.7^\circ$. The mean radius of the rotor is $r = 17 \text{ cm}$, and the rotor turns at 20000 rpm. (a) Find the work done and the drop in stagnation temperature across the stage. (b) Determine the flow angles of the relative velocity at the inlet and exit of the rotor. (c) Calculate the contribution of internal energy and flow work in increasing the kinetic energy through the stator. (d) Calculate the contributions of internal energy, flow work, and kinetic energy to work delivered by the stage.

Solution: (a, b) The specific heats at constant pressure and volume for the gas are

$$c_p = \frac{\gamma R}{\gamma - 1} = 4 \cdot 287 = 1148 \text{ J/(kg K)}$$

$$c_v = c_p - R = 1148 - 287 = 861 \text{ J/(kg K)}$$

The blade velocity is

$$U = r \Omega = \frac{0.17 \cdot 20000 \cdot \pi}{30} = 356.0 \text{ m/s}$$

The tangential component and the magnitude of the absolute velocity leaving the stator are

$$V_{u2} = V_x \tan \alpha_2 = 280 \tan(57.7^\circ) = 442.9 \text{ m/s}$$

$$V_2 = \sqrt{V_x^2 + V_{u2}^2} = \sqrt{280^2 + 442.9^2} = 524.0 \text{ m/s}$$

The tangential component and the flow angle of the relative velocity at the stator exit are

$$W_{u2} = V_{u2} - U = 442.9 - 356.0 = 86.9 \text{ m/s}$$

$$\beta_2 = \tan^{-1} \left(\frac{W_{u2}}{W_x} \right) = \tan^{-1} \left(\frac{86.9}{280} \right) = 17.2^\circ$$

At the exit of the rotor, the tangential component of the flow velocity is

$$V_{u3} = V_x \tan \alpha_3 = 280 \tan(-14.4^\circ) = -71.9 \text{ m/s}$$

and its speed is

$$V_3 = \sqrt{V_x^2 + V_{u3}^2} = \sqrt{280^2 + 71.9^2} = 289.1 \text{ m/s}$$

The tangential component and the flow angle of the relative velocity there are

$$W_{u3} = V_{u3} - U = -71.9 - 356.0 = -427.9 \text{ m/s}$$

$$\beta_3 = \tan^{-1} \left(\frac{W_{u3}}{W_x} \right) = \tan^{-1} \left(-\frac{427.9}{280} \right) = -56.8^\circ$$

Work delivered by the turbine is

$$w = U(V_{u2} - V_{u3}) = 356.0 (442.9 + 71.9) = 183.3 \text{ kJ/kg}$$

and the stagnation temperature drop across the rotor is

$$\Delta T_0 = \frac{w}{c_p} = \frac{183.3}{1.148} = 159.7 \text{ K}$$

(c) At the inlet to the stator, the static temperature is given by

$$T_1 = T_{01} - \frac{V_1^2}{2c_p} = 1200 - \frac{289.1^2}{2 \cdot 1148} = 1200 - 36.4 = 1163.6 \text{ K}$$

At the exit of the stator, the static temperature is

$$T_2 = T_{02} - \frac{V_2^2}{2c_p} = 1200 - \frac{524.0^2}{2 \cdot 1148} = 1200 - 119.6 = 1080.4 \text{ K}$$

so that

$$u_1 - u_2 = c_v(T_1 - T_2) = 0.861 (1163.6 - 1080.4) = 71.6 \text{ kJ/kg}$$

and

$$p_1 v_1 - p_2 v_2 = R(T_1 - T_2) = 0.287 (1163.6 - 1080.4) = 23.9 \text{ kJ/kg}$$

Increase in the kinetic energy across the stator is

$$\frac{1}{2}(V_2^2 - V_1^2) = \frac{1}{2}(524.0^2 - 289.1^2) = 95.5 \text{ kJ/kg}$$

which also equals the sum of the previous two terms.

(d) Since the stagnation temperature drop across the rotor is $\Delta T_0 = 159.7 \text{ K}$, the stagnation temperature after the rotor is

$$T_{03} = T_{02} - \Delta T_0 = 1200 - 159.7 = 1040.3 \text{ K}$$

and

$$T_3 = T_{03} - \frac{V_3^2}{2c_p} = 1040.3 - \frac{289.1^2}{2 \cdot 1148} = 1040.3 - 36.4 = 1003.9 \text{ K}$$

The contributions to work are

$$u_2 - u_3 = c_v(T_2 - T_3) = 0.861 (1080.4 - 1003.9) = 65.8 \text{ kJ/kg}$$

and

$$p_2 v_2 - p_3 v_3 = R(T_2 - T_3) = 0.287 (1080.4 - 1003.9) = 21.9 \text{ kJ/kg}$$

In a normal stage, the increase in kinetic energy across the stator is equal to its decrease across the rotor. Hence, the decrease in kinetic energy across the rotor is

$$\frac{1}{2}(V_2^2 - V_3^2) = \frac{1}{2}(524.0^2 - 289.1^2) = 95.5 \text{ kJ/kg}$$

The sums of internal energy changes and pv -work, and the change in kinetic energy across the rotor, add up to the work delivered by the stage. ■

7.3 FLOW AND LOADING COEFFICIENTS AND REACTION RATIO

The work delivered by a stage is given by

$$w = U(V_{u2} - V_{u3}) = U(W_{u2} - W_{u3})$$

which, if $V_x = W_x$ is constant across the stage, then, this may be written as

$$w = UV_x(\tan \alpha_2 - \tan \alpha_3) = UV_x(\tan \beta_2 - \tan \beta_3) \quad (7.4)$$

Let $\phi = V_x/U$ denote a *flow coefficient* and $\psi = w/U^2$ a *blade-loading coefficient*. Then, dividing both sides of this equation by U^2 gives the Euler turbine equation in a nondimensional form as

$$\psi = \phi(\tan \alpha_2 - \tan \alpha_3) \quad (7.5)$$

Other names for the blade-loading coefficient are *work coefficient* and *loading factor*. In addition to ψ and ϕ , a third nondimensional quantity of importance in the theory is the *reaction ratio* R , introduced previously. It was defined as the *ratio of the static enthalpy change across the rotor to that across the entire stage*. Hence,

$$R = \frac{h_2 - h_3}{h_1 - h_3} = \frac{h_1 - h_3 - (h_1 - h_2)}{h_1 - h_3} = 1 - \frac{h_1 - h_2}{h_1 - h_3} \quad (7.6)$$

Reaction naturally falls into the range $0 \leq R \leq 1$, but it was seen to be slightly negative for a pure impulse stage. This equation shows that the reaction is zero, if the entire static enthalpy drop takes place in the stator.

Recalling that the stagnation enthalpy of the relative motion, given by Eq. (5.17), remains constant across a rotor in an axial stage, it follows that

$$h_2 + \frac{1}{2}W_2^2 = h_3 + \frac{1}{2}W_3^2$$

or

$$h_2 - h_3 = \frac{1}{2}(W_3^2 - W_2^2)$$

Hence, if $W_2 = W_3$, the reaction is zero. Across the stator, the stagnation enthalpy is constant so that

$$h_1 - h_2 = \frac{1}{2}(V_2^2 - V_1^2)$$

The value of V_1 is smallest for an axial entry, and this equation shows that the static enthalpy drop across the stator increases and reaction decreases for increasing V_2 . In addition, a large deflection of the flow across the stator leads to a large V_2 .

It is useful also to think of R in the incompressible limit, for then in an isentropic flow across the stator, internal energy remains constant, and in the pv -work, only the pressure changes. Thus, pressure changes are directly proportional to changes in static enthalpy. Hence, in this limit, a large reaction means a small pressure drop across the stator and a large decrease in pressure across the rotor.

The reaction may be related to the flow angles by noting first that $V_1^2 = V_{x1}^2 + V_{u1}^2$ and $V_2^2 = V_{x2}^2 + V_{u2}^2$. Then, for constant axial velocity, $V_{x1} = V_{x2}$, the change in enthalpy across the stator may be written as

$$h_1 - h_2 = \frac{1}{2}(V_{u2}^2 - V_{u1}^2) = \frac{1}{2}V_x^2(\tan^2\alpha_2 - \tan^2\alpha_1)$$

For a *normal stage*, $V_1 = V_3$, and therefore, $h_1 - h_3 = h_{01} - h_{03}$. With $w = h_{01} - h_{03}$, Eq. (7.6) for the reaction may be written as

$$R = 1 - \frac{V_x^2}{2} \frac{(\tan^2\alpha_2 - \tan^2\alpha_3)}{\psi U^2}$$

or as

$$R = 1 - \frac{\phi^2}{2\psi}(\tan^2\alpha_2 - \tan^2\alpha_3) \quad (7.7)$$

Substituting ψ from Eq. (7.5) into this gives

$$R = 1 - \frac{1}{2}\phi(\tan\alpha_2 + \tan\alpha_3) \quad (7.8)$$

Next, α_2 is eliminated, again using Eq. (7.5), and the important result

$$\psi = 2(1 - R - \phi \tan\alpha_3) \quad (7.9)$$

is obtained. It shows that a decreasing R increases the loading. A small R means that the pressure drop across the rotor is small, but the large loading is the result of a large deflection. In the stator, the flow leaves at high speed at large angle α_2 . The high kinetic energy obtained this way becomes available for doing work on the rotor blades. The flow is then deflected back toward the axis and beyond to a negative value of α_3 , so that the last term in this equation is positive. Hence, for R fixed, an increase in the absolute value of α_3 , obtained by increasing it in the direction opposite to U , leads to a large deflection and a large value for the blade-loading factor ψ . Thus, a fairly low value of R and high turning gives heavily loaded blades and a compact design.

Equations (7.5) and (7.8) can be written as

$$\tan \alpha_2 - \tan \alpha_3 = \frac{\psi}{\phi} \quad (7.10)$$

$$\tan \alpha_2 + \tan \alpha_3 = \frac{2 - 2R}{\phi} \quad (7.11)$$

when solved for the unknown angles give

$$\tan \alpha_3 = \frac{1 - R - \psi/2}{\phi} \quad \tan \alpha_2 = \frac{1 - R + \psi/2}{\phi} \quad (7.12)$$

Experienced turbomachinery designers choose the flow and loading coefficients and the degree of reaction at the outset and then determine the flow angles from these equations. These are true only for a normal stage. If the axial velocity does not remain constant, the proper equations need to be redeveloped from the fundamental concepts.

Similar expressions are next developed for the flow angles of the relative velocity. The Euler turbine equation may be written as

$$w = U(W_{u2} - W_{u3}) = UV_x(\tan \beta_2 - \tan \beta_3)$$

which after dividing through by U^2 gives

$$\psi = \phi(\tan \beta_2 - \tan \beta_3) \quad (7.13)$$

To arrive at the second equation relating the relative flow angles to the nondimensional parameters, the reaction ratio

$$R = \frac{h_2 - h_3}{h_1 - h_3}$$

is converted into an appropriate form. Since the stagnation enthalpy of the relative motion is constant across the rotor, the relation

$$h_2 - h_3 = \frac{1}{2}W_3^2 - \frac{1}{2}W_2^2$$

follows. Then, since $W_{x2} = W_{x3}$, the term on the right may be rewritten in the form

$$h_2 - h_3 = \frac{1}{2}(W_{x3}^2 + W_{u3}^2 - W_{x2}^2 - W_{u2}^2) = \frac{1}{2}(W_{u3}^2 - W_{u2}^2) = \frac{1}{2}V_x^2(\tan^2 \beta_3 - \tan^2 \beta_2)$$

In addition, for a normal stage, $h_1 - h_3 = h_{01} - h_{03} = w = U^2\psi$. When this and the previous equation are substituted into the definition of reaction ratio, it becomes

$$R = \frac{V_x^2 (\tan^2 \beta_3 - \tan^2 \beta_2)}{2U^2\psi} \quad \text{or} \quad R = \frac{\phi^2}{2\psi}(\tan^2 \beta_3 - \tan^2 \beta_2)$$

Substituting ψ from Eq. (7.13) into this gives

$$R = -\frac{\phi}{2}(\tan \beta_3 + \tan \beta_2)$$

This and Eq. (7.13) written as

$$\tan \beta_2 - \tan \beta_3 = \frac{\psi}{\phi} \quad (7.14)$$

$$\tan \beta_2 + \tan \beta_3 = -\frac{2R}{\phi} \quad (7.15)$$

when solved for the flow angles of the relative velocity give

$$\tan \beta_3 = -\frac{R + \psi/2}{\phi} \quad \tan \beta_2 = -\frac{R - \psi/2}{\phi} \quad (7.16)$$

The flow angles may now be determined if the value of the parameters ϕ , ψ , and R are specified. With four equations and seven variables, any three may be specified, and the other four calculated from them. One such calculation is illustrated in the next example.

■ EXAMPLE 7.2

Combustion gases with $\gamma = \frac{4}{3}$ and $c_p = 1148 \text{ J/(kg K)}$ flow through an axial turbine stage with $\phi = 0.80$ as the design value for the flow coefficient and $\psi = 1.7$ for the blade-loading coefficient. The stage is repeating with flow into the stator at angle $\alpha_1 = -21.2^\circ$. The absolute velocity of the gases leaving the stator is $V_2 = 463 \text{ m/s}$. The inlet stagnation temperature is $T_{01} = 1200 \text{ K}$, and the total-to-total efficiency is 0.89. (a) Find the flow angles for this repeating stage and the amount of turning by the stator and the rotor. (b) Calculate the work delivered by the stage and the drop in the stagnation temperature. (c) Determine the static pressure ratio across the stage.

Solution: (a) With $\alpha_3 = \alpha_1$, solving

$$\psi = 2(1 - R - \phi \tan \alpha_3)$$

for R gives

$$R = 1 - \frac{\psi}{2} - \phi \tan \alpha_3 = 1 - 0.85 - 0.8 \tan(-21.2^\circ) = 0.46$$

The remaining flow angles are

$$\begin{aligned} \tan \alpha_2 &= \frac{1 - R + \psi/2}{\phi} = 1.737 & \alpha_2 &= 60.08^\circ \\ \tan \beta_3 &= \frac{-(R + \psi/2)}{\phi} = -1.638 & \beta_3 &= -58.59^\circ \\ \tan \beta_2 &= \frac{-(R - \psi/2)}{\phi} = 0.487 & \beta_2 &= 25.97^\circ \end{aligned}$$

The amounts of turning by the stator and the rotor are

$$\alpha_2 - \alpha_3 = 81.27^\circ \quad \beta_2 - \beta_3 = 84.57^\circ$$

(b) The axial velocity is

$$V_x = V_2 \cos \alpha_2 = 463 \cos(60.08^\circ) = 231.0 \text{ m/s},$$

and now the inlet and exit velocity to the stage may be determined. It is

$$V_3 = V_1 = \frac{V_x}{\tan \alpha_1} = \frac{231.0}{\cos(-21.2^\circ)} = 247.8 \text{ m/s}$$

The blade speed is

$$U = \frac{V_x}{\phi} = \frac{231.0}{0.8} = 288.7 \text{ m/s}$$

Hence, the work done may be calculated from

$$w = \psi U^2 = 1.7 \cdot 288.7^2 = 141.7 \text{ kJ/kg}$$

and the drop in stagnation temperature is

$$\Delta T_0 = \frac{w}{c_p} = \frac{141.7}{1.148} = 123.4 \text{ K}$$

The isentropic work is obtained by dividing the work w by the stage efficiency, which is the total-to-total efficiency,

$$w_s = \frac{w}{\eta_{tt}} = \frac{141.7}{0.89} = 159.2 \text{ kJ/kg}$$

(c) The static temperature at the inlet is

$$T_1 = T_{01} - \frac{V_1^2}{2c_p} = 1200 - \frac{247.8^2}{2 \cdot 1148} = 1173.3 \text{ K}$$

Neither the static nor the stagnation pressure is known at the inlet, but their ratio can be calculated from

$$\frac{p_1}{p_{01}} = \left(\frac{T_1}{T_{01}} \right)^{\gamma/(\gamma-1)} = \left(\frac{1173.3}{1200} \right)^4 = 0.9139$$

The stagnation temperature at the exit of the stage comes out to be

$$T_{03} = T_{01} - \frac{w}{c_p} = 1200 - \frac{141.7}{1.148} = 1076.6 \text{ K}$$

The static temperature at the exit is

$$T_3 = T_{03} - \frac{V_3^2}{2c_p} = 1076.6 - \frac{247.8^2}{2 \cdot 1148} = 1049.8 \text{ K}$$

This can be used to calculate the ratio of static to stagnation pressure at the exit:

$$\frac{p_3}{p_{03}} = \left(\frac{T_3}{T_{03}} \right)^{\gamma/(\gamma-1)} = \left(\frac{1049.8}{1076.6} \right)^4 = 0.9043$$

The stagnation temperature at the isentropic end state is determined to be

$$T_{03s} = T_{01} - \frac{w_s}{c_p} = 1200 - \frac{159.2}{1.148} = 1061.3 \text{ K}$$

and the stagnation pressure ratio across the stage is therefore

$$\frac{p_{01}}{p_{03}} = \left(\frac{T_{01}}{T_{03s}} \right)^{\gamma/(\gamma-1)} = \left(\frac{1200}{1061.3} \right)^4 = 1.635$$

The ratio of static pressures across the stage can now be determined:

$$\frac{p_1}{p_3} = \frac{p_1}{p_{01}} \frac{p_{01}}{p_{03}} \frac{p_{03}}{p_3} = \frac{0.9138 \cdot 1.635}{0.9043} = 1.652$$

The representative values for an axial turbine stage $\psi = 1.7$, $\phi = 0.8$, and $R = 0.46$ give these values for the stagnation and static pressure ratios and the amount of turning comes out to be about $80\text{--}85^\circ$. In addition, the stagnation temperature drop of $\Delta T_0 = 123.4$ K is representative for a stage. ■

7.3.1 Fifty percent (50%) stage

A 50% reaction stage has equal static enthalpy drops across the stator and the rotor. For such a stage, Eq. (7.9) reduces to

$$\psi = 1 - 2\phi \tan \alpha_3 \quad (7.17)$$

The blades and velocity triangles are shown in Figure 7.4. To achieve a high efficiency, the flow angle at the inlet is kept only slightly negative, but if some of the efficiency is sacrificed to achieve higher performance, the inlet flow angle may reach $\alpha_1 = -45^\circ$. For such a stage, a flow coefficient may have a value of $\phi = 0.75$, which then gives $\psi = 2.5$. Gas turbines for aircraft are designed for high performance and low weight. Hence, the number of stages is kept as low as possible, and materials that withstand high stresses are used for the turbine blades.

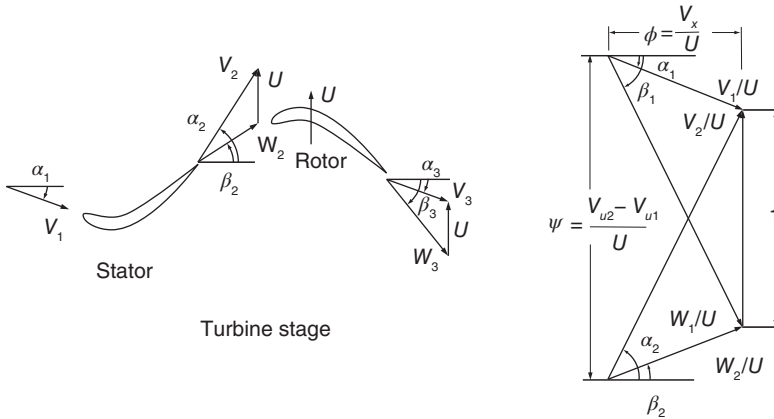


Figure 7.4 Blading for a 50% reaction turbine.

For a 50% reaction stage, Eqs. (7.12) and (7.16) for absolute and relative flow angles reduce to

$$\tan \alpha_3 = \frac{1 - \psi}{2\phi} \quad \tan \alpha_2 = \frac{1 + \psi}{2\phi} \quad (7.18)$$

and

$$\tan \beta_3 = -\frac{1 + \psi}{2\phi} \quad \tan \beta_2 = -\frac{1 - \psi}{2\phi} \quad (7.19)$$

From these, it is seen that

$$\tan \alpha_3 = -\tan \beta_2 \quad \tan \alpha_2 = -\tan \beta_3 \quad (7.20)$$

With their absolute values less than 90° , these equations are satisfied if $\alpha_3 = -\beta_2$ and $\alpha_2 = -\beta_3$. Since $W_x = V_x$, it follows that

$$\begin{aligned} W_3^2 &= W_x^2 + W_{u3}^2 = V_x^2 + W_x^2 \tan^2 \beta_3 \\ &= V_x^2 + V_x^2 \tan^2 \alpha_2 = V_x^2 + V_{u2}^2 = V_2^2 \end{aligned}$$

By a similar argument, it can be shown that $W_2^2 = V_3^2$. Hence,

$$W_3 = V_2 \quad W_2 = V_3$$

A *combined velocity diagram* is shown on the right half of Figure 7.4. It is constructed by drawing the inlet and exit velocity diagrams with U as a base of common length. If all velocities are then divided by U , the diagram is *normalized*, and the base has unity for its length. The blade-loading coefficient ψ can be identified as the vertical distance between the left vertices of the two triangles. For a constant axial velocity, widths of the triangles are the same and in a normalized diagram equal to the flow coefficient ϕ . The results for the angles and velocities show that the velocity triangles for 50% reaction stage are symmetric.

■ EXAMPLE 7.3

Combustion gases, with $\gamma = \frac{4}{3}$ and $R = 287 \text{ J/(kg K)}$, flow through a 50% repeating reaction stage of an axial turbine with the design flow coefficient $\phi = 0.80$ and blade-loading coefficient $\psi = 1.4$. The axial velocity is constant across the stage and equal to $V_x = 220 \text{ m/s}$, and the mass flow rate is $\dot{m} = 15 \text{ kg/s}$. The inlet stagnation temperature is $T_{01} = 1200 \text{ K}$, and pressure is $p_{01} = 400 \text{ kPa}$. The shaft turns at $\Omega = 10000 \text{ rpm}$. Since the stage has 50% reaction, the enthalpy loss coefficients are nearly equal with an estimated value for the stator $\zeta_N = 0.070$, and owing to tip leakage, the loss coefficient for the rotor is estimated to be slightly higher, with the value $\zeta_R = 0.072$. (a) Find the flow angles for a normal stage, and the amount of turning by the stator and the rotor. (b) Find the work delivered by the stage and the drop in the stagnation temperature. (c) Find the flow areas entering the stator and those entering and leaving the rotor. Find also the blade heights for a design with constant mean radius for the stage.

Solution: (a) The blade angles are

$$\tan \alpha_3 = \frac{1 - \psi}{2\phi} = -0.25 \quad \text{so that } \alpha_3 = -14.04^\circ$$

The other angles are

$$\tan \alpha_2 = \frac{1 + \psi}{2\phi} = 1.50 \quad \text{so that } \alpha_2 = 56.31^\circ$$

and

$$\beta_3 = -\alpha_2 = -56.31^\circ \quad \beta_2 = -\alpha_3 = 14.04^\circ$$

The amount turning by the stator and rotor are

$$\alpha_2 - \alpha_3 = 70.35^\circ \quad \beta_2 - \beta_1 = 70.35^\circ$$

(b) The blade speed is

$$U = \frac{V_x}{\phi} = \frac{220}{0.8} = 275.0 \text{ m/s}$$

Hence, the work delivered may be calculated from

$$w = \psi U^2 = 1.40 \cdot 275^2 = 105.9 \text{ kJ/kg}$$

and the drop in stagnation temperature becomes $\Delta T_0 = w/c_p = 92.2 \text{ K}$, since $c_p = 1148 \text{ J/(kg K)}$.

(c) In order to calculate the flow areas, density is needed at each station. At the inlet to stator,

$$V_1 = \frac{V_x}{\cos \alpha_1} = \frac{220}{\cos(-14.04^\circ)} = 226.8 \text{ m/s}$$

For a repeating stage, $V_3 = 226.8 \text{ m/s}$ as well. The static temperature at the inlet to the stator is

$$T_1 = T_{01} - \frac{V_1^2}{2c_p} = 1200 - \frac{226.8^2}{2 \cdot 1148} = 1177.6 \text{ K}$$

and the static pressure is

$$p_1 = p_{01} \left(\frac{T_1}{T_{01}} \right)^{\gamma/(\gamma-1)} = 400 \left(\frac{1177.6}{1200} \right)^4 = 371.0 \text{ kPa}$$

Hence, the density is $\rho_1 = p_1/(RT_1) = 371.0/(0.287 \cdot 1177.6) = 1.10 \text{ kg/m}^3$. The inlet area is therefore

$$A_1 = \frac{\dot{m}}{\rho_1 V_x} = \frac{15}{1.10 \cdot 220} = 0.0621 \text{ m}^2$$

At the entrance to the rotor

$$V_2 = \frac{V_x}{\cos \alpha_2} = \frac{220}{\cos(56.31^\circ)} = 396.6 \text{ m/s}$$

and since $T_{02} = T_{01}$, the static temperature is

$$T_2 = T_{02} - \frac{V_2^2}{2c_p} = 1200 - \frac{396.6^2}{2 \cdot 1148} = 1131.5 \text{ K}$$

The corresponding isentropic state is given by

$$T_{2s} = T_2 - \zeta_s \frac{V_2^2}{2c_p} = 1131.5 - 0.07 \frac{396.6^2}{2 \cdot 1148} = 1126.7 \text{ K}$$

Now, the static pressure is obtained from

$$p_2 = p_{01} \left(\frac{T_{2s}}{T_{01}} \right)^{\gamma/(\gamma-1)} = 400 \left(\frac{1126.7}{1200} \right)^4 = 310.9 \text{ kPa}$$

A schematic diagram of these states can be found by looking ahead to Figure 7.10. The density at the inlet to the rotor is $\rho_2 = p_2/(RT_2) = 310.9/(0.287 \cdot 1131.5) = 0.957 \text{ kg/m}^3$. The corresponding area is

$$A_2 = \frac{\dot{m}}{\rho_2 V_x} = \frac{15}{0.957 \cdot 220} = 0.0712 \text{ m}^2$$

The stagnation temperature after the rotor is given by

$$T_{03} = T_{02} - \frac{w}{c_p} = 1200 - \frac{105.9}{1.148} = 1107.8 \text{ K}$$

and the velocity at this location is

$$V_3 = \frac{V_x}{\cos \alpha_3} = \frac{220}{\cos(-14.04^\circ)} = 226.8 \text{ m/s}$$

Hence, the static temperature is

$$T_3 = T_{03} - \frac{V_3^2}{2c_p} = 1107.8 - \frac{226.8^2}{2 \cdot 1148} = 1085.4 \text{ K}$$

To establish the corresponding isentropic state, the relative velocity at this location is needed. It is given by

$$W_3 = \frac{V_x}{\cos \beta_3} = \frac{220}{\cos(-56.3^\circ)} = 396.6 \text{ m/s}$$

Now, the temperature T_{3s} is obtained from

$$T_{3s} = T_3 - \zeta_R \frac{W_3^2}{2c_p} = 1085.4 - 0.072 \frac{396.6^2}{2 \cdot 1148} = 1080.4 \text{ K}$$

The static pressure after the rotor is then

$$p_3 = p_{02} \left(\frac{T_{3s}}{T_{03}} \right)^{\gamma/(\gamma-1)} = 393.3 - \left(\frac{1080.4}{1107.8} \right)^4 = 258.4 \text{ kPa}$$

and the density is $\rho_3 = p_3/(RT_3) = 258.4/(0.287 \cdot 1085.4) = 0.830 \text{ kg/m}^3$. The flow area after the rotor is thus

$$A_3 = \frac{\dot{m}}{\rho_3 V_x} \frac{15}{0.80 \cdot 220} = 0.0797 \text{ m}^2$$

To find the blade heights, the mean radius is first determined from

$$r_m = \frac{U}{\Omega} = \frac{275 \cdot 30}{10000 \cdot \pi} = 0.263 \text{ m}$$

By denoting the hub to casing ratio by $\kappa = r_h/r_m$, these are calculated from

$$\kappa_1 = \frac{2\pi r_m^2 - A_1}{2\pi r_m^2 + A_1} = 0.749, \quad \kappa_2 = \frac{2\pi r_m^2 - A_2}{2\pi r_m^2 + A_2} = 0.718,$$

$$\kappa_3 = \frac{2\pi r_m^2 - A_3}{2\pi r_m^2 + A_3} = 0.689$$

The blade heights at the inlet to the stator is

$$b_1 = 2r_m \frac{1 - \kappa_1}{1 + \kappa_1} = 0.0753 \text{ m}$$

and at the inlet and exit of the rotor, they are $b_2 = 0.0863 \text{ m}$ and $b_3 = 0.0966 \text{ m}$. The stator blade has therefore the average height $b_S = (b_1 + b_2)/2 = 0.0808 \text{ m}$, and the for the rotor, it is $b_R = (b_2 + b_3)/2 = 0.0915 \text{ m}$. ■

7.3.2 Zero percent (0%) reaction stage

Consider a stage for which $R = 0$. Equation (7.16) then shows that

$$\tan \beta_3 = -\tan \beta_2 \quad \text{or} \quad \beta_3 = -\beta_2$$

Assuming that the axial velocity is constant, it follows from these that $W_2 = W_3$. If the flow angles were to be equal to the blade angles, then the blade would have a symmetric bucket shape, as shown in Figure 7.5. With low reaction, the blades are heavily loaded.

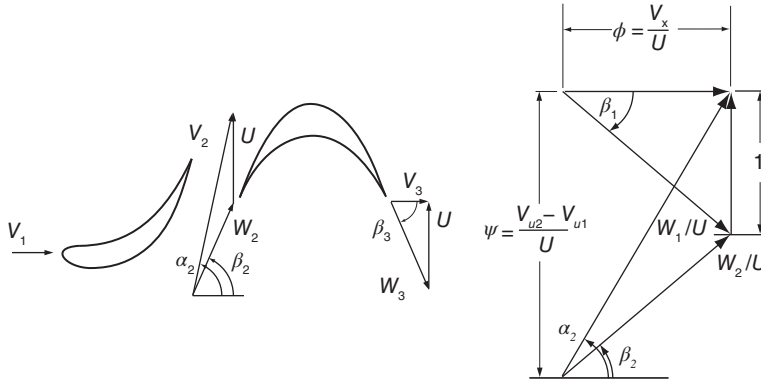


Figure 7.5 Blades for a 0% reaction stage.

This stage reaction and the impulse stage were discussed in Chapter 5 for steam turbines, and the differences between them were shown to be slight. Since the flow enters the nozzles from a steam chest, the inlet to the nozzles is naturally axial, and if most of the pressure drop takes place across the nozzles, the stage reaction is close to zero. Here, the 0% reaction stage is considered as a special case of a stage with an arbitrary reaction.

The normalized velocity diagram for a stage with $\alpha_3 = 0$ is shown on the right-hand side (RHS) of Figure 7.5. For a normal stage with axial entry and with $R = 0$, the relation

$$\psi = 2(1 - R + \phi \tan \alpha_3)$$

reduces to $\psi = 2$. Thus, the line indicating the blade loading is twice as long as blade speed line.

■ EXAMPLE 7.4

A repeating stage with $R = 0$ operates with axial entry. The nozzle turns the flow by 64° . (a) Find the flow coefficient. (b) What is the discharge velocity from the nozzles, if the axial velocity is $V_x = 240$ m/s? (c) Calculate the work delivered by the stage and the drop in the stagnation temperature, given gases with $c_p = 1148$ J/(kg K).

Solution: (a) From

$$\psi = 2(1 - R - \phi \tan \alpha_3)$$

a stage with $R = 0$ and axial entry has $\psi = 2$. Next, solving

$$\tan \alpha_2 = \frac{1 + \psi/2}{\phi}$$

for ϕ , gives

$$\phi = 2 \cot \alpha_2 = 2 \cot(64^\circ) = 0.9755$$

(b) The discharge velocity is

$$V_2 = \frac{V_x}{\cos \alpha_2} = \frac{240}{\cos(64^\circ)} = 547.5 \text{ m/s}$$

(c) The blade speed is

$$U = \frac{V_x}{\phi} = \frac{240}{0.9755} = 246.0 \text{ m/s}$$

and the work delivered and the drop in the stagnation temperature are

$$w = \psi U^2 = 121.1 \text{ kJ/kg} \quad \Delta T_0 = \frac{w}{c_p} = \frac{121.1}{1.148} = 105.5 \text{ K}$$

■

7.3.3 Off-design operation

When a turbine is operated away from its design conditions, the incidence of the flow entering the blades changes, and this will increase the thermodynamic losses in the flow. The angle at which the flow leaves the stator tends not to change, however; nor does the angle of the relative velocity leaving the rotor. By recasting the Euler turbine equation

$$w = U(V_{u2} - V_{u3})$$

in terms of the exit angles gives an equation that shows how the turbine performs under off-design conditions. Replacing the exit velocity by

$$V_{u3} = U + W_{u3}$$

gives

$$w = U(-U - W_{u3} + V_{u2}) = -U^2 + UV_x(\tan \alpha_2 - \tan \beta_3)$$

Dividing though by U^2 yields

$$\psi = -1 + \phi(\tan \alpha_2 - \tan \beta_3) \quad (7.21)$$

The departure angle from the stator α_2 is positive, and the exit angle of the relative velocity β_3 from the rotor is usually negative. Therefore, the term in parentheses is positive. As these angles are close to the metal angles that are set by the design, they are fixed, and the trigonometric terms in Eq. (7.21) tend to remain constant when the machine is operated away from its design condition. Thus, Eq. (7.21) represents an operating line through the design point.

Figure 7.6b shows this operating line. As the flow rate is increased beyond its design value, the flow will eventually choke, and the flow coefficient no longer increases. In Figure 7.6a, the velocity triangles illustrate how the incidence changes as the flow rate decreases. The design condition is denoted by subscript d and off-design, by o. With the exit flow angles held constant, the value of $\psi + 1$ drops in proportion to a drop in ϕ , and as the sketch shows, both α_3 and β_2 decrease in absolute value as the flow coefficient is reduced. This means that incidence of the flow to the vanes and the blades decreases. Although the improper incidence leads to larger losses, these can be reduced by making the leading edges of the blades and vanes well rounded.

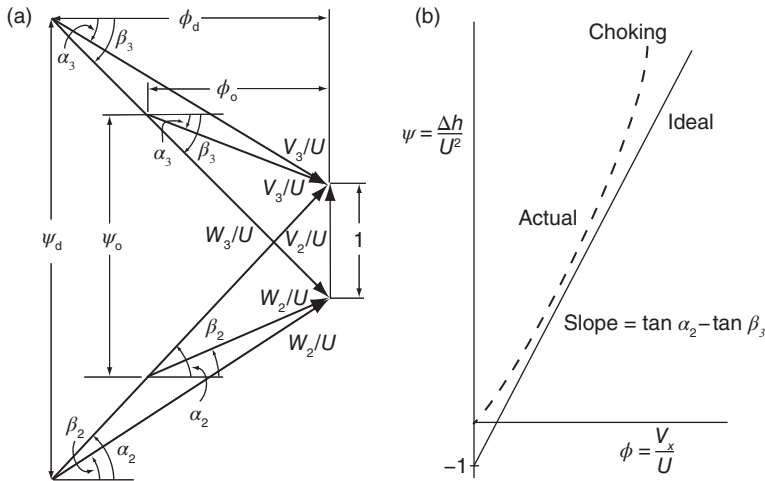


Figure 7.6 (a) Velocity diagrams for off-design performance. (b) A sketch of an ideal and an actual performance characteristic.

EXAMPLE 7.5

In an axial turbine stage, flow leaves the stator at $V_2 = 350$ m/s in the direction $\alpha_2 = 60^\circ$. Its blade-loading coefficient is $\psi = 1.8$, and flow coefficient is $\phi = 0.7$. Assuming that the axial velocity is reduced by 25 m/s from its design condition, find the percent reduction in the reaction.

Solution: The axial velocity at the design condition is

$$V_x = V_2 \cos \alpha_2 = 350 \cos(60^\circ) = 175 \text{ m/s}$$

and the reaction is

$$R = 1 + \frac{\psi}{2} - \phi \tan \alpha_2 = 1 + 0.9 - 0.7 \tan(60^\circ) = 0.688$$

Hence, the angle of the relative flow leaving the rotor is

$$\tan \beta_3 = -\frac{R + \psi/2}{\phi} = -\frac{0.688 + 0.9}{0.7} = -2.2678 \quad \beta_3 = -66.2^\circ$$

Reduction of the axial velocity by 25 m/s gives $V_{xn} = 150 \text{ m/s}$, and with the blade speed constant, the *new* value of flow coefficient is

$$\phi_n = \frac{V_{xn}}{V_x} \phi = \frac{150}{175} 0.7 = 0.6$$

Assuming that the flow angles α_2 and β_3 remain constant, the new value for blade-loading coefficient is

$$\psi_n = -1 + \frac{\phi_n}{\phi}(\psi + 1) = -1 + \frac{0.6}{0.7}(1.8 + 1) = 1.4$$

A new value for reaction is then obtained from the equality

$$\tan \beta_3 = -\frac{R + \psi/2}{\phi} = -\frac{R_n + \psi_n/2}{\phi_n}$$

and it gives

$$R_n = -\frac{\psi_n}{2} + \frac{\phi_n}{\phi} \left(R + \frac{\psi}{2} \right) = -\frac{1.4}{2} + \frac{0.6}{0.7} \left(0.688 + \frac{1.8}{2} \right) = 0.661$$

Hence, the percent reduction for the reaction is $(0.688 - 0.661)/0.688 = 0.039$ or about 4% when the axial velocity is reduced by 14.3%. ■

The values of the flow coefficients in the foregoing examples were chosen to be in their typical range $0.5 < \phi < 1.0$, and the blade-loading coefficients were in the range $1.4 < \psi < 2.2$. The reaction turned out to be generally close to 0.5, except, of course, for the zero-reaction stage. The typical stagnation temperature drop across the rotor is 120–150 K.

7.3.4 Variable axial velocity

Although axial turbines are designed to have constant axial velocity, the development discussed earlier can be generalized to allow the axial velocity to vary across the stage. The definition of a *repeating stage* required the axial velocity to be constant, and the definition that the stage be *normal* requires that $V_1 = V_3$. If the flow coefficient varies,

then the normal stage is still obtained by assuming that $V_3 = V_1$, but except when both are axial, it is no longer possible to have α_1 equal to α_3 . Still, the angle α_1 may be specified independently, and its value does not change the main results of this subsection. The requirement that $V_1 = V_3$ is assumed in the following development, for then the reaction becomes independent of the conditions at the inlet to the stage.

Work delivered by the stage is

$$w = U(V_{x2} \tan \alpha_2 - V_{x3} \tan \alpha_3)$$

and dividing by U^2 gives

$$\psi = \phi_2 \tan \alpha_2 - \phi_3 \tan \alpha_3 \quad (7.22)$$

in which $\phi_2 = V_{x2}/U$ and $\phi_3 = V_{x3}/U$.

From the definition of reaction

$$R = \frac{h_2 - h_3}{h_1 - h_3} = 1 - \frac{h_1 - h_2}{h_1 - h_3} = 1 - \frac{h_{01} - h_{02} - \frac{1}{2}V_1^2 + \frac{1}{2}V_2^2}{h_{01} - h_{03} - \frac{1}{2}V_1^2 - \frac{1}{2}V_3^2}$$

Invoking the assumption that $V_1 = V_3$ and noting that $h_{01} = h_{02}$ and that $w = h_{01} - h_{03}$ reduces this to

$$\begin{aligned} R &= 1 - \frac{V_2^2 - V_3^2}{2w} = 1 - \frac{V_{x2}^2 + V_{u2}^2 - V_{x3}^2 - V_{u3}^2}{2w} \\ &= 1 - \frac{V_{x2}^2(1 + \tan^2 \alpha_2) - V_{x3}^2(1 + \tan^2 \alpha_3)}{2w} \end{aligned}$$

and dividing through by U^2 gives

$$R = 1 - \frac{\phi_2^2(1 + \tan^2 \alpha_2) - \phi_3^2(1 + \tan^2 \alpha_3)}{2\psi}$$

From Eq. (7.22), substituting $\phi_3 \tan \alpha_3 = \phi_2 \tan \alpha_2 - \psi$ into this equation and simplifying gives

$$R = 1 - \frac{\phi_2^2 - \phi_3^2 + 2\psi\phi_2 \tan \alpha_2 - \psi^2}{2\psi}$$

from which

$$\tan \alpha_2 = \frac{2(1 - R)\psi + \psi^2 - (\phi_2^2 - \phi_3^2)}{2\phi_2\psi}$$

Similarly, substituting $\phi_2 \tan \alpha_2 = \phi_3 \tan \alpha_3 + \psi$ into the equation for the reaction gives

$$\tan \alpha_3 = \frac{2(1 - R)\psi - \psi^2 - (\phi_2^2 - \phi_3^2)}{2\phi_3\psi}$$

The development of the relative flow angles follows similarly. The definition

$$R = \frac{h_2 - h_3}{h_1 - h_3}$$

can be recast into a more convenient form by noting that trothalpy is constant across the rotor so that $h_2 - h_3 = \frac{1}{2}(W_3^2 - W_2^2)$ and $V_1 = V_3$. Making use of these and the enthalpy

change across the stage $h_1 - h_3 = h_{01} - h_{03} = w$ to simplify this equation gives

$$R = \frac{W_{x3}^2 + W_{u3}^2 - W_{x2}^2 - W_{u2}^2}{2w} = \frac{V_{x2}^2(1 + \tan^2 \beta_3) - V_{x2}^2(1 + \tan^2 \beta_2)}{2\psi U^2}$$

or

$$R = \frac{\phi_3^2(1 + \tan^2 \beta_3) - \phi_2^2(1 + \tan^2 \beta_2)}{2\psi}$$

The expression for work done may be written as

$$w = U(V_{u2} - V_{u3}) = U(W_{u2} - W_{u3}) = U(V_{x2} \tan \beta_2 - V_{x3} \tan \beta_3)$$

or as

$$\psi = \phi_2 \tan \beta_2 - \phi_3 \tan \beta_3$$

Writing this as $\phi_3 \tan \beta_3 = \phi_2 \tan \beta_2 - \psi$ and substituting it into the expression for reaction and simplifying gives

$$\tan \beta_2 = \frac{-2R\psi + \psi^2 + (\phi_3^2 - \phi_2^2)}{2\phi_2\psi}$$

Similarly,

$$\tan \beta_3 = \frac{-2R\psi - \psi^2 + (\phi_3^2 - \phi_2^2)}{2\phi_3\psi}$$

Now, four parameters are needed to determine the flow angles. If V_1 is not equal to V_3 , then such simple equations no longer can be found.

7.4 THREE-DIMENSIONAL FLOW AND RADIAL EQUILIBRIUM

In the last stages of gas turbines, and certainly for steam turbines that exhaust to below atmospheric pressure, the blades are long in order to accommodate the large volumetric flow rate. Since the blade speed increases with radius, a simple approach is to construct velocity triangles at each element of the blade. As a consequence, the blade loading and reaction may vary considerably along the span of the blade. But this approach does not take into account the pressure variation properly. The aim of this section is to take into account the influence of the pressure increase from the hub to the casing in a flow with a swirl velocity and as a result also of the variation of the reaction and the blade loading along the span of long blades.

Consider a flow in which fluid particles move on cylindrical surfaces. Applying the momentum balance in the radial direction to the control volume shown in Figure 7.7 gives

$$-2V_u \sin\left(\frac{d\theta}{2}\right) \rho V_u dr = pr d\theta - (p + dp)(r + dr)d\theta + 2\left(p + \frac{1}{2}dp\right) dr \sin\left(\frac{d\theta}{2}\right)$$

The left side represents the net rate at which the radial component of momentum leaves the control volume, and the right side is the net pressure force. Viscous terms have been neglected. Noting that $\sin(d\theta/2) \approx d\theta/2$ for small $d\theta$, simplifying, and dropping higher

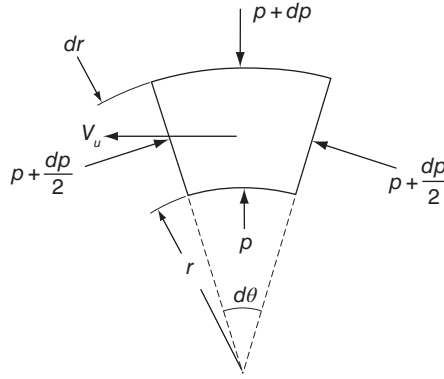


Figure 7.7 Radial equilibrium condition on a fluid element.

order terms reduces this equation to

$$-\frac{1}{\rho} \frac{dp}{dr} + \frac{V_u^2}{r} = 0 \quad (7.23)$$

The first term represents the net pressure force on a fluid particle of unit mass. The second term is the centrifugal force. Since the second term is positive, pressure must increase in the radial direction for this equation to be satisfied. Therefore, if the flow has a swirl component, its pressure must increase from the hub to the casing.

If the radial velocity is small, then, the definition of stagnation enthalpy can be written as

$$h_0 = h + \frac{1}{2}(V_x^2 + V_u^2) \quad (7.24)$$

Differentiating with respect to r gives

$$\frac{dh_0}{dr} = \frac{dh}{dr} + V_x \frac{dV_x}{dr} + V_u \frac{dV_u}{dr} \quad (7.25)$$

The Gibbs equation $Tds = dh - dp/\rho$ may also be written as

$$T \frac{ds}{dr} = \frac{dh}{dr} - \frac{1}{\rho} \frac{dp}{dr} \quad (7.26)$$

and substituting into this dh/dr from Eq. (7.25) and dp/dr from Eq. (7.23) gives

$$\frac{dh_0}{dr} - T \frac{ds}{dr} = V_x \frac{dV_x}{dr} + V_u \frac{dV_u}{dr} + \frac{V_u^2}{r}$$

which may be rewritten as

$$\frac{dh_0}{dr} - T \frac{ds}{dr} = V_x \frac{dV_x}{dr} + \frac{V_u}{r} \frac{d}{dr}(rV_u)$$

If neither h_0 nor s varies with r , then the left side is zero, and this equation reduces to

$$V_x \frac{dV_x}{dr} + \frac{V_u}{r} \frac{d}{dr}(rV_u) = 0 \quad (7.27)$$

For a given radial variation of V_u , the variation of the *axial velocity* with r can be determined by solving this equation.

7.4.1 Free vortex flow

Let the radial variation of the tangential velocity be given by $V_u = K/r$. In this situation, the second term in Eq. (7.27) vanishes, and V_x is independent of the radial coordinate. The work done on the blades by the fluid passing through a streamtube at radial location r of the rotor is given by

$$w = U(V_{u2} - V_{u3}) = \Omega r \left(\frac{K_2}{r} - \frac{K_3}{r} \right) = \Omega(K_2 - K_3)$$

Since this is independent of r , the work done is the same at each radial location. The mean-line analysis that has been used in the previous chapters is thus justified if the tangential velocity has the *free vortex distribution* $V_u = K/r$.

The degree of reaction has been shown to be

$$\begin{aligned} R &= 1 - \frac{1}{2}\phi(\tan \alpha_2 + \tan \alpha_3) = 1 - \frac{1}{2U}(V_x \tan \alpha_2 + V_x \tan \alpha_3) \\ &= 1 - \frac{1}{2U}(V_{u2} + V_{u3}) \end{aligned}$$

or

$$R = 1 - \frac{K_2 + K_3}{2\Omega r^2}$$

Hence, the degree of reaction increases from the hub to the casing. The mass flow rate through the annulus is given by

$$\dot{m} = 2\pi V_x \int_{r_h}^{r_c} \rho r \, dr$$

since V_x does not depend on r . The integration could be carried out were the density variation with the radial position known. It is found by noting first that a free vortex design leads to equal work done on each blade element, and therefore, the stagnation temperature will remain uniform in the annulus. The loss of stagnation pressure takes place in the wake as the flow leaves a blade row. There is also a loss in the endwall boundary layers and in the tip region of the blades. Secondary flow losses are more evenly distributed across the annulus. To make analytical progress, it is assumed that entropy and thus also stagnation pressure are uniform across the flow channel. This can be achieved by good lateral mixing of the flow. Even if such mixing cannot be justified, if this assumption is made, the stagnation density is also uniform. Of course, irreversibilities still cause the stagnation pressure loss in the flow direction. The density ratio may be written as

$$\frac{\rho}{\rho_0} = \left(\frac{T}{T_0} \right)^{1/(\gamma-1)} = \left(\frac{T_0 - V^2/2c_p}{T_0} \right)^{1/(\gamma-1)} = \left(1 - \frac{V^2}{2c_p T_0} \right)^{1/(\gamma-1)}$$

The velocity in this expression is seen to vary with radius according to

$$V^2 = V_x^2 + V_u^2 = V_x^2 + V_{um}^2 \frac{r_m^2}{r^2}$$

Here, r_m is the mean radius, at which the tangential velocity is V_{um} . Defining $y = r/r_m$, the mass balance can be converted to the form

$$\dot{m} = 2\pi V_x r_m^2 \rho_0 \int_{2\kappa/(1+\kappa)}^{2/(1+\kappa)} \left(1 - \frac{V_x^2}{2c_p T_0} - \frac{V_{um}^2}{2c_p T_0} \frac{1}{y^2} \right)^{1/(\gamma-1)} y dy \quad (7.28)$$

in which $r_c/r_m = 2/(1+\kappa)$, $r_h/r_m = 2\kappa/(1+\kappa)$, and $\kappa = r_h/r_c$. This integral can be evaluated in closed form, at least for values of γ for which $1/(\gamma-1)$ is an integer. But, for example, if $\gamma = \frac{4}{3}$, the result of the integration is sufficiently complicated, that it is better to proceed by numerical integration.

Cohen et al. [15] use the mean radius as a reference value and express at the inlet to the rotor the free vortex velocity distribution in the form

$$r_{2m} V_{u2m} = r_2 V_{u2}$$

which can be recast as

$$r_{2m} V_{x2} \tan \alpha_{2m} = r_2 V_{x2} \tan \alpha_2$$

from which it follows that

$$\tan \alpha_2 = \frac{r_{2m}}{r_2} \tan \alpha_{2m} \quad (7.29)$$

Here, r_2 denotes an arbitrary radial position at the inlet of the rotor. Similarly, at the exit,

$$\tan \alpha_3 = \frac{r_{3m}}{r_3} \tan \alpha_{3m} \quad (7.30)$$

The relative velocity at the inlet is $W_{u2} = V_{u2} - U$, from which

$$\tan \beta_2 = \tan \alpha_2 - \frac{U}{V_{x2}}$$

or

$$\tan \beta_2 = \tan \alpha_2 - \frac{r_2}{r_{2m}} \frac{1}{\phi_{2m}} \quad (7.31)$$

Similarly,

$$\tan \beta_3 = \tan \alpha_3 - \frac{r_3}{r_{3m}} \frac{1}{\phi_{3m}} \quad (7.32)$$

These equations are valid even if the axial velocity differs between the inlet and exit of the rotor. When $r_{2m} = r_{3m}$, then $U_{2m} = U_{3m}$, and if the axial velocity is the same at the inlet and outlet of the rotor, then also $\phi_{2m} = \phi_{3m}$.

■ EXAMPLE 7.6

Combustion gases with $\gamma = \frac{4}{3}$ and $R = 287 \text{ J/(kg K)}$ expand through a turbine stage with free vortex blading. The inlet stagnation temperature is $T_{01} = 1100 \text{ K}$, and the stagnation pressure is $p_{01} = 420 \text{ kPa}$. The mean radius is $r_m = 0.17 \text{ m}$. The turbine is flared so that the axial velocity remains constant, and the mean radius is the same at the inlet and outlet of the rotor. The hub-to-casing radius is $\kappa_2 = 0.7$ at

the inlet and $\kappa_3 = 0.65$ at exit of the rotor. The flow angles at the mean radius at the inlet are $\alpha_{2m} = 60.08^\circ$ and $\beta_{2m} = 25.98^\circ$. At the exit, the corresponding angles are $\alpha_{3m} = -21.20^\circ$ and $\beta_{3m} = -58.59^\circ$. The axial velocity is $V_x = 231$ m/s. (a) Plot the inlet and exit flow angles along the span of the blades. (b) Determine the reaction at the hub. (c) Calculate the mass flow rate using both numerical integration and the mean density.

Solution: (a) The reaction at the mean radius of this stage can be obtained by adding both parts of Eq. (7.16) together and doing the same for Eq. (7.12) and then dividing one by the other. This gives

$$1 - \frac{1}{R_m} = \frac{\tan \alpha_{2m} + \tan \alpha_{3m}}{\tan \beta_{2m} + \tan \beta_{3m}}$$

Substituting the values of the angles gives $R_m = 0.460$. The flow coefficient is then obtained from

$$\phi_m = \frac{1}{\tan \alpha_{2m} - \tan \beta_{2m}} = 0.800$$

and the blade-loading coefficient is

$$\psi_m = 2(1 - R_m - \phi_m \tan \alpha_{3m}) = 1.700$$

The flow angles are next calculated using Eqs. (7.29)–(7.32). At the hub,

$$\tan \alpha_{2h} = \frac{1 + \kappa_2}{2\kappa_2} \tan \alpha_{2m} = \frac{1.7}{1.4} \tan(60.08^\circ) = 2.11 \quad \alpha_{2h} = 64.64^\circ$$

$$\tan \beta_{2h} = \frac{1 + \kappa_2}{2\kappa_2} \tan \alpha_{2m} - \frac{2\kappa_2}{1 + \kappa_2} \frac{1}{\phi_m} = 1.08 \quad \beta_{2h} = 47.22^\circ$$

At the casing,

$$\tan \alpha_{2c} = \frac{1 + \kappa_2}{2} \tan \alpha_{2m} = \frac{1.7}{2} \tan(60.08^\circ) = 1.48 \quad \alpha_{2c} = 55.90^\circ$$

$$\tan \beta_{2c} = \frac{1 + \kappa_2}{2} \tan \alpha_{2m} - \frac{2}{1 + \kappa_2} \frac{1}{\phi_m} = 0.0064 \quad \beta_{2c} = 0.37^\circ$$

The exit angles are calculated similarly. They are

$$\alpha_{3h} = -26.21^\circ \quad \beta_{3h} = -55.90^\circ \quad \alpha_{3c} = -17.74^\circ \quad \beta_{3c} = -61.41^\circ$$

The variation in flow angles along the span is obtained from Eqs. (7.29)–(7.32), which, together with the blade shapes, are shown in Figure 7.8.

(b) The reaction at the hub at the inlet to the rotor is

$$R_{2h} = 1 - (1 - R_m) \left(\frac{1 + \kappa_2}{2\kappa_2} \right)^2 = 1 - 0.54 \left(\frac{1.7}{1.4} \right)^2 = 0.2038$$

(c) The mass flow rate is calculated from Eq. (7.28). The stagnation density is

$$\rho_{01} = \frac{p_{01}}{RT_{01}} = \frac{420000}{287 \cdot 1100} = 1.330 \text{ kg/m}^3$$

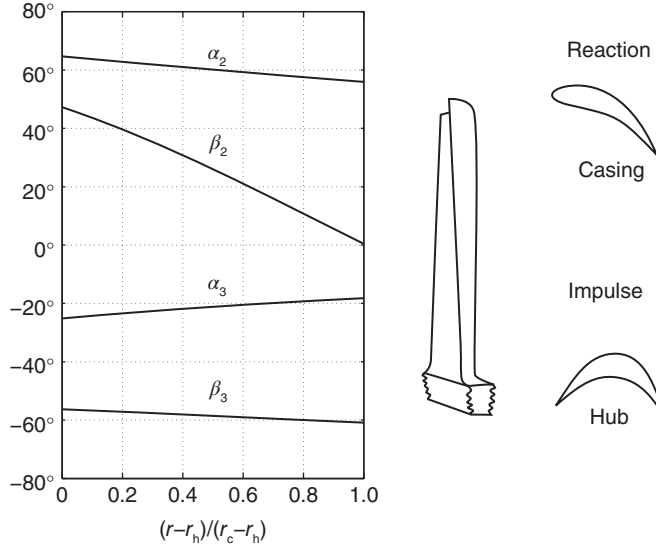


Figure 7.8 Variation of flow angles along the span for a gas with $\gamma = 1.4$.

With hub radius $r_h = 0.14$ m, and casing radius, $r_c = 0.20$ m, numerical integration of Eq. (7.28) gives

$$\dot{m} = 15.068 \text{ kg/s}$$

Cohen et al. [15] suggested that a very good approximation may be obtained by ignoring the density variation along the span and using its value at the mean radius. Since

$$V_{u2m} = V_x \tan \alpha_{2m} = 231 \tan(60.08^\circ) = 401.40 \text{ m/s}$$

the mean temperature is

$$T_{2m} = T_{02} - \frac{V_x^2 + V_{u2m}^2}{2c_p} = 1100 - \frac{231^2 + 401.4^2}{2 \cdot 1148} = 1006.6 \text{ K}$$

Hence,

$$\rho_{2m} = \rho_{02} \left(\frac{T_{2m}}{T_{02}} \right)^{1/(\gamma-1)} = 1.33 \left(\frac{1006.6}{1100} \right)^3 = 1.019 \text{ kg/m}^3$$

The flow rate is then

$$\begin{aligned} \dot{m} &= \pi(r_c^2 - r_h^2)\rho_{2m}V_x = 2\pi r_m(r_c - r_h)\rho_{2m}V_x \\ &= 2\pi \cdot 0.17 \cdot 0.06 \cdot 1.019 \cdot 231 = 15.086 \text{ kg/s} \end{aligned}$$

The approximation of using the density at the mean radius is seen to be excellent. ■

7.4.2 Fixed blade angle

A design with a free vortex tangential velocity distribution has the attractive feature that each blade element delivers the same amount of work and that the axial velocity remains constant. On the other hand, the reaction varies quite strongly along the span of the blade. Other design possibilities exist. For example, if the nozzle angle is kept constant along the span, manufacturing cost of nozzles can be reduced. As the flow moves through the nozzles, its stagnation enthalpy will not change, and, if the radial entropy gradients may be neglected, the equation for radial equilibrium

$$\frac{dh_0}{dr} - T \frac{ds}{dr} = V_x \frac{dV_x}{dr} + V_u \frac{dV_u}{dr} + \frac{V_u^2}{r}$$

reduces to

$$V_x \frac{dV_x}{dr} + V_u \frac{dV_u}{dr} + \frac{V_u^2}{r} = 0$$

as before. This can also be written as

$$\frac{d}{dr} \left(\frac{1}{2} V_x^2 + \frac{1}{2} V_u^2 \right) + \frac{V_u^2}{r} = 0$$

Since $V_u = V \sin \alpha$ and $V_x^2 + V_u^2 = V^2$, this becomes

$$V \frac{dV}{dr} + \frac{V^2 \sin^2 \alpha}{r} = 0$$

or

$$\frac{dV}{V} = -\sin^2 \alpha \frac{dr}{r} \quad (7.33)$$

If the angle α is constant, integrating gives

$$\frac{V(r)}{V_m} = \left(\frac{r_m}{r} \right)^{\sin^2 \alpha}$$

In addition, $V_u = V \sin \alpha$ and $V_x = V \cos \alpha$, so that for constant α

$$r^{\sin^2 \alpha} V_u = r_m^{\sin^2 \alpha} V_{um}$$

For nozzles, the exit flow angle is quite large (often between 60° and 70°). Therefore, $\sin^2 \alpha_2$ is in the range 0.75–0.88, and the velocity distribution is nearly the same as for a free vortex. The rotor blades may then be twisted properly to give the free vortex distribution at their exit.

7.4.3 Constant mass flux

It has been seen that, if the tangential velocity varies inversely with radius, axial velocity is independent of radius. Since the density also varies, Horlock [42] suggested that a designer

might decide to hold the axial *mass flux* ρV_x constant. This requires the blade angle to vary in such a way that

$$\rho V \cos \alpha = \rho_m V_m \cos \alpha_m$$

remains independent of radius. The flow angle in terms of the velocity and density ratios is therefore

$$\frac{\cos \alpha}{\cos \alpha_m} = \frac{V_m \rho_m}{V \rho} \quad (7.34)$$

From the definition of stagnation temperature,

$$T_0 = T \left(1 + \frac{\gamma - 1}{2} M^2 \right) = T_m \left(1 + \frac{\gamma - 1}{2} M_m^2 \right)$$

the ratio of the static temperature to its value at the mean radius is

$$\frac{T}{T_m} = \frac{2 + (\gamma - 1) M_m^2}{2 + (\gamma - 1) M^2} \quad (7.35)$$

It then follows that

$$\frac{\rho}{\rho_m} = \left(\frac{2 + (\gamma - 1) M_m^2}{2 + (\gamma - 1) M^2} \right)^{1/(\gamma - 1)} \quad (7.36)$$

and

$$\frac{p}{p_m} = \left(\frac{2 + (\gamma - 1) M_m^2}{2 + (\gamma - 1) M^2} \right)^{\gamma/(\gamma - 1)} \quad (7.37)$$

The velocity ratio is obtained from the definition of Mach number:

$$\frac{V}{V_m} = \frac{M}{M_m} \sqrt{\frac{T}{T_m}} = \frac{M}{M_m} \left(\frac{2 + (\gamma - 1) M_m^2}{2 + (\gamma - 1) M^2} \right)^{1/2} \quad (7.38)$$

The ratio of cosines of the flow angles can now be written as

$$\frac{\cos \alpha}{\cos \alpha_m} = \frac{M_m}{M} \left(\frac{2 + (\gamma - 1) M^2}{2 + (\gamma - 1) M_m^2} \right)^{(\gamma + 1)/2(\gamma - 1)} \quad (7.39)$$

From the equation for radial equilibrium, it follows that

$$\frac{dV}{V} = -\sin^2 \alpha \frac{dr}{r} = (\cos^2 \alpha - 1) \frac{dr}{r}$$

and by logarithmically differentiating Eq. (7.38) yields the equation

$$\frac{dM^2}{M^2[2 + (\gamma - 1) M^2]} = (\cos^2 \alpha - 1) \frac{dr}{r} \quad (7.40)$$

Dividing through by $\cos^2 \alpha - 1$ and integrating both sides gives

$$I = \int_{M_h}^{M_c} \frac{2dM}{M[2 + (\gamma - 1) M^2](\cos^2 \alpha - 1)} = \ln \frac{r_c}{r_h} = \ln \frac{1}{\kappa} \quad (7.41)$$

so that

$$\kappa = e^{-I}$$

Since the highest Mach number is at the hub, the way to proceed is to set it at an acceptable value. This may be slightly supersonic. Then, if the flow angle and Mach number are known at the average radius, Eq. (7.39) can be used to find the value of α_h . After that Eq. (7.39) is rewritten as

$$\frac{\cos \alpha}{\cos \alpha_h} = \frac{M_h}{M} \left(\frac{2 + (\gamma - 1)M^2}{2 + (\gamma - 1)M_h^2} \right)^{(\gamma+1)/2(\gamma-1)} \quad (7.42)$$

and this is substituted for $\cos \alpha$ in the integrand of Eq. (7.41). Finally, by trial, the value of M_c needs to be chosen so that the numerical integration gives the desired radius ratio κ . For a flow at the exit of the nozzle, the stagnation temperature is known, and with the mean Mach number known, the mean temperature T_m can be determined. After that, the other ratios are calculated from Eqs. (7.35)–(7.38).

To obtain the radial locations that correspond to the calculated values of the thermodynamic properties, Eq. (7.40) is written as

$$\frac{2dM}{M[2 + (\gamma - 1)M^2](\cos^2 \alpha - 1)} = \frac{dr}{r} \quad (7.43)$$

and this is solved numerically using a fine grid.

Results from a sample calculation for $M_h = 1.15$ are shown in Figure 7.9. Panel (a) shows the variation of the thermodynamic variables, normalized with respect to their values

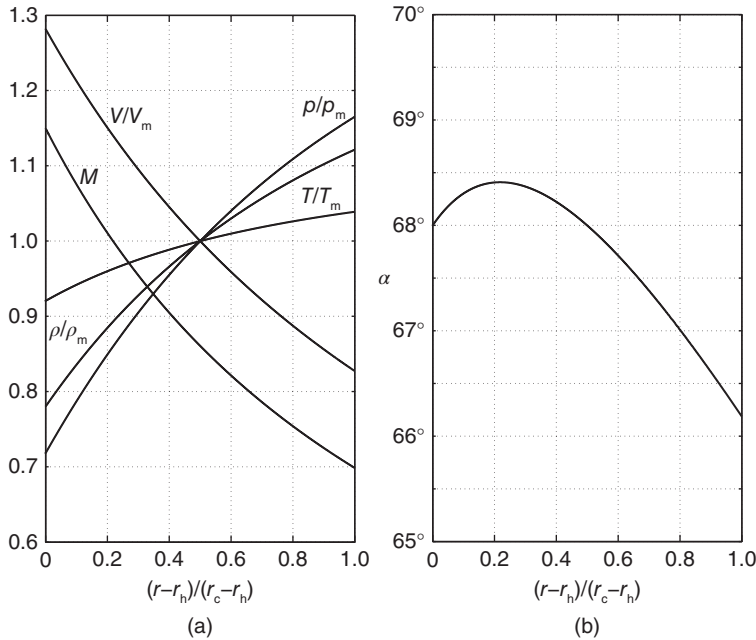


Figure 7.9 (a) Temperature, density, pressure, and velocity along the span for a gas with $\gamma = 1.4$ and (b) flow angle leaving a nozzle as a function of the radial location.

at the mean radius. Since the flow resembles a free vortex type, the largest velocity is at the hub. The temperature there has the smallest value, since the stagnation temperature is constant across the span. Hence, the Mach number is largest at the hub and drops to a value $M_c = 0.6985$ at the casing for a flow with radius ratio $\kappa = 0.6$. Four significant figures were used to make sure that κ was also accurate to the same number of significant figures. Radial equilibrium theory shows that pressure increases from the hub to the casing in a flow with a swirl component of velocity. The density follows the ideal gas law, and it increases from the hub to the casing. The flow angles are shown in Figure 7.9b. The value at the mean radius was set at $\alpha_m = 68^\circ$, and its value at the hub happens to come out to be the same. At the casing, the flow angle drops to $\alpha_c = 66.18^\circ$, and the entire variation is seen to be quite slight.

7.5 TURBINE EFFICIENCY AND LOSSES

Three methods are in common use for the calculation of losses in axial turbines. The correlation by Soderberg was introduced in Chapter 6. The other two methods are based on the original work of Ainley and Mathieson [3] and the studies of Craig and Cox [16]. The former is discussed in the following; the latter is presented by Wilson and Korakianitis [97] in their text on gas turbines. In this section, analytical results are developed that relate the stage efficiency to the flow parameters. They enable the calculation of efficiency contours by methods introduced by Hawthorne [40] and Smith [84], and further developed by Lewis [57]. Horlock [42] gives a comprehensive review of the early work.

7.5.1 Soderberg loss coefficients

The loss correlation of Soderberg makes use of the static enthalpy loss coefficient

$$\zeta = \frac{h - h_s}{\frac{1}{2}V^2}$$

with V replaced by V_2 for the stator and by W_3 for the rotor, and enthalpy h is similarly identified. The nominal value of the loss coefficient is calculated from

$$\zeta^* = 0.04 + 0.06 \left(\frac{\varepsilon}{100} \right)^2$$

in which ε is the amount of turning, $\varepsilon_S = \alpha_2 - \alpha_3$ for the stator and $\varepsilon_R = \beta_2 - \beta_3$ for the rotor. The angles are in degrees. The nominal value, identified with superscript star, is for a blade height-to-axial chord ratio $b/c_x = 3.0$ and Reynolds number equal to 10^5 . For different values of blade height to axial-chord-ratio, a new value for stator vanes is calculated from

$$\bar{\zeta} = (1 + \zeta^*) \left(0.993 + 0.021 \frac{c_x}{b} \right) - 1$$

and for the rotor, from

$$\bar{\zeta} = (1 + \zeta^*) \left(0.975 + 0.075 \frac{c_x}{b} \right) - 1$$

If Reynolds number differs from 10^5 , then the Reynolds number correction is obtained from

$$\zeta = \left(\frac{10^5}{Re} \right)^{1/4} \bar{\zeta}$$

The Reynolds number is based on the hydraulic diameter, which is given approximately by the expression

$$D_h = \frac{2sb \cos \alpha_2}{s \cos \alpha_2 + b}$$

for the stator and by

$$D_h = \frac{2sb \cos \beta_3}{s \cos \beta_3 + b}$$

for the rotor.

7.5.2 Stage efficiency

The process lines for a turbine stage are shown in Figure 7.10. The states of static enthalpy are drawn such that the enthalpy drop across the rotor is slightly larger than that across the stator. The reaction therefore is slightly larger than one-half. An isentropic expansion through the stator takes the process from state 1 to state 2s, whereas the actual end state is at state 2. The stagnation enthalpy remains constant through the stator, and its process line is horizontal. The stagnation pressure in the interblade gap is denoted by p_{02} .

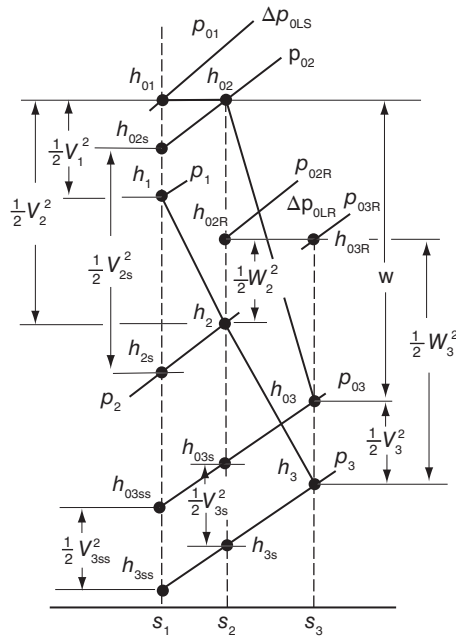


Figure 7.10 Thermodynamic states for expansion across a turbine stage.

The irreversible expansion across the rotor takes the process to state 3, with a corresponding stagnation enthalpy h_{03} and stagnation pressure p_{03} . The loss of stagnation pressure is discussed in the next subsection. The losses can be related to efficiency by first writing (as was done for steam turbines) the efficiency as

$$\eta_{tt} = \frac{h_{01} - h_{03}}{h_{01} - h_{03ss}}$$

and then manipulating it into the form

$$\frac{1}{\eta_{tt}} - 1 = \frac{h_{03} - h_{03ss}}{h_{01} - h_{03}} = \frac{h_3 - h_{3ss}}{w} + \frac{V_3^2 - V_{3ss}^2}{2w}$$

This can be further rearranged as

$$\frac{1}{\eta_{tt}} - 1 = \frac{(h_3 - h_{3s}) + (h_{3s} - h_{3ss})}{w} + \left(1 - \frac{V_{3ss}^2}{V_3^2}\right) \frac{V_3^2}{2w}$$

The first term in the numerator is simply

$$h_3 - h_{3s} = \frac{1}{2} \zeta_R W_3^2$$

Next, integrating the Gibbs equation along the constant-pressure line p_3 from state 3ss to 3s gives

$$s_2 - s_1 = c_p \ln \frac{T_{3s}}{T_{3ss}}$$

Similarly, integration along the constant pressure line p_2 yields

$$s_2 - s_1 = c_p \ln \frac{T_2}{T_{2s}}$$

Equating the RHSs gives

$$\frac{T_{3s}}{T_{3ss}} = \frac{T_2}{T_{2s}} \quad (7.44)$$

Subtracting one from each side, rearranging, and multiplying by c_p gives

$$h_{3s} - h_{3ss} = \frac{T_{3ss}}{T_{2s}} (h_2 - h_{2s})$$

Since $T_{3ss}/T_{2s} = T_{3s}/T_2$ and

$$h_2 - h_{2s} = \frac{1}{2} \zeta_S V_2^2$$

the expression for efficiency can be written as

$$\frac{1}{\eta_{tt}} - 1 = \frac{1}{2w} \left[\zeta_R W_3^2 + \frac{T_{3ss}}{T_2} \zeta_S V_2^2 + \left(1 - \frac{T_{3ss}}{T_3}\right) V_3^2 \right]$$

In the last term, the equality $V_{3ss}^2/V_3^2 = T_{3ss}/T_3$ was used, which follows from the fact that $M_3 = M_{3ss}$, as was shown in Chapter 6. Furthermore, since $V_x = W_3 \cos \beta_3 = V_2 \cos \alpha_2 = V_3 \cos \alpha_3$, the expression for efficiency can be recast as

$$\frac{1}{\eta_{tt}} - 1 = \frac{\phi^2}{2\psi} \left[\frac{\zeta_R}{\cos^2 \beta_3} + \frac{T_{3s}}{T_2} \frac{\zeta_S}{\cos^2 \alpha_2} + \left(1 - \frac{T_{3ss}}{T_3}\right) \frac{1}{\cos^2 \alpha_3} \right] \quad (7.45)$$

Often, this is approximated by

$$\frac{1}{\eta_{tt}} - 1 = \frac{\phi^2}{2\psi} \left(\frac{\zeta_R}{\cos^2 \beta_3} + \frac{\zeta_S}{\cos^2 \alpha_2} \right) \quad (7.46)$$

It will be shown in an example that the error in using this approximation is very small.

7.5.3 Stagnation pressure losses

The stagnation pressure drop across the stator can be related to the static enthalpy loss coefficient by first integrating the Gibbs equation along the constant-stagnation-enthalpy line $h_{01} = h_{02}$:

$$s_2 - s_1 = R \ln \left(\frac{p_{01}}{p_{02}} \right)$$

Similarly, integrating the Gibbs equation along the constant-pressure line p_2 gives

$$s_2 - s_1 = \frac{\gamma R}{\gamma - 1} \ln \left(\frac{T_2}{T_{2s}} \right)$$

Equating the RHSs gives

$$\frac{p_{01}}{p_{02}} = \left(\frac{T_2}{T_{2s}} \right)^{\gamma/(\gamma-1)}$$

The definition for the static enthalpy loss coefficient

$$h_2 - h_{2s} = \frac{1}{2} \zeta_S V_2^2$$

can be written as

$$T_2 - T_{2s} = \frac{\gamma - 1}{2\gamma R} \zeta_S M_2^2 \gamma R T_2$$

from which

$$\frac{T_2}{T_{2s}} = \left(1 - \frac{\gamma - 1}{2} \zeta_S M_2^2 \right)^{-1}$$

Since the second term involving the Mach number is small, this can be expanded as

$$\frac{T_2}{T_{2s}} = 1 + \frac{\gamma - 1}{2} \zeta_S M_2^2$$

The pressure ratio p_{01}/p_{02} is therefore

$$\frac{p_{01}}{p_{02}} = \left(1 + \frac{\gamma - 1}{2} \zeta_S M_2^2 \right)^{\gamma/(\gamma-1)}$$

and expanding this for small values of $\zeta_S M^2$ gives

$$\frac{p_{01}}{p_{02}} = 1 + \frac{\gamma}{2} \zeta_S M_2^2$$

The expression for the stagnation pressure loss now takes the form

$$\Delta p_{0LS} = \frac{\gamma}{2} p_{02} \zeta_S M_2^2 = \frac{1}{2} \frac{T_{02}}{T_2} \rho_{02} \zeta_S V_2^2$$

or

$$\Delta p_{0LS} = \rho_{02} \left(1 + \frac{\gamma - 1}{2} M_2^2 \right) \frac{1}{2} \zeta_S V_2^2 \quad (7.47)$$

Since the loss coefficient ζ_S is rather insensitive to Mach number, this shows how the stagnation pressure loss increases as compressibility becomes important.

The development of the stagnation pressure loss across the rotor is similar. It will be carried out in detail in order to highlight the use of stagnation properties on the basis of relative velocity. First, the stagnation enthalpy of relative motion is defined as

$$h_{03R} = h_3 + \frac{1}{2} W_3^2$$

and in using the Mach number in terms of W_3 , defined as

$$M_{3R} = \frac{W_3}{\sqrt{\gamma R T_3}}$$

this can be rewritten in the form

$$\frac{T_{03R}}{T_3} = 1 + \frac{\gamma - 1}{2} M_{3R}^2$$

The relative stagnation pressure is calculated from

$$\frac{p_{03R}}{p_3} = \left(1 + \frac{\gamma - 1}{2} M_{3R}^2 \right)^{\gamma/(\gamma-1)}$$

Since $h_{02R} = h_{03R}$ across the rotor, integrating the Gibbs equation along the line of constant relative stagnation enthalpy and also along the constant-pressure line p_3 gives

$$s_3 - s_2 = R \ln \frac{p_{02R}}{p_{03R}} \quad s_3 - s_2 = c_p \ln \frac{T_3}{T_{3s}}$$

so that

$$\frac{p_{02R}}{p_{03R}} = \left(\frac{T_3}{T_{3s}} \right)^{\gamma/(\gamma-1)}$$

From the definition for static enthalpy loss coefficient for the rotor

$$h_3 - h_{3s} = \frac{1}{2} \zeta_R W_3^2$$

the temperature ratio

$$\frac{T_3}{T_{3s}} = \left(1 - \frac{\gamma - 1}{2} \zeta_R M_{3R}^2\right)^{-1}$$

is obtained. Noting again that the term involving the Mach number is small and expanding the RHS gives

$$\frac{T_3}{T_{3s}} = 1 + \frac{\gamma - 1}{2} \zeta_R M_{3R}^2$$

and the pressure ratio p_{02R}/p_{03R} is therefore

$$\frac{p_{02R}}{p_{03R}} = \left(1 + \frac{\gamma - 1}{2} \zeta_R M_{3R}^2\right)^{\gamma/(\gamma-1)}$$

Expanding this gives

$$\frac{p_{02R}}{p_{03R}} = 1 + \frac{\gamma}{2} \zeta_R M_{3R}^2$$

The stagnation pressure loss across the rotor is therefore

$$\Delta p_{0LR} = \frac{\gamma}{2} p_{03R} \zeta_R M_{3R}^2 = \frac{1}{2} \frac{T_{03R}}{T_3} \rho_{03R} \zeta_R W_3^2$$

or

$$\Delta p_{0LR} = \rho_{03R} \left(1 + \frac{\gamma - 1}{2} M_{3R}^2\right) \frac{1}{2} \zeta_R W_3^2 \quad (7.48)$$

■ EXAMPLE 7.7

Combustion gases with $\gamma = \frac{4}{3}$ and $c_p = 1148 \text{ J/(kg K)}$ flow through a normal turbine stage with $R = 0.60$. The flow enters the stator at $\alpha_1 = -33.0^\circ$ and leaves at velocity $V_2 = 450 \text{ m/s}$. The inlet stagnation temperature is 1200 K , and the inlet stagnation pressure is 15 bar . The flow coefficient is $\phi = 0.7$, the blade height-to-axial chord ratio is $b/c_x = 3.5$, and the Reynolds number is 10^5 . Find the efficiency of the stage.

Solution: The blade-loading coefficient is first determined from

$$\psi = 2(1 - R - \phi \tan \alpha_3) = 2(1 - 0.6 - 0.7 \tan(-33^\circ)) = 1.709$$

The flow angle leaving the stator is

$$\alpha_2 = \tan^{-1} \left(\frac{1 - R + \psi/2}{\phi} \right) = \tan^{-1} \left(\frac{1 - 0.6 + 1.709/2}{0.7} \right) = 60.84^\circ$$

and the angle of the relative velocity leaving the stage is

$$\beta_3 = \tan^{-1} \left(\frac{-R - \psi/2}{\phi} \right) = \tan^{-1} \left(\frac{-0.6 - 1.709/2}{0.7} \right) = -64.30^\circ$$

The angle of the relative velocity at the inlet of the rotor is

$$\beta_2 = \tan^{-1} \left(\frac{-R + \psi/2}{\phi} \right) = \tan^{-1} \left(\frac{-0.6 + 1.709/2}{0.7} \right) = 19.99^\circ$$

The deflections are therefore

$$\begin{aligned}\varepsilon_S &= \alpha_2 - \alpha_1 = 60.84 + 33.00 = 93.84^\circ \\ \varepsilon_R &= \beta_2 - \beta_3 = 19.99 + 64.30 = 84.29^\circ\end{aligned}$$

and the loss coefficients can now be calculated. First, the nominal values are

$$\bar{\zeta}_S = 0.04 + 0.06 \left(\frac{\varepsilon_S}{100} \right)^2 = 0.04 + 0.06 \left(\frac{93.84}{100} \right)^2 = 0.0928$$

and

$$\bar{\zeta}_R = 0.04 + 0.06 \left(\frac{\varepsilon_R}{100} \right)^2 = 0.04 + 0.06 \left(\frac{84.29}{100} \right)^2 = 0.0826$$

When corrected for $b/c_x = 3.5$, they are

$$\begin{aligned}\zeta_S &= (1 + \bar{\zeta}_S) \left(0.993 + 0.021 \frac{c_x}{b} \right) - 1 = (1 + 0.0928) \left(0.993 + \frac{0.021}{3.5} \right) - 1 \\ &= 0.0917 \\ \zeta_R &= (1 + \bar{\zeta}_R) \left(0.975 + 0.075 \frac{c_x}{b} \right) - 1 = (1 + 0.0826) \left(0.975 + \frac{0.075}{3.5} \right) - 1 \\ &= 0.0788\end{aligned}$$

The axial velocity is

$$V_x = V_2 \cos \alpha_2 = 450 \cos(60.84^\circ) = 219.26 \text{ m/s}$$

and the tangential velocity leaving the rotor is

$$V_{u3} = V_x \tan \alpha_3 = 219.26 \tan(-33^\circ) = -142.39 \text{ m/s}$$

so that

$$V_3 = \sqrt{V_x^2 + V_{u3}^2} = \sqrt{219.26^2 + 142.39^2} = 261.44 \text{ m/s}$$

The blade speed is $U = V_x/\phi = 219.26/0.7 = 313.23 \text{ m/s}$. The tangential component of the relative velocity leaving the stage is

$$W_{u3} = V_{u3} - U = -142.39 - 313.23 = -455.62 \text{ m/s}$$

so that

$$W_3 = \sqrt{W_x^2 + W_{u3}^2} = \sqrt{219.26^2 + 455.62^2} = 505.63 \text{ m/s}$$

The work done by the stage is $w = \psi U^2 = 1.709 \cdot 313.23^2 = 167.69 \text{ kJ/kg}$. An approximate value for the stage efficiency may now be obtained by setting $T_{3ss} = T_{2s}$ and $T_{3ss} = T_3$ in

$$\frac{1}{\eta_{tt}} - 1 = \frac{\zeta_R W_3^2 + \frac{T_{3s}}{T_2} \zeta_S V_2^2 + \left(1 - \frac{T_{3ss}}{T_3}\right) V_3^2}{2w}$$

so that this expression evaluates to

$$\frac{1}{\eta_{tt}} - 1 = \frac{0.0788 \cdot 505.63^2 + 0.0917 \cdot 450^2}{2 \cdot 167690} = 0.1154$$

with the result that $\eta_{tt} = 0.8965$.

To see the extent to which neglecting the temperature ratio T_{3ss}/T_3 and the kinetic energy correction changes the efficiency, these terms are calculated next. The isentropic stage work is $w_s = w/\eta_{tt} = 167.69/0.8965 = 187.05 \text{ kJ/kg}$. With $T_{02} = T_{01} = 1200 \text{ K}$, the exit temperature is

$$T_{03} = T_{02} - \frac{w}{c_p} = 1200 - \frac{167690}{1148} = 1053.9 \text{ K}$$

and for an isentropic process, it is

$$T_{03ss} = T_{02} - \frac{w_s}{c_p} = 1200 - \frac{187050}{1148} = 1037.1 \text{ K}$$

The static temperature at the exit is

$$T_3 = T_{03} - \frac{V_3^2}{2c_p} = 1053.9 - \frac{252.09^2}{2 \cdot 1148} = 1024.2 \text{ K}$$

Integrating the Gibbs equation along the constant pressure line p_3 and along the constant pressure line p_{03} gives

$$s_3 - s_1 = c_p \ln \frac{T_3}{T_{3ss}} \quad s_3 - s_1 = c_p \ln \frac{T_{03}}{T_{03ss}}$$

from which

$$T_{3ss} = \frac{T_{03ss}}{T_{03}} T_3 = \frac{1037.1}{1053.9} 1024.2 = 1007.8 \text{ K}$$

From the definition of static enthalpy loss coefficient across the rotor,

$$T_{3s} = T_3 - \frac{\zeta_R W_3^2}{2c_p} = 1024.2 - \frac{0.0788 \cdot 505.63^2}{2 \cdot 1148} = 1015.4 \text{ K}$$

In addition,

$$T_2 = T_{02} - \frac{V_2^2}{2c_p} = 1200 - \frac{450^2}{2 \cdot 1148} = 1111.8 \text{ K}$$

so that

$$\frac{1}{\eta_{tt}} - 1 = \frac{0.0788 \cdot 505.63^2 + \frac{1015.4}{1111.8} 0.0917 \cdot 450^2 + (1 - \frac{1007.8}{1024.2}) 261.44^2}{2 \cdot 167690}$$

$$= 0.1139$$

Therefore, the total-to-total efficiency of the stage is $\eta_{tt} = 0.8978$, which is nearly the same as that without the temperature and velocity correction. The temperature correction makes the loss through the rotor lower, but the velocity correction adds slightly to the losses, with the net result that these are compensating errors, and the shorter calculation gives an accurate result.

The stagnation pressure at the exit of the stator is obtained from

$$\frac{p_{01}}{p_{02}} = 1 + \frac{\gamma}{2} \zeta_S M_2^2$$

The Mach number is

$$M_2 = \frac{V_2}{\sqrt{\gamma R T_2}} = \frac{450}{\sqrt{1.333 \cdot 287 \cdot 1111.8}} = 0.690$$

so that

$$\frac{p_{01}}{p_{02}} = 1 + \frac{2 \cdot 0.0917 \cdot 0.690^2}{3} = 1.0291 \quad p_{02} = \frac{1500}{1.0291} = 1457.6 \text{ kPa}$$

and the stagnation pressure loss across the stator is

$$\Delta p_{0LS} = 1500 - 1457.6 = 42.4 \text{ kPa}$$

To calculate the loss of stagnation pressure across the rotor, the absolute and relative Mach numbers at the exit are determined first. They are as follows:

$$M_3 = \frac{V_3}{\sqrt{\gamma R T_3}} = \frac{261.44}{\sqrt{1.333 \cdot 287 \cdot 1024.2}} = 0.4176$$

$$M_{3R} = \frac{W_3}{\sqrt{\gamma R T_3}} = \frac{505.63}{\sqrt{1.333 \cdot 287 \cdot 1024.2}} = 0.8077$$

Then, stagnation pressure at the exit is

$$p_{03} = p_{01} \left(\frac{T_{03ss}}{T_{01}} \right)^{\gamma/(\gamma-1)} = 1500 \left(\frac{1037.1}{1200} \right)^4 = 836.8 \text{ kPa}$$

and p_3 is

$$p_3 = p_{03} \left(1 + \frac{\gamma-1}{2} M_3^2 \right)^{-\gamma/(\gamma-1)} = 836.8 \left(1 + \frac{0.4176^2}{6} \right)^{-4} = 746.14 \text{ kPa}$$

The stagnation pressure p_{03R} is obtained from

$$p_{03R} = p_3 \left(1 + \frac{\gamma - 1}{2} M_{3R}^2 \right)^{\gamma/(\gamma-1)} = 746.14 \left(1 + \frac{0.8077^2}{6} \right)^4 = 1127.5 \text{ kPa}$$

and the value of p_{02R} is then

$$p_{02R} = p_{03R} \left(1 + \frac{\gamma}{2} \zeta_R M_{3R}^2 \right) = 1127.5 \left(1 + \frac{2}{3} 0.088 \cdot 0.8077^2 \right) = 1166.1 \text{ kPa}$$

so that the loss of stagnation pressure across the rotor is

$$\Delta p_{0LR} = 1166.1 - 1127.5 = 38.6 \text{ kPa}$$

7.5.4 Performance charts

A useful collection of turbine performance characteristics was compiled by Smith [84] in 1965. His chart is shown in Figure 7.11. Each design is labeled in a small circle by the value of efficiency that may be achieved for a given choice of flow coefficient $\phi = V_x/U$ and a stage-loading coefficient $\psi = w/U^2 = \Delta h_0/U^2$. The curves of constant efficiency are based on a theory by Smith. He took blade losses other than tip losses into account, and for this reason, the actual values of efficiency are expected to drop slightly.

The flow coefficients in the range from $0.6 \leq \phi \leq 1.0$ give uncorrected efficiencies in a range from 90% to 94%, depending on how heavily loaded the blades are. Typical turbines have a blade-loading coefficient in the range $1.5 < \psi < 2.2$, but there are designs outside this range.

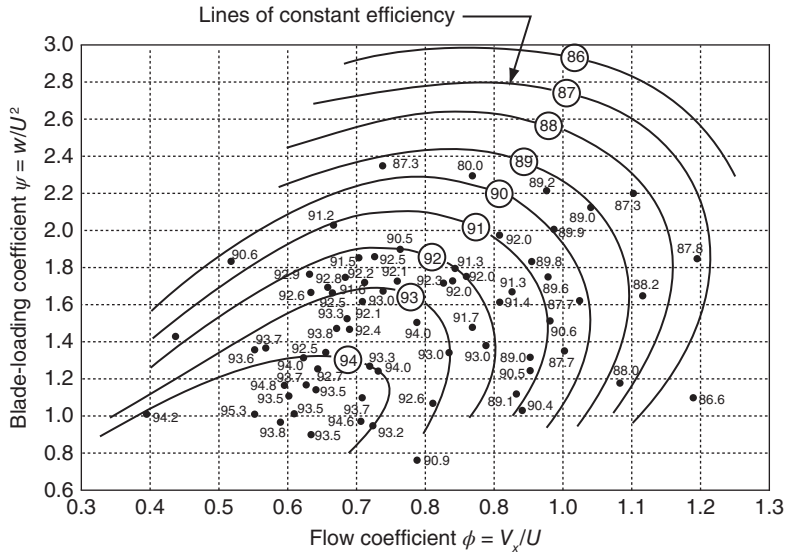


Figure 7.11 Variation of measured stage efficiency with stage-loading coefficient and flow coefficient for axial-flow turbines. Source: Adapted from Smith [84].

Smith's method for calculating the main features of the performance characteristics has been extended by Lewis [57]. The present discussion follows Lewis, who suggests writing the efficiency in the form

$$\eta_{tt} = \frac{1}{1 + f_L} \quad (7.49)$$

The calculations in the foregoing example show that f_L can be approximated by

$$f_L = \frac{\zeta_R W_3^2 + \zeta_S V_2^2}{2w} = \frac{1}{2\psi} \left[\zeta_R \left(\frac{W_3}{U} \right)^2 + \zeta_S \left(\frac{V_2}{U} \right)^2 \right] \quad (7.50)$$

Since

$$\tan \alpha_2 = \frac{1 - R + \psi/2}{\phi} \quad \tan \beta_3 = \frac{-(R + \psi/2)}{\phi}$$

it follows that

$$\cos \alpha_2 = \frac{\phi}{\sqrt{\phi^2 + (1 - R + \psi/2)^2}} \quad \cos \beta_3 = \frac{R + \psi/2}{\sqrt{\phi^2 + (R + \psi/2)^2}}$$

and the velocity ratios may be written as

$$\left(\frac{V_2}{U} \right)^2 = \phi^2 + \left(1 - R + \frac{\psi}{2} \right)^2$$

and

$$\left(\frac{W_3}{U} \right)^2 = \phi^2 + \left(R + \frac{\psi}{2} \right)^2$$

so that

$$f_L = \frac{1}{2\psi} \left[\zeta_R \left(\phi^2 + \left(R + \frac{\psi}{2} \right)^2 \right) + \zeta_S \left(\phi^2 + \left(1 - R + \frac{\psi}{2} \right)^2 \right) \right]$$

This may be expressed in a more convenient form by defining $\nu = \zeta_S/\zeta_R$ and $F_L = f_L/\zeta_R$, so that

$$F_L = \frac{1}{2\psi} \left[\phi^2 + \left(R + \frac{\psi}{2} \right)^2 + \nu \left(\phi^2 + \left(1 - R + \frac{\psi}{2} \right)^2 \right) \right] \quad (7.51)$$

and the efficiency can now be written as

$$\eta_{tt} = \frac{1}{1 + F_L \zeta_R}$$

The maximum efficiency is obtained by minimizing F_L with respect to ψ with the value of ζ_R assumed to remain constant. Then, if the ratio ν is also assumed to remain constant,

differentiating and setting the result to zero gives

$$\left(\frac{\partial F_L}{\partial \psi}\right)_{\nu, \phi, R} = \frac{1}{\psi} \left[\left(R + \frac{\psi}{2}\right) + \nu \left(1 - R + \frac{\psi}{2}\right) \right] - \frac{1}{\psi^2} \left[\phi^2 + \left(R + \frac{\psi}{2}\right)^2 + \nu \left(\phi^2 + \left(1 - R + \frac{\psi}{2}\right)^2 \right) \right] = 0$$

which, when solved for ψ , leads to

$$\psi_m = 2\sqrt{\frac{\phi^2 + R^2 + \nu(\phi^2 + (1 - R)^2)}{1 + \nu}} \quad (7.52)$$

For $\nu = 1$ and $R = \frac{1}{2}$, this reduces to

$$\psi_m = \sqrt{4\phi^2 + 1} \quad (7.53)$$

Contours of constant F_L are obtained by rearranging Eq. (7.51) first as

$$\psi^2 + \frac{4[\nu(1 - R) + R - 2F_L]}{1 + \nu}\psi + \frac{4[\phi^2 + R^2 + \nu(\phi^2 + (1 - R)^2)]}{1 + \nu} = 0$$

and solving it for ψ . This gives

$$\psi = \frac{2 \left[2F_L - \nu(1 - R) - R \pm \sqrt{4F_L^2 - 4F_L[\nu(1 - R) + R] + 4\nu R(1 - R) - \nu - (1 + \nu)^2 \phi^2} \right]}{1 + \nu}$$

For $R = 0.5$ and $\zeta_S = \zeta_R = 0.09$, the two branches of each of the curves are shown in Figure 7.12. The knee of the curves is where the discriminant is zero, namely, at

$$\phi_m = \frac{\sqrt{4F_L^2 - 4F_L[\nu(1 - R) + R] + \nu - 4\nu R(1 - R)}}{1 + \nu}$$

The locus of points of the blade-loading coefficient for which the losses are minimum, obtained from Eq. (7.53), is also shown. As stressed by Lewis, when the efficiency is written as

$$\eta_{tt} = \frac{1}{1 + F_L \zeta_R}$$

the factor F_L depends primarily on the shape of the velocity diagrams, which, in turn, are completely determined by ψ , ϕ , and R . The irreversibilities are taken into account by ζ_R and ζ_S . These depend on the amount of turning, but their influence on the shape of the efficiency contours is less than the influence of the flow angles.

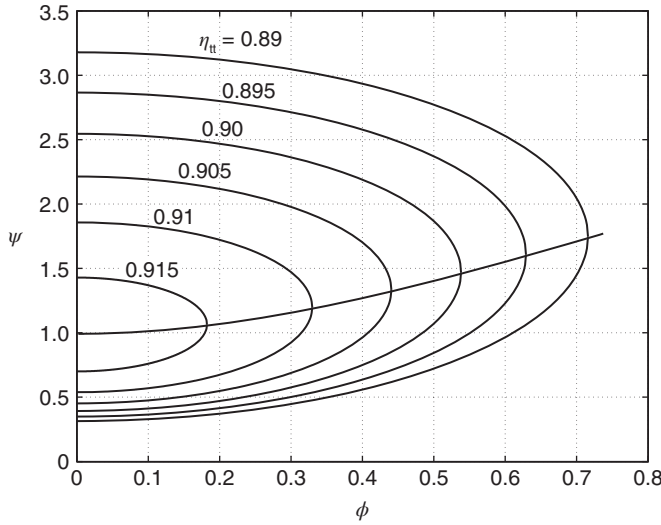


Figure 7.12 Contours of constant efficiency for an axial turbine stage with $R = 0.5$, $\zeta_s = 0.09$, and $\zeta_R = 0.09$; also shown is the curve of least losses.

The results in Figure 7.12 are qualitatively similar to those in Figure 7.11, but they differ in important details. In the calculations, the loss coefficients were assumed to be constant with values $\zeta_R = \zeta_s = 0.09$. They clearly depend on the amount of turning and thus on the values of ψ , ϕ , and R . As mentioned, Smith subtracted out the tip losses, and they are not included in Soderberg's correlation, either. The experiments on which the Smith plot is based were carried out on a test rig at low temperature, and therefore, the results do not represent real operating conditions. The amount of turning today is approaching 90° or even higher [19]. This is achieved by using computational fluid dynamic analysis to design highly three-dimensional blades. In fact, the high efficiencies achieved today make further increases in efficiency more and more difficult to achieve [21].

The actual loss coefficients using the Soderberg correlation are easily included in the calculations, and the contours of constant efficiency and the deflection for a 50% reaction are shown in Figure 7.13. The results are based on a blade height-to-axial chord ratio of $b/c_x = 3$, and the Reynolds number was set at $Re = 10^5$. From the expression

$$\psi = 2(1 - R - \phi \tan \alpha_3)$$

it is seen that when $\phi = 0$ and $R = \frac{1}{2}$, the blade-loading coefficient is $\psi = 1$. If this stage has an axial entry with $\alpha_3 = 0$, the loading coefficient is $\psi = 1$ for any value of ϕ . Examination of the figure shows that for an axial entry, as ϕ is increased to 0.5, the efficiency increases to slightly over 0.92 and decreases from there as ϕ is increased. Since the stage reaction is 50%, the flow turns across the rotor and stator by an equal amount. At $\phi = 0.5$ and $\psi = 1$, since $\alpha_3 = \alpha_1 = 0$, the flow angle α_2 is

$$\alpha_2 = \tan^{-1} \left(\frac{1 - R + \psi/2}{\phi} \right) = \tan^{-1}(2) = 63.4^\circ$$

On the other hand, if the entry angle is chosen to be $\alpha_3 = \alpha_1 = -45^\circ$, then

$$\psi = 1 + 2\phi$$

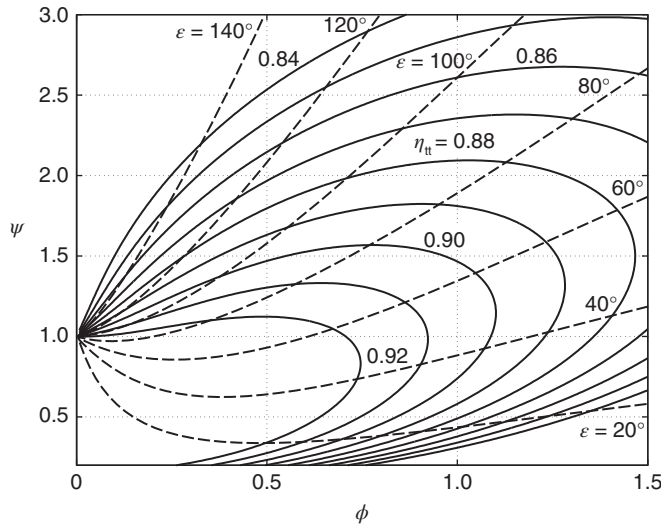


Figure 7.13 Contours of constant efficiency and deflection for a stage with $R = 0.5$, $b/c_x = 3$, and $Re = 10^5$.

and at $\phi = 0.5$, the blade-loading coefficient would be $\psi = 2$. The flow angle leaving the nozzle would then be $\alpha_2 = 71.56^\circ$, and the flow angles for the rotor would have the values $\beta_2 = 45^\circ$ and $\beta_3 = -71.56^\circ$. Hence, the deflection would reach $\varepsilon_R = 116.56^\circ$. This is larger than that recommended, and the inlet angle is too steep. These calculations show that good designs are obtained for a range of flow coefficients of $0.5 < \phi < 1.5$ and the blade-loading coefficient in the range $0.8 < \psi < 2.7$, for then the deflection is less than 80° . As the flow coefficient is increased from 0.5 to 1.5, the inlet flow angle may be changed from an axial entry to one with $\alpha_3 = -30^\circ$.

Contours of constant-rotor-loss coefficients are shown in Figure 7.14. They are seen to follow the shape of the deflection lines in Figure 7.13. When there is no turning,

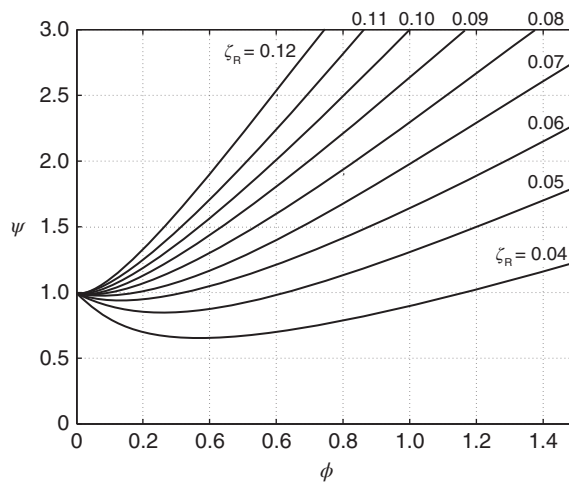


Figure 7.14 Lines of constant rotor loss coefficients for a stage with $R = 0.5$, $b/c_x = 3$, and $Re = 10^5$.

the loss coefficient is $\zeta_R = 0.04$, and the line for $\zeta_R = 0.05$ corresponds to a turning of $\beta_2 - \beta_3 = 40^\circ$.

For a zero-reaction stage, the contours of constant efficiency are given in Figure 7.15. Since $R = 0$, the equation

$$\psi = 2(1 - R - \phi \tan \alpha_3)$$

shows that at $\phi = 0$, the loading coefficient is $\psi = 2$. The lines of constant turning for the rotor are now straight lines, owing to the relationship $\beta_3 = -\beta_2$ and

$$\psi = \phi(\tan \beta_2 - \tan \beta_3) = 2\phi \tan \beta_2$$

If the deflection is kept at 70° , then $\beta_2 = 35^\circ$, and at $\phi = 1.5$, the blade-loading coefficient is $\psi = 2.1$, and the efficiency is close to 0.87. At $\phi = 0.5$, the blade-loading coefficient has the value $\psi = 0.7$, and the efficiency is slightly over 0.92. For axial entry, $\psi = 2$ independent of ϕ , and an efficiency of slightly under 0.89 may be maintained for the range of ϕ from 0.3 to 0.8.

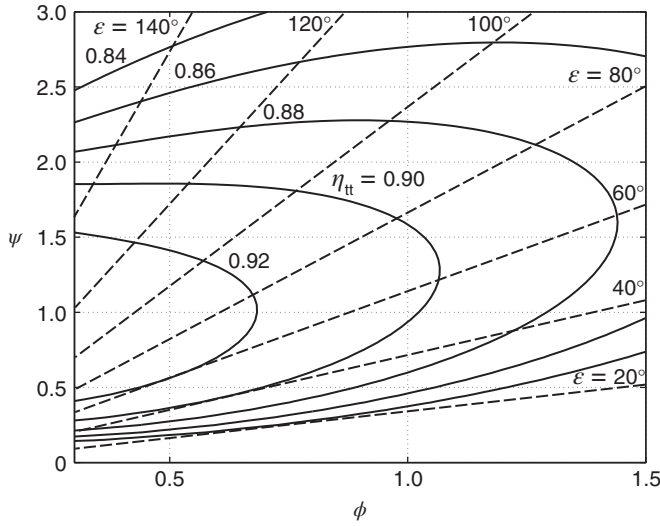


Figure 7.15 Contours of constant efficiency and deflection for a stage with $R = 0$, $b/c_x = 3$, and $Re = 10^5$.

7.5.5 Zweifel correlation

Zweifel [109] examined losses in turbines and developed a criterion for the space-to-axial chord ratio at which losses are the smallest. He put the loading of the blades into a nondimensional form by dividing the driving force by an ideal one defined as the pressure difference $p_{02} - p_3$ times the axial chord. The stagnation pressure p_{02} is the maximum possible pressure encountered, and p_3 is close to the minimum one as the flow accelerates through the passage. The ratio becomes

$$\psi_T = \frac{\rho V_x s (V_{u2} - V_{u3})}{(p_{02} - p_3) c_x}$$

in which c_x is the axial chord length. This can be written as

$$\psi_T = \frac{s}{c_x} \frac{\rho V_x^2 (\tan \alpha_2 - \tan \alpha_3)}{\frac{1}{2} \rho V_3^2}$$

or as

$$\psi_T = 2 \frac{s}{c_x} \cos^2 \alpha_3 (\tan \alpha_2 - \tan \alpha_3) \quad (7.54)$$

In examining the performance of various turbines, Zweifel determined that the losses are minimized when $\psi_T = 0.8$. With this value for ψ_T , this equation is used to determine the spacing of the blades. With the spacing known, the cross-sectional area of the flow channel and its wetted area may be calculated, and the Reynolds number is determined. This may then be used to obtain the loss coefficients from the Soderberg correlation. For the rotor, the flow angles of the absolute velocities are replaced by the relative flow angles. Alternatively, the losses may be determined by results from experiments of Ainley and Mathieson that are discussed next. Their correlations are based on the spacing to chord ratio, whereas in the Zweifel's formula, the spacing-to-axial chord is used. The angle between the chord line and the axial chord is called the stagger angle.

7.5.6 Further discussion of losses

Ainley [2] carried out an experimental study of losses in turbines at about the same time as Soderberg. His loss estimates are shown in Figure 7.16 for a flow that turns only by about 40° and thus has fairly small losses at the design condition. He presented the results in the form of a stagnation pressure loss coefficient, defined as

$$Y_p = \frac{p_{01} - p_{02}}{p_{02} - p_2}$$

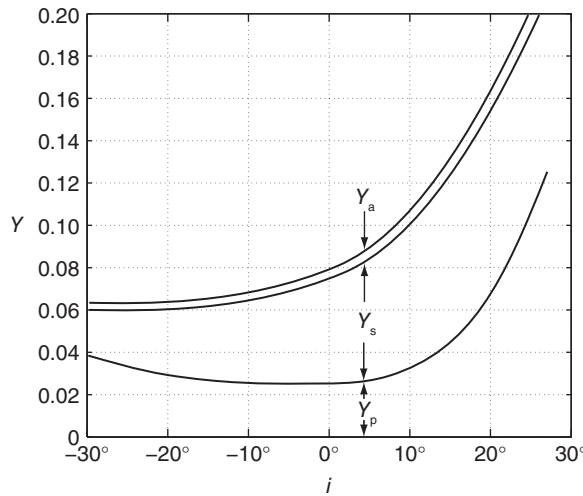


Figure 7.16 Stagnation pressure loss coefficients for turbine blades as a function of incidence (flow angle minus the metal angle), with $s/c = 0.77$ and $b/c = 2.7$ at Reynolds number $Re = 2 \cdot 10^5$. Source: From measurements by Ainley [2].

The denominator of this expression clearly depends on the Mach number, and therefore, so does the value of the loss coefficient. The losses are separated into profile losses, Y_p , secondary flow losses, Y_s , and the losses in the annulus boundary layers, Y_a . The profile losses, associated with the growth of the boundary layers along the blades, are lowest at a few degrees of negative incidence. The secondary flow losses dominate at all values of incidence. The losses in the annulus boundary layers represent a small addition to the secondary flow losses, and they are typically grouped together as it is difficult to separate them from each other.

The physical cause of the secondary flows is the curvature along the flow path. From study of fundamentals of fluid dynamics, it is known that pressure increases from concave to convex side of curved streamlines. This transverse pressure gradient gives rise to secondary flows for the following reason. In the inviscid stream far removed from the solid surfaces, viscous forces are small, and inertial forces are balanced by pressure forces. The transverse component of pressure force points from the pressure side of one blade to the suction side of the next one, and the transverse component of the inertial force is equal and opposite to this.

In the endwall boundary layer, viscous forces in the main flow direction retard the flow, with the result that inertial forces in the boundary layers are smaller than those in the inviscid stream. However, owing to the thinness of the endwall boundary layers, pressure distribution in these layers is the same as in the inviscid stream. For this reason, the unbalanced part of the pressure force causes a transverse flow in the endwall boundary layers toward the suction side of the blade. This is shown schematically in Figure 7.17. This secondary flow takes place in both endwall boundary layers. Continuity requires that there be a return flow across the inviscid stream. The return flow is more diffuse than that in the boundary layers as it occupies a large flow area. The effect is the development of two counterrotating secondary vortices, with axes in the direction of the main stream. Thus, a secondary flow exists in these vortices. If this were all, the secondary flow would be easy to understand. But the flow in the boundary layer near the casing is also influenced by a vortex that develops at the tips of the rotor blades. This interaction increases the

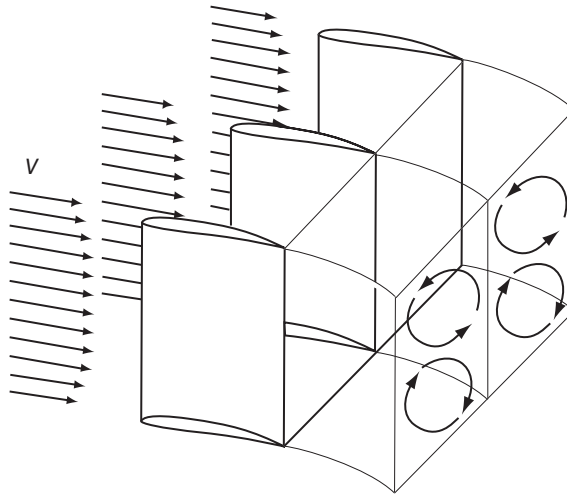


Figure 7.17 Secondary flows in a channel between two blades.

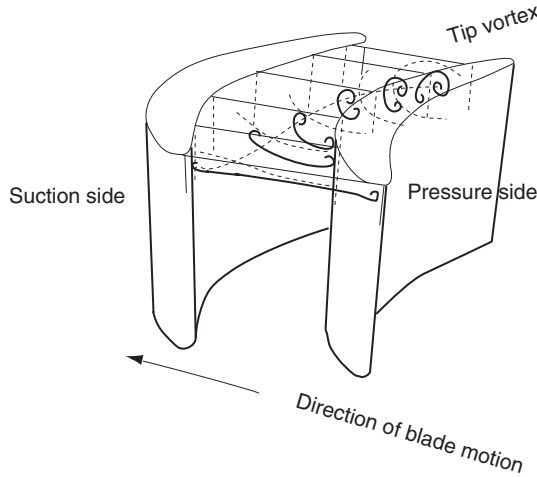


Figure 7.18 Distortion of tip vortex as it moves through the passage.

intensity of the secondary flow, and the axis of the vortex migrates from the pressure side of the blade to the suction side as it traverses the flow passage. A sketch of this is shown in Figure 7.18. Further complication arises from the unsteadiness of the flow caused by a discrete set of rotor blades passing by the row of stator vanes.

7.5.7 Ainley–Mathieson correlation

Ainley and Mathieson [3] continued the work of Ainley [2] on turbine cascades. Their results are shown in Figure 7.19. The flow enters the nozzles axially and leaves at the angle α_2 indicated. The profile loss coefficient Y_{pa} is seen to vary both with the space-to-chord ratio and the amount of turning of the flow. The two curves in the figure, for which the flow is seldom turned this much, are marked with dashed line, for the flow is seldom turned this much.

To facilitate the use of these results with hand calculators (or in short computer calculations), they have been fitted with two parabolas. The data in Figure 7.19 are

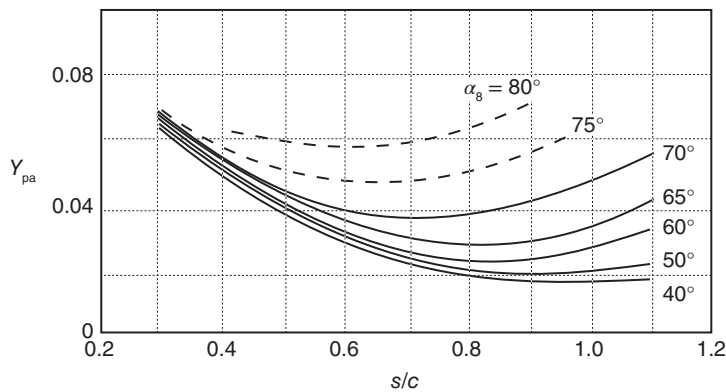


Figure 7.19 Stagnation pressure loss coefficients for nozzles. Source: Measurements by Ainley and Mathieson [3].

correlated reasonably well by the biquadratic fit

$$\begin{aligned}
 Y_{\text{pa}} = & \left[-0.627 \left(\frac{\alpha_2}{100} \right)^2 + 0.821 \left(\frac{\alpha_2}{100} \right) - 0.129 \right] \left(\frac{s}{c} \right)^2 \\
 & + \left[1.489 \left(\frac{\alpha_2}{100} \right)^2 - 1.676 \left(\frac{\alpha_2}{100} \right) + 0.242 \right] \left(\frac{s}{c} \right) \\
 & - 0.356 \left(\frac{\alpha_2}{100} \right)^2 + 0.399 \left(\frac{\alpha_2}{100} \right) + 0.0077
 \end{aligned} \quad (7.55)$$

■ EXAMPLE 7.8

A nozzle row is tested with air. The air enters the row axially and leaves it at angle 60° . The space-to-chord ratio is $s/c = 0.7$. The inlet pressure is $p_{01} = 200$ kPa, stagnation temperature at the inlet is $T_{01} = 540$ K, and the exit static pressure is $p_2 = 160$ kPa. Find (a) the exit stagnation pressure and (b) the static enthalpy loss coefficient.

Solution: (a) For $s/c = 0.7$, the stagnation pressure loss coefficient is

$$\begin{aligned}
 Y_{\text{pa}} = & \left[-0.627 \left(\frac{60}{100} \right)^2 + 0.821 \left(\frac{60}{100} \right) - 0.129 \right] 0.7^2 \\
 & + \left[1.489 \left(\frac{60}{100} \right)^2 - 1.676 \left(\frac{60}{100} \right) + 0.242 \right] 0.7 \\
 & - 0.356 \left(\frac{60}{100} \right)^2 + 0.399 \left(\frac{60}{100} \right) + 0.0077 = 0.0272
 \end{aligned}$$

Examination of Figure 7.19 shows that this value is smaller than what can be read from the figure, which suggests that it should be increased to 0.032. If this error can be tolerated, solving next

$$Y_{\text{pa}} = \frac{p_{01} - p_{02}}{p_{02} - p_2}$$

for p_{02} gives

$$p_{02} = \frac{p_{01} + Y_{\text{pa}} p_2}{1 + Y_{\text{pa}}} = \frac{200 + 0.0272 \cdot 160}{1.0272} = 198.94 \text{ kPa}$$

so that $\Delta p_{0S} = 1.06$ kPa. A more accurate value using the actual charts is 1.24 kPa.

(b) The exit static temperature is

$$T_2 = T_{02} \left(\frac{p_2}{p_{02}} \right)^{(\gamma-1)/\gamma} = 540 \left(\frac{160000}{198940} \right)^{1/3.5} = 507.41 \text{ K}$$

and velocity is therefore

$$V_2 = \sqrt{2c_p(T_{02} - T_2)} = \sqrt{2 \cdot 1004.5(540 - 507.41)} = 255.85 \text{ m/s}$$

These give a Mach number value of $M_2 = V_2/\sqrt{\gamma RT_2} = 0.567$. The stagnation density at the exit is

$$\rho_{02} = \frac{p_{02}}{RT_{02}} = \frac{198940}{287 \cdot 540} = 1.284 \text{ kg/m}^3$$

The static enthalpy loss coefficient is calculated from

$$\zeta_s = \frac{2\Delta p_{0s}}{p_{01}\gamma M_2^2} = 0.0236$$

These calculated loss coefficients only include profile losses, and as Figure 7.16 shows, secondary flow losses contribute the major part of the total losses. Secondary flow losses are discussed in the next section. ■

The experiments of Ainley and Mathieson [3] also included the influence of the space-to-chord ratio for *impulse blades*. This is shown in Figure 7.20. Again, the approach velocity is at zero incidence. Since the rotor blades have the shape of impulse blades, the different curves are labeled by the relative flow angles. In a two-stage velocity compounded steam turbine, the stator between the two rotors has equiangular vanes as well, but this is an exceptional situation in turbines. Ainley and Mathieson showed that the results from the nozzles with axial entry and the impulse blades can be combined for use in other situations. This is discussed in the following.

The data shown in Figure 7.20 when fitted to a biquadratic expression, results in

$$\begin{aligned} Y_{pe} = & \left[-1.56 \left(\frac{\alpha_2}{100} \right)^2 + 1.55 \left(\frac{\alpha_2}{100} \right) - 0.064 \right] \left(\frac{s}{c} \right)^2 \\ & + \left[3.73 \left(\frac{\alpha_2}{100} \right)^2 - 3.43 \left(\frac{\alpha_2}{100} \right) + 0.290 \right] \left(\frac{s}{c} \right) \\ & - 0.83 \left(\frac{\alpha_2}{100} \right)^2 + 0.78 \left(\frac{\alpha_2}{100} \right) + 0.078 \end{aligned} \quad (7.56)$$

This is a reasonably good fit even if it was forced to a simple second-order polynomial form. On the basis of values obtained from Eqs. (7.55) and (7.56), Ainley and Mathieson recommend that for blades for which the inlet angle is between the axial entry of nozzles and that of the impulse blades, the stagnation pressure loss coefficient can be estimated from

$$Y_p = \left[Y_{pa} + \left(\frac{\alpha_1}{\alpha_2} \right)^2 (Y_{pe} - Y_{pa}) \right] \left(\frac{t/c}{0.2} \right)^{|\alpha_1/\alpha_2|} \quad (7.57)$$

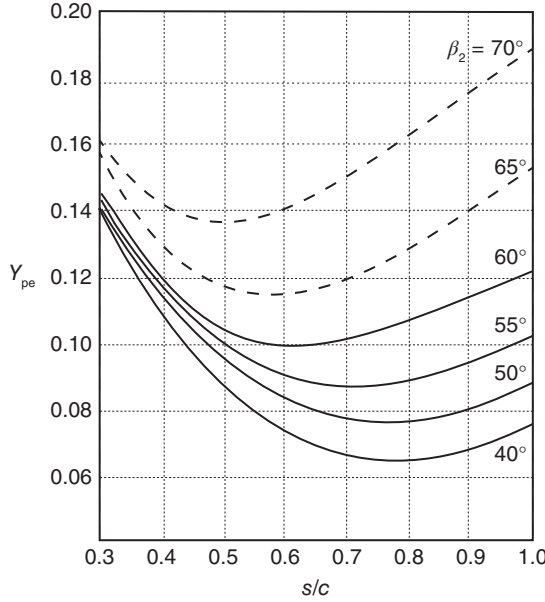


Figure 7.20 Loss coefficients for impulse blades, $\beta_3 = -\beta_2$, and $Re = 2 \cdot 10^5$, $M < 0.6$. Source: Measurements by Ainley and Mathieson [3].

The subscripts in this expression have the following meaning: Y_p is the *profile* loss at zero incidence; Y_{pa} is the profile loss coefficient for *axial* entry, and Y_{pe} is the profile loss coefficient for *equiangular* impulse blades. The absolute values are needed in the exponent because α_1 could be negative.

For a rotor, the angle α_1 is replaced by β_2 , and α_2 is replaced by β_3 . Thus, Eq. (7.57) takes the form

$$Y_p = \left[Y_{pa} + \left(\frac{\beta_2}{\beta_3} \right)^2 (Y_{pe} - Y_{pa}) \right] \left(\frac{t/c}{0.2} \right)^{|\beta_2/\beta_3|} \quad (7.58)$$

In evaluating the loss coefficient from Eq. (7.56) for impulse blades, α_2 is replaced by β_2 for rotor blades, since β_2 will be positive and $\beta_3 = -\beta_2$. The ratio of maximum thickness to the length of the chord in these expressions is t/c , with a nominal value of 20%. Should it be greater than 25%, the value $t/c = 0.2$ is used. If it is less than 15%, its value is set at $t/c = 0.15$.

7.5.8 Secondary loss

Secondary and tip losses require examination of lift and drag on the rotor blades. Unlike for airfoils, for which lift is the force component perpendicular to incoming flow direction, in turbomachinery flows, the direction of the lift is defined as the force perpendicular to a *mean flow direction*. This, together with other important geometric parameters, is shown in Figure 7.21. The mean direction is obtained by first defining the mean tangential component of the relative velocity as

$$W_{um} = \frac{1}{2}(W_{u2} + W_{u3})$$

which can be rewritten in the form

$$W_{um} = \frac{1}{2} W_x (\tan \beta_2 + \tan \beta_3)$$

Next, writing $W_{um} = W_x \tan \beta_m$ gives

$$\tan \beta_m = \frac{1}{2} (\tan \beta_2 + \tan \beta_3)$$

and β_m defines the mean direction. For the situation shown in Figure 7.21, $\tan \beta_m$ is negative and so is W_{um} .

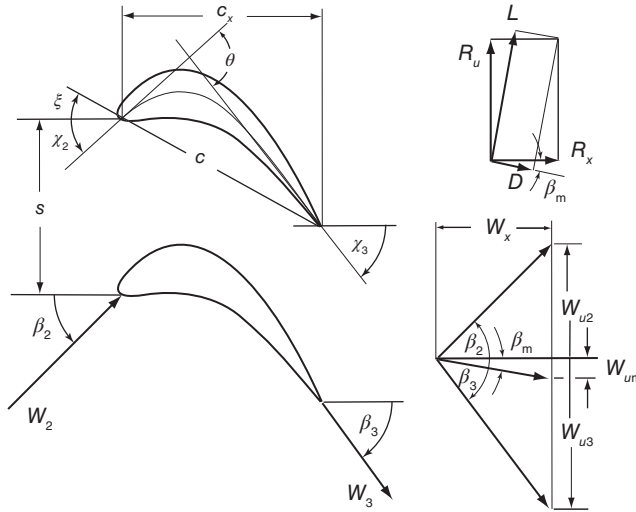


Figure 7.21 Illustration of flow angles, blade metal angles χ , mean direction, and lift and drag forces on a rotor.

Next, applying the momentum theorem to the rotor, the force in the direction of the wheel motion is given by

$$F_u = \rho s W_x (W_{u3} - W_{u2}) = \rho s W_x^2 (\tan \beta_3 - \tan \beta_2)$$

This is the force that the blade exerts on the fluid per unit height of the blade. The reaction force $R_u = -F_u$ is the force by the fluid on the blade, and it is given by

$$R_u = \rho s W_x^2 (\tan \beta_2 - \tan \beta_3) \quad (7.59)$$

The component of the reaction forces are related to lift L and drag D by

$$R_x = L \sin \beta_m + D \cos \beta_m \quad R_u = L \cos \beta_m - D \sin \beta_m$$

The magnitude of the drag force has been drawn larger in the figure than its actual size, to make the sketch clearer. If it is neglected, the reaction R_u is related to lift by

$$R_u = L \cos \beta_m$$

and Eq. (7.59) can be written as

$$L \cos \beta_m = \rho s W_x^2 (\tan \beta_2 - \tan \beta_3)$$

Introducing the lift coefficient leads to the expression

$$C_L = \frac{L/c}{\frac{1}{2} \rho W_m^2} = 2 \left(\frac{s}{c} \right) \frac{W_x^2 (\tan \beta_2 - \tan \beta_3)}{W_m^2 \cos \beta_m}$$

Since $W_x = W_m \cos \beta_m$, this reduces to

$$C_L = 2 \left(\frac{s}{c} \right) (\tan \beta_2 - \tan \beta_3) \cos \beta_m \quad (7.60)$$

The secondary flow and tip losses according to Dunham and Came [26] are expressed as

$$Y_s + Y_k = \frac{c}{b} \left[0.0334 \frac{\cos \beta_3}{\cos \beta_2} + B \left(\frac{k}{c} \right)^{0.78} \right] \left(\frac{C_L}{s/c} \right)^2 \frac{\cos^2 \beta_3}{\cos^3 \beta_m} \quad (7.61)$$

The second term, in which the gap width k appears, accounts for the tip losses. The parameter $B = 0.47$ for standard blades and $B = 0.37$ for shrouded blades. A shrouded blade is shown in Figure 3.8.

The loss coefficients are similar for the stator. The mean flow direction is given by

$$\tan \alpha_m = \frac{1}{2} (\tan \alpha_1 + \tan \alpha_2)$$

and the lift coefficient is

$$C_L = 2 \left(\frac{s}{c} \right) (\tan \alpha_2 - \tan \alpha_1) \cos \alpha_m$$

The loss coefficient of the secondary flows is

$$Y_s = \frac{c}{b} \left(0.0334 \frac{\cos \alpha_2}{\cos \alpha_1} \right) \left(\frac{C_L}{s/c} \right)^2 \frac{\cos^2 \alpha_2}{\cos^3 \alpha_m} \quad (7.62)$$

as there are no tip losses.

■ EXAMPLE 7.9

Combustion gases, with $\gamma = \frac{4}{3}$ and $c_p = 1148 \text{ J/(kg K)}$, flow through a normal turbine stage with $R = 0.60$. The flow enters the stator at $\alpha_1 = -33^\circ$ and leaves at velocity $V_2 = 450 \text{ m/s}$. The inlet stagnation temperature is $T_{01} = 1200 \text{ K}$, and the inlet stagnation pressure is 15 bar. The flow coefficient is $\phi = 0.7$, blade height-to-chord ratio is $b/c = 3$, the space-to-chord ratio $s/c = 0.9$, and the Reynolds number is 10^5 . The blades are unshrouded with $B = 0.47$, the tip-gap-to-blade height ratio is $k/b = 0.02$, and the thickness-to-chord ratio is $t/c = 0.2$. Find the stagnation pressure loss across the stator and the rotor based on Ainley–Mathieson correlations.

Solution: The blade-loading coefficient is first determined from

$$\psi = 2(1 - R - \phi \tan \alpha_3) = 2(1 - 0.6 - 0.7 \tan(-33^\circ)) = 1.709$$

The flow angle leaving the stator is

$$\alpha_2 = \tan^{-1} \left(\frac{1 - R + \psi/2}{\phi} \right) = \tan^{-1} \left(\frac{1 - 0.6 + 1.709/2}{0.7} \right) = 60.84^\circ$$

Hence, the mean flow angle is

$$\alpha_m = \tan^{-1} \left[\frac{1}{2} (\tan \alpha_1 + \tan \alpha_2) \right] = 29.74^\circ$$

The lift coefficient is

$$\begin{aligned} C_{LN} &= 2 \left(\frac{s}{c} \right) (\tan \alpha_2 - \tan \alpha_1) \cos \alpha_m \\ &= 2 \cdot 0.9 (\tan(60.84^\circ) - \tan(-33^\circ)) \cos(29.74^\circ) = 3.816 \end{aligned}$$

The secondary loss coefficient for the nozzles is

$$\begin{aligned} Y_{sN} &= \frac{c}{b} \left(0.0334 \frac{\cos \alpha_2}{\cos \alpha_1} \right) \left(\frac{C_{LN}}{s/c} \right)^2 \frac{\cos^2 \alpha_2}{\cos^3 \alpha_m} \\ &= \frac{1}{3} \left(0.0334 \frac{\cos(60.84^\circ)}{\cos(-33.00^\circ)} \right) \left(\frac{3.816}{0.9} \right)^2 \frac{\cos^2(60.84^\circ)}{\cos^3(29.74^\circ)} = 0.0434 \end{aligned}$$

The value of profile losses obtained from Eqs. (7.55) and (7.56) are

$$Y_{paN} = 0.0269 \quad Y_{peN} = 0.1151$$

so that for the particular nozzle row

$$Y_{pN} = \left[Y_{paN} + \left(\frac{\alpha_1}{\alpha_2} \right)^2 (Y_{peN} - Y_{paN}) \right] \left(\frac{t/c}{0.2} \right)^{|\alpha_1/\alpha_2|}$$

comes out to be

$$Y_{pN} = \left[0.0269 + \left(\frac{-33.00}{60.84} \right)^2 (0.1151 - 0.0269) \right] = 0.0529$$

Thus, the stagnation pressure loss coefficient is $Y_N = Y_{pN} + Y_{sN} = 0.0963$.

For the rotor, the angle of the relative velocity leaving the stage is

$$\beta_3 = \tan^{-1} \left(\frac{-R - \psi/2}{\phi} \right) = \tan^{-1} \left(\frac{-0.6 - 1.709/2}{0.7} \right) = -64.3^\circ$$

and the angle of the relative velocity at the inlet of the rotor is

$$\beta_2 = \tan^{-1} \left(\frac{-R + \psi/2}{\phi} \right) = \tan^{-1} \left(\frac{-0.6 + 1.709/2}{0.7} \right) = 20.0^\circ$$

The mean flow angle is

$$\beta_m = \tan^{-1} \left[\frac{1}{2} (\tan \beta_2 + \tan \beta_3) \right] = -40.6^\circ$$

The lift coefficient is

$$\begin{aligned} C_{LR} &= 2 \left(\frac{s}{c} \right) (\tan \beta_2 - \tan \beta_3) \cos \beta_m \\ &= 2 \cdot 0.9 [\tan(20^\circ) - \tan(-64.32^\circ)] \cos(-40.6^\circ) = 3.34 \end{aligned}$$

The secondary flow and tip losses can then be determined from

$$\begin{aligned} Y_{sR} + Y_{kR} &= \frac{c}{b} \left[0.0334 \frac{\cos \beta_3}{\cos \beta_2} + B \left(\frac{k}{c} \right)^{0.78} \right] \left(\frac{C_{LR}}{s/c} \right)^2 \frac{\cos^2 \beta_3}{\cos^3 \beta_m} \\ Y_{sR} + Y_{kR} &= \frac{1}{3} \left[0.0334 \frac{\cos(-64.3^\circ)}{\cos(20.0^\circ)} + 0.47 \cdot 0.02^{0.78} \right] \left(\frac{3.34}{0.9} \right)^2 \frac{\cos^2(-64.3^\circ)}{\cos^3|-40.6^\circ|} \\ &= 0.075 \end{aligned}$$

From Eqs. (7.55) and (7.56), the profile losses coefficients are

$$Y_{paR} = 0.0322 \quad Y_{peR} = 0.1334$$

so that

$$Y_{pR} = \left[Y_{paR} + \left(\frac{\beta_2}{\beta_3} \right)^2 (Y_{peR} - Y_{paR}) \right] \left(\frac{t/c}{0.2} \right)^{|\beta_2/\beta_3|}$$

is

$$Y_{pR} = \left[0.0322 + \left(\frac{-20.0}{-64.3} \right)^2 (0.1334 - 0.0322) \right] = 0.0419$$

The stagnation pressure loss coefficient for the rotor is therefore $Y_R = Y_{pR} + Y_{sR} + Y_{kR} = 0.1170$.

The stagnation pressure loss across the nozzle row is obtained from

$$Y_N = \frac{p_{01} - p_{02}}{p_{02} - p_2} \quad p_{01} - p_{02} = Y_N (p_{02} - p_2)$$

Dividing through by p_{02} gives

$$\frac{p_{01}}{p_{02}} = 1 + Y_N \left(1 - \frac{p_2}{p_{02}} \right) = 1 + Y_N \left[1 - \left(\frac{T_2}{T_{02}} \right)^{\gamma/(\gamma-1)} \right]$$

Since the temperature T_2 is

$$T_2 = T_{02} - \frac{V_2^2}{2c_p} = 1200 - \frac{450^2}{2 \cdot 1148} = 1111.8 \text{ K}$$

and $M_2 = V_2/\sqrt{\gamma RT_2} = 0.690$, the stagnation pressure ratio is

$$\frac{p_{01}}{p_{02}} = 1 + 0.0963 \left[1 - \left(\frac{1111.8}{1200} \right)^4 \right] = 1.02534$$

Hence, $p_{02} = 1500/1.02534 = 1462.9 \text{ kPa}$, and the stagnation pressure loss is $\Delta p_{0LS} = 37.1 \text{ kPa}$.

The static pressure at the exit is

$$p_2 = p_{02} \left(1 + \frac{\gamma - 1}{2} M_2^2 \right)^{-\gamma/(\gamma-1)} = 1462.9 \left(1 + \frac{0.690^2}{2} \right)^{-4} = 1078.0 \text{ kPa}$$

Some preliminary calculations are necessary for the rotor. First,

$$V_x = V_2 \cos \alpha_2 = 450 \cos(60.84^\circ) = 219.3 \text{ m/s}$$

and then,

$$W_2 = \frac{V_x}{\cos \beta_2} = \frac{219.3}{\cos(20^\circ)} = 233.3 \text{ m/s}$$

$$W_3 = \frac{V_x}{\cos \beta_3} = \frac{219.3}{\cos(-64.3^\circ)} = 505.6 \text{ m/s}$$

$$V_3 = \frac{V_x}{\cos \alpha_3} = \frac{219.3}{\cos(-33^\circ)} = 261.4 \text{ m/s}$$

Also

$$U = \frac{V_x}{\phi} = \frac{219.3}{0.7} = 313.3 \text{ m/s} \quad w = \psi U^2 = 1.709 \cdot 313.3^2 = 167.69 \text{ kJ/kg}$$

so that

$$T_{03} = T_{02} - \frac{w}{c_p} = 1200 - \frac{167.69}{1148} = 1053.9 \text{ K}$$

and

$$T_3 = T_{03} - \frac{V_3^2}{2c_p} = 1053.9 - \frac{261.4^2}{2 \cdot 1148} = 1024.2 \text{ K}$$

Next,

$$T_{03R} = T_3 + \frac{W_3^2}{2c_p} = 1024.2 + \frac{505.6^2}{2 \cdot 1148} = 1135.5 \text{ K}$$

and since $T_{02R} = T_{03R}$

$$p_{02R} = p_2 \left(\frac{T_{02R}}{T_2} \right)^{\gamma/(\gamma-1)} = 1078.0 \left(\frac{1135.5}{1111.8} \right)^4 = 1172.9 \text{ kPa}$$

The stagnation pressure loss coefficient for the rotor is

$$Y_R = \frac{p_{02R} - p_{03R}}{p_{03R} - p_3}$$

so that

$$\frac{p_{02R}}{p_{03R}} = 1 + Y_R \left(1 - \frac{p_3}{p_{03R}} \right) = 1 + Y_R \left[1 - \left(\frac{T_3}{T_{03R}} \right)^{\gamma/(\gamma-1)} \right]$$

The numerical value for the pressure ratio is

$$\frac{p_{02R}}{p_{03R}} = 1 + 0.1169 \left[1 - \left(\frac{1024.2}{1135.5} \right)^4 \right] = 1.040$$

and $p_{03R} = 1172.9/1.040 = 1128.28$ kPa. Hence, the stagnation pressure loss across the rotor is $\Delta p_{0LR} = 44.6$ kPa. The value obtained by Soderberg correlation was 38.6 kPa, but that correlation neglects the tip losses. For the nozzle row, the loss is $\Delta p_{0LS} = 37.1$ kPa, and the Soderberg correlation gave 42.4 kPa. Ainley–Mathieson and Soderberg correlations are therefore in reasonable agreement. ■

7.6 MULTISTAGE TURBINE

7.6.1 Reheat factor in a multistage turbine

Consider next a multistage turbine with process lines as shown in Figure 7.22. The isentropic work delivered by the j th stage is denoted as w_{js} , whereas the actual stage work is w_j . The stage efficiency is defined to be

$$\eta_s = \frac{w_j}{w_{js}}$$

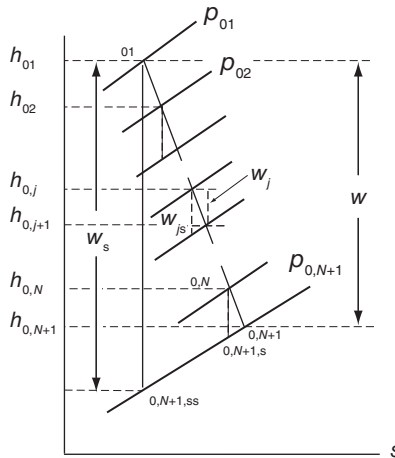


Figure 7.22 Processes in a multistage turbine.

and it is assumed to be the same for each stage. With

$$w_{js} = h_{0j} - h_{0j+1,s}$$

the sum over all the stages gives

$$\sum_{j=1}^N w_{js} = \sum_{j=1}^N (h_{0j} - h_{0j+1,s})$$

The isentropic work delivered by the turbine is $w_s = h_{01} - h_{0,N+1,ss}$. A *reheat factor* is defined as

$$\text{RF} = \frac{\sum_{j=1}^N w_{js}}{w_s} = \frac{\eta}{\eta_s} \frac{\sum_{j=1}^N w_j}{w}$$

in which $w = \sum_{j=1}^N w_j$, so that

$$\text{RF} = \frac{\eta}{\eta_s}$$

Since the slope of constant-pressure line increases as temperature increases, it follows that

$$\sum_{j=1}^N w_{js} > w_s$$

and $\text{RF} > 1$. Hence $\eta > \eta_s$, and the overall efficiency of a turbine is greater than the stage efficiency. The reason is the internal heating, for the increase in static enthalpy by irreversibilities becomes *partly available* as the expansion proceeds over the next stage. The increase in the overall efficiency depends on the number of stages.

If the ideal gas model can be used, then the actual and ideal work delivered by the first stage are

$$w = c_p(T_{01} - T_{02}) \quad w_s = c_p(T_{01} - T_{02s})$$

Since

$$\frac{T_{02s}}{T_{01}} = \left(\frac{p_{02}}{p_{01}} \right)^{(\gamma-1)/\gamma}$$

the temperature difference for the isentropic process becomes

$$T_{01} - T_{02s} = T_{01} \left[1 - \left(\frac{p_{02}}{p_{01}} \right)^{(\gamma-1)/\gamma} \right]$$

Letting

$$x = 1 - \left(\frac{p_{02}}{p_{01}} \right)^{(\gamma-1)/\gamma} \quad \text{then} \quad T_{01} - T_{02s} = xT_{01}$$

The actual temperature drop is then

$$T_{01} - T_{02} = \eta_s x T_{01} \quad \text{so that} \quad T_{02} = T_{01}(1 - \eta_s x)$$

Assuming that the pressure ratio and the efficiency are the same for each stage, similar analysis for the next stage gives

$$T_{02} - T_{03} = \eta_s x T_{02} \quad \text{so that} \quad T_{03} = T_{02}(1 - \eta_s x) = T_{01}(1 - \eta_s x)^2$$

and for the Nth stage,

$$T_{0,N} - T_{0,N+1} = \eta_s x T_{0,N} \quad \text{so that} \quad T_{0,N+1} = T_{01}(1 - \eta_s x)^N$$

The work delivered by the entire turbine can then be expressed as

$$w = c_p(T_{01} - T_{02}) + c_p(T_{02} - T_{03}) + \cdots + c_p(T_{0,N} - T_{0,N+1}) = c_p(T_{01} - T_{0,N+1})$$

which can be written as

$$w = c_p T_{01} [1 - (1 - \eta_s x)^N]$$

The isentropic work by the entire turbine is given by this same equation when $\eta_s = 1$, or

$$w_s = c_p T_{01} [1 - (1 - x)^N]$$

The isentropic work can also be written as

$$w_s = c_p T_{01} \left[1 - \left(\frac{p_{0,N+1}}{p_{01}} \right)^{(\gamma-1)/\gamma} \right]$$

and therefore,

$$\eta = \frac{w}{w_s} = \frac{1 - (1 - \eta_s x)^N}{1 - \left(\frac{p_{0,N+1}}{p_{01}} \right)^{(\gamma-1)/\gamma}}$$

so that the reheat factor becomes

$$\text{RF} = \frac{\eta}{\eta_s} = \frac{1 - (1 - \eta_s x)^N}{\eta_s \left[1 - \left(\frac{p_{0,N+1}}{p_{01}} \right)^{(\gamma-1)/\gamma} \right]}$$

7.6.2 Polytropic or small-stage efficiency

The polytropic process was introduced in Chapter 3. Here, it is used for a small stage. If the stagnation enthalpy change is small across a stage, then the stage efficiency approaches the polytropic efficiency. Consider the situation for which the ideal gas relation is valid and for which an incremental process is as shown in Figure 7.23. The temperature drops for actual and ideal processes are related and given by

$$\eta_p dT_{0s} = dT_0$$

For an isentropic expansion,

$$c_p \frac{dT_{0s}}{T_0} = R \frac{dp_0}{p_0} \quad \text{or} \quad \frac{\gamma}{\eta_p(\gamma-1)} \frac{dT_0}{T_0} = \frac{dp_0}{p_0}$$

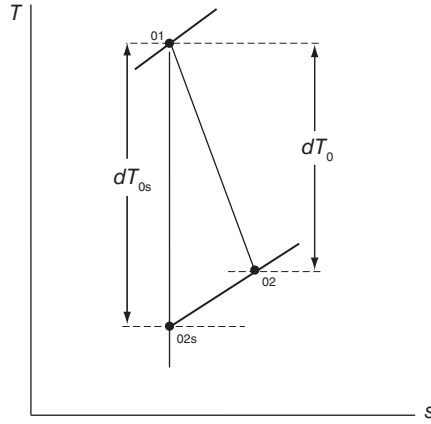


Figure 7.23 Processes across a small stage.

Integrating this between the inlet and the exit gives

$$\frac{T_{0,N+1}}{T_{01}} = \left(\frac{p_{0,N+1}}{p_{01}} \right)^{(\gamma-1)\eta_p/\gamma}$$

The reheat factor can then be written as

$$\text{RF} = \frac{\eta}{\eta_p} = \frac{1 - \left(\frac{p_{0,N+1}}{p_{01}} \right)^{(\gamma-1)\eta_p/\gamma}}{\eta_p \left[1 - \left(\frac{p_{0,N+1}}{p_{01}} \right)^{(\gamma-1)/\gamma} \right]}$$

The relationship between the turbine efficiency and polytropic or small-stage efficiency is

$$\eta = \frac{1 - \left(\frac{1}{r} \right)^{(\gamma-1)\eta_p/\gamma}}{1 - \left(\frac{1}{r} \right)^{(\gamma-1)/\gamma}}$$

in which $r = p_{01}/p_{0e}$ is the overall pressure ratio of the turbine. This relationship is shown in Figure 7.24.

This completes the study of axial turbines, which began in the previous chapter on steam turbines. Wind turbines and some hydraulic turbines are also axial machines. They are discussed later. Many of the concepts introduced in this chapter are carried over to the next one on axial compressors.

EXERCISES

7.1 Combustion gases enter the inlet of a rotor in a single-stage axial-flow turbine at the absolute velocity of 610 m/s. Their direction is 61° as measured from the cascade front in the direction of the blade motion. The values $\gamma = 4/3$ and $c_p = 1148 \text{ kJ}/(\text{kg K})$ are suitable for these gases. At exit of this rotor, the absolute velocity of the fluid is 305 m/s

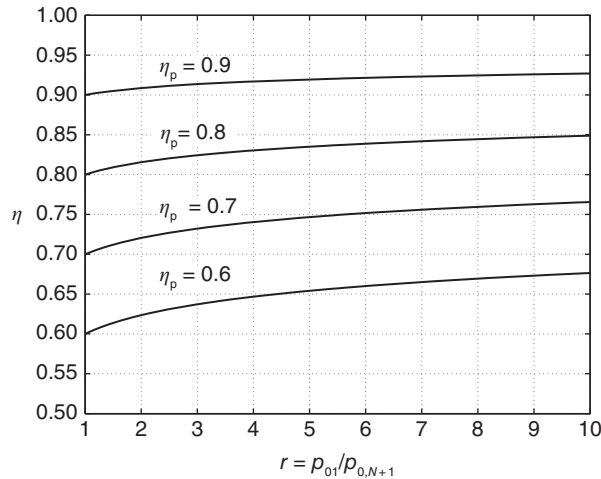


Figure 7.24 Turbine efficiency as a function of pressure ratio and polytropic efficiency for a gas with $\gamma = 1.4$.

directed such that its tangential component is negative. The axial velocity is constant, the blade speed is 305 m/s, and the flow rate through the rotor is 5 kg/s. (a) Construct the rotor inlet and exit velocity diagrams showing the axial and tangential components of the absolute and relative velocities, as well as the flow angles. (b) Evaluate the change in total enthalpy across the rotor. (c) Evaluate the power delivered by the rotor. (d) Evaluate the average driving force exerted on the blades. (e) Evaluate the change in static and stagnation temperature of the fluid across the rotor. (f) Calculate the flow coefficient and the blade-loading coefficient. Are they reasonable? [Ans: (b) 185.48 kJ/kg, (c) 927.4 kW, (d) 3040.6 N, (e) 40 and 161.6 K, (f) 0.97, 2.0]

7.2 Show that for a normal stage

$$\frac{V_2}{U} = \sqrt{\phi^2 + (1 - R + \psi/2)^2} \quad \frac{W_3}{U} = \sqrt{\phi^2 + (R + \psi/2)^2}$$

7.3 A small axial-flow turbine must have an output power of 37 kW when the mass flow rate of combustion gases is 0.5 kg/s, and the inlet total temperature is 410 K. The value of the gas constant is 287 J/(kg K) and $\gamma = 4/3$. The total-to-total efficiency of the turbine is 80%. The rotor operates at 50000 rpm, and the mean blade diameter is 10 cm. Evaluate (a) the average driving force on the turbine blades, (b) the change in the tangential component of the absolute velocity across the rotor, and (c) the required total pressure ratio across the turbine. [Ans: (a) 141.3N, (b) 282.7 m/s, (c) 2.4]

7.4 A turbine stage of a multistage axial turbine is shown in Figure 7.3. The inlet gas angle to the stator is $\alpha_1 = -36.8^\circ$, and the outlet angle from the stator is $\alpha_2 = 60.3^\circ$. The flow angle of the relative velocity at the inlet to the rotor is $\beta_2 = 36.8^\circ$, and the flow leaves at $\beta_3 = -60.3^\circ$. The value of the gas constant is 287 J/(kg K) and $\gamma = 4/3$. (a) Assuming that the blade speed is $U = 220$ m/s, find the axial velocity, which is assumed constant throughout the turbine. (b) Find the work done by the fluid on the rotor blades for one stage. (c) The inlet stagnation temperature to the turbine is 950 K, and the mass flow rate is $\dot{m} = 400$ kg/s. Assuming that this turbine produces a power output of 145 MW,

find the number of stages. (d) Find the overall stagnation pressure ratio, given that its isentropic efficiency is $\eta_{tt} = 0.85$. (e) Why does the static pressure fall across the stator and the rotor? [Ans: (a) 218.9 m/s, (b) 120.4 kJ/kg, (c) 3, (d) 7.2]

7.5 A single-stage axial turbine has a total pressure ratio of 1.5:1, with an inlet total pressure 300 kPa and temperature of 600 K. The absolute velocity at the inlet to the stator row is in the axial direction. The adiabatic total-to-total efficiency is 80%. The relative velocity is at an angle of 30° at the inlet of the Rotor, and at the exit, it is -35° . If the flow coefficient is $\phi = 0.9$, find the blade velocity. Use compressible flow analysis with $c_p = 1148 \text{ J/(kg K)}$, $\gamma = \frac{4}{3}$, and $R = 287 \text{ J/(kg K)}$. [Ans: 215 m/s]

7.6 An axial turbine has a total pressure ratio of 4:1, with an inlet total pressure 650 kPa and total temperature of 800 K. The combustion gases that pass through the turbine have $\gamma = \frac{4}{3}$, and $R = 287 \text{ J/(kg K)}$. (a) Justify the choice of two stages for this turbine, and assume repeating stages, both designed the same way, with the blade-loading coefficient equal to 1.1 and the flow coefficient equal to 0.6. The absolute velocity at the inlet to the stator row is at angle 5° from the axial direction. The adiabatic total-to-total efficiency is 91.0%. Find, (b) the angle at which the absolute velocity leaves the stator, (c) the angle of the relative velocity at the inlet of the rotor, and (d) the angle at which the relative velocity leaves the rotor. (e) Draw the velocity diagrams at the inlet and outlet of the rotor. (f) What are the blade speed and the axial velocity? A consequence of the design is that each stage has the same work output and efficiency. Find, (g) the stage efficiency and (h) the pressure ratio for each stage. [Ans: (b) 62.5° , (c) 14.3° , (d) -57.7° , (f) 333.6 and 200.1 m/s, (g) 0.902, (h) 1.895 and 2.111]

7.7 For a steam turbine rotor, the blade speed at the casing is $U = 300 \text{ m/s}$, and at the hub, its speed is 240 m/s . The absolute velocity at the casing section at the inlet to the rotor is $V_{2c} = 540 \text{ m/s}$, and at the hub section, it is $V_{2h} = 667 \text{ m/s}$. The angle of the absolute and relative velocities at the inlet and exit of the casing and hub sections are $\alpha_{2c} = 65^\circ$, $\beta_{3c} = -60^\circ$, $\alpha_{2h} = 70^\circ$, and $\beta_{3h} = -50^\circ$. The exit relative velocity at the casing is $W_{3c} = 456 \text{ m/s}$ and at the hub, it is $W_{3h} = 355 \text{ m/s}$. For the tip section, evaluate (a) the axial velocity at the inlet and exit; (b) the change in total enthalpy of the steam across the rotor; and (c) the outlet total and static temperatures at the tip and hub, assuming that the inlet static temperature is 540°C and inlet total pressure is 7 MPa, and they are the same at all radii. Assume that the process is adiabatic, and steam can be considered a perfect gas with $\gamma = 1.3$. The static pressure at the exit of the rotor is the same for all radii and is equal to the static pressure at inlet of the hub section. Repeat the calculations for the hub section. (d) Find the stagnation pressure at the outlet at the tip and the hub. (e) Find the reaction at the tip and hub sections. [Ans: (a) 228 m/s, (b) average between tip and hub 166.6 kJ/kg, (c) tip 783.2 and 798.4 K hub 832.0 and 845.3 K, (d) 4368 and 4303 kPa, (e) 0.343 and -0.239 . Note that reaction increases along the blade but is too low at the hub.]

7.8 Combustion gases, with $\gamma = \frac{4}{3}$ and $R = 287 \text{ kJ/(kg K)}$, flow through a repeating turbine stage. The inlet flow angle for a normal stage is $\alpha_1 = 0^\circ$. The flow coefficient is $\phi = 0.52$, and the blade-loading coefficient is $\psi = 1.4$. (a) Draw the velocity diagrams for the stage. (b) Determine the angle at which relative velocity leaves the rotor. (c) Find the flow angle at the exit of the stator. (d) A two-stage turbine has an inlet stagnation temperature of $T_{01} = 1250 \text{ K}$ and blade speed $U = 320 \text{ m/s}$. Assuming that the total-to-total efficiency of the turbine is $\eta_{tt} = 0.89$, find the stagnation temperature of the gas at the exit of the turbine and the stagnation pressure ratio for the turbine. (e) Assuming

that the density ratio across the turbine based on static temperature and pressure ratios is the same as that based on the stagnation temperature and stagnation pressure ratios, find the ratio of the exit cross-sectional area to that of the inlet to the two-stage turbine. [Ans: (b) -62.5° , (c) 69.6° , (d) 1000 K, 2.765, (e) 2.229]

7.9 Steam enters a 10-stage 50%-reaction turbine at the stagnation pressure 0.8 MPa and stagnation temperature 200°C and leaves at pressure 5 kPa and with quality equal to 0.86. (a) Assuming that the steam flow rate is 7 kg/s, find the power output and the overall efficiency of the turbine. (b) The steam enters each stator stage axially with velocity of 75 m/s. The mean rotor diameter for all stages is 1.4 m, and the axial velocity is constant through the machine. Find the rotational speed of the shaft. (c) Find the absolute and relative inlet and exit flow angles at the mean blade height assuming equal enthalpy drops for each stage. [Ans: (a) 4328 kW, 0.812, (b) 3392 rpm, (c) 0° , 73.2° , -73.2° , 0°]

7.10 Combustion gases, with $\gamma = 4/3$ and $R = 287 \text{ kJ}/(\text{kg K})$ enter axially into a normal stage at stagnation temperature $T_{01} = 1200 \text{ K}$ and stagnation pressure $p_{01} = 1500 \text{ kPa}$. The flow coefficient is $\phi = 0.8$, and the reaction is $R = 0.4$. The inlet Mach number to the stator is $M_1 = 0.4$. Find, (a) the blade speed and (b) the Mach number leaving the stator and the relative Mach number leaving the rotor. (c) Using the Zweifel criterion, determine the ratio of spacing to the axial chord. (d) Using the Soderberg loss coefficients, and assuming that $Re = 10^5$, find the efficiency of the stage. (e) Repeat the calculations with inlet Mach number $M_1 = 0.52$ and explain the differences in the results, if any. [Ans: (a) 334.4 m/s, (b) 0.744, 0.675, (c) 0.267, (d) 0.912, (e) 430.9 m/s, 0.99, 0.912]

7.11 Combustion gases, with $\gamma = 4/3$ and $R = 287 \text{ kJ}/(\text{kg K})$, enter the stator of a normal stage at angle 10° . The relative velocity has an angle -40° as it leaves the rotor. The blade-loading factor is 1.6. (a) Determine the exit angle of the flow leaving the stator and the angle of the relative velocity as it enters the rotor. (b) Find the degree of reaction and the flow coefficient. (c) Calculate the total-to-total efficiency using Soderberg correlations. Take the blade height to axial chord ratio to be $b/c_x = 3.5$. (d) Determine the stagnation pressure loss across the stator, given that the inlet conditions are $T_{01} = 700 \text{ K}$ and $p_{01} = 380 \text{ kPa}$, and the velocity after the stator is $V_2 = 420 \text{ m/s}$. [Ans: (a) 61.0° and 38.1° , (b) 0.026 and 0.985, (c) 0.903, (d) 9.95 kPa]

7.12 Show that the total-to-static efficiency can be expressed as

$$\frac{1}{\eta_{ts}} = \frac{1}{\eta_{tt}} + \frac{\phi^2}{2\psi \cos^2 \alpha_3}$$

What kind of approximation is needed to arrive at this result?

7.13 Consider the Example 7.3. Assume that the gap between the blades is one quarter of the average width of the stator and rotor blades and that the blade width is one third its height. Find the angle at which the casing of the stage is increasing. [Ans: 25°]

7.14 For Example 7.6, write a computer program to calculate the mass flow rate and plot the blade angles as shown in Figure 7.8.

7.15 For Example 7.6, write a computer program to (a) calculate and plot the variation of the reaction from the hub to the casing at the inlet and exit to the rotor. Define the nondimensional abscissa as $\bar{r}_2 = (r_2 - r_{2h})/(r_{2c} - r_{2h})$, and $\bar{r}_3 = (r_3 - r_{3h})/(r_{3c} - r_{3h})$. (b) Calculate and plot the blade-loading coefficient similarly. [Ans: (a) $R_{2h} = 0.2040$,

$R_{2c} = 0.6099$, $R_{3h} = 0.1303$, and $R_{3c} = 0.6325$, (b) $\psi_{2h} = 2.506$, $\psi_{2c} = 1.228$, $\psi_{3h} = 2.738$, and $\psi_{3c} = 1.157$

7.16 For a normal turbine stage, the exit blade angle of the stator at 70° and relative velocity has angle -60° as it leaves the rotor. For a range of flow coefficients $\phi = 0.2 - 0.8$, calculate and plot the gas exit angle from the rotor, the angle the relative velocity makes as it leaves the stator, the blade-loading coefficient, and the degree of reaction. Comment on what is a good operating range and what are the deleterious effects in flow over the blades if the mass flow rate is reduced too much, or if it is increased far beyond this range.

7.17 Combustion gases, with $\gamma = 4/3$ and $c_p = 1148 \text{ kJ/(kg K)}$, enter into a normal stage with a degree of reaction 50%. The ratio of the blade speed to the absolute velocity at the inlet is $U/V_2 = 0.75$, and the flow angle of the relative velocity is $\beta_2 = 34^\circ$. The shaft speed is 12000 rpm. The inlet stagnation temperature is $T_{01} = 1400 \text{ K}$, and stagnation pressure is $p_{01} = 2200 \text{ kPa}$. Find the stagnation pressure ratio across this stage if the total-to-total efficiency is $\eta_{tt} = 0.92$. [Ans: 1.604]

7.18 Combustion gases with $\gamma = 4/3$ and $c_p = 1148 \text{ kJ/(kg K)}$ flow through a turbine. The inlet stagnation temperature is $T_{01} = 1400 \text{ K}$, and stagnation pressure is $p_{01} = 1100 \text{ kPa}$. Blade speed is $U = 300 \text{ m/s}$, and the blade height to axial chord ratio is $b/c_x = 3.5$. The axial velocity is not constant, and the flow coefficients for the stator is $\phi_2 = V_{x2}/U = 0.50$. For the rotor it is $\phi_3 = V_{x3}/U = 0.56$. The absolute velocity enters the rotor at the angle $\alpha_2 = 68^\circ$, and the relative velocity leaves it at angle $\beta_3 = -65^\circ$. Assuming that $Re = 10^5$ and using the Soderberg correlations to establish the loss coefficients, find the areas entering the rotor and leaving the rotor. [Ans: $A_2 = 0.0434 \text{ m}^2$ and $A_3 = 0.0450 \text{ m}^2$]

7.19 Combustion gases with $\gamma = 4/3$ and $R = 297 \text{ kJ/(kg K)}$, enter a normal single stage turbine with stagnation temperature $T_{01} = 1100 \text{ K}$. At the inlet to the rotor, the absolute velocity is $V_2 = 400 \text{ m/s}$, and flow angle is $\alpha_2 = 79^\circ$. The relative velocity at the exit of the stage is $W_3 = -310 \text{ m/s}$, and the flow angle is $\beta_3 = -65^\circ$. (a) Find the flow coefficients $\phi_1 = V_{x1}/U$, $\phi_2 = V_{x2}/U$, and $\phi_3 = V_{x3}/U$ and the blade-loading coefficient. (b) Find the temperature after the stage. [Ans: (a) $\phi = 0.578$, $\phi_2 = 0.547$, $\phi_3 = 0.578$, $\psi = 1.744$, (b) 994.4 K]

7.20 In a normal single-stage turbine, the gas with $\gamma = 4/3$ and $R = 287 \text{ kJ/(kg K)}$ enters the rotor at angle $\alpha_2 = 74.5^\circ$. The blade-loading coefficient is $\psi = 1.8$, and the flow coefficients are $\phi_2 = 0.50$ and $\phi_3 = 0.52$. The blade speed is $U = 340 \text{ m/s}$. (a) Find the reaction. (b) Find the flow angles of the absolute and relative velocities. (c) Find the Mach number M_2 if the flow entering the stage is $T_{01} = 1100 \text{ K}$. (d) Find the velocity entering the stator, and calculate the flow coefficient $\phi_1 = V_{x1}/U$ assuming that the flow at the entrance is axial. [Ans: (a) 0.103, (b) $\alpha_3 = 0.3^\circ$, $\beta_2 = 58.1^\circ$, $\beta_3 = -62.5^\circ$, (c) 1.07, (d) 176.8 m/s , $\phi_1 = 0.52$]

7.21 In a normal single-stage turbine, the gas with $\gamma = 4/3$ and $R = 287 \text{ kJ/(kg K)}$ leaves the rotor axially. The blade-loading coefficient is $\psi = 1.8$, and the flow coefficients are $\phi_2 = 0.7$ and $\phi_3 = 0.72$. The blade speed is $U = 220 \text{ m/s}$. (a) Find the reaction. (b) Find the flow angles of the absolute and relative velocities. (c) Find the Mach number M_2 if the flow entering the stage is $T_{01} = 1100 \text{ K}$. [Ans: (a) 0.108, (b) $\alpha_2 = 68.7^\circ$, $\beta_2 = 48.8^\circ$, $\beta_3 = -54.2^\circ$, (c) 0.68]

7.22 For a normal turbine stage, fluid enters the stator with the inlet conditions $T_{01} = 1100$ K and $p_{01} = 380$ kPa. The inlet flow angle is -10° , and the velocity after the stator is $V_2 = 420$ m/s. The relative velocity has angle -60° as it leaves the rotor. The blade-loading factor is 1.6. (a) Determine the exit angle of the flow leaving the stator and (b) the angle of the relative velocity as it enters the rotor. (c) Determine the degree of reaction. (d) Calculate the stagnation pressure losses across the stator using Ainley–Mathieson correlations. Take the space to axial chord ratio equal to $s/c_x = 0.75$, and assume that the maximum thickness-to-chord ratio is $t/c = 0.22$. [Ans: (a) 66.6° , (b) 37.1° , (c) 0.313, (d) 3.46]

7.23 Examination of Example 7.8 shows that $Y_N \approx \zeta_N$. Derive an expression that shows that for $\zeta_N \ll 1$,

$$\zeta_N = Y_N \frac{2}{\gamma M_2^2} \left[1 - \left(1 + \frac{\gamma - 1}{2} M_2^2 \right)^{-\gamma/(\gamma-1)} \right]$$

and that for $M_2 \ll 1$, this reduces to $\zeta_N \approx Y_N$.

CHAPTER 8

AXIAL COMPRESSORS

In Chapter 5 it was pointed out that axial compressors are well suited for high flow rates and centrifugal machines are used when a large pressure rise is needed at a relatively low flow rate. To obtain the high flow rate, gas enters the compressor at a large radius. The gas is often atmospheric air and as it is compressed, it becomes denser and the area is reduced from stage to stage, often in such a way that the axial velocity remains constant. As in axial turbines, this may be accomplished by keeping the mean radius constant and by reducing the casing radius and increasing the hub radius. In jet engines, high-pressure ratios are obtained by pairing one multistage compressor with a turbine sufficiently powerful to turn that compressor. This arrangement of a turbine and compressor running on the same shaft is called a *spool*. A two- spool engine has a low pressure (LP) compressor and a turbine to drive it on the separate hollow shaft that is concentric with the shaft of a high-pressure (HP) spool. In a three-spool engine, an intermediate (IP) spool is added. The high and intermediate pressure spools then serve as *gas generators* to provide a flow to an LP turbine that drives the fan in a turbofan jet aircraft or a generator for electricity production in a power plant [77].

The larger LP and IP compressors turn at a lower speed than the HP spool in order to keep the blade speed sufficiently low to ensure that compressibility effects do not deteriorate the performance of the machine. In a typical spool, one turbine stage drives six or seven compressor stages. The stage pressure ratio has increased with improved designs, reaching 1.3 and 1.4 in modern jet engine core compressors [77].

Pipeline compressors are often driven by a power turbine that uses a jet engine spool as the gas generator. Alternatively, a diesel engine may provide the power to the compressor. An industrial compressor manufactured by MAN Diesel & Turbo SE in Germany is shown in Figure 8.1. It has 14 axial stages and one centrifugal compressor stage with shrouded blades.

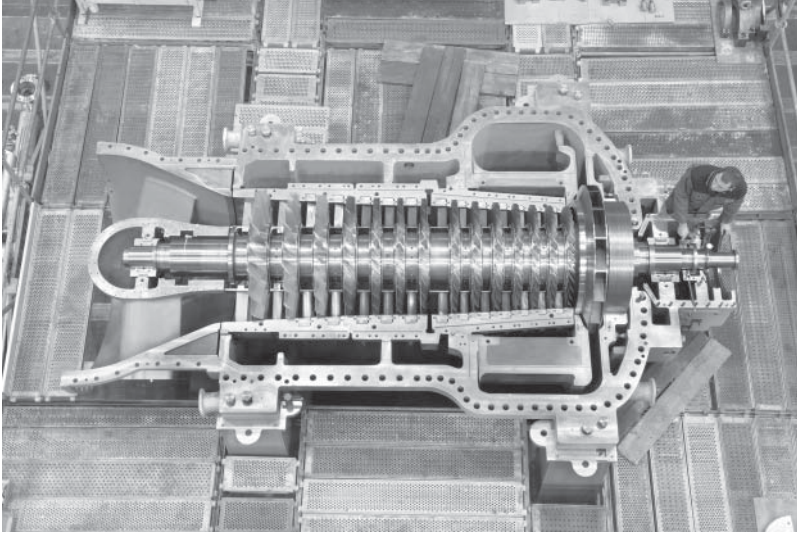


Figure 8.1 A 14-stage axial compressor with a single centrifugal stage. Source: Photo courtesy MAN Diesel & Turbo SE.

The first section of this chapter is on the stage analysis of axial compressors. The theory follows closely that which is discussed in the previous chapter for axial turbines. Then empirical methods for calculating the flow deflection across the stator and rotor are introduced. After that a semiempirical method for allowable diffusion limit is discussed. Too much diffusion leads to separation of boundary layers, which may be catastrophic, with complete deterioration of the compressor performance. Next, the efficiency of a compressor stage is defined, followed by methods to calculate stagnation pressure losses. Three-dimensional effects will receive mention as well. Once the stagnation pressure losses have been related to flow angles, reaction, blade loading, and flow coefficient, an estimate of the stage efficiency can be obtained. The task of a compressor engineer is to use this information to design a well-performing multistage axial compressor.

8.1 COMPRESSOR STAGE ANALYSIS

A compressor stage consists of a rotor that is followed by a stator. In contrast to the flow in turbines, in which pressure decreases in the direction of the flow, in compressors flow is against an adverse pressure gradient. The blade-loading coefficient is kept fairly low in order to prevent separation, with design range $0.35 \leq \psi \leq 0.5$. As a result, the amount of turning is about 20° and does not exceed 45° [19]. A typical range for the flow coefficient is $0.4 \leq \phi \leq 0.7$. If the flow is drawn into the compressor directly from an atmosphere, it enters the first stage axially. However, a set of inlet guide vanes may be used to change the flow angle α_1 to the first stage to a small positive value [18].

8.1.1 Stage temperature and pressure rise

Figure 8.2 shows a typical compressor stage. Since the rotor now precedes the stator, the inlet to the rotor is station 1, and its outlet is station 2. The outlet from the stator is station 3, and for a repeating stage, the flow angles and velocity magnitudes there are equal to those at the inlet to the rotor.

Work done by the blades is

$$w = U(V_{u2} - V_{u1}) \quad (8.1)$$

or

$$w = h_{02} - h_{01} = UV_x(\tan \alpha_2 - \tan \alpha_1) = UV_x(\tan \beta_2 - \tan \beta_1)$$

With $w = c_p(T_{03} - T_{01})$, this can also be expressed in the form

$$\frac{w}{c_p T_{01}} = \frac{\Delta T_0}{T_{01}} = \frac{UV_x}{c_p T_{01}}(\tan \beta_2 - \tan \beta_1)$$

which gives the nondimensional stagnation temperature rise. From the definition of stage efficiency

$$\eta_{tt} = \frac{T_{03s} - T_{01}}{T_{03} - T_{01}}$$

the stage stagnation pressure ratio can be written as

$$\frac{p_{03}}{p_{01}} = \left(1 + \eta_{tt} \frac{\Delta T_0}{T_{01}}\right)^{\gamma/(\gamma-1)}$$

The stage stagnation temperature rise can also be written in the form

$$\frac{\Delta T_0}{T_{01}} = (\gamma - 1) \frac{U}{V_x} \frac{V_x^2}{c_{01}^2} (\tan \beta_2 - \tan \beta_1)$$

For axial entry, V_x is the inlet velocity. In terms of the flow coefficient and stagnation Mach number, defined as

$$\phi = \frac{V_x}{U} \quad M_{01} = \frac{V_x}{c_{01}}$$

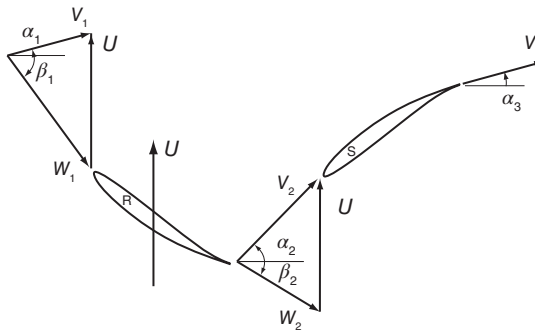


Figure 8.2 A typical axial compressor stage.

and the temperature rise takes the form

$$\frac{\Delta T_0}{T_{01}} = (\gamma - 1) \frac{M_{01}^2}{\phi} (\tan \beta_2 - \tan \beta_1)$$

A typical inlet velocity is $V_x = 150$ m/s, and an inlet stagnation temperature is $T_{01} = 300$ K. The stagnation Mach number is therefore

$$M_{01} = \frac{V_x}{c_{01}} = \frac{150}{\sqrt{1.4 \cdot 287 \cdot 300}} = 0.432$$

The actual Mach number is obtained by noting that

$$M_1 = \frac{V_x}{c_1} = \frac{V_x}{c_{01}} \frac{c_{01}}{c_1} = M_{01} \sqrt{\frac{T_{01}}{T_1}} = M_{01} \left(1 + \frac{\gamma - 1}{2} M_{01}^2 \right)^{1/2}$$

so that

$$M_{01} = \frac{M_1}{\sqrt{1 + \frac{\gamma - 1}{2} M_1^2}} \quad \text{and} \quad M_1 = \frac{M_{01}}{\sqrt{1 - \frac{\gamma - 1}{2} M_{01}^2}}$$

Hence, for this value of the stagnation Mach number, $M_1 = 0.440$. For a flow coefficient $\phi = 0.56$ (and axial entry), the relative velocity is at an angle

$$\begin{aligned} \beta_1 &= \tan^{-1} \left(\frac{W_{u1}}{W_{x1}} \right) = \tan^{-1} \left(-\frac{U}{V_x} \right) = \tan^{-1} \left(-\frac{1}{\phi} \right) \\ &= \tan^{-1} \left(-\frac{1}{0.56} \right) = -60.75^\circ \end{aligned}$$

If the relative velocity is turned by 12° , the exit flow angle is $\beta_2 = -48.75^\circ$. With these values, nondimensional stagnation temperature rise is

$$\begin{aligned} \frac{\Delta T_0}{T_{01}} &= (\gamma - 1) \frac{M_{01}^2}{\phi} (\tan \beta_2 - \tan \beta_1) \\ &= \frac{0.4 \cdot 0.432^2}{0.56} (\tan(-48.75^\circ) - \tan(-60.75^\circ)) = 0.086 \end{aligned}$$

so that the actual stagnation temperature rise is $\Delta T_0 = 25.8^\circ$. Assuming a stage efficiency $\eta_{tt} = 0.9$, the stage pressure rise is

$$\frac{p_{03}}{p_{01}} = (1 + 0.9 \cdot 0.086)^{3.5} = 1.30$$

This falls into the typical range of 1.3–1.4 for core compressors.

The relative Mach number may be quite high at the casing, owing to the large magnitude of the relative velocity there. With $\kappa = r_h/r_c$, the blade speed at the casing is $U_c = 2U/(1 + \kappa)$. Hence, the relative flow angle, for $\kappa = 0.4$, at the casing is

$$\beta_{1c} = \tan^{-1} \left[-\frac{2}{(1 + \kappa)\phi} \right] = \tan^{-1} \left(-\frac{2}{1.4 \cdot 0.56} \right) = -68.6^\circ$$

and the relative mach number is

$$M_{1Rc} = \frac{M_1}{\cos \beta_{1c}} = \frac{0.44}{0.365} = 1.21$$

Hence, the flow is supersonic (or transonic). As has been mentioned earlier, shock losses in transonic flows do not impose a heavy penalty on the performance of the machine and are therefore tolerable. In Figure 8.3 is shown the relative Mach numbers for typical blade speeds and axial velocities and how mild amount of pre-rotation reduces the relative Mach number.

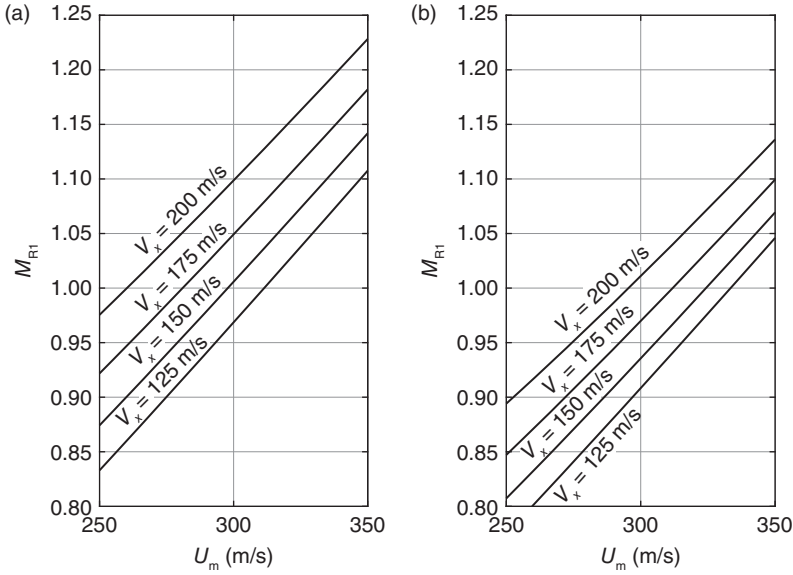


Figure 8.3 Compressor inlet conditions with (a) $\alpha_1 = 0^\circ$ and (b) $\alpha_1 = 10^\circ$.

8.1.2 Analysis of a repeating stage

Equation (8.1) for work can be rewritten in a nondimensional form by dividing both sides by U^2 , leading to

$$\psi = \phi(\tan \alpha_2 - \tan \alpha_1) = \phi(\tan \beta_2 - \tan \beta_1) \quad (8.2)$$

The reaction R is the ratio of the enthalpy increase across the rotor to that over the stage

$$R = \frac{h_2 - h_1}{h_3 - h_1} = \frac{h_3 - h_1 + h_2 - h_3}{h_3 - h_1} = 1 - \frac{h_3 - h_2}{h_3 - h_1}$$

The work done by the blades causes the static enthalpy and kinetic energy (as seen from Figure 8.2) to increase across the rotor. In the stator stagnation enthalpy remains constant, and the static enthalpy and, therefore, also a pressure increases are obtained by decreasing the kinetic energy. In a design in which the areas are adjusted to keep the axial flow constant, the reduction in kinetic energy and increase in pressure result from turning the flow toward the axis. A similar argument holds for the rotor, but now it is the stagnation

enthalpy of the relative flow that is constant. Hence, pressure is increased by turning the relative velocity toward the axis. The velocity vectors in Figure 8.2 show this turning. The amount of turning of the flow through the rotor and stator is quite mild. A large deflection could lead to rapid diffusion and likelihood of stalled blades. Since compression is obtained in both the stator and the rotor, intuition suggests that the reaction ratio ought to be fixed to a value close to 50% in a good design. But in the first two stages, at least, where density is low and blades long, reaction increases from the hub to the casing and the average reaction is made sufficiently large to ensure that the reaction at the hub is not too low.

In Figure 8.4, the thermodynamic states are displayed on a Mollier diagram. The distances that represent the absolute and relative kinetic energies are also shown. The relative stagnation enthalpy across the rotor remains constant at the value $h_{01R} = h_1 + W_1^2/2 = h_2 + W_2^2/2$. The relative Mach number and the relative stagnation temperature are related by

$$\frac{T_{0R}}{T} = 1 + \frac{\gamma - 1}{2} M_R^2$$

and the corresponding stagnation pressure and density are

$$\frac{p_{0R}}{p} = \left(\frac{T_{0R}}{T} \right)^{\gamma/(\gamma-1)} \quad \frac{\rho_{0R}}{\rho} = \left(\frac{T_{0R}}{T} \right)^{1/(\gamma-1)}$$

The loss of stagnation pressure across the rotor is given by $p_{01R} - p_{02R}$. Across the stator, the loss is $p_{02} - p_{03}$.

For the stator $h_{02} = h_{03}$ and therefore

$$h_2 + \frac{1}{2}V_2^2 = h_3 + \frac{1}{2}V_3^2 \quad \text{or} \quad h_3 - h_2 = \frac{1}{2}V_2^2 - \frac{1}{2}V_3^2$$

Since $V_2^2 = V_{x2}^2 + V_{u2}^2$ and $V_3^2 = V_{x3}^2 + V_{u3}^2$ and the axial velocity V_x is constant

$$h_3 - h_2 = \frac{1}{2}(V_{u2}^2 - V_{u3}^2) = \frac{1}{2}V_x^2(\tan^2\alpha_2 - \tan^2\alpha_3)$$

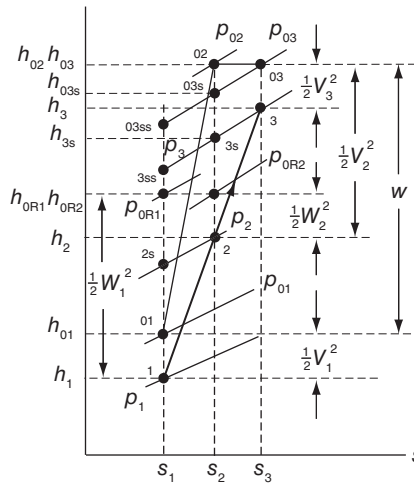


Figure 8.4 A Mollier diagram for an axial compressor stage.

For *normal stage* $V_1 = V_3$ and $h_{03} - h_{01} = h_3 - h_1$. Since no work is done by the stator, across a stage

$$w = h_{03} - h_{01} = h_3 - h_1 = \psi U^2$$

Using these equations the reaction ratio, with $\alpha_1 = \alpha_3$, may be expressed as

$$R = 1 - \frac{V_x^2 (\tan^2 \alpha_2 - \tan^2 \alpha_1)}{U^2 \psi} \quad \text{or} \quad R = 1 - \frac{\phi^2}{2\psi} (\tan^2 \alpha_2 - \tan^2 \alpha_1)$$

Substituting ψ from Eq. (8.2) into this gives

$$R = 1 - \frac{1}{2} \phi (\tan \alpha_2 + \tan \alpha_1) \quad (8.3)$$

Eliminating next α_2 from this, with the help of Eq. (8.2), yields

$$\psi = 2(1 - R - \phi \tan \alpha_1) \quad (8.4)$$

Equations (8.2) – (8.4) are identical to Eqs. (7.5), (7.8), and (7.9) for turbines, provided α_1 is replaced by α_3 . Hence, the flow angles for the stator can be calculated from

$$\tan \alpha_1 = \frac{1 - R - \psi/2}{\phi} \quad \tan \alpha_2 = \frac{1 - R + \psi/2}{\phi} \quad (8.5)$$

Similarly, for the rotor, the flow angles can be determined from

$$\tan \beta_1 = -\frac{R + \psi/2}{\phi} \quad \tan \beta_2 = -\frac{R - \psi/2}{\phi} \quad (8.6)$$

In these four equations, there are seven variables. Thus, once three have been specified, the other four can be determined. For example, specifying R , ψ , and ϕ , it is easy to obtain the flow angles. Suggested design ranges for these have already been mentioned. The situation changes if the axial velocity is not constant because then two flow coefficients need to be introduced. Equations (8.5) and (8.6) no longer hold, and as was done in the previous chapter, the appropriate equations need to be developed. This can be done for a normal stage, and the task is left as an exercise. If the stage is not normal, then the fundamental definitions need to be used.

There are two situations of particular interest. First, for a 50% normal reaction stage, these equations show that

$$\begin{aligned} \tan \alpha_1 &= -\tan \beta_2 & \alpha_1 &= -\beta_2 \\ \tan \alpha_2 &= -\tan \beta_1 & \alpha_2 &= -\beta_1 \end{aligned}$$

and the velocity triangles are symmetric. Second, from Eq. (8.4), it is seen that for axial entry, with $\alpha_1 = 0$, the blade-loading coefficient is related to reaction by $\psi = 2(1 - R)$ and thus it cannot be specified independently of the reaction. If the loading coefficient is to be in the range $0.35 < \psi < 0.5$, the stage would have to be designed for a reaction greater than 50%. But if the flow enters the stator at a small positive angle, then the blade loading can also be reduced by reducing the flow coefficient. The calculations for this situation are illustrated in the following example.

■ EXAMPLE 8.1

A normal compressor stage is designed for an inlet flow angle $\alpha_1 = 15.8^\circ$, reaction $R = 0.63$, and the flow coefficient $\phi = 0.6$. (a) Find the blade-loading factor. (b) Determine the inlet and exit flow angles of the relative velocity to the rotor and the inlet flow angle to the stator.

Solution: (a) The value

$$\psi = 2(1 - R - \phi \tan \alpha_1) = 2(1 - 0.63 - 0.6 \tan(15.8^\circ)) = 0.400$$

for a blade loading coefficient falls into a typical range.

(b) The flow angles are

$$\alpha_2 = \tan^{-1} \left(\frac{1 - R + \psi/2}{\phi} \right) = \tan^{-1} \left(\frac{1 - 0.63 + 0.2}{0.6} \right) = 43.54^\circ$$

$$\beta_1 = \tan^{-1} \left(\frac{-R - \psi/2}{\phi} \right) = \tan^{-1} \left(\frac{-0.63 - 0.2}{0.6} \right) = -54.14^\circ$$

$$\beta_2 = \tan^{-1} \left(\frac{-R + \psi/2}{\phi} \right) = \tan^{-1} \left(\frac{-0.63 + 0.2}{0.6} \right) = -35.61^\circ$$

The rotor turns the relative velocity by $\Delta\beta = \beta_2 - \beta_1 = 18.53^\circ$, and the stator turns the flow by $\Delta\alpha = 27.74^\circ$. These are also in the acceptable range. The velocity triangles in Figure 8.2 were drawn to have these angular values. A similar calculation shows that for a 50% reaction, the blade-loading coefficient would increase to 0.66 and the amount of turning would be 38.34° in both the stator and the rotor. ■

A simple criterion, developed by de Haller, may be used to check whether the flow diffuses excessively [38]. He suggested that the ratios V_1/V_2 and W_2/W_1 should be kept above 0.72. These ratios can be expressed in terms of the flow angles, and for a normal stage, they give the following conditions:

$$\frac{V_1}{V_2} = \frac{\cos \alpha_2}{\cos \alpha_1} > 0.72 \qquad \frac{W_2}{W_1} = \frac{\cos \beta_1}{\cos \beta_2} > 0.72$$

In the foregoing example, when $R = 0.63$

$$\frac{V_1}{V_2} = \frac{\cos \alpha_2}{\cos \alpha_1} = \frac{\cos(43.54^\circ)}{\cos(15.80^\circ)} = 0.75 \qquad \frac{W_2}{W_1} = \frac{\cos \beta_1}{\cos \beta_2} = \frac{\cos(-54.14^\circ)}{\cos(-35.63^\circ)} = 0.72$$

so the de Haller criterion is satisfied. If the reaction is reduced to $R = 0.5$, then for both the rotor and the stator, these ratios are

$$\frac{\cos \alpha_2}{\cos \alpha_1} = \frac{\cos(54.14^\circ)}{\cos(15.80^\circ)} = 0.61$$

and now the de Haller criterion is violated. On the basis of this comparison, the higher reaction keeps the diffusion within acceptable limits.

It has been mentioned that there is another reason why the reaction should be relatively large for the first two stages. Since the gas density there is low, to keep the axial velocity constant through the compressor, a large area and thus long blades are needed. This causes

reaction to vary greatly from the blade root to its tip. To see this, consider again the equation

$$w = U(V_{u2} - V_{u1}) = \Omega(rV_{u2} - rV_{u1})$$

If the tangential velocity distribution is given by free vortex flow for which rV_u is constant, then each blade section does the same amount of work. For a blading of this kind the equation for reaction

$$R = 1 - \frac{1}{2}\phi(\tan \alpha_2 + \tan \alpha_1)$$

may also be written as

$$R = 1 - \frac{V_{u2} + V_{u1}}{2U} = 1 - \frac{C_2 + C_1}{2rU}$$

where $C_1 = rV_{u1}$ and $C_2 = rV_{u2}$. Since $U = rU_m/r_m$, in which subscript m designates a condition at the mean radius, for this flow, the reaction takes the form

$$R = 1 - \frac{A}{r^2}$$

which shows that the reaction is low at the hub and increases along the blades. Thus, if the reaction at the mean radius is to be 50%, then low reaction at the hub causes a large loading and greater deflection of the flow. This leads to a greater diffusion.

If guide vanes are absent, the flow enters the stage axially. Hence, $\alpha_1 = 0$ and Eq. (8.4) reduces to $\psi = 2(1 - R)$. When this is substituted into Eqs. (8.5) and (8.6), the following relations are obtained:

$$\tan \alpha_2 = \frac{2(1 - R)}{\phi} \quad \tan \beta_1 = -\frac{1}{\phi} \quad \tan \beta_2 = -\frac{2R - 1}{\phi}$$

Two of the parameters could now be assigned values and the rest calculated from these equations.

Another way to proceed is to use the de Haller criterion for the rotor flow angles and set

$$\frac{\cos \beta_1}{\cos \beta_2} = \sqrt{\frac{\phi^2 + (2R - 1)^2}{\phi^2 + 1}} = D_R \quad (8.7)$$

in which $D_R = 0.72$, or slightly larger than this. This method of designing a stage is discussed in the next example.

■ EXAMPLE 8.2

A compressor stage is to be designed for axial entry and a reaction $R = 0.82$. Use the de Haller criterion to fix the flow angles for the stage design.

Solution: With $\alpha_1 = 0$ and $R = 0.82$, the blade loading coefficient is $\psi = 0.36$. Using the de Haller criterion, with $D_R = 0.72$, for limiting the amount of diffusion in the rotor, the flow coefficient can be solved from Eq. (8.7). This yields

$$\phi = \sqrt{\frac{D_R^2 - (2R - 1)^2}{1 - D_R^2}} = \sqrt{\frac{0.72^2 - (2 \cdot 0.82 - 1)^2}{1 - 0.72^2}} = 0.4753$$

The remaining calculations give

$$\alpha_2 = \tan^{-1} \left(\frac{2 - 2R}{\phi} \right) = \tan^{-1} \left(\frac{0.36}{0.4753} \right) = 37.14^\circ$$

$$\beta_1 = \tan^{-1} \left(-\frac{1}{\phi} \right) = \tan^{-1} \left(-\frac{1}{0.4753} \right) = -64.58^\circ$$

$$\beta_2 = \tan^{-1} \left(\frac{1 - 2R}{\phi} \right) = \tan^{-1} \left(-\frac{0.64}{0.4753} \right) = -53.40^\circ$$

Thus, the de Haller criterion for the stator becomes

$$D_S = \frac{\cos \alpha_2}{\cos \alpha_1} = \frac{\cos(37.14^\circ)}{\cos(0^\circ)} = 0.797$$

and for the rotor, it is

$$D_R = \frac{\cos \beta_1}{\cos \beta_2} = \frac{\cos(-64.58^\circ)}{\cos(-53.40^\circ)} = 0.720$$

in agreement with its specified value. The deflection across the stator is $\Delta\alpha = 37.14^\circ$, and across the rotor it is $\Delta\beta = -53.40^\circ + 64.58^\circ = 11.18^\circ$. ■

The velocity triangles of the foregoing example, drawn with U as a common side, are shown in Figure 8.5. The example shows that even if the flow turns by a greater amount through the stator, it diffuses less than in the rotor. The reason is that the turning takes place at a low mean value of α . In fact, were the flow to turn from, say, -10° to 10° , there would be no diffusion at all, because the magnitude of the absolute velocity would be the same before and after the stator. Thus, it is the higher stagger of the rotor that leads to large diffusion even at low deflection. For this reason, the de Haller criterion needs to be checked.

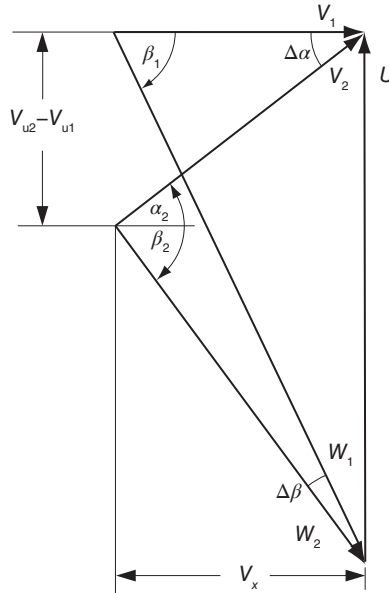


Figure 8.5 Velocity triangles on a common base for an axial compressor stage.

The deflection, represented by the change in the swirl velocity, is shown as the vertical distance in the top left of the diagram. Dividing it by the blade speed gives the loading coefficient. The ratio of the horizontal V_x to blade speed is the flow coefficient. Thus, a glance at the horizontal width of the triangles and comparison with the blade speed shows that the flow coefficient is slightly less than 0.5. The extents of turning across the stator and the rotor are shown as angles $\Delta\alpha$ and $\Delta\beta$, respectively. The decrease in magnitude of the velocity across the stator is slightly larger than the length of the side opposite to the angle $\Delta\beta$ in the triangle with sides W_1 and W_2 . Similarly, the length of the side opposite to the angle $\Delta\alpha$ in the triangle with V_1 and V_2 as its sides indicates the extent of reduction of the relative velocity. Hence, inspection confirms that even a slight turning may lead to a large diffusion when the blades are highly staggered.

8.2 DESIGN DEFLECTION

Figure 8.6 shows typical results from experiments carried out in a cascade tunnel [44]. It shows the deflection and losses from irreversibilities for a given blade as a function of incidence. The incidence is $i = \alpha_2 - \chi_2$, in which χ_2 is the metal angle. The losses increase with both positive and negative incidence, but there is a large range of incidence for which the losses are quite low. The deflection increases with incidence up to the stalling incidence ε_s , at which the maximum deflection is obtained. At this value, losses have reached about twice their minimum value. This correspondence is not exact, but since the losses increase rapidly beyond this, a stage is designed for a nominal deflection of $\varepsilon^* = 0.8\varepsilon_s$, which also corresponds to an incidence at which the loss is near its minimum. As shown in the figure, at this condition, the incidence is slightly negative. But for another cascade, it may be zero, or slightly positive. The loss coefficients have been defined as

$$\omega_R = \frac{\Delta p_{0LR}}{\frac{1}{2}\rho_1 W_1^2} \quad \omega_S = \frac{\Delta p_{0LS}}{\frac{1}{2}\rho_2 V_2^2}$$

These are closely related to the loss coefficients Y_R and Y_S , defined by

$$Y_R = \frac{\Delta p_{0LR}}{p_{01R} - p_1} \quad Y_S = \frac{\Delta p_{0LS}}{p_{02} - p_2}$$

because at low Mach numbers, the denominators may be replaced by $p_{01R} - p_1 = \frac{1}{2}\rho_1 W_1^2$ and $p_{02} - p_2 = \frac{1}{2}\rho_2 V_2^2$. The stagnation and static pressures can be measured in a cascade tunnel.

The conclusion from a large number of experiments is that the nominal deflection is mainly a function of the gas outlet angle and the space-chord ratio of the cascade. The camber and incidence are additive and both contribute to the size of the flow deflection. For the cascade shown in Figure 8.6, the nominal deflection is 30° with incidence at -4° . Thus, the camber is quite low, making the blades rather flat. From such experiments, a universal correlation was developed by Howell [44]. It is shown in Figure 8.7, and it relates the deflection to the exit angle with solidity $\sigma = c/s$ as a parameter. Solidity is the ratio of the length of the blade chord to the spacing of the blades. It increases with reduced spacing, and the term suggests that in this case, the solid blades fill the flow annulus more than the open passages. As the solidity increases, the flow follows the blades better.

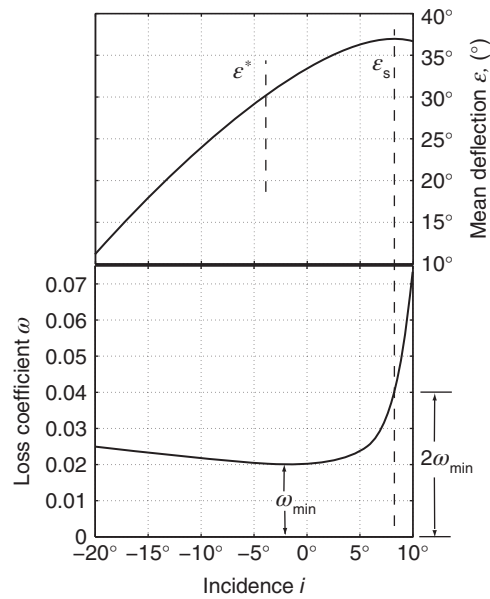


Figure 8.6 Mean deflection and stagnation loss coefficient as a function of incidence. Source: Drawn after Howell [43].

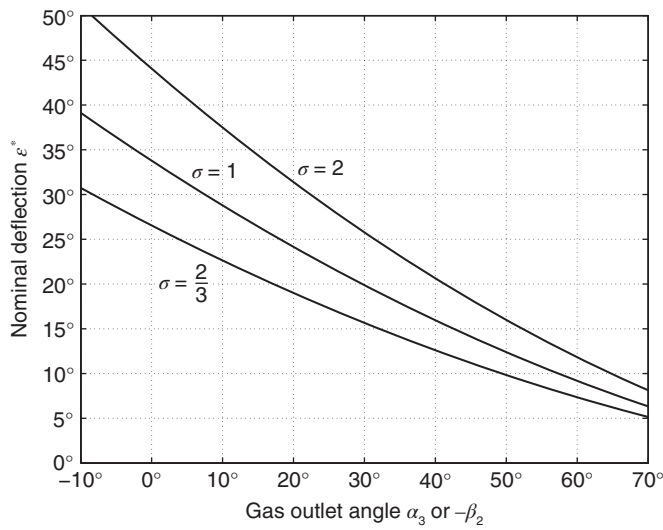


Figure 8.7 Nominal deflection as a function of gas outlet angle and solidity. Source: Drawn after Howell [44].

A curve fit for the nominal deflection, suitable for computer calculations, is

$$\begin{aligned} \varepsilon^* = & (-3.68\sigma^2 + 17.2\sigma + 4.3) \left(\frac{\alpha_3^*}{100} \right)^2 + (12.6\sigma^2 - 54.3\sigma - 10.0) \frac{\alpha_3^*}{10} \\ & - 8.7\sigma^2 + 36.4\sigma + 6.1 \end{aligned} \quad (8.8)$$

For example, for a cascade with $\sigma = 1.2$, if the relative velocity leaves the rotor at angle $\alpha_3 = 30^\circ$, the nominal deflection is $\varepsilon^* = 21.92^\circ$. For a cascade with solidity $\sigma = \frac{2}{3}$ and the flow leaving the stator at $\alpha_3 = -10^\circ$, the nominal deflection is $\varepsilon^* = 30.7^\circ$. For a given ε^* and α_3 , this equation is quadratic in σ . Its solution has an extraneous root with a value greater than 3, and it needs to be rejected.

This equation can also be used to calculate the deflection across a rotor by replacing α_3 with $-\beta_2$. The two examples worked out earlier in this chapter show that the deflection is larger across the stator than across rotor and that the angle at which the gas leaves the stator is not large. The flow over the rotor is turned less, and the absolute value of its exit angle is quite large. These are consistent with the results shown in Figure 8.7.

An alternative to Eq. (8.8) is the *tangent difference formula*, which for the rotor is

$$\tan \beta_2^* - \tan \beta_1^* = \frac{1.55}{1 + 1.5/\sigma_R} \quad (8.9)$$

and a similar equation

$$\tan \alpha_2^* - \tan \alpha_3^* = \frac{1.55}{1 + 1.5/\sigma_S} \quad (8.10)$$

holds for a stator. They provide a quick way to calculate the nominal deflection and fit the data well over most of the outlet angles. At low deflections, they underpredict the deflection, by about 3° at $\alpha_3^* = -10^\circ$ and low solidity. Indeed, at $\alpha_3^* = -10^\circ$ and $\sigma = \frac{2}{3}$ the tangent difference formula gives $\varepsilon^* = 26.7^\circ$, whereas Eq. (8.8) yields 30.7° . Typically, the flow does not leave the stator at negative angle so that such exit angles are just outside the range of usual designs.

For a normal stage with constant axial velocity, the nondimensional equation for work is

$$\psi = \phi(\tan \alpha_2 - \tan \alpha_1) = \phi(\tan \beta_2 - \tan \beta_1)$$

The tangent difference formulas now show that the solidity for the rotor is the same as that for the stator, as the design is based on nominal conditions. It is determined by solving

$$\frac{\psi^*}{\phi^*} = \frac{1.55}{1 + 1.5/\sigma}$$

for σ . In order to prevent resonance vibrations, the number of blades in the rotor is slightly different from the number of stator blades. Thus, the spacing is changed, but the same solidity can still be achieved by changing the length of the chord.

■ EXAMPLE 8.3

A normal compressor stage is designed to have the flow leave the stator at the angle $\alpha_1 = 12.60^\circ$. Assume that the optimum design condition for least losses is achieved when the reaction is $R = 0.68$, and the flow coefficient is $\phi = 0.56$. For a normal

stage, find the blade loading factor and the optimum value for the solidity. Check also that the de Haller criterion is satisfied.

Solution: The loading coefficient is first determined from

$$\psi = 2(1 - R - \phi \tan \alpha_1) = 2(1 - 0.68 - 0.56 \tan(12.6^\circ)) = 0.39,$$

and the flow angles are

$$\begin{aligned}\alpha_2 &= \tan^{-1} \left(\frac{1 - R + \psi/2}{\phi} \right) = \tan^{-1} \left(\frac{1 - 0.68 + 0.195}{0.56} \right) = 42.59^\circ \\ \beta_1 &= \tan^{-1} \left(\frac{-R - \psi/2}{\phi} \right) = \tan^{-1} \left(\frac{-0.68 - 0.195}{0.56} \right) = -57.38^\circ \\ \beta_2 &= \tan^{-1} \left(\frac{-R + \psi/2}{\phi} \right) = \tan^{-1} \left(\frac{-0.68 + 0.195}{0.56} \right) = -40.91^\circ\end{aligned}$$

The deflections are therefore

$$\varepsilon_S^* = 30.00^\circ \quad \varepsilon_R^* = 16.47^\circ$$

The diffusion factors are

$$\frac{\cos \alpha_2}{\cos \alpha_1} = \frac{\cos(42.60^\circ)}{\cos(12.60^\circ)} = 0.754 \quad \frac{\cos \beta_1}{\cos \beta_2} = \frac{\cos(-57.38^\circ)}{\cos(-40.90^\circ)} = 0.713$$

so that the diffusion in the rotor is marginally too high. If the solidity is calculated from the tangent difference formula, it yields

$$\sigma = \frac{1.5 \psi}{1.55 \phi - \psi} = 1.22$$

■

The values of ϕ , ψ , and R vary across the span, owing to the change in the blade velocity with the radius, and ψ tends to be high near the hub and low near the casing. The reaction is low near the hub and high near the casing, as R moves in opposite direction to the loading coefficient. The blade angles are adjusted to counteract the natural tendency that causes the values to change so that the loading can be kept more uniform. A 50% reaction ratio is common, and the blade-loading coefficient is typically in the range $0.3 < \psi < 0.45$.

8.2.1 Compressor performance map

Compressor blades tend to be quite thin, with maximum thickness-to-chord ratio of 5%. If the solidity is high, the blades guide the flow well. An operating condition in which the flow coefficient, ϕ_0 , is larger than its design value, ϕ_d , is shown in Figure 8.8. It is seen that an increase in the flow rate causes a decrease in the blade-loading coefficient. This effect becomes amplified downstream as the density does not change according to design, and the difference cumulates from stage to stage. This subject is discussed by Cumpsty [18], who shows that the last stage is one that is likely to choke. Similarly, examination of Figure 8.8 shows that if the flow coefficient decreases, then the blade loading coefficient increases. The blades now become susceptible to stall, and the last stage controls the stall margin.

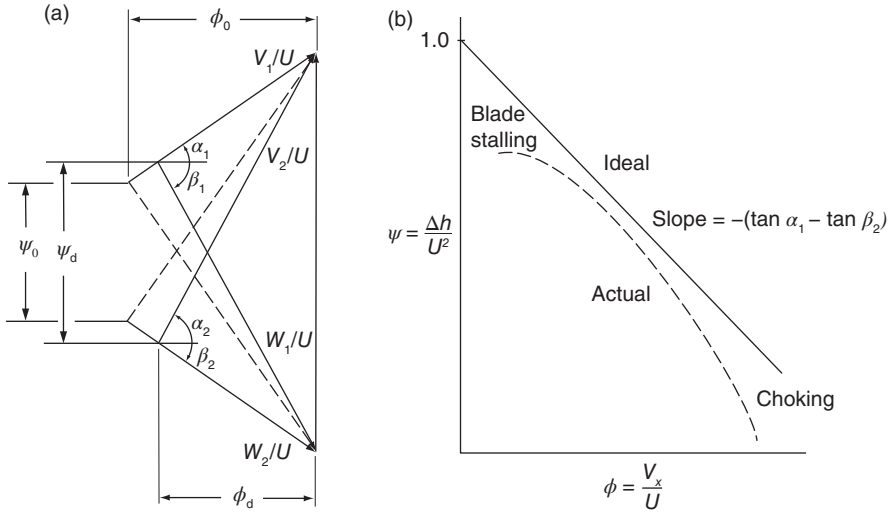


Figure 8.8 Normalized velocity triangles at design and off-design conditions and (b) their operating characteristics.

This reasoning can be carried out analytically by rewriting the Euler equation of turbomachinery

$$w = U(V_{u2} - V_{u1})$$

into a different form. Substituting

$$V_{u2} = U + W_{u2}$$

into the previous equation gives

$$w = U(U + W_{u2} - V_{u1}) = U[U - V_x(\tan \alpha_1 - \tan \beta_2)]$$

and dividing next each term by U^2 gives

$$\psi = 1 - \phi(\tan \alpha_1 - \tan \beta_2)$$

For a normal stage, the exit angle from the stator is α_1 , and the exit angle of the relative velocity from the rotor is β_2 . These then tend to remain constant even at off-design conditions. Furthermore, the latter angle is usually negative so that the term in parentheses is positive. With the trigonometric factors constant, this means that increasing the flow coefficient decreases the loading.

This equation gives the compressor characteristic for an ideal compressor. It is a straight-line with a negative slope when the blade-loading coefficient is plotted against the flow coefficient. This is shown in Figure 8.8b. The actual compressor characteristic is also shown, and the differences away from the design point are caused by irreversibilities. Far away from the design point to the left, the blades stall, and at even lower flow rates (smaller ϕ), the compressor may experience surge. This means that the flow can actually reverse its direction and flow out of the front of the compressor. For this reason, compressors are operated some distance away from the stall line. To the right of the design point, irreversibilities again cause deviation from the theoretical curve, and as the flow rate increases, the blade row will choke.

8.3 RADIAL EQUILIBRIUM

The mean line analysis on which most of the calculations in this text are based ignores the cross-stream variation in the flow. In axial-flow machines, this means that only the influence of the blade speed, that increases with radius, is taken into account. Today, it is possible to carry out calculations by computational fluid dynamics (CFD) methods to resolve the three-dimensional aspects of the flow. However, as was seen in the discussion of axial turbines, the elementary radial equilibrium theory advances the understanding on how the important variables, such as the reaction and the loading, vary from the hub to the casing. There (and in Appendix A) it is shown that the principal equation to be solved is

$$\frac{dh_0}{dr} = T \frac{ds}{dr} + V_x \frac{dV_x}{dr} + V_u \frac{dV_u}{dr} + \frac{V_u^2}{r} \quad (8.11)$$

The first term on the right represents the entropy variation in the radial direction. Owing to the entropy production in the endwall boundary layers, tip vortices, and possible shocks, this is likely to be important near the walls. However, if the flow mixes well in the radial direction, entropy gradients diminish and it may be reasonable to neglect this term. Of course, irreversibilities would still cause entropy to increase in the downstream direction, even if it does not have radial gradients.

The stagnation enthalpy is uniform at the entrance to the first row of rotor blades, and if every blade section does an equal amount of work on the flow, it will remain uniform even if the stagnation enthalpy increases in the direction of the stream. As a consequence, the term on the left side of this equation may be neglected, and the equation reduces to

$$V_x \frac{dV_x}{dr} + V_u \frac{dV_u}{dr} + \frac{V_u^2}{r} = 0 \quad (8.12)$$

This is a relationship between the velocity components V_u and V_x . If the radial variation of one of them is assumed, the variation of the other is obtained by solving this equation. For example, as was seen in the discussion of axial turbines, if the axial component V_x is assumed to be uniform, then the radial component must satisfy the equation

$$\frac{dV_u}{V_u} = -\frac{dr}{r}$$

the solution of which is $rV_u = \text{constant}$. This is the *free vortex* velocity distribution. Before and after a row of blades, the tangential velocity is

$$V_{u1} = \frac{c_1}{r} \quad V_{u2} = \frac{c_2}{r}$$

It was observed earlier that the expression for work is now

$$w = U(V_{u2} - V_{u1}) = r\Omega \left(\frac{c_2}{r} - \frac{c_1}{r} \right) = \Omega(c_2 - c_1)$$

so that the work is independent of radius. This justifies dropping the term dh_0/dr in Eq. (8.11).

8.3.1 Modified free vortex velocity distribution

The free vortex velocity distribution is a special case of the family of distributions

$$V_{u1} = cr^n - \frac{d}{r} \quad V_{u2} = cr^n + \frac{d}{r} \quad (8.13)$$

in which n is a parameter. Regardless of the value of n , each member of this family has a velocity distribution for which each blade section does an equal amount of work, as seen from

$$w = U(V_{u2} - V_{u1}) = \Omega r \left(\frac{d}{r} + \frac{d}{r} \right) = 2\Omega d$$

With the mean radius r_m , the same at the inlet and the exit, a nondimensional radius may be introduced as $y = r/r_m$. The tangential velocity components for a free vortex distribution with $n = -1$ may now be written as

$$V_{u1} = \frac{a}{y} - \frac{b}{y} = \frac{a-b}{y} \quad V_{u2} = \frac{a}{y} + \frac{b}{y} = \frac{a+b}{y}$$

When the Eq. (8.12) for radial equilibrium is recast into the form,

$$V_x \frac{dV_x}{dy} = -\frac{V_u}{y} \frac{d}{dy}(yV_u)$$

it shows that for this velocity distribution right-hand side (RHS) vanishes at the inlet, as the substitution shows

$$V_x \frac{dV_x}{dy} = -\frac{a-b}{y^2} \frac{d(a-b)}{dy} = 0 \quad V_x \neq V_x(y)$$

Clearly, the same result is obtained for the outlet, as only the sign of b needs to be changed to describe the tangential velocity there. This reduced equation now shows that the axial velocity is constant along the span of the blade, but it does not follow that it has the same constant value before and after the blade row. The axial velocities can be made the same by proper taper of the flow channel.

The reaction is given by

$$R = 1 - \frac{1}{2} \frac{V_x}{U} (\tan \alpha_2 + \tan \alpha_1) = 1 - \frac{1}{2} \frac{V_{u2} + V_{u1}}{U_m y}$$

Here $U = r\Omega = rU_m/r_m$, or $U = U_m y$ was used. Since $V_{u2} + V_{u1} = 2a/y$, the reaction is

$$R = 1 - \frac{a}{U_m y^2}$$

If R_m is the reaction at the mean radius $y = 1$, then $a = U_m(1 - R_m)$ and the reaction can be written as

$$R(y) = 1 - (1 - R_m) \frac{1}{y^2}$$

The parameter b can be related to the work done. From

$$w = U(V_{u2} - V_{u1}) = 2U_m b$$

and $b = w/2U_m = \frac{1}{2}\psi_m U_m$, in which $\psi_m = w/U_m^2$.

Another way to represent the data is to introduce a nondimensional radial coordinate $z = (r - r_h)/(r_c - r_h)$, so that

$$z = \frac{1 + \kappa}{1 - \kappa} \frac{y}{2} - \frac{\kappa}{1 - \kappa}$$

in which $\kappa = r_h/r_c$. Clearly, the hub is now at $z = 0$ and the casing, at $z = 1$. The variation in the reaction as a function of this variable is shown in Figure 8.9, for the hub to tip radius ratio is $\kappa = 0.4$, and for values of the mean reaction in the range $0.5 \leq R_m \leq 0.8$. The graphs show that increasing the mean reaction lifts the negative reaction at the hub to a positive value.

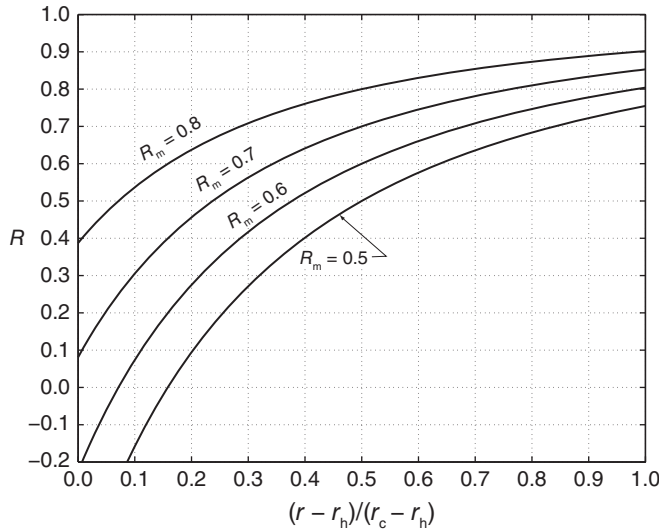


Figure 8.9 Reaction as a function of the radial position on the blade for a free vortex velocity distribution for $\kappa = 0.4$.

Since the axial velocity is constant, the mean flow angles are given by Eqs. (8.5) and (8.6) for specified values of reaction, flow coefficient, and blade-loading coefficient. In this flow, the flow coefficient and blade-loading coefficient vary along the blade only because the blade speed varies. Their local values, and that of the reaction, are given by

$$\phi = \frac{\phi_m}{y} \quad \psi = \frac{\psi_m}{y^2} \quad R = 1 - (1 - R_m) \frac{1}{y^2}$$

The angles are then obtained from

$$\begin{aligned} \alpha_1 &= \tan^{-1} \left(\frac{1 - R - \psi/2}{\phi} \right) & \beta_1 &= \tan^{-1} \left(-\frac{R + \psi/2}{\phi} \right) \\ \alpha_2 &= \tan^{-1} \left(\frac{1 - R + \psi/2}{\phi} \right) & \beta_2 &= \tan^{-1} \left(-\frac{R - \psi/2}{\phi} \right) \end{aligned}$$

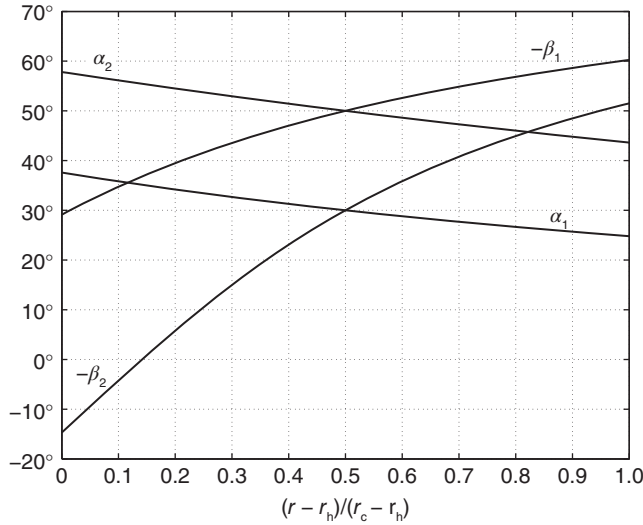


Figure 8.10 Flow angles as a function of the radial position on the blade for a free vortex velocity distribution for a stage with $\kappa = 0.6$. At the mean radius $R_m = 0.5$, $\alpha_{1m} = 30^\circ$ and $\beta_{1m} = -50^\circ$, $\alpha_{2m} = 50^\circ$ and $\beta_{2m} = -30^\circ$, with $\phi_m = 0.565$ and $\psi_m = 0.347$.

They are shown in Figure 8.10 for the situation for which $R_m = 0.5$, $\alpha_{1m} = 30^\circ$, $\beta_{1m} = -50^\circ$, $\alpha_{2m} = 50^\circ$, and $\beta_{2m} = -30^\circ$. This stage is a typical one deeper into the compressor, where blades are shorter ($\kappa = 0.6$) and reaction can be kept at 50% without becoming negative at the hub. In fact, the reaction at the hub is $R_h = 0.111$, and the blade-loading coefficient and flow coefficient are $\psi_h = 0.617$ and $\phi_h = 0.754$. The relative flow undergoes a large deflection at the hub of the rotor, as the flow angle changes by 43.8° . Furthermore, as the hub is approached, β_2 changes sign, and at $(r - r_h)/(r_c - r_h) = 0.1415$, the relative flow is exactly in the axial direction.

Since the axial velocity is independent of the radius in the free vortex blading,

$$V_1 \cos \alpha_1 = V_{1m} \cos \alpha_{1m} \quad W_2 \cos \beta_2 = W_{2m} \cos \beta_{2m}$$

and dividing the first equation by c_{01} and the second by c_{02} gives

$$M_{01} = M_{01m} \frac{\cos \alpha_{1m}}{\cos \alpha_1} \quad M_{02R} = M_{02mR} \frac{\cos \beta_{2m}}{\cos \beta_2}$$

The stagnation Mach numbers can be calculated from

$$M_{01m} = \frac{M_{1m}}{\sqrt{1 + \frac{\gamma-1}{2} M_{1m}^2}} \quad M_{02mR} = \frac{M_{2mR}}{\sqrt{1 + \frac{\gamma-1}{2} M_{2mR}^2}}$$

The absolute and relative Mach numbers are then obtained from

$$M_1 = \frac{M_{01}}{\sqrt{1 - \frac{\gamma-1}{2} M_{01}^2}} \quad M_{2R} = \frac{M_{02R}}{\sqrt{1 - \frac{\gamma-1}{2} M_{02R}^2}}$$

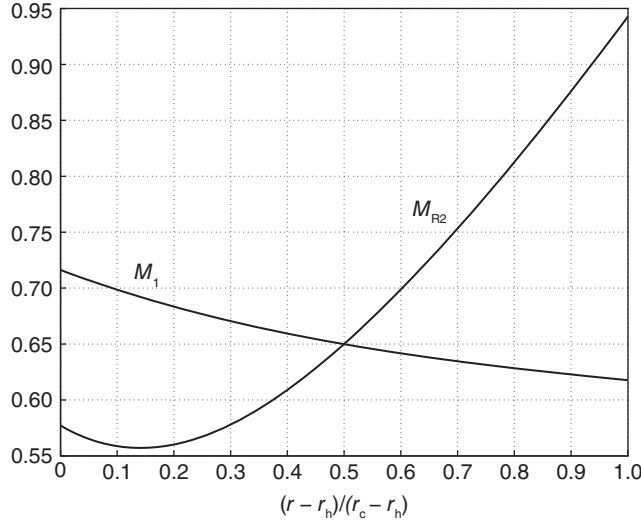


Figure 8.11 Variation of the Mach number as a function of radial position on the blade at the entrance to the stator and the relative Mach number at the entrance to the rotor. In both cases, the respective Mach numbers were 0.65 at the mean radius. The other parameters are the same as in Figure 8.10.

Figure 8.11 shows that the relative Mach number has a minimum near the hub, where the relative velocity changes sign. It rises rapidly to a very high value at the casing. For this reason, its design value at the mean radius cannot be very large. It was convenient to assign the same value 0.65 for Mach numbers M_1 and M_{2R} at the average radius to show their trends along the blade. In actuality, for a given value of M_1 , the value of M_{2R} needs to be calculated, because the relative velocity decreases and static temperature increases across the rotor, leading to a lower value for M_{2R} .

8.3.2 Velocity distribution with zero-power exponent

Another member of the velocity profiles given by Eq. (8.13) is

$$V_{u1} = a - \frac{b}{y} \quad V_{u2} = a + \frac{b}{y}$$

for which $n = 0$. At the inlet, the radial equilibrium equation in this case reduces to

$$V_x \frac{dV_x}{dy} = - \left(\frac{a}{y} - \frac{b}{y^2} \right) \frac{d}{dy} (ay - b) = - \left(\frac{a^2}{y} - \frac{ab}{y^2} \right)$$

Integrating both sides from $y = 1$ to some arbitrary location gives

$$V_{x1}^2 - V_{x1m}^2 = -2 \left[a^2 \ln y + ab \left(\frac{1}{y} - 1 \right) \right]$$

Corresponding expression at the exit is obtained by changing the sign of b . It is

$$V_{x2}^2 - V_{x2m}^2 = -2 \left[a^2 \ln y - ab \left(\frac{1}{y} - 1 \right) \right]$$

The axial velocity now depends on the radial coordinate. For this reason, the reaction is calculated from

$$R = 1 - \frac{h_3 - h_2}{h_3 - h_1} = 1 - \frac{V_2^2 - V_1^2}{2w} = 1 - \frac{V_{x2}^2 - V_{x1}^2 + V_{u2}^2 - V_{u1}^2}{2U(V_{u2} - V_{u1})}$$

If the taper is set such that the axial velocity at the mean radius is the same at the inlet and the outlet, then subtracting the two equations for the axial velocity gives

$$V_{x2}^2 - V_{x1}^2 = 4ab \left(\frac{1}{y} - 1 \right)$$

and the sum and difference terms in $V_{u2}^2 - V_{u1}^2 = (V_{u2} - V_{u1})(V_{u2} + V_{u1})$ are

$$V_{u2} - V_{u1} = \frac{2b}{y} \quad V_{u2} + V_{u1} = 2a$$

Hence, with $U = U_m y$, the reaction may be written as

$$R = 1 - \frac{a}{U_m} \left(1 - \frac{2}{y} \right)$$

and, with the reaction equal to R_m at $y = 1$, the parameter a is obtained from the expression $a = U_m(R_m - 1)$. The reaction depends on the radius as

$$R(y) = 1 + (1 - R_m) \left(1 - \frac{2}{y} \right)$$

As shown above, work done is uniform and $b = \frac{1}{2}\psi U_m$.

8.3.3 Velocity distribution with first-power exponent

A velocity distribution with $n = 1$ in Eq. (8.13) can be expressed as

$$V_{u1} = ay - \frac{b}{y} \quad V_{u2} = ay + \frac{b}{y}$$

The radial equilibrium equation at the inlet now reduces to the form

$$V_x \frac{dV_x}{dy} = - \left(a - \frac{b}{y^2} \right) \frac{d}{dy} (ay^2 - b) = \frac{2ab}{y} - 2a^2 y$$

Integrating this from $y = 1$ to an arbitrary location gives

$$V_{x1}^2 - V_{x1m}^2 = 4ab \ln y - 2a^2(y^2 - 1)$$

and the same operations at the exit yield

$$V_{x2}^2 - V_{x2m}^2 = -4ab \ln y - 2a^2(y^2 - 1)$$

The reaction is calculated from

$$R = 1 - \frac{h_3 - h_2}{h_3 - h_1} = 1 - \frac{V_2^2 - V_1^2}{2w} = 1 - \frac{V_{x2}^2 - V_{x1}^2 + V_{u2}^2 - V_{u1}^2}{2U(V_{u2} - V_{u1})}$$

Again, if the taper of the annulus is such that the axial velocities at the common mean radius are equal, then the difference of the squares of the axial velocities is

$$V_{x2}^2 - V_{x1}^2 = -8ab \ln y$$

and the difference and the sum of the swirl velocities are

$$V_{u2} - V_{u1} = \frac{2b}{y} \quad V_{u2} + V_{u1} = 2ay$$

Hence, the reaction may be written as

$$R = 1 + \frac{2a}{U_m} \ln y - \frac{a}{U_m}$$

With $R = R_m$ at $y = 1$, the parameter $a = U_m(1 - R_m)$. Similarly, $b = \frac{1}{2}\psi U_m$. The reaction, shown in Figure 8.12, can be written as

$$R(y) = 1 - (1 - R_m)(1 - 2 \ln y)$$

Also shown are the axial velocities before and after the rotor. They are given by the expressions

$$\frac{V_{x1}}{U_m} = \sqrt{\phi_m^2 + 2(1 - R_m)\psi \ln y - 2(1 - R_m)^2(y^2 - 1)}$$

$$\frac{V_{x2}}{U_m} = \sqrt{\phi_m^2 - 2(1 - R_m)\psi \ln y - 2(1 - R_m)^2(y^2 - 1)}$$

in which $\phi_m = V_{xm}/U_m$ is the flow coefficient at the mean radius.

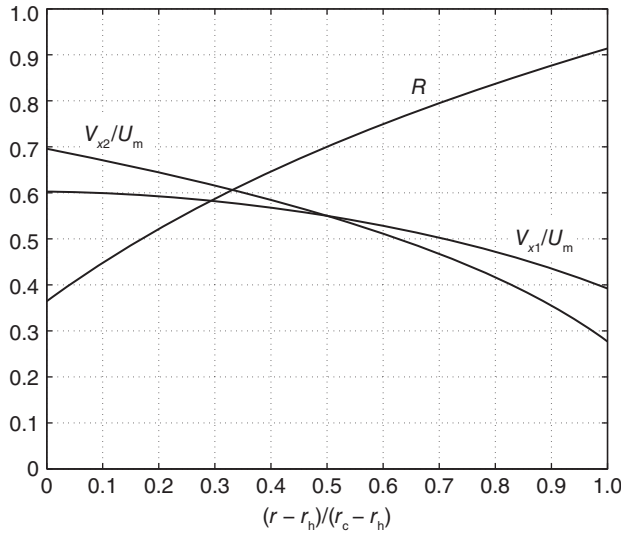


Figure 8.12 Normalized axial velocities before and after the rotor and reaction as a function of the radial position on the blade for a first power velocity distribution, for $\phi_m = 0.55$, $\psi = 0.18$, $R_m = 0.7$, and $\kappa = 0.4$.

8.4 DIFFUSION FACTOR

Earlier in this chapter the de Haller criterion was used as a criterion to ensure that the diffusion in the flow passages would not be so severe to cause separation of the boundary layers. The adverse pressure gradient associated with diffusion is seen in Figure 8.13, which shows a typical stator blade surface pressure measurement, plotted as a pressure coefficient $C_p = (p - p_2)/(p_{02} - p_2)$ against the fractional distance along the chord for three different values of solidity $\sigma = c/s$. The bottom branch of the curve gives the suction-side pressure distribution and the top branch the same for the pressure side of the blade. Under ideal conditions at low Mach number, the spike in the pressure coefficient on the top branch should reach unity at the stagnation point located near the leading edge. From there the pressure falls as the flow accelerates to a location of maximum blade thickness followed by diffusion toward the trailing edge. Near the trailing edge, the flow may accelerate slightly owing to the blade orientation and camber. On the suction side of the blade, the negative spike is caused by the need for the flow to negotiate the blunt leading edge of the blade as it flows from the location of the stagnation point to the suction side. Pressure then increases sharply from the suction spike all the way to the trailing edge as the flow diffuses. This diffusion must be kept within acceptable limits. The difference in the value of pressure at any given chord location is a measure of the *local loading* on the blade and, as seen from Figure 8.13, the blade becomes *unloaded* as the trailing edge is approached.

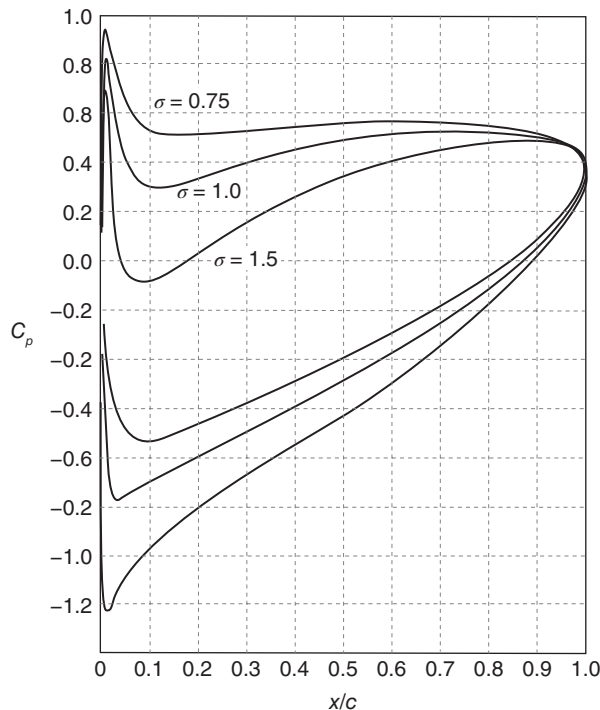


Figure 8.13 Pressure coefficient for a cascade with different solidities.

Since the blade force is obtained by integrating the pressure acting over the blade surface, the area inscribed by the curves represents the blade force normal to the chord. As the solidity increases, this force is reduced, but now with reduced spacing, more blades

can be fitted to the rotor wheel to carry the load. Increased solidity lifts the value of the minimum pressure, with the result that the pressure gradient decreases. Therefore, the flow can be turned by a greater amount without danger of boundary-layer separation.

A local *diffusion factor* is defined as

$$D_{\text{loc}} = \frac{V_{\text{max}} - V_3}{V_2}$$

in which V_{max} is the velocity at the location of minimum pressure. This definition would be useful, if the profile shape were known and V_{max} could be easily calculated. It can, in fact, be done quite readily with a computer code for inviscid flows. But before this became a routine task, an alternative was sought. Lieblein and Roudebush [58] suggested a diffusion factor of the form

$$\text{DF} = \frac{V_2 - V_3}{V_2} + \frac{1}{2\sigma} \frac{V_{u2} - V_{u3}}{V_2} \quad (8.14)$$

The first part is similar to the local diffusion factor, and the second part accounts for the amount of turning and the solidity of the blade row. Since reduced turning and higher solidity both contribute to lighter loading on the blades, diffusion is expected to diminish by both effects. The Lieblein diffusion factor for the stator can be expressed as

$$\text{DF}_S = \frac{\cos \alpha_3 - \cos \alpha_2}{\cos \alpha_3} + \frac{1}{2\sigma_S} (\tan \alpha_2 - \tan \alpha_3) \cos \alpha_2 \quad (8.15)$$

For the rotor, since the relative flow angles are negative and the flow turns toward the axis, the diffusion factor needs to be written as

$$\text{DF}_R = \frac{\cos \beta_2 - \cos \beta_1}{\cos \beta_2} + \frac{1}{2\sigma_R} (\tan \beta_2 - \tan \beta_1) \cos \beta_1 \quad (8.16)$$

It is known that boundary layers thicken faster in a flow with an adverse pressure gradient than when there is none. A relationship may be developed between diffusion and the boundary-layer thickness. Figure 8.14 is a plot of the diffusion factor as a function of the ratio, θ/c , of the *momentum thickness* of the boundary layer (discussed in the next subsection) to the length of the chord. The curve begins its upward bend at the momentum thickness-to-chord ratio of about 0.007, and this corresponds to $\text{DF} = 0.45$. Thus values below these give good designs. For larger DF values, the stagnation pressure losses grow appreciably.

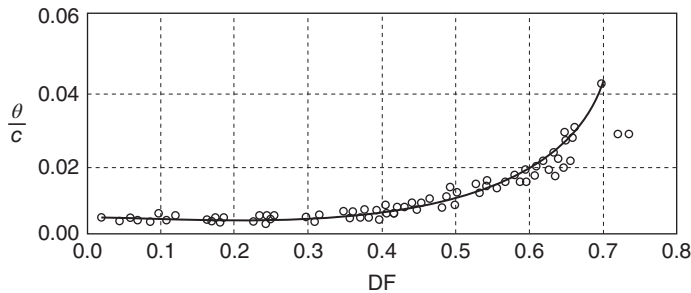


Figure 8.14 Dependence of the momentum thickness of the boundary layer on diffusion factor. Source: Drawn after Lieblein and Roudebush [58].

Equations (8.15) and (8.16) are two additional equations among the design variables. In an earlier section, it was shown that specifying the values for R , ψ , ϕ fixes the flow angles. With the tangent difference formulas and the two diffusion factor formulas, three more equations are added, but solidity is the only new unknown. Hence, in principle, the designer has the freedom to choose only one of the parameters, such as reaction, or else violate either the tangent difference equation, or one of the diffusion factor equations. However, if the design is such that either DF_S or DF_R , or both are less than 0.42, then the tangent difference formula fixes the solidity. Thus the choice for the acceptable range of values of reaction, blade loading, and the flow coefficient to achieve the mild diffusion restricts the design parameter space. The typical design ranges $0.35 \leq \psi \leq 0.5$ and $0.4 \leq \phi \leq 0.7$ reflect this.

8.4.1 Momentum thickness of a boundary layer

The *momentum thickness of a boundary layer* is related to the diffusion factor in Figure 8.14. It and the *displacement thickness* are now discussed further. The latter is denoted by δ^* and is introduced by the expression

$$\delta^* V_f = \int_0^\delta (V_f - V(y)) dy \quad (8.17)$$

in which V_f is the uniform velocity outside the boundary layer of thickness δ . Clearly, this equation can be rewritten as

$$\int_0^\delta V(y) dy = V_f (\delta - \delta^*) \quad (8.18)$$

and its interpretation is shown with the aid of Figure 8.15, in which the shadowed areas in parts (a) and (b) are equal according to Eq. (8.17). Figure 8.15b shows the *blocking effect* of the boundary layer; that is, the flow can be envisioned to have velocity V_f to the edge of δ^* and inside the layer to have zero velocity, as if the flow were completely blocked. Another way to say this is that if the wall were to be *displaced* by δ^* , the same mass flow rate would exist in the inviscid flow as in a real flow without a displacement of the wall.

The momentum thickness θ is defined by the equation

$$\theta V_f^2 = \int_0^\delta V(y)(V_f - V(y)) dy \quad (8.19)$$

This can be written as

$$\theta V_f^2 = V_f \int_0^\delta V(y) dy - \int_0^\delta V^2(y) dy = V_f^2 (\delta - \delta^*) - \int_0^\delta V^2(y) dy$$

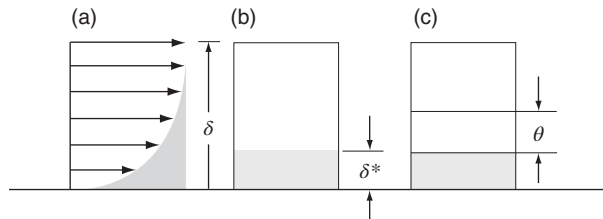


Figure 8.15 Illustration of (a) boundary layer, (b) its displacement thickness, and (c) its momentum thickness.

and reduced to the form

$$\int_0^\delta V^2(y)dy = V_f^2(\delta - \delta^* - \theta) \quad (8.20)$$

This is also illustrated in Figure 8.15, and it shows that the momentum thickness contributes a further blockage. Because the integrand in Eqs. (8.18) and (8.20) vanishes beyond the boundary layer thickness, δ can be replaced by the channel width L , in which case these become

$$\int_0^L V(y)dy = V_f(L - \delta^*) \quad (8.21)$$

and

$$\int_0^L V^2(y)dy = V_f^2(L - \delta^* - \theta) \quad (8.22)$$

The boundary layer at the wall $y = L$ is ignored for now.

Consider next the flow in a compressor cascade. Figure 8.16a shows two blades and boundary layers along them. As the boundary layers leave the blades, they form a wake behind the cascade. On the suction side, the boundary layer is thicker than on the pressure side owing to the strongly decelerating flow there. Consider next the control volume in Figure 8.16b. The inflow boundary is at some location just before the trailing edge, and the outflow boundary is sufficiently far in the wake where mixing has made the velocity uniform. The side boundaries are streamlines that divide one flow channel from the next. Mass balance for this control volume gives

$$\dot{m}' = \int_0^L \rho V(y)dy = \rho L V_3$$

or

$$\dot{m}' = (L - \delta^*)\rho V_f = L\rho V_3$$

in which \dot{m}' is the mass flow rate per unit width. The displacement thickness δ^* is that of the boundary layer on the suction side of the blade; the boundary layer along the pressure side has been ignored. Dividing through by L gives

$$\frac{\dot{m}'}{L} = \left(1 - \frac{\delta^*}{L}\right)\rho V_f = \rho V_3 \quad (8.23)$$

The x component of the momentum equation gives

$$\int_0^L \rho V_3^2 dy - \int_0^L \rho V^2(y)dy = (p - p_3)L$$

in which the shear stress has been neglected, as it is very small along the dividing streamlines in the wake and also small along the blade surfaces, which now account for a small fraction of the control surface. This can be expressed as

$$\rho V_3^2 L - \rho V_f^2(L - \delta^* - \theta) = (p - p_3)L$$

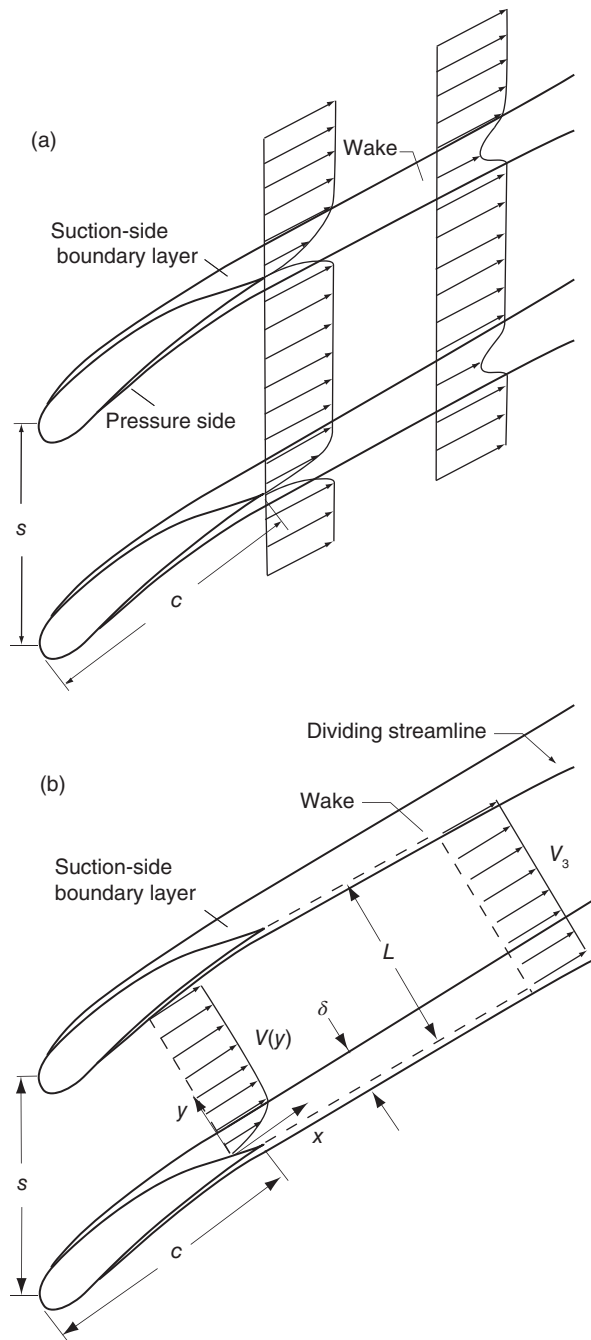


Figure 8.16 (a) Flow in the wake of a compressor cascade and (b) a sketch for its analysis.

Dividing through by L gives

$$p - p_3 = \rho V_3^2 - \left(1 - \frac{\delta^*}{L}\right) \rho V_f^2 + \frac{\theta}{L} \rho V_f^2$$

Adding the term $\rho V_f^2/2$ to both sides, and subtracting $\rho V_3^2/2$ from both sides, gives

$$p_0 - p_{03} = p + \frac{1}{2} \rho V_f^2 - (p_3 + \frac{1}{2} \rho V_3^2) = \frac{1}{2} \rho V_3^2 - (1 - \frac{\delta^*}{L}) \rho V_f^2 + \frac{1}{2} \rho V_f^2 + \frac{\theta}{L} \rho V_f^2$$

Making use of Eq. (8.23) puts this into the form

$$p_0 - p_{03} = \frac{1}{2} \left(1 - \frac{\delta^*}{L}\right)^2 \rho V_f^2 - \left(\frac{1}{2} - \frac{\delta^*}{L}\right) \rho V_f^2 + \frac{\theta}{L} \rho V_f^2$$

Simplifying this gives

$$\frac{p_0 - p_{03}}{\frac{1}{2} \rho V_f^2} = \left(\frac{\delta^*}{L}\right)^2 + \frac{2\theta}{L}$$

The stagnation pressure loss takes place mainly in the decelerating boundary layer and the wake, so that it is reasonable to take $p_0 = p_{02}$. Also, the first term on the right is much smaller than the second one and can be neglected. Thus the stagnation pressure loss is related to the momentum boundary-layer thickness by

$$\frac{p_{02} - p_{03}}{\frac{1}{2} \rho V_f^2} = \frac{2\theta}{L}$$

Finally, V_f is approximately V_3 and $L = s \cos \alpha_3$, so that

$$\frac{p_{02} - p_{03}}{\frac{1}{2} \rho V_3^2} = \frac{2\theta}{s \cos \alpha_3} \quad (8.24)$$

and

$$\omega_S = \frac{2\theta}{s \cos \alpha_3} \left(\frac{\cos \alpha_2}{\cos \alpha_3}\right)^2 \quad \omega_R = \frac{2\theta}{s \cos \beta_2} \left(\frac{\cos \beta_1}{\cos \beta_2}\right)^2 \quad (8.25)$$

The boundary-layer thickness on the pressure side of the blade was neglected in the analysis. If it is included, as it should, the only change is that the momentum thickness is now the sum of the momentum boundary-layer thicknesses on both sides of the blade. It is, in fact, this thickness that is shown in the experimental data relating it to the diffusion factor. If $DF = 0.45$ is taken as the design value, then at this value, the momentum boundary-layer thickness is given as $\theta = 0.007c$, so that the stagnation pressure losses for the stator and the rotor are

$$\frac{p_{02} - p_{03}}{\frac{1}{2} \rho V_2^2} = \frac{0.014 \sigma_S}{\cos \alpha_3} \left(\frac{\cos \alpha_2}{\cos \alpha_3}\right)^2 \quad \frac{p_{01R} - p_{02R}}{\frac{1}{2} \rho W_1^2} = \frac{0.014 \sigma_R}{\cos \beta_2} \left(\frac{\cos \beta_1}{\cos \beta_2}\right)^2 \quad (8.26)$$

The stagnation pressure losses and their relation to stage efficiency are discussed further in the next section.

8.5 EFFICIENCY AND LOSSES

Various stagnation pressure losses in a compressor stage are shown in Figure 8.17. It dates from 1945, and the estimates reflect the way in which compressors were designed then. Today, the design flow coefficient has been lowered to the range $0.4 \leq \phi \leq 0.7$, and the losses are expected to be smaller as designs have improved. The data show that, owing to boundary-layer separation and blade stall, profile losses become a major loss component when a compressor is operated far from its design condition. *Profile losses* are associated with the boundary layers along the blades, and the *annular losses* come from the boundary layers along the endwalls of the flow annulus. *Secondary flow* arises from the interaction of the annulus boundary layers and the inviscid stream, which set up a circulation in the plane normal to the primary flow. Dissipation in the secondary flow accounts for these losses.

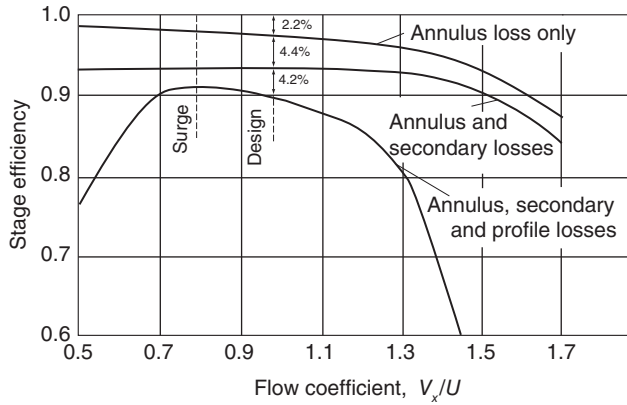


Figure 8.17 Losses in a typical compressor stage. Source: Drawn after Howell [44].

8.5.1 Efficiency

The stage efficiency is defined by

$$\eta_{tt} = \frac{h_{03ss} - h_{01}}{h_{03} - h_{01}} \quad \text{so that} \quad 1 - \eta_{tt} = \frac{h_{03} - h_{03ss}}{h_{03} - h_{01}}$$

where the states are as shown in Figure 8.4. This can be written as

$$1 - \eta_{tt} = \frac{h_3 - h_{3ss}}{w} + \frac{V_3^2 - V_{3ss}^2}{2w}$$

The numerator of the first term on the right is

$$h_3 - h_{3ss} = h_3 - h_{3s} + h_{3s} - h_{3ss}$$

From the definition of static enthalpy loss coefficient, the first of these can be written as

$$h_3 - h_{3s} = \frac{1}{2} \zeta_s V_3^2,$$

and the second term is

$$h_{3s} - h_{3ss} = c_p T_{3s} \left(1 - \frac{T_{3ss}}{T_{3s}} \right)$$

Integrating the Gibbs equation along the constant-pressure lines p_2 and p_3 between states with entropies s_1 and s_2 gives

$$\frac{T_{2s}}{T_2} = \frac{T_{3ss}}{T_{3s}}$$

so that the previous equation can be recast as

$$h_{3s} - h_{3ss} = \frac{T_{3s}}{T_2} (h_2 - h_{2s})$$

When written in terms of the static enthalpy loss coefficient, this becomes

$$h_{3s} - h_{3ss} = \frac{1}{2} \zeta_R W_2^2 \frac{T_{3s}}{T_2}$$

The velocity term on the right in the expression for efficiency is

$$\frac{V_3^2 - V_{3ss}^2}{2w} = \left(1 - \frac{V_{3ss}^2}{V_3^2} \right) \frac{V_3^2}{2w}$$

But it has been shown in Chapter 5 that $M_{3ss} = M_3$. Therefore $V_{3ss}^2/V_3^2 = T_{3ss}/T_3$, and the expression for the efficiency now takes the form

$$1 - \eta_{tt} = \frac{\zeta_S V_3^2 + \zeta_R W_2^2 \frac{T_{3s}}{T_2} + \left(1 - \frac{T_{3ss}}{T_3} \right) V_3^2}{2w}$$

The first and the last term have a common factor in V_3^2 , and they could be combined. However, for a typical stage, the temperature factor of the last term has a value of about 0.008. If this is neglected and the term T_{3s}/T_2 is set to unity, the right side is simplified somewhat. Therefore, the reduced equation

$$1 - \eta_{tt} = \frac{\zeta_S V_3^2 + \zeta_R W_2^2}{2w};$$

although simple to use, underestimates the losses by about 1.5%.

The relationship to stagnation pressure loss can be developed by writing for the stator

$$h_3 - h_{3s} = c_p (T_3 - T_{3s}) = c_p T_3 \left(1 - \frac{T_{3s}}{T_3} \right) = c_p T_3 \left[1 - \left(\frac{p_{03}}{p_{02}} \right)^{(\gamma-1)\gamma} \right]$$

which can be rewritten and then expanded for small stagnation pressure loss as

$$\begin{aligned} h_3 - h_{3s} &= c_p T_3 \left[1 - \left(\frac{p_{03}}{p_{03} + \Delta p_{0LS}} \right)^{(\gamma-1)/\gamma} \right] = c_p T_3 \left[1 - \left(1 + \frac{\Delta p_{0LS}}{p_{03}} \right)^{-(\gamma-1)/\gamma} \right] \\ &= c_p T_3 \frac{\gamma-1}{\gamma} \frac{\Delta p_{0LS}}{p_{03}} = \frac{p_3}{p_{03}} \frac{\Delta p_{0LS}}{\rho_3} \end{aligned}$$

Thus

$$h_3 - h_{3s} = \frac{\Delta p_{0LS}/\rho_3}{\left(1 + \frac{\gamma-1}{2} M_3^2\right)^{\gamma/(\gamma-1)}}$$

A similar analysis for the rotor gives

$$h_2 - h_{2s} = c_p(T_2 - T_{2s}) = c_p T_2 \left(1 - \frac{T_{2s}}{T_2}\right) = c_p T_2 \left[1 - \left(\frac{p_{02R}}{p_{01R}}\right)^{(\gamma-1)/\gamma}\right]$$

which can be rewritten and then expanded for small stagnation pressure loss as

$$\begin{aligned} h_2 - h_{2s} &= c_p T_2 \left[1 - \left(\frac{p_{02R}}{p_{02R} + \Delta p_{0LR}}\right)^{(\gamma-1)/\gamma}\right] = c_p T_2 \left[1 - \left(1 + \frac{\Delta p_{0LR}}{p_{02R}}\right)^{-(\gamma-1)/\gamma}\right] \\ &= c_p T_2 \frac{\gamma-1}{\gamma} \frac{\Delta p_{0LR}}{p_{02R}} = \frac{p_2}{p_{02R}} \frac{\Delta p_{0LR}}{\rho_2} \end{aligned}$$

Therefore

$$h_2 - h_{2s} = \frac{\Delta p_{0LR}/\rho_2}{\left(1 + \frac{\gamma-1}{2} M_{2R}^2\right)^{\gamma/(\gamma-1)}}$$

The stagnation pressure losses can now be written as

$$\frac{\Delta p_{0LS}}{\rho_3} = \frac{1}{2} \zeta_S V_3^2 \left(1 + \frac{\gamma-1}{2} M_3^2\right)^{\gamma/(\gamma-1)} \quad (8.27)$$

and

$$\frac{\Delta p_{0LR}}{\rho_2} = \frac{1}{2} \zeta_R W_2^2 \left(1 + \frac{\gamma-1}{2} M_{2R}^2\right)^{\gamma/(\gamma-1)} \quad (8.28)$$

Since the rotor turns the flow toward the axis, the magnitude of the relative velocity diminishes and the relative Mach number leaving the rotor is fairly small. The same is true for the absolute Mach number leaving the stator. Hence, if the Mach number terms in Eqs. (8.27) and (8.28) are neglected, then with some loss of accuracy, substituting these expressions for the stagnation pressure losses into Eq. (8.26), gives

$$\zeta_R = \frac{0.014 \sigma_R}{\cos \beta_2} \quad \zeta_S = \frac{0.014 \sigma_S}{\cos \alpha_3} \quad (8.29)$$

These show that

$$\omega_S = \zeta_S \left(\frac{\cos \alpha_2}{\cos \alpha_3}\right)^2 \quad \omega_R = \zeta_R \left(\frac{\cos \beta_1}{\cos \beta_2}\right)^2 \quad (8.30)$$

Since $V_x = V_3 \cos \alpha_3 = W_2 \cos \beta_2$ the efficiency may be rewritten in the form

$$1 - \eta_{tt} = \left(\frac{\zeta_R}{\cos^2 \alpha_3} + \frac{\zeta_S}{\cos^2 \beta_1}\right) \frac{\phi^2}{2\psi} \quad (8.31)$$

8.5.2 Parametric calculations

The development of the theory for axial compressors has been carried out in terms of assumed values for a flow coefficient ϕ , a blade-loading factor ψ , and a reaction ratio R . These three quantities are *nondimensional parameters* and are sufficient for calculating the flow angles. Solidity was obtained from experimental measurements of deflection for given flow outlet angle. It was used to establish the permissible diffusion, and the stagnation pressure coefficient for profile losses was established. The efficiency can then be cast in terms of the loss coefficients for the rotor and the stator. This is the most effective way to display results, and when the actual parameters for a machine are given, all the important results are quickly calculated from the nondimensional ones. Thus flow angles for a compressor stator and rotor have been shown to be

$$\begin{aligned}\tan \alpha_1 &= \frac{1 - R - \psi/2}{\phi} & \tan \alpha_2 &= \frac{1 - R + \psi/2}{\phi} \\ -\tan \beta_1 &= \frac{R + \psi/2}{\phi} & -\tan \beta_2 &= \frac{R - \psi/2}{\phi}\end{aligned}$$

Hence, with ϕ, ψ , and R given, they can be determined. The rest of the calculations then follow directly. Results from such calculations are shown in Figure 8.18. The flow coefficient was taken to be $\phi = 0.6$ and the degree of reaction, $R = 0.4$. For Figure 8.18a–c, the Lieblein diffusion factor was taken to be equal to 0.45, and solidities of the rotor and stator were calculated in terms of this value. Figure 8.18a represents the diffusion in the flow.

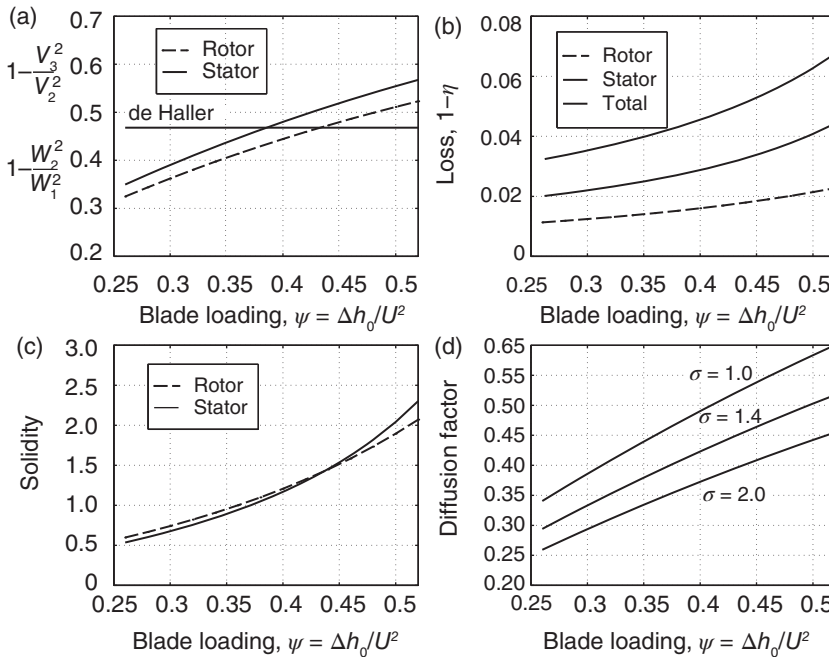


Figure 8.18 Design study for a compressor cascade with diffusion factor, DF = 0.45, flow coefficient $\phi = 0.6$, and reaction $R = 0.4$. (a) de Haller criterion, (b) losses, (c) solidity, and (d) diffusion factor.

If the stagnation pressure losses are neglected and the flow is assumed incompressible, then

$$p_2 + \frac{1}{2}\rho V_2^2 = p_3 + \frac{1}{2}\rho V_3^2$$

and

$$\frac{p_3 - p_2}{\frac{1}{2}\rho V_2^2} = 1 - \frac{V_3^2}{V_2^2}$$

Hence, this also gives the pressure rise in a nondimensional form. A similar expression applies for the rotor. This nondimensional pressure rise should not be greater than 0.48, according to the recommendation by de Haller [38]. The de Haller criterion shows that the blade-loading factor must be kept below 0.39.

Figure 8.18b shows that if the de Haller criterion is obeyed, the stage efficiency is around 0.96. This efficiency calculation should not be considered conclusive, as it ignores the *annulus and secondary flow losses*, as well as *losses from the tip region*. Furthermore, in the calculations the values of $\omega_S = 0.014\sigma_S / \cos \alpha_3$ and $\omega_R = 0.014\sigma_R / \cos \beta_2$ were used following Cumpsty [18, p. 55]. Had Eqs. (8.30) been used instead, the efficiency would have been higher. Figure 8.18c shows solidity to be near unity for both the rotor and the stator if the Lieblein diffusion factor is kept at 0.45. It turns out that Howell's criterion is also satisfied under these conditions. To be sure, the Howell's criterion shows that the solidity ought to be the same for the rotor and stator, so that the system is overconstrained. The diffusion factor then becomes a check that the design parameters have been reasonably chosen. Figure 8.18d shows what happens to the diffusion factor as the solidity is varied independently. For a blade row of high solidity, diffusion is reduced, as the load per blade is reduced.

8.6 CASCADE AERODYNAMICS

The development of axial compressor blade shapes has been carried out in extensive experiments in cascade tunnels. Such tunnels are designed to test in a two-dimensional arrangement, either a row of rotor blades, or a row of stator vanes. Both are shown in Figure 8.19 in which the flow moves from left to right. The blades are characterized by their chord, camber, thickness, and height. The axial chord c_x is the chord's projection along the x axis. In Figure 8.19b, the blade (or metal) angle at the inlet is χ_2 , and at the outlet, it is χ_3 . The flow *incidence* is defined as the difference between the flow angle and the metal angle. Thus $i = \alpha_2 - \chi_2$ at the inlet to the stator, and since the angles are negative, incidence is $i = |\beta_1 - \chi_1|$ at the inlet to the rotor. The figure is drawn to show a positive incidence for both. The angle $\delta = \alpha_3 - \chi_3$ at the exit of the stator is called *deviation*. Although the flow tends to leave at the exit metal angle, it turns slightly toward the suction surface.

The general orientation of the blades is given by the *stagger* angle ξ , and their curvature by the camber angle θ . The lines that form a triangle on the stator blade in Figure 8.19b has the included angle $\chi_2 - \xi$ on the left, $\xi - \chi_3$ on the right, and $\pi - \theta$ at the top. These add up to π . Hence, $\theta = \chi_2 - \chi_3$. These relationships are also true for the rotor in which negative angles are encountered. The exit metal angle χ_2 of the rotor has the same designation as the inlet metal angle to the stator. It will always be clear whether the rotor row or stator row is analyzed, so separate symbols are not needed.

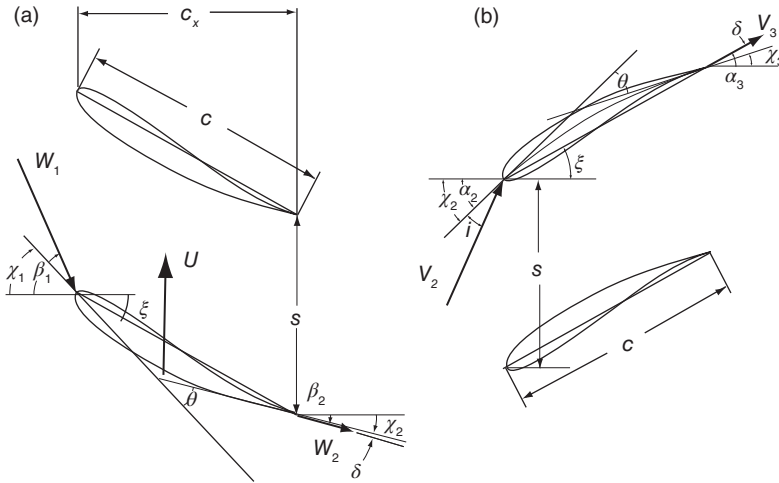


Figure 8.19 (a) Rotor and (b) stator cascade for an axial compressor.

8.6.1 Blade shapes and terms

Today, the designer is no longer constrained to the blade shapes that were in use during the early period of compressor development. Members from the NACA-65 series of blades in the United States were adopted as the base profiles. In the Great Britain, blade designation, such as 6C7/25P40, carries with it the pertinent information about the maximum thickness b and its location from the leading edge a . The notation means that the maximum thickness is 6% of the chord, so that $b/c = 0.06$. The next item C7 describes how the thickness is distributed over the blade. Next is the camber angle, which here is 25° . After that the letter P designates this to be a blade with a parabolic camber, with the location of maximum thickness at 40% from the leading edge; that is, $a/c = 0.4$. The circular arc profile 10C4/30C50 has 10% thickness and 30° camber. Its maximum thickness always occurs at the midchord point.

For parabolic arc profiles defining $\theta_1 = \chi_1 - \xi$ and $\theta_2 = \xi - \chi_2$, the angles θ_1 and θ_2 are given by

$$\tan \theta_1 = \frac{cb}{a^2} \quad \tan \theta_2 = \frac{cb}{a(c-a)}$$

and, if the location of maximum camber a is close to the midchord position, these can be approximated by

$$\tan \theta_1 = \frac{4b}{4a-c} \quad \tan \theta_2 = \frac{4b}{3c-4a}$$

From these follow the relation

$$\frac{b}{c} = \frac{1}{4 \tan \theta} \left[\sqrt{(1 + 16 \tan^2 \theta) \left(\frac{a}{c} - \frac{a^2}{c^2} - \frac{3}{16} \right)} - 1 \right]$$

where $\theta = \theta_1 + \theta_2$. For blades for which the position of maximum camber is near the midchord point, useful approximations [18] to these are

$$\theta = 8 \frac{b}{c} \quad \theta_1 = \frac{1}{2} \theta \left[1 + 2 \left(1 - 2 \frac{a}{c} \right) \right] \quad \theta_2 = \frac{1}{2} \theta \left[1 - 2 \left(1 - 2 \frac{a}{c} \right) \right]$$

8.6.2 Blade forces

Figure 8.20 shows a typical stator of an axial compressor. The x component of the momentum equation applied to a control volume consisting of the flow channel for the stator gives

$$\rho s V_{x2}(V_{x3} - V_{x2}) = s(p_2 - p_3) + F_x$$

and if the axial velocity remains constant, this reduces to

$$F_x = s(p_3 - p_2)$$

Using the definition of stagnation pressure for an incompressible flow, this becomes

$$\frac{F_x}{s} = \frac{1}{2}(V_2^2 - V_3^2) - \Delta p_{0L} \quad (8.32)$$

in which Δp_{0L} is the loss in stagnation pressure.

The force F_x is per unit height of the blade. Since the axial velocity is taken to be constant and $\alpha_3 < \alpha_2$, inspection of the magnitudes of V_2 and V_3 shows that $V_3 < V_2$ and therefore, also $p_3 > p_2$, as it ought to be in a compressor. Hence, the force F_x that blades exert on the fluid is positive. The y component gives

$$\rho s V_{x2}(V_{u3} - V_{u2}) = -F_y$$

and the minus sign is inserted on the right side to render the numerical value of F_y positive, because $V_{u3} < V_{u2}$. This equation may also be written as

$$\frac{F_y}{s} = \rho V_x^2 (\tan \alpha_2 - \tan \alpha_3) \quad (8.33)$$

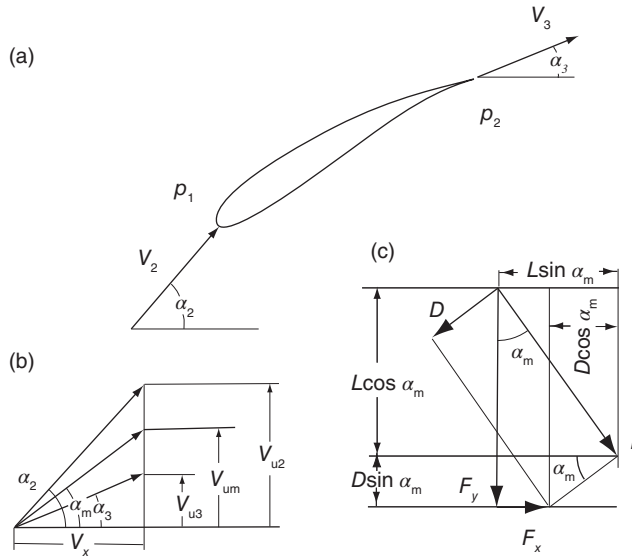


Figure 8.20 (a) A compressor stator blade, (b) velocity vectors and definition of mean velocity, and (c) construction of lift and drag forces.

Since $V_{x2} = V_{x3}$, the kinetic energy difference in Eq. (8.32) may be expressed as

$$\begin{aligned} V_2^2 - V_3^2 &= (V_{x2}^2 + V_{u2}^2) - (V_{x3}^2 + V_{u3}^2) \\ &= V_{u2}^2 - V_{u3}^2 = (V_{u2} - V_{u3})(V_{u2} + V_{u3}) \end{aligned}$$

Next, let the mean tangential velocity be

$$V_{um} = \frac{1}{2}(V_{u2} + V_{u3})$$

then using this definition and inspection of Figure 8.20 gives

$$V_{um} = V_x \tan \alpha_m = \frac{V_x}{2}(\tan \alpha_2 + \tan \alpha_3)$$

in which the mean gas angle α_m is defined by the expression

$$\tan \alpha_m = \frac{1}{2}(\tan \alpha_2 + \tan \alpha_3) \quad (8.34)$$

The x component of the force may now be written as

$$F_x = \rho s V_x^2 (\tan \alpha_2 - \tan \alpha_3) \tan \alpha_m - s \Delta p_{0L} \quad (8.35)$$

In addition to the axial and tangential components of forces, the lift and the drag force are also shown in Figure 8.20. They are the forces that the blades exert on the fluid. Lift and drag are obtained by resolving the resultant along the direction of the mean flow angle and one perpendicular to it. With the resultant expressed as

$$\mathbf{F} = F_x \mathbf{i} - F_y \mathbf{j}$$

the component D parallel and L normal to the mean flow vector, as shown in Figure 8.20c, are

$$L = F_x \sin \alpha_m + F_y \cos \alpha_m \quad (8.36)$$

$$D = -F_x \cos \alpha_m + F_y \sin \alpha_m \quad (8.37)$$

Introducing Eqs. (8.35) and (8.33) into Eq. (8.36) gives

$$L = \rho s V_x^2 (\tan \alpha_2 - \tan \alpha_3) \sec \alpha_m - s \Delta p_{0L} \sin \alpha_m$$

The lift coefficient now becomes

$$C_L = \frac{L}{\frac{1}{2} \rho V_m^2 c} = \frac{2}{\sigma} (\tan \alpha_2 - \tan \alpha_3) \cos \alpha_m - \frac{\Delta p_{0L}}{\frac{1}{2} \rho V_m^2} \frac{\sin \alpha_m}{\sigma}$$

Substituting Eqs. (8.32) and (8.33) into Eq. (8.37) gives

$$D = s \Delta p_{0L} \cos \alpha_m \quad (8.38)$$

The choice in defining the direction of drag and lift as parallel and perpendicular to the mean flow direction as given by the angle α_m is guided exactly by this result, since the stagnation pressure drop from profile losses should depend mainly on the drag and not the lift.

Defining next the drag coefficient as

$$C_D = \frac{D/c}{\frac{1}{2}\rho V_m^2} \quad (8.39)$$

in which c is the chord, and making use of the preceding equation, gives

$$C_D = \frac{\Delta p_{0L} \cos \alpha_m}{\frac{1}{2}\rho V_m^2 \sigma}$$

For the stator, the stagnation pressure loss can be written as

$$\Delta p_{0LS} = \frac{1}{2}\rho \zeta_S V_3^2 = \frac{1}{2}\rho V_m^2 \frac{\sigma_S C_D}{\cos \alpha_m}$$

so that

$$\zeta_S = \frac{\sigma_S \cos^2 \alpha_3}{\cos^3 \alpha_m} C_D \quad (8.40)$$

in which $V_m/V_3 = \cos \alpha_3 / \cos \alpha_m$ has been used. For the rotor similarly

$$\zeta_R = \frac{\sigma_R \cos^2 \beta_2}{\cos^3 \beta_m} C_D \quad (8.41)$$

The drag coefficients in these expressions are not the same, but are the appropriately calculated ones for the stator and the rotor. As will be seen below, the various losses are expressed in terms of the drag coefficients, and their sum gives the total. The two preceding equations can then be used to relate the drag coefficients to the static enthalpy loss coefficients.

The expression for the lift coefficient for the stator can now be written as

$$C_L = \frac{2}{\sigma_S} (\tan \alpha_2 - \tan \alpha_3) \cos \alpha_m - C_D \tan \alpha_m$$

In a typical unstalled blade $C_D \sim 0.025 C_L$, and, as will be shown shortly, it is advantageous to keep α_m less than 45° . Under these conditions, the drag term may be neglected. This gives the following expression for the lift-to-drag ratio:

$$\frac{C_L}{C_D} = \frac{L}{D} = \frac{2}{\zeta_S} (\tan \alpha_2 - \tan \alpha_3) \frac{\cos^2 \alpha_3}{\cos^2 \alpha_m}$$

To make use of these expressions for compressor rotors, the flow angle α_2 is replaced by β_1 and α_3 by β_2 and the rotor loss coefficient ζ_R is substituted for ζ_S .

8.6.3 Other losses

The drag coefficient for annulus losses is given by

$$C_{Da} = 0.02 \frac{s}{b}$$

in which b is the blade height. The annulus losses become a smaller fraction of the total losses as the blade height increases. Secondary losses are a complicated subject, but all

these complications are sidestepped by calculating the loss coefficient from the expression

$$C_{Ds} = 0.018C_L^2$$

The tip losses arise from a tip vortex and leakage loss through the tip clearance for the rotor. They are taken into account by the empirical relation

$$C_{Dt} = 0.29 \frac{k}{b} C_L^{3/2}$$

where k is the tip clearance.

The total loss coefficient is then obtained by summing these

$$C_D = C_{Dp} + C_{Da} + C_{Ds} + C_{Dt}$$

The equivalent drag coefficients for secondary and tip losses are a way of expressing the total pressure loss on the same basis for profile and annulus losses. With the sum of drag coefficients determined, the total static enthalpy loss coefficient can be calculated from either Eq. (8.40) or (8.41). The calculation of losses using the method outlined above has been questioned over the years [18, 21], for it is clear that in the complicated flow structure with highly staggered blades, dividing the losses neatly into constituent parts and adding them is suspect. Modern CFD analysis gives a powerful alternative that can be used to calculate stagnation pressure losses. Even if the modern methods are an improvement over what has been done in the past, there are still hurdles to overcome. One important advancement has been to develop methods to include unsteady interactions between moving and stationary blade rows. The theory still hinges on accurate methods to calculate local entropy production of a turbulent velocity and temperature fields. New turbulence models and large-eddy-simulation methods show promise, and for this reason, industry has moved to rely more and more on CFD to resolve the flow fields in compressors and turbines.

8.6.4 Diffuser performance

The expression for the lift-to-drag ratio can be used to assess under which conditions a compressor cascade performs well as a diffuser. The diffuser efficiency is defined as

$$\eta_D = \frac{p_3 - p_2}{p_{3s} - p_2}$$

which is the ratio of the static pressure rise to the maximum possible. The labels are chosen to reflect that diffusion through the stator is considered. In a reversible adiabatic flow, the stagnation pressure remains constant and

$$p_{02} - p_{03s} = p_2 - p_{3s} + \frac{1}{2}\rho(V_2^2 - V_{3s}^2) = 0$$

Hence,

$$p_{3s} - p_2 = \frac{1}{2}\rho(V_2^2 - V_{3s}^2)$$

Assuming that $V_3 = V_{3s}$, the diffuser efficiency can thus be written as

$$\eta_D = \frac{p_3 - p_2}{\frac{1}{2}\rho(V_2^2 - V_3^2)}$$

Now

$$F_x = s(p_3 - p_2) \quad F_x = F_y \tan \alpha_m - s \Delta p_{0S} \quad F_y = \rho s V_x^2 (\tan \alpha_2 - \tan \alpha_3)$$

so that

$$p_3 - p_2 = \rho V_x^2 \tan \alpha_m (\tan \alpha_2 - \tan \alpha_3) - \Delta p_{0LS}$$

Thus

$$\eta_D = 1 - \frac{\Delta p_{0LS}}{\rho V_x^2 \tan \alpha_m (\tan \alpha_2 - \tan \alpha_3)}$$

or in terms of C_D and C_L the diffuser efficiency can be written as

$$\eta_D = 1 - \frac{2C_D}{C_L \sin 2\alpha_m}$$

The maximum efficiency is determined by differentiating. Thus

$$\frac{d\eta_D}{d\alpha_m} = \frac{4C_D \cos 2\alpha_m}{C_L \sin^2 2\alpha_m} = 0$$

Hence, $\alpha_m = 45^\circ$ at the condition of maximum diffuser Efficiency, and for $C_D/C_L = 0.05$ the efficiency is 90%. This result is due to Horlock [41].

8.6.5 Flow deviation and incidence

Before the blade angle can be set, the deviation at the exit from the blade row must be established. The flow deviation from a stator is given by $\delta = \alpha_3 - \chi_3$, in which χ_3 is the blade angle. Deviation is positive when the flow deflects from the pressure side toward the suction side. A positive deviation for the stator is shown in Figure 8.19, and for the rotor, the flow is deflected in the opposite direction.

Deviation is an inviscid flow effect and not related to viscosity and, therefore, to losses. It can be regarded as incomplete turning of the flow. Hence, to obtain the desired turning, blades need to be curved more than in the absence of deviation.

Carter [14] recommends that deviation be calculated from

$$\delta^* = m\theta \sqrt{\frac{s}{c}}$$

at the design conditions, and Howell [44] proposed the formula

$$m = 0.92 \frac{a^2}{c^2} + \frac{\alpha_3^*}{500}$$

for m , in which α_3^* is given in degrees and a/c is the ratio of maximum thickness to the chord and the superscript star denotes nominal conditions.

■ EXAMPLE 8.4

A compressor state has a stator outlet metal angle $\chi_3 = 3^\circ$, camber angle $\theta = 34^\circ$, pitch chord ratio $s/c = 0.88$, and the position of maximum camber $a/c = 0.5$. The ratio of the blade height to the chord is $b/c = 2$. Find (a) the deviation of the flow

leaving the stator, (b) the deflection, and (c) the flow coefficient and blade-loading coefficient, assuming that the inflow is at zero incidence. (d) Find the reaction.

Solution: (a) The flow deviation is calculated first. Since $\alpha_3^* = \chi_3 + \delta^*$, the flow angle can be calculated from

$$\alpha_3^* = \chi_3 + m\theta\sqrt{\frac{s}{c}} = \chi_3 + 0.92\frac{a^2}{c^2}\theta\sqrt{\frac{s}{c}} + \frac{\alpha_3^*}{500}\theta\sqrt{\frac{s}{c}}$$

Solving this for α_3^* gives

$$\alpha_3^* = \frac{\chi_3 + 0.92\frac{a^2}{c^2}\theta\sqrt{\frac{s}{c}}}{1 - \frac{\theta}{500}\sqrt{\frac{s}{c}}} = \frac{3 + 0.92 \cdot 0.25 \cdot 34\sqrt{0.88}}{1 - \frac{34}{500}\sqrt{0.88}} = 11.04^\circ$$

so that $\delta^* = \alpha_3^* - \chi_3 = 11.04^\circ - 3^\circ = 8.04^\circ$.

(b) The nominal deflection is calculated by first solving

$$\tan \alpha_2^* - \tan \alpha_3^* = \frac{1.55}{1 + 1.5s/c}$$

for α_2^* . It yields

$$\alpha_2^* = \tan^{-1} \left(\tan \alpha_3^* + \frac{1.55}{1 + 1.5s/c} \right) = \tan^{-1} \left(0.1951 + \frac{1.55}{1 + 1.5 \cdot 0.88} \right) = 40.8^\circ$$

Thus the nominal deflection is

$$\epsilon^* = \alpha_2^* - \alpha_3^* = 40.8^\circ - 11.0^\circ = 29.8^\circ$$

If the metal angle at the inlet to the stator is set at $\chi_2 = 40.8^\circ$, then the flow enters the stator at *zero incidence*. If the metal angle is set, say, to $\chi_2 = 37^\circ$, then the incidence angle is $i^* = \alpha_2^* - \chi_2 = 40.8 - 37 = 3.8^\circ$.

(c) Since for a normal stage $\alpha_1^* = \alpha_3^*$, the flow coefficients is obtained from

$$\phi = \frac{1}{\tan \alpha_1^* + \tan \alpha_2^*} = \frac{1}{0.1951 + 0.8632} = 0.945$$

and the blade-loading coefficient, from

$$\psi = \phi(\tan \alpha_2^* - \tan \alpha_1^*) = 0.945(0.8632 - 0.1951) = 0.631$$

Both of these are above the high end of the usual range of industrial practice which is $0.4 \leq \phi \leq 0.7$ and $0.35 \leq \psi \leq 0.5$, as was mentioned at the beginning of this chapter.

(d) The reaction is

$$R = 1 - \frac{1}{2}\phi(\tan \alpha_2^* + \tan \alpha_1^*) = 1 - 0.5 \cdot 0.945(0.8632 + 0.1950) = 0.500$$

■

8.6.6 Multi-stage compressor

The polytropic efficiency was introduced for turbines in the previous chapter. For a small change in the stagnation enthalpy across a stage, the stage efficiency approaches the polytropic efficiency. For an ideal gas, the incremental process is as shown in Figure 8.21.

The relation between the stagnation temperature increases for an actual and an ideal process is given by

$$dT_{0s} = \eta_p dT_0$$

For an isentropic expansion

$$c_p \frac{dT_{0s}}{T_0} = R \frac{dp_0}{p_0} \quad \text{or} \quad \frac{\gamma \eta_p}{(\gamma - 1)} \frac{dT_0}{T_0} = \frac{dp_0}{p_0}$$

Integrating this across an infinite number of infinitesimally small stages gives

$$\frac{T_{0,N+1}}{T_{01}} = \left(\frac{p_{0,N+1}}{p_{01}} \right)^{(\gamma-1)\eta_p/\gamma}$$

A reheat factor, defined as $RF = \eta_p/\eta$, can then be written as

$$RF = \frac{\eta_p}{\eta} = \frac{\eta_p \left[\left(\frac{p_{0,N+1}}{p_{01}} \right)^{(\gamma-1)/\eta_p\gamma} - 1 \right]}{\left(\frac{p_{0,N+1}}{p_{01}} \right)^{(\gamma-1)/\gamma} - 1}$$

The relationship between the compressor efficiency and polytropic or small-stage efficiency is

$$\eta = \frac{r^{(\gamma-1)/\gamma} - 1}{r^{(\gamma-1)/\eta_p\gamma} - 1}$$

in which $r = p_{0e}/p_{01}$ is the overall pressure ratio of the compressor. This relationship is shown in Figure 8.22.

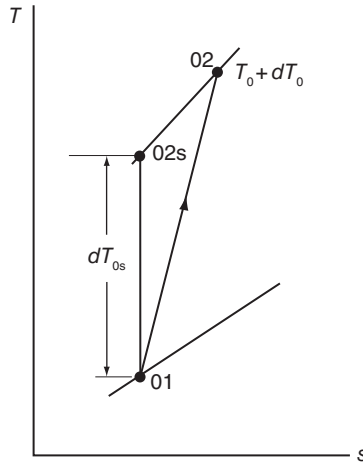


Figure 8.21 Processes across a small compressor stage.

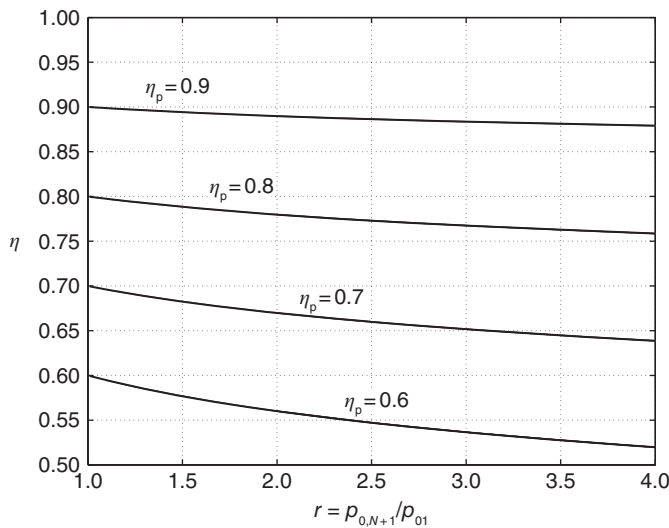


Figure 8.22 Compressor efficiency as a function of pressure ratio and polytropic efficiency for a gas with $\gamma = 1.4$.

In a multistage compressor, the upstream stages influence those downstream. Smith [85] measured velocity and temperature profiles after each stage of a 12-stage compressor. These are shown in Figure 8.23, and examination shows that annulus boundary layers cause large decrease in the axial velocity and increase in total temperature. Although it has been assumed that average stagnation temperature does not change in adiabatic flow, the local values may change. These influences are taken into account by modifying the Euler equation for compressor work by introducing a *work-done factor* λ and expressing the work done as

$$h_{03} - h_{01} = \lambda U(V_{u2} - V_{u1})$$

Comparing different compressors Howell and Bonham recommend a work-done factors shown in Table 8.1 [45].

Table 8.1 Work-done factor λ of various stages of an axial compressors.

| | | | | | | | | | |
|-----------|-------|-------|-------|-------|-------|-------|-------|-------|-------|
| stages | 1 | 2 | 3 | 4 | 5 | 6 | 7 | 8 | 9 |
| λ | 0.982 | 0.952 | 0.929 | 0.910 | 0.895 | 0.883 | 0.875 | 0.868 | 0.863 |
| stages | 10 | 11 | 12 | 13 | 14 | 15 | 16 | 17 | 18 |
| λ | 0.860 | 0.857 | 0.855 | 0.853 | 0.851 | 0.850 | 0.849 | 0.848 | 0.847 |

8.6.7 Compressibility effects

The influence of Mach number on losses is substantial, and the loss coefficient increases rapidly with the incidence angle as Mach number at the inlet is increased from 0.4 to 0.8. A way in which a designer can help the situation is to choose a blade for which the location of maximum thickness is nearer to the leading edge.

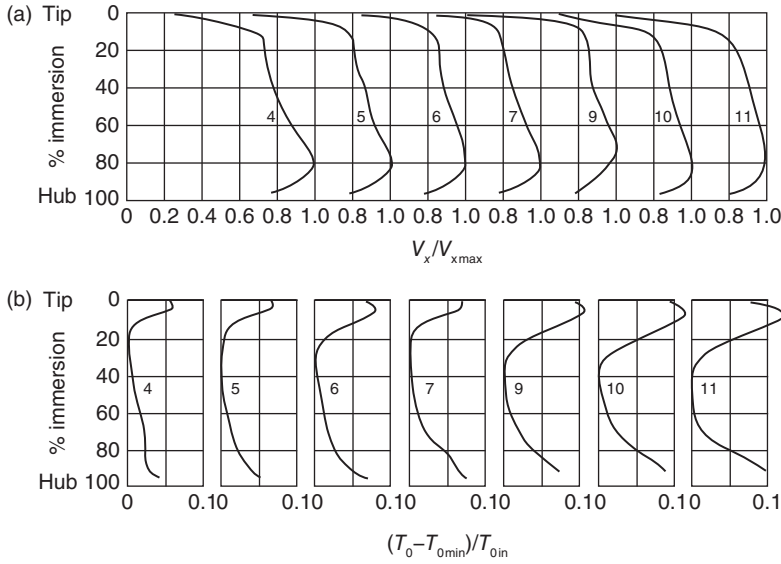


Figure 8.23 (a) Velocity and (b) temperature profiles in a 12-stage compressor. Source: From Smith [85].

8.6.8 Design of a compressor

In this last subsection of this chapter steps are given for a design of a multistage compressor. The analysis of the first two stages of a five-stage compressor are carried out in the next example and the last three are reserved for the exercises. It is expected that the reaction varies from stage to stage, so the stages are not normal. Hence, the equations developed for normal stage cannot be used, but the calculations are carried from the fundamental relations between blade loading and flow coefficients and the flow angles. The reaction is an additional parameter, and its value may be related to these.

It is assumed that the axial velocity is constant. The definition for reaction leads to

$$R = \frac{h_2 - h_1}{h_3 - h_1} = 1 - \frac{h_3 - h_2}{h_3 - h_1} = 1 - \frac{h_{03} - h_{02} - \frac{1}{2}(V_3^2 - V_2^2)}{h_{03} - h_{01} - \frac{1}{2}(V_3^2 - V_1^2)}$$

Since the stagnation enthalpy is constant across the stator $h_{03} = h_{02}$ and work done is $w = h_{03} - h_{01}$. Because the stage is not normal $V_1 \neq V_3$, and the reaction may be written as

$$R = 1 - \frac{V_2^2 - V_3^2}{2w + V_1^2 - V_3^2} = 1 - \frac{\phi^2(\tan^2\alpha_2 - \tan^2\alpha_3)}{2\psi + \phi^2(\tan^2\alpha_1 - \tan^2\alpha_3)} \quad (8.42)$$

Solving this for $\tan \alpha_3$ gives

$$\tan \alpha_3 = \sqrt{\frac{\tan^2\alpha_2}{R} - \left(\frac{2\psi}{\phi^2} + \tan^2\alpha_1\right) \left(\frac{1-R}{R}\right)} \quad (8.43)$$

from which α_3 may be determined when the other parameters are known.

EXAMPLE 8.5

A multistage axial compressor with axial inlet delivers air at total pressure ratio of $p_{0e}/p_{0i} = 3.5$, when the inlet conditions are $T_{0i} = 300$ K and $p_{0i} = 100$ kPa. The mass flow rate is $\dot{m} = 12$ kg/s, the axial flow is constant at $V_x = 175$ m/s, and the blade speed at the mean radius is $U = 300$ m/s. Determine the number of stages needed, the physical properties, flow angles and dimensions of the blades for the first two stages, assuming that the radius ratio at the inlet is $r_h/r_c = 0.5$ and that the stage efficiency is $\eta_p = 0.9$.

Solution: In the introductory section of this chapter, a stage compression ratio in the range 1.3–1.4 was stated to be typical for core compressors and since $3.5^{1/5} = 1.28$, a five-stage compressor is a reasonable design aim. With the stage efficiency assumed to be $\eta_p = 0.9$, then the polytropic exponent for air, from the definition $(n-1)/n = (\gamma-1)/\eta_p\gamma$ becomes $n = 1.465$. The stagnation temperature ratio across the entire compressor may be calculated from

$$\frac{T_{0e}}{T_{0i}} = \left(\frac{p_{0e}}{p_{0i}} \right)^{(n-1)/n} = 3.5^{0.465/1.465} = 1.488$$

which yields $T_{0e} = 446.52$ K. The difference $T_{0e} - T_{0i} = 146.52$ K divided into the five stages gives a 29.30 K stagnation temperature rise across each stage. The axial entrance to the first stage makes the relative Mach number at the casing quite large. Following the suggestion of Cohen et al. [15], the first stage is designed to have a lower temperature rise, so that the flow turns less and the reaction is not unduly high. By fixing $\Delta T_0 = 25$ K for the first stage and $\Delta T_0 = 32$ K for the three middle stages, would leave $\Delta T_0 = 25.52$ K for the last stage. It will not be exactly this because the compressor has only five stages so that the small stage theory is not strictly applicable.

Stage 1: The values $V_x = 175$ m/s and $U = 300$ m/s were chosen by examining the data in Figure 8.3. These give for the flow coefficient and blade loading coefficients the values

$$\phi = \frac{V_x}{U} = \frac{175}{300} = 0.5833 \quad \psi = \frac{c_p \Delta T_0}{U^2} = \frac{1004.5 \cdot 25}{300^2} = 0.2790$$

Mass balance gives the expression for the entrance area the expression

$$A_i = \frac{\dot{m}}{\rho_i V_x}$$

The static density is obtained from the ideal gas relation, in which the static temperature is

$$T_i = T_{0i} - \frac{V_i^2}{2c_p} = 300 - \frac{175^2}{2 \cdot 1004.5} = 284.76 \text{ K}$$

and the static pressure is

$$p_i = p_{0i} \left(\frac{T_i}{T_{0i}} \right)^{\gamma/(\gamma-1)} = 1000 \left(\frac{284.76}{300} \right)^{3.5} = 83.32 \text{ kPa}$$

The static density is therefore

$$\rho_i = \frac{p_i}{R_a T_i} = \frac{83.32}{0.287 \cdot 284.76} = 1.0195 \text{ kg/m}^3$$

The inlet area can now be calculated from

$$A_i = \frac{\dot{m}}{\rho_i V_x} = \frac{12}{1.0195 \cdot 175} = 0.1009 \text{ m}^2$$

This gives for the casing radius the value

$$r_c = \sqrt{\frac{A}{\pi(1 - \kappa^2)}} = 0.2069 \text{ m}$$

in which $\kappa = r_h/r_c$ is the radius ratio. The hub radius is $r_h = \kappa r_c = 0.1035 \text{ m}$ and the mean radius is $r_m = (r_c + r_h)/2 = 0.1552 \text{ m}$. The shaft speed is $\Omega = U/r_m = 300/0.1552 = 1933 \text{ rad/s} = 18459 \text{ rpm}$.

Since the flow is axial at the inlet, the relative velocity is

$$W_1 = \sqrt{V_x^2 + U^2} = \sqrt{175^2 + 300^2} = 347.3 \text{ m/s}$$

and the relative Mach number at the mean line has the value

$$M_{1R} = \frac{W_1}{\sqrt{\gamma R_a T_1}} = \frac{347.3}{\sqrt{1.4 \cdot 287 \cdot 284.76}} = 1.027$$

At the casing $U_c = r_c U/r_m = 0.2069 \cdot 300/0.1552 = 400 \text{ m/s}$, so the relative velocity at the casing is

$$W_{1c} = \sqrt{V_x^2 + U_c^2} = \sqrt{175^2 + 400^2} = 436.6 \text{ m/s}$$

and the relative Mach number is then $M_{1R} = 436.6/\sqrt{1.4 \cdot 287 \cdot 284.76} = 1.291$. This makes the inlet transonic, but this high Mach number can be tolerated, as the losses are not too high.

To obtain the flow angles, the inlet relative velocity is calculated first. To make sure that the algebraic sign is correct, write $W_{u1} = -U$ and then the angle of the relative velocity at the inlet is

$$\beta_1 = \tan^{-1} \left(\frac{W_{u1}}{W_x} \right) = \tan^{-1} \left(-\frac{1}{\phi} \right) = \tan^{-1} \left(-\frac{1}{0.5833} \right) = -59.74^\circ$$

The flow angle of the absolute velocity from the rotor is obtained by solving

$$c_p \Delta T_0 = \lambda_1 V_x U \tan \alpha_2 \quad \psi = \lambda_1 \phi \tan \alpha_2$$

for α_2 . It gives

$$\alpha_2 = \tan^{-1} \left(\frac{\psi}{\lambda_1 \phi} \right) = \tan^{-1} \left(\frac{0.2790}{0.982 \cdot 0.5833} \right) = 25.97^\circ$$

in which the work-done factor $\lambda_1 = 0.982$ was obtained from Table 8.1.

The angle of the relative velocity leaving the rotor is

$$\beta_2 = \tan^{-1} \left(\tan \alpha_2 - \frac{1}{\phi} \right) = \tan^{-1} \left(\tan(25.97^\circ) - \frac{1}{0.5833} \right) = -50.82^\circ$$

Next the outflow angle from the stage may be specified. In order to bring the reaction toward the 50% range, the inlet angle for the next stage should be such that the flow has a swirl component. The inlet angle for the second stage is equal to the exit angle of the first stage. This is chosen to be $\alpha_3 = 10^\circ$. The de Haller criterion can now be checked for the rotor and the stator. They are

$$\frac{\cos \beta_1}{\cos \beta_2} = \frac{\cos(-59.74^\circ)}{\cos(-50.82^\circ)} = 0.798 \quad \frac{\cos \alpha_2}{\cos \alpha_3} = \frac{\cos(25.97^\circ)}{\cos(10.00^\circ)} = 0.913$$

and both are clearly satisfied.

The reaction may be calculated using Eq. (8.42). It is

$$\begin{aligned} R &= 1 - \frac{\phi^2(\tan^2 \alpha_2 - \tan^2 \alpha_3)}{2\psi + \phi^2(\tan^2 \alpha_1 - \tan^2 \alpha_3)} \\ &= 1 - \frac{0.5833^2[\tan^2(25.97^\circ) - \tan^2(10^\circ)]}{2 \cdot 0.2790 + 0.5833^2[\tan^2(0^\circ) - \tan^2(10^\circ)]} = 0.872 \end{aligned}$$

The stagnation properties entering the second stage are $T_{02i} = 300 + 25 = 325$ K and

$$p_{02i} = p_{0i} \left(1 + \frac{\eta_p \Delta T_0}{T_{0i}} \right)^{\gamma/(\gamma-1)} = 100 \left(1 + \frac{0.9 \cdot 25}{300} \right)^{3.5} = 128.80 \text{ kPa}$$

Stage 2: For the second stage, the outlet angle is increased to $\alpha_3 = 20^\circ$, and the calculations are carried out identically to those for the first stage. The angle of the relative flow entering the rotor is

$$\beta_1 = \tan^{-1} \left(\tan \alpha_1 - \frac{1}{\phi} \right) = \tan^{-1} \left(\tan(10.0^\circ) - \frac{1}{0.5833} \right) = -56.97^\circ$$

Since $\Delta T_0 = 32$ K, the value of $\psi = c_p \Delta T_0 / U^2 = 1004.5 \cdot 32 / 300^2 = 0.3572$ and

$$\alpha_2 = \tan^{-1} \left(\frac{\psi}{\lambda_1 \phi} \right) = \tan^{-1} \left(\frac{0.3572}{0.952 \cdot 0.5833} \right) = 39.33^\circ$$

for the Table 8.1 shows that the work-done factor $\lambda_1 = 0.952$.

The relative velocity leaves the rotor at the angle

$$\beta_2 = \tan^{-1} \left(\tan \alpha_2 - \frac{1}{\phi} \right) = \tan^{-1} \left(\tan(39.33^\circ) - \frac{1}{0.5833} \right) = -41.82^\circ$$

Now the outflow angle is fixed to a value greater than from the first stage, say $\alpha_3 = 20^\circ$ and the de Haller criterion is checked for both the rotor and the stator. They are

$$\frac{\cos \beta_1}{\cos \beta_2} = \frac{\cos(-56.97^\circ)}{\cos(-41.82^\circ)} = 0.731 \quad \frac{\cos \alpha_2}{\cos \alpha_3} = \frac{\cos(39.33^\circ)}{\cos(20.00^\circ)} = 0.823$$

and both are still satisfied.

Again, the reaction may be calculated by Eq. (8.42). It is

$$R = 1 - \frac{\phi^2(\tan^2\alpha_2 - \tan^2\alpha_3)}{2\psi + \phi^2(\tan^2\alpha_1 - \tan^2\alpha_3)}$$

$$= 1 - \frac{0.5833^2[\tan^2(39.33^\circ) - \tan^2(20.00^\circ)]}{2 \cdot 0.3572 + 0.5833^2[\tan^2(10.00^\circ) - \tan^2(20.00^\circ)]} = 0.730$$

The stagnation properties entering the third stage are $T_{02i} = 325 + 32 = 357$ K and

$$p_{02i} = p_{0i} \left(1 + \frac{\eta_p \Delta T_0}{T_{0i}} \right)^{\gamma/(\gamma-1)} = 128.80 \left(1 + \frac{0.9 \cdot 32}{325} \right)^{3.5} = 173.38 \text{ kPa}$$

Mass balance gives the expression for the entrance area the expression

$$A_{2i} = \frac{\dot{m}}{\rho_{2i} V_x}$$

The static temperature is

$$T_{2i} = T_{02i} - \frac{V_{2i}^2}{2c_p} = 325 - \frac{177.70^2}{2 \cdot 1004.5} = 309.28 \text{ K}$$

in which $V_1 = V_x / \cos \alpha_1 = 175 / \cos(10.00^\circ) = 177.70$ m/s was used. The static pressure is

$$p_{2i} = p_{02i} \left(\frac{T_{2i}}{T_{02i}} \right)^{\gamma/(\gamma-1)} = 128.80 \left(\frac{309.28}{325} \right)^{3.5} = 108.29 \text{ kPa}$$

and the static density is

$$\rho_{2i} = \frac{p_{2i}}{R_a T_{2i}} = \frac{108.29}{0.287 \cdot 309.28} = 1.220 \text{ kg/m}^3$$

The flow area is therefore

$$A_2 = \frac{\dot{m}}{\rho_{2i} V_x} = \frac{12}{1.220 \cdot 175} = 0.0843 \text{ m}^2$$

Since $A_2 = \pi(r_c^2 - r_h^2) = 2\pi r_m b$, the blade height is

$$b = \frac{A_2}{2\pi r_m} = 0.0865 \text{ m}$$

so that

$$r_c = r_m + \frac{1}{2}b = 0.1552 + \frac{1}{2}0.0865 = 0.1984 \text{ m}$$

$$r_h = r_m - \frac{1}{2}b = 0.1552 - \frac{1}{2}0.0865 = 0.1120 \text{ m}$$

and the radius ratio is $\kappa_2 = 0.564$.

Table 8.2 A multistage axial compressor.

| Property | Stage 1 | Stage 2 | Stage 3 | Stage 4 | Stage 5 |
|------------------|---------|---------|---------|---------|---------|
| T_{0in} (K) | 300 | 325 | 357 | 389 | 421 |
| p_{0in} (kPa) | 100 | 128.8 | 173.4 | 227.47 | 292.07 |
| λ | 0.982 | 0.952 | 0.929 | 0.910 | 0.895 |
| ΔT_0 (K) | 25 | 32 | 32 | 32 | 24.82 |
| ψ | 0.279 | 0.357 | 0.357 | 0.357 | 0.277 |
| R | 0.872 | 0.730 | 0.588 | 0.500 | 0.500 |
| α_1 | 0 | 10.00 | 20.00 | 25.00 | 27.83 |
| α_2 | 25.97 | 39.33 | 45.65 | 48.72 | 46.63 |
| β_1 | -59.74 | -56.97 | -53.48 | -51.30 | -49.87 |
| β_2 | -50.82 | -41.82 | -34.65 | -29.91 | -33.25 |
| r_c (m) | 0.2069 | 0.1984 | 0.1905 | 0.1844 | 0.1798 |
| r_h (m) | 0.1035 | 0.1120 | 0.1199 | 0.1260 | 0.1306 |
| κ | 0.500 | 0.564 | 0.630 | 0.683 | 0.727 |

Stage 3: For the stage three $\Delta T_0 = 32$ K, $\lambda = 0.929$, and outlet angle is taken to be $\alpha_3 = 25^\circ$. Carrying out the calculations gives the results shown in Table 8.2.

Stage 4: For the stage four $\Delta T_0 = 32$ K, $\lambda = 0.910$. Now the reaction is set to $R = 0.5$, and the outlet flow angle α_3 is calculated from Eq. (8.43). The results for this set of calculations can be shown in the next column of Table 8.2.

Stage 5: Since the stage five is the last stage, the stagnation temperature rise across it is obtained by first calculating its pressure ratio. With $p_{0e} = 350$ kPa it becomes

$$\frac{p_{0e}}{p_{05in}} = \frac{350}{292.07} = 1.1983$$

and then the stagnation temperature increase is obtained from

$$\Delta T_0 = \left[\left(\frac{p_{0e}}{p_{05in}} \right)^{(\gamma-1)/\gamma} - 1 \right] \frac{T_{05in}}{\eta_p} = (1.1983^{1/3.5} - 1) \frac{421}{0.9} = 24.82 \text{ K}$$

With this stagnation temperature rise and $\lambda = 0.895$, and again assigning the reaction the value $R = 0.5$ gives the results listed in Table 8.2. In addition, the flow leaves the last stage at angle $\alpha_3 = 30.04$ K.

The work-done factor varies from stage to stage, and this is the reason the flow angles are not the same in absolute value even when the reaction is 50%. When the calculations are carried out with the aid of a computer, it is quite simple to change the assumed outlet angles or reactions, whichever is specified. Hence, the designer is free to adjust the design to check, for example how well the de Haller criteria is satisfied. The stage efficiency was assumed to have a value $\eta_p = 0.9$. The blade shapes would need to be chosen next and then the detailed loss calculations carried out to establish more accurate values for the efficiency of each stage. Today, this is followed by CFD-calculations to check the design. ■

EXERCISES

8.1 The inlet and exit stagnation pressures of air flowing through an axial compressor are 100 and 1000 kPa. The inlet stagnation temperature is 281 K. What is the work of compression if the adiabatic total-to-total efficiency is 0.75? [Ans: 350 kJ/kg]

8.2 Air flows through an axial fan rotor at mean radius of 15 cm. The tangential component of the absolute velocity is increased by 15 m/s through the rotor. The rotational speed of the shaft is 3000 rpm. (a) Evaluate the torque exerted on the air by the rotor, assuming that the flow rate is $0.48 \text{ m}^3/\text{s}$ and the inlet pressure and temperature of the air are 100 kPa and 300 K. (b) What is the rate of energy transfer to the air? [Ans: (a) 1.25 N m, (b) 394 W]

8.3 The blade speed of an axial compressor rotor is $U = 280 \text{ m/s}$, and the total enthalpy change across a normal stage is 31.6 kJ/kg . If the flow coefficient $\phi = 0.5$ and the inflow to the rotor is axial, what are the absolute and relative gas angles leaving the rotor? [Ans: 38.9° , -50.1°]

8.4 Air flows through an axial-flow fan, with an axial velocity of 40 m/s . The absolute velocities at the inlet and the outlet of the stator are at angles of 60° and 30° , respectively. The relative velocity at the outlet of the rotor is at an angle -25° . Assume reversible adiabatic flow and a repeating stage. (a) Draw the velocity diagrams at the inlet and outlet of the rotor. (b) Determine the flow coefficient. (c) Determine the blade-loading coefficient. (d) Determine at what angle the relative velocity enters the rotor. (e) Determine the static pressure increase across the rotor. The inlet total temperature is 300 K and the inlet total pressure is 101.3 kPa. (f) Determine the degree of reaction. [Ans: (b) 0.455, (c) 0.525, (d) -58.3° , (e) 2.27 kPa, (f) 0.475]

8.5 Air flows through an axial-flow compressor. The axial velocity is 60% of the blade speed at the mean radius. The reaction ratio is 0.4. The absolute velocity enters the stator at an angle of 55° from the axial direction. Assume a normal stage. (a) Draw the velocity diagrams at the inlet and outlet of the rotor. (b) Determine the flow coefficient. (c) Determine the blade-loading coefficient. (d) Determine at what angle the relative velocity enters the rotor. (e) Determine at what angle the relative velocity leaves the rotor. (f) Determine at what angle the absolute velocity leaves the stator. [Ans: (b) 0.600, (c) 0.514, (d) -47.6° , (e) -13.4° , (f) 29.8°]

8.6 A single stage of a multistage axial compressor is shown in Figure 8.2. The angle at which the absolute velocity enters the rotor is $\alpha_1 = 40^\circ$, and the relative velocity at the inlet of the rotor is $\beta_1 = -60^\circ$. These angles at the inlet of the stator are $\alpha_2 = 60^\circ$ and $\beta_2 = -40^\circ$. The mean radius of the rotor is 30 cm, and the hub-to-tip radius is 0.8. The axial velocity is constant and has a value $V_x = 125 \text{ m/s}$. The inlet air is atmospheric at pressure 101 kPa and temperature 293 K. (a) Find the mass flow rate. (b) What is the rotational speed of the shaft under these conditions? (c) What is the power requirement of the compressor? [Ans: (a) 16.81 kg/s, (b) 10230 rpm, (c) 602.85 kW]

8.7 A single stage of a multistage axial compressor is shown in Figure 8.2. The angle at which the absolute velocity enters the rotor is $\alpha_1 = 35^\circ$, and the relative velocity makes an angle of $\beta_1 = -60^\circ$. The corresponding angles at the inlet to the stator are $\alpha_2 = 60^\circ$ and

$\beta_2 = -35^\circ$. The stage is normal, and the axial velocity is constant through the compressor. (a) Why does the static pressure rise across both the rotor and the stator? (b) Draw the velocity triangles. (c) If the blade speed is $U = 290$ m/s, what is the axial velocity? (d) Find the work done per unit mass for a stage and the increase in stagnation temperature across it, if the stage efficiency is $\eta_p = 0.914$. (e) The stagnation temperature at the inlet is 300 K and pressure is 1 bar. The overall adiabatic efficiency of the compressor is $\eta_c = 0.756$, and the overall stagnation pressure ratio is 5.5. Determine the number of stages in the compressor. (f) How many axial turbine stages will it take to power this compressor? [Ans: (c) 119 m/s, (d) 35.68 kJ/kg, 35.5 K, (e) 7]

8.8 The blade speed of a rotor of an axial air compressor is $U = 150$ m/s. The axial velocity is constant and equal to $V_x = 75$ m/s. The tangential component of the relative velocity leaving the rotor is $W_{u2} = -30$ m/s; the tangential component of the absolute velocity entering the rotor is $V_{u1} = 55$ m/s. The stagnation temperature and pressure at the inlet to the rotor are 340 K and 185 kPa. The stage efficiency is 0.9, and one-half of the loss in stagnation pressure takes place through the rotor. (a) Draw the velocity diagrams at the inlet and exit of the rotor. (b) Find the work done per unit mass flow through the compressor. (c) Draw the states on an h - s -diagram. (d) Find the stagnation and static temperatures between the rotor and the stator. (e) Find the stagnation pressure between the rotor and the stator. [Ans: (b) 9.75 kJ/kg (d) 349.7 K and 339.7 K, (e) 203.25 kPa]

8.9 Air from ambient at 1 bar and temperature 20°C enters into a blower with the velocity 61 m/s. The blade tip radius is 60 cm, and the hub radius is 42 cm. The shaft speed is 1800 rpm. The air enters a stage axially and leaves it axially at the same speed. The rotor turns the relative velocity 18.7° toward the direction of the blade movement. The total-to-total stage efficiency is 0.87. (a) Draw the inlet and exit velocity diagrams for the rotor. (b) Draw the blade shapes. (c) Determine the flow coefficient and the blade-loading factor. (d) Determine the mass flow rate. (e) What is the specific work required? (f) What is the total pressure ratio for the stage? (g) Determine the degree of reaction. [Ans: (c) 0.635, 0.488, (d) 41.8 kg/s, (e) 4.51 kJ/kg, (f) 1.047, (g) 0.756]

8.10 Air from ambient at 1 bar and temperature 300 K enters an axial-flow compressor stage axially with velocity 122 m/s. The blade casing radius is 35 cm, and the hub radius is 30 cm. The shaft speed is 6000 rpm. At the exit, relative velocity is at an angle -45° . The total-to-total stage efficiency is 0.86. (a) Draw the inlet and exit velocity diagrams for the rotor. (b) Draw the blade shapes. (c) Determine the flow coefficient and the blade-loading factor. (d) Determine the mass flow rate. (e) What is the total pressure ratio for the stage? (f) Determine the degree of reaction. [Ans: (c) 0.60, 0.40, (d) 14.47 kg/s, (e) 1.178, (f) 0.80]

8.11 Air from ambient at 1 bar and temperature 300 K enters an axial-flow compressor at angle 15° , through a set of guide vanes, and the relative velocity is at angle -65° . The axial velocity has a constant value $V_x = 100$ m/s and the ratio of the blade speed to the exit angle from the rotor is $U/V_2 = 0.85$. The relative velocity leaves the rotor at angle -5° . (a) Find the angle at which the absolute velocity leaves the rotor. (b) Find the blade loading coefficient, the flow coefficient, and the reaction. (c) If the total-to-total efficiency of the stage is $\eta_{tt} = 0.9$, find the pressure p_2 leaving the rotor. [Ans: (a) 52.86° , (b) 0.436, 0.415, 0.671, (c) 81.5 kPa]

8.12 Air enters a repeating stage of an axial compressor with stagnation temperature 310 K. The reaction is 0.5, and the flow coefficient has the value 0.45. The relative

Mach number entering the rotor is 0.65 and the flow leaves the rotor at angle $\beta_2 = -25^\circ$. (a) Assuming the axial velocity to be constant, find its value. (b) Find the stagnation temperature rise across the stage. [Ans: (a) 112 m/s, (b) 35.9 K]

8.13 Show that when the axial velocity changes across the rotor from V_{x1} to V_{x2} , the flow angles are the following:

$$\begin{aligned}\tan \alpha_1 &= \frac{2(1-R)\psi - \psi^2 - \phi_2^2 + \phi_1^2}{2\phi_1\psi} \\ \tan \alpha_2 &= \frac{2(1-R)\psi + \psi^2 - \phi_2^2 + \phi_1^2}{2\phi_2\psi} \\ \tan \beta_1 &= \frac{-2R\psi - \psi^2 - \phi_2^2 + \phi_1^2}{2\phi_1\psi} \\ \tan \beta_2 &= \frac{-2R\psi + \psi^2 - \phi_2^2 + \phi_1^2}{2\phi_2\psi}\end{aligned}$$

8.14 Show that the solidity is related to the diffusion ratio and the flow angles by the equations

$$\begin{aligned}\sigma_S &= \frac{\frac{1}{2} \sin(\alpha_2 - \alpha_3)}{\cos \alpha_2 - (1 - \text{DF}) \cos \alpha_3} \\ \sigma_R &= \frac{\frac{1}{2} \sin(\beta_2 - \beta_1)}{\cos \beta_1 - (1 - \text{DF}) \cos \beta_2}\end{aligned}$$

8.15 Perform design calculations for a compressor stage with blade loading factor in the range $\psi = 0.25$ to $\psi = 0.55$, flow coefficient $\phi = 0.7$, and reaction $R = 0.6$. Keep the diffusion factor equal to 0.45. Calculate and plot $1 - \eta$, solidity, and the static pressure rise $1 - V_2^2/V_1^2$ for rotor and stator (including the de Haller criterion) as functions of ψ . What are the stagnation pressure losses across stator and rotor? [Ans: for $\psi = 0.25$, $\Delta p_{0LS} = 0.0145$ kPa, $\Delta p_{0LR} = 0.0206$ kPa, for $\psi = 0.55$, $\Delta p_{LS} = 0.0267$ kPa, $\Delta p_{LR} = 0.0436$ kPa]

8.16 A normal compressor stage has a reaction $R = 0.54$ and a stator outlet metal angle $\chi_3 = 14.5^\circ$. The camber angle is $\theta = 32^\circ$, pitch chord ratio is $s/c = 0.82$, and the position of maximum camber $a/c = 0.45$. The ratio of the blade height to the chord is $b/c = 1.7$. (a) Find the deviation of the flow leaving the stator. (b) Find the deflection. (c) Find the flow coefficient and blade-loading coefficient by assuming the inflow at zero incidence. [Ans: (a) 6.62° , (b) 26.1° , (c) 0.681, 0.474]

8.17 The circular arc blades of a compressor cascade have camber $\theta = 30^\circ$ and maximum thickness at $a/c = 0.5$. The space-to-chord ratio is $s/c = 1.0$. The nominal outflow angle is $\alpha_3^* = 25^\circ$. (a) Determine the nominal incidence. (b) Determine the lift coefficient at the nominal incidence given a drag coefficient of $C_D = 0.016$. [Ans: (a) 0.77° , (b) 0.967]

8.18 Air with density 1.21 kg/m³ flows into a compressor stator with velocity $V_2 = 120$ m/s and leaves at angle $\alpha_3 = 30^\circ$. If the Lieblein diffusion factor is to be held at 0.5 and the stagnation pressure loss across a compressor stator is 0.165 kPa, assuming incompressible flow and $s/c = 0.8$, what is the static pressure increase across the stage? [Ans: 4.46 kPa]

8.19 Air at temperature 288 K and at pressure 101 kPa flows into a compressor with 10 stages. The overall pressure ratio is $p_{0e}/p_{0i} = 4.3$. The efficiency of the first stage is 0.920 and the second stage, 0.916. For the remaining stages, the stage efficiency drops by 0.004 successively so that the last stage has an efficiency of 0.884. The axial velocity is constant, and the flow angles are the same at the inlet and exit of each of the stages. Hence, the work done by each stage is the same. (a) Find the overall efficiency of the compressor. (b) Find the overall efficiency by using the theory for a polytropic compression with small stage efficiency $\eta_p = 0.902$. [Ans: (a) 0.8846, (b) 0.8804]

8.20 Air at pressure 101 kPa and temperature 293 K flows into an axial flow fan of free vortex design, with hub radius $r_h = 7.5$ cm and casing radius 17 cm. The fan operates at 2400 rpm. The volumetric flow rate $Q = 1.1$ m³/s and the stagnation pressure rise is 3 cm H₂O. The fan efficiency is $\eta_{tt} = 0.86$. (a) Find the axial velocity. (b) Find the work done on the fluid. (c) Find the absolute and relative flow angles at the mean radius of the inlet and exit of the rotor when the inlet is axial. [Ans: (a) 15 m/s, (b) 284.3 J/kg, (c) $\alpha_1 = 0^\circ$, $\alpha_2 = 31.5^\circ$, $\beta_1 = -64.0^\circ$, $\beta_2 = -55.1^\circ$]

8.21 Consider an axial-flow compressor in which flow leaves the stator with a tangential velocity distributed as a free vortex. The hub radius is 10 cm and the static pressure at the hub is 94 kPa, and the static temperature there is 292 K. The radius of the casing is 15 cm, and the static pressure at the casing is 97 kPa. The total pressure at the hub and the casing are both 101.3 kPa. Find the exit flow angles at the hub and the casing. [Ans: 59.3° , 48.3°]

8.22 Air enters axially to a compressor from atmosphere at temperature 288 K and pressure 101.3 kPa. The axial velocity is $V_x = 175$ m/s, and the mass flow rate is $\dot{m} = 20$ kg/s. The blade speed at the mean radius is $U_m = 280$ m/s. (a) Calculate the relative Mach number at the mean radius and at the casing, when the radius ratio $\kappa = 0.5$. (b) If the inlet is fitted with a set of guide vanes that give some inlet swirl, so that the absolute velocity enters at $\alpha_1 = 10^\circ$, find the value for the axial velocity, by assuming that the shaft speed and the flow rate are the same. (c) Calculate the relative Mach number at the mean radius and at the casing. Check your results with Figure 8.3. [Ans: (a) 0.997, 1.245, (b) 176.07 m/s, (c) 0.922, 1.164]

8.23 Consider a three-stage axial compressor with total pressure ratio $p_{0e}/p_{0i} = 2.5$. The inlet stagnation temperature is $T = 300$ K and stagnation pressure 100 kPa. The mass flow rate is $\dot{m} = 15$ kg/s. The hub to tip ratio of the first stage of the blades is $\kappa = r_h/r_t = 0.5$. Assume that the stage efficiency is $\eta_p = 0.9$. The blade speed at the mean radius is $U_m = 300$ m/s and the axial velocity is constant and has the value $V_x = 200$ m/s. The absolute velocity at the inlet to the compressor is axial. (a) Find the relative Mach number at the tip radius of the blade at the inlet. (b) The blade height of the first stage assuming that the mean radius remains constant. (c) Assume that the stagnation temperature rise for the first two stages is 25 K, and design the exit flow angle from the first stage be 10° and from the second stage 20° . Design the first two stages. Make a table listing the flow angles, the reaction, and the casing and hub radii assuming that the mean radius remains constant. (d) Determine the stagnation temperature rise for the third stage and for $R = 0.55$, find the angles α_3 leaving this stage. What happens if the reaction is set to $R = 0.5$. (e) Determine diffusion factors for each stage making sure that de Haller criterion is. [Ans: (a) 1.33, (b) 9.02 cm, (c) stage 1: $R = 0.877$, $r_c = 0.1804$ m, $r_h = 0.0902$ m stage 2: $R = 0.786$, $r_c = 0.188$ m, $r_h = 0.1224$ m, (d) 24.14 K]

8.24 Carry out the calculations to confirm the results in Table 8.2 for stages 3, 4 and 5.

CHAPTER 9

CENTRIFUGAL COMPRESSORS AND PUMPS

This chapter is on centrifugal compressors and centrifugal pumps. Both achieve in a single stage a much higher pressure ratio than their axial counterparts. Large booster compressors are used in natural gas transmission across continental pipelines and in offshore natural gas production. Multistage centrifugal compressors, also known as *barrel compressors*, are employed when very high delivery pressure is required. When compressed air at high pressure is needed for industrial processes, a radial compressor fits this application well. Centrifugal compressors are often an integral part of a refrigeration plant to provide chilled water in heating, ventilating, and air conditioning (HVAC) systems. In contrast to these large compressors, in cars and trucks small centrifugal compressors are used as turbochargers and superchargers. They provide a machine of low inertia that is suitable for rapidly changing operating conditions.

Centrifugal pumps operate on the same principles as compressors, but handle liquids in various industrial, agricultural, and sanitary applications. Small pumps perform a variety of tasks in households. The number of various kinds of compressors and pumps in the world is very large, making their manufacture an important industry.

A sketch of a centrifugal compressor is shown in Figure 9.1. The axial part of the impeller at the inlet is called an *inducer*. The flow enters the impeller axially, or perhaps with a small amount of swirl, and leaves the wheel peripherally. From there, it flows through a vaned or vaneless diffuser and then enters a *volute*. Thus, in this machine, the flow at the inlet has no radial component of velocity and at the outlet, the axial component vanishes. In many blowers and fans, the inducer section is left out. An example is the

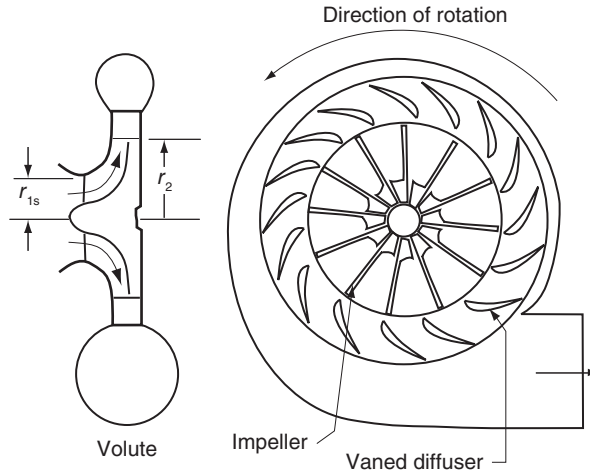


Figure 9.1 A sketch of a centrifugal compressor.

so-called *squirrel cage fan*, which provides large flow rates with modest pressure rise for certain industrial needs and which is also familiar as a small exhaust fan in a bathroom and a kitchen.

The blades in the impeller may be shrouded (as in the last stage of the compressor in Figure 1.6). Such impellers are used in multistage compressors, which, owing to the large load, require a large shaft, and the possible axial movement is better tolerated by a shrouded impeller than an unshrouded one. In an impeller with many vanes, some of the vanes do not reach all the way into the inducer, for the finite thickness of the blades leaves less flow area and causes possible choking of the flow. The vanes that extend all the way to the inlet of the inducer are curved at the inlet sufficiently that the relative velocity enters the vanes tangentially when the absolute velocity is axial.

9.1 COMPRESSOR ANALYSIS

The velocity triangles at the inlet and outlet of a centrifugal compressor are shown in Figure 9.2. At the inlet, the axial direction is to the right; at the outlet, the radial direction is to the right and normal to U . When the work done is written in terms of kinetic energies, it is

$$w = \frac{1}{2}(V_2^2 - V_1^2) + \frac{1}{2}(U_2^2 - U_1^2) + \frac{1}{2}(W_1^2 - W_2^2)$$

It is clear that in order to obtain a high pressure increase in the compressor, the work transfer must be large. Only the first term on the right accounts for an actual increase in kinetic energy, and the other two represent increases in other thermodynamic properties. If the work done is written as

$$w = h_{02} - h_{01} = h_2 - h_1 + \frac{1}{2}(V_2^2 - V_1^2),$$

then equating the right sides of this and the previous equation gives

$$h_1 + \frac{1}{2}(W_1^2 - U_1^2) = h_2 + \frac{1}{2}(W_2^2 - U_2^2)$$

This is a statement that the *trothalpy* remains constant across the compressor wheel. Writing this as

$$h_2 - h_1 = u_2 - u_1 + p_2 v_2 - p_1 v_1 = \frac{1}{2}(U_2^2 - U_1^2 + W_1^2 - W_2^2) \quad (9.1)$$

shows that the two kinetic energy terms on the right represent an increase in the internal energy of the gas and the difference in the flow work between the exit and the inlet.

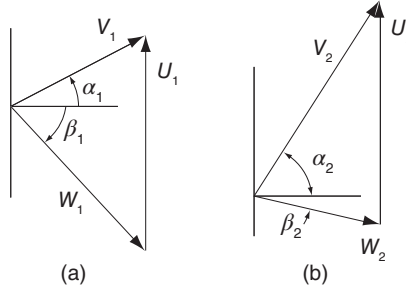


Figure 9.2 Velocity triangles for a centrifugal compressor. (a) Inlet and (b) outlet.

Comparing Eq. (9.1) to the equation obtained for a rotor of an axial machine, it is seen to reduce to it when U at the inlet and the outlet is the same. In that case, the increase in static enthalpy across the rotor was seen to arise from the decrease in relative velocity across the rotor. This effect is still there, but more importantly, enthalpy and thus pressure now rises owing to the centrifugal effect of a larger outlet radius. This increase in pressure is present even in the absence of any flow, and thus does not have a loss associated with it. It is substantially larger than the diffusional effect of the relative velocity.

The expression for work in the form

$$w = U_2 V_{u2} - U_1 V_{u1}$$

shows that a large amount of work can be done on the air if both the blade speed U_2 and V_{u2} are large. However, a flow with a large V_{u2} and, therefore, a large V_2 , may be difficult to diffuse to a slow speed in the volute. This must be taken into consideration in the design. The velocity diagrams in Figure 9.2 have been drawn to illustrate a general situation. Typically, in air compressors, air is drawn from the atmosphere, and it is without a tangential component and, therefore, enters the compressor with $\alpha_1 = 0$. However, a maldistribution of the flow through the impeller and the vaned space at the exit may influence the upstream condition and lead to some swirl. In addition, in the second and the subsequent stages of a multistage compressor, the inlet air might have some *pre-rotation*, and there are also single-stage compressors with special vanes at the inlet that give the flow a small amount of swirl, with positive swirl decreasing the work and negative swirl increasing it.

9.1.1 Slip factor

At the exit of the blades of a centrifugal compressor, the flow *deviates* in much the same way as was encountered in axial compressors. To account for it, a *slip factor* is introduced as

$$\sigma = 1 - \frac{V'_{u2} - V_{u2}}{U_2} = 1 - \frac{V_{us}}{U_2}$$

Here V_{u2} is the actual velocity, and V'_{u2} the velocity if there were no slip. The slip velocity is defined as $V_{us} = V'_{u2} - V_{u2}$. The flow angle of the relative velocity at the outlet is typically negative and greater in absolute value than the blade angle χ_2 . The deviation is from the pressure side toward the suction side of the blades. From the equations,

$$V'_{u2} = U_2 + V_{r2} \tan \chi_2 \qquad V_{u2} = U_2 + V_{r2} \tan \beta_2$$

the slip velocity can be determined, and then the slip coefficient may be expressed as

$$\sigma = 1 - \frac{V_{r2}}{U_2} (\tan \chi_2 - \tan \beta_2)$$

This can also be written as

$$\sigma U_2 = U_2 + W_{u2} - V_{r2} \tan \chi_2 = V_{u2} - V_{r2} \tan \chi_2$$

or in the more convenient form

$$V_{u2} = \sigma U_2 + V_{r2} \tan \chi_2 \tag{9.2}$$

In addition, writing $V_{r2} = V_{u2} / \tan \alpha_2$, substituting and solving for V_{u2} , gives

$$V_{u2} = \frac{\sigma U_2}{1 - \frac{\tan \chi_2}{\tan \alpha_2}} \tag{9.3}$$

If there is no inlet swirl, then $w = U_2 V_{u2}$, and this equation becomes

$$\psi = \frac{\sigma}{1 - \frac{\tan \chi_2}{\tan \alpha_2}} \tag{9.4}$$

For radial blades $\chi_2 = 0$, and Eq. (9.3) reduces to

$$V_{u2} = \sigma U_2$$

The range of slip factor is $0.83 < \sigma < 0.95$, and the higher value is obtained if the number of blades is large and the flow is guided well. The actual and ideal velocities are shown in Figure 9.3.

Stodola gave the following argument to estimate the slip factor [89]. The fluid flow through the rotor is irrotational in the laboratory frame, except for that part of the flow that moves right next to the solid surfaces. Therefore, relative to the blade, the spin of the fluid particles (i.e. their vorticity) must be equal and opposite to that caused by the rotating coordinates. Hence, a secondary forced vortex that rotates at the angular velocity Ω , as shown, can be assumed to exist in the flow channel. If s is the spacing between the blades along the peripheral circle, the diameter of the secondary vortex is roughly $D_s = s \cos \chi_2$, as the construction in Figure 9.3b shows. Hence, the slip velocity can be taken to be

$$V_{us} = \frac{D_s}{2} \Omega = \frac{D_s U_2}{D} = \frac{U_2 s \cos \chi_2}{D}$$

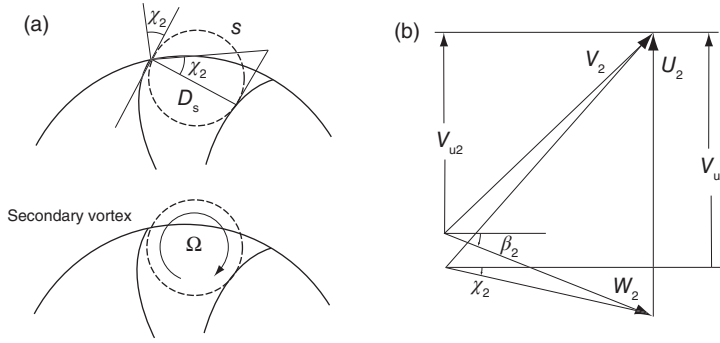


Figure 9.3 Illustration of slip.

If Z is the number of blades, then $\pi D = sZ$, so that $s/D = \pi/Z$ and the slip velocity takes the form

$$V_{us} = \frac{\pi U_2 \cos \chi_2}{Z}$$

and the slip factor is

$$\sigma = 1 - \frac{\pi \cos \chi_2}{Z} \quad (9.5)$$

Stanitz [87] recommends

$$\sigma = 1 - \frac{0.63\pi}{Z} \quad (9.6)$$

for the slip coefficient and assures it to be good in the range $-45^\circ < \chi_2 < 45^\circ$. Other efforts to establish the value for the slip velocity include those by Busemann for blades of logarithmic spiral shape. A synthesis of this and other results was carried out by Wiesner [96], who recommends the expression

$$\sigma = 1 - \frac{\sqrt{\cos \chi_2}}{Z^{0.7}} \quad (9.7)$$

9.1.2 Pressure ratio

The Euler equation for turbomachinery is

$$w = h_{03} - h_{01} = U_2 V_{u2} - U_1 V_{u1}$$

and the ideal work is

$$w_s = h_{03ss} - h_{01}$$

The states for the compression process are shown in the Mollier diagram in Figure 9.4. With $\eta_{tt} = w_s/w$ from these equations, it follows that

$$\left(\frac{p_{03}}{p_{01}} \right)^{(\gamma-1)/\gamma} = 1 + \frac{\gamma-1}{\gamma R T_{01}} \eta_{tt} (U_2 V_{u2} - U_1 V_{u1}) \quad (9.8)$$

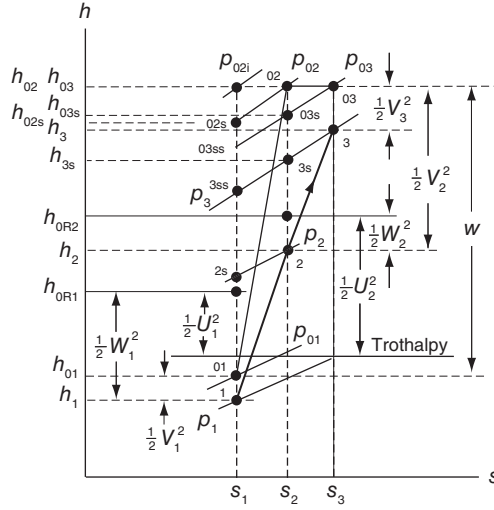


Figure 9.4 The thermodynamic states in a centrifugal compressor.

When the inlet velocity is axial and therefore small, the stagnation enthalpy h_{01} is only slightly larger than h_1 . The line of constant trothalpy

$$h_1 + \frac{1}{2}W_1^2 - \frac{1}{2}U_1^2 = h_2 + \frac{1}{2}W_2^2 - \frac{1}{2}U_2^2$$

is shown in Figure 9.4, as well as the magnitudes of the various kinetic energies. In particular, the blade velocity U_1 is smaller than U_2 , and the relative velocity diffuses across the rotor so that $W_1 > W_2$. The kinetic energy leaving the rotor is quite large. The loss of stagnation pressure across the rotor is $\Delta p_{0LR} = p_{02i} - p_{02}$, and across the volute, it is $\Delta p_{0LS} = p_{02} - p_{03}$. The pressure p_{02i} is the stagnation pressure for an isentropic compression process in which the same amount of work has been done as in the actual process.

The rotor efficiency is given by

$$\eta_R = \frac{h_{02s} - h_{01}}{h_{02} - h_{01}} \quad (9.9)$$

With η_R known, the stagnation temperature T_{02s} can be calculated from Eq. (9.9), and the stagnation pressure p_{02} can then be determined from

$$p_{02} = p_{01} \left(\frac{T_{02s}}{T_{01}} \right)^{\gamma/(\gamma-1)}$$

In addition, integrating the Gibbs equation along the line of constant p_{02} and along the line of constant h_{02} between the states with entropies s_1 and s_2 gives

$$\frac{p_{02i}}{p_{02}} = \left(\frac{T_{02}}{T_{02s}} \right)^{\gamma/(\gamma-1)}$$

from which p_{02i} is obtained.

For an axial inlet flow $V_{u1} = 0$ and introducing $V_{u2} = \psi U_2$ into Eq. (9.8), the pressure ratio may be written as

$$\frac{p_{03}}{p_{01}} = [1 + (\gamma - 1)\psi\eta_{tt}M_{0u}^2]^{\gamma/(\gamma-1)} \quad (9.10)$$

in which $M_{0u} = U_2/c_{01}$. A plot of this relation is shown in Figure 9.5. Similarly, the pressure ratio across the rotor alone is

$$\frac{p_{02}}{p_{01}} = [1 + (\gamma - 1)\psi\eta_R M_{0u}^2]^{\gamma/(\gamma-1)} \quad (9.11)$$

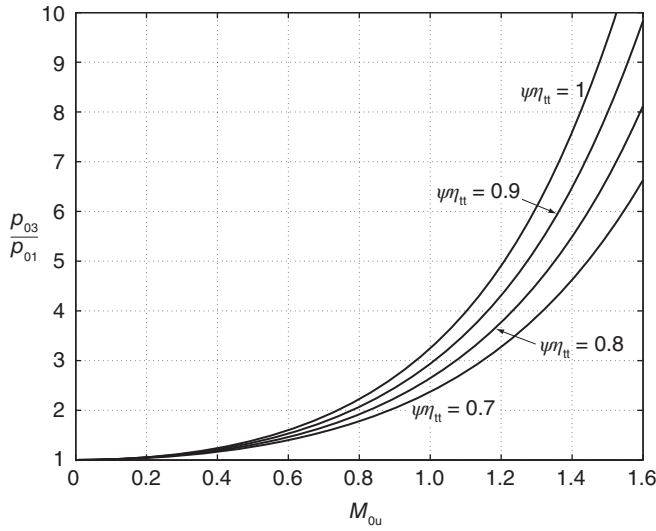


Figure 9.5 Pressure ratio as a function of blade stagnation Mach number, for various values of $\psi\eta_{tt}$ and for gas with $\gamma = 1.4$.

It was seen earlier that in the expression for constant trothalpy

$$h_2 - h_1 = \frac{1}{2}(U_2^2 - U_1^2) + \frac{1}{2}(W_1^2 - W_2^2)$$

the first term on the right side is a kinematic effect and therefore represents a reversible process. If the left side is written as

$$h_2 - h_1 = h_2 - h_{2s} + h_{2s} - h_1,$$

then the reversible enthalpy change may be written as

$$h_{2s} - h_1 = \frac{1}{2}(U_2^2 - U_1^2) + (1 - f)\frac{1}{2}(W_1^2 - W_2^2),$$

and for the irreversible change,

$$h_2 - h_{2s} = f\frac{1}{2}(W_1^2 - W_2^2)$$

in which f is the fraction of the change in relative kinetic energy lost to irreversibility. The static enthalpy loss coefficient ζ_R in

$$h_2 - h_{2s} = \frac{1}{2} \zeta_R W_2^2$$

is related to f by the equation

$$\zeta_R = f \left(\frac{W_1^2}{W_2^2} - 1 \right)$$

The ratio $(1 - \eta_R)/(1 - \eta_{tt})$ of rotor losses to the total losses is between 0.5 and 0.6. Hence, for $\eta_{tt} = 0.8$, the rotor efficiency is about $\eta_R = 0.89$.

Writing the rotor efficiency as

$$\eta_R = \frac{h_{2s} - h_1 + \frac{1}{2}(V_{2s}^2 - V_1^2)}{h_2 - h_1 + \frac{1}{2}(V_2^2 - V_1^2)}$$

and assuming that $V_{2s} = V_2$, this becomes

$$\eta_R = \frac{h_{2s} - h_2 + h_2 - h_1 + \frac{1}{2}(V_2^2 - V_1^2)}{h_2 - h_1 + \frac{1}{2}(V_2^2 - V_1^2)}$$

which can also be written as

$$\eta_R = 1 - \frac{h_2 - h_{2s}}{w} = 1 - \frac{\zeta_R W_2^2}{2w} = 1 - \frac{\zeta_R W_2^2}{2\psi U_2^2}$$

Squaring and adding the component equations

$$W_2 \sin \beta_2 = V_{u2} - U_2 \quad W_2 \cos \beta_2 = V_{r2}$$

gives

$$W_2^2 = V_{u2}^2 - 2V_{u2}U_2 + U_2^2 + V_{r2}^2$$

In addition,

$$V_{r2} = \frac{V_{u2}}{\tan \alpha_2}$$

so that

$$\frac{W_2^2}{U_2^2} = 1 - 2\psi + \frac{\psi^2}{\sin^2 \alpha_2} \quad (9.12)$$

and the rotor efficiency can be written as

$$\eta_R = 1 - \zeta_R \frac{(1 - 2\psi + \psi^2/\sin^2 \alpha_2)}{2\psi}$$

in which

$$\psi = \frac{\sigma}{1 - \frac{\tan \chi_2}{\tan \alpha_2}} \quad (9.13)$$

Solving the equation for rotor efficiency for ζ_R gives

$$\zeta_R = \frac{(1 - \eta_R)2\psi}{1 - 2\psi + \psi^2/\sin^2\alpha_2}$$

For a typical case, $\chi_2 = -40^\circ$ and $\alpha_2 = 67^\circ$. With $\sigma = 0.85$, these equations give $\psi = 0.627$, and for a rotor efficiency $\eta_R = 0.89$, the loss coefficient is $\zeta_R = 0.656$. The latter appears to be quite large, but when calculating the stagnation pressure losses, this is multiplied by W_2^2 , which is small because the flow will have been diffused through the rotor. In addition, a typical value for $W_1/W_2 = 1.6$. For these values, the fraction of the relative kinetic energy lost to irreversibility is $f = 0.38$. This number accords with Cumpsty's [18] review of the field. Although this number appears to be large, in a typical compressor, the centrifugal effect accounts for over three quarters of the pressure rise and the diffusion of the relative velocity the rest. Hence, 38% loss keeps the rotor efficiency still over 90%.

■ EXAMPLE 9.1

Air flows from atmosphere at pressure 101.3 kPa and temperature 288 K into a centrifugal compressor with radial blades at the exit of the impeller and without any swirl at the inlet. The compressor wheel has 18 blades, and it turns at 15000 rpm. The exit radius is $r_2 = 26$ cm, and the inlet hub radius is $r_h = 8.5$ cm and the shroud radius is $r_s = 17$ cm. The total-to-total efficiency is $\eta_{tt} = 0.79$. (a) Find the power required assuming that the mass flow rate is $\dot{m} = 8$ kg/s. Use the Stanitz formula to find the slip coefficient. (b) Find the stagnation pressure ratio. (c) Find the blade height at the exit for a design in which the radial velocity at the exit is equal to the uniform axial velocity at the inlet. In addition, as is stated in the text, one may also assume that the losses in the impeller are equal to those in the volute. (d) Find the Mach number at the inlet based on the relative velocity at the hub, the mean radius, and the shroud.

Solution: (a) Since the air comes from the atmosphere, where it is stagnant, the atmospheric pressure and temperature are the inlet stagnation properties. The blade speeds at the exit and inlet are obtained from $U = r\Omega$, and these are

$$U_2 = r_2\Omega = \frac{0.26 \cdot 15000 \cdot \pi}{30} = 408.4 \text{ m/s} \quad U_m = \frac{0.1275 \cdot 15000 \cdot \pi}{30} = 200.3 \text{ m/s}$$

$$U_s = r_s\Omega = \frac{0.17 \cdot 15000 \cdot \pi}{30} = 267.0 \text{ m/s} \quad U_h = \frac{0.085 \cdot 15000 \cdot \pi}{30} = 133.5 \text{ m/s}$$

At the outlet, the tangential velocity is $V_{u2} = \sigma U_2$ and the slip coefficient is

$$\sigma = 1 - \frac{0.63 \cdot \pi}{Z} = 1 - \frac{0.63 \cdot \pi}{18} = 0.89$$

Since the inlet flow is axial, the work done is

$$w = V_{u2}U_2 = \sigma U_2^2 = 0.89 \cdot 408.4^2 = 148.46 \text{ kJ/kg}$$

and the power to the compressor is

$$\dot{W} = \dot{m}w = 8 \cdot 148.46 = 1187.6 \text{ kW}$$

(b) The isentropic work is

$$w_s = \eta_{tt} w = 0.79 \cdot 146.46 = 117.3 \text{ kJ/kg}$$

so that

$$T_{03s} = T_{01} + \frac{w_s}{c_p} = 288 + \frac{117.3}{1.0045} = 404.78 \text{ K},$$

and the pressure ratio across the compressor is

$$\frac{p_{03}}{p_{01}} = \left(\frac{T_{03s}}{T_{01}} \right)^{\gamma/(\gamma-1)} = \left(\frac{404.78}{288} \right)^{3.5} = 3.29$$

(c) To determine the blade height at the exit, the radial velocity at the exit is needed. In the statement of this example, it is suggested that for preliminary design it may be assumed that it is equal to the axial velocity at the inlet. Thus, the inlet velocity needs to be determined first. This is obtained from the mass balance at the inlet.

$$\dot{m} = \rho_1 V_x A_1$$

in which both V_x and ρ_1 are unknowns, since the inlet area is simply

$$A_1 = \pi(r_s^2 - r_h^2) = \pi(0.17^2 - 0.085^2) = 0.0681 \text{ m}^2$$

The mass balance may be written in terms of the flow function, and doing so leaves the inlet Mach number as the only unknown. The flow function is

$$F = \frac{\dot{m} \sqrt{c_p T_{01}}}{A_1 p_{01}} = \frac{8 \sqrt{1004.5 \cdot 288}}{0.0681 \cdot 101000} = 0.624$$

and now from its definition

$$F = \frac{\gamma M_1}{\sqrt{\gamma - 1}} \left(1 + \frac{\gamma - 1}{2} M_1^2 \right)^{-(\gamma+1)/(2\gamma-2)}$$

the inlet Mach number may be determined iteratively by hand or with the computer software's FZERO-function. It is determined to be $M_1 = 0.297$. Next the static temperature at the inlet is

$$T_1 = T_{01} \left(1 + \frac{\gamma - 1}{2} M_1^2 \right)^{-1} = \frac{288}{1 + 0.2 \cdot 0.297^2} = 283.0 \text{ K}$$

The inlet velocity is now $V_x = M_1 \sqrt{\gamma R T_1} = 0.297 \sqrt{1.4 \cdot 287 \cdot 283} = 100.1 \text{ m/s}$.

Just to check the work, the static pressure is seen to be

$$p_1 = p_{01} \left(\frac{T_1}{T_{01}} \right)^{\gamma/(\gamma-1)} = 101.3 \left(\frac{283}{288} \right)^{3.5} = 95.28 \text{ kPa},$$

and the density at the inlet is

$$\rho_1 = \frac{p_1}{RT_1} = \frac{95.29}{0.287 \cdot 283} = 1.173 \text{ kg/m}^3$$

These give for the mass flow rate

$$\dot{m} = \rho_1 V_x A_1 = 1.173 \cdot 100.1 \cdot 0.0681 = 8 \text{ kg/s}$$

which accords with the mass flow rate given in the problem statement.

The mass balance at the exit of the impeller can be used to determine the blade height. For this, the static density is needed, which in turn depends on the static temperature and pressure. To determine them, the radial velocity at the exit may be assumed in preliminary design to be equal to the inlet velocity, so that $V_{r2} = V_x = 100.1 \text{ m/s}$. Since $V_{u2} = \sigma U_2 = 0.89 \cdot 408.4 = 363.5 \text{ m/s}$, the velocity at the exit is

$$V_2 = \sqrt{V_{2r}^2 + V_{2u}^2} = \sqrt{100.1^2 + 363.5^2} = 377.0 \text{ m/s}$$

Next assuming that half of the losses take place in the flow across the impeller and the half after it, the rotor efficiency may be calculated from

$$\frac{1 - \eta_R}{1 - \eta_{tt}} = 0.5 \quad \eta_R = 1 - 0.5(1 - \eta_{tt}) = 1 - 0.5(1 - 0.79) = 0.895$$

Hence, with $T_{02} = T_{03} = 435.8 \text{ K}$

$$T_{02s} = T_{01} + \eta_R(T_{02} - T_{01}) = 288 + 0.895(435.8 - 288) = 420.3 \text{ K}$$

and

$$p_{02} = p_{01} \left(\frac{T_{02s}}{T_{01}} \right)^{\gamma/(\gamma-1)} = 101.3 \left(\frac{420.3}{288} \right)^{3.5} = 380.3 \text{ kPa}$$

The static properties are therefore

$$T_2 = T_{02} - \frac{V_2^2}{2c_p} = 435.8 - \frac{377^2}{2 \cdot 1000.45} = 365.0 \text{ K}$$

$$p_2 = p_{02} \left(\frac{T_2}{T_{02}} \right)^{\gamma/(\gamma-1)} = 380.3 \left(\frac{365.0}{435.6} \right)^{3.5} = 204.5 \text{ kPa}$$

$$\rho_2 = \frac{p_2}{RT_2} = \frac{204.5}{0.287 \cdot 365} = 1.952 \text{ kg/m}^3$$

The area at the impeller exit is thus

$$A_2 = \frac{\dot{m}}{\rho_2 V_{r2}} = \frac{8}{1.952 \cdot 100.1} = 0.0409 \text{ m}^2$$

and the blade height is

$$b = \frac{A_2}{2\pi r_2} = \frac{0.0409}{2 \cdot \pi \cdot 0.26} = 0.025 \text{ m} = 2.5 \text{ cm}$$

(d) At the inlet, the flow angle of the relative velocity is at the hub, shroud, and mean radii

$$\begin{aligned}\beta_{1h} &= \tan^{-1} \left(-\frac{U_h}{V_x} \right) = \tan^{-1} \left(-\frac{133.5}{100.1} \right) = -53.13^\circ \\ \beta_{1s} &= \tan^{-1} \left(-\frac{U_s}{V_x} \right) = \tan^{-1} \left(-\frac{267.0}{100.1} \right) = -69.44^\circ \\ \beta_{1m} &= \tan^{-1} \left(-\frac{U_m}{V_x} \right) = \tan^{-1} \left(-\frac{200.3}{100.1} \right) = -63.43^\circ,\end{aligned}$$

and the corresponding relative velocities are

$$\begin{aligned}W_{1h} &= \frac{V_x}{\cos \beta_{1h}} = \frac{100.1}{\cos(-53.13)} = 166.6 \text{ m/s} \\ W_{1m} &= \frac{V_x}{\cos \beta_{1m}} = \frac{100.1}{\cos(-63.43)} = 223.9 \text{ m/s} \\ W_{1s} &= \frac{V_x}{\cos \beta_{1s}} = \frac{100.1}{\cos(-69.44)} = 285.2 \text{ m/s}\end{aligned}$$

The relative Mach numbers are

$$M_{1Rh} = \frac{W_{1h}}{c_1} = 0.495 \quad M_{1Rm} = \frac{W_{1m}}{c_1} = 0.664 \quad M_{1Rs} = \frac{W_{1s}}{c_1} = 0.846$$

It is desirable to keep the relative Mach number at the shroud to value less than 0.8, and in this example, it is slightly higher than that. The radial velocity at the exit was taken to be equal to the axial velocity at the inlet. This, of course, does not need to be exactly the case. ■

9.2 INLET DESIGN

Similar design limitations are encountered in the design of centrifugal compressors as in axial compressors. Namely, absolute and relative velocities must be kept sufficiently low to ensure that shock losses do not become excessive. The blade speed for high-performance compressors with a stainless-steel wheel is kept below 450 m/s owing to limitations caused by high stresses.

Typically, the inlet stagnation pressure and temperature are known, and when atmospheric air is compressed, they are the ambient values. If the compressor is not equipped with vanes to introduce pre-swirl into the flow, the absolute velocity is axial. This velocity is also uniform across the inlet. The inlet hub and shroud radii are r_{1h} and r_{1s} , and the inlet area is

$$A_1 = \pi(r_{1s}^2 - r_{1h}^2) = \pi r_{1s}^2(1 - \kappa^2) \quad \text{where} \quad \kappa = \frac{r_{1h}}{r_{1s}}$$

The flow rate

$$\dot{m} = \rho_1 A_1 V_1$$

may be expressed in a nondimensional form by dividing it by the product $\rho_{01}\pi r_2^2 c_{01}$. Following Whitfield and Baines [95], this is written as

$$\Phi = \frac{\dot{m}}{\rho_{01}\pi r_2^2 c_{01}} = \frac{\rho}{\rho_{01}} \frac{r_{1s}^2}{r_2^2} (1 - \kappa^2) \frac{W_{1s}}{c_{01}} \cos \beta_{1s} \quad (9.14)$$

in which the inlet velocity V_1 has been related to the relative velocity at the shroud by $V_1 = W_{1s} \cos \beta_{1s}$. In addition, $W_{1s} = \sqrt{U_{1s}^2 + V_1^2}$, and since the blade speed is largest at the shroud, so is W_{1s} , and β_{1s} has the largest absolute value there. With $r_{1s}/r_2 = U_{1s}/U_2$, the nondimensional mass flow rate may be written as

$$\Phi = \frac{\rho_1}{\rho_{01}} \frac{U_{1s}^2}{U_2^2} (1 - \kappa^2) \frac{W_{1s}}{c_{01}} \cos \beta_{1s},$$

and it can be further manipulated into the form

$$\Phi = \frac{\rho_1}{\rho_{01}} \left(\frac{W_{1s}^2 - V_1^2}{c_1^2} \right) \frac{c_{01}^2}{U_2^2} \frac{c_1^2}{c_{01}^2} (1 - \kappa^2) \frac{W_{1s}}{c_1} \frac{c_1}{c_{01}} \cos \beta_{1s} \quad (9.15)$$

which can be written as

$$\Phi = \frac{\rho_1}{\rho_{01}} \left(\frac{T_1}{T_{01}} \right)^{3/2} \frac{M_{1Rs}^3}{M_{0u}^2} (1 - \kappa^2) (1 - \cos^2 \beta_{1s}) \cos \beta_{1s}$$

Here, $M_{1Rs} = W_{1s}/c_1$ is the relative Mach number at the shroud. Defining next

$$\Phi_f = \frac{\Phi M_{0u007D^2}}{1 - \kappa^2},$$

the preceding equation can be written as

$$\Phi_f = \frac{M_{1Rs}^3 (1 - \cos^2 \beta_{1s}) \cos \beta_{1s}}{\left(1 + \frac{\gamma-1}{2} M_{1Rs}^2 \cos^2 \beta_{1s} \right)^{(3\gamma-1)/(2\gamma-2)}} \quad (9.16)$$

Graphs calculated from Eq. (9.16) are shown in Figure 9.6. The angle β_{1s} at which the flow rate reaches its maximum value is obtained by differentiating this equation with respect to $\cos \beta_{1s}$ and setting the derivative to zero:

$$\cos^4 \beta_{1s} - \frac{3 + \gamma M_{1Rs}^2}{M_{1Rs}^2} \cos^2 \beta_{1s} + \frac{1}{M_{1Rs}^2} = 0 \quad (9.17)$$

The solution is

$$\cos^2 \beta_{1s} = \left(\frac{3 + \gamma M_{1Rs}^2}{2M_{1Rs}^2} \right) \left(1 - \sqrt{1 - \frac{4M_{1Rs}^2}{(3 + \gamma M_{1Rs}^2)^2}} \right) \quad (9.18)$$

Another way to plot the data is shown in Figure 9.7. For $M_{1Rs} = 0.6$, the optimum angle from Eq. (9.18) is $\beta_{1s} = -57.15^\circ$, and if the relative Mach number is increased to $M_{1Rs} = 1.2$, the optimum angle is $\beta_{1s} = -62.56^\circ$. In the incompressible limit, the optimum angle is $\beta_{1s} = -54.74^\circ$.

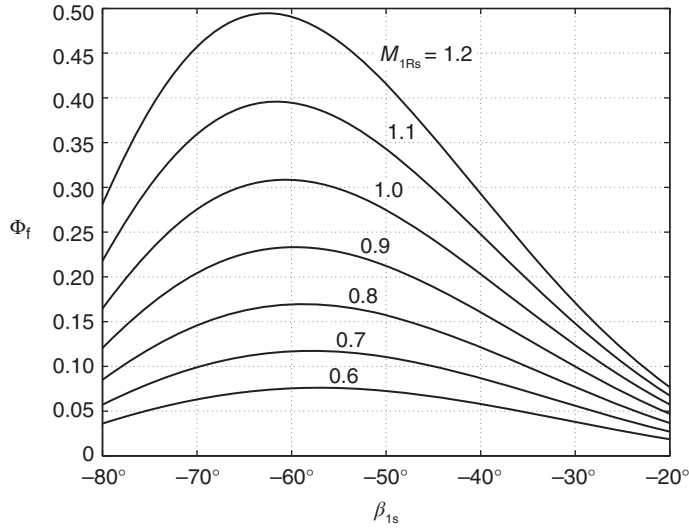


Figure 9.6 Nondimensional mass flow rate for given inlet angle of relative flow with relative Mach number as a parameter, for a gas with $\gamma = 1.4$.

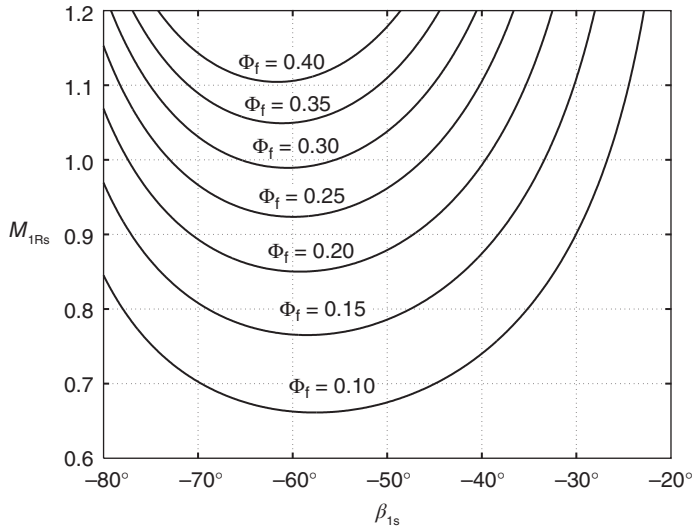


Figure 9.7 Relative Mach number for a given inlet angle of relative flow with nondimensional flow rate as a parameter, for a gas with $\gamma = 1.4$.

Equation (9.16) can be recast also in the form

$$\Phi_f = \frac{\rho_1}{\rho_{01}} \left(\frac{W_{1s}^2 - V_1^2}{c_1^2} \right) \frac{c_1^2}{c_{01}^2} \frac{V_1}{c_1} \frac{c_1}{c_{01}}$$

and further as

$$\Phi_f = \frac{(M_{1Rs}^2 - M_1^2) M_1}{\left(1 + \frac{\gamma-1}{2} M_1^2\right)^{(3\gamma-1)/(2\gamma-2)}}$$

Solving this for M_{IRs}^2 gives

$$M_{\text{IRs}}^2 = M_1^2 + \frac{\Phi_f}{M_1} \left(1 + \frac{\gamma - 1}{2} M_1^2 \right)^{(3\gamma - 1)/(2\gamma - 2)}$$

This result is displayed in Figure 9.8. Since $M_1 = M_{\text{IRs}} \cos \beta_{1s}$, the lines of constant $\cos \beta_{1s}$ are straight on this set of graphs and the optimum angle is at the minima of the curves.

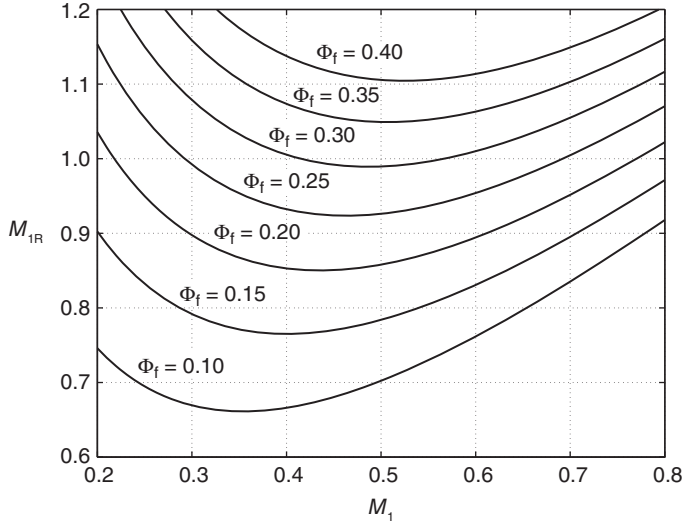


Figure 9.8 Relative Mach number for given inlet Mach number with nondimensional flow rate as a parameter and for a gas with $\gamma = 1.4$.

EXAMPLE 9.2

In an air compressor, the relative Mach number is $M_{\text{IRs}} = 0.9$ at the shroud of the impeller. The inlet stagnation pressure and temperature are 101.3 kPa and 288 K. The mass flow rate is $\dot{m} = 8$ kg/s. The hub-to-shroud radius ratio is 0.4, and the inlet flow is axial. Determine (a) the rotational speed of the impeller, (b) the axial velocity, and (c) the inducer shroud diameter, assuming that the inducer is designed for optimum relative flow angle, and that the compressor operates at the design point.

Solution: The stagnation density is

$$\rho_{01} = \frac{p_{01}}{RT_{01}} = \frac{101.3}{0.287 \cdot 288} = 1.2256 \text{ kg/m}^3$$

and the stagnation speed of sound is

$$c_{01} = \sqrt{\gamma RT_{01}} = \sqrt{1.4 \cdot 287 \cdot 288} = 340.17 \text{ m/s}$$

The optimum relative flow angle can be found from

$$\cos^2 \beta_{1s} = \left(\frac{3 + \gamma M_{\text{IRs}}^2}{2 M_{\text{IRs}}^2} \right) \left(1 - \sqrt{1 - \frac{4 M_{\text{IRs}}^2}{(3 + \gamma M_{\text{IRs}}^2)^2}} \right)$$

With $\gamma = 1.4$ and $M_{1Rs} = 0.9$ this gives

$$\cos^2 \beta_{1s} = \frac{3 + 1.4 \cdot 0.81}{2 \cdot 0.81} \left(1 - \sqrt{1 - \frac{4 \cdot 0.81}{(3 + 1.4 \cdot 0.81)^2}} \right) = 0.2546$$

and therefore $\beta_{1s} = -59.70^\circ$. Next value of Φ_f is calculated from

$$\Phi_f = \frac{M_{1Rs}^3 (1 - \cos^2 \beta_{1s}) \cos \beta_{1s}}{\left(1 + \frac{\gamma-1}{2} M_{1Rs}^2 \cos^2 \beta_{1s} \right)^{(3\gamma-1)/(2\gamma-2)}},$$

and it yields the value

$$\Phi_f = \frac{0.9^3 (1 - \cos^2(-59.7^\circ)) \cos(-59.7^\circ)}{(1 + 0.2 \cdot 0.81 \cos^2(-59.7^\circ))^4} = 0.2333$$

The equality

$$\Phi = \frac{\Phi_f (1 - \kappa^2)}{M_{0u}^2}$$

can next be rewritten as

$$\frac{\dot{m}}{\rho_{01} c_{01} \pi r_2^2} = \frac{\Phi_f (1 - \kappa^2) c_{01}^2}{U_2^2}$$

After $U_2 = r_2 \Omega$ is substituted and r_2^2 canceled from both sides, this can be solved for Ω with the result:

$$\Omega = \sqrt{\frac{\Phi_f (1 - \kappa^2) \rho_{01} c_{01}^3 \pi}{\dot{m}}} = \sqrt{\frac{0.2333 \cdot 0.84 \cdot 1.226 \cdot 340.17^3 \pi}{8}} = 18400 \text{ rpm}$$

(b) The inlet Mach number is

$$M_1 = M_{1Rs} \cos \beta_{1s} = 0.9 \cos(-59.7^\circ) = 0.454$$

and hence, the inlet static temperature has the value

$$T_1 = \frac{T_{01}}{1 + \frac{\gamma-1}{2} M_1^2} = \frac{288}{1 + 0.2 \cdot 0.454^2} = 276.6 \text{ K}$$

The static density comes out to be

$$\rho_1 = \rho_{01} \left(\frac{T_1}{T_{01}} \right)^{1/(\gamma-1)} = 1.2259 \left(\frac{276.6}{288} \right)^{2.5} = 1.108 \text{ kg/m}^3$$

and the axial velocity is

$$V_1 = M_1 \sqrt{\gamma R T_1} = 0.454 \sqrt{1.4 \cdot 287 \cdot 276.6} = 151.4 \text{ m/s}$$

The mass flow rate,

$$\dot{m} = \rho_1 A_1 V_1 = \rho_1 \pi r_{1s}^2 (1 - \kappa^2) V_1$$

when solved for r_{1s} gives

$$r_{1s} = \sqrt{\frac{\dot{m}}{\rho_1 \pi (1 - \kappa^2) V_1}} = \sqrt{\frac{8}{1.108 \cdot \pi \cdot 0.84 \cdot 151.4}} = 0.1344 \text{ m}$$

so that the inducer diameter of the impeller is $D_{1s} = 26.9 \text{ cm}$. ■

9.2.1 Choking of the inducer

The inducer is shown in Figure 9.9. The flow is axial at the inlet, and the relative velocity forms an angle β_1 at the mean radius and β_{1s} at the shroud. The corresponding blade velocities are U_1 and U_{1s} , with $U_{1s} = r_{1s} U_1 / r_{1m}$. The blade angle is χ_1 , and the stagger is ξ . The throat width is denoted by t . From the shape of the blade, its thickness distribution, and the stagger, the width of the throat can be determined. As the sketch shows, a reasonable estimate is given by $t = s \cos \chi_1$. A typical value for incidence $i = \beta_1 - \chi_1$ is -4° to -6° [75].

Mass balance in the form

$$\dot{m} = \rho_1 A_1 W_1 \cos \beta_1 = \frac{p_1}{RT_1} A_1 M_{1R} \sqrt{\gamma R T_1} \cos \beta_1$$

can be written in terms of functions of the relative Mach number, by introducing the ratios

$$\frac{T_{0R}}{T_1} = 1 + \frac{\gamma - 1}{2} M_{1R}^2$$

and

$$\frac{p_{0R}}{p_1} = \left(1 + \frac{\gamma - 1}{2} M_{1R}^2 \right)^{\gamma/(\gamma-1)}$$

with the result that the mass balance takes the form

$$\dot{m} = \frac{p_{0R} A_1 \cos \beta_1}{\sqrt{c_p T_{0R}}} \frac{\gamma}{\sqrt{\gamma - 1}} M_{1R} \left(1 + \frac{\gamma - 1}{2} M_{1R}^2 \right)^{-(\gamma+1)/2(\gamma-1)}$$

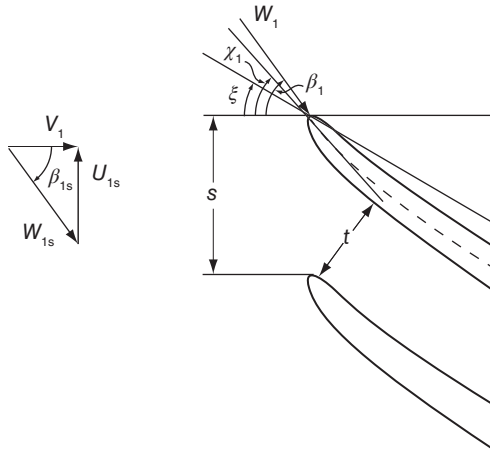


Figure 9.9 Detail of the inlet to the inducer.

At the throat, the mass flow rate can be expressed as

$$\dot{m} = \rho_t A_t W_t = \frac{p_{0R} A_t}{\sqrt{c_p T_{0R}}} \frac{\gamma}{\sqrt{\gamma-1}} M_{tR} \left(1 + \frac{\gamma-1}{2} M_{tR}^2 \right)^{-(\gamma+1)/2(\gamma-1)}$$

Equating the mass flow rates in the two preceding equations gives

$$\frac{A_1 M_{1R} \cos \beta_1}{\left(1 + \frac{\gamma-1}{2} M_{1R}^2 \right)^{(\gamma+1)/2(\gamma-1)}} = \frac{A_t M_{tR}}{\left(1 + \frac{\gamma-1}{2} M_{tR}^2 \right)^{(\gamma+1)/2(\gamma-1)}} \quad (9.19)$$

If the flow is choked, $M_{tR} = 1$, and this equation reduces to

$$\frac{A_t}{A_1 \cos \beta_1} = M_{1R} \left(\frac{2}{\gamma+1} + \frac{\gamma-1}{\gamma+1} M_{1R}^2 \right)^{-(\gamma+1)/2(\gamma-1)} \quad (9.20)$$

Figure 9.10 shows the graphs of the relative Mach number as a function of the effective area ratio for various values of the relative throat Mach number. If more accurate numerical values are needed than can be read from the graphs, they are easily calculated from Eq. (9.19).

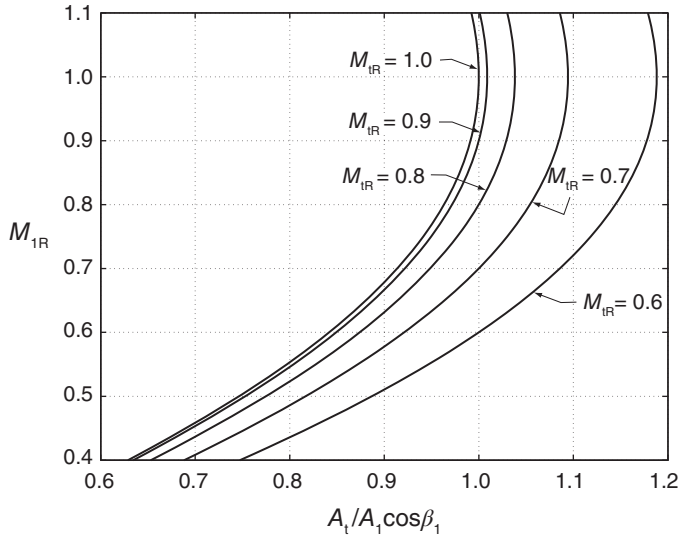


Figure 9.10 Throat area for a choked inducer for a gas with $\gamma = 1.4$.

Substituting $A_1 \cos \beta_1$ from Eq. (9.19) into

$$\dot{m} = \rho_1 A_1 W_1 \cos \beta_1$$

gives

$$\dot{m} = \rho_1 c_1 A_t M_{tR} \frac{\left(1 + \frac{\gamma-1}{2} M_{tR}^2 \right)^{(\gamma+1)/2(\gamma-1)}}{\left(1 + \frac{\gamma-1}{2} M_{1R}^2 \right)^{(\gamma+1)/2(\gamma-1)}}$$

which, when multiplied and divided by $\rho_{01}c_{01}$, can be written as

$$\dot{m} = \rho_{01}c_{01}A_tM_{tR} \frac{\left(1 + \frac{\gamma-1}{2}M_{tR}^2\right)^{(\gamma+1)/2(\gamma-1)}}{\left(1 + \frac{\gamma-1}{2}M_1^2\right)^{(\gamma+1)/2(\gamma-1)}\left(1 + \frac{\gamma-1}{2}M_{tR}^2\right)^{(\gamma+1)/2(\gamma-1)}}$$

In this equation, the ratio of the two terms involving relative and absolute Mach numbers can be written as

$$\frac{1 + \frac{\gamma-1}{2}M_{tR}^2}{1 + \frac{\gamma-1}{2}M_1^2} = \frac{h_1 + \frac{1}{2}W_1^2}{h_1 + \frac{1}{2}V_1^2} = \frac{h_1 + \frac{1}{2}V_1^2 + \frac{1}{2}U_1^2}{h_1 + \frac{1}{2}V_1^2} = 1 + \frac{U_1^2}{2h_{01}} = 1 + \frac{\gamma-1}{2} \frac{U_1^2}{c_{01}^2}$$

so that

$$\dot{m} = \rho_{01}c_{01}A_tM_{tR} \frac{\left(1 + \frac{\gamma-1}{2} \frac{U_1^2}{c_{01}^2}\right)^{(\gamma+1)/2(\gamma-1)}}{\left(1 + \frac{\gamma-1}{2}M_{tR}^2\right)^{(\gamma+1)/2(\gamma-1)}}$$

This shows that the mass flow rate increases as the blade speed increases. This happens even after the flow chokes, for then this equation becomes

$$\dot{m} = \rho_{01}c_{01}A_t \left(\frac{2}{\gamma+1} + \frac{\gamma-1}{\gamma+1} \frac{U_1^2}{c_{01}^2} \right)^{(\gamma+1)/2(\gamma-1)}$$

With increased blade speed, more compression work is done on the gas, and its pressure, temperature, and density, all increase in the flow channel. Thus, at the choked throat the higher velocity, given by $V_t = \sqrt{\gamma RT_t}$, and higher density result in an increased flow rate.

9.3 EXIT DESIGN

The characteristic design calculation in turbomachinery flows involves the relationship between the flow angles and the flow and blade loading coefficients. Density differences between the inlet and the exit of the impeller are considered only when the blade heights are determined. This was largely ignored in the axial compressor theory, as the annulus area could be reduced to keep the axial velocity constant. In radial compressor calculations, the situation is somewhat more complicated, as the comparable criterion of constant axial velocity is absent. To be sure, the design is often such that the radial velocity leaving the impeller is reasonably close to the axial velocity at the inlet and when this is taken into account, the range in the design parameters is reduced. In this section, the characteristics of the exit of the impeller are discussed.

9.3.1 Performance characteristics

If the inlet is axial, the work done is

$$w = U_2 V_{u2} \quad (9.21)$$

Since $V_{u2} = U_2 + W_2 \sin \beta_2$ and $V_{r2} = W_2 \cos \beta_2$, where V_{r2} is the radial velocity at the exit, this can be written as

$$w = U_2(U_2 + W_2 \sin \beta_2) = U_2^2 + V_{r2}U_2 \tan \beta_2$$

Defining the blade-loading coefficient for a centrifugal machine as $\psi = w/U_2^2$ and the flow coefficient as $\phi = V_{r2}/U_2$, this equation can be recast in the form

$$\psi = 1 + \phi \tan \beta_2 \quad (9.22)$$

This is a straight line in the performance plot shown in Figure 9.11. If $\beta_2 > 0$, the characteristic is rising, and for $\beta_2 < 0$, it is falling. The outlet velocity diagrams in the same figure show what happens to the absolute velocity in these two cases. It is clearly much larger in a machine with a rising characteristic.

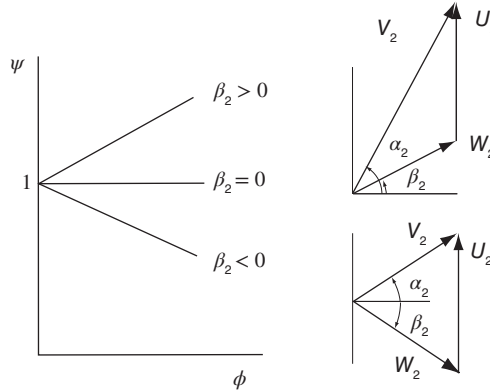


Figure 9.11 Idealized characteristic of a centrifugal machine.

Pressure rise in a centrifugal compressor takes place not only across the impeller but also in a vaned or vaneless diffuser and a volute. The latter consists of the stationary components of the machine and can be viewed as the stator. This is a useful way of thinking about the machine, and the degree of reaction can again be defined as the ratio of the static enthalpy rise across the rotor to the total.

If the outlet velocity from the impeller is large, then the flow needs to be diffused by a large amount in the stationary components of the machine. In order to prevent the flow separation and the irreversibilities associated with it, the diffusion in the volute must be kept sufficiently mild. This can be controlled by curving the blades backward, in order to reduce the absolute velocity at the outlet of the impeller.

Backward-swept blades have another decisive advantage; namely, the operation of the machine is *stable*. If the flow rate is reduced by increasing the load, for example by partially closing a valve downstream, on a falling characteristic of backward-swept blades, the blade-loading coefficient increases leading to higher enthalpy and thus also pressure at the outlet of the impeller. Hence, a higher pressure rise is obtained across the machine. This counteracts the increase in flow resistance, and a new stable operating point is established. On the other hand, for forward-swept blades a drop in the flow rate decreases the pressure across the machine and thus leads to further drop in the flow rate in the system. Thus the operation of a compressor with forward-swept blades is inherently unstable.

If the flow angle α_2 of the absolute velocity at the outlet is in the range 63° – 72° , a good design is obtained; the best designs being in the range 67° – 69° . For radial blades, which are common, there is a wide range of fairly high efficiency. Radial blades have the added advantage that they experience no bending by centrifugal loads, and the state of stress tends to be dominated by tensile stresses.

The pressure ratio has been shown to obey the equation

$$\left(\frac{p_{03}}{p_{01}}\right)^{(\gamma-1)/\gamma} = 1 + (\gamma - 1)\eta_{tt} \frac{U_2 V_{u2}}{c_{01}^2} = 1 + (\gamma - 1)\eta_{tt} \psi M_{0u}^2$$

and the temperature ratio is

$$\frac{T_{03}}{T_{01}} = 1 + (\gamma - 1)\psi M_{0u}^2$$

in which the blade-loading coefficient is given by Eq. (9.13). The exit Mach number can also be expressed in terms of the blade stagnation Mach number M_{0u} . The definition of exit Mach number can be rewritten as

$$M_2 = \frac{V_2}{c_2} = \frac{V_{u2}}{c_{01} \sin \alpha_2} \frac{c_{01}}{c_{02}} \frac{c_{02}}{c_2}$$

which can be rearranged to the form

$$M_2 = \frac{V_{u2}}{c_{01} \sin \alpha_2} \left(\frac{T_{01}}{T_{02}}\right)^{1/2} \left(\frac{T_{02}}{T_2}\right)^{1/2} = \frac{\psi M_{0u}}{\sin \alpha_2} \sqrt{\frac{1 + \frac{\gamma-1}{2} M_2^2}{1 + (\gamma - 1)\psi M_{0u}^2}}$$

Solving this for M_2 gives

$$M_2 = \frac{\psi M_{0u}}{\sqrt{\sin^2 \alpha_2 + (\gamma - 1)\psi M_{0u}^2 (\sin^2 \alpha_2 - \frac{1}{2}\psi)}} \quad (9.23)$$

The inlet Mach number can be written in terms of M_{0u} as well. First, the definition of M_1 can be written in the form

$$M_1^2 = \frac{V_1^2}{c_1^2} = \frac{U_{1s}^2}{c_{01}^2} \frac{c_{01}^2}{c_1^2} \frac{1}{\tan^2 \beta_{1s}}$$

and then using $U_{1s} = r_{1s} U_2 / r_2$ and $c_{01}^2 / c_1^2 = T_{01} / T_1$ in this leads to

$$\tan^2 \beta_{1s} M_1^2 = M_{0u}^2 \frac{r_{1s}^2}{r_2^2} \left(1 + \frac{\gamma - 1}{2} M_1^2\right)$$

Solving this for M_1 gives

$$M_1 = \frac{M_{0u} r_{1s} / r_2}{\sqrt{\tan^2 \beta_{1s} - \frac{\gamma - 1}{2} M_{0u}^2 \frac{r_{1s}^2}{r_2^2}}} \quad (9.24)$$

The relative inlet Mach number at the shroud is $M_{1Rs} = M_1 / \cos \beta_{1s}$. These relations are shown graphically in Figure 9.12 in the manner following Whitfield [94]. The blade angle varies from $\chi_2 = 0^\circ$ for radial blades in increments of -10° to $\chi_2 = -60^\circ$. The outlet angle was assumed to be $\alpha_2 = 67^\circ$ and the inlet flow angle, $\beta_{1s} = -60^\circ$ at the shroud. The slip factor was assumed to be $\sigma = 0.85$, and the total-to-total efficiency was taken to be $\eta_{tt} = 0.8$. The radius ratio has the value $r_{1s} / r_2 = 0.6$. With these values fixed, a typical design would have $M_{0u} = 1.4$ and, say $\chi_2 = -30^\circ$. These give a blade-loading coefficient of $\psi = 0.683$, an exit Mach number of $M_2 = 0.9$, a pressure ratio of $p_{03} / p_{01} = 3.84$, and a relative Mach number at the inlet shroud of $M_{1Rs} = 1.17$.

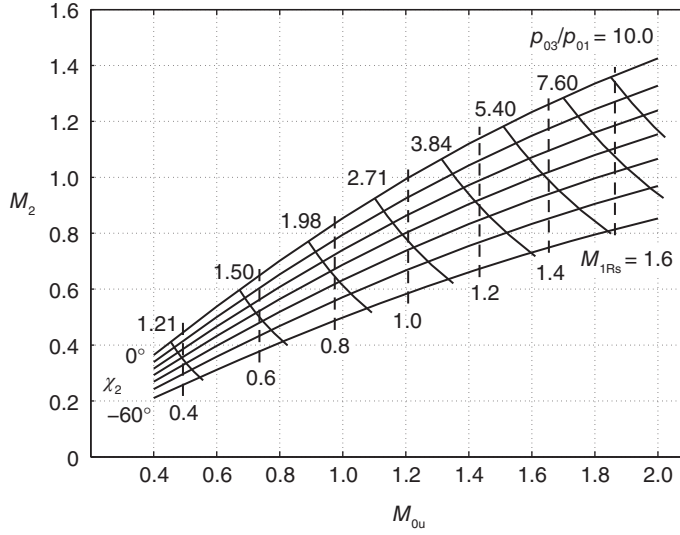


Figure 9.12 Exit Mach number, pressure ratio, and relative inlet Mach number as functions of blade stagnation Mach number for various blade angles χ_2 . The exit flow angle is $\alpha_2 = 67^\circ$, and at the inlet, $\beta_{1s} = 60^\circ$. The slip factor is $\sigma = 0.85$ and $\eta_{tt} = 0.8$. The radius ratio is $r_{1s}/r_2 = 0.6$, and $\gamma = 1.4$.

9.3.2 Diffusion ratio

The diffusion ratio for the relative velocity is discussed next. It is obtained by first writing at the inlet

$$-W_{1s} \sin \beta_{1s} = U_{1s}$$

and then developing the relative velocity at the outlet into a convenient form. Starting with

$$W_2 \sin \beta_2 = V_{u2} - U_2 \quad W_2 \cos \beta_2 = V_{r2}$$

and squaring and adding them gives

$$W_2^2 = V_{u2}^2 - 2V_{u2}U_2 + U_2^2 + V_{r2}^2$$

Noting that $V_{r2} = V_{u2}/\tan \alpha_2$, and dividing by U_2^2 , gives

$$\frac{W_2^2}{U_2^2} = 1 - 2\psi + \frac{\psi^2}{\sin^2 \alpha_2}$$

a result that was developed earlier in this chapter. Hence, the diffusion ratio becomes

$$\frac{W_{1s}}{W_2} = -\frac{U_{1s}/U_2}{\sin \beta_{1s} \sqrt{1 - 2\psi + \frac{\psi^2}{\sin^2 \alpha_2}}}$$

which in terms of the radius ratio is clearly

$$\frac{W_{1s}}{W_2} = - \frac{r_{1s}/r_2}{\sin \beta_{1s} \sqrt{1 - 2\psi + \frac{\psi^2}{\sin^2 \alpha_2}}}$$

This ratio should be kept below $W_{1s}/W_2 < 1.9$. For radius ratio, $r_{1s}/r_2 = 0.7$, graphs of the diffusion ratio as a function of χ_2 are plotted in Figure 9.13 for various values of the exit flow angle α_2 . A typical design might have $\alpha_2 = 67^\circ$, and if the diffusion ratio $W_{1s}/W_2 = 1.9$ is chosen, then $\chi_2 = -28.2^\circ$.

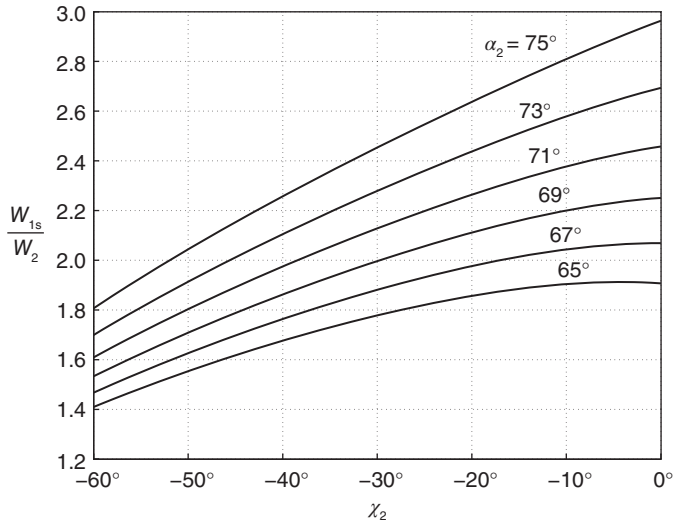


Figure 9.13 Diffusion ratio for $\sigma = 0.85$, inlet flow angle $\beta_{1s} = -60^\circ$, $r_{1s}/r_2 = 0.7$, and $\gamma = 1.4$, as a function of χ_2 and for various values of α_2 .

9.3.3 Blade height

The blade height at the exit is determined by equating the mass flow rates at the inlet and the outlet of the rotor. Writing the mass flow rates in terms of the flow functions as

$$\frac{\dot{m} \sqrt{c_p T_{01}}}{p_{01} A_1} = F_1(M_1)$$

and

$$\frac{\dot{m} \sqrt{c_p T_{02}}}{p_{02} A_2} = F_2(M_2)$$

Dividing the former by the latter gives

$$\frac{A_2}{A_1} = \sqrt{\frac{T_{02}}{T_{01}}} \frac{p_{01}}{p_{02}} \frac{F_1(M_1)}{F_2(M_2)} \quad (9.25)$$

The area ratio is seen to depend on the pressure ratio across the rotor, which is

$$\frac{p_{02}}{p_{01}} = [1 + (\gamma - 1)\eta_R \psi M_{0u}^2]^{\gamma/(\gamma-1)}$$

and the temperature ratio, which is

$$\frac{T_{02}}{T_{01}} = 1 + (\gamma - 1)\psi M_{0u}^2$$

The area ratio

$$\frac{A_2}{A_1} = \frac{2\pi b r_2}{\pi r_{1s}^2 (1 - \kappa^2)}$$

yields the blade height to radius ratio b_2/r_2 , as

$$\frac{b}{r_2} = \frac{A_2}{A_1} \frac{r_{1s}^2}{r_2^2} \frac{(1 - \kappa^2)}{2}$$

To establish the area ratio in Eq. (9.25), the flow function $F_1(M_1)$ can be calculated in terms of M_{0u} , since Eq. (9.24) gives the relationship between M_1 and M_{0u} , provided the other parameters are known. Similarly, Eq. (9.23) is a relationship between M_2 and M_{0u} . Thus the blade height-to-radius ratio can now be calculated for various values of M_{0u} . The graphs shown in Figure 9.14 are again patterned after Whitfield [94].

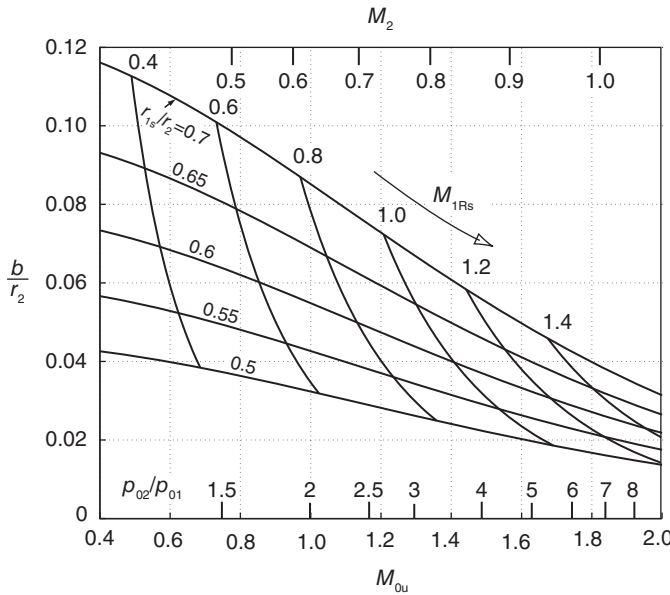


Figure 9.14 Blade height-to-radius ratio for $\sigma = 0.85$, $\eta_R = 0.9$ and $\eta_{tt} = 0.8$. At the inlet $\beta_{1s} = -60^\circ$ and at the exit $\chi_2 = -40^\circ$ and $\alpha_2 = 65^\circ$. The hub-to-shroud radius ratio is $\kappa = 0.4$, and the gas has $\gamma = 1.4$.

9.4 VANELESS DIFFUSER

As the compressed gas leaves the rotor, it enters a vaneless space in which it diffuses to a lower velocity. The mass balance at the exit of the rotor can be written as

$$\dot{m} = \rho_2 2\pi r_2 b_2 V_2 \cos \alpha_2$$

A similar equation at the end of the diffusion process at r_{2e} is

$$\dot{m} = \rho_{2e} 2\pi r_{2e} b_{2e} V_{2e} \cos \alpha_{2e}$$

so that

$$\rho_2 r_2 b_2 V_2 \cos \alpha_2 = \rho_{2e} r_{2e} b_{2e} V_{2e} \cos \alpha_{2e} \quad (9.26)$$

These mass balances can also be cast in the nondimensional forms:

$$\begin{aligned} \frac{\dot{m} \sqrt{c_p T_{02}}}{p_{02} 2\pi} &= r_2 b_2 F_2 \cos \alpha_2 \\ \frac{\dot{m} \sqrt{c_p T_{02e}}}{p_{02e} 2\pi} &= r_{2e} b_{2e} F_{2e} \cos \alpha_{2e} \end{aligned}$$

The stagnation temperature is constant so that $T_{02e} = T_{02}$. If it assumed that there are no losses, then since no work is done, $p_{02e} = p_{02}$. In addition, if the channel has a constant height, equating the foregoing two equations gives

$$r_{2e} F_{2e} \cos \alpha_{2e} = r_2 F_2 \cos \alpha_2 \quad (9.27)$$

For a free vortex velocity distribution,

$$r_{2e} V_{u2e} = r_2 V_{u2}$$

or

$$r_{2e} V_{2e} \sin \alpha_{2e} = r_2 V_2 \sin \alpha_2 \quad (9.28)$$

For a channel of constant width $b_2 = b_{2e}$, so that dividing this equation by Eq. (9.26), yields

$$\frac{\tan \alpha_{2e}}{\rho_{2e}} = \frac{\tan \alpha_2}{\rho_2} \quad (9.29)$$

Since both T_0 and p_0 are taken as constant, it then follows from the ideal gas relation that $\rho_{02} = \rho_{02e}$. Multiplying the left side of this equation by ρ_{02e} and the right side by ρ_{02} gives

$$\left(1 + \frac{\gamma - 1}{2} M_{2e}^2\right)^{1/(\gamma-1)} \tan \alpha_{2e} = \left(1 + \frac{\gamma - 1}{2} M_2^2\right)^{1/(\gamma-1)} \tan \alpha_2 \quad (9.30)$$

When the conditions at the exit of the rotor are known, this equation and Eq. (9.27) are two equations for the two unknowns M_{2e} and α_{2e} for a specified location r_{2e} .

Mach number M_{2e} as a function of the radius ratio is shown in Figure 9.15 for a flow with $M_2 = 1.2$ at the exit of the rotor and flow angles in the range $62^\circ < \alpha_2 < 70^\circ$. The value of M_{2e} at $r_{2e}/r_2 = 1.30$ is seen to be in the range 0.82–0.85, as the flow angle is increased from 62° to 70° . The diffusion of velocity is shown in Figure 9.16.

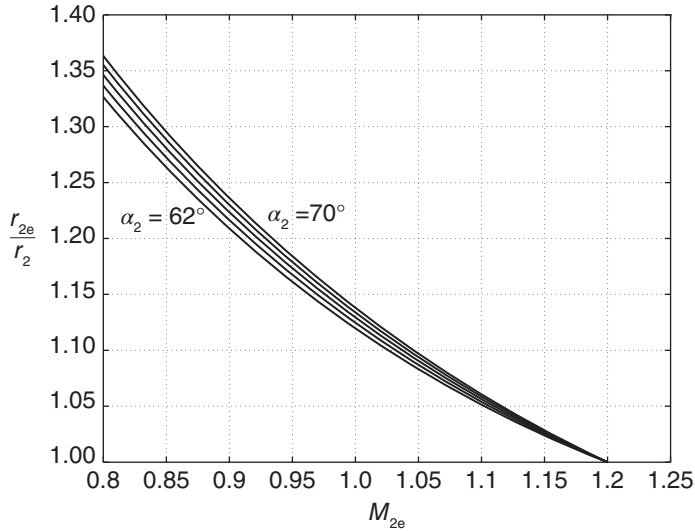


Figure 9.15 Mach number for a gas with $\gamma = 1.4$ as a function of radius ratio r_{2e}/r_2 for flow angles at the exit of the rotor in the range $62^\circ < \alpha_2 < 70^\circ$ and $M_2 = 1.2$.

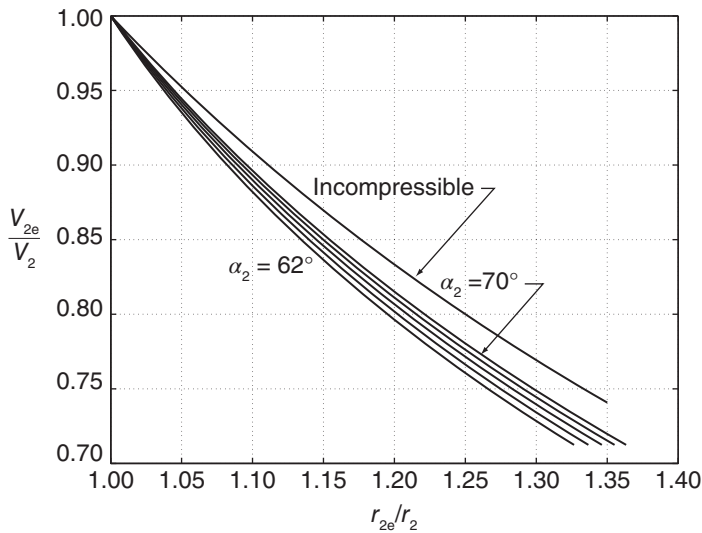


Figure 9.16 Diffusion ratio for a gas with $\gamma = 1.4$ as a function of radius ratio r_{2e}/r_2 for flow angles at the exit of the rotor in the range $62^\circ < \alpha_2 < 70^\circ$ and $M_2 = 1.2$; the incompressible flow case corresponds to constant flow angle.

In the incompressible limit, the mass balance and the irrotational flow condition give

$$r_2 V_2 \cos \alpha_2 = r_{2e} V_{2e} \cos \alpha_{2e} \quad r_2 V_2 \sin \alpha_2 = r_{2e} V_{2e} \sin \alpha_{2e}$$

Taking ratio of these two equations gives $\tan \alpha_2 = \tan \alpha_{2e}$ indicating that the flow angle remains constant. In this case,

$$\frac{V_{2e}}{V_2} = \frac{r_2}{r_{2e}}$$

and the diffusion varies inversely with the radius ratio. The compressible flow approaches this condition as the flow angle moves toward 90° . Since the Mach number at any given radius is higher for the larger flow angles, density is lower, and Eq. (9.29) shows that the flow angle is now smaller. The change in flow angles is shown in Figure 9.17. That the flow angle α_{2e} increases with radius means that the flow remains longer in the vaneless space and, therefore, experiences losses as the boundary layers grow in a decelerating flow in a narrow channel. For this reason, the vaneless space is kept small, and vanes are inserted to guide the flow into the volute.

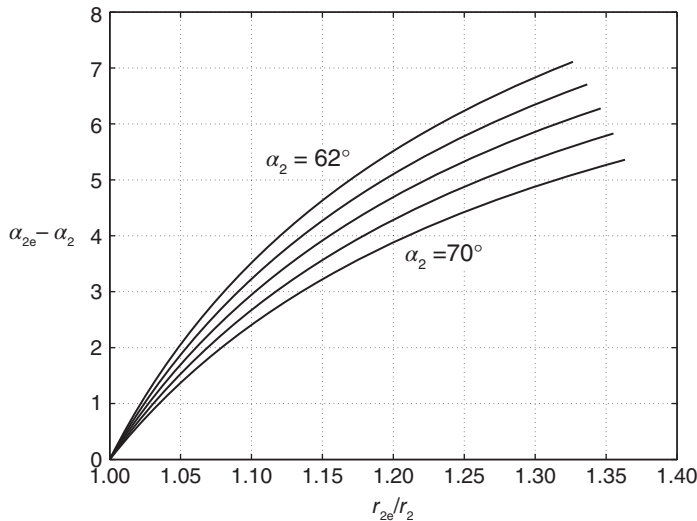


Figure 9.17 Difference in flow angles during the diffusion process, with angle at exit of the rotor in the range $62^\circ < \alpha_2 < 70^\circ$ and $M_2 = 1.2$, and the ratio of specific heats $\gamma = 1.4$.

More information on losses can be found in Cumpsty [18] and in Whitfield and Baines [95]. The function of the vaned diffuser is to reduce the area over which the diffusion takes place. The vanes may be in the form of airfoils, triangular channels, or what are called *island diffusers*. For the triangular channels a rule of thumb is to keep the opening angle at less than 12° . Again, Whitfield and Baines give more information, including results from a more advanced analysis.

■ EXAMPLE 9.3

Air from a centrifugal compressor leaves the blades at angle $\alpha_2 = 67.40^\circ$ and $M_2 = 1.1$ at the radius $r_2 = 7.5$ cm as it enters a vaneless diffuser. (a) Find the radial location at which the flow reaches the sonic condition. (b) Find the Mach number at radius $r_{2e} = 10$ cm.

Solution: (a) It is assumed that there are no losses, so that the stagnation state does not change, then by denoting the sonic state by star, and multiplying both sides of Eq. (9.29) by ρ_{02} gives

$$\frac{\rho_{02}}{\rho_2} \tan \alpha_2 = \frac{\rho_{02}}{\rho^*} \tan \alpha^*$$

The density ratio at the inlet to the vaneless diffuser is

$$\frac{\rho_{02}}{\rho_2} = \left(1 + \frac{\gamma-1}{2} M_2^2\right)^{1/(\gamma-1)} = (1 + 0.2 \cdot 1.1^2)^{2.5} = 1.719$$

and at the sonic state, it is therefore

$$\frac{\rho_{02}}{\rho^*} = \left(\frac{\gamma+1}{2}\right)^{1/(\gamma-1)} = 1.2^{2.5} = 1.577$$

The flow angle at the sonic state is

$$\alpha^* = \tan^{-1} \left(\frac{\rho_{02}}{\rho_2} \frac{\rho^*}{\rho_{02}} \tan \alpha_2 \right) = \tan^{-1} \left[\frac{1.719}{1.577} \tan(67.40^\circ) \right] = 69.09^\circ$$

The radial location where $M = 1$ is

$$r^* = r_2 \frac{F_2 \cos \alpha_2}{F^* \cos \alpha^*} = 0.075 \frac{1.271 \cos(67.40^\circ)}{1.281 \cos(69.09^\circ)} = 0.0801 \text{ m}$$

in which

$$F_2 = \frac{\gamma}{\sqrt{\gamma-1}} M_2 \left(1 + \frac{\gamma-1}{2} M_2^2\right)^{-(\gamma+1)/2(\gamma-1)} = \frac{1.4}{\sqrt{0.4}} 1.1 (1 + 0.2 \cdot 1.1^2)^{-3} = 1.271$$

and

$$F^* = \frac{\gamma}{\sqrt{\gamma-1}} \left(\frac{\gamma+1}{2}\right)^{-(\gamma+1)/2(\gamma-1)} = \frac{1.4}{\sqrt{0.4}} (1.2)^{-3} = 1.281$$

(b) The two equations

$$r_{2e} \cos \alpha_{2e} F_{2e} = r_2 \cos \alpha_2 F_2$$

and

$$\tan \alpha_{2e} = \frac{\left(1 + \frac{\gamma-1}{2} M_2^2\right)^{1/(\gamma-1)}}{\left(1 + \frac{\gamma-1}{2} M_{2e}^2\right)^{1/(\gamma-1)}} \tan \alpha_2$$

are to be solved simultaneously for α_{2e} and M_{2e} . The angle can be eliminated using

$$\cos \alpha_{2e} = \frac{1}{\sqrt{1 + \tan^2 \alpha_{2e}}}$$

Substituting, simplifying, and rearranging gives

$$\frac{r_{2e} \gamma M_{2e}}{\sqrt{\gamma-1} \sqrt{1 + \frac{\gamma-1}{2} M_{2e}^2}} -$$

$$r_2 \cos \alpha_2 F_2 \sqrt{\left(1 + \frac{\gamma - 1}{2} M_{2e}^2\right)^{2/(\gamma-1)} + \left(1 + \frac{\gamma - 1}{2} M_2^2\right)^{2/(\gamma-1)}} \tan^2 \alpha_2 = 0$$

Finding the root of this equation by iteration gives $M_{2e} = 0.764$. ■

A well-designed vaned diffuser improves the efficiency by 2% or 3% over a vaneless one. However, this comes at a cost, for at off-design operation, the efficiency of a vaned diffuser will deteriorate; that is, a compressor with a vaned diffuser will have a narrow operating range at the peak efficiency, owing to stalling of the vanes. To widen the range, adjustable vanes can be implemented into the design at added complexity and initial cost. The payback is reduction in operating costs at higher efficiency. A low-cost option is to have a vaneless diffuser, which has a lower efficiency but a flatter operating range near peak efficiency.

As the flow leaves the vaneless, or vaned, diffuser, it enters a volute. Its design for pumps is discussed at the end of this chapter. Also the use of specific diameter and specific speed in the selection of a power absorbing turbomachine is deferred to the next section for incompressible fluids. When using these for compressible flows, a difficulty arises as to which volumetric flow rate to use. This is removed by adopting the volumetric flow rate at the exit of a machine (or a stage) as the standard. The difference in the volumetric flow, if other slightly different definitions are used, are unlikely to change the choice of the machine.

9.5 CENTRIFUGAL PUMPS

The operation and design of pumps follow principles similar to those of centrifugal compressors. Compressibility can be clearly ignored in pumping liquids, but it may also be neglected in fans in which the pressure rise is slight.

The first law of thermodynamics across a pump is

$$w = h_{02} - h_{01} = \left(u_2 + \frac{p_2}{\rho} + \frac{1}{2} V_1^2 + g z_1\right) - \left(u_1 + \frac{p_1}{\rho} + \frac{1}{2} V_2^2 + g z_2\right)$$

In incompressible fluids, as was discussed in Chapter 2, internal energy increases only as a result of irreversibilities in an adiabatic flow. Hence, if the flow through the pump is reversible and adiabatic, internal energy does not increase and $u_2 = u_1$. In this situation, the preceding equation reduces to

$$w_s = \left(\frac{p_2}{\rho} + \frac{1}{2} V_2^2 + g z_2\right) - \left(\frac{p_1}{\rho} + \frac{1}{2} V_1^2 + g z_1\right)$$

The *total head* developed by a pump is defined as

$$H = \left(\frac{p_2}{\rho g} + \frac{1}{2g} V_2^2 + z_2\right) - \left(\frac{p_1}{\rho g} + \frac{1}{2g} V_1^2 + z_1\right)$$

so it represents the work done by a reversible pump per unit weight of the fluid. On the unit mass basis, the reversible work is

$$w_s = gH$$

Since the total head is readily measurable, the pump industry reports it, as well as the overall efficiency, in the pump specifications.

The shaft power to the pump is given by

$$\dot{W}_o = \frac{\rho Q g H}{\eta}$$

in which the overall efficiency η in the denominator is the product

$$\eta = \eta_m \eta_v \eta_h$$

Here η_h is a hydraulic efficiency, η_v is a volumetric efficiency, and η_m is a mechanical efficiency. The hydraulic efficiency accounts for the irreversibilities in the flow through the pump. If the loss term is written as

$$gH_L = u_2 - u_1,$$

then

$$w = w_s + gH_L = gH + gH_L,$$

and the *hydraulic efficiency* is defined as

$$\eta_h = \frac{w_s}{w} = \frac{gH}{gH + gH_L}$$

The hydraulic efficiency may be calculated from the empirical equation

$$\eta_h = 1 - \frac{0.4}{Q^{1/4}} \quad (9.31)$$

in which Q is in liters per second. If the volumetric flow rate is given in gallons per minute, as is still done in part of the pump industry today, the constant 0.4 has to be replaced by 0.8. It is in this form that this expression for hydraulic efficiency appears in the *Pump Handbook* [52].

A typical set of pump performance curves is given in Figure 9.18. (The quantity on the right ordinate axis, $[NPSH_R]$ = required net positive suction head, and its significance is

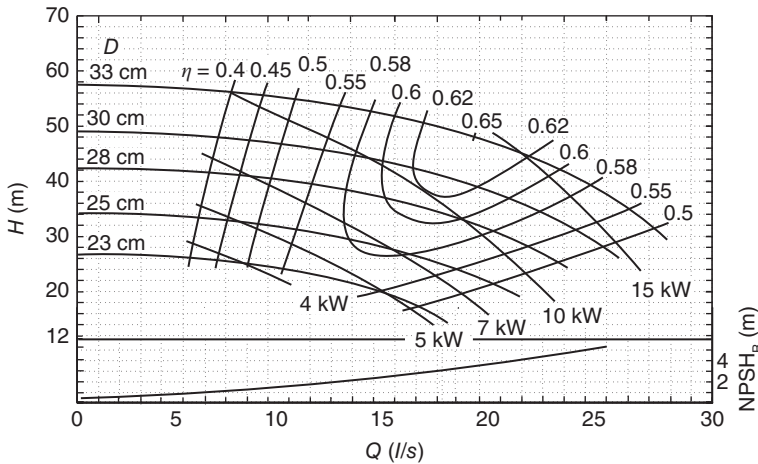


Figure 9.18 A typical set of performance curves for a centrifugal pump at 1750 rpm.

discussed later in conjunction with consideration of cavitation.) For an impeller diameter of 31 cm and flow rate of 18 L/s, the delivered head is 48 m at the shaft speed of 1750 rpm. The efficiency at this condition is about 0.63. The contours of constant efficiency and the power for pumping water are shown.

There is some leakage from the exit of the impeller back to the inlet and thus work will be redone on leakage flow as it crosses the impeller. To correct for this, the power into the impeller is obtained from

$$\dot{W}_R = (\dot{m} + \dot{m}_L)w$$

in which \dot{m}_L is the leakage flow. The power transferred to the fluid is

$$\dot{W} = \dot{m}w$$

and the ratio of these two expression for power is defined as the volumetric efficiency. Hence, it also equals the ratio of the mass flow rates and can be written as

$$\eta_v = \frac{\dot{m}}{\dot{m} + \dot{m}_L} = \frac{Q}{Q + Q_L} = \frac{Q}{Q_R} = \frac{\dot{W}}{\dot{W}_R}$$

in which Q_R is the flow that passes over the blade passage. The volumetric efficiency for large pumps with flow rates of 600 L/s reaches 0.99 and for small pumps with flow rates of 3 L/s it drops to 0.86. Logan [59] correlated the volumetric efficiency according to

$$\eta_v = 1 - \frac{C}{Q^n} \quad (9.32)$$

The constants are given in Table 9.1 as a function of the specific speed $\Omega_s = \Omega\sqrt{Q}/w_s^{3/4}$, with the flow rate in liters per second.

Table 9.1 Correlation for volumetric efficiency

| Ω_s | C | n |
|------------|-------|-------|
| 0.20 | 0.250 | 0.500 |
| 0.37 | 0.122 | 0.380 |
| 0.73 | 0.047 | 0.240 |
| 1.10 | 0.023 | 0.128 |

Finally, there is bearing friction and disk drag that are not taken into account in the impeller losses. Hence, if the power needed from the prime mover to power the pump is \dot{W}_o , then the power delivered to the rotor \dot{W}_R is less than this. Their ratio is defined as the mechanical efficiency

$$\eta_m = \frac{\dot{W}_R}{\dot{W}_o}$$

The power loss from mechanical friction can be estimated. But if the overall efficiency, hydraulic efficiency, and the volumetric efficiency are obtained from empirical relations, then the mechanical efficiency can be determined from the equation $\eta = \eta_h\eta_v\eta_m$.

As reported by Cooper and coworkers in the *Pump Handbook* [52], the overall efficiency has been correlated by Anderson and is given by

$$\eta = 0.94 - 0.08955 \left[\left(\frac{1.66Q}{\Omega} \right) \left(\frac{3.56}{e_{\text{rms}}} \right)^2 \right]^{-0.21333} - 0.29 \left[\log_{10} \left(\frac{0.8364}{\Omega_s} \right) \right]^2 \quad (9.33)$$

The original correlation is in a mixed set of units, and even after it has been converted here to a form in which Q is given in liters per second and Ω in radians per second, it is not in a dimensionless form. Be it as it may, according to Cooper, it gives satisfactory values for the overall efficiency, except at the upper half of the specific speed range, and he suggests that for large-capacity pumps the dashed line in Figure 9.19 be used. This figure gives a graphical representation of Eq. (9.33). The surface roughness of the flow passage is denoted by e_{rms} , and its value is in micrometers, with $e_{\text{rms}} = 3.56 \mu\text{m}$ for the graphs shown.

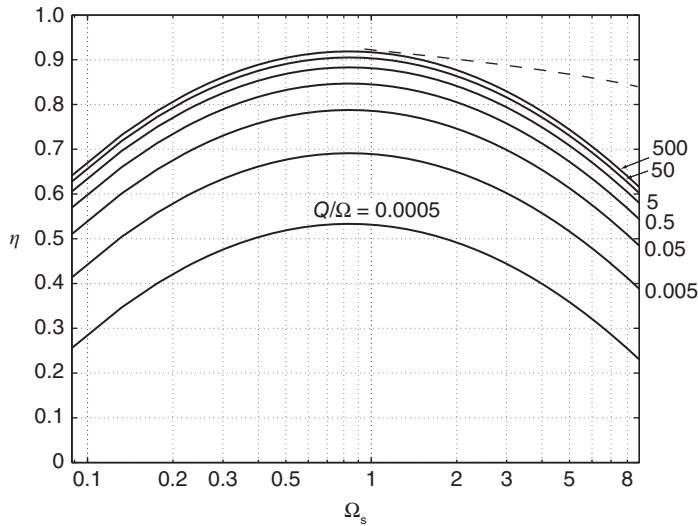


Figure 9.19 Efficiency of centrifugal pumps according to the correlation of Anderson, as quoted by Cooper and coworkers [52].

The number of blades in the impeller is in the range $5 < Z < 12$, and the empirical equation of Pfleiderer and Petermann [70]

$$Z = 6.5 \left(\frac{r_2 + r_{1s}}{r_2 - r_{1s}} \right) \cos \left(\frac{1}{2} (\chi_2 + \beta_{1s}) \right) \quad (9.34)$$

can be used to calculate this number. It shows that Z increases as r_{1s}/r_2 increases.

Analysis of a double-flow (double-suction) pump, a sketch of which is shown in Figure 9.20, follows closely the analysis of a single-flow pump. The flow rate $Q/2$ is used to calculate the hydraulic and volumetric efficiencies as well as the specific speed. The mechanical efficiency is close to that for a single-flow pump. In the next section, Cordier diagram is used to determine the size of a pump. When it is used for a double-flow pump, the entire flow rate Q is used in the definition of the specific diameter.

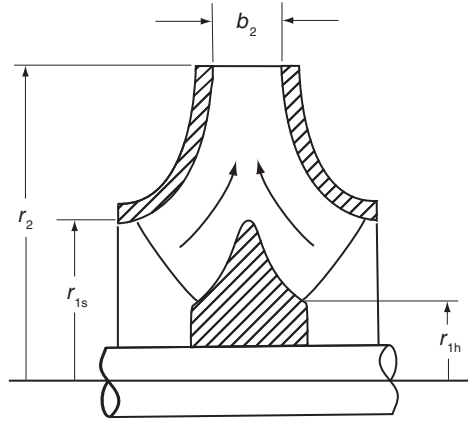


Figure 9.20 A double-flow pump.

9.5.1 Specific speed and specific diameter

A useful chart for pump selection was developed by Cordier. Its modified form is shown in Figure 9.21. The abscissa in the chart is the specific diameter, and the ordinate is the specific speed. These are defined as

$$D_s = \frac{D(gH)^{1/4}}{\sqrt{Q}} \quad \Omega_s = \frac{\Omega\sqrt{Q}}{(gH)^{4/3}}$$

It was seen in Chapter 5 that specific speed is used to select a pump of certain shape. Once selected, the size of the pump can be obtained using the Cordier diagram. The curve has been constructed such that for the size selected, optimal efficiency is obtained.

Since the total head is reported, it is more convenient to define the blade loading coefficient in terms of the reversible work rather than the actual work. Therefore, the loading coefficient is defined as

$$\psi_s = \frac{w_s}{U_2^2} = \frac{gH}{U_2^2},$$

and the subscript *s* serves as a reminder that this definition differs from the conventional one. With $\psi = w/U_2^2$, the relation $\psi_s = \eta\psi$ relates the two definitions.

Another way to size pumps is given by Cooper and coworkers [52]. With a specified flow rate and head rise across a pump, the rotational speed is first chosen, with the understanding that the higher the speed, the more compact is the pump. Once the rotational speed is fixed, the flow coefficient $\phi = V_{m2}/U_2$ can be obtained from the correlation

$$\phi = 0.1715\sqrt{\Omega_s} \quad (9.35)$$

A correlation for the blade-loading coefficient is

$$\psi_s = \frac{0.386}{\Omega_s^{1/3}} \quad (9.36)$$

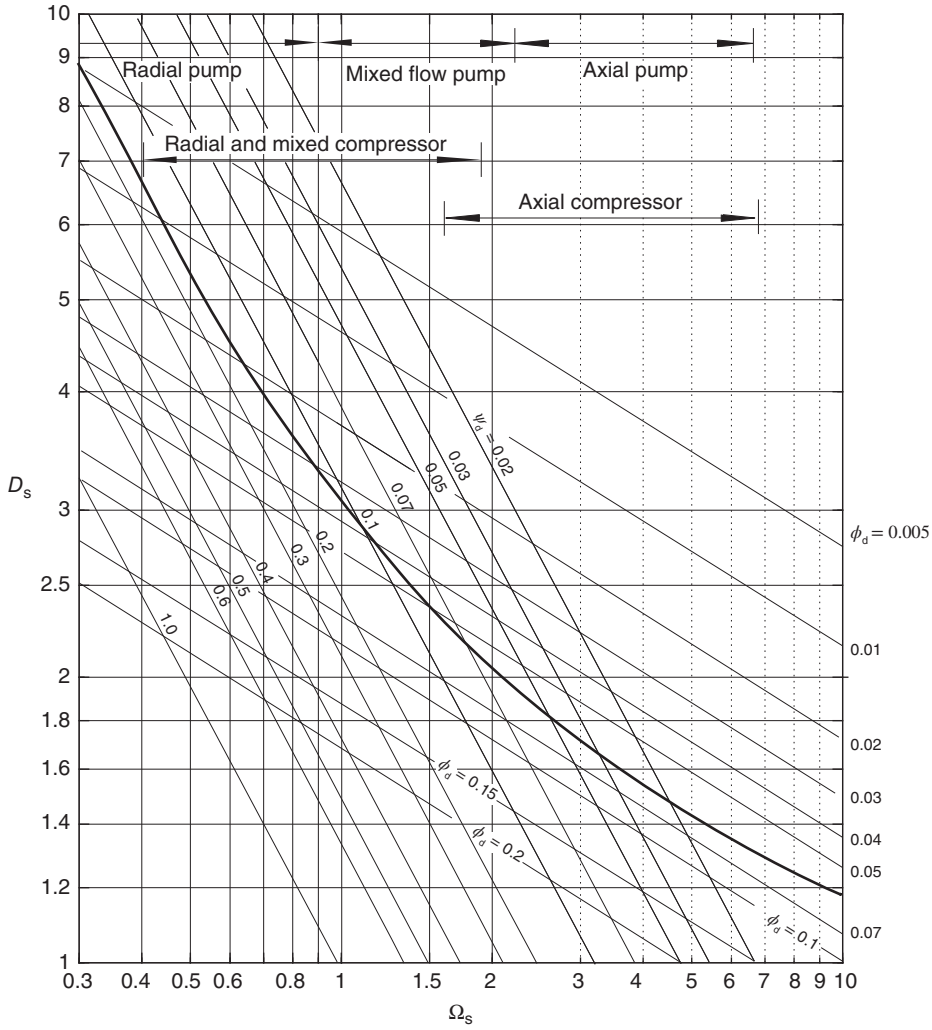


Figure 9.21 Cordier diagram for fans and pumps. Source: Adapted from Dibelius and Stoff [22].

and after the loading coefficient is determined, the blade speed is obtained from

$$U_2 = \sqrt{\frac{gH}{\psi_s}}$$

After that, the impeller radius is calculated as $r_2 = U_2/\Omega$ and the flow meridional velocity determined is $V_{m2} = \phi U_2$. Finally, the blade height b_2 is determined from

$$b_2 = \frac{Q_R}{2\pi r_2 V_{m2}}$$

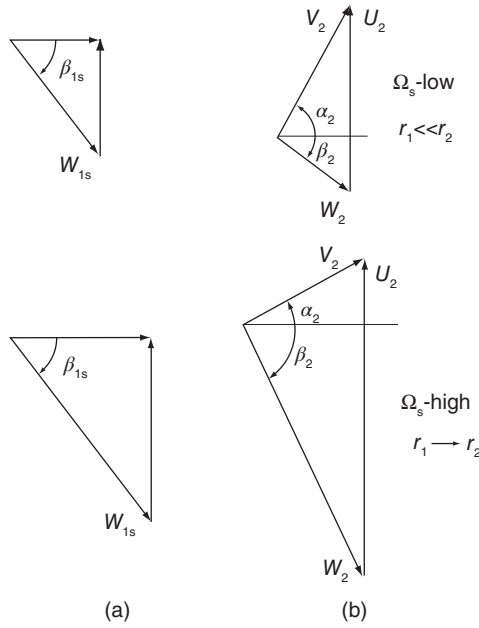


Figure 9.22 Velocity triangles for a low- and high-specific speed centrifugal pump. (a) inlet and (b) exit.

where Q_R is the sum of the delivered flow Q and the leakage flow Q_L . Shapes of the velocity diagrams for low- and high-specific speeds are shown in Figure 9.22. Since

$$\psi_s = \frac{w_s}{U_2^2} = \frac{\eta w}{U_2^2} = \frac{\eta V_{u2} U_2}{U_2^2}$$

the relationship

$$\frac{V_{u2}}{U_2} = \frac{\psi_s}{\eta} = \frac{0.383}{\Omega_s^{1/3} \eta}$$

is obtained. When the specific speed is high, V_{u2} becomes much smaller than U_2 and vanes have a large backsweep. The backsweep reduces as the specific speed decreases. It also decreases because lowering the specific speed lowers the efficiency. A sufficient reduction in the specific speed leads to forward-swept vanes, and such pumps are prone to unstable operation if the load changes. When the specific speed becomes very low, the centrifugal pump is no longer suitable for the application, and it should be replaced by a positive displacement pump, such as a screw pump or a rotary vane pump. In typical designs, V_{u2} is slightly over 0.5 of U_2 , and then the absolute values of both flow angles are quite large. For such pumps, the exit relative flow angle ranges from -65° to -73° .

In the discussion of compressors, an optimum inlet flow angle for the relative velocity was found, which gives the largest flow rate with a given relative Mach number. In the incompressible limit, this gives $\beta_{1s} = -54.74^\circ$. A range from -65° to -80° is typical for pumps, which means that a flow rate lower than the optimum is obtained for a fixed relative velocity.

For axial entry, the volumetric flow rate can be written as

$$Q = A_1 V_1 = \pi r_{1s}^2 (1 - \kappa^2) \sqrt{W_{1s}^2 - r_{1s}^2 \Omega^2}$$

Solving this for W_{1s}^2 gives

$$W_{1s}^2 = r_{1s}^2 \Omega^2 + \frac{Q^2}{\pi^2 (1 - \kappa^2)^2 r_{1s}^4}$$

When r_{1s} is small, the second term causes W_{1s} to be large, and when r_{1s} is large, the first term increases the value of W_{1s} . The value of r_{1s} for which W_{1s} is minimum, is given by

$$r_{1s} = \left(\frac{\sqrt{2}Q}{\pi(1 - \kappa^2)\Omega} \right)^{1/3}$$

An alternative way to optimize the inlet is given by Dixon [24]. Typical values of κ are in the range from very small to about 0.5. The smallest value of the hub radius r_{1h} depends on the size of the shaft. Once the torque is known, the shaft diameter is easily determined from torsion theory, discussed in books on strength of materials. For double-suction pumps, in which the shaft penetrates the entire hub, κ is typically 0.5. These guidelines are illustrated next with examples.

■ EXAMPLE 9.4

A pump is to be selected to pump water at the rate of 50 L/s. The increase in total head across the pump is to be 35 m. An electric motor, connected with a direct drive and a rotational speed of 3450 rpm, provides the power to the pump. Water is drawn from a pool at atmospheric temperature and pressure. Its density is $\rho = 1000 \text{ kg/m}^3$. (a) Determine the type of pump for this application and its efficiency, assuming $e_{\text{rms}} = 3.56 \text{ } \mu\text{m}$. (b) Calculate the pump diameter. (c) Estimate the pump efficiency and the power needed.

Solution: (a) The specific speed of this pump is

$$\Omega_s = \frac{\Omega \sqrt{Q}}{(gH)^{3/4}} = \frac{3450 \cdot \pi}{30} \frac{\sqrt{0.05}}{(9.81 \cdot 35)^{3/4}} = 1.013$$

From Figure 5.9, a pump with Francis-type impeller is chosen. The efficiency, calculated from Eq. (9.33), is $\eta = 0.815$.

(b) To determine the size of the pump, a Cordier diagram may be consulted. The specific diameter is estimated to be $D_s = 3.1$ so that the impeller diameter is

$$D = D_s \frac{Q}{(gH)^{1/4}} = \frac{3.1 \sqrt{0.05}}{(9.81 \cdot 35)^{1/4}} = 16.1 \text{ cm}$$

(c) The power required is

$$\dot{W} = \frac{\rho Q g H}{\eta} = \frac{1000 \cdot 0.05 \cdot 9.81 \cdot 35}{0.815} = 21.0 \text{ kW}$$

■

The specific speed of the pump in Example 9.4 is at the upper limit for centrifugal pumps. Beyond this value pumps fall into the category of mixed-flow type. In mixed-flow pumps, the edge of the blade on the meridional plane is inclined with respect to the radial

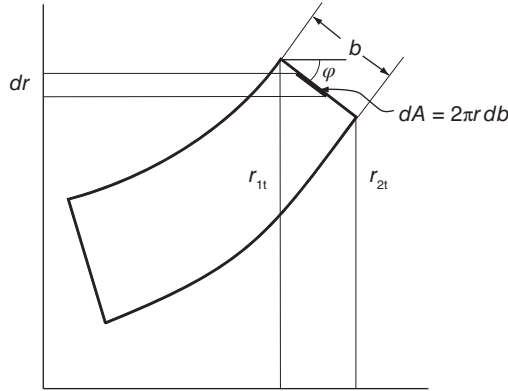


Figure 9.23 Sketch for calculation of blade width.

(or axial) direction. If the meridional velocity is perpendicular to the edge, then the effective radius for calculating the volumetric flow rate is determined from the construction shown in Figure 9.23.

The differential area is $dA = 2\pi r db$ and $dr = \sin \varphi db$. Hence

$$A = \int_{r_{1t}}^{r_{2t}} \frac{2\pi r}{\sin \varphi} dr = \frac{\pi(r_{1t}^2 - r_{2t}^2)}{\sin \varphi} = \frac{\pi(r_{1t} - r_{2t})(r_{1t} + r_{2t})}{\sin \varphi} = \pi(r_{1t} + r_{2t})b$$

Thus the effective radius is the mean radius $r_m = \frac{1}{2}(r_{1t} + r_{2t})$ and $A_2 = 2\pi r_m b$.

EXAMPLE 9.5

A pump handles water at the rate of 10 L/s with a head of 100 m across the pump. The power is provided by an electric motor with shaft speed 3450 rpm. Water is at 20°C with density $\rho = 1000 \text{ m}^3/\text{kg}$. (a) Calculate the specific speed of the pump. (b) Determine the flow coefficient and the blade-loading coefficient. (c) Find the directions of the absolute velocity and the relative velocity of water leaving the impeller. (d) Find the tip radius of the impeller. (e) Find the power needed.

Solution: (a) The specific speed of this pump is

$$\Omega_s = \frac{\Omega \sqrt{Q}}{(gH)^{3/4}} = \frac{3450 \cdot \pi}{30} \frac{\sqrt{0.01}}{(9.81 \cdot 100)^{3/4}} = 0.2061$$

(b) The flow coefficient is determined from

$$\phi = 0.1715 \sqrt{\Omega_s} = 0.1715 \sqrt{0.2061} = 0.0779$$

and the blade loading coefficient is obtained from

$$\psi_s = \frac{0.386}{\Omega_s^{1/3}} = \frac{0.386}{0.2061^{1/3}} = 0.6535$$

From $\psi_s = gH/U_2^2$, the blade tip speed is

$$U_2 = \sqrt{\frac{gH}{\psi_s}} = \sqrt{\frac{9.81 \cdot 100}{0.6535}} = 38.7 \text{ m/s}$$

(c) The hydraulic efficiency is

$$\eta_h = 1 - \frac{0.4}{Q^{1/4}} = 1 - \frac{0.4}{10^{1/4}} = 0.775$$

and the work done is therefore

$$w = \frac{w_s}{\eta_h} = \frac{9.81 \cdot 100}{0.775} = 1.266 \text{ kJ/kg}$$

The tangential and radial components of the velocity are

$$V_{u2} = \frac{w}{U_2} = \frac{1266}{38.74} = 32.67 \text{ m/s} \quad V_{r2} = \phi U_2 = 0.0779 \cdot 38.7 = 3.02 \text{ m/s}$$

so that the flow angle is

$$\alpha_2 = \tan^{-1} \left(\frac{V_{u2}}{V_{r2}} \right) = \tan^{-1} \left(\frac{32.7}{3.01} \right) = 84.72^\circ$$

The tangential and radial components of the relative velocity are

$$W_{u2} = V_{u2} - U_2 = 32.67 - 38.74 = -6.08 \text{ m/s} \quad W_{r2} = V_{r2} = 3.02 \text{ m/s}$$

and therefore

$$\beta_2 = \tan^{-1} \left(\frac{W_{u2}}{W_{r2}} \right) = \tan^{-1} \left(-\frac{6.08}{3.02} \right) = -63.61^\circ$$

(d) The impeller radius can be calculated to be

$$r_2 = \frac{U_2}{\Omega} = \frac{38.7 \cdot 30}{3450 \cdot \pi} = 0.1072 \text{ m}$$

The volumetric efficiency is obtained by first finding the constants in Eq. (9.32) by interpolation. They are $C = 0.2454$ and $n = 0.4957$ for $\Omega_s = 0.2061$. The volumetric efficiency is then

$$\eta_v = 1 - \frac{C}{Q^n} = 1 - \frac{0.2454}{10^{0.4957}} = 0.9216$$

so that $Q_R = Q/\eta_v = 0.01/0.9216 = 0.01085 \text{ m}^3/\text{s}$. The blade width is therefore

$$b_2 = \frac{Q_R}{2\pi r_2 V_{r2}} = \frac{0.01085}{2\pi \cdot 0.1077 \cdot 3.01} = 0.0053 \text{ m} \quad b_2 = 0.53 \text{ cm}$$

(e) The overall efficiency is determined from Eq. (9.33) to be $\eta = 0.66$. Hence the power to the pump is

$$\dot{W} = \frac{\rho Q g H}{\eta} = \frac{1000 \cdot 10 \cdot 9.81 \cdot 100}{1000 \cdot 0.66} = 14.86 \text{ kW}$$

■

In the next example, the number of blades and their metal angle are also considered.

EXAMPLE 9.6

Water flows axially into a double-suction centrifugal pump at the rate of $2Q = 0.120 \text{ m}^3/\text{s}$. The pump delivers a head of 20 m while operating at 880 rpm. The hub-to-shroud ratio at the inlet is 0.50, and the relative velocity makes an angle -73° at the shroud of the inlet. (a) Find the reversible work done by the pump. (b) What is the work done by the impeller? (c) Find the radius of the impeller and the inlet radius of the shroud. (d) Determine the blade width at the exit of the impeller. (e) Assume a reasonable number of blades and calculate the blade angle at the exit. Use the Pfleiderer equation to check this.

Solution: (a) The reversible work is

$$w_s = gH = 9.81 \cdot 20 = 196.2 \text{ J/kg}$$

(b) The hydraulic efficiency is

$$\eta_h = 1 - \frac{0.4}{Q^{1/4}} = 1 - \frac{0.4}{60^{1/4}} = 0.856$$

and the actual work by the impeller is

$$w = \frac{w_s}{\eta_h} = \frac{196.2}{0.856} = 229.1 \text{ J/kg}$$

(c) The specific speed is

$$\Omega_s = \frac{\Omega \sqrt{Q}}{w_s^{3/4}} = \frac{880 \cdot \pi \sqrt{0.060}}{30 \cdot 196.2^{3/4}} = 0.431$$

and the loading coefficient is

$$\psi_s = \frac{0.386}{\Omega_s^{1/3}} = \frac{0.386}{0.431^{1/3}} = 0.511$$

Therefore, the impeller tip speed is

$$U_2 = \sqrt{\frac{w_s}{\psi_s}} = \sqrt{\frac{196.2}{0.511}} = 19.59 \text{ m/s}$$

and the impeller radius is

$$r_2 = \frac{U_2}{\Omega} = \frac{19.59 \cdot 30}{880 \cdot \pi} = 0.213 \text{ m}$$

The volumetric flow rate can be written as

$$Q = A_1 V_1 = \frac{\pi r_{1s}^2 (1 - \kappa^2) U_{1s}}{\tan(-\beta_{1s})} = \frac{\pi (1 - \kappa^2) \Omega r_{1s}^3}{\tan(-\beta_{1s})}$$

Solving this for r_{1s} gives

$$r_{1s} = \left[\frac{Q \tan(-\beta_{1s})}{\pi(1 - \kappa^2)\Omega} \right]^{1/3}$$

so that

$$r_{1s} = \left[\frac{60 \cdot \tan(73^\circ) \cdot 30}{1000 \cdot \pi^2(1 - 0.50^2) \cdot 880} \right]^{1/3} = 0.0967 \text{ m}$$

and

$$r_{1h} = \kappa r_{1s} = 0.5 \cdot 0.0967 = 0.0483 \text{ m}$$

and thus the blade speed at the shroud is

$$U_{1s} = r_{1s}\Omega = \frac{0.0967 \cdot 880 \cdot \pi}{30} = 8.91 \text{ m/s}$$

(d) The flow coefficient is

$$\phi = 0.1715\sqrt{\Omega_s} = 0.1715\sqrt{0.431} = 0.1125$$

and the radial velocity at the exit is then

$$V_{r2} = \phi U_2 = 0.1125 \cdot 19.59 = 2.20 \text{ m/s}$$

To calculate the leakage flow, the coefficients for the expression of volumetric are interpolated to be

$$C = 0.1094 \quad n = 0.3564$$

so that

$$\eta_v = 1 - \frac{C}{Q^n} = 1 - \frac{0.1094}{60^{0.3564}} = 0.975$$

and the flow through the exit is

$$Q_R = \frac{2Q}{\eta_v} = \frac{120}{0.975} = 0.123 \text{ m}^3/\text{s}$$

Hence, the blade height has the value

$$b_2 = \frac{Q_R}{2\pi r_2 V_{r2}} = \frac{0.123}{2 \cdot \pi \cdot 0.213 \cdot 2.20} = 4.18 \text{ cm}$$

(e) The tangential component of the exit velocity is calculated to be

$$V_{u2} = \frac{w}{U_2} = \frac{229.1}{19.59} = 11.70 \text{ m/s}$$

and the flow angle at the exit is

$$\alpha_2 = \tan^{-1} \left(\frac{V_{u2}}{V_{r2}} \right) = \tan^{-1} \left(\frac{11.70}{2.20} \right) = 79.3^\circ$$

The tangential component of the relative velocity becomes

$$W_{u2} = V_{u2} - U_2 = 11.70 - 19.59 = -7.90 \text{ m/s}$$

so that the flow angle is

$$\beta_2 = \tan^{-1} \left(\frac{W_{u2}}{W_{r2}} \right) = \tan^{-1} \left(-\frac{7.90}{2.20} \right) = -74.4^\circ$$

Next, the number of blades is assumed. Let $Z = 6$, and the blade angle is guessed to be, say, $\chi_2 = -60^\circ$. Then the slip coefficient is calculated from

$$\sigma = 1 - \frac{\sqrt{\cos \chi_2}}{Z^{0.7}} = 1 - \frac{\sqrt{\cos(-60^\circ)}}{6^{0.7}} = 0.798$$

and the equation

$$V_{u2} = \sigma U_2 + V_{r2} \tan \chi_2$$

is solved for χ_2 , giving

$$\chi_2 = \tan^{-1} \left(\frac{V_{u2} - \sigma U_2}{V_{r2}} \right) = \tan^{-1} \left(\frac{11.70 - 0.798 \cdot 19.59}{2.20} \right) = -60.79^\circ$$

Now a new value of σ is obtained from

$$\sigma = 1 - \frac{\sqrt{\cos \chi_2}}{Z^{0.7}} = 1 - \frac{\sqrt{\cos(-60.79^\circ)}}{6^{0.7}} = 0.801$$

With this value for σ , repeating the calculation gives $\chi_2 = -61.19^\circ$ and $\sigma = 0.802$. The number of blades can now be calculated from Pfleiderer's equation

$$Z = 6.5 \left(\frac{1 + r_{1s}/r_2}{1 - r_{1s}/r_2} \right) \cos \left(\frac{\beta_{1s} + \chi_2}{2} \right) = 6.75$$

so that the initial guess is close to being correct. Thus six (or seven) is an acceptable number. ■

9.6 FANS

An industrial fan with a wide impeller and blades in the shape of airfoils is shown in Figure 9.24. The impeller has no inducer, and the flow enters the fan axially. It then turns and enters the blade passage radially. The increase in radius between the inlet and outlet is quite modest, and for this reason, such fans also have a low pressure rise and the flow can be considered incompressible. The blades can be made quite long, which gives a large flow area. Since the flow at the inlet is radial, at the inlet $W_{r1} = V_1$ and $W_{u1} = -U_1$. The blades are oriented such that the relative flow enters at the angle β_1 obtained by solving

$$\tan \beta_1 = \frac{W_{u1}}{W_{r1}}$$

Since the width of the flow areas at the inlet and exit are the same, and the density change is ignored, the radial velocities are related by $r_1 V_{r1} = r_2 V_{r2}$. With an inlet velocity without swirl, the work done is calculated in the same way as for centrifugal pumps.

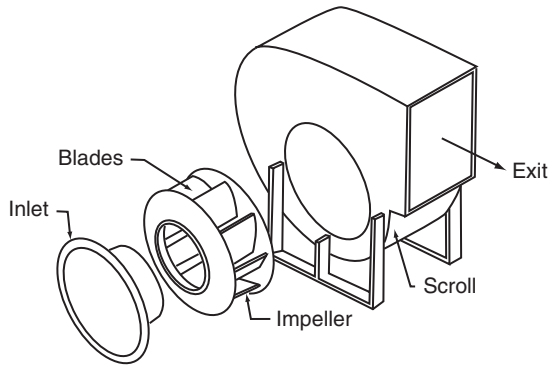


Figure 9.24 A centrifugal fan.

9.7 CAVITATION

Common experience shows that water pressure increases with depth in a quiescent pool of water. Similarly, pressure decreases in a vertical pipe flow if the fluid moves to a higher elevation, not only because of this hydrostatic effect but as a result of irreversibilities caused by turbulence and wall friction. If the inlet of the suction pipe is a short distance below a surface of a body of water, the pressure at the inlet to the pump is below atmospheric pressure by the sum of the hydrostatic head, the drop caused by the dynamic head, and the frictional pressure loss. As a consequence, for an upward-moving flow, the pressure in a sufficiently long pipe may drop enough to reach the saturation pressure corresponding to the prevailing temperature. The saturation pressure for water at 20 °C is 2.34 kPa.

After the saturation pressure has been crossed, vapor bubbles begin to form in the stream. When this happens in the blade passage of a turbomachine, the flow is said to undergo *cavitation*. The effects of cavitation are harmful, and the performance of the pump deteriorates. The work done by each element of the impeller vane increases the fluid pressure, and as the flow moves in the flow passages, it carries the bubbles into regions of higher pressure. There they collapse. The collapse is a consequence of an instability in the size and shape of the bubble. As the instability develops, the bubble flattens out, and a liquid from the back accelerates toward the center, forming a jet that pierces through the bubble. These impinging jets from the bubbles located next to the impeller of the pump cause erosion. This kind of cavitation damage is seen also in marine propellers.

Any dissolved air tends to come out of the liquid at low pressures. These small air bubbles act as nucleation sites for vapor bubble formation. They are aided in turbulent flow by local negative pressure spikes. The kinetics of nucleation, turbulence, and growth rates of bubbles are complicated subjects and make prediction of cavitation difficult. Hence, pump manufacturers rely on experimentation to determine when the pump performance is significantly affected. A comprehensive review of the mechanisms of cavitation is given by Arakeri [4] and Brennen [9, 10].

A pressure difference called *net positive suction pressure* (NPSP) is defined as

$$p_N = p + \frac{1}{2}\rho V^2 - p_v$$

in which p_v is the saturation pressure, p is the static pressure, and V is the velocity at the pump end of the suction pipe (which is the inlet to the pump). When expressed in units of

a height of water, the net positive suction pressure is called the *net positive suction head* (NPSH).

The manufacturer tests the pump and gives a value for the *required* net positive suction head (NPSH_R). This increases with the flow rate as the accelerating flow into the inlet causes the pressure to drop. The application engineer can now determine what is the minimum total head at the pump end of the suction pipe and from this determine the *actual* net positive suction head NPSH_A. In order to avoid cavitation, NPSH_A > NPSH_R. In the lower half of Figure 9.18 is a curve showing values (on the ordinate on the right) for the NPSH_R as a function of the flow rate.

A suction specific speed is defined as

$$\Omega_{ss} = \frac{\Omega \sqrt{Q}}{(g \text{ NPSH})^{3/4}}$$

For a single-flow pump a rough rule is to keep the suction specific speed under $\Omega_{ss} = 0.3$ and for a double flow, under $\Omega_{ss} = 0.4$.

■ EXAMPLE 9.7

A pump draws water with at temperature $T = 20^\circ\text{C}$ and density $\rho = 1000 \text{ kg/m}^3$ at the rate of 20 L/s from a large reservoir open to atmosphere with pressure 101.3 kPa . As shown in Figure 9.25, the pump is situated a height $z_1 = 4 \text{ m}$ above the reservoir surface. The pipe diameter is 7.6 cm , and the suction pipe is 10 m in length. The entrance loss coefficient is $K_i = 0.8$, the loss coefficient of the elbow is $K_e = 0.6$, and the pipe roughness is $45 \mu\text{m}$. Find the suction specific speed, given a shaft speed is of 1800 rpm . The viscosity of water is $1.0 \cdot 10^{-3} \text{ kg/(m s)}$.

Solution: A control volume containing the water in the reservoir and in the suction pipe is

$$\frac{p_a}{\rho} = \frac{p_1}{\rho} + \frac{1}{2}V_p^2 + gz_1 + \left(f \frac{L_p}{D_p} + K_i + K_e\right) \frac{1}{2}V_p^2$$

so that

$$p_1 + \frac{1}{2}\rho V_p^2 - p_v = p_a - \rho g z_1 - \left(f \frac{L_p}{D_p} + K_i + K_e\right) \frac{1}{2}\rho V_p^2 - p_v$$

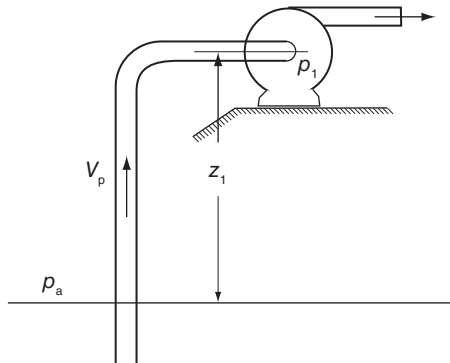


Figure 9.25 A pumping example illustrating possible cavitation.

and the positive suction head is

$$\text{NPSH} = \frac{p_a}{\rho g} - z_1 - \left(f \frac{L_p}{D_p} + K_i + K_e \right) \frac{V_p^2}{2g} - \frac{p_v}{\rho g}$$

The velocity in the pipe is calculated as

$$V_p = \frac{Q}{A_p} = \frac{4Q}{\pi D_p^2} = \frac{4 \cdot 20}{1000 \cdot \pi \cdot 0.076^2} = 4.41 \text{ m/s}$$

and the Reynolds number has the value

$$Re = \frac{\rho V_p D_p}{\mu} = \frac{1000 \cdot 4.41 \cdot 0.076}{1.0 \cdot 10^{-3}} = 334392$$

The friction factor can now be calculated from Eq. (3.29). For a commercial steel pipe with roughness 0.045 mm, its value is $f = 0.0186$, and the net positive suction head is therefore

$$\begin{aligned} \text{NPSH} &= \frac{101300}{1000 \cdot 9.81} - 4 - \left(0.0187 \frac{10}{0.076} + 0.6 + 0.8 \right) \frac{4.41^2}{2 \cdot 9.81} - \frac{2.34 \cdot 1000}{998 \cdot 9.81} \\ &= 2.29 \text{ m} \end{aligned}$$

The value of the suction-specific speed becomes

$$\Omega_{ss} = \frac{\Omega \sqrt{Q}}{(g \text{NPSH})^{3/4}} = \frac{1800 \cdot \pi \sqrt{0.020}}{30(9.81 \cdot 2.29)^{3/4}} = 2.58$$

Since the suction specific speed is lower than the criterion $\Omega_{ss} = 3.0$, the pump on this basis will not experience cavitation. However, if the pump in Figure 9.18 is used, then this flow rate shows the value of $\text{NPSH}_R = 2.1 \text{ m}$ to be close to that calculated here, so that inception of the cavitation is close. ■

9.8 DIFFUSER AND VOLUTE DESIGN

9.8.1 Vaneless diffuser

In the vaneless space in a flow without spin, the tangential component of the velocity follows the free vortex distribution. This is a consequence of the law of conservation of angular momentum, if no moment is applied to the fluid particles. Thus

$$rV_u = r_2 V_{u2}$$

and, if the vaneless diffuser has a constant width, then, for an incompressible flow, the equation

$$\rho 2\pi r b V_r = \rho 2\pi r_2 b V_{r2}$$

reduces to

$$rV_r = r_2 V_{r2}$$

This and the condition for irrotationality $rV_u = \text{constant}$ then yields

$$rV = r_2 V_2$$

This is a special case of the general result discussed for centrifugal compressors. Since $V_u = V_r \tan \alpha$, the flow angle α remains constant.

From the flow trajectories in Figure 9.26, it is easy to see that the flow angle is given by

$$\tan \alpha = \frac{r d\theta}{dr}$$

which for a constant flow angle can be integrated to

$$\theta_2 - \theta_1 = \ln \frac{r_2}{r_1} \tan \alpha$$

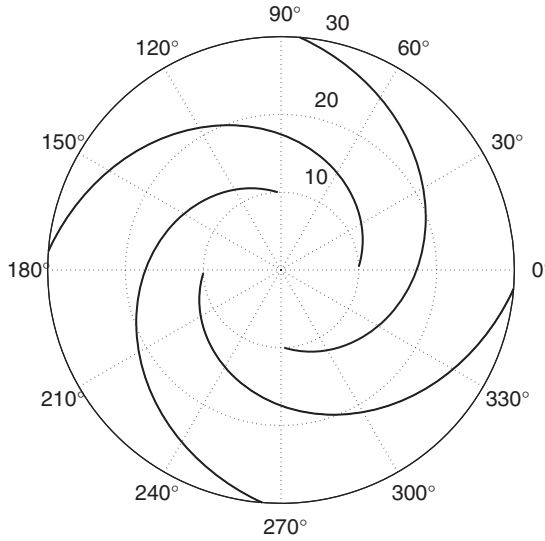


Figure 9.26 Logarithmic spiral with $\alpha = 70^\circ$ and $10 \text{ cm} < r < 30 \text{ cm}$.

The curve traced out is a *logarithmic spiral*. The incremental length of the path is

$$dL = \sqrt{dr^2 + r^2 d\theta^2} = \sqrt{(1 + \tan^2 \alpha) dr} = \frac{dr}{\cos \alpha}$$

and integrating this gives $r_2 - r_1 = L \cos \alpha$. In the spirals shown in the Figure 9.26 $\alpha = 70^\circ$. Therefore, a spiral that starts at $r_1 = 10 \text{ cm}$ and $\theta = 0$ and ends at $r_2 = 30 \text{ cm}$ will have traversed an angular distance $\theta = 172.9^\circ$. As the flow angle approaches 90° , the length of the path increases greatly.

9.8.2 Volute design

In this section, the calculations involved in the design of a volute are discussed. A schematic of a volute cross section for a centrifugal pump is shown Figure 9.27, in which the various radii are indicated. The diffuser includes a constant-width vaneless space, followed by a section with a linearly increasing gap, and then a circular volute. Although the principles for the calculation are straightforward, the details lead to complicated equations.

The side view of the pump is shown in Figure 9.28. The volute is a channel around the impeller in which the flow area increases slowly, leading to a decrease in velocity and thus

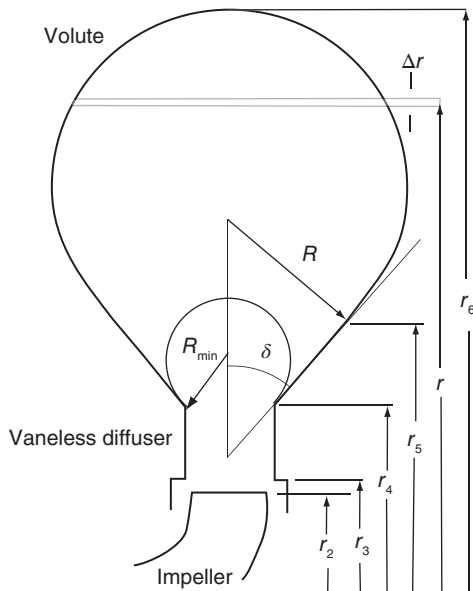


Figure 9.27 Sketch for volute design.

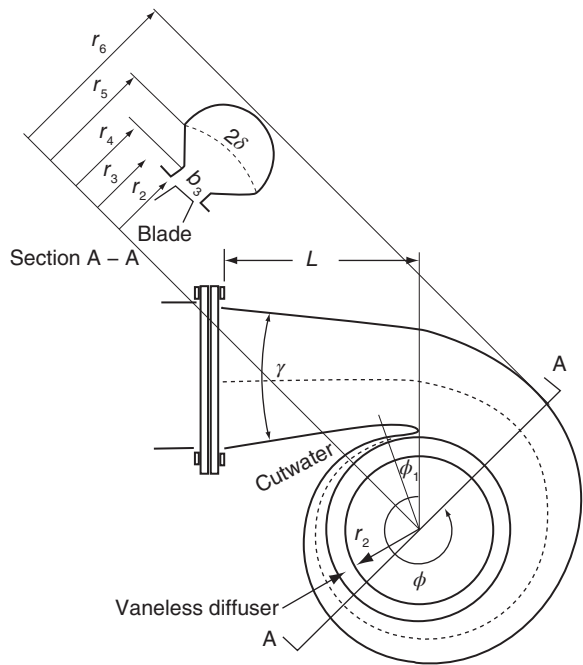


Figure 9.28 Centrifugal pump and its volute.

an increase in pressure. The upstream section of the volute begins at a *tongue*, or *cutwater*, and the volute returns to the same location after turning 360° . It then transitions into a conical diffuser that is connected to a high pressure delivery pipe.

The exit blade radius is labeled r_2 , and the blade height is designated as b_2 . The vaneless diffuser begins at radius r_3 and has a width b_3 . In order to slide the impeller into the casing, radius r_3 is made slightly larger than r_2 . For large pumps for which the casing is split in half, the impeller and the shaft can be lowered into place, and for a such a pump, r_2 can be larger than r_3 . The width of the vaneless diffuser b_3 is just a couple of millimeters larger than the blade height b_2 . For purposes of illustration, the radii r_2 and r_3 are assumed to be equal. With the radius r_3 decided, how the volute is developed depends on the design practice of each pump manufacturer. One possibility is to have the volute begin with a diffuser of trapezoidal cross section. The half-angle δ of the sidewalls and the height of the trapezoid is chosen such that a volute of circular cross section is fitted to the trapezoid in such a way that the slope of the circular section is the same as that of the sidewalls of the trapezoid at the point where they join. This is shown in Figure 9.27. The radii r_5 and r_6 increase in the flow direction in order to accommodate the increase in flow entering the volute. The calculations for this kind of design are illustrated in Wirzenius [99], and his analysis is partly repeated below.

The angle around the volute is ϕ , and it is convenient to measure this angle from the *tongue* or *lip* of the volute. The design of the tongue region requires special attention to make a smooth transition to the main part of the volute. The volute is to be designed in such a way that the pressure at the exit of the impeller is uniform and independent of ϕ . In such a situation, the rate of flow into the volute is the same at every angular location, and, if Q_ϕ is the volumetric flow rate through the volute at the angle ϕ , then by simple proportionality

$$Q_\phi = \frac{\phi}{2\pi} Q$$

where Q is the total flow rate. Let V_u be the tangential component of the velocity in the volute. Then

$$Q_\phi = \int_{A_\phi} V_u dA = \int_{r_3}^{r_6} V_u b(r) dr$$

in which $b(r)$ is the volute width at the radius r .

The flow is assumed to be irrotational, and the tangential velocity, therefore, varies with r as

$$V_u = V_{u2} \frac{r_2}{r}$$

with V_{u2} the tangential velocity leaving the impeller. Hence,

$$Q_\phi = \frac{\phi}{2\pi} Q = V_{u2} r_2 \int_{r_3}^{r_6} \frac{b(r)}{r} dr$$

Solving this for ϕ gives

$$\phi = \frac{2\pi V_{u2} r_2}{Q} \left[\int_{r_3}^{r_4} \frac{b(r)}{r} dr + \int_{r_4}^{r_5} \frac{b(r)}{r} dr + \int_{r_5}^{r_6} \frac{b(r)}{r} dr \right]$$

It remains to evaluate the integrals. To organize the work, let

$$I_1 = \int_{r_3}^{r_4} \frac{b(r)}{r} dr \quad I_2 = \int_{r_4}^{r_5} \frac{b(r)}{r} dr \quad I_3 = \int_{r_5}^{r_6} \frac{b(r)}{r} dr$$

For the first integral $b(r) = b_3$. Hence,

$$I_1 = b_3 \int_{r_3}^{r_4} \frac{dr}{r} = b_3 \ln \frac{r_4}{r_3}$$

The channel width $b(r)$ for the linearly diverging part is given by

$$b(r) = b_3 + 2(r - r_4) \tan \delta$$

Hence,

$$I_2 = \int_{r_4}^{r_5} \frac{b_3 + 2 \tan \delta (r - r_4)}{r} dr = (b_3 - 2r_4 \tan \delta) \ln \frac{r_5}{r_4} + 2(r_5 - r_4) \tan \delta$$

With the aid of trigonometric relationships

$$r_5 = r_4 + R \frac{\cos \delta}{\tan \delta} - \frac{b_3}{2 \tan \delta} \quad (9.37)$$

the second integral therefore evaluates to

$$I_2 = (b_3 - 2r_4 \tan \delta) \ln \left(1 + \frac{R \cos \delta}{r_4 \tan \delta} - \frac{b_3}{2r_4 \tan \delta} \right) + 2R \cos \delta - b_3$$

The radius that gives $I_2 = 0$ is the minimum radius $R_{\min} = b_3/2 \cos \delta$; that is, the triangular section of the volute increases as the volute radius increases in the downstream direction. Therefore, the radius r_5 also increases as R increases, whereas the radii r_4 and r_3 remain fixed, as does the angle δ .

The integral I_3 is the most complicated of the three integrals. The width of the volute at location r is given by $b(r) = 2R \sin \theta$. Also $r = r_6 - R + R \cos \theta$. Let

$$c = \frac{r_6}{R} - 1 = \frac{r_5}{R} + \sin \delta = \frac{r_4}{R} + \frac{\cos \delta}{\tan \delta} - \frac{b_3}{2R \tan \delta} + \sin \delta$$

so that

$$c = \frac{r_4}{R} + \frac{1}{\sin \delta} - \frac{b_3}{2R \tan \delta} \quad (9.38)$$

The integral I_3 now can be written as

$$I_3 = \int_{r_5}^{r_6} \frac{b(r)}{r} dr = 2R \int_0^{\pi/2+\delta} \frac{\sin^2 \theta}{\frac{r_5}{R} + \sin \delta + \cos \theta} d\theta = 2R \int_0^{\pi/2+\delta} \frac{\sin^2 \theta}{c + \cos \theta} d\theta$$

Evaluation of this leads to

$$I_3 = 2R \left[c \left(\frac{\pi}{2} + \delta \right) - \cos \delta - 2\sqrt{c^2 - 1} \tan^{-1} \left(\sqrt{\frac{c-1}{c+1}} \frac{1 + \tan(\delta/2)}{1 - \tan(\delta/2)} \right) \right]$$

Collecting the results gives the design formula

$$\phi = \frac{2\pi r_2 r_4 V_{u2}}{Q} \left\{ \frac{b_3}{r_4} \left(\ln \frac{r_4}{r_3} - \frac{1}{2} \right) + \left(\frac{b_3}{r_4} - 2 \tan \delta \right) \ln \left(1 + \frac{R \cos \delta}{r_4 \tan \delta} - \frac{b_3}{2r_4 \tan \delta} \right) + 2 \frac{R}{r_4} \left[1 + c \left(\frac{\pi}{2} + \delta \right) - \cos \delta - 2\sqrt{c^2 - 1} \tan^{-1} \left(\sqrt{\frac{c-1}{c+1}} \frac{1 + \tan(\delta/2)}{1 - \tan(\delta/2)} \right) \right] \right\} \quad (9.39)$$

The calculation now proceeds by starting with R_{\min} and incrementing R by ΔR , so that the new value of R is $R_{\min} + \Delta R$. Next, the value of c is determined from Eq. (9.38) and r_5 is calculated from Eq. (9.37). Then r_6 , the outer extent of the volute, is determined from $r_6 = (1 + c)R$, but this is not needed in the calculation of angle ϕ . The value of angle ϕ is finally determined from Eq. (9.39). These values then trace out the volute and its trapezoidal base.

EXERCISES

9.1 An industrial air compressor has 29 backward-swept blades with blade angle -21° . The tip speed of the blades is 440 m/s, and the radial component of the velocity is 110 m/s. Air is inducted from atmospheric conditions at 101.3 kPa and 298 K with an axial velocity equal to 95 m/s. The hub-to-tip ratio at the inlet is 0.4. The total-to-total efficiency of the compressor is 0.83, and the mass flow rate is 2.4 kg/s. Find: (a) The total pressure ratio using the Stodola slip factor and (b) the tip radius of the impeller. [Ans: (a) 3.5, (b) 9.16 cm]

9.2 A centrifugal compressor has 23 radial vanes and an exit area equal to 0.12 m^2 , where the radial velocity is 27 m/s, and the tip speed of the impeller is 350 m/s. The total-to-total efficiency is 0.83. (a) Find the mass flow rate of air, given that the total pressure and temperature are 101.3 kPa and 298 K at the inlet. (b) What is the exit Mach number? (c) If the blade height at the exit is $b = 3 \text{ cm}$ and there is no leakage flow, what is the tip radius of the impeller? (d) Find the rotational speed of the compressor wheel, and the required power neglecting mechanical losses. [Ans: (a) 5.16 kg/s, (b) 0.8, (c) 0.637 m, (d) 5250 rpm, 545.7 kW]

9.3 A centrifugal compressor has an axial inlet and the outlet blades at an angle such that the tangential component of the velocity at the exit has a value equal to 0.9 times the blade speed. The outlet radius is 30 cm, and the desired pressure ratio is 3.5. The inlet stagnation temperature is $T_{01} = 298 \text{ K}$. If the total-to-total efficiency of the compressor is 0.8, at what angular speed does it need to be operated? [Ans: 13464 rpm]

9.4 Air flows from atmosphere at pressure 101.3 kPa and temperature 288 K into a centrifugal compressor with radial blades at the exit of the impeller. The inlet velocity is $V_1 = 93 \text{ m/s}$, and there is no pre-swirl. The compressor wheel has 33 blades, and its tip speed is $U_2 = 398 \text{ m/s}$. The total-to-total efficiency is $\eta_{tt} = 0.875$. Find (a) the stagnation pressure ratio and (b) the power required assuming that the mass flow rate is $\dot{m} = 2.2 \text{ kg/s}$. Use the Stanitz formula to find the slip coefficient. [Ans: (a) 3.67, (b) 327.6 kW]

9.5 A small centrifugal compressor as a part of a turbocharger operates at 55000 rpm. It draws air from atmosphere at temperature 288 K and pressure 101.325 kPa. The inlet

Mach number is $M_1 = 0.4$, and the flow angle of the relative velocity is $\beta_{1s} = -60^\circ$ at the shroud. The radius ratio at the inlet is $\kappa = r_{1h}/r_{1s} = 0.43$. (a) Find the blade speed at the inlet shroud and (b) the mass flow rate. (c) If the inducer is choked, what is the throat area? [Ans: (a) 232.0 m/s, (b) 0.630 kg/s, (c) 20 cm²]

9.6 A centrifugal compressor in a turbocharger operates at 40000 rpm and inlet Mach number $M_1 = 0.35$. It draws air from atmosphere at temperature 293 K and pressure 101.325 kPa. The radius ratio is $r_{1s}/r_2 = 0.71$, and the diffusion ratio is $W_{1s}/W_2 = 1.8$. The inlet angle of the relative velocity at the shroud is $\beta_{1s} = -63^\circ$. The slip factor is $\sigma = 0.85$, and the flow angle at the exit is $\alpha_2 = 69^\circ$. Find (a) the blade speed at the inlet shroud, (b) the tip speed of the blade at the outlet, (c) the loading coefficient, and (d) the metal angle at the exit. [Ans: (a) 232.9 m/s, (b) 328.0 m/s, (c) 0.629, (d) -42.48°]

9.7 A small centrifugal compressor draws atmospheric air at 293 K and 101.3 kPa. At the inlet $r_{1h} = 3.2$ cm and $r_{1s} = 5$ cm. The rotor efficiency of the compressor is 0.88. The relative Mach number at the inlet shroud is 0.9 and the corresponding relative flow angle is $\beta_{1s} = -62^\circ$. At the outlet the absolute velocity is at angle $\alpha_2 = 69^\circ$. The diffusion ratio is $W_{1s}/W_2 = 1.8$ and the radius ratio is $r_{1s}/r_2 = 0.72$. Find, (a) the rotational speed of the shaft, (b) the blade-loading coefficient w/U_2^2 , (c) the flow coefficient $\phi = V_{r2}/U_2$, and (d) the blade width at the exit. [Ans: (a) 12720 rpm, (b) 0.534, (c) 0.205, (d) 3.1 cm]

9.8 Show that in the incompressible limit, the angle of the relative velocity at the inlet is optimum at 54.7° .

9.9 Show that the expression for the dimensionless mass flow rate for a compressor with pre-swirl at angle α_1 is

$$\Phi_f = \frac{M_{1R}^3 (\tan \alpha_1 - \tan \beta_{1s})^2 \cos^3 \beta_{1s}}{\left(1 + \frac{\gamma - 1}{2} M_{1R}^2 \frac{\cos^2 \beta_{1s}}{\sin^2 \alpha_1}\right)}$$

Plot the results for $\alpha_1 = 30^\circ$, with β_{1s} on the abscissa and Φ_f on the ordinate, for relative Mach numbers 0.6, 0.7, 0.8. For a given mass flow rate, does the pre-swirl increase or decrease the allowable relative Mach number, and does the absolute value of the relative flow angle increase or decrease with pre-swirl?

9.10 Show that for a centrifugal compressor without any inlet swirl, the stagnation temperature ratio is given by

$$\frac{T_{03}}{T_{01}} = 1 + (\gamma - 1) \psi M_{0u}^2$$

9.11 Air from atmosphere at pressure 101.3 kPa and temperature 288 K enters a centrifugal axially with speed $V_x = 145$ m/s and flow rate of $\dot{m} = 10$ kg/s. The blade speed at the exit is $U_2 = 205$ m/s. If the Mach relative Mach number at the throat is $M_{tR} = 0.7$, find (a) rotational speed of the shaft, (b) the area of the throat. [Ans: (a) 16126 rpm, (b) 0.0368 m²]

9.12 (a) Carry out the calculations to determine the ratio b/r_2 for air entering a centrifugal compressor axially at conditions $\sigma = 0.85$, $r_{1s}/r_2 = 0.65$, $\beta_{1s} = -60^\circ$, $\alpha_2 = 65^\circ$, $\chi_2 = -40^\circ$, $\eta_R = 0.9$, $\kappa = 0.4$ and $M_{0u} = 0.82$. (b) Determine the ratio V_{r2}/V_x . [Ans: (a) 0.0774, (b) 0.759]

9.13 Atmospheric air at 288 K and 101.2 kPa enters axially at the rate $\dot{m} = 9 \text{ kg/s}$ into a centrifugal compressor, with an inlet velocity 95 m/s. The blades are curved backward with blade angle $\chi_2 = -37^\circ$. The radius ratio $r_{1s}/r_2 = 0.65$ and the radial velocity is $v_{r2} = 0.8V_x$. Assume that the rotor efficiency $\eta_R = 0.91$. The ratio of the shroud to the hub radii is $\kappa = 0.52$ and the mean radius is $r_m = 0.10 \text{ m}$. The angle of the relative velocity at the inlet shroud is $\beta_{1s} = -62^\circ$. (a) Find the blade height at the exit. [Ans: 1.19 cm]

9.14 Atmospheric air at 288 K and 101.3 kPa enters axially into a centrifugal compressor. The impeller mean radius is $r_m = 5 \text{ cm}$, and its radius ratio is $\kappa = 0.4$. The relative velocity makes an angle $\beta_{1s} = -60^\circ$ at the inlet shroud, where the relative Mach number is to be no more than $M_{1Rs} = 0.9$. Find the rotational speed of the shaft. [Ans: (a) 17680 rpm]

9.15 Water with density 998 kg/m^3 flows through the inlet pipe of a centrifugal pump at a velocity of 6 m/s. The inlet shroud radius is 6.5 cm, and the hub radius is 5 cm. The entry is axial. The relative velocity at the exit of the impeller is 15 m/s and is directed by backward-curved impeller blades such that the exit angle of the absolute velocity is $\alpha_2 = 65^\circ$. The impeller rotates at 1800 rpm and has a tip radius of 15 cm. Assume that the rotor efficiency of the pump is 75%. Evaluate (a) the power into the pump, (b) the increase in total pressure of the water across the impeller, and (c) the change in static pressure of the water between the inlet and outlet of the impeller. (d) What is the ratio of the change in kinetic energy of the water across the impeller to the total enthalpy of the water across the pump, the change in the relative kinetic energy, and the change in the kinetic energy owing to the centrifugal effect as a fraction of work done? (e) If the velocity at the exit of the volute is 6 m/s, what is the ratio of change in static pressure across the rotor to the change in static pressure across the entire pump? [Ans: (a) 24 kW, (b) 318 kPa, (c) 199 kPa, (d) 0.281, 0.837, -0.118 , (e) 0.626]

9.16 A centrifugal-pump that handles water operates with backward-curving blades. The angle between the relative velocity and the tip section is 45° . The radial velocity at the tip section is 4.5 m/s, the flow at the inlet is axial, and the impeller rotational speed is 1800 rpm. Assume that there is no leakage and that the mechanical friction may be neglected, and that the total-to-total efficiency is 70%. (a) Construct the velocity diagram at the impeller exit and (b) evaluate the required tip radius for a water pressure rise of 600 kPa across the pump. (c) For the total pressure rise of 600 kPa, evaluate the difference between the total and static pressure of water at the impeller tip section. [Ans: (a) 16.8 cm, (b) 377.7 kPa]

9.17 A centrifugal water pump has an impeller diameter $D_2 = 27 \text{ cm}$, and when its shaft speed is 1750 rpm, it produces a head $H = 33 \text{ m}$. Find, (a) the volumetric flow rate, (b) the blade height at the exit of the impeller assuming that there are no leakage losses, and (c) the blade angle at the exit of the impeller, given that it has 11 blades. [Ans: (a) 26.2 L/s (b) 1.17 cm, (c) -58.9°]

9.18 A centrifugal water pump has an impeller diameter of $D_2 = 25 \text{ cm}$, and when its shaft speed is 1750 rpm, it delivers 20 L/s of water. Find, (a) the head of water delivered by the pump and (b) the power needed to drive the pump. (c) The impeller has nine blades. Use the Stanitz slip factor to find the blade angle at the exit of the impeller. (d) Use the Wiesner slip factor to find the blade exit blade angle. [Ans: (a) 28.25 m, (b) 6.83 kW, (c) -50.6° , (d) -62.4°]

9.19 A centrifugal pump delivers water at $0.075 \text{ m}^3/\text{s}$ with a head of 20 m while operating at 880 rpm. The hub-to-shroud radius ratio at the inlet is 0.35, and the relative velocity makes an angle of -52° at the inlet. (a) Find the reversible work done by the pump. (b) What is the work done by the impeller? (c) Find the impeller radius and the inlet radius of the shroud. (d) Determine the blade height at the exit of the impeller. (e) Assume a reasonable number of blades, and calculate the blade angle at the exit. Use the Pfleiderer equation to determine more accurately the number of blades and recalculate the blade angle at the exit if needed. (f) What is the power required to drive the pump? [Ans: (a) 196 J/kg, (b) 227 J/kg, (c) 23.4 cm, 7.23 cm (d) 2.04 cm, (e) 6 blades, -71.2° , (f) 17.53 kW]

9.20 A fan draws in atmospheric air at $0.4 \text{ m}^3/\text{s}$ at pressure 101.32 kPa, and temperature 288 K. The total pressure rise across the fan, which has 30 radial blades, is 2.8 cm of water. The inner radius is 14.8 cm and outer radius is 17.0 cm. The rotational speed of the fan is 980 rpm and the hydraulic efficiency is the fan is 0.78. Use the Stanitz slip factor. (a) Assuming that velocity into the fan is radially outward, find the angle of the relative velocity at the shroud at the inlet. (b) Determine the power to the fan, given that 4% is lost to mechanical friction. (c) Find the angle blade angle at the exit. [Ans: (a) -79.7° , (b) 0.147 kW, (c) 4.16°]

9.21 A pump draws water at the rate of 75 L/s from a large tank with the air pressure above the free surface at 98.00 kPa. The pump is $z = 2 \text{ m}$ above the water level in the tank. The pipe diameter is 14.0 cm, and the suction pipe is 20 m in length. The entrance loss coefficient is $K_i = 0.2$, and the loss coefficient of the elbow is $K_e = 0.6$ and the pipe roughness is $55 \mu\text{m}$. Find the suction specific speed given a shaft speed of 1800 rpm. The viscosity of water is $1.08 \cdot 10^{-3} \text{ kg}/(\text{m s})$. [Ans: 3.46]

9.22 Consider a volute consisting only a of circular section in which the tangential velocity varies as $V_u = K/r$, and r is the location from the center of the volute to a location on the circular section. (a) Show that the value of K in terms of the volumetric flow rate Q , the radius of the circular section R , and the radius to the center of the of the circular section a , is given by

$$K = \frac{Q}{2\pi R(\lambda - \sqrt{\lambda^2 - 1})}$$

in which $\lambda = a/R$. (b) For $R = 0.5 \text{ m}$, $a = 2 \text{ m}$, and $Q = 1.5 \text{ m}^3/\text{s}$, find the pressure difference $p_2 - p_1$ at the centerline, between the outside and inside edges of the section. [Ans: 2 kPa]

CHAPTER 10

RADIAL INFLOW TURBINES

The best known use of radial inflow turbines is in automobile turbochargers, but they also appear as auxiliary power turbines and, for example in turboprop aircraft engines. They are used in processing industries (including refineries), natural-gas processing, air liquefaction, and geothermal energy production. In the automotive application, burned gases from the engine exhaust manifold are directed into a radial inflow turbine of the turbocharger, which powers a centrifugal compressor on the same axis. The compressor, in turn, increases the pressure and density of the supply air to the engine. As the engine speed may change quite rapidly, turbochargers must respond to the changing operating conditions nimbly. Centrifugal machines are inherently short and thus light in weight and low in inertia.

A sketch on the left side in Figure 10.1 is a radial cross-section of radial inflow turbine. It looks like a centrifugal compressor, but with a reversed flow direction. Hot gases enter through a volute and move into a vaned stator, which redirects them into a vaneless space and then into the rotor. On the right is a front view of the rotor. The velocity diagrams at the inlet and exit are shown in Figure 10.2. For best efficiency, the inflow angle β_2 is negative. But the blades at the inlet are typically radial, which means that the entering flow is at a negative incidence. Since the blades operate in a high-temperature environment and material strength diminishes as temperature increases, radial blades can withstand the imposed loads better than curved blades. It is for this reason that the blade angle at the inlet is set at $\chi_2 = 0$. The rotor turns the flow toward the axis as it passes through the flow channel, so that its radial velocity is zero at the exit and if the swirl component of

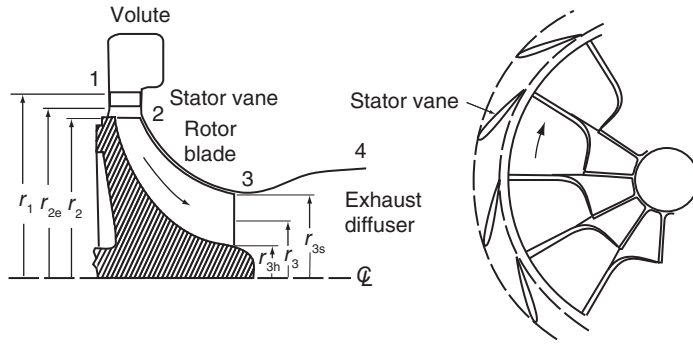


Figure 10.1 Radial inflow turbine.

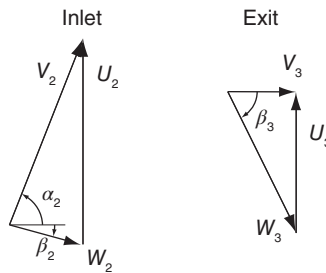


Figure 10.2 Velocity diagrams for a radial inflow turbine.

the absolute velocity vanishes at the exit, then the flow leaves the turbine axially. For this reason, these machines are also called 90° *inward-flow radial* (IFR) turbines.

10.1 TURBINE ANALYSIS

The velocity diagrams in Figure 10.2 are similar to those for centrifugal compressors, and at the exit, the absolute velocity is axial, as it is at the inlet of a compressor. Work delivered by the turbine, if written in terms of kinetic energies, is given by

$$w = \frac{1}{2}(V_2^2 - V_3^2) + \frac{1}{2}(U_2^2 - U_3^2) + \frac{1}{2}(W_3^2 - W_2^2) \quad (10.1)$$

This equation shows that increasing the inlet velocity V_2 increases the work. The increase in velocity is achieved by orienting the stator blades such that the flow enters the rotor at a large nozzle angle α_2 . Similarly, a small value for W_2 increases the work, and this is obtained by directing the relative velocity radially inward at the inlet. The same reasoning leads to a design in which the exit velocity V_3 is axial and therefore as small as possible and in which the relative velocity W_3 is large. This can be obtained by making the magnitude of the flow angle of the relative velocity $|\beta_3|$ large. Finally, a large U_2 and a small U_3 increase the work delivered.

The usual expression for work

$$w = U_2 V_{u2} - U_3 V_{u3} \quad (10.2)$$

leads to same conclusions, namely, V_{u3} should be small and V_{u2} large. Similarly, U_2 should be large and U_3 small, which means that the ratio r_3/r_2 ought to be fairly small. It falls into the range from 0.53 to 0.66 for common designs. Work could be increased by making V_{u3} negative, but this would also increase the absolute value of β_3 , and the exit relative Mach number might become so large as to cause the flow to choke. If the exit swirl is eliminated, the expression for work becomes

$$w = U_2 V_{u2}$$

When this equation is compared to Eq. (10.1) it is clear that the terms involving the exit station in that equation must cancel.

Since the blade speed $U_3 = r_3 \Omega$ is smallest at the hub, if the exit velocity V_3 is designed to be uniform across the exit plane, then the flow angle β_{3s} and therefore also the magnitude of the blade angle must be larger at the shroud than at the hub. This means that the relative velocity and the relative Mach number M_{3R} at the shroud will be the largest on the exit plane. The equation for work delivered by a turbine

$$w = c_p(T_{01} - T_{03})$$

when written in the form

$$s_w = \frac{w}{c_p T_{01}} = 1 - \frac{T_{03}}{T_{01}}$$

defines a nondimensional specific work intensity $s_w = w/c_p T_{01} = \dot{W}/\dot{m}c_p T_{01}$, also known as a *power ratio*. If the exit kinetic energy is wasted (as is often the case), it is appropriate to use the total-to-static efficiency as the proper measure of efficiency. It is defined as

$$\eta_{ts} = \frac{T_{01} - T_{03}}{T_{01} - T_{3ss}} = \frac{1 - \frac{T_{03}}{T_{01}}}{1 - \frac{T_{3ss}}{T_{01}}}$$

which is clearly also

$$\eta_{ts} = \frac{1 - \frac{T_{03}}{T_{01}}}{1 - \left(\frac{p_3}{p_{01}}\right)^{(\gamma-1)/\gamma}}$$

Solving this for the pressure ratio gives

$$\frac{p_{01}}{p_3} = \left(1 - \frac{s_w}{\eta_{ts}}\right)^{-\gamma/(\gamma-1)} \quad (10.3)$$

Graphs of the pressure ratio as a function of s_w are shown in Figure 10.3. Power ratios in the range $0.15 < s_w < 0.25$ correspond to pressure ratios in the range of $2 < p_{01}/p_3 < 3$ for typical values of efficiency. From the pressure ratio, and an estimate of the efficiency, the power ratio can be calculated.

The expression for work can be written as

$$w = c_p T_{01} s_w$$

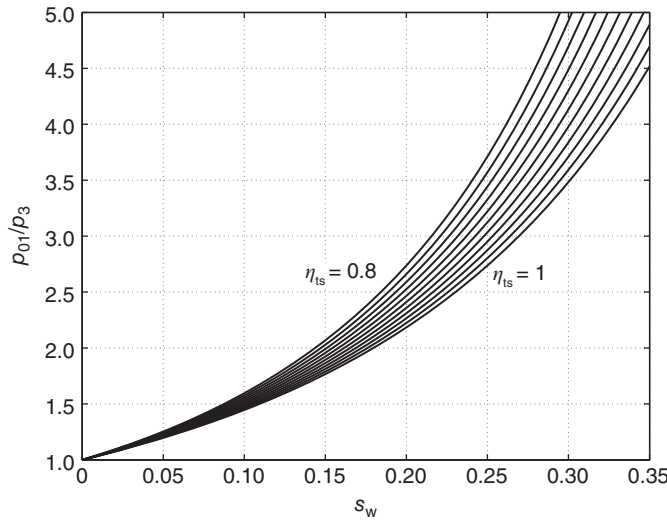


Figure 10.3 Pressure ratio for a gas with $\gamma = 1.4$ as a function of power ratio, or total-to-static efficiency $\eta_{ts} = 0.8$ to $\eta_{ts} = 1.0$ with adjacent graphs incremented by 0.02.

and with a typical power ratio $s_w = 0.2$ and inlet stagnation temperature $T_{01} = 1000$ K, the specific work is $w = 229.60$ kJ/kg in expansion of combustion gases with $c_p = 1148$ J/(kg K). Thus the stagnation temperature drop is 200 K. If the relative flow is radially inward and there is no exit swirl, the Euler turbine equation shows that $w = U_2^2$, so that a typical blade speed is 479 m/s. The size of the machine depends on the mass flow rate. Thus, as a rough estimate, a turbocharger operating at shaft speed of 40000 rpm gives an inlet radius of about 10 cm, and one operating at 200000 rpm gives a radius of 2 cm. An automotive turbocharger with a rotor diameter of approximately 3 cm is shown in Figure 10.4.

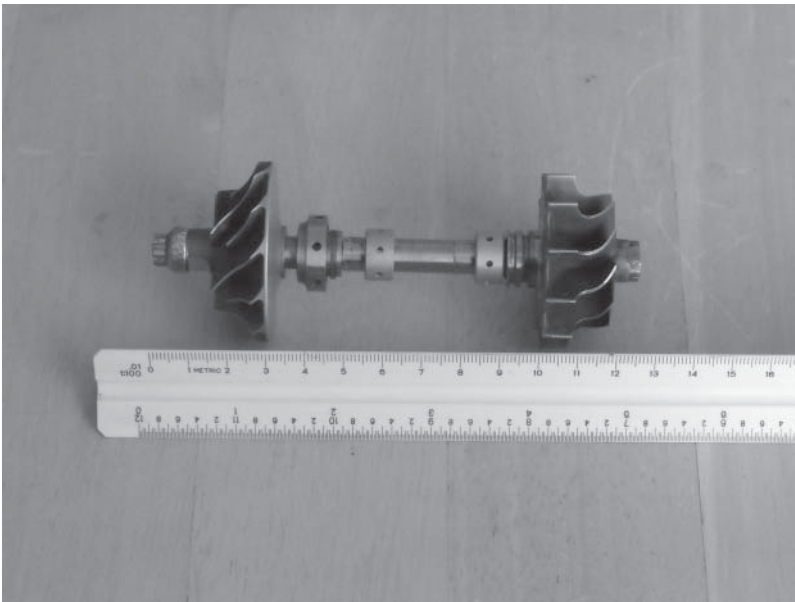


Figure 10.4 An automotive turbocharger.

At the exit, in addition to being uniform, the axial velocity V_3 should be small so that the exit kinetic energy is small. Whatever exit kinetic energy is left in the exit stream may be recovered in an exit diffuser. Ideally, the exit diffuser would reduce the velocity to zero as the flow enters the atmosphere. For isentropic flow, the work delivered in this situation is

$$w_s = h_{01} - h_{3ss} = \frac{1}{2}V_0^2 \quad (10.4)$$

and the quantity V_0 is called a *spouting velocity*. The kinetic energy associated with the spouting velocity is a convenient replacement for the maximum work that this turbine can deliver. This equation can also be interpreted as defining what velocity would be reached in a frictionless *nozzle* as the flow expands from pressure p_{01} to the exit static pressure p_3 . The equation for isentropic work can now be written as

$$\frac{1}{2}V_0^2 = c_p T_{01} \left(1 - \frac{T_{3ss}}{T_{01}} \right)$$

or as

$$\frac{V_0^2}{2c_p T_{01}} = 1 - \left(\frac{p_3}{p_{01}} \right)^{(\gamma-1)/\gamma}$$

If the relative flow entering the turbine is radial and there is no exit swirl, then, the definition of total-to-static efficiency can be written as

$$\eta_{ts} = \frac{w}{w_s} = \frac{2U_2^2}{V_0^2} \quad (10.5)$$

The largest value for U_2/V_0 according to this equation is 0.707, but since the highest efficiency is obtained with β_2 in the range from -20° to -40° , and the nozzle angle is typically $\alpha_2 = 70^\circ$, this result needs some modification and a typical range for this ratio is $0.55 < U_2/V_0 < 0.77$.

Since the isentropic work is given by Eq. (10.4), the value of the spouting velocity gives a way to calculate an initial estimate for the blade speed. With the value of blade speed U_2 known, the magnitude of the stresses can then be calculated.

■ EXAMPLE 10.1

A radial inflow turbine with radial blades at the inlet operates at 62000 rpm. Its inlet diameter is $D_2 = 12.6$ cm. The gases enter the blades radially and leave without exit swirl. The supply temperature is $T_{01} = 1150$ K, the pressure ratio of the turbine is $p_{01}/p_3 = 2$, and the mass flow rate is $\dot{m} = 0.31$ kg/s. The ratio of specific heats is $\gamma = 1.35$ and the gas constant is $R = 287$ J/(kg K). Find (a) the ratio U_2/V_0 , in which V_0 is the spouting velocity, (b) the total-to-static efficiency, and (c) the power delivered by the turbine.

Solution: (a) The specific heat is

$$c_p = \frac{\gamma R}{\gamma - 1} = \frac{1.35 \cdot 287}{0.35} = 1107 \text{ J/(kg K)}$$

and the isentropic static temperature at the exit is

$$T_{3ss} = T_{01} \left(\frac{p_3}{p_{01}} \right)^{(\gamma-1)/\gamma} = 1150 \cdot 0.5^{0.35/1.35} = 960.84 \text{ K}$$

The isentropic work is, therefore,

$$w_s = c_p(T_{01} - T_{3ss}) = 1107(1150 - 960.84) = 209.40 \text{ kJ/kg}$$

and the spouting velocity is

$$V_0 = \sqrt{2w_s} = \sqrt{2 \cdot 209400} = 647.1 \text{ m/s}$$

The blade speed at the inlet is

$$U_2 = r_2 \Omega = \frac{12.6 \cdot 62000 \cdot \pi}{2 \cdot 100 \cdot 30} = 409.0 \text{ m/s}$$

so that the ratio $U_2/V_0 = 0.632$.

(b) Since there is no exit swirl, the work becomes

$$w = U_2^2 = 167.31 \text{ kJ/kg}$$

and the stagnation temperature drop amounts to $T_{01} - T_{02} = w/c_p = 151^\circ\text{C}$. The total-to-static efficiency comes out to be

$$\eta_{ts} = \frac{w}{w_s} = \frac{167.31}{209.40} = 0.799$$

(c) The power delivered is

$$\dot{W} = \dot{m}w = 0.31 \cdot 167.31 = 51.87 \text{ kW}$$

■

The next example gives an analysis for a choked rotor passage.

■ EXAMPLE 10.2

Combustion gases with $\gamma = 1.35$, $c_p = 1107 \text{ J/(kg K)}$ and $R = 287 \text{ J/(kg K)}$ flow from conditions $p_{01} = 390 \text{ kPa}$ and $T_{01} = 1150 \text{ K}$ through a radial inflow turbine to an exit pressure $p_3 = 100 \text{ kPa}$. The total-to-static efficiency is $\eta_{ts} = 0.8$, and the flow leaving the stator is choked with $M_2 = 1$. (a) Find the work delivered by the turbine, given that the relative velocity at the inlet of the rotor is radial and that flow leaves without swirl. (b) Find the angle of the absolute velocity at the inlet of the rotor.

Solution: Since the stator is choked, and $T_{02} = T_{01}$, the static temperature at the exit of the stator is

$$T_2 = \frac{2}{\gamma + 1} T_{02} = \frac{2}{2.35} 1150 = 978.7 \text{ K}$$

and the velocity, since $M_2 = 1$, is

$$V_2 = \sqrt{\gamma R T_2} = \sqrt{1.35 \cdot 287 \cdot 978.7} = 615.8 \text{ m/s}$$

Solving the definition of total-to-static efficiency

$$\eta_{ts} = \frac{T_{01} - T_{03}}{T_{01} - T_{3ss}}$$

for the exit stagnation temperature gives

$$\frac{T_{03}}{T_{01}} = 1 - \eta_{ts} \left[1 - \left(\frac{p_{01}}{p_3} \right)^{-(\gamma-1)/\gamma} \right]$$

so that

$$T_{03} = 1150 [1 - 0.8 (1 - 3.9^{-0.35/1.35})] = 876.5 \text{ K}$$

Work delivered by the turbine is, therefore,

$$w = c_p (T_{01} - T_{03}) = 1107(1150 - 876.5) = 302.80 \text{ kJ/kg}$$

This is also

$$w = U_2^2$$

so that

$$U_2 = \sqrt{w} = \sqrt{302800} = 550.27 \text{ m/s}$$

The flow angle at the inlet to the rotor is

$$\alpha_2 = \sin^{-1} \left(\frac{U_2}{V_2} \right) = \sin^{-1}(0.893) = 63.3^\circ$$

■

The foregoing two examples assumed that the relative velocity at the inlet to the rotor is radial and that there is no exit swirl. In the next section, a general development based on this assumption is carried out in order to relate the important flow parameters to the total-to-static efficiency.

10.2 EFFICIENCY

The total-to-static efficiency of a turbine is

$$\eta_{ts} = \frac{h_{01} - h_{03}}{h_{01} - h_{3ss}}$$

with the thermodynamic states as shown in Figure 10.5. This can be written as

$$\frac{1}{\eta_{ts}} - 1 = \frac{h_{03} - h_{3ss}}{h_{01} - h_{03}}$$

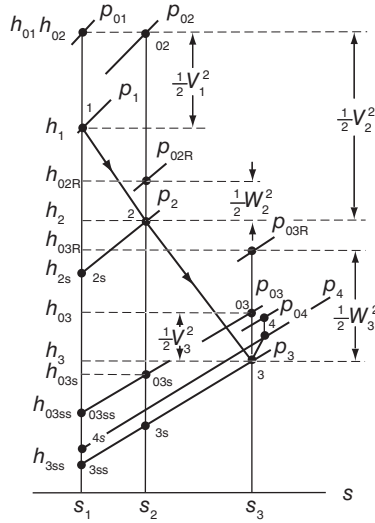


Figure 10.5 Velocity triangles and Mollier chart for a radial inflow turbine.

If the turbine is fitted with a diffuser and its exit pressure is p_4 , then, if the flow exhausts to the atmosphere, the pressure p_4 is the atmospheric pressure and the small amount of residual kinetic energy is lost into the atmosphere. In this situation, the pressure p_3 is below the atmospheric value. If the flow through this diffuser were reversible, then the pressure p_4 would correspond to the stagnation pressure p_{03} . In this case, the appropriate efficiency to use is the total-to-total efficiency. On the other hand, if the flow is not diffused and the flow is exhausted to the atmosphere directly, then the exit pressure p_3 is the atmospheric pressure and the residual kinetic energy is lost. In this case, the efficiency is the total-to-static efficiency. The numerator can be rewritten as

$$h_{03} - h_{3ss} = \frac{1}{2}V_3^2 + h_3 - h_{3s} + h_{3s} - h_{3ss}$$

Next, integrating the Gibbs equation along the constant pressure lines p_2 and p_3 gives

$$\frac{T_2}{T_{2s}} = \frac{T_{3s}}{T_{3ss}} \quad \text{thus} \quad \frac{T_{3ss}}{T_{2s}} = \frac{T_{3s}}{T_2}$$

Adding minus one to both sides of the first of these equations, multiplying by c_p , rearranging, and using the second equation, gives

$$h_{3s} - h_{3ss} = \frac{T_{3ss}}{T_{2s}}(h_2 - h_{2s}) = \frac{T_{3s}}{T_2}(h_2 - h_{2s})$$

As a consequence the expression for efficiency is

$$\frac{1}{\eta_{ts}} - 1 = \frac{V_3^2}{2w} + \frac{\zeta_R W_3^2}{2w} + \frac{T_{3s}}{T_2} \frac{\zeta_S V_2^2}{2w}$$

in which the enthalpy changes have been written in terms of the loss coefficients as

$$h_3 - h_{3s} = \frac{1}{2}\zeta_R W_3^2 \quad h_2 - h_{2s} = \frac{1}{2}\zeta_S V_2^2,$$

and they have been substituted for the internal heating terms. Making use of the relationships $w = U_2^2$, $U_2 = V_2 \sin \alpha_2$, $U_3 = -V_3 \tan \beta_3$, $U_3 = -W_3 \sin \beta_3$, and $U_3 = r_3 U_2 / r_2$ turns this equation into

$$\frac{1}{\eta_{ts}} - 1 = \frac{1}{2} \left[\left(\frac{r_3}{r_2} \right)^2 (\cot^2 \beta_3 + \zeta_R \csc^2 \beta_3) + \frac{T_{3s}}{T_2} \zeta_S \csc^2 \alpha_2 \right] \quad (10.6)$$

The temperature ratio in this expression can be written in a form from which it is easy to calculate. First, it is recast as

$$\frac{T_{3s}}{T_2} = 1 - \frac{1}{T_2} (T_2 - T_3 + T_3 - T_{3s})$$

in which temperature difference $T_2 - T_3$ is obtained from

$$w = U_2^2 = h_{02} - h_{03} = c_p (T_2 - T_3) + \frac{1}{2} V_2^2 - \frac{1}{2} V_3^2$$

Solving this for $T_2 - T_3$ gives

$$T_2 - T_3 = \frac{1}{c_p} \left(U_2^2 - \frac{1}{2} V_2^2 + \frac{1}{2} V_3^2 \right)$$

But from the velocity diagrams in Figure 10.2, since $\beta_2 = 0$ and $\alpha_3 = 0$, it is seen that

$$V_2^2 = W_2^2 + U_2^2 \quad W_3^2 = V_3^2 + U_3^2$$

so that

$$T_2 - T_3 = \frac{1}{2c_p} (W_3^2 - W_2^2 + U_2^2 - U_3^2)$$

and therefore

$$\frac{T_{3s}}{T_2} = 1 - \frac{1}{2c_p T_2} (W_3^2 - W_2^2 + U_2^2 - U_3^2 + \zeta_R W_3^2)$$

in which $\zeta_R = 2c_p (T_3 - T_{3s}) / W_3^2$ has been used. This can now be written as

$$\frac{T_{3s}}{T_2} = 1 - \frac{1}{2c_p T_2} (U_3^2 \csc^2 \beta_3 - U_2^2 \cot^2 \alpha_2 + U_2^2 - U_3^2 + \zeta_R U_3^2 \csc^2 \beta_3)$$

and, with $U_3 = U_2 r_3 / r_2$, as

$$\frac{T_{3s}}{T_2} = 1 - \frac{U_2^2}{2c_p T_2} \left[1 + \left(\frac{r_3}{r_2} \right)^2 ((1 + \zeta_R) \csc^2 \beta_3 - 1) - \cot^2 \alpha_2 \right]$$

From

$$T_2 = T_{02} - \frac{1}{2c_p} V_2^2 \quad 2c_p T_2 = 2c_p T_{02} - U_2^2 \csc^2 \alpha_2$$

so that

$$\frac{U_2^2}{2c_p T_2} = \left(\frac{T_{02}}{T_2} - 1 \right) \sin^2 \alpha_2 = \frac{\gamma - 1}{2} M_2^2 \sin^2 \alpha_2,$$

and it follows that the temperature ratio can also be written as

$$\frac{T_{3s}}{T_2} = 1 - \frac{\gamma - 1}{2} M_2^2 \sin^2 \alpha_2 \left[1 + \left(\frac{r_3}{r_2} \right)^2 ((1 + \zeta_R) \csc^2 \beta_3 - 1) - \cot^2 \alpha_2 \right]$$

The value of ζ_S is measured in a stationary test apparatus, and the total-to-static efficiency can be measured from the overall balance for the turbine [15]. The value of ζ_R can then be determined from the theory developed above. These calculations are illustrated in the following example.

■ EXAMPLE 10.3

In a radial-inflow turbine, combustion gases, with $\gamma = \frac{4}{3}$ and $c_p = 1148 \text{ J/(kg K)}$, leave the stator at the angle $\alpha_2 = 67^\circ$. The rotor blades at the inlet are radial, with a radius $r_2 = 5.8 \text{ cm}$. At the outlet the shroud radius of the blade is $r_{3s} = 4.56 \text{ cm}$, the hub-to-shroud radius ratio is $\kappa = 0.35$, and the relative flow makes an angle $\beta_3 = -38^\circ$ with the axial direction at the exit. The relative velocity at the inlet to the rotor is radial. The power delivered by the turbine is $\dot{W} = 58.2 \text{ kW}$ when the mass flow rate is $\dot{m} = 0.34 \text{ kg/s}$ and the rotational speed is 64000 rpm. The stagnation temperature and pressure at the inlet to the stator are $T_{01} = 1100 \text{ K}$ and $p_{01} = 2.5 \text{ bar}$. The static enthalpy loss coefficient for the flow across the stator is $\zeta_S = 0.08$. The outlet static pressure is $p_3 = 1 \text{ bar}$. Find (a) the Mach number at the inlet of the rotor, (b) the total-to-static efficiency, and (c) the static enthalpy loss coefficient of the rotor.

Solution: (a) The blade speed at the inlet is

$$U_2 = r_2 \Omega = \frac{0.058 \cdot 64000 \cdot \pi}{30} = 388.72 \text{ m/s},$$

and since the relative flow is radial, $V_{u2} = U_2$ and

$$V_2 = \frac{V_{u2}}{\sin \alpha_2} = \frac{388.72}{\sin(67^\circ)} = 422.29 \text{ m/s}$$

Since $T_{02} = T_{01}$, the static temperature at the inlet is

$$T_2 = T_{02} - \frac{V_2^2}{2c_p} = 1100 - \frac{422.29^2}{2 \cdot 1148} = 1022.3 \text{ K}$$

and the Mach number becomes

$$M_2 = \frac{V_2}{\sqrt{\gamma R T_2}} = \frac{422.29}{\sqrt{1.333 \cdot 287 \cdot 1022.3}} = 0.675$$

(b) The specific work is given by

$$w = \frac{\dot{W}}{\dot{m}} = \frac{58200}{0.34} = 171.18 \text{ kJ/kg}$$

and the stagnation temperature at the outlet is therefore

$$T_{03} = T_{01} - \frac{w}{c_p} = 1100 - \frac{171.18}{1.148} = 950.9 \text{ K}$$

In an isentropic process to the exit pressure, the static temperature at the exit is

$$T_{3ss} = T_{01} \left(\frac{p_3}{p_{01}} \right)^{(\gamma-1)/\gamma} = 1100 \left(\frac{1}{2.5} \right)^{0.25} = 874.8 \text{ K}$$

and the total-to-static efficiency is therefore

$$\eta_{ts} = \frac{T_{01} - T_{03}}{T_{01} - T_{3ss}} = \frac{1100 - 950.9}{1100 - 874.8} = 0.662$$

(c) If in the expression for efficiency the temperature ratio T_{3s}/T_2 is set to 1, then the static enthalpy loss coefficient ζ_R can be solved from

$$\frac{1}{\eta_{ts}} - 1 = \frac{1}{2 \tan^2 \beta_3} \left(\frac{r_3}{r_2} \right)^2 + \frac{\zeta_R}{2 \sin^2 \beta_3} \left(\frac{r_3}{r_2} \right)^2 + \frac{\zeta_S}{2 \sin^2 \alpha_2}$$

With $\zeta_S = 0.08$, $\beta_3 = -38^\circ$, and $r_3 = (r_{3s} + r_{3h})/2 = 0.0308 \text{ m}$, solving this equation gives $\zeta_R = 0.6256$. Now the temperature ratio is calculated as

$$\frac{T_{3s}}{T_2} = 1 - \frac{\gamma - 1}{2} M_2^2 \sin^2 \alpha_2 \left[1 + \left(\frac{r_3}{r_2} \right)^2 ((1 + \zeta_R) \csc^2 \beta_3 - 1) - \cot^2 \alpha_2 \right] = 0.8876$$

Substituting this into Eq. (10.6) and repeating the calculation with the new temperature ratio gives $\zeta_R = 0.6399$. The static loss coefficient for the rotor is larger than that for the stator not only because the flow path is long but also because the flow undergoes a great deal of turning through the rotor. ■

10.3 SPECIFIC SPEED AND SPECIFIC DIAMETER

The specific speed, defined as

$$\Omega_s = \frac{\Omega \sqrt{Q_3}}{w_s}^{3/4}$$

characterizes the shape of a turbomachine, and a machine with a small specific speed has a low flow rate and a large specific work. A related quantity is the specific diameter given by

$$D_s = \frac{D w_s^{1/4}}{\sqrt{Q_3}}$$

It is small in axial turbines because the flow rate is large and the work per stage is relatively small. For radial inflow turbines, this quantity is large because the work per stage is large and the volumetric flow rate is rather small. The product of specific speed and specific diameter is

$$\Omega_s D_s = \frac{D \Omega}{\sqrt{w_s}} = 2^{3/2} \frac{U_2}{V_0}$$

When the work is given by $w = U_2^2$, this reduces to

$$\Omega_s D_s = 2\sqrt{\eta_{ts}} \quad (10.7)$$

Balje [5] has constructed a large number of diagrams with specific speed on the abscissa and specific diameter as the ordinate. A Balje diagram for radial inflow turbines is shown in Figure 10.6, and the region of highest efficiency falls into the range $0.2 < \Omega_s < 0.8$. The corresponding specific diameter can be calculated according to Eq. (10.7). Lines of constant r_3/r_2 are also drawn with an optimum value near 0.7. The recommended range is $0.53 < r_3/r_2 < 0.66$. The slight discrepancy in this range and the optimum value 0.7 arises from different loss model being used to calculate the results and scant experimental data to verify them. Here the radius

$$r_3 = \sqrt{\frac{1}{2}(r_{3h}^2 + r_{3s}^2)}$$

is used to define the mean exit radius. The line $\Omega_s D_s = 2$ corresponding to $\eta_{ts} = 1$ has been drawn into the Balje diagram as well.

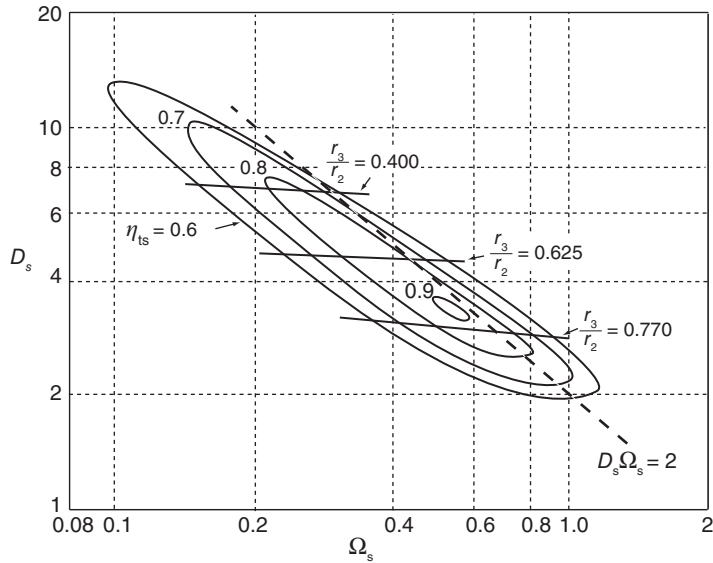


Figure 10.6 A Balje diagram for a radial inflow turbine, with β_2 . Source: Drawn after Balje [5].

EXAMPLE 10.4

Combustion gases, with $\gamma = \frac{4}{3}$, $R = 287 \text{ J}/(\text{kg K})$, and $c_p = 1148 \text{ J}/(\text{kg K})$, flow through a radial inflow turbine. It is designed to deliver 352 kW of power. The exit pressure is atmospheric at $p_3 = 101.3 \text{ kPa}$. The stagnation temperature to the turbine is $T_{01} = 960 \text{ K}$, and the loss coefficient of the stator is $\zeta_s = 0.08$. The ratio of the blade radii at the exit is $\kappa = r_{3h}/r_{3s} = 0.35$. The rotor speed is 35000 rpm, the blade speed is $U_2 = 440 \text{ m/s}$, and the flow angle to the inlet of the rotor is $\alpha_2 = 72.1^\circ$.

Use a design point from the Balje diagram with $D_s = 2.65$, $\Omega_s = 0.68$, and choose $r_{3s} = 0.86r_2$. Find (a) the mass flow rate, (b) the inlet Mach number, (c) supply stagnation pressure p_{01} and the blade height at the inlet. Assuming that the absolute velocity is uniform at the exit, find (d) the relative Mach number at the exit at the shroud and the hub, and (e) the ratios W_{3s}/W_2 , W_{3h}/W_2 and V_{r2}/V_{x3} .

Solution: (a) The spouting velocity is first determined from the ratio

$$\frac{U_2}{V_0} = \frac{\Omega_s D_s}{2^{3/2}} = \frac{0.68 \cdot 2.65}{2^{3/2}} = 0.6371$$

so that

$$V_0 = \frac{440}{0.6371} = 690.6 \text{ m/s}$$

The specific work is

$$w = U_2^2 = 440^2 = 193.60 \text{ kJ/kg}$$

and the mass flow rate is, therefore,

$$\dot{m} = \frac{\dot{W}}{w} = \frac{352.00}{193.60} = 1.818 \text{ kg/s}$$

(b) The inlet radius of the rotor has the value

$$r_2 = \frac{U_2}{\Omega} = \frac{440 \cdot 30}{35000 \cdot \pi} = 0.120 \text{ m}$$

and the relative and absolute velocities at the inlet are

$$W_2 = U_2 \cot \alpha_2 = 440 \cot(72.1^\circ) = 142.1 \text{ m/s}$$

$$V_2 = \frac{U_2}{\sin \alpha_2} = \frac{440}{\sin(72.1^\circ)} = 462.38 \text{ m/s}$$

The inlet Mach number is obtained by first calculating the static temperature at the inlet

$$T_2 = T_{02} - \frac{V_2^2}{2c_p} = 960 - \frac{462.38^2}{2 \cdot 1148} = 866.9 \text{ K}$$

and then the Mach number at the inlet is

$$M_2 = \frac{V_2}{\sqrt{\gamma R T_2}} = \frac{462.38}{\sqrt{1.333 \cdot 287 \cdot 866.9}} = 0.803$$

(c) From the definition of the stator loss coefficient, the isentropic inlet static temperature is

$$T_{2s} = T_2 - \zeta_s \frac{V_2^2}{2c_p} = 866.9 - 0.08 \frac{462.38^2}{2 \cdot 1148} = 859.4 \text{ K}$$

and the isentropic static temperature at the exit is

$$T_{3ss} = T_{01} - \frac{V_0^2}{2c_p} = 960 - \frac{690.6^2}{2 \cdot 1148} = 752.3 \text{ K}$$

Hence, the inlet stagnation pressure to the stator has the value

$$p_{01} = p_3 \left(\frac{T_{01}}{T_{3ss}} \right)^{\gamma/(\gamma-1)} = 101.3 \left(\frac{960}{752.2} \right)^4 = 268.7 \text{ kPa}$$

At the inlet to the rotor the static pressure is

$$p_2 = p_{01} \left(\frac{T_{2s}}{T_{02}} \right)^{\gamma/(\gamma-1)} = 268.7 \left(\frac{859.4}{960.0} \right)^4 = 172.6 \text{ kPa}$$

so that the density at the inlet becomes

$$\rho_2 = \frac{p_2}{RT_2} = \frac{172.6}{0.287 \cdot 866.9} = 0.694 \text{ kg/m}^3$$

The blade height can now be determined from the mass balance

$$b_2 = \frac{\dot{m}}{2\pi r_2 \rho_2 V_2 \cos \alpha_2} = \frac{1.818}{2\pi \cdot 0.120 \cdot 0.694 \cdot 462.4 \cos(72.1^\circ)} = 0.0245 \text{ m}$$

The ratio of the inlet blade height to the inlet radius is $b_2/r_2 = 0.204$.

(d) The rotor shroud and hub radii are

$$r_{3s} = 0.86r_2 = 0.86 \cdot 0.12 = 0.1032 \text{ m} \quad r_{3h} = \kappa r_{3s} = 0.35 \cdot 0.1032 = 0.0361 \text{ m}$$

When the Balje diagram is used, the average exit radius is its root mean square value

$$r_3 = \sqrt{\frac{1}{2}(r_{3h}^2 + r_{3s}^2)} = 0.0773 \text{ m}$$

The blade speed at the mean radius is therefore

$$U_3 = r_3 \Omega = \frac{0.0773 \cdot 35000 \cdot \pi}{30} = 283.5 \text{ m/s}$$

At the shroud and the hub, the blade speeds are

$$U_{3s} = r_{3s} \Omega = \frac{0.1032 \cdot 35000 \cdot \pi}{30} = 378.4 \text{ m/s}$$

and

$$U_{3h} = U_{3s} \frac{r_{3h}}{r_{3s}} = 378.4 \frac{0.0361}{0.1032} = 132.4 \text{ m/s}$$

To calculate the exit velocity, the exit Mach number is needed. First, the exit stagnation temperature is found to be

$$T_{03} = T_{02} - \frac{w}{c_p} = 960 - \frac{193600}{1148} = 791.4 \text{ K}$$

Rearranging the mass balance

$$\dot{m} = \rho_3 V_3 A_3 = \frac{p_3 A_3}{RT_3} M_3 \sqrt{\gamma RT_3}$$

leads to

$$\frac{\dot{m}}{p_3 A_3} \sqrt{\frac{RT_{03}}{\gamma}} = M_3 \left(1 + \frac{\gamma-1}{2} M_3^2 \right)^{1/2}$$

which on squaring can be written as a quadratic equation in M_3^2

$$M_3^4 + \frac{2}{\gamma-1} M_3^2 - \frac{2RT_{03}\dot{m}^2}{\gamma(\gamma-1)p_3^2 A_3^2} = 0,$$

and after numerical values are inserted, this reduces to

$$M_3^4 + 6M_3^2 - 0.3813 = 0$$

Solution of this is $M_3 = 0.251$.

(e) The exit velocity can now be determined by first calculating the static temperature at the exit

$$T_3 = T_{03} \left(1 + \frac{\gamma-1}{2} M_3^2 \right)^{-1} = 791.4 \left(1 + \frac{0.251^2}{2} \right)^{-1} = 783.1 \text{ K}$$

which gives the exit velocity

$$V_3 = M_3 \sqrt{\gamma R T_3} = 0.251 \sqrt{1.333 \cdot 287 \cdot 783.1} = 137.3 \text{ m/s}$$

Since the absolute velocity is axial at the exit, the angles that the relative flow makes at the shroud and the hub at the exit are

$$\begin{aligned} \beta_{3s} &= \tan^{-1} \left(-\frac{U_{3s}}{V_3} \right) = \tan^{-1} \left(-\frac{378.4}{137.3} \right) = -70.06^\circ \\ \beta_{3h} &= \tan^{-1} \left(-\frac{U_{3h}}{V_3} \right) = \tan^{-1} \left(-\frac{132.4}{137.3} \right) = -43.97^\circ \end{aligned}$$

The relative velocities at the shroud and hub are

$$W_{3s} = \sqrt{U_{3s}^2 + V_3^2} = \sqrt{378.4^2 + 137.3^2} = 402.5 \text{ m/s}$$

$$W_{3h} = \sqrt{U_{3h}^2 + V_3^2} = \sqrt{132.4^2 + 137.3^2} = 190.8 \text{ m/s}$$

and at the inlet, the relative velocity is

$$W_2 = \sqrt{V_2^2 - U_2^2} = \sqrt{462.4^2 - 440^2} = 142.1 \text{ m/s}$$

Hence, the relative velocity ratios are $W_{3s}/W_2 = 2.83$ and $W_{3h}/W_2 = 1.34$. Since $V_{r2} = V_2 \cos \alpha_2 = 462.4 \cos(72.1) = 142.1 \text{ m/s}$ and $V_{x3} = V_3 = 137.3$, their ratio is $V_{r2}/V_{x3} = 1.035$. The relative Mach numbers are $M_{3Rs} = 0.735$ and $M_{3Rh} = 0.348$. ■

In the foregoing example, only the product $\Omega_s D_s = 1.802$ was used. If the volumetric flow rate is based on the exit condition, then

$$D_s = \frac{D_2 w_s^{1/4}}{\sqrt{Q_3}} = \frac{2 \cdot 0.12 \cdot (2.385 \cdot 10^5)^{1/4}}{\sqrt{4.034}} = 2.64$$

$$\Omega_s = \frac{\Omega \sqrt{Q_3}}{w_s^{3/4}} = \frac{35000 \cdot \pi \sqrt{4.034}}{30 \cdot \sqrt{2.385 \cdot 10^5}} = 0.682$$

The mass balance was used to link the upstream and downstream states. Depending on what kind of information is known, this may become a somewhat involved calculation. The general approach is to express the mass balance in terms of the flow function. Upstream, this leads to

$$\frac{\dot{m} \sqrt{c_p T_{02}}}{p_{02} A_2} = F_2 \cos \alpha_2$$

and downstream the corresponding statement is

$$\frac{\dot{m} \sqrt{c_p T_{03}}}{p_{03} A_3} = F_3$$

in which the flow function is

$$F = \frac{\gamma}{\sqrt{\gamma-1}} M \left(1 + \frac{\gamma-1}{2} M^2 \right)^{-(\gamma+1)/(2\gamma-2)}$$

The term $\cos \alpha_2$ appears in the upstream expression because it is the radial inflow velocity, $V_{r2} = V_2 \cos \alpha_2$, that enters the expression for the mass flow rate. Downstream the corresponding factor is missing because it is assumed that the absolute velocity is axial.

Dividing these gives

$$\frac{A_2}{A_3} = \frac{F_3}{F_2 \cos \alpha_2} \sqrt{\frac{T_{02} p_{03}}{T_{03} p_{02}}}$$

The temperature ratio is

$$\frac{T_{02}}{T_{03}} = \frac{1}{1 - s_w}$$

and the pressure ratios may be written as

$$\frac{p_{03}}{p_{02}} = \frac{p_{03}}{p_3} \frac{p_3}{p_{01}} \frac{p_{01}}{p_{02}}$$

in which

$$\frac{p_{03}}{p_3} = \left(1 + \frac{\gamma-1}{2} M_3^2 \right)^{\gamma/(\gamma-1)}$$

and

$$\frac{p_{01}}{p_3} = \left(1 - \frac{s_w}{\gamma-1} \right)^{\gamma/(\gamma-1)}$$

In addition,

$$\frac{p_{01}}{p_{02}} = \left(\frac{T_2}{T_{2s}} \right)^{\gamma/(\gamma-1)} = \left(1 - \zeta_s \frac{\gamma-1}{2} M_2^2 \right)^{-\gamma/(\gamma-1)}$$

Substituting gives

$$\frac{A_2}{A_3} = \frac{F_3}{F_2 \cos \alpha_2} \left(\frac{1 + \frac{\gamma-1}{2} M_3^2}{1 - \zeta_s \frac{\gamma-1}{2} M_2^2} \right)^{\gamma/(\gamma-1)} \left(1 - \frac{s_w}{\eta_{ts}} \right)^{\gamma/(\gamma-1)} \frac{1}{\sqrt{1 - s_w}}$$

From this, it is clear that if the power ratio s_w can be determined and the total-to-static efficiency and the stator loss coefficient can be estimated, then the mass balance in this form involves only M_2 , M_3 , and the area ratio A_2/A_3 as unknowns. Hence, if two of these can be determined in other ways, this equation may be solved for the third. Clearly, if the area ratio is the only unknown, then it can be solved from this explicitly. However, if one of the Mach numbers is unknown, then an iterative solution of a nonlinear equation must be carried out. This can be readily performed with the aid of a computer. In hand calculations, it may be worthwhile to calculate the results directly from

$$\dot{m} = \rho_2 A_2 V_{r2} = \rho_3 A_3 V_3$$

by assuming one of the unknowns and then using the mass balance to check that the other converges by iterations to its correct value.

A collection of typical ranges of parameters for a well-designed radial inflow turbines has been compiled by Logan [59]. It is reproduced as Table 10.1.

Table 10.1 Design parameters for a radial inflow turbine.

| Parameter | Typical range |
|-----------------|----------------------------|
| α_2 | $68^\circ - 76^\circ$ |
| β_3 | -50° to -70° |
| r_{3h}/r_{3s} | < 0.4 |
| r_{3h}/r_2 | < 0.7 |
| r_3/r_2 | $0.53 - 0.66$ |
| b_2/r_2 | $0.1 - 0.3$ |
| U_2/V_0 | $0.55 - 0.8$ |
| W_3/W_2 | $2 - 2.5$ |
| V_3/U_2 | $0.15 - 0.5$ |
| ζ_R | $0.4 - 0.8$ |
| ζ_N | $0.06 - 0.24$ |

Source: Logan [59].

10.4 STATOR FLOW

The flow enters the stator row from a volute and leaves into a vaneless space. In the vaneless space, if losses are neglected, the flow may be assumed to be irrotational. The same assumption was made when the flow in the vaneless space of a centrifugal compressor

was considered. In such an irrotational flow the tangential component of velocity varies inversely with radius, and thus rV_u is constant. Since mass flow rate is constant

$$\dot{m} = 2\pi r_{2e} b_{2e} \rho_{2e} V_{r2e} = 2\pi r_2 b_2 \rho_2 V_{r2}$$

and, as Figure 10.1 shows, the subscript in r_{2e} refers to a radius at the exit of the stator blades, and r_2 is the exit of the vaneless space and therefore also the inlet to the rotor. This equation can be recast as

$$V_{r2} = V_{r2e} \frac{b_{2e} \rho_{2e} r_{2e}}{b_2 \rho_2 r_2}$$

For a gap of constant width $b_{2e} = b_2$. The density ratio influences only the radial component of velocity, and since this component is much smaller than the tangential component only a small error is made if the density is assumed constant. If the density difference is ignored, then this equation and $rV_u = \text{constant}$ can be written as

$$V_{r2} = V_{r2e} \frac{r_{2e}}{r_2} \quad V_{u2} = V_{u2e} \frac{r_{2e}}{r_2}$$

Dividing gives

$$\frac{V_{u2}}{V_{r2}} = \frac{V_{u2e}}{V_{r2e}} = \tan \alpha_2$$

so the flow angle α_2 remains constant. The calculations are illustrated next.

■ EXAMPLE 10.5

A combustion gas mixture, with the ratio of specific heats $\gamma = \frac{4}{3}$ and gas constant $R = 287 \text{ J/(kg K)}$, has a specific heat $c_p = 1148 \text{ J/(kg K)}$. These gases flow through a radial inflow turbine with the inlet stagnation temperature $T_{01} = 1015 \text{ K}$, and the stagnation pressure at the exit of the stator is $p_{02e} = 8.5 \text{ bar}$. The mass flow rate is $\dot{m} = 2.8 \text{ kg/s}$. The outlets of the stator blades are at the circle of radius $r_{2e} = 11.2 \text{ cm}$, where the flow angle is $\alpha_{2e} = 74.0^\circ$. The stator blade height is $b = 1.7 \text{ cm}$. The inlet of the rotor blade is at $r_2 = 9.8 \text{ cm}$, and at the exit of the rotor, the shroud radius is $r_{3s} = 7.7 \text{ cm}$ and the hub radius is $r_{3h} = 2.7 \text{ cm}$. The shaft rotates at 40000 rpm, and the turbine rotor efficiency is $\eta_{tt} = 0.89$. At the exit, the absolute velocity is axial. Find (a) the Mach number at the inlet to the rotor; (b) the power delivered by the turbine; (c) the Mach number at the exit of the turbine, assuming that the exit static pressure is 1 bar; (d) the flow angle of the relative velocity at the inlet to the rotor; and (e) the blade-loading coefficient $\psi = w/U_2^2$, the flow coefficient $\phi = V_{r2}/U_2$, and the specific speed of the turbine.

Solution: (a) If the thickness of the trailing edge of the stator blades is ignored, the flow area leaving the stator is

$$A_{2e} = 2\pi r_{2e} b = \frac{2\pi \cdot 11.2 \cdot 1.7}{100 \cdot 100} = 0.01196 \text{ m}^2$$

To determine the exit Mach number, the flow function is first calculated. Since $T_{02} = T_{01}$, it has the value

$$F_{2e} = \frac{\dot{m} \sqrt{c_p T_{02}}}{A_{2e} p_{02e} \cos \alpha_{2e}} = \frac{2.8 \sqrt{1148 \cdot 1015}}{0.01196 \cdot 850000 \cdot \cos(74^\circ)} = 1.078$$

Now the exit Mach number is obtained by iteration from the nonlinear equation

$$F_{2e} = \frac{\gamma}{\sqrt{\gamma-1}} M_{2e} \left(1 + \frac{\gamma-1}{2} M_{2e}^2 \right)^{-(1/2)[(\gamma+1)/(\gamma-1)]} = 1.078$$

With $\gamma = \frac{4}{3}$, its solution is $M_{2e} = 0.557$. The temperature can now be determined from

$$T_{2e} = T_{02} \left(1 + \frac{\gamma-1}{2} M_{2e}^2 \right)^{-1} = 1015 \left(1 + \frac{0.557^2}{2} \right)^{-1} = 965.1 \text{ K},$$

and the pressure is

$$p_{2e} = p_{02} \left(\frac{T_{2e}}{T_{02}} \right)^{\gamma/(\gamma-1)} = 8.5 \left(\frac{965.1}{1015} \right)^4 = 6.948 \text{ bar}$$

The static density is, therefore,

$$\rho_{2e} = \frac{p_{2e}}{RT_{2e}} = \frac{6.948 \cdot 10^5}{287 \cdot 965.1} = 2.508 \text{ kg/m}^3$$

The exit velocity is next determined from

$$V_{2e} = M_{2e} \sqrt{\gamma RT_{2e}} = 0.557 \sqrt{1.333 \cdot 287 \cdot 965.1} = 338.5 \text{ m/s}$$

and the radial and tangential velocity components are

$$V_{r2e} = V_{2e} \cos \alpha_{2e} = 338.5 \cos(74^\circ) = 93.3 \text{ m/s}$$

$$V_{u2e} = V_{2e} \sin \alpha_{2e} = 338.5 \sin(74^\circ) = 325.4 \text{ m/s}$$

The tangential velocity component of the flow leaving the gap is

$$V_{u2} = \frac{r_{2e}}{r_2} V_{u2e} = \frac{11.2}{9.8} 325.4 = 371.9 \text{ m/s}$$

and ignoring the density change in the radial term, the corresponding value of the velocity component entering the blade is

$$V_{r2} = \frac{r_{2e}}{r_2} V_{r2e} = \frac{11.2}{9.8} 93.3 = 106.6 \text{ m/s}$$

The magnitude of the absolute velocity is therefore

$$V_2 = \sqrt{V_{r2}^2 + V_{u2}^2} = \sqrt{106.6^2 + 371.9^2} = 386.9 \text{ m/s}$$

The static temperature at this location is

$$T_2 = T_{02} - \frac{V_2^2}{2c_p} = 1015 - \frac{386.9^2}{2 \cdot 1148} = 949.8 \text{ K}$$

and the Mach number is, therefore,

$$M_2 = \frac{V_2}{\sqrt{\gamma RT_2}} = \frac{386.9}{\sqrt{1.333 \cdot 287 \cdot 949.8}} = 0.642$$

If the density difference had been taken into account in the radial term, Mach number would have increased only to $M_2 = 0.644$.

(b) The tip speed of the rotor blade is

$$U_2 = r_2 \Omega = \frac{9.8 \cdot 40000 \cdot \pi}{100 \cdot 30} = 410.5 \text{ m/s}$$

and the tangential component of the relative velocity is

$$W_{u2} = V_{u2} - U_2 = 371.9 - 410.5 = -38.6 \text{ m/s}$$

Since $W_{r2} = V_{r2}$, the flow angle of the relative velocity has the value

$$\beta_2 = \tan^{-1} \left(\frac{W_{u2}}{W_{r2}} \right) = \tan^{-1} \left(-\frac{38.6}{106.6} \right) = -19.9^\circ$$

(c) Since there is no exit swirl, the work delivered becomes

$$w = U_2 V_{u2} = 410.5 \cdot 371.9 = 152.67 \text{ kJ/kg}$$

and the isentropic work is

$$w_s = \frac{w}{\eta_{tt}} = \frac{152.67}{0.89} = 171.54 \text{ kJ/kg}$$

The power delivered by the turbine is therefore

$$\dot{W} = \dot{m} w = 2.8 \cdot 152.67 = 427.5 \text{ kW}$$

(d) The stagnation temperature at the exit drops to

$$T_{03} = T_{02} - \frac{w}{c_p} = 1015 - \frac{152670}{1148} = 882.0 \text{ K}$$

and the corresponding temperature for an isentropic flow is

$$T_{03s} = T_{02} - \frac{w_s}{c_p} = 1015 - \frac{171540}{1148} = 865.6 \text{ K}$$

The exit stagnation pressure is therefore

$$p_{03} = p_{02e} \left(\frac{T_{03s}}{T_{02}} \right)^{\gamma/(\gamma-1)} = 8.5 \left(\frac{865.6}{1015} \right)^4 = 449.5 \text{ kPa}$$

With the exit area

$$A_3 = \pi(r_{3s}^2 - r_{3h}^2) = \pi(0.077^2 - 0.027^2) = 0.01634 \text{ m}^2,$$

the exit flow function is equal to

$$F_3 = \frac{\dot{m} \sqrt{c_p T_{03}}}{A_3 p_{03}} = \frac{2.8 \sqrt{1148 \cdot 882.0}}{0.01634 \cdot 449550} = 0.384$$

and the Mach number can then be obtained by iteration from the nonlinear equation

$$F_3 = \frac{\gamma}{\sqrt{\gamma-1}} M_3 \left(1 + \frac{\gamma-1}{2} M_3^2 \right)^{-(\gamma+1)/(2\gamma-2)} = 0.384$$

in which $\gamma = \frac{4}{3}$. The solution is $M_3 = 0.169$. The exit static temperature is then

$$T_3 = T_{03} \left(1 + \frac{\gamma-1}{2} M_3^2 \right)^{-1} = 882.0 \left(1 + \frac{0.169^2}{2} \right)^{-1} = 877.8 \text{ K}$$

so that the exit velocity becomes

$$V_3 = M_3 \sqrt{\gamma R T_3} = 0.315 \sqrt{1.333 \cdot 287 \cdot 877.8} = 97.9 \text{ m/s}$$

The volumetric flow rate is, therefore,

$$Q_3 = V_3 A_3 = 97.9 \cdot 0.01634 = 1.60 \text{ m}^3/\text{s}$$

(e) The blade-loading coefficient is

$$\psi = \frac{w}{U_2^2} = \frac{152670}{410.5^2} = 0.906$$

and the flow coefficient is

$$\phi = \frac{V_{r2}}{U_2} = \frac{106.6}{410.5} = 0.260$$

The flow coefficient for radial inflow turbines is usually less than 0.5. The specific speed is

$$\Omega_s = \frac{\Omega \sqrt{Q_3}}{w_s^{3/4}} = \frac{40000 \cdot \pi \sqrt{1.60}}{30 \cdot 171540^{3/4}} = 0.628$$

and the specific diameter turns out to be

$$D_s = \frac{D_2 w_s^{1/4}}{\sqrt{Q_3}} = \frac{0.196 \cdot 171540^{1/4}}{\sqrt{1.60}} = 3.15$$

These are in the range for good radial inflow turbine designs. ■

In the foregoing example, losses in the stator and vaneless gap were not taken into account explicitly. In the next section, methods to include them in the analysis are discussed.

10.4.1 Loss coefficients for stator flow

Baskharone [6] gives a correlation for the velocity coefficient for a flow through the stator:

$$c_v^2 = 1 - 1.8 \left(\frac{\theta}{s \cos \alpha_{2e} - t_e - \delta^*} \right) \left(1 + \frac{s \cos \alpha_m}{b} \right) \left(\frac{Re}{Re_f} \right)$$

in which $Re_f = 2.74 \cdot 10^6$ is a reference Reynolds number, that is based on the blade chord c and exit velocity V_{2e} . The angle α_m is the average flow angle between α_1 and α_{2e} . The spacing of the blades is s , and their height is b . The trailing-edge thickness of the blades is t_e . The sum of the pressure- and suction-side displacement thicknesses is $\delta^* = \delta_p^* + \delta_s^*$ and similarly for the total momentum thickness θ . It is assumed that the suction-side thicknesses are $\delta_s^* = 3.5\delta_p^*$ and $\theta_s = 3.5\theta_p$. The pressure-side values are obtained from

$$\frac{\delta_p^*}{c} = \frac{1.72}{\sqrt{Re}} \quad \frac{\theta_p}{c} = \frac{0.664}{\sqrt{Re}}$$

which are valid for laminar flow when $Re < 2 \cdot 10^5$, and for turbulent boundary layers, when $Re > 2 \cdot 10^5$, they are

$$\frac{\delta_p^*}{c} = \frac{0.057}{Re^{1/6}} \quad \frac{\theta_p}{c} = \frac{0.022}{Re^{1/6}}$$

Baskharone also recommends a model proposed by Khalil et al. [55] for taking into account the losses in the gap. It can be written as

$$Y_g = Y_r Y_\alpha Y_M Y_b$$

in which

$$Y_g = \frac{p_{02e} - p_{02}}{p_{02e} - p_{2e}}$$

is the stagnation pressure loss coefficient and

$$\begin{aligned} Y_r &= 0.193 \left(1 - \frac{r_2}{r_{2e}} \right) \\ Y_\alpha &= 1 + 0.0641(\alpha_{2e} - \alpha_{2f}) + 0.0023(\alpha_{2e} - \alpha_{2f})^2 \\ Y_M &= 1 + 0.6932(M_{02e} - M_{02f}) + 0.4427(M_{02e} - M_{02f})^2 \\ Y_b &= 1 + 0.0923\left(\frac{r_{2e}}{b} - \frac{r_{2e}}{b_f}\right) + 0.0008\left(\frac{r_{2e}}{b} - \frac{r_{2e}}{b_f}\right)^2 \end{aligned}$$

Here $M_{02e} = V_{2e}/\sqrt{\gamma RT_{02}}$ and the reference values are

$$\alpha_{2f} = 70^\circ \quad M_{02f} = 0.8 \quad b_f = r_{2e}/10$$

The angle α_{2e} is measured in degrees.

EXAMPLE 10.6

A gas with $\gamma = \frac{4}{3}$ and $c_p = 1148 \text{ J/(kg K)}$ flows through a radial inflow turbine. The conditions at the inlet to the stator are $T_{01} = 1015 \text{ K}$ and $p_{01} = 7.5 \text{ bar}$. At the inlet, the flow angle is $\alpha_1 = 20^\circ$ and Mach number is $M_1 = 0.14$. The gas leaves the stator at angle $\alpha_{2e} = 71^\circ$. The number of stator vanes is $Z = 37$, their trailing edge thickness is $t_e = 1.5 \text{ mm}$, their chord length is $c = 2.8 \text{ cm}$, and their height is $b = 0.9 \text{ cm}$. The radii are $r_1 = 12.0 \text{ cm}$, $r_{2e} = 10.5 \text{ cm}$, and $r_2 = 10.0 \text{ cm}$. Assume the kinematic viscosity to be $\nu = 90 \cdot 10^{-6} \text{ m}^2/\text{s}$. Find the stagnation pressure loss across the stator and the gap.

Solution: The static temperature at the inlet is

$$T_1 = T_{01} \left(1 + \frac{\gamma - 1}{2} M_1^2 \right)^{-1} = 1015 \left(1 + \frac{0.14^2}{2} \right)^{-1} = 1011.7 \text{ K}$$

and the static pressure is

$$p_1 = p_{01} \left(\frac{T_1}{T_{01}} \right)^{\gamma/(\gamma-1)} = 7.5 \left(\frac{1011.7}{1015} \right)^4 = 7.40 \text{ bar}$$

which gives for the static density the value

$$\rho_1 = \frac{p_1}{RT_1} = \frac{7.4 \cdot 10^5}{287 \cdot 1011.7} = 2.55 \text{ kg/m}^3$$

The velocity at the inlet is

$$V_1 = M_1 \sqrt{\gamma R T_1} = 0.14 \sqrt{1.333 \cdot 287 \cdot 1011.7} = 87.1 \text{ m/s}$$

and its radial component is

$$V_{r1} = V_1 \cos \alpha_1 = 87.1 \cos(20^\circ) = 81.86 \text{ m/s}$$

Mass balance may be written as

$$\dot{m} = \rho_1 2\pi r_1 b V_{r1} = \rho_{2e} 2\pi r_{2e} b V_{r2e}$$

Introducing the flow function, the nondimensional mass flow rate may be written as

$$\frac{\dot{m} \sqrt{c_p T_{01}}}{A_1 p_{01}} = \frac{\gamma M_1}{\sqrt{\gamma - 1}} \cos \alpha_1 \left(1 + \frac{\gamma - 1}{2} M_1^2 \right)^{-(\gamma+1)/(2\gamma-2)} = F_1 \cos \alpha_1$$

at the inlet and at the exit it is

$$\frac{\dot{m} \sqrt{c_p T_{02}}}{A_{2e} p_{02e}} = \frac{\gamma M_{2e}}{\sqrt{\gamma - 1}} \cos \alpha_{2e} \left(1 + \frac{\gamma - 1}{2} M_{2e}^2 \right)^{-(\gamma+1)/(2\gamma-2)} = F_{2e} \cos \alpha_{2e}$$

Since the flow is adiabatic, $T_{01} = T_{02}$, and if it is assumed to be isentropic, then it follows that $p_{01} = p_{02e}$. With $A_1 = 2\pi r_1 b$ and $A_{2e} = 2\pi r_{2e} b$, the mass balance gives the relationship

$$F_{2e} = F_1 \frac{r_1 \cos \alpha_1}{r_{2e} \cos \alpha_{2e}}$$

The value of F_1 is

$$F_1 = \frac{\gamma M_1}{\sqrt{\gamma - 1}} \left(1 + \frac{\gamma - 1}{2} M_1^2 \right)^{-(\gamma+1)/(2\gamma-2)} = \frac{4\sqrt{3} \cdot 0.14}{3} \left(1 + \frac{0.14^2}{6} \right)^{-3.5} = 0.3196$$

and therefore,

$$F_{2e} = 0.3196 \frac{12.0 \cos(20^\circ)}{10.5 \cos(71^\circ)} = 1.054$$

Solving the nonlinear equation

$$F_{2e} = \frac{\gamma M_{2e}}{\sqrt{\gamma - 1}} \left(1 + \frac{\gamma - 1}{2} M_{2e}^2 \right)^{-(\gamma+1)/(2\gamma-2)}$$

with this value of F_{2e} and $\gamma = \frac{4}{3}$, yields $M_{2e} = 0.539$. Static temperature at the exit of the stator is

$$T_{2e} = T_{02} \left(1 + \frac{\gamma - 1}{2} M_{2e}^2 \right)^{-1} = 1015 \left(1 + \frac{0.538^2}{6} \right)^{-1} = 968.7 \text{ K}$$

and the velocity is

$$V_{2es} = M_{2e} \sqrt{\gamma R T_{2e}} = 0.539 \sqrt{1.333 \cdot 287 \cdot 968.7} = 327.85 \text{ m/s}$$

Introduction of the flow function into the development assumes that the flow is isentropic. It is anticipated that no correction is needed, as V_{2e} is only used to calculate the Reynolds number in the loss correlation. The value of the Reynolds number is

$$Re = \frac{V_{2e} c}{\nu} = \frac{327.85 \cdot 2.8}{90 \cdot 10^{-6} \cdot 100} = 1.02 \cdot 10^5$$

so the flow is laminar. The displacement thickness on the pressure side is, therefore,

$$\delta_p^* = \frac{1.72c}{Re^{1/2}} = \frac{1.72 \cdot 2.8}{100 \cdot (1.02 \cdot 10^5)^{1/2}} = 1.51 \cdot 10^{-4} \text{ m}$$

Since the suction side displacement thickness is assumed to be $3.5\delta_p^*$, the sum becomes $\delta^* = 6.79 \cdot 10^{-4} \text{ m}$. The momentum thickness on the pressure side is

$$\theta_p = \frac{0.644c}{Re^{1/2}} = \frac{0.644 \cdot 2.8}{100 \cdot (1.02 \cdot 10^5)^{1/2}} = 5.65 \cdot 10^{-5} \text{ m}$$

and with the suction side thickness assumed again to be $3.5\theta_p$, the sum is $\theta = 2.54 \cdot 10^{-4} \text{ m}$. Next, the spacing can be obtained from

$$s_2 = \frac{2\pi r_{2e}}{Z} = \frac{2\pi \cdot 10.5}{100 \cdot 37} = 0.0178 \text{ m}$$

The average flow angle is $\alpha_{2m} = \frac{1}{2}(\alpha_1 + \alpha_{2e}) = 45.5^\circ$, and the velocity coefficient is obtained from

$$c_v^2 = 1 - 1.8 \left(\frac{\theta}{s_2 \cos \alpha_{2e} - t_e - \delta^*} \right) \left(1 + \frac{s_2 \cos \alpha_{2m}}{b} \right) \frac{Re}{Re_f}$$

with

$$\frac{\theta}{s_2 \cos \alpha_{2e} - t_e - \delta^*} = \frac{2.54 \cdot 10^{-4}}{0.0178 \cos(71^\circ) - 1.5 \cdot 10^{-3} - 6.79 \cdot 10^{-4}} = 0.0700$$

and

$$1 + \frac{s_2 \cos \alpha_{2m}}{b} = 1 + \frac{0.178 \cos(45.5^\circ)}{0.009} = 2.389$$

The square of the velocity coefficient becomes

$$c_v^2 = 1 - 1.8 \cdot 0.070 \cdot 2.389 \frac{102000}{2740000} = 0.989 \quad \text{so that} \quad c_v = 0.994$$

The actual exit velocity is therefore

$$V_{2e} = c_v V_{2es} = 0.994 \cdot 327.85 = 326.0 \text{ m/s}$$

and the enthalpy loss coefficient is $\zeta = 1/c_v^2 - 1 = 0.0113$. As anticipated, the difference from the ideal is such that no correction is needed. The static temperature at the exit of the stator is now

$$T_{2e} = T_{02} - \frac{V_{2e}^2}{2c_p} = 1015 - \frac{326.0^2}{2 \cdot 1148} = 968.7 \text{ K}$$

and the Mach number at the exit does not change significantly, and it is $M_{2e} = 0.539$. The stagnation pressure ratio across the stator ratio is now

$$\frac{p_{01}}{p_{02e}} = \left(1 + \frac{\gamma - 1}{2} \zeta M_{2e}^2\right)^{\gamma/(\gamma-1)} = \left(1 + \frac{0.0113 \cdot 0.539^2}{6}\right)^4 = 1.0022$$

and the loss of stagnation pressure across the stator is therefore

$$\Delta p_{0LS} = p_{01} - p_{02e} = 750.0(1 - 1/1.0022) = 1.64 \text{ kPa}$$

To determine the stagnation pressure loss across the gap, the stagnation Mach number at the inlet to the gap is needed. With $T_{02e} = T_{01}$, it is

$$M_{02e} = \frac{V_{2e}}{\sqrt{\gamma R T_{02}}} = \frac{326.0}{\sqrt{1.333 \cdot 287 \cdot 1015}} = 0.523$$

The stagnation loss coefficients for the gap are

$$Y_r = 0.193 \left(1 - \frac{10.0}{10.5}\right) = 0.00919$$

$$Y_\alpha = 1 + 0.0641(71 - 70) + 0.0023(71 - 70)^2 = 1.0664$$

$$Y_M = 1 + 0.6932(0.523 - 0.8) + 0.4427(0.523 - 0.8)^2 = 0.8420$$

$$Y_b = 1 + 0.0923 \left(\frac{10.5}{0.9} - 10\right) + 0.0008 \left(\frac{10.5}{0.9} - 10\right)^2 = 1.1561$$

and the overall loss coefficient comes out as

$$Y_g = 0.00919 \cdot 1.0664 \cdot 0.8420 \cdot 1.1561 = 0.00954$$

With the static pressure at the inlet of the rotor

$$p_{2e} = p_{02e} \left(\frac{T_{2e}}{T_{02}} \right)^{\gamma/(\gamma-1)} = 748.36 \left(\frac{968.7}{1015} \right)^4 = 620.9 \text{ kPa}$$

so that the stagnation pressure there is

$$p_{02} = p_{02e} - Y_g(p_{02e} - p_{2e}) = 748.36 - 0.00954(748.36 - 620.9) = 747.14 \text{ kPa}$$

and the stagnation pressure loss across the gap is

$$\Delta p_{0LG} = p_{02e} - p_{02} = 748.36 - 747.14 = 1.22 \text{ kPa}$$

Hence, upstream of the rotor the stagnation pressure loss is

$$\Delta p_{0LS} + \Delta p_{0LG} = 1.64 + 1.22 = 2.86 \text{ kPa}$$

■

Note that the Mach number increases across the stator from 0.14 to 0.539 owing to the acceleration of the flow as a result of the turning. There is a significant density change associated with this acceleration.

As has been shown above, across the gap the flow angle does not change for irrotational flow. Since the gap is also quite narrow, the area does not decrease greatly and the acceleration of the flow is rather slight. For this reason, it is possible to assume the flow to be incompressible across the gap and calculate it by the formula

$$V_{r2} = V_{r2e} \frac{r_{2e}}{r_2}$$

This cannot be used for the stator flow, and using it in the foregoing example would have yielded for the radial component of the stator exit velocity the value

$$V_{r2e} = V_{r1} \frac{r_1}{r_{2e}} = 81.86 \frac{12.0}{10.5} = 93.55 \text{ m/s}$$

and the exit velocity would have been

$$V_{2e} = \frac{V_{r2e}}{\cos \alpha_2} = \frac{93.55}{\cos(71^\circ)} = 287.4 \text{ m/s}$$

This would have been a significant error as the correct value came out to be 326.0 m/s.

10.5 DESIGN OF THE INLET OF A RADIAL INFLOW TURBINE

The foregoing developments and examples illustrate the basic methods for carrying out design calculations for radial inflow turbines. The loss calculations for the stator and

interblade gap, together with the expression for the overall efficiency and its appropriate value obtained from the Balje diagram, are sufficient to determine the loss through the rotor. Table 10.1 gives the appropriate geometric length ratios for a design. Methods to obtain some of these values are developed from the theory discussed in this section. This work has been carried out, among others, by Rodgers and Geiser [75], Rohlik [76], and Whitfield [94]. The extensive study by Whitfield has been included in the book by Whitfield and Baines [95]. The following development follows their studies.

Since

$$s_w = \frac{w}{c_p T_{01}}$$

the blade loading coefficient is

$$\psi = \frac{w}{U_2^2} = \frac{s_w c_p T_{01}}{U_2^2} = \frac{1}{M_{0u}^2} \frac{s_w}{\gamma - 1}$$

in which the blade stagnation Mach number is

$$M_{0u} = \frac{U_2}{\sqrt{\gamma R T_{01}}}$$

This is based on the inlet stagnation temperature as a reference value.

If at the exit, the flow has no swirl component and at the inlet, the relative velocity is radially inward, then $w = U_2^2$, and the blade-loading coefficient is

$$\psi = \frac{w}{U_2^2} = 1$$

Experiments have shown that efficiency is increased if $-40^\circ < \beta_2 < -20^\circ$. This introduces a negative incidence into the flow since the blade angle χ_2 is invariably zero. The blade-loading coefficient is now given by

$$\psi = \frac{V_{u2}}{U_2} = \frac{U_2 + W_{u2}}{U_2} = 1 + \phi \tan \beta_2$$

in which the flow coefficient is defined as

$$\phi = \frac{V_{r2}}{U_2}$$

The flow angle of the relative velocity is in the range $\beta_{2 \min} \leq \beta_2 \leq 0$, in which $\beta_{2 \min}$ is chosen such that the blade loading coefficient falls into the range $0 \leq \psi \leq 1$.

10.5.1 Minimum inlet Mach number

Whitfield [94] has shown how to optimize the inlet to the rotor by choosing (for a given power ratio) the absolute and relative flow angles that give the smallest inlet Mach number. Improper flow angles might lead to high inlet Mach numbers, and a possibility for choking. Following his development, the tangential velocity is first written as

$$V_{u2} = U_2 + W_{u2} = U_2 + V_{u2} \frac{\tan \beta_2}{\tan \alpha_2}$$

in which the second equation follows by using

$$V_{u2} = V_{r2} \tan \alpha_2 \quad W_{u2} = W_{r2} \tan \beta_2$$

together with $V_{r2} = W_{r2}$. Multiplying through by V_{u2} and rearranging gives

$$V_{u2}^2 \left(1 - \frac{\tan \beta_2}{\tan \alpha_2} \right) = U_2 V_{u2}$$

The right side is the work delivered, and since this is related to the power ratio, it will be taken to be a fixed quantity. Dividing both sides by V_2^2 leads to

$$\sin^2 \alpha_2 \left(1 - \frac{\tan \beta_2}{\tan \alpha_2} \right) = u \quad (10.8)$$

in which

$$u = \frac{U_2 V_{u2}}{V_2^2} = \frac{U_2 V_{u2}}{c_{02}^2} \frac{c_{02}^2}{V_2^2}$$

or

$$u = \frac{s_w}{(\gamma - 1)} \frac{1}{M_{02}^2} = \frac{s}{m}$$

where the following notation has been introduced:

$$s = \frac{s_w}{\gamma - 1} \quad m = M_{02}^2$$

The inlet stagnation Mach number has been defined as

$$M_{02} = \frac{V_2}{\sqrt{\gamma R T_{02}}}$$

which can be written also as

$$M_{02}^2 = \frac{V_2^2}{c_{02}^2} = \frac{V_2^2}{c_2^2} \frac{c_2^2}{c_{02}^2} = M_2^2 \frac{T_2}{T_{02}}$$

so that

$$M_{02}^2 = \frac{M_2^2}{1 + \frac{\gamma-1}{2} M_2^2} \quad (10.9)$$

Dividing Eq. (10.8) next by $\cos^2 \alpha_2$, and noting that $1/\cos^2 \alpha_2 = \tan^2 \alpha_2 + 1$, gives

$$(1 - u) \tan^2 \alpha_2 - \tan \beta_2 \tan \alpha_2 - u = 0$$

or

$$(m - s) \tan^2 \alpha_2 - m \tan \beta_2 \tan \alpha_2 - s = 0 \quad (10.10)$$

For given values of s_w , M_2 , and β_2 , this quadratic equation can be solved for $\tan \alpha_2$. The solution is displayed in Figure 10.7 with β_2 and s_w as parameters.

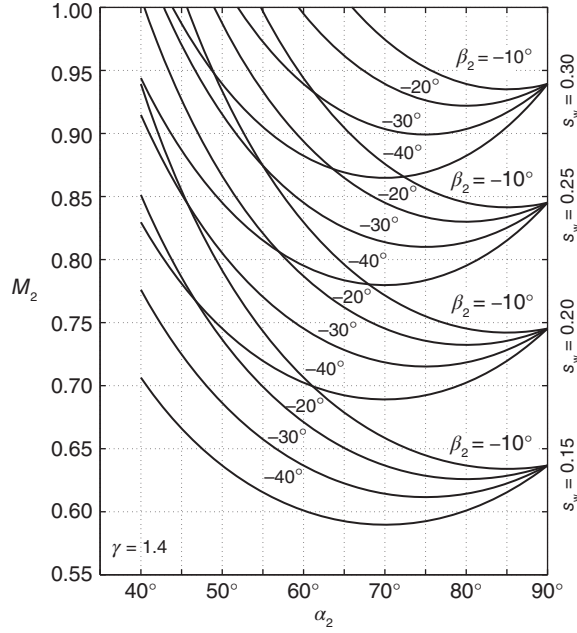


Figure 10.7 Inlet Mach number as a function of the nozzle angle for different relative flow angles and the power ratio with $\gamma = 1.4$.

For a given power ratio and relative flow angle, the minimum of each curve is sought next. To find it, let $a = \tan \alpha_2$ and $b = \tan \beta_2$. This puts Eq. (10.10) into the form

$$(m - s)a^2 - mba - s = 0 \quad m = \frac{s(1 + a^2)}{a(a - b)} \quad (10.11)$$

The minimum for m , for a fixed s and b , is obtained by setting the derivative of this with respect to a to zero. Thus

$$\frac{dm}{da} = \frac{2s(a - b)a^2 - s(2a - b)(1 + a^2)}{a^2(b - a)^2} = 0,$$

and this reduces to

$$ba^2 + 2a - b = 0$$

Solving this quadratic equation gives

$$a = \frac{-1 \pm \sqrt{1 + b^2}}{b} \quad (10.12)$$

Substituting this value of a into Eq. (10.11) gives

$$m = \frac{2s}{1 \mp \sqrt{1 + b^2}} \quad (10.13)$$

for the minimum of m as a function of s and β_2 . Since

$$\sqrt{1+b^2} = \sqrt{1+\tan^2\beta_2} = \frac{1}{\cos\beta_2}$$

Eq. (10.12) becomes

$$\tan\alpha_2 = \frac{-\cos\beta_2 \pm 1}{\sin\beta_2} \quad (10.14)$$

Next, making use of the identities

$$\cos\beta_2 = \cos^2\frac{\beta_2}{2} - \sin^2\frac{\beta_2}{2} \quad \sin\beta_2 = 2\sin\frac{\beta_2}{2}\cos\frac{\beta_2}{2}$$

in Eq. (10.14) leads to

$$\tan\alpha_2 = \frac{-\cos^2(\beta_2/2) + \sin^2(\beta_2/2) \pm 1}{2\sin(\beta_2/2)\cos(\beta_2/2)}$$

The positive sign gives

$$\tan\alpha_2 = \tan\frac{\beta_2}{2}$$

which is rejected because Figure 10.7 shows that $\alpha_2 > 0$ and $\beta_2 < 0$. The negative sign gives

$$\tan\alpha_2 = -\cot\frac{\beta_2}{2} \quad \text{or} \quad \tan\alpha_2 = \tan\left(\frac{\pi}{2} + \frac{\beta_2}{2}\right)$$

hence,

$$\alpha_2 = \frac{\pi}{2} + \frac{\beta_2}{2}$$

when m is minimum. Substituting this into Eq. (10.13) gives

$$m = \frac{2s\cos\beta_2}{\cos\beta_2 \mp 1}$$

Since the minus sign gives a negative m , the positive sign is chosen. This then gives

$$M_{02\min}^2 = \frac{2s\cos\beta_2}{1+\cos\beta_2} \quad (10.15)$$

Equation (10.9) shows that

$$M_2^2 = \frac{M_{02}^2}{1 - \frac{\gamma-1}{2}M_{02}^2} \quad (10.16)$$

Substituting the value of $M_{02\min}$ from Eq. (10.15) into this gives, after simplification

$$M_{2\min} = \left[\left(\frac{2s_w}{\gamma-1} \right) \frac{\cos\beta_2}{1+(1-s_w)\cos\beta_2} \right]^{1/2} \quad (10.17)$$

The minima for the curves, as seen from Figure 10.7, are at nozzle angles in their usual range between $60^\circ < \alpha_2 < 80^\circ$. For a given M_2 , s_w , and β_2 , there may be two angles α_2 that satisfy Eq. (10.10). The smaller angle is to be chosen. The larger angles put a limit on how large the inlet Mach number can be. As $\alpha_2 \rightarrow 90^\circ$, $\tan \alpha_2 \rightarrow \infty$, and the second of Eqs. (10.11) shows that $m = s$. This means that at $\alpha_2 = 90^\circ$ the inlet Mach number is

$$M_2 = \left[\frac{2s_w}{(\gamma - 1)(2 - s_w)} \right]^{1/2}$$

In particular, for $\gamma = 1.4$ and $s_w = 0.15$, $M_2 = 0.637$, as the graph shows. Figure 10.8 shows how the minimum Mach number depends on the power ratio and that its dependence on the angle β_2 , and correspondingly on α_2 , is weak.

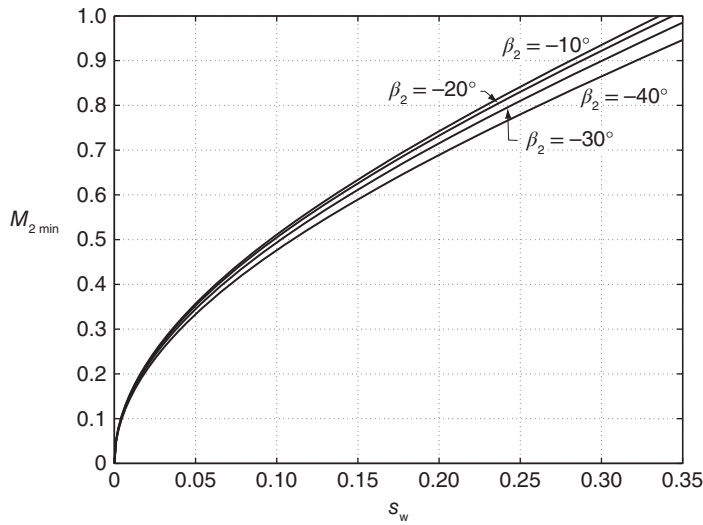


Figure 10.8 Minimum Mach number as a function of the power ratio for $\gamma = 1.4$ with angle β_2 as a parameter.

EXAMPLE 10.7

Gas with $\gamma = 1.4$, and $R = 287 \text{ J/(kg K)}$ flows into a radial inflow turbine. The inlet stagnation temperature is $T_{01} = 1100 \text{ K}$, and the design-specific work is $w = 165.74 \text{ kJ/kg}$. (a) Find the value of the total-to-static efficiency that would give a pressure ratio of $p_{01}/p_3 = 2.0$. (b) At what angle should the flow leave the stator in order for $M_2 = 0.62$ be the minimum possible Mach number at the exit of the stator? (c) Find the blade speed at this condition. (d) Assume that the blade speed is increased to $U_2 = 460 \text{ m/s}$ and that the flow angle and the magnitude of the exit velocity from the stator remain the same. Find the new value for the relative flow angle β_2 entering the rotor.

Solution: (a) From the expression

$$w = s_w c_p T_{01}$$

the power ratio is

$$s_w = \frac{165740}{1004.5 \cdot 1100} = 0.15$$

The pressure ratio is related to the power ratio and the total-to-static efficiency by Eq. (10.3), so that

$$\eta_{ts} = \frac{s_w}{1 - \left(\frac{p_3}{p_{01}}\right)^{(\gamma-1)/\gamma}} = \frac{0.15}{1 - 0.5^{1/3.5}} = 0.835$$

(b) The flow angle at the minimum inlet Mach number is obtained from the equation

$$M_2 = \left[\left(\frac{2s_w}{\gamma - 1} \right) \frac{\cos \beta_2}{1 + (1 - s_w) \cos \beta_2} \right]^{1/2}$$

which, when solved for $\cos \beta_2$, gives

$$\cos \beta_2 = \frac{M_2^2}{2s_w/(\gamma - 1) - (1 - s_w)M_2^2} \quad \beta_2 = -24.74^\circ$$

The minus sign must be chosen for the angle. At the minimum

$$\alpha_2 = \frac{\pi}{2} + \frac{\beta_2}{2} = 90^\circ - 12.37^\circ = 77.63^\circ$$

(c) To determine the blade speed, the velocity leaving the nozzle is needed, and therefore the stagnation Mach number is calculated first as follows:

$$M_{02} = \frac{M_2}{\sqrt{1 + \frac{\gamma - 1}{2} M_2^2}} = \frac{0.62}{\sqrt{1 + 0.2 \cdot 0.62^2}} = 0.5975$$

The exit velocity from the stator is therefore

$$V_2 = M_{02} \sqrt{\gamma R T_{02}} = 0.5975 \sqrt{1.4 \cdot 287 \cdot 1100} = 397.2 \text{ m/s}$$

and the tangential and radial components are

$$V_{u2} = V_2 \sin \alpha_2 = 397.2 \sin(77.63^\circ) = 388.0 \text{ m/s}$$

$$V_{r2} = V_2 \cos \alpha_2 = 397.2 \cos(77.63^\circ) = 85.10 \text{ m/s}$$

The blade speed can be obtained, for example, from

$$U_2 = \frac{w}{V_{u2}} = \frac{165740}{388} = 427.2 \text{ m/s}$$

(d) If the blade speed is increased to $U_2 = 460 \text{ m/s}$ and the nozzle exit speed and direction are the same, then the new work done is

$$w = U_2 V_{u2} = 460 \cdot 388 = 178.48 \text{ kJ/kg}$$

The new value for the tangential component of the relative velocity is

$$W_{u2} = V_{u2} - U_2 = 388.0 - 460.0 = -72.0 \text{ m/s}$$

Since the radial component of the inlet velocity remains the same, the flow angle is

$$\beta_2 = \tan^{-1} \left(\frac{W_{u2}}{W_{r2}} \right) = \tan^{-1} \left(-\frac{72.0}{85.1} \right) = -40.2^\circ$$

It is expected that the total-to-static efficiency will be somewhat lower at this angle. If the efficiency drops greatly, adjustable stator blades may be used to adjust the exit stator angle, which then influences the incidence. However, in a turbocharger, an increase in blade speed comes from a larger cylinder pressure and a larger flow rate through the engine. Hence, the radial component of the inlet velocity to the rotor also increases. The control of the stator blade angle must account for this as well. ■

10.5.2 Blade stagnation Mach number

The blade stagnation Mach number is yet another parameter of interest. It is obtained from the definition of the power ratio, which may be written as

$$\frac{U_2}{c_{01}} \frac{V_{u2}}{c_{01}} = \frac{s_w}{\gamma - 1}$$

so that

$$M_{0u} = \frac{U_2}{c_{01}} = \frac{s_w}{\gamma - 1} \frac{c_{01}}{c_2} \frac{c_2}{V_2 \sin \alpha_2}$$

Since $T_{01} = T_{02}$, this may be written as

$$M_{0u} = \frac{s_w}{\gamma - 1} \frac{1}{M_2 \sin \alpha_2} \sqrt{\frac{T_{02}}{T_2}}$$

and further as

$$M_{0u} = \frac{s_w}{\gamma - 1} \frac{\left(1 + \frac{\gamma - 1}{2} M_2^2 \right)^{1/2}}{M_2 \sin \alpha_2} \quad (10.18)$$

For a given power factor $s_w/(\gamma - 1)$, the relative flow angle β_2 , and Mach number M_2 , Eq. (10.10) can be solved for α_2 and the nondimensional blade speed M_{0u} can be calculated from Eq. (10.18). These results are shown in Figure 10.9. Even if the blade speed is higher than the absolute velocity, the blade stagnation Mach number is based on the larger sonic speed and therefore for large M_2 it does not become as high as the inlet Mach number. This graph is useful when it is linked to the maximum attainable efficiency.

Experimental data for the total-to-static efficiency, measured by Rodgers and Geiser [75], are shown in Figure 10.10. The abscissa in this figure is the ratio of the blade speed to spouting velocity. Since

$$\frac{1}{2} V_0^2 = c_p T_{01} \left(1 - \frac{T_{3ss}}{T_{01}} \right) = c_p T_{01} \frac{s_w}{\eta_{ts}}$$

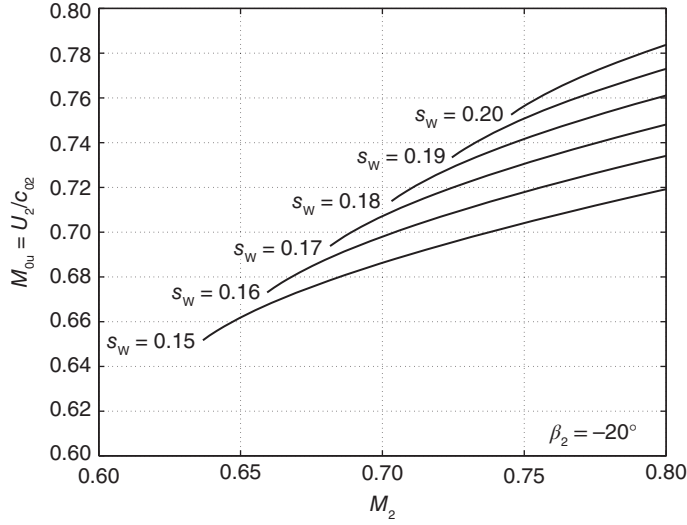


Figure 10.9 Blade stagnation Mach number as a function of M_2 for $\gamma = 1.4$ and for various power ratios and $\beta_2 = -20^\circ$.

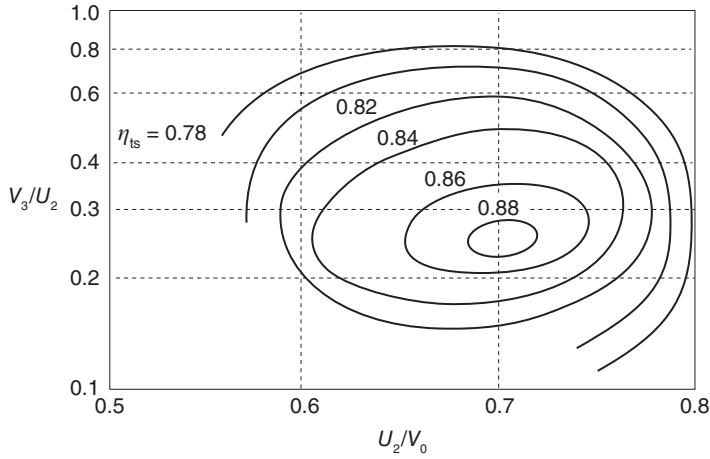


Figure 10.10 Total-to-static efficiency contours. Source: Redrawn from the data of Rodgers and Geiser [75].

the ratio of the spouting velocity to the stagnation speed of sound is

$$\frac{V_0}{c_{01}} = \sqrt{\frac{2s_w}{(\gamma - 1)\eta_{ts}}}$$

hence,

$$M_{0u} = \frac{U_2}{V_0} \sqrt{\frac{2s_w}{(\gamma - 1)\eta_{ts}}}$$

For $\gamma = \frac{4}{3}$, $\eta_{ts} = 0.9$, and $s_w = 0.15$, the factor involving the square root is unity. For values $\eta_{ts} = 0.8$ and $s_w = 0.2$, this equation yields $M_{0u} = 1.22U_2/V_0$. Hence, a turbine

with a reasonably low power ratio and stagnation blade Mach number in the range $0.70 < M_{0u} < 0.75$ operates in the region of highest efficiency. Also, Figure 10.9 shows that under these conditions M_2 is quite high.

10.5.3 Inlet relative Mach number

The inlet relative Mach number can be calculated by first writing the component equations

$$V_2 \sin \alpha_2 = U_2 + W_2 \sin \beta_2 \quad V_2 \cos \alpha_2 = V_2 \cos \beta_2$$

and then squaring and adding them. This yields

$$V_2^2 = U_2^2 + W_2^2 + 2U_2W_2 \sin \beta_2$$

and after each term is divided $c_2^2 = \gamma RT_2$, and the definition $M_u = U_2/c_2$ is substituted, then after rearrangement this reduces to

$$M_{2R}^2 + 2M_u \sin \beta_2 M_{2R} + M_u^2 - M_2^2 = 0$$

The solution of this is

$$M_{2R} = -M_u \sin \beta_2 + \sqrt{M_2^2 - M_u^2 \cos^2 \beta_2}$$

in which the term M_u may be related to M_2 by

$$M_u = M_{0u} \sqrt{\frac{T_{02}}{T_2}} = M_{0u} \left(1 + \frac{\gamma - 1}{2} M_2^2 \right)^{1/2} = \left(\frac{s_w}{\gamma - 1} \right) \frac{1 + \frac{\gamma - 1}{2} M_2^2}{M_2 \sin \alpha_2}$$

because the blade stagnation Mach number M_{0u} is given by Eq. (10.18). These results are plotted in Figure 10.11.

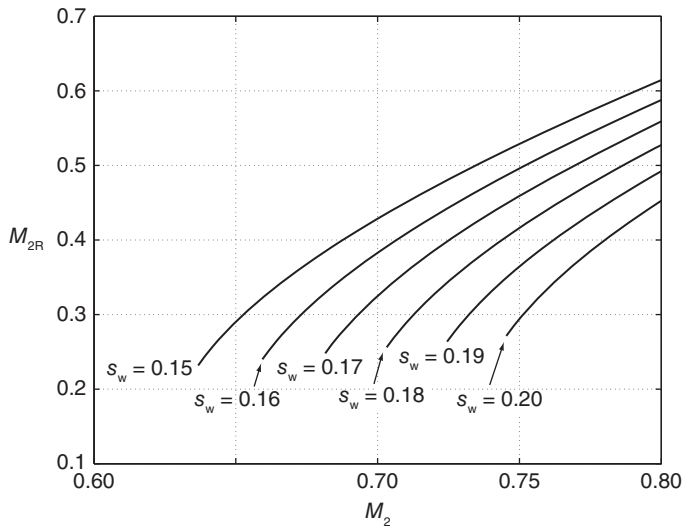


Figure 10.11 The relative inlet Mach number M_{2R} as a function of M_2 for various power ratios and for $\beta_2 = -20^\circ$ and $\gamma = 1.4$.

10.6 DESIGN OF THE EXIT

The blade height at the exit is to be chosen sufficiently large to reduce the relative velocity low enough that the relative Mach number at the shroud does not reach unity. In this section, its value is related to a nondimensional mass flow rate and the exit Mach number. In addition, the optimum angle of the relative flow at the exit is found.

10.6.1 Minimum exit Mach number

If the turbine operates under conditions such that the absolute velocity at the exit is axial, then the mass balance can be written as

$$\dot{m} = \rho_3 V_3 A_3 = \rho_3 V_3 \pi (r_{3s}^2 - r_{3h}^2) = \rho_3 V_3 \pi r_{3s}^2 (1 - \kappa^2)$$

in which $\kappa = r_{3h}/r_{3s}$. This can be changed to

$$\dot{m} = \frac{p_3}{RT_3} M_3 \sqrt{\gamma RT_3} \pi r_{3s}^2 (1 - \kappa^2)$$

Multiplying and dividing the right side by $p_{01} = \rho_{01} RT_{01}$ and introducing the inlet stagnation speed of sound $c_{01}^2 = \gamma RT_{01}$ converts this equation into

$$\dot{m} = \rho_{01} c_{01} \pi r_{3s}^2 (1 - \kappa^2) \frac{p_3}{p_{01}} \left(\frac{T_{01}}{T_3} \right)^{1/2} M_3$$

A form of a flow coefficient may now be defined as

$$\Phi = \frac{\dot{m}}{\rho_{01} c_{01} \pi r_2^2} = \frac{p_3}{p_{01}} \left(\frac{T_{01}}{T_3} \right)^{1/2} M_3 \frac{r_{3s}^2}{r_2^2} (1 - \kappa^2)$$

in which the denominator is large because it is a product of the stagnation density and the speed of sound at the upstream conditions (conditions at which both of these are large) and a fictitious large flow area πr_2^2 . Substituting $U_{3s}/U_2 = r_{3s}/r_2$ into this gives

$$\Phi = \frac{p_3}{p_{01}} \left(\frac{T_{01}}{T_3} \right)^{1/2} M_3 \frac{U_{3s}^2}{U_2^2} (1 - \kappa^2) \quad (10.19)$$

Next, the absolute Mach number at the exit is related to the exit relative Mach number at the shroud of the blade. The relative velocity at the shroud is

$$W_{3s}^2 = V_3^2 + U_{3s}^2$$

Dividing through by U_2^2 leads to the following expression

$$\begin{aligned} \frac{U_{3s}^2}{U_2^2} &= \frac{W_{3s}^2}{U_2^2} - \frac{V_3^2}{U_2^2} \\ &= \frac{W_{3s}^2}{c_3^2} \frac{c_3^2}{c_{01}^2} \frac{c_{01}^2}{U_2^2} - \frac{V_3^2}{c_3^2} \frac{c_3^2}{c_{01}^2} \frac{c_{01}^2}{U_2^2} \\ &= \frac{M_{3Rs}^2}{M_{0u}^2} - \frac{M_3^2}{M_{0u}^2} \frac{T_3}{T_{01}} \end{aligned}$$

Substituting this into Eq. (10.19) leads to

$$\Phi = \frac{p_3}{p_{01}} \left(\frac{T_3}{T_{01}} \right)^{1/2} M_3 \frac{M_{3Rs}^2 - M_3^2}{M_{0u}^2} (1 - \kappa^2)$$

which when solved for M_{3Rs}^2 gives

$$M_{3Rs}^2 = M_3^2 + \frac{\Phi M_{0u}^2}{1 - \kappa^2} \frac{1}{M_3} \left(1 + \frac{\gamma - 1}{2} M_3^2 \right)^{1/2} \left(\frac{p_{01}}{p_3} \right) \left(\frac{T_{01}}{T_{03}} \right)^{1/2}$$

where the pressure ratio and the stagnation temperature ratio are given by

$$\frac{p_{01}}{p_3} = \left(1 - \frac{s_w}{\eta_{ts}} \right)^{-\gamma/(\gamma-1)} \quad \frac{T_{01}}{T_{03}} = \frac{1}{1 - s_w}$$

Defining B as

$$B = \Phi_f \left(1 - \frac{s_w}{\eta_{ts}} \right)^{-\gamma/(\gamma-1)} \frac{1}{\sqrt{1 - s_w}}$$

in which

$$\Phi_f = \Phi M_{0u}^2 / (1 - \kappa^2) \quad (10.20)$$

the relative Mach number at the exit has the form

$$M_{3Rs}^2 = M_3^2 + B \left(\frac{1}{M_3^2} + \frac{\gamma - 1}{2} \right)^{1/2}$$

The minimum value of M_{3Rs}^2 as a function of M_3^2 , with other parameters held fixed, is obtained by differentiation:

$$\frac{dM_{3Rs}^2}{dM_3^2} = 1 - \frac{B}{2M_3^4} \left(\frac{1}{M_3^2} + \frac{\gamma - 1}{2} \right)^{-1/2}$$

Setting this to zero gives the following equation for M_3 ,

$$M_3^8 + \frac{2}{\gamma - 1} M_3^6 - \frac{B^2}{2(\gamma - 1)} = 0$$

This fourth-order polynomial equation in M_3^2 is now numerically solved for M_3^2 , and then M_{3Rs} is determined from

$$M_{3Rs} = \left[M_3^2 + \frac{B}{M_3} \left(1 + \frac{\gamma - 1}{2} M_3^2 \right)^{1/2} \right]^{1/2}$$

The results are shown graphically in Figure 10.12, with the minima of M_{3Rs} marked by small circles. Since the absolute velocity at the exit is axial, it follows that

$$\frac{M_3}{M_{3Rs}} = \frac{V_3}{W_{3s}} = \cos \beta_{3s}$$

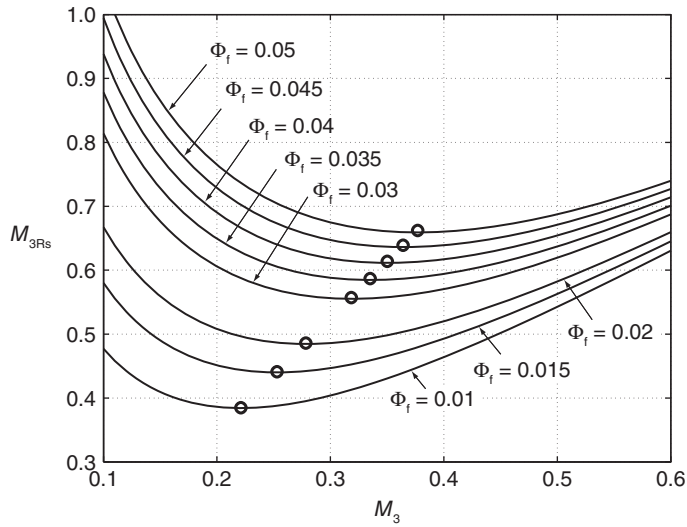


Figure 10.12 Relative Mach number as a function of Mach number, with Φ_f as a parameter. The pressure ratio is $p_{01}/p_3 = 2$, with $\eta_{ts} = 0.85$ and $\gamma = 1.4$. The locations of the minima of M_{3Rs} are marked by circles.

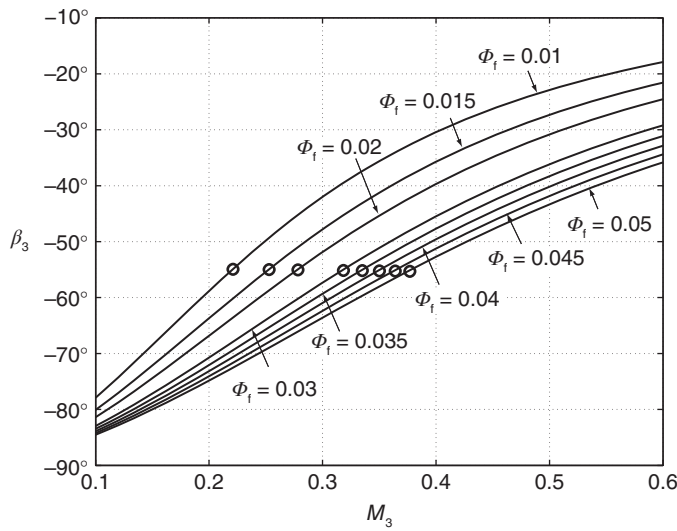


Figure 10.13 The flow angle of the relative velocity at the exit as a function of Mach number, with Φ_f as a parameter. The pressure ratio is $p_{01}/p_3 = 2$, with $\eta_{ts} = 0.85$ and $\gamma = 1.4$. The locations of the angle corresponding to minima of M_{3Rs} are marked by circles.

This equation shows that lines of constant β_{3s} are straight-lines in Figure 10.12. The relative flow angle is plotted in Figure 10.13. It shows that the minimum relative Mach number at the exit occurs when $\beta_3 = -56^\circ$ for $p_{01}/p_3 = 2$ and $\eta_{ts} = 0.85$. Clearly, since the absolute velocity is axial, the Mach number for the absolute flow is less than that for the relative flow.

10.6.2 Radius ratio r_{3s}/r_2

From the exit velocity diagram,

$$\sin |\beta_3| = \frac{U_3}{W_3}$$

This equation applies at every radial location r_3 of the exit, and r_3 now denotes a radius that varies from the hub to the tip. It is assumed that the angle β_3 changes with radius such that the exit velocity V_3 is uniform. With $U_3 = U_2 r_3/r_2$, this may be written as

$$\sin |\beta_3| = \frac{U_2}{W_2} \frac{W_2}{W_3} \frac{r_3}{r_2}$$

Therefore, the radius ratio can be written as

$$\frac{r_3}{r_2} = \frac{W_3}{W_2} \frac{W_2}{U_2} \sin |\beta_3|$$

From the inlet velocity diagram, the tangential components give

$$U_2 = V_2 \sin \alpha_2 - W_2 \sin \beta_2$$

or

$$\frac{U_2}{W_2} = \frac{V_2}{W_2} \sin \alpha_2 - \sin \beta_2$$

From the radial components,

$$V_2 \cos \alpha_2 = W_2 \cos \beta_2 \quad \frac{V_2}{W_2} = \frac{\cos \beta_2}{\cos \alpha_2}$$

Substituting this into the previous expression gives

$$\frac{U_2}{W_2} = \frac{\sin \alpha_2 \cos \beta_2 - \cos \alpha_2 \sin \beta_2}{\cos \alpha_2} = \frac{\sin(\alpha_2 - \beta_2)}{\cos \alpha_2}$$

which is just the law of sines.

The radius ratio may now be written as

$$\frac{r_3}{r_2} = \frac{W_3}{W_2} \frac{\cos \alpha_2 \sin |\beta_3|}{\sin(\alpha_2 - \beta_2)}$$

If the angle β_2 is chosen to be that for a minimum inlet Mach number, then $\beta_2 = 2\alpha_2 - \pi$, and $\sin(\alpha_2 - \beta_2) = \sin \alpha_2$, and this expression reduces to

$$\frac{r_3}{r_2} = \frac{W_3}{W_2} \frac{\sin |\beta_3|}{\tan \alpha_2} \quad (10.21)$$

At the shroud, it is clearly

$$\frac{r_{3s}}{r_2} = \frac{W_{3s}}{W_2} \frac{\sin |\beta_{3s}|}{\tan \alpha_2}$$

Substituting $\alpha_2 = \pi/2 + \beta_2/2$ gives the alternative form

$$\frac{r_{3s}}{r_2} = \frac{W_{3s}}{W_2} \tan \frac{\beta_2}{2} \sin \beta_{3s} \quad (10.22)$$

Rohlik [76] suggested that the relative velocity ratio $W_3/W_2 = 2$ gives a good design, or if the relative velocity at the shroud is used, then $W_{3s}/W_2 = 2.5$ is appropriate [95].

10.6.3 Blade height-to-radius ratio b_2/r_2

The final parameter to be determined is the blade height-to-radius ratio b_2/r_2 at the inlet. By casting the mass balance

$$\dot{m} = \rho_2 V_{r2} A_2 = \rho_3 V_3 A_3$$

in terms of the flow functions, the area ratio becomes

$$\frac{A_3}{A_2} = \frac{F_2 \cos \alpha_3}{F_3} \sqrt{\frac{T_{03}}{T_{02}}} \frac{p_{02}}{p_{03}} = \frac{F_2 \cos \alpha_3}{F_3} \sqrt{\frac{T_{03}}{T_{02}}} \frac{p_{02}}{p_{01}} \frac{p_{01}}{p_3} \frac{p_3}{p_{03}}$$

The stagnation pressure ratio p_{02}/p_{01} is related to the static temperature ratio T_2/T_{2s} by integrating the Gibbs equation along the constant-pressure line p_2 and along the line of constant stagnation temperature $T_{01} = T_{02}$. Equality of entropy changes then gives

$$\frac{p_{02}}{p_{01}} = \left(\frac{T_{2s}}{T_2} \right)^{\gamma/(\gamma-1)}$$

From the definition of the static enthalpy loss coefficient in the stator

$$\zeta_S = \frac{h_2 - h_{2s}}{\frac{1}{2} V_2^2}$$

the relationship

$$\frac{T_{2s}}{T_2} = 1 - \zeta_S \frac{\gamma - 1}{2} M_2^2$$

is obtained. In addition,

$$\frac{T_{03}}{T_{01}} = 1 - s_w \quad \text{and} \quad \frac{p_3}{p_{01}} = \left(1 - \frac{s_w}{\eta_{ts}} \right)^{\gamma/(\gamma-1)}$$

so the area ratio can now be written as

$$\frac{A_3}{A_2} = \frac{F_2 \sin \alpha_2}{F_3} \left(1 - \frac{s_w}{\eta_{ts}} \right)^{-\gamma/(\gamma-1)} \sqrt{1 - s_w} \left(\frac{1 - \zeta_S \frac{\gamma - 1}{2} M_2^2}{1 + \frac{\gamma - 1}{2} M_3^2} \right)^{\gamma/(\gamma-1)} \quad (10.23)$$

The blade height at the inlet is now obtained by writing the reciprocal of the area ratio as

$$\frac{A_2}{A_3} = \frac{2\pi r_2 b_2}{\pi(r_{3s}^2 - r_{3h}^2)} = 2 \left(\frac{r_2}{r_{3s}} \right)^2 \frac{b_2}{r_2} \frac{1}{1 - \kappa^2}$$

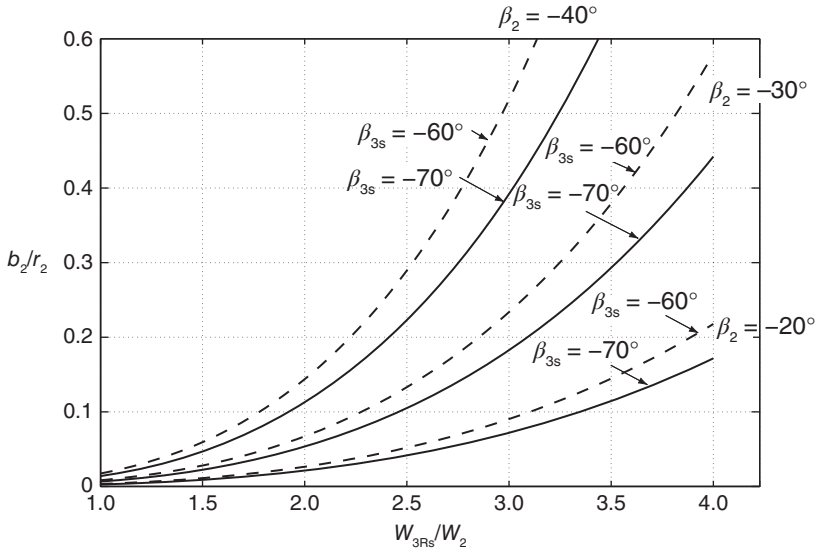


Figure 10.14 Blade width-to-radius ratio as a function of the relative velocity ratio W_{3s}/W_2 for relative flow angles corresponding to minimum Mach number at the inlet and at axial exit. The pressure ratio is $p_{01}/p_3 = 2$, with $\eta_{ts} = 0.85$, $\gamma = 1.4$, and the static enthalpy loss coefficient of the stator is $\zeta_s = 0.15$. The exit hub to shroud radius ratio is $\kappa = 0.2$.

in which $\kappa = r_{3h}/r_{3s}$. Solving for the blade height gives

$$\frac{b_2}{r_2} = \frac{1}{2} \left(\frac{r_{3s}}{r_2} \right)^2 (1 - \kappa_2) \frac{A_2}{A_3}$$

For a radial inflow turbine with a pressure ratio $p_{01}/p_3 = 2$, total-to-static efficiency $\eta_{ts} = 0.85$, the stator static enthalpy loss coefficient $\zeta_s = 0.15$, $\kappa = 0.2$, and $\gamma = 1.4$, the graphs for b_2/r_2 are shown in Figure 10.14. Turbines operated at low power factor have a blade height of about one-fourth the inlet radius r_2 .

10.6.4 Optimum incidence angle and the number of blades

For centrifugal compressors, the Stanitz slip factor was given as

$$\sigma = \frac{V_{u2}}{V'_{u2}} \quad \text{with} \quad \sigma = 1 - \frac{0.63\pi}{Z}$$

in which Z is the number of blades and V'_{u2} is the tangential velocity component in the absence of slip. For radial blades $V'_{u2} = U_2$. Using this expression at the inlet to the rotor gives

$$\frac{V_{u2}}{U_2} = 1 - \frac{0.63\pi}{Z}$$

Since

$$V_{u2} = U_2 + W_{u2} = U_2 + W_{r2} \tan \beta_2 = U_2 + V_{r2} \tan \beta_2 = U_2 + V_{u2} \frac{\tan \beta_2}{\tan \alpha_2}$$

the ratio V_{u2}/U_2 becomes

$$\frac{V_{u2}}{U_2} = \frac{\tan \alpha_2}{\tan \alpha_2 - \tan \beta_2}$$

At the condition of minimum inlet Mach number, at which $\alpha_2 = \pi/2 - \beta_2/2$, this reduces to

$$\frac{V_{u2}}{U_2} = \cos \beta_2$$

Hence, the number of blades is related to the β_2 by

$$\cos \beta_2 = 1 - \frac{0.63\pi}{Z}$$

If this angle corresponds to the optimum nozzle angle for a minimum Mach number at the entry, then the substitution $\beta_2 = 2\alpha_2 - \pi$ gives

$$\cos \alpha_2 = \frac{1}{\sqrt{Z}}$$

This formula for the optimum nozzle angle was developed by Whitfield [94]. The second half of this chapter has been based on his original research on how the rotor blade design might proceed. The optimum angle is plotted in Figure 10.15 along with Glassman's suggestion

$$Z = \frac{\pi}{3}(110 - \alpha_2) \tan \alpha_2$$

These results agree when the number of blades is 13, but the incidence in the Glassman correlation decreases more rapidly as the number of blades increases.

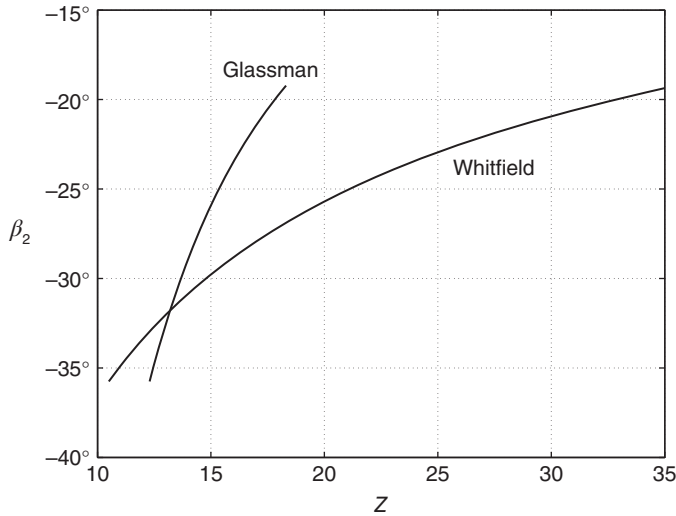


Figure 10.15 Optimum incidence angle β_2 as a function of the number of blades Z according to Glassman [30] and Whitfield [94].

EXAMPLE 10.8

Combustion gases with $\gamma = \frac{4}{3}$ and $R = 287 \text{ J/(kg K)}$ enter the stator of an radial inflow turbine at $T_{01} = 1050 \text{ K}$ and $p_{01} = 250 \text{ kPa}$. The power produced by the turbine is $\dot{W} = 232 \text{ kW}$ at shaft speed of 35000 rpm. The Mach number at the exit of the stator is $M_2 = 0.69$, and the flow angle there is $\alpha_2 = 67^\circ$. The efficiency of the turbine is $\eta_{ts} = 0.89$, and the static enthalpy loss coefficient for the stator is $\zeta_s = 0.15$. There is no swirl in the exit flow, and the design seeks to have the incidence at the inlet to be at angle $\beta_2 = -18.9^\circ$. Find (a) the exit blade radius entering the turbine and (b) the exit static pressure. (c) Given the exit Mach number $M_3 = 0.5$ and a ratio of the hub-to-shroud radius of blade of $\kappa = 0.3$, find the angle of the relative flow at the shroud radius of the exit. Find (d) the ratio W_{3s}/W_2 for the machine and (e) the blade height b_2 at the inlet.

Solution: (a) The stagnation speed of sound at the exit of the stator is

$$c_{01} = \sqrt{\gamma R T_{01}} = \sqrt{1.333 \cdot 287 \cdot 1050} = 633.9 \text{ m/s}$$

and the stagnation Mach number leaving the stator is therefore

$$M_{02} = \frac{M_2}{\sqrt{1 + \frac{\gamma-1}{2} M_2^2}} = \frac{0.69}{\sqrt{1 + \frac{0.69^2}{6}}} = 0.664$$

This gives the velocity leaving the stator the value

$$V_2 = M_{02} c_{01} = 0.664 \cdot 633.9 = 421.0 \text{ m/s}$$

The velocity components are then

$$V_{u2} = V_2 \sin \alpha_2 = 421.0 \sin(67^\circ) = 387.5 \text{ m/s}$$

$$V_{r2} = V_2 \cos \alpha_2 = 421.0 \cos(67^\circ) = 164.5 \text{ m/s}$$

With $W_{r2} = V_{r2}$, the relative velocity is

$$W_2 = \frac{W_{r2}}{\cos \beta_2} = \frac{164.49}{\cos(-18.9^\circ)} = 173.9 \text{ m/s}$$

and its tangential component is

$$W_{u2} = W_2 \sin \beta_2 = 173.9 \cdot \sin(-18.9^\circ) = -56.3 \text{ m/s}$$

The blade speed comes out to be

$$U_2 = V_{u2} - W_{u2} = 387.5 + 56.3 = 443.8 \text{ m/s},$$

and the radius has the value

$$r_2 = \frac{U_2}{\Omega} = \frac{443.8 \cdot 30}{35000 \cdot \pi} = 0.121 \text{ m}$$

(b) The work delivered by the turbine is

$$w = U_2 V_{u2} = 443.8 \cdot 387.5 = 172.00 \text{ kJ/kg}$$

and the stagnation temperature at the exit is therefore,

$$T_{03} = T_{02} - \frac{w}{c_p} = 1050 - \frac{172.00}{1.148} = 900.2 \text{ K}$$

With the total-to-static efficiency $\eta_{ts} = 0.89$, the isentropic work becomes

$$w_s = \frac{w}{\eta_{ts}} = \frac{172.0}{0.89} = 193.26 \text{ kJ/kg}$$

so that the exit static temperature at the end of the isentropic process has the value

$$T_{3ss} = T_{01} - \frac{w_s}{c_p} = 1050 - \frac{193.26}{1.148} = 881.7 \text{ K}$$

and the static pressure at the exit is

$$p_3 = p_{01} \left(\frac{T_{3ss}}{T_{01}} \right)^{\gamma/(\gamma-1)} = 250 \left(\frac{881.7}{1050} \right)^4 = 124.3 \text{ kPa}$$

(c) To calculate the conditions at the shroud, first the mass flow rate is obtained from

$$\dot{m} = \frac{\dot{W}}{w} = \frac{232}{172} = 1.349 \text{ kg/s}$$

and the stagnation density at the inlet is

$$\rho_{01} = \frac{p_{01}}{RT_{01}} = \frac{250000}{287 \cdot 1050} = 0.830 \text{ kg/m}^3$$

Using these, the nondimensional mass flow rate becomes

$$\Phi = \frac{\dot{m}}{\rho_{01} c_{01} \pi r_2^2} = \frac{1.349}{0.830 \cdot 633.9 \cdot \pi \cdot 0.121^2} = 0.0557$$

The stagnation blade Mach number has the value

$$M_u = \frac{U_2}{c_{01}} = \frac{443.8}{633.9} = 0.70$$

which is used to calculate the modified nondimensional flow rate

$$\Phi_f = \frac{\Phi M_u^2}{(1 - \kappa^2)} = \frac{0.0557 \cdot 0.70^2}{1 - 0.09} = 0.030$$

With the exit Mach number $M_3 = 0.5$, the relative shroud Mach number can now be obtained from

$$\begin{aligned} M_{3Rs} &= \left[M_3^2 + \frac{\Phi_f}{M_3} \left(1 + \frac{\gamma-1}{2} M_3^2 \right)^{1/2} \frac{p_{01}}{p_3} \left(\frac{T_{01}}{T_{03}} \right)^{1/2} \right]^{1/2} \\ &= \left[0.5^2 + \frac{0.03}{0.5} \sqrt{1 + \frac{0.5^2}{6}} \frac{250}{124.3} \sqrt{\frac{1050}{900.2}} \right]^{1/2} = 0.619 \end{aligned}$$

The flow angle is therefore

$$\beta_{3s} = -\cos^{-1} \left(\frac{M_3}{M_{3Rs}} \right) = -\cos^{-1} \left(\frac{0.50}{0.619} \right) = -36.1^\circ$$

(d) To calculate the relative velocity at the shroud, the temperature T_3 is needed. It is given by

$$T_3 = \frac{T_{03}}{1 + \frac{\gamma-1}{2} M_3^2} = \frac{900.2}{1 + \frac{0.5^2}{6}} = 864.2 \text{ K}$$

The relative velocity at the shroud is therefore

$$W_{3s} = M_{3Rs} \sqrt{\gamma R T_3} = 0.619 \sqrt{1.333 \cdot 287 \cdot 864.2} = 355.9 \text{ m/s}$$

and the ratio of relative velocities is

$$\frac{W_{3s}}{W_2} = \frac{355.9}{173.86} = 2.05$$

This is in the typical range for good designs.

(e) To determine the blade height at the inlet, the flow areas are calculated next. At the exit, the shroud radius is obtained by first calculating the blade speed there. Its value is

$$U_{3s} = W_{3s} \sin |\beta_{3s}| = 355.9 \sin |36.1^\circ| = 209.7 \text{ m/s}$$

The shroud radius is now obtained as

$$r_{3s} = r_2 \frac{U_{3s}}{U_2} = 0.121 \frac{209.7}{443.8} = 0.0572 \text{ m}$$

The exit area is of size

$$A_3 = \pi(r_{3s}^2 - r_{3h}^2) = \pi r_{3s}^2 (1 - \kappa^2) = \pi \cdot 0.0572^2 (1 - 0.3^2) = 0.00936 \text{ m}^2$$

The flow functions at the inlet and exit of the turbine blade are

$$F_2 = \frac{\gamma M_2}{\sqrt{\gamma-1}} \left(1 + \frac{\gamma-1}{2} M_2^2 \right)^{-(\gamma+1)/(2\gamma-2)} = \frac{4 \cdot 0.69 \sqrt{3}}{3} \left(1 + \frac{0.69^2}{6} \right)^{-3.5} = 1.220$$

$$F_3 = \frac{\gamma M_3}{\sqrt{\gamma-1}} \left(1 + \frac{\gamma-1}{2} M_3^2 \right)^{-(\gamma+1)/(2\gamma-2)} = \frac{4 \cdot 0.5 \sqrt{3}}{3} \left(1 + \frac{0.5^2}{6} \right)^{-3.5} = 1.001$$

The area ratio is now

$$\begin{aligned} \frac{A_3}{A_2} &= \frac{F_2 \cos \alpha_2}{F_3} \sqrt{\frac{T_{03} p_{01}}{T_{01} p_3}} \left(\frac{1 - \zeta_S \frac{\gamma-1}{2} M_2^2}{1 + \frac{\gamma-1}{2} M_3^2} \right)^{\gamma/(\gamma-1)} \\ &= \frac{1.220 \cos 67^\circ}{1.001} \sqrt{\frac{900.2}{1050} \frac{250}{124.3}} \left(\frac{1 - 0.15 \frac{0.69^2}{6}}{1 + \frac{0.5^2}{6}} \right)^4 = 0.718 \end{aligned}$$

so that

$$A_2 = \frac{A_3}{A_3} A_3 = \frac{0.00936}{0.718} = 0.01304 \text{ m}^2$$

and the blade height is

$$b_2 = \frac{A_2}{2\pi r_2} = \frac{0.01304}{2\pi \cdot 0.121} = 0.0171 \text{ m}$$

or $b_2 = 1.71 \text{ cm}$. ■

EXERCISES

10.1 Combustion gases with $\gamma = \frac{4}{3}$ and $c_p = 1148 \text{ J/(kg K)}$, at $T_{01} = 1050 \text{ K}$ and $p_{01} = 220 \text{ kPa}$ enter a turbine with radial blades at the inlet of the rotor. At the exit of the stator $M_2 = 0.9$. The flow leaves the turbine without exit swirl and is diffused to atmospheric pressure at $p_4 = 101.3 \text{ kPa}$. The total-to-total efficiency of the turbine is $\eta_{tt} = 0.89$. Find the stator exit angle. [Ans: 54.3°]

10.2 During a test, air flows through a radial inflow turbine at the rate of $\dot{m} = 0.323 \text{ kg/s}$ when the shaft speed is 55000 rpm . The inlet stagnation temperature is $T_{01} = 1000 \text{ K}$, and the pressure ratio is $p_{01}/p_3 = 2.1$. At the inlet, the blades are radial with the blade radius $r_2 = 6.35 \text{ cm}$. The flow leaves the blades without swirl. Find (a) the spouting velocity, (b) the total-to-static efficiency, and (c) the power delivered. [Ans: (a) 623.5 m/s , (b) 0.688 , (c) 43.2 kW]

10.3 A radial turbine delivers $\dot{W} = 80 \text{ kW}$ as its shaft turns at 44000 rpm . Combustion gases with $\gamma = \frac{4}{3}$ and $c_p = 1148 \text{ J/(kg K)}$ enter the rotor with relative velocity radially inward at radius $r_2 = 8.10 \text{ cm}$. At the exit, the shroud radius is $r_{3s} = 6.00 \text{ cm}$ and at this location $M_{3Rs} = 0.59$. The exit pressure is $p_3 = 101.3 \text{ kPa}$ and exit temperature is $T_3 = 650 \text{ K}$. Find the hub-to-shroud ratio $\kappa = r_{3h}/r_{3s}$ at the exit. [Ans: 0.268]

10.4 Combustion gases with $c_p = 1148 \text{ J/(kg K)}$ and gas constant $R = 287 \text{ J/(kg K)}$ enter the stator of a radial inflow turbine at the stagnation pressure $p_{01} = 205 \text{ kPa}$ and stagnation temperature $T_{01} = 980 \text{ K}$. They enter the rotor at the Mach number $M_2 = 0.8$ and exhaust into the atmosphere at 101.3 kPa . The total-to-total efficiency of the turbine is $\eta_{ts} = 0.83$. Find (a) the angle at which the flow enters the rotor if the angle $\beta_2 = 0$ and also determine the value of U_2 . (b) Repeat part (a) if the angle $\beta_2 = -10^\circ$. [Ans: (a) 56.52° , 388.4 m/s , (b) 51.33° , 414.9 m/s]

10.5 Air enters a radial inflow turbine at $T_{01} = 400 \text{ K}$ and $p_{01} = 200 \text{ kPa}$. The absolute velocity is at an angle $\alpha_2 = 65^\circ$ at the inlet, where the blades are radial. The relative velocity at the exit is axial and the air flows from there to atmosphere at $p_3 = 101.3 \text{ kPa}$. The shaft operates at 30000 rpm and the inlet radius is $r_2 = 10.5 \text{ cm}$. The mean radius at the exit is $r_3 = 5.7 \text{ cm}$. If the power output is $\dot{W} = 75 \text{ kW}$, find the mass flow rate. [Ans: 0.977 kg/s]

10.6 A radial inflow turbine rotor, with rotor inlet radius $r_2 = 9.3 \text{ cm}$ and blade height $b_2 = 1.8 \text{ cm}$, turns at 42000 rpm . Its working fluid is a gas mixture with $c_p = 1148 \text{ J/(kg K)}$ and $\gamma = \frac{4}{3}$. The exhaust pressure is $p_3 = 101.3 \text{ kPa}$, and the total-to-static efficiency is $\eta_{ts} = 0.82$. The nozzle (stator) angle is $\alpha_2 = 67^\circ$, and the velocity coefficient for the flow through the stator is $c_v = 0.96$. The Mach number at the exit of the stator is 0.8 . Find (a) the inlet stagnation pressure to the stator, and (b) the stagnation pressure loss across the stator. [Ans: (a) 237.5 kPa , (b) 8.8 kPa].

10.7 Determine the rotor loss coefficient ζ_R in Example 10.4. Also, show that the volumetric flow rate at the exit is $Q_3 = 0.916 \text{ m}^3/\text{s}$. [Ans: 0.626]

10.8 Gas with $\gamma = \frac{4}{3}$ and $c_p = 1148 \text{ K}/(\text{kg K})$ flows in a radial inflow turbine, in which the inlet stagnation temperature is $T_{01} = 980 \text{ K}$ and the inlet stagnation pressure is $p_{01} = 205.0 \text{ kPa}$. The exit pressure is $p_3 = 101.3 \text{ kPa}$, and the exit temperature is $T_3 = 831.5 \text{ K}$. The stagnation temperature at the exit is $T_{03} = 836.7 \text{ K}$. The pressure at the inlet to the rotor is $T_2 = 901.6 \text{ K}$, and the pressure is $p_2 = 142.3 \text{ kPa}$. The shaft speed is 160000 rpm, and the radius ratio is $r_3/r_2 = 0.57$. Assume that the relative velocity is radial at the inlet and that there is no exit swirl. Find (a) the total-to-static efficiency, (b) the flow angles α_2 and β_3 , and (c) ζ_S and ζ_R . [Ans: (a) 0.905, 72.9°, -64.7°, (c) 0.0903, 0.0914]

10.9 For an exit with no swirl, show that

$$\frac{W_3(r)}{W_2} = \frac{\sin(\alpha_2 - \beta_2)}{\cos \alpha_2} \frac{r_3}{r_2} \sqrt{\frac{r^2}{r_3^2} + \cot^2 \beta_3}$$

in which r is the radius at an arbitrary location of the exit plane of the blade and r_3 and β_3 are the mean values of the exit radius and angle. Show further that at the mean radius

$$\frac{W_3}{W_2} = -\frac{\sin(\alpha_2 - \beta_2)}{\cos \alpha_2 \sin \beta_3} \frac{r_3}{r_2}$$

and plot the angle β_3 for the range $0.53 < r_3/r_2 < 0.65$ when $W_3/W_2 = 2$ and $\alpha_2 = 70^\circ$ and $\beta_2 = -40^\circ$. [Ans: $r_3/r_2 = 0.62$, $\beta_3 = -58.4^\circ$]

10.10 An inexpensive radial inflow turbine has flat radial blades at both the inlet and the exit of the rotor. The shaft speed is 20000 rpm. The radius of the inlet to the rotor is 10 cm, and the mean radius at the exit is 6 cm. The ratio of blade widths is $b_3/b_2 = 1.8$ and the flow angle is $\alpha_{2e} = 75^\circ$. The inlet stagnation temperature is $T_{01} = 420 \text{ K}$ and the exhaust flows into the atmospheric pressure 101.3 kPa. Assume that the gases that flow through the turbine have $\gamma = \frac{4}{3}$ and $c_p = 1148 \text{ J}/(\text{kg K})$ and the velocity coefficient of the nozzle is $c_N = 0.97$ and the rotor loss coefficient is $\zeta_R = 0.5$. (a) If the power output is 10 kW, what is the mass flow rate? Find (b) the static temperature at the exit of the stator and the static temperature at the exit of the rotor, (c) the blade height at the inlet and the exit, (d) the total-to-total efficiency, and the total-to-static efficiency. [Ans: (a) 0.356 kg/s, (b) 399.5 K, 387.2 K, (c) 0.100 m, 0.018 m (d) 0.924, 0.704]

10.11 Combustion gases with $\gamma = \frac{4}{3}$ and $c_p = 1148 \text{ J}/(\text{kg K})$ enter a stator of a radial flow turbine with $T_{01} = 1150 \text{ K}$, $p_{01} = 1300 \text{ kPa}$, and $M_1 = 0.5$, and with a flow rate of $\dot{m} = 5.2 \text{ kg/s}$ and leave with the flow angle $\alpha_{2e} = 72^\circ$. The radius of the inlet is $r_1 = 17.4 \text{ cm}$, the exit from the stator is at $r_{2e} = 15.8 \text{ cm}$, and the inlet to the rotor is at $r_2 = 15.2 \text{ cm}$. The chord of the stator is $c = 4.8 \text{ cm}$, and the width of the channel is $b = 1.2 \text{ cm}$. The rotational speed of the rotor is 31000 rpm and the blade loading coefficient is $\psi = 1.3$. The exit static pressure is $p_3 = 320 \text{ kPa}$. The trailing-edge thickness of the 17 stator vanes can be ignored. Find (a) the total-to-static efficiency of the turbine, (b) the stagnation pressure loss across the stator, and (c) the stagnation pressure loss across the gap. [Ans: (a) 0.811, (b) 6.98 kPa, (c) 4.22 kPa]

10.12 Combustion gases with $c_p = 1148 \text{ J/(kg K)}$ and gas constant $R = 287 \text{ J/(kg K)}$ flow at the rate $\dot{m} = 3.4 \text{ kg/s}$ from a stagnation state with $T_{01} = 1050 \text{ K}$ and $p_{01} = 620 \text{ kPa}$ into a stator. The loss coefficient for the stator and the vaneless space is $\zeta_s = 0.12$. The absolute velocity enters the rotor at angle $\alpha_2 = 71^\circ$, where the blade speed is $U_2 = 450 \text{ m/s}$. The shaft turns at 40000 rpm. The loss coefficient for the rotor is $\zeta_R = 0.4$. The flow leaves the rotor without any swirl at a relative flow angle of $\beta_3 = 60^\circ$. The radius ratio at the exit is $\kappa = 0.44$, and the rotor is designed such that $r_{3h}/r_2 = 0.31$. The flow areas are sized such that the relative velocity ratio is $W_3/W_2 = 1.79$. (a) Find the angle of the relative velocity at the entrance to the rotor and the radial velocity V_{r2} there. (b) Find the stagnation pressure drop across the stator and the rotor. (c). Find the blade height b_2 at the inlet to the rotor. (d) Assuming that the flow after the rotor is decelerated isentropically to the ambient pressure find the total-to-total efficiency η_{tt} . (e) Calculate the ratio V_{r2}/V_{x3} and comment. [Ans: Two possible solutions: First solution: (a) -13.2° , (b) 25.62 kPa, 32.01 kPa, (c) 2.29 cm, (d) 0.850, (e) 1.088, Second solution: (a) -24.8° , (b) 22.08 kPa, 31.86 kPa, (c) 2.36 cm, (d) 0.847, (e) 1.014]

10.13 Rework the previous exercise replacing the condition W_3/W_2 by the condition $V_{r2}/V_{x3} = 1$. Find the value of W_3/W_2 . [Ans: 1.782]

CHAPTER 11

HYDRAULIC TURBINES

Hydroelectric power plants are important providers of electricity in those countries in which there are large rivers or rainy high mountain regions, or both. In the United States, large hydropower installations exist in the western states of Washington, Oregon, Idaho, and Nevada. The Tennessee Valley Authority (TVA) has a large network of dams and hydropower stations in Tennessee and other southeastern states. Smaller plants in New England account for the rest of the installed capacity. In addition to the United States, large hydropower installations exist in Canada, Brazil, Russia, and China. Norway, Switzerland, Sweden, and Iceland obtain a large part of their power needs from hydroelectricity, and Norway in particular exports its excess generation. About 7% of primary energy production and 17% of total electricity generation in the world are obtained by hydropower. Hydropower plants exceeding 30 MW are designated as large plants. Plants with generation from 0.1 to 30 MW fall into a range of small plants, and those with capacity below 0.1 MW are classified as micro-hydropower. Although hydropower is a clean form of energy, its negative aspects relate to blocking of fish migration paths and displacement of populations from valleys that have been cultivated for hundreds of years by local communities.

11.1 HYDROELECTRIC POWER PLANTS

The preliminary design of a power plant begins with the siting analysis, which consists of determining the available flow rate of water and its head. The rate of water flow depends on the season, and for large power plants with high capital costs, dams are used not only

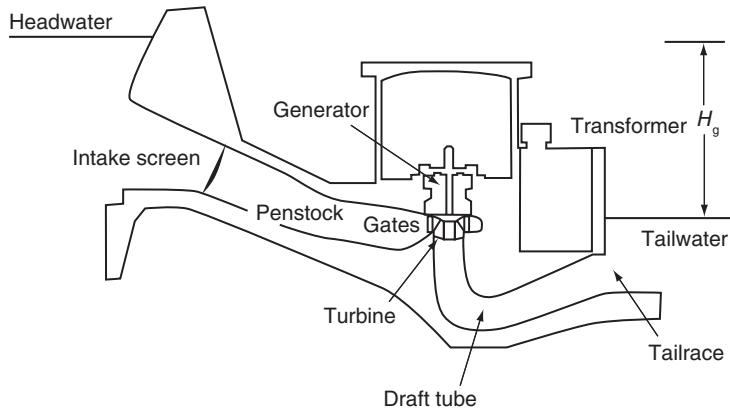


Figure 11.1 Hydroelectric power plant.

to increase the head, but to store water for the dry season. When there is ample water flow, several turbines can be housed in the same plant. For example, in the Three Gorges Dam station in China, there are 32 turbines, each rated at 700 MW, and 2 smaller 50 MW turbines. Similarly the Itaipu power station at the border of Brazil and Paraguay has 20 turbines, each 700 MW.

A schematic of a hydroelectric power plant is shown in Figure 11.1. In small installations with high head, a forebay is included and is made large enough that debris flowing into it will settle to the bottom. The floating debris is caught by an inlet screen. In a large installation, the reservoir formed by an impound dam serves the same purpose. When the waterflow is regulated into the forebay, the head can be held constant and the turbine can be operated at its design condition. From the forebay, the flow passes through a penstock into an inlet volute. After this, the water is directed through a set of adjustable wicket or inlet gates to the runner. From the turbine, the water is discharged into a draft tube and from there through a tailrace to the tailwater reservoir.

The elevation difference between the headwater and tailwater, denoted by H_g , is called the *gross head*. For a control volume with an inlet just below the free surface at the upper reservoir and an exit just below the free surface of the lower reservoir, the pressures at the inlet and exit are both atmospheric. Owing to the size of these reservoirs, the entering and leaving flow velocities are negligibly small. Hence, the energy balance reduces to

$$gH_g = w_s + \sum_i gH_{Li}$$

in which $\sum_i H_{Li}$ is the head loss in the headwater, the penstock, the draft tube, and the exit to the tailwater. If the losses were absent, $w_s = gH_g$ would be the reversible work delivered by the turbine. It is customary, however, to include the spiral volute and the draft tube as part of the turbine and call the difference $H_e = H_g - H_{Lp}$ the *effective head*, in which H_{Lp} represents these losses. Then only the exit kinetic energy from the draft tube is a loss not attributed to the turbine. Efficiency now might be called the *total-to-static efficiency*, but this is not a customary practice. Clearly, the exit kinetic energy loss can be made small by making the draft tube long with a mild increase in area along its length.

In the same way as for centrifugal pumps, the overall efficiency η is given by the product of three terms

$$\eta = \eta_m \eta_v \eta_h$$

in which η_m is the mechanical efficiency and η_v is the volumetric efficiency. The hydraulic efficiency η_h takes into account the various losses in the equipment downstream of the penstock. The overall efficiency can be written as

$$\eta = \frac{\dot{W}_o}{\dot{W}_R} \frac{\dot{W}_R}{\dot{W}} \frac{\dot{W}}{\rho Q g H_e}$$

in which \dot{W}_o is the power delivered by the output shaft, \dot{W}_R is the actual power delivered to the runner, and \dot{W} is the rate at which the water does work on the turbine blades.

The hydraulic efficiency is defined as

$$\eta_h = \frac{\dot{W}}{\rho Q g H_e} = \frac{w}{g H_e}$$

There is some leakage flow that does no work on the turbine blades. For this reason, the power delivered to the runner is

$$\dot{W}_R = \rho(Q - Q_L)w$$

in which Q_L is the volumetric flow rate of the leakage. The ratio

$$\frac{\dot{W}_R}{\dot{W}} = \frac{\rho(Q - Q_L)w}{\rho Q w} = \frac{Q - Q_L}{Q}$$

shows that the volumetric efficiency is also

$$\eta_v = \frac{Q - Q_L}{Q}$$

The mechanical efficiency is defined as the ratio

$$\eta_m = \frac{\dot{W}_o}{\dot{W}_R}$$

and the difference between \dot{W}_R and \dot{W}_o is caused by bearing friction and windage.

11.2 HYDRAULIC TURBINES AND THEIR SPECIFIC SPEED

The operating ranges for the three main types of hydraulic turbines are shown in Figure 11.2. In rivers with large flow rates, Kaplan turbines and Francis turbines are used, and Pelton wheels are the appropriate technology in very mountainous regions. A Pelton wheel is an impulse turbine in which a high-velocity jet impinges on buckets and the flow enters and leaves them at atmospheric pressure. Kaplan turbines are axial machines and handle

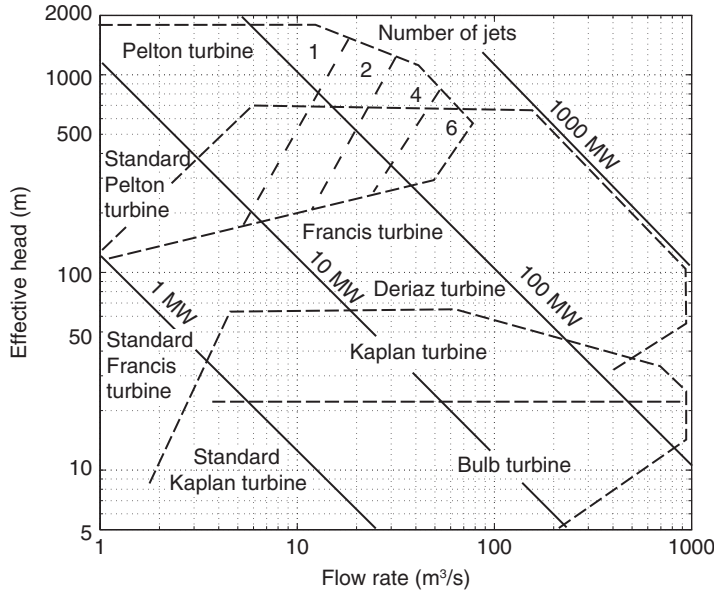


Figure 11.2 Types of hydraulic turbine and their operating ranges. Source: Drawn after charts by Sulzer Hydro Ltd. and Voith Hydro.

large flow rates at relatively low head. They are mounted vertically with the electrical generators on the floor above the turbine bay. A bulb turbine is similar to a Kaplan turbine, but mounted horizontally. It handles even larger flow rates than does a Kaplan turbine at lower head. For Francis turbines, the runner can be designed to accommodate a large variation in flow rates and elevation. A Deriaz turbine is similar to a Kaplan turbine, but with a conical runner. Turbines are classified according to their specific speed, defined as

$$\Omega_s = \frac{\Omega \sqrt{Q}}{(gH_e)^{3/4}}$$

The power specific speed is given by

$$\Omega_{sp} = \frac{\Omega \sqrt{\dot{W}/\rho}}{(gH_e)^{5/4}}$$

Since

$$\dot{W} = \eta \rho Q g H_e$$

the power specific speed reduces to

$$\Omega_{sp} = \frac{\Omega \sqrt{\eta Q}}{(gH_e)^{3/4}}$$

so that $\Omega_{sp} = \sqrt{\eta} \Omega_s$. For a well-designed hydropower station, the overall efficiency at design condition is often greater than 0.9, and for this reason, there is only slight difference between the two forms of specific speed.

Examination of Figure 11.2 shows that in the range where Pelton wheels are appropriate, the increased flow rate at a given head is accomplished by increasing the number of jets. In addition, if the flow rate is sufficient, multiple penstocks and Pelton wheels may be located at the same site. A Pelton wheel with a horizontal shaft may have one or two jets. If the shaft is vertical even six jets can be employed, as shown in Figure 11.3.

The power-specific speeds of various machines are given in Table 11.1, obtained from Nechleba [67, p. 477]. It shows that the specific speed increases as the effective head decreases. Thus, the high-specific-speed Francis runners operate at lower heads. For calculation of the specific speed, the shaft speed is needed. Since hydraulic turbines are used for electricity generation, the shaft speed must be synchronous with the frequency of the electric current. With some exceptions, the frequency f is 50 Hz in Europe and Asia and 60 Hz in North and South America. To match the shaft speed to the proper value for the line frequency, the shaft speed needs to be

$$\Omega = \frac{120f}{P}$$

in which the number of poles in the electric generator is P , which may vary from 2 to 48, and there is no fundamental reason why it could not be even higher. The number 120 is twice the 60 seconds in a minute, and the factor 2 arises from the fact that both ends of a magnet in an electric machine behave similarly. Thus, a generator with 16 poles delivering energy at line frequency 50 Hz needs a turbine shaft speed of 375 rpm according to this formula. This is a typical shaft speed for large turbines.

Table 11.1 Power specific speed ranges of hydraulic turbines.

| Type | Ω_{sp} | η (%) |
|----------------|---------------|------------|
| Pelton wheel | | |
| Single jet | 0.02–0.18 | 88–90 |
| Twin jet | 0.09–0.26 | 89–92 |
| Three jet | 0.10–0.30 | 89–92 |
| Four jet | 0.12–0.36 | 86 |
| Francis | | |
| Low-speed | 0.39–0.65 | 90–92 |
| Medium-speed | 0.65–1.2 | 93 |
| High-speed | 1.2–1.9 | 93–96 |
| Extreme-speed | 1.9–2.3 | 89–91 |
| Kaplan turbine | 1.55–5.17 | 87–94 |
| Bulb turbine | 3–8 | |

11.3 PELTON WHEEL

A Pelton wheel is shown in Figure 11.3. This machine provides an excellent way of producing power if the water reservoir is high. Water from the reservoir flows down a *penstock* and then through a set of nozzles that are directed against *buckets* fastened to a wheel. Penstocks are constructed from steel or reinforced concrete. Early ones were made of wood stave. Pelton wheels have been generally used if the total head is greater than 300 m. There is one installation in Switzerland in which the water head is 1700 m.

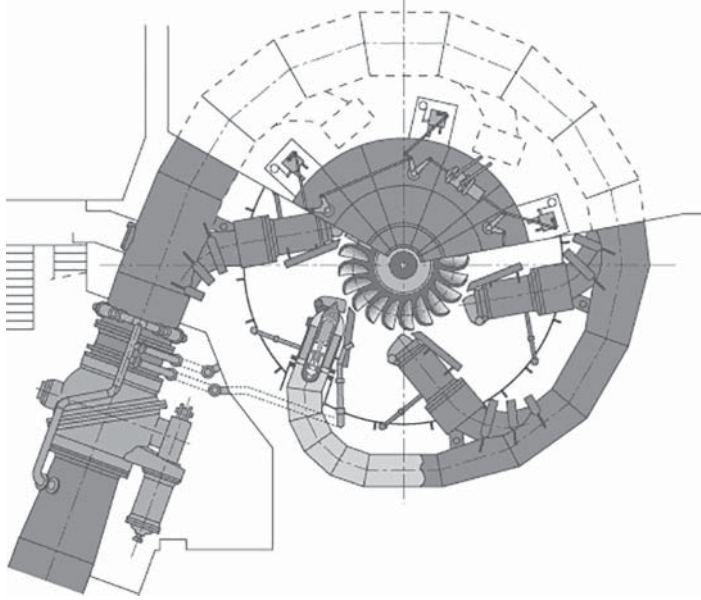


Figure 11.3 A six-jet Pelton wheel. Source: Drawing courtesy Voith Siemens Hydro.

An important advantage of Pelton wheels is that the machine can accommodate water laden with silt, for the erosion damage of the blades is easy to repair.

A Pelton wheel with six jets is shown in Figure 11.3. The number of buckets in the wheel can be calculated by an empirical formula of Tygun (cited by Kadambi and Prasad [51]), namely,

$$Z = \frac{D}{2d} + 15$$

in which D is the wheel diameter and d is the jet diameter. In the analysis of a Pelton wheel, the exit velocity is close to being axial, and therefore, is as small as possible. Generally, the exit losses are ignored. The calculations are illustrated next.

■ EXAMPLE 11.1

A Pelton wheel generates $\dot{W}_o = 1$ MW of power as it operates under the effective head of $H_e = 410$ m and at 395 rpm. Its overall efficiency is $\eta = 0.84$, the nozzle velocity coefficient is $c_N = 0.98$, and the blade speed is $U = 37$ m/s. Find (a) the specific speed and the recommended number of jets, (b) the wheel diameter, the diameter of the jet, as well as the recommended number of blades, and (c) the mechanical efficiency.

Solution: (a) The shaft power

$$\dot{W}_o = \eta \rho Q g H_e$$

solved for the flow rate gives

$$Q = \frac{\dot{W}_o}{\eta \rho g H_e} = \frac{10^6}{0.84 \cdot 1000 \cdot 9.81 \cdot 410} = 0.296 \text{ m}^3/\text{s}$$

and the specific speed comes out to as

$$\Omega_s = \frac{\Omega \sqrt{Q}}{(gH_e)^{3/4}} = \frac{395 \cdot \pi \sqrt{0.296}}{30 \cdot (9.81 \cdot 410)^{3/4}} = 0.0446$$

For this value of specific speed, one jet is sufficient.

(b) The jet velocity is given by

$$V_2 = c_N \sqrt{2gH_e} = 0.98 \sqrt{2 \cdot 9.81 \cdot 410} = 87.90 \text{ m/s}$$

so that the cross sectional area is

$$A = \frac{Q}{V_2} = \frac{0.297}{87.90} = 0.00337 \text{ m}^2$$

and the jet diameter is

$$d = \sqrt{\frac{4A}{\pi}} = \sqrt{\frac{4 \cdot 0.00337}{\pi}} = 0.0655 \text{ m} = 6.55 \text{ cm}$$

The diameter of the wheel is

$$D = \frac{2U}{\Omega} = \frac{2 \cdot 37 \cdot 30}{395 \cdot \pi} = 1.79 \text{ m}$$

and the number of buckets comes out to be

$$Z = \frac{D}{2d} + 15 = \frac{1.79}{2 \cdot 0.0655} + 15 = 28.6 \quad \text{or} \quad Z = 29$$

When using Tygun's formula for calculating the number of buckets, the typical range of diameter ratio $6 < D/d < 28$ gives the range $18 < Z < 29$ for a single wheel.

Consider a Pelton wheel in which the work done by the jet is

$$w = U(V_{u2} - V_{u3})$$

Owing to symmetry, only the stream deflected to the right needs to be analyzed. The inlet and outlet velocity diagrams are shown in Figure 11.4.

The fluid pressure at the inlet and exit is atmospheric, and frictional effects along the blades reduce the relative velocity to $W_3 = c_v W_2$, in which c_v is the velocity coefficient. At the inlet, the flow is entirely tangential and thus $V_{u2} = V_2$ and $W_2 = V_2 - U$. The tangential component at the exit is

$$V_{u3} = U + W_3 \sin \beta_3 = U + c_v W_2 \sin \beta_3$$

Substituting $W_2 = V_2 - U$, gives

$$w = U(V_2 - U)(1 - c_v \sin \beta_3)$$

From this equation, it is clear that the maximum power is obtained for $\beta_3 = -90^\circ$, with other parameters held constant. It is not feasible to construct the buckets with such a large amount of turning, as the water would not clear the wheel. For this reason, in actual installations β_3 is in the neighborhood of -65° . Any water that is partly spilled during the operation does no work on the blades. This spillage is taken into account by the volumetric efficiency.

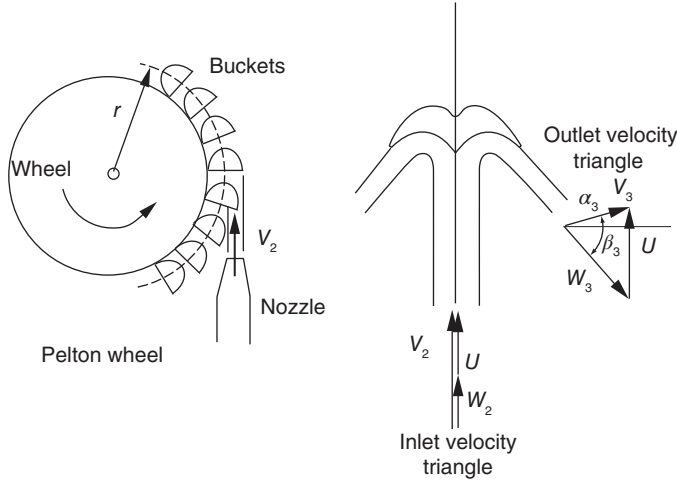


Figure 11.4 Setup for Pelton wheel analysis.

In the expression for the overall efficiency

$$\eta = \eta_h \eta_v \eta_m$$

the hydraulic efficiency can be written as the sum of the nozzle efficiency and the rotor efficiency

$$\eta_h = \eta_N \eta_R$$

in which

$$\eta_N = \frac{V_2^2}{V_0^2}$$

and $V_0 = \sqrt{2gH_e}$ is the spouting velocity. The rotor efficiency is then

$$\eta_R = \frac{w}{\frac{1}{2}V_2^2}$$

The mechanical losses are taken to be proportional to U^2 , with the proportionality constant denoted by K_u . The fluid dynamic losses in turbulent flows are often proportional to the square of the flow velocity, and therefore, the windage losses should have this dependence on the blade speed. Then

$$\eta_m \eta_v = \frac{\dot{W}_o}{\dot{W}} = \frac{\dot{W}_R - \rho Q \frac{1}{2} K_u U^2}{\dot{W}} = \eta_v - \frac{K_u U^2}{2w}$$

Hence,

$$\eta = \eta_h \left(\eta_v - \frac{K_u U^2}{2w} \right) = \left(\eta_v - \frac{K_u U^2}{2w} \right) \frac{w}{gH_e}$$

or

$$\eta = \frac{2\eta_v w}{2gH_e} - \frac{K_u U^2}{2gH_e} = \frac{1}{V_0^2} (2\eta_v w - K_u U^2)$$

Substituting the expression for work into this and replacing V_0 by $V_2/\sqrt{\eta_N}$ gives

$$\eta = \frac{\eta_N}{V_2^2} [2\eta_v U(V_2 - U)(1 - c_v \sin \beta_3) - K_u U^2]$$

This can be written in terms of the ratio of the blade speed to the nozzle velocity $\lambda = U/V_2$, as follows:

$$\eta = \eta_N (2\eta_v \lambda(1 - \lambda)(1 - c_v \sin \beta_3) - K_u \lambda^2)$$

To determine the rotational speed at which the power is maximum, this expression is differentiated with respect to λ while other parameters are held fixed. Setting the result to zero gives

$$\frac{d\eta}{d\lambda} = 2\eta_v(1 - 2\lambda)(1 - c_v \sin \beta_3) - 2K_u \lambda = 0$$

from which

$$\lambda_m = \frac{\eta_v(1 - c_v \sin \beta_3)}{2\eta_v(1 - c_v \sin \beta_3) + K_u}$$

At this value, the maximum efficiency is

$$\eta_{\max} = \frac{\eta_N \eta_v^2 (1 - c_v \sin \beta_3)^2}{2\eta_v(1 - c_v \sin \beta_3) + K_u}$$

If $K_u = 0$, then $\eta_m = 1$, and this reduces to

$$\eta_{\max} = \frac{1}{2} \eta_N \eta_v (1 - c_v \sin \beta_3) = \eta_N \eta_{R \max} \eta_v$$

in which the maximum rotor efficiency is

$$\eta_{R \max} = \frac{1}{2} (1 - c_v \sin \beta_3)$$

The efficiency of the Pelton wheel as a function of the speed ratio $\lambda = U/V_2$ is shown in Figure 11.5.

■ EXAMPLE 11.2

A Pelton wheel operates with a gross head of 530 m and a flow rate of $9 \text{ m}^3/\text{s}$. The penstock length is 400 m, its diameter is 1.5 m. Minor losses increase the equivalent length of the penstock to 630 m. The hydraulic efficiency is $\eta_h = 0.84$, and the shaft speed is 650 rpm. The volumetric and mechanical losses may be neglected. Find (a) the effective head and the power delivered by the turbine if the pipe roughness is 0.7 mm and (b) the specific speed and from it the recommended number of jets and the number of buckets in the wheel. The nozzle coefficient is $c_N = 0.97$, and the ratio of the blade speed to the discharge velocity is $\lambda = U/V_2 = 0.45$.

Solution: (a) The velocity of water in the penstock is

$$V_p = \frac{Q}{A} = \frac{4Q}{\pi D_p^2} = \frac{4 \cdot 9}{\pi \cdot 1.5^2} = 5.1 \text{ m/s}$$

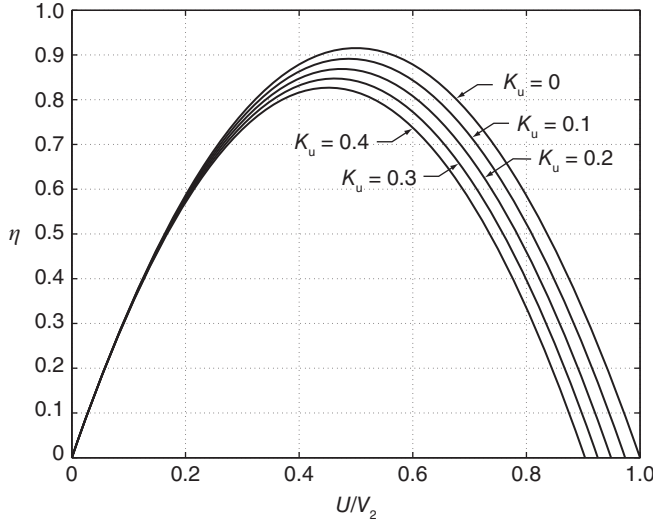


Figure 11.5 Efficiency of a Pelton wheel for various values of the windage loss coefficient.

The Reynolds number is therefore

$$Re = \frac{\rho V_p D_p}{\mu} = \frac{1000 \cdot 5.1 \cdot 1.5}{1.01 \cdot 10^{-3}} = 7.56 \cdot 10^6$$

The Colebrook formula gives the friction factor the value $f = 0.0165$, so that the head loss is

$$H_L = f \frac{L}{D_p} \frac{V_p^2}{2g} = \frac{0.0165 \cdot 630 \cdot 5.1^2}{1.5 \cdot 2 \cdot 9.81} = 9.2 \text{ m}$$

The gross head is measured as the elevation difference between the headwater and the nozzle. Only the upstream losses are included in the calculation of the effective head, and whatever kinetic energy is left after the water is discharged from the wheel is taken into account in the turbine efficiency. Thus, the turbine efficiency is the total-to-static efficiency. The effective head is $H_e = 530 - 9.2 = 520.8 \text{ m}$.

The power delivered, since $\eta = \eta_h$, is

$$\dot{W}_o = \eta \rho Q g H_e = 0.84 \cdot 1000 \cdot 9 \cdot 9.81 \cdot 520.8 = 38.6 \text{ MW}$$

(b) The specific speed comes out to be

$$\Omega_s = \frac{\Omega \sqrt{Q}}{(g H_e)^{3/4}} = \frac{650 \cdot \pi \sqrt{9}}{30 \cdot (9.81 \cdot 520.8)^{3/4}} = 0.338$$

The recommended number of jets is four. Hence, the discharge from each jet is $Q_j = 2.25 \text{ m}^3/\text{s}$. By calculating the discharge velocity as

$$V_2 = c_N \sqrt{2g H_e} = 0.97 \sqrt{2 \cdot 9.81 \cdot 520.8} = 98.05 \text{ m/s},$$

the nozzle diameter can be determined to be

$$d = \sqrt{\frac{4Q_j}{\pi V_2}} = \sqrt{\frac{4 \cdot 2.25}{\pi \cdot 98.05}} = 0.171 \text{ m}$$

and the blade speed is $U = 0.45V_2 = 44.1 \text{ m/s}$. Therefore, the diameter of the wheel is

$$D = \frac{2U}{\Omega} = \frac{2 \cdot 44.1 \cdot 30}{650 \cdot \pi} = 1.3 \text{ m}$$

and the number of buckets is

$$Z = \frac{D}{2d} + 15 = \frac{130}{2 \cdot 17.1} + 15 = 18.8 \quad \text{or} \quad Z = 19$$

EXAMPLE 11.3

A Pelton wheel operates with an effective head of 310 m producing 15 MW of power. The overall efficiency of the turbine is $\eta = 0.84$, the velocity coefficient of the nozzle is $c_N = 0.98$, and the velocity coefficient of the rotor is $c_v = 0.85$. The angle of the relative velocity leaving the rotor is $\beta_3 = -73^\circ$. The wheel rotates at 500 rpm, and the ratio of the blade speed to nozzle velocity is 0.46. (a) Give a recommended number of jets to which the supply flow should be split and the number of blades on the wheel. (b) Find the mechanical and volumetric efficiencies given the value of $K_u = 0.05$. (c) Find also the optimum speed ratio.

Solution: (a) The volumetric flow rate can be calculated from

$$\dot{W}_o = \eta \rho Q g H_e$$

which gives

$$Q = \frac{\dot{W}_o}{\eta \rho g H_e} = \frac{15 \cdot 10^6}{0.84 \cdot 1000 \cdot 9.81 \cdot 310} = 5.87 \text{ m}^3/\text{s}$$

The spouting velocity is

$$V_0 = \sqrt{2gH_e} = \sqrt{2 \cdot 9.81 \cdot 310} = 78.0 \text{ m/s}$$

so that the nozzle velocity comes out as

$$V_2 = c_N V_0 = 0.98 \cdot 78.0 = 76.43 \text{ m/s}$$

The blade speed is therefore $U = \lambda V_2 = 0.46 \cdot 76.43 = 35.16 \text{ m/s}$. With the specific speed equal to

$$\Omega_s = \frac{\Omega \sqrt{Q}}{(gH_e)^{3/4}} = \frac{500 \cdot \pi \sqrt{5.87}}{30 \cdot (9.81 \cdot 310)^{3/4}} = 0.310$$

the suitable number of jets is $N = 4$. The flow rate from each jet is therefore $Q_j = Q/N = 1.47 \text{ m}^3/\text{s}$, and for this flow rate and velocity, the nozzle diameter is

$$d = \sqrt{\frac{4Q_j}{\pi V_2}} = \sqrt{\frac{4 \cdot 1.47}{\pi \cdot 76.43}} = 0.156 \text{ m} = 15.6 \text{ cm}$$

The wheel diameter is

$$D = \frac{2U}{\Omega} = \frac{2 \cdot 35.15 \cdot 30}{500 \cdot \pi} = 1.343 \text{ m}$$

so that the recommended number of buckets on the wheel is

$$Z = \frac{D}{2d} + 15 = \frac{134.3}{2 \cdot 15.6} + 15 = 19.3 \quad \text{or} \quad Z = 20$$

(b) The specific work done by the jet on the rotor is

$$\begin{aligned} w &= U(V_2 - U)(1 - c_v \sin \beta_3) \\ &= 35.16(76.43 - 35.16)(1 - 0.85 \sin(-73^\circ)) = 2630.4 \text{ J/kg} \end{aligned}$$

The nozzle efficiency and rotor efficiencies are

$$\eta_N = c_N^2 = 0.98^2 = 0.960 \quad \eta_R = \frac{w}{\frac{1}{2}V_2^2} = \frac{2 \cdot 2630.6}{76.43^2} = 0.901$$

Hence, the hydraulic efficiency is $\eta_h = \eta_N \eta_R = 0.960 \cdot 0.901 = 0.865$. The mechanical efficiency is obtained from

$$\eta_m = 1 - \frac{K_u U^2}{2\eta_v w}$$

Solving for η_v from

$$\eta = \eta_h \eta_v \eta_m \quad \text{gives} \quad \eta_v = \frac{\eta}{\eta_h \eta_m}$$

and substituting this into the previous equation leads to

$$\eta_m = 1 - \frac{K_u U^2 \eta_h \eta_m}{2\eta w}$$

which when solved for η_m results in

$$\eta_m = \left(1 + \frac{K_u U^2 \eta_h}{2\eta w}\right)^{-1} = \left(1 + \frac{0.05 \cdot 35.16^2 \cdot 0.865}{2 \cdot 0.84 \cdot 2630.4}\right)^{-1} = 0.988$$

The volumetric efficiency is therefore

$$\eta_v = \frac{\eta}{\eta_h \eta_m} = \frac{0.84}{0.865 \cdot 0.988} = 0.983$$

The optimum speed ratio is

$$\begin{aligned}\lambda_{\text{opt}} &= \frac{\eta_v(1 - c_v \sin \beta_3)}{2\eta_v(1 - c_v \sin \beta_3) + K_u} \\ &= \frac{0.983(1 - 0.85 \sin(-73^\circ))}{2 \cdot 0.983(1 - 0.85 \sin(-73^\circ)) + 0.05} = 0.487\end{aligned}$$

11.4 FRANCIS TURBINE

A schematic of a Francis turbine is shown in Figure 11.6. It is a radial inward turbine similar in principle to the radial turbine discussed in Chapter 10. The flow enters the turbine through a set of adjustable inlet guide vanes, located downstream of a spiral volute and a penstock. The spiral volute is absent in Figure 11.1. Both the volute and the penstock may be absent if the head is low, but the flow capacity is large. In that case, the turbine can be placed into a pit. The shape of the draft tube is conical with a straight axis. An alternative is to curve the axis as is shown in Figure 11.1. This way, the draft tube can be longer and the diffusion milder over its length.

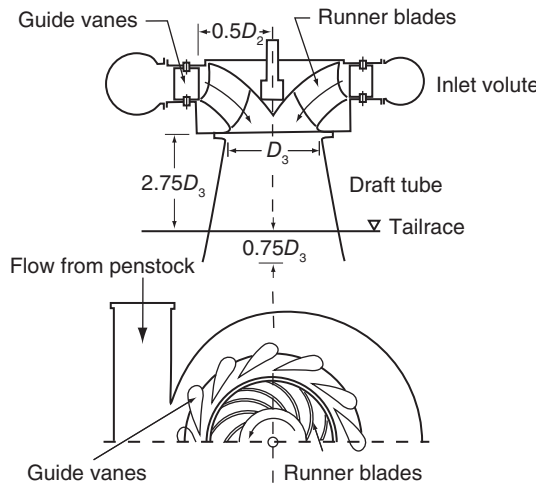


Figure 11.6 Francis turbine.

The shape of the runner depends on the specific speed and thus on the flow rate and the effective head, with a low speed-runner having radial inlet and outlet. As the specific speed increases, the flow is turned such that it leaves in the axial direction. These modifications are illustrated in Figure 11.7.

The flow leaves a low-specific-speed runner in a radial direction, and it receives no further guidance from the blades as it turns toward the axial direction and then enters the draft tube. When the flow rate increases, the velocity in this turning region also increases, and in order to reduce it, the flow must be guided into the axial direction by properly shaped blades. The blade design aims to reduce the tangential component of the velocity to zero.

For a given flow rate and effective head, Figure 11.2 is a guide to what kind of turbine is best suited to the proposed power plant site. There is some latitude in the choices.

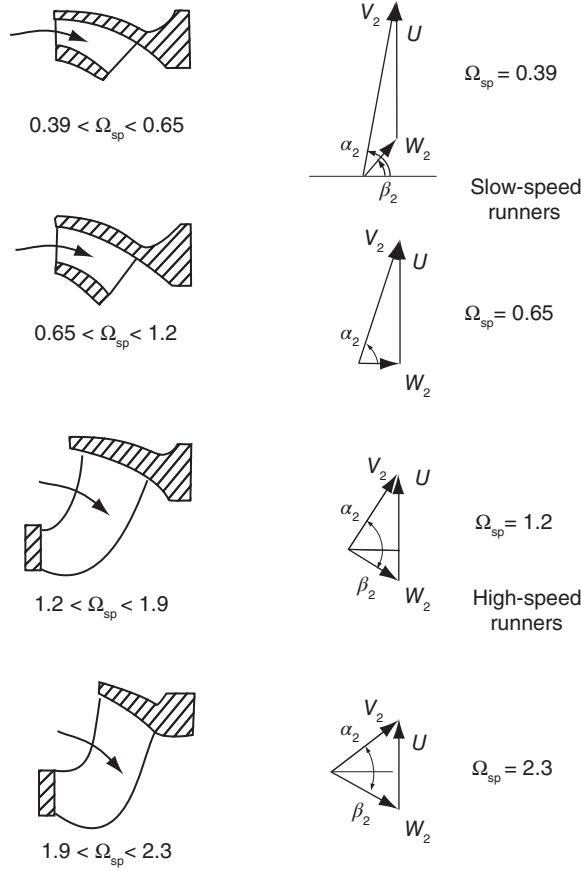


Figure 11.7 Shapes of Francis turbine runners.

The axes in the figure are in terms of extensive properties and, as usual, an engineering design proceeds also in terms of not only intensive properties but, if possible, in terms of nondimensional parameters. The specific speed is one of them. The other is the specific diameter, defined by

$$D_s = \frac{D_2 (gH_e)^{1/4}}{\sqrt{Q}}$$

The loading coefficient, ψ_d and the flow coefficient ϕ_d , defined as

$$\psi_d = \frac{gH_e}{\Omega^2 D_2^2} \quad \phi_d = \frac{Q}{\Omega D_2^3}$$

can be related to the specific speed and the specific diameter. It is readily shown that

$$\psi_d = \frac{1}{\Omega_s^2 D_s^2} \quad \phi_d = \frac{1}{\Omega_s D_s^3}$$

The ratio of the blade speed to the spouting velocity $V_0 = \sqrt{2gH_e}$ is

$$\frac{U_2}{V_0} = \frac{\Omega D_2}{2\sqrt{2gH_e}} = \frac{1}{\sqrt{8}} \Omega_s D_s = \frac{1}{\sqrt{8\psi_d}}$$

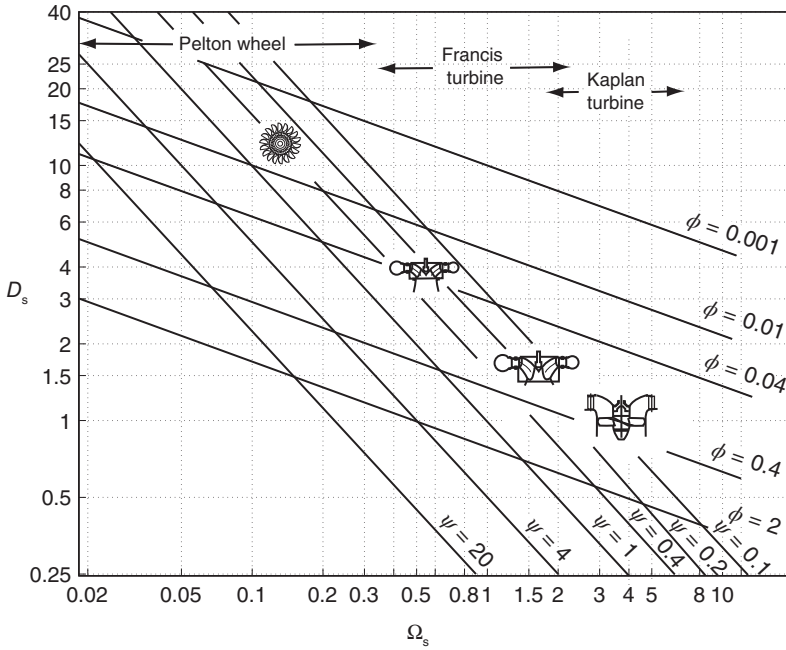


Figure 11.8 Specification map of hydraulic turbines. (See also the Cordier diagram, Figure 5.10.)

Balje [5] gives the locus of maximum efficiency that tends to be in the range $0.6 < U_2/V_0 < 1.1$. This is equivalent to $0.1 < \psi_d < 0.35$, with Francis turbines in the high end of this range for ψ_d and Kaplan turbines in the low end. Figure 11.8 is a plot with specific speed on the abscissa and specific diameter on the ordinate, with some lines of constant loading and flow coefficient added. The figures of different runners are placed close to where their efficiency is the highest. Pelton wheels with multiple jets are not shown.

The flow angles shown for the different runners in Figure 11.7 can be calculated by noting that

$$\tan \alpha_2 = \frac{V_{u2}}{V_{r2}} = \frac{U_2 V_{u2}}{U_2 V_{r2}} = \frac{w}{U_2 V_{r2}}$$

and since $Q = \pi D_2 b_2 V_{r2}$, and $w = \eta_h g H_e$, this can be written as

$$\tan \alpha_2 = \frac{\eta_h g H_e \pi D_2 b_2}{U_2 Q}$$

From the definition of the specific speed, the ratio

$$\frac{g H_e}{Q} = \frac{\Omega^2}{\Omega_s^2 \sqrt{g H_e}}$$

follows immediately, and with $\Omega = 2U_2/D_2$ and $V_0 = \sqrt{2gH_e}$, the formula for the tangent of α_2 can further be written as

$$\tan \alpha_2 = \frac{4\eta_h \sqrt{2\pi} b_r}{\Omega_s^2} \frac{U_2}{V_0}$$

in which the ratio $b_r = b/D_2$ appears. A graph of this ratio appears in the book by Nechleba [[67], p. 100]. A quadratic curve fit over the range of the power-specific speeds for Francis turbines gives

$$b_r = -0.0505\Omega_{sp}^2 + 0.26\Omega_{sp} + 0.018 \quad (11.1)$$

In addition, the formula

$$\frac{U_2}{V_0} = 0.74\Omega_{sp}^{0.238} \quad (11.2)$$

can be used to relate the range

$$0.60 < \frac{U_2}{V_0} < 0.90$$

for which the efficiency is near the maximum to the range of specific speeds for Francis turbines

$$0.39 < \Omega_s < 2.3$$

This range for the speed ratio, given by Daugherty [20, p. 394], is in agreement with that obtained from the graphs of Balje [5], mentioned above. The results of the calculations are shown in the Table 11.2. For these, the hydraulic efficiency was taken to have the constant value $\eta_h = 0.9$, and for simplicity, the mechanical and volumetric losses were neglected.

Table 11.2 Flow angles for various power-specific speeds
for a Francis turbine of hydraulic efficiency $\eta_h = 0.9$.

| Ω_{sp} | b_r | U/V_0 | α_2 | β_2 |
|---------------|-------|---------|------------|-----------|
| 0.39 | 0.11 | 0.59 | 80.0° | 49.5° |
| 0.65 | 0.17 | 0.67 | 73.8° | −2.9° |
| 1.20 | 0.26 | 0.77 | 61.1° | −33.3° |
| 1.90 | 0.33 | 0.86 | 46.0° | −35.8° |
| 2.30 | 0.35 | 0.90 | 38.0° | −34.0° |

The angle β_2 can be determined from the exit velocity diagram, which yields

$$\tan \beta_2 = \frac{\sin \alpha_2 - U_2/V_2}{\cos \alpha_2}$$

and it is easy to show that the ratio U_2/V_2 is

$$\frac{U_2}{V_2} = \frac{\Omega_{sp}^4}{(4\pi b_r)^2 \eta_h^5} \tan^2 \alpha_2 \sin \alpha_2$$

For low-specific-speed runners, the flow angle α_2 is quite large and the angle β_2 at first drops quite quickly as Ω_{sp} increases, but then it settles to a value around -35° for the high-speed runners.

It may be of some interest to relate also the degree of reaction to the specific speed, as well as the blade loading coefficient. Here, the formulas simplify substantially if another definition of reaction ratio is used; namely the change in enthalpy across the runner to the change is stagnation enthalpy across the entire machine. The two are the same for a

repeated stage of axial machines, in which case $V_1 = V_3$. This alternative definition of reaction ratio is thus given by

$$R_t = \frac{h_2 - h_3}{h_{01} - h_{03}} = \frac{h_{02} - h_{03} - \frac{1}{2}(V_2^2 - V_3^2)}{h_{01} - h_{03}}$$

Since $h_{01} = h_{02}$ and $w = h_{02} - h_{03}$, this may be written as

$$R_t = 1 - \frac{V_2^2 - V_3^2}{2w}$$

But $V_2^2 = V_{x2}^2 + V_{u2}^2$ and if there is no exit swirl, $V_3^2 = V_{m3}^2$. Assuming next, as discussed by Dick [23], that the meridional components are approximately equal: i.e. $V_{x2} \approx V_{m3}$, then

$$1 - R_t = \frac{V_{u2}^2}{2U_2 V_{u2}} = \frac{V_{u2}}{2U_2}$$

Since the blade loading coefficient is

$$\psi = \frac{w}{U_2^2} = \frac{V_{u2} U_2}{U_2^2} = \frac{V_{u2}}{U_2}$$

it follows that

$$1 - R_t = \frac{\psi}{2}$$

The speed ratio can then be written as

$$\lambda = \frac{U_2}{V_0} = \frac{U_2}{\sqrt{2gH_e}} = \frac{\sqrt{\eta}}{\sqrt{2\psi}} = \frac{\sqrt{\eta}}{2\sqrt{1 - R_t}}$$

This equated to and Eq. (11.2) gives then a semi-empirical relationship between the reaction and the specific speed. It shows that the specific speed increases as the reaction ratio increases.

The specific speed, the speed ratio, reaction, and blade height to diameter ratio are nondimensional parameters, but to determine them, the head, the volumetric flow rate, and the rotational speed of the shaft are needed. Typically, the head is known and suitable power is chosen based on either the available flow rate, or how many turbines are needed if the flow cannot be accommodated with a single turbine. There exist empirical relations that relate the specific speed to the effective head. One such equation by Morozov (cited by Nechleba [67, p. 80]) can be written as

$$\Omega_{sp} = 0.82 \left(\frac{H_r}{H_e} \right)^{0.57}$$

in which $H_r = 100$ m has been chosen as a reference head. Similarly, by gathering data from a large number of installations, Lugaresi and Massa [60] carried out a statistical analysis and developed the correlation

$$\Omega_s = 1.14 \left(\frac{H_r}{H_e} \right)^{0.512}$$

The reference head is again $H_r = 100$ m. This correlation is based on the specific speed rather than power-specific speed, and is to be preferred over the proposal of Morozov, as it is based on a more recent and larger set of turbines. It is important to note that these correlations are to be used as a guide, for turbine manufacturers has its own design manual that is based on designs that have been improved over many years. The use of the correlations is illustrated next.

■ EXAMPLE 11.4

A Francis turbine is contemplated for a small power plant with an effective head of 220 m and capacity of $1.9 \text{ m}^3/\text{s}$. The anticipated overall efficiency is $\eta = 0.94$. Neglect mechanical and volumetric losses. (a) Determine the power delivered by the turbine. (b) What is your recommendation for the shaft speed if the electric line frequency is 60 Hz? (c) What should the diameter D_2 of the runner be, and what is the tip speed of the blade?

Solution: (a) The power can be calculated readily as

$$\dot{W}_o = \eta \rho Q g H_e = 0.94 \cdot 1000 \cdot 1.9 \cdot 9.81 \cdot 220 = 3.85 \text{ MW}$$

(b) Examination of Figure 11.2 shows that a single-jet Pelton wheel and a Francis wheel are suitable for the site. It is therefore anticipated that a Francis turbine of low-specific speed is a reasonable choice. Using the correlation for specific speed in terms of the effective head gives

$$\Omega_s = 1.14 \left(\frac{100}{220} \right)^{0.512} = 0.7614$$

and then from the definition of the specific speed, the shaft speed can be determined to be

$$\Omega = \frac{\Omega_s (g H_e)^{3/4}}{\sqrt{Q}} = \frac{0.7614 (9.81 \cdot 220)^{3/4} 30}{\pi \sqrt{1.9}} = 1670 \text{ rpm}$$

If the shaft speed is taken to be 1800 rpm, then the number of poles in the generator is

$$P = \frac{120f}{\Omega} = \frac{120 \cdot 60}{1800} = 4$$

(c) With this shaft speed, the specific speed is

$$\Omega_s = \frac{\Omega \sqrt{Q}}{(g H_e)^{3/4}} = \frac{1800 \cdot \pi \sqrt{1.9}}{30 \cdot (9.81 \cdot 220)^{3/4}} = 0.821$$

and the power-specific speed is $\Omega_{sp} = \sqrt{\eta} \Omega_s = \sqrt{0.94} 0.821 = 0.796$. The velocity ratio is

$$\frac{U_2}{V_0} = 0.74 \Omega_{sp}^{0.238} = 0.701$$

The specific diameter can then be calculated from

$$D_s = \frac{\sqrt{8} U_2 / V_0}{\Omega_s} = \frac{0.701 \cdot \sqrt{8}}{0.821} = 2.415,$$

and the diameter is

$$D_2 = \frac{D_s \sqrt{Q}}{(gH_e)^{1/4}} = \frac{2.415 \sqrt{1.9}}{(9.81 \cdot 220)^{1/4}} = 0.488 \text{ m}$$

The blade speed is therefore $U_2 = D_2 \Omega / 2 = 46.0 \text{ m/s}$. ■

To obtain more accurate results, the volumetric flow rate at the inlet to the runner can be calculated from

$$Q = \left(\pi D_2 - \frac{Zt}{\cos \beta_2} \right) b_2 W_{r2}$$

in which t is the blade thickness, Z is the number of blades, and W_{r2} is the radial component of the relative velocity with the flow angle β_2 , at the inlet. The number of blades can be taken to be between $Z = 11V_0/U_2$ and $Z = 13V_0/U_2$, which for the typical range of U_2/V_0 comes close to 16 blades. The runner in Figure 11.9 has 17 blades, which is appropriately a prime number to prevent some resonance vibrations.



Figure 11.9 Francis turbine viewed from downstream.

As the flow enters the draft tube, the axial velocity V_{x3} can be obtained from the expression for the volumetric flow rate, which is

$$Q = \frac{\pi D_3^2}{4} V_{x3} \quad (11.3)$$

It is assumed that the flow enters without swirl so that $V_{x3} = V_3$. For the conical draft tube shown in Figure 11.6, the length of the tube is 2.5–3 times the diameter D_3 and its submerged length into the tailwater ranges from $0.5D_3$ to D_3 . Since the function of the draft tube is to diffuse the flow, its flare must be kept small enough to prevent separation.

The diffuser efficiency is defined as

$$\eta_d = 1 - \frac{2gH_d}{V_3^2 - V_4^2} = 1 - \frac{2gH_d/V_3^2}{1 - A_3^2/A_4^2}$$

in which H_d is the head loss in the diffuser. For a conical diffuser, the peak efficiency is at the cone angle $2\theta = 6^\circ$ and has a value of about $\eta_{d \max} = 0.9$. Defining the loss coefficient K_d via the equation

$$H_d = K_d \frac{V_3^2}{2g}$$

it is readily seen that it can be expressed in terms of the diffuser efficiency as

$$K_d = (1 - \eta_d) \left(1 - \frac{A_3^2}{A_4^2} \right)$$

Since all the kinetic energy leaving the draft tube is dissipated in the tailwater pool, the exit loss is

$$H_e = \frac{V_4^2}{2g} = \frac{V_4^2}{V_3^2} \frac{V_3^2}{2g} = \frac{A_3^2}{A_4^4} \frac{V_3^2}{2g}$$

so that the loss coefficient based on the velocity V_3 is

$$K_e = \frac{A_3^2}{A_4^2}$$

The draft tube and exit loss coefficients and their sum are shown as a function of the ratio A_4/A_3 in Figure 11.10. If the inlet and exit diameters D_3 and D_4 are known, so is the area ratio, and the inlet velocity V_3 to the draft tube is determined from Eq. (11.3). These then give a way to calculate the head loss in the draft tube. The true reversible work is given by

$$w_s = g \left(H_e - H_d - \frac{V_4^2}{2g} \right)$$

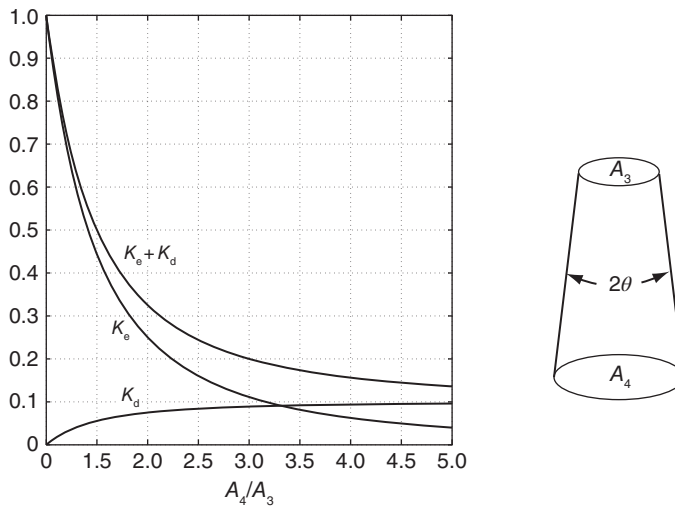


Figure 11.10 Loss coefficients for a draft tube.

which can then be compared to the actual work so that the true efficiency of the turbine can be determined.

11.5 KAPLAN TURBINE

A Kaplan turbine is shown in Figure 11.11. It is an axial-flow turbine suitable for large installations, and it generally operates under a head ranging from 20 to 70 m. The guide vanes are similarly adjustable as in a Francis turbine. Its runner is a propeller type, typically having 3–6 blades, but for smaller flow rates, the number may reach 10. Each blade can be adjusted to the proper flow conditions by rotating it about its axis. This makes the power plant perform well also at off-design flow rates. In a typical installation the runner, turning at 120 rpm, might have a blade with 1 m hub radius and 3 m tip radius, with a volumetric flow rate of $200 \text{ m}^3/\text{s}$ through a turbine. One such a turbine produces around 74.5 MW of power.

A bulb turbine is similar to a Kaplan turbine but with a horizontal axis. A power plant based on a bulb turbine can be constructed at a lower cost than one with a Kaplan turbine. It can be used at low heads of 4–10 m when the speed of the flow is increased by proper design of the inlet channel. The design output power ranges between 100 kW and 50 MW for blade diameters between 0.8 and 8.4 m.

As the flow moves through the axial turbine, its relative velocity is turned only moderately and by differing amounts at the hub and the tip of the blade. The blades extend over a considerable distance, and the local velocity of the blade $U = r\Omega$ increases outward. For this reason, for shockless entry, the absolute value of the blade angle must increase

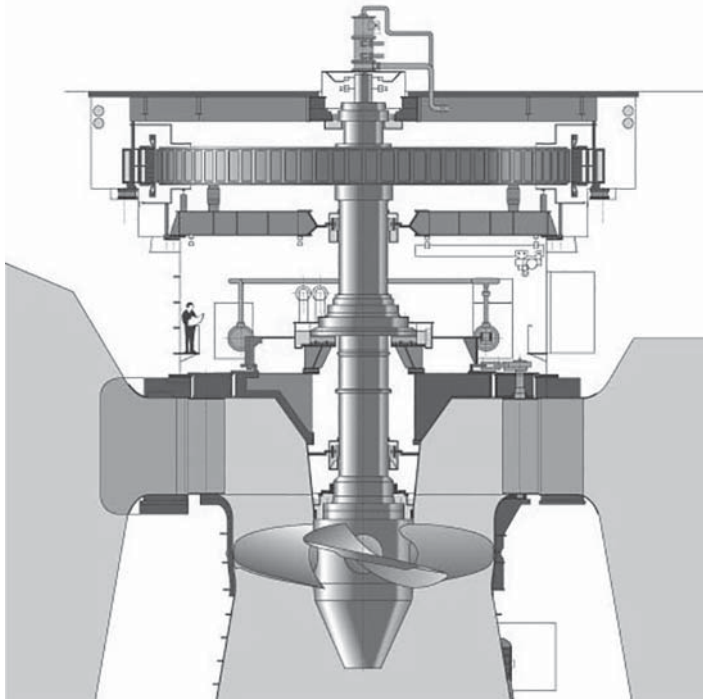


Figure 11.11 Kaplan turbine.

toward the tip. Thus, the blade is oriented quite broadside to the flow at the tip. The flow, having started from stationary conditions at the headwater, remains free of vorticity as it flows into the turbine. Hence, the tangential velocity has the *free vortex* distribution

$$K = rV_{u2}(r) = r_{2t}V_{u2t}$$

in which r_{2t} refers to the tip radius. If the exit swirl is absent, then the work delivered is

$$w = U_2V_{u2} = r\Omega V_{u2t} \frac{r_{2t}}{r} = \Omega V_{u2t} r_{2t} = K\Omega$$

which is independent of the radial location. This is the same result as was found when the axial turbines were discussed in Chapter 7.

An equation similar to that of Morozov for Francis turbines, can be obtained from the graphical result in Nechleba [67] for Kaplan turbines. However, by using data from more recent installations, Schweiger and Gregory [81] give the equation

$$\Omega_s = 2.76 \left(\frac{H_r}{H_e} \right)^{0.486} \quad (11.4)$$

in which the reference head has been chosen to be $H_r = 30$ m. In addition, the hub-to-tip radii ratio may be correlated as

$$\frac{r_h}{r_t} = 0.8 - 0.1 \Omega_{sp}$$

The number of blades increases with decreasing specific speed, with 3 blades when the power specific speed is 5.2 and 10 blades when the power-specific speed drops to 1.7.

■ EXAMPLE 11.5

The Otari power plant in Japan delivers 100 MW of power when the flow rate is $220 \text{ m}^3/\text{s}$ and the effective head is 51 m. The diameter of the Kaplan turbine is $D_{2t} = 6.1$ m, and the hub-to-tip ratio is $\kappa = 0.6$. The generator has 48 poles and delivers power at a line frequency of 50 Hz. (a) Find the efficiency of the turbine. (b) Calculate the flow angles entering and leaving the rotor.

Solution: (a) The efficiency is

$$\eta = \frac{\dot{W}_0}{\rho Q g H_e} = \frac{10^8}{1000 \cdot 220 \cdot 9.81 \cdot 51} = 0.91$$

(b) Since the line frequency is 50 Hz and the generator was chosen to have 48 poles, the shaft speed is $\Omega = 120 \cdot 50/48 = 125$ rpm. The tip speed of the runner blade is

$$U_{2t} = \frac{D_{2t}}{2} \Omega = \frac{6.1 \cdot 125 \cdot \pi}{2 \cdot 30} = 39.9 \text{ m/s}$$

The axial velocity is uniform and is given by

$$V_{x2} = \frac{4Q}{\pi D_{2t}^2 (1 - \kappa^2)} = \frac{4 \cdot 220}{\pi \cdot 6.1^2 (1 - 0.6^2)} = 11.76 \text{ m/s}$$

Since each blade element delivers the same amount of work, the tangential velocity at the tip can be determined from

$$V_{u2t} = \frac{\eta g H_e}{U_{2t}} = \frac{0.91 \cdot 9.81 \cdot 51}{39.9} = 11.39 \text{ m/s}$$

The flow angles for the absolute and relative velocities can now be determined. They are shown in Figure 11.12 across the span of the blades. To illustrate the calculations, at the mean radius $r_{2m} = 2.44 \text{ m}$ the absolute velocity makes an angle

$$\alpha_{2m} = \tan^{-1} \left(\frac{V_{u2t} r_{2t}}{V_{x2} r_{2m}} \right) = \tan^{-1} \left(\frac{11.39 \cdot 3.05}{11.76 \cdot 2.44} \right) = 50.4^\circ$$

The tangential component of the relative velocity at this location is

$$W_{u2m} = V_{x2} \tan \alpha_{2m} - U_{2t} \frac{r_{2m}}{r_{2t}} = 11.76 \tan(50.4^\circ) - \frac{39.9 \cdot 2.44}{3.05} = -17.71 \text{ m/s}$$

and the flow angle is

$$\beta_{2m} = \tan^{-1} \left(\frac{W_{u2m}}{W_{x2}} \right) = \tan^{-1} \left(-\frac{17.71}{11.76} \right) = -56.4^\circ$$

The flow leaves the runner axially. Therefore the tangential component of the relative velocity is $W_{u3m} = -U_{2t} r_m / r_t$ and with the axial velocity constant, the flow angle is

$$\beta_{3m} = \tan^{-1} \left(\frac{W_{u3m}}{W_{x3}} \right) = \tan^{-1} \left(-\frac{39.9 \cdot 2.44}{11.76 \cdot 3.05} \right) = -69.8^\circ$$

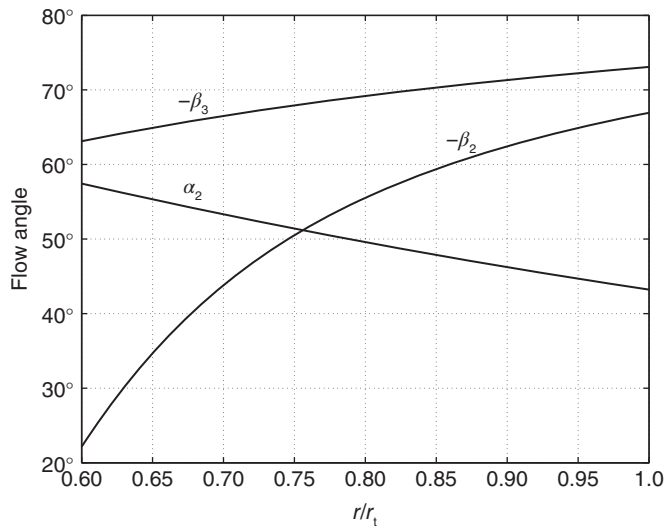


Figure 11.12 Flow angles for the turbine

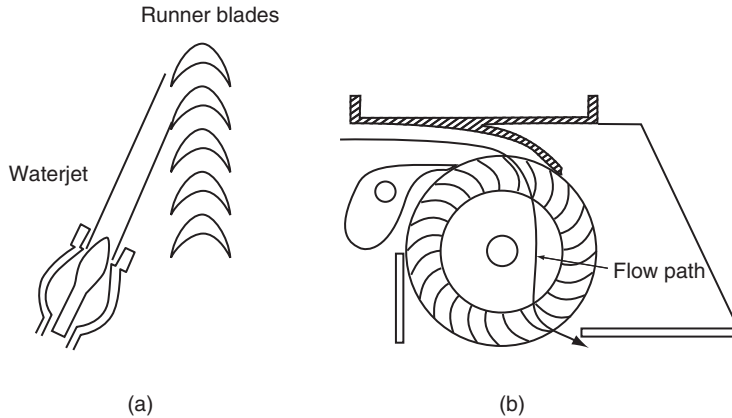


Figure 11.13 (a) Turgo turbine. (b) Crossflow or a Banki–Mitchell turbine.

Small turbines have been excluded from Figure 11.2. The single-jet Pelton wheels are appropriate for flow rates lower than shown on this graph of the graph. Some who live far from the electricity grid and have access to streams with headwaters in high hills have built power plants using such small Pelton wheels. An alternative is a turgo turbine, shown in Figure 11.13a. It operates at the effective head of 50–250 m. The analysis is similar to that of a single stage steam turbines and a Pelton wheel. The nozzle angle is about 70° .

A crossflow turbine, also called a *Banki–Mitchell turbine*, can be operated under heads between 5 and 200 m, but it is generally used in rural settings with ample flow rates and low head. It is shown in Figure 11.13b. It looks like a waterwheel, but the blades are designed is such a way that as water flows through the turbine, it does work on both the leading set of blades and on the trailing set. Because the axis is horizontal, the shaft and the blades can be made long to accommodate a large flow.

11.6 CAVITATION

Cavitation takes place in a hydraulic turbine if the minimum pressure drops below the vapor pressure of water at the prevailing temperature. For this reason, elevation of the plant in relation to the tailwater needs to be properly chosen. In addition, since the atmospheric pressure drops with increasing elevation, the margin between the minimum pressure and the vapor pressure diminishes, and this is to be taken into account. With large runners in hydroelectric power plants, the cavitation damage can become very expensive, not only in equipment repair but also in the unavailability of the plant during repairs.

The physical basis of cavitation is discussed in the review paper by Arakeri [4], who also proposes alternative criteria that factor in more precisely the location of the local minimum in pressure. In this section, however, the typical engineering criterion is used. The static pressure at the exit of the turbine is given by

$$\frac{p_3}{\rho g} + \frac{V_3^2}{2g} + H_s = \frac{p_a}{\rho g} + \frac{V_4^2}{2g} + H_d$$

in which the last two terms represent the exit head loss and the head loss in the diffuser and H_s is the elevation of the turbine above the tailwater. The net positive suction pressure

is defined as the sum of the static pressure head and the dynamic head minus the vapor pressure head of water at the ambient temperature

$$H_{sv} = \frac{p_3}{\rho g} + \frac{V_3^2}{2g} - \frac{p_v}{\rho g}$$

Substituting from the previous equation gives

$$H_{sv} = \frac{p_a - p_v}{\rho g} - H_s + \frac{V_4^2}{2g} + H_d$$

The head loss in the draft tube has been shown to be

$$H_d = (1 - \eta_d) \frac{(V_3^2 - V_4^2)}{2g}$$

Dividing through by the effective head leads to the definition of the Thoma cavitation parameter σ , as

$$\sigma = \frac{H_{sv}}{H_e} = \frac{p_a - p_v}{\rho g H_e} - \frac{H_s}{H_e} + \frac{V_4^2}{2g H_e} - \frac{H_d}{H_e}$$

Critical values for this parameter have been given by Moody and Zowski [65] for Francis turbines as

$$\sigma_c = 0.006 + 0.123\Omega_{sp}^{1.8}$$

and for Kaplan turbines as

$$\sigma_c = 0.100 + 0.037\Omega_{sp}^{2.5}$$

They are shown in Figure 11.14.

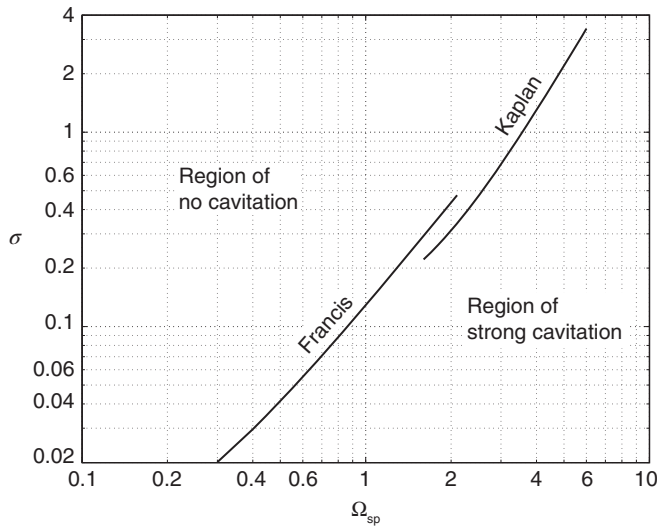


Figure 11.14 Critical Thoma parameter for Francis and Kaplan turbines.

EXERCISES

11.1 A Pelton wheel operates from an effective head of $H_e = 300$ m and at a flow rate of $4.2 \text{ m}^3/\text{s}$. The wheel radius is $r_2 = 0.75$ m, and rotational speed is 450 rpm. The water that leaves the penstock is divided into five streams. The nozzle coefficient is $c_N = 0.98$ for each nozzle. Impulse blades turn the flow into the direction $\beta_3 = -65^\circ$, and as a result of friction, the relative velocity reduces by an amount that gives a velocity coefficient $c_v = 0.90$. Find (a) the efficiency of the turbine, (b) the power-specific speed, and (c) the nozzle diameter and the number of buckets in the wheel. [Ans: (a) 0.869, (b) 0.225, (c) 11.9 cm, 21]

11.2 For Example 11.2 assume that the blade coefficient is $c_v = 0.93$ and find (a) the blade angle at the exit assuming that the relative velocity leaves the wheel at this angle. (b) Determine the exit kinetic energy head as a percentage of the potential energy head in the reservoir. [Ans: (a) -58.9° , (b) 6.2%]

11.3 The velocity diagrams for the runner of a small Francis turbine are shown in Figure 11.15. The discharge is $4.5 \text{ m}^3/\text{s}$, the head is 150 m of water, and the rotational speed is 450 rpm. The inlet radius is $r_2 = 0.6$ m, and the water leaves the guide vanes at angle $\alpha_2 = 72^\circ$ and velocity $V_2 = 53.3$ m/s. It leaves the turbine without swirl. (a) Find the velocity coefficient of the stator (inlet spiral and gates). (b) Find the inlet angle of the relative velocity β_2 . (c) What is the output power? (d) What is the torque on the shaft? (e) Determine the power-specific speed. [Ans: (a) 0.982, (b) 53.7° , (c) 6.45 MW, (d) 136.9 kN m, (e) 0.415]

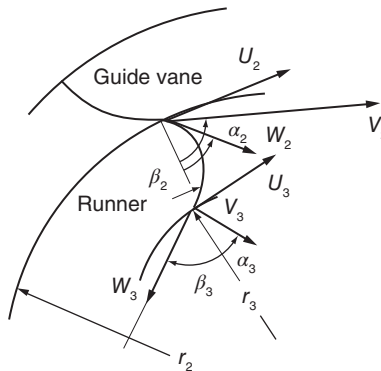


Figure 11.15 A runner of a Francis turbine.

11.4 The pressure at the entrance of a Francis turbine runner is 238.6 kPa, and at the exit it is 22.6 kPa. The shaft turns at 210 rpm. At the exit the flow leaves without swirl. The inlet radius is $r_2 = 910$ mm, and the exit radius is $r_3 = 760$ mm. The relative velocity entering the runner is $W_2 = 10.2$ m/s, and the flow angle of the relative velocity leaving the runner is $\beta_3 = -72^\circ$. The blade height at the inlet is $b_2 = 0.6$ m. (a) Compute the stagnation pressure loss in the runner. (b) Find the power delivered by the turbine. [Ans: (a) 53.0 kPa, (b) 9.1 MW]

11.5 A Francis turbine has an inlet radius of $r_2 = 1450$ mm and outlet radius of $r_3 = 1220$ mm. The blade width is constant at $b = 370$ mm. The shaft speed is 360 rpm and the volumetric flow rate is $Q = 16.7$ m³/s. The flow enters the runner at $\alpha_2 = 78^\circ$. Water leaves the turbine without swirl, and the outlet pressure is $p_3 = 35$ kPa. The loss through the runner is $0.20W_2^3/2g$. Find the pressure p_2 at the inlet and the head loss through the runner. [Ans: 1257 kPa, 21.92 m]

11.6 The relative velocities at the inlet and the exit of a Francis turbine are $W_2 = 10.0$ m/s and $W_3 = 33.7$ m/s. The shaft speed is $\Omega = 200$ rpm. The inlet radius of the runner is $r_2 = 1880$ mm, and the outlet radius is $r_3 = 1500$ mm. The runner blade height is constant at $b = 855$ mm. Find (a) the flow rate through the turbine and (b) the torque, assuming that the flow leaves without exit swirl. [Ans: (a) 98.3 m³/s, (b) 7713 kN m]

11.7 A Francis runner is to be designed for an effective head of $H_e = 140$ m and flow rate $Q = 20$ m³/s. Assume that the efficiency is $\eta = 0.9$ and that there is no exit swirl. Use the formula of Lugaresi and Massa to calculate the specific speed. Use the other formulas in the text to obtain b_1 and U_2/V_0 from Ω_{sp} . Assume that the mechanical and volumetric losses are negligible. Find, (a) the specific diameter on this basis, (b) the diameter at the inlet, (c) the blade speed at the inlet, and (d) the flow angles of the absolute and relative velocities at the inlet. [Ans: (a) 0.960, (b) 1.57 m, (c) 37.9 m/s, (d) $69.5^\circ, -23.6^\circ$]

11.8 Determine the modified reaction ratio for each of the runners shown in Table 11.2. Assume that the efficiency of each is $\eta = 0.92$.

11.9 A hydro power plant with effective head $H_e = 153$ m and power output of $\dot{W} = 330$ MW has a runner diameter $D_2 = 5.2$ m, and operates at 150 rpm. Its efficiency is $\eta = 0.93$. (a) Find its specific speed using the fundamental definitions and compare it with the correlation of Lugaresi and Massa. (b) Determine the blade height from the correlation given in the chapter. (c) Assume that the meridional velocity across the runner does not change and determine the angle of the relative velocity after the runner. (d) Determine the modified reaction. [Ans: (a) 1.00, (b) 1.203 m, (c) -73.0° , (d) 0.582]

11.10 The Itaipu power plant on the border of Brazil and Paraguay has a Francis turbine that generates 715 MW of power at the volumetric flow rate of $Q = 666$ m³/s. The inlet diameter of the turbine is $D_2 = 10.5$ m, and the shaft speed is 92.3 rpm. The line frequency is 60 Hz. (a) How many poles does the electric generator have? (b) Find its specific speed and efficiency. (c) What is the blade height at the inlet to the runner. (d) Assuming that the meridional velocity remains constant across the runner, find the flow angles α_2 , β_2 , and β_3 , assuming that the flow leaves the turbine without swirl. [Ans: (a) 78, (b) 1.254, 0.924 (c) 2.65 m, (d) $\alpha_2 = 70.2^\circ$, $\beta_2 = -75.5^\circ$, $\beta_3 = -81.5^\circ$]

11.11 Water enters the runner of a Francis turbine with a relative velocity at angle -12° . The inlet radius is 2.29 m, and the mean radius at the exit is 1.37 m. The rotational speed is 200 rpm. The blade height at the inlet is $b_2 = 1.22$ m, and at the exit the inclined width of the blade is $b_3 = 1.55$ m. The radial velocity at the runner inlet is 10.0 m/s, and the flow leaves the runner without swirl. Evaluate (a) the change in total specific enthalpy of the water across the runner, (b) the specific torque exerted by the water on the runner. (c) the power developed, (d) the flow rate of water, and (e) the change in total pressure across the runner

when the total-to-total efficiency is 95%, and the volumetric and mechanical losses can be neglected. (f) What is the change in static pressure across the runner? [Ans: (a) 2198 kJ/kg, (b) 105 kNm/kg, (c) 385 MW, (d) $175.5 \text{ m}^3/\text{s}$, (e) 2198 kPa, (f) 1184.5 kPa]

11.12 The Otari number 2 power plant in Japan delivers 89.5 MW of power when the flow rate is $207 \text{ m}^3/\text{s}$ and the head is 48.1 m. The diameter of the Kaplan turbine is $D_{2t} = 5.1 \text{ m}$ and the hub to tip ratio $\kappa = 0.56$. The generator has 36 poles and delivers power at a line frequency of 50 Hz. (a) Find the efficiency of the turbine. (b) Calculate and flow angles entering and leaving the rotor, and construct a graph to show their variation across the span. [Ans: (a) 0.916, (b) $\alpha_{2m} = 40.15^\circ$, $\beta_{2m} = -56.45^\circ$, $\beta_{3m} = -66.96^\circ$]

CHAPTER 12

HYDRAULIC TRANSMISSION OF POWER

The subject matter of this chapter is *hydraulic transmission* of power by fluid couplings and torque converters. In these the *driver shaft* turns impeller blades of a centrifugal pump, and the *driven shaft* is powered by a radial turbine. The pump and its driver shaft are also called a *primary* and the turbine and the driven shaft, a *secondary*. The working fluid is oil, and the work done by the pump increases the oil pressure, which then drops as the oil flows through the turbine. The work done by the pump is greater than that delivered by the turbine; the difference is lost to irreversibilities.

Transmission of power by hydraulic means offers the advantages of quiet operation, damping of torsional vibrations, and low wear. As both the pump and the turbine are in a common casing, these machines are compact and safe to use in industrial settings. Such advantages come with some loss in efficiency when hydraulic transmissions are compared to rigid couplings.

12.1 FLUID COUPLINGS

A fluid coupling was invented by Hermann Föttinger while he was an engineer at AG Vulcan in Stettin, Germany.¹ Such a coupling is shown in Figure 12.1. It is toroidal in shape

¹H. Föttinger (1877–1945) received a PhD from TH München in 1904 and moved to work at AG Vulcan. In 1909, he left the company to assume a professorship in marine engineering at the Technical University of Danzig. From there he moved to the Chair of Turbomachinery of the Technical University of Berlin in 1924.

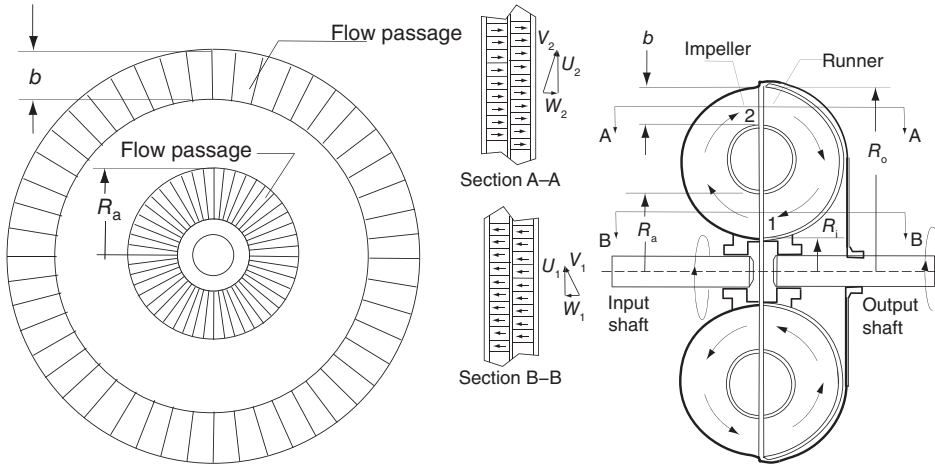


Figure 12.1 Sketch of a fluid coupling.

with a centrifugal pump on the primary side and a radial inflow turbine on the secondary side. There are no guide vanes in the torus, and absence of a fixed member means that there is no restraining torque on the housing. Hence, a free body diagram, cutting across both the driver and the driven shaft, shows that the torques in these shafts are equal. This result is independent of the shape of the blades.

12.1.1 Fundamental relations

The flow moves outward to a larger radius in the pump and inward in the turbine through a set of straight *radial blades* in both. Since the fluid flows from the primary to the secondary, the flow rate in each is the same. The torque *exerted by the impeller blades on the fluid* is

$$T_p = \rho Q(r_2 V_{u2} - r_1 V_{u1})$$

Similarly, the torque that *the fluid exerts on the turbine blades* is

$$T_s = \rho Q(r_2 V_{u2} - r_1 V_{u1})$$

Owing to irreversibilities in the coupling, the transmitted power is lower than the power inflow on the driver shaft. Therefore, with power given by $\dot{W} = T\Omega$, the output shaft must rotate at a lower speed than the input shaft. The difference in rotational speeds is called *slip*, and it is written in normalized form as follows:

$$s = \frac{\Omega_p - \Omega_s}{\Omega_p} = 1 - \frac{\Omega_s}{\Omega_p}$$

From the equation for power,

$$\dot{W}_p = T\Omega_p \quad \dot{W}_s = T\Omega_s$$

the efficiency is given as

$$\eta = \frac{\dot{W}_s}{\dot{W}_p} = \frac{\Omega_s}{\Omega_p}$$

The dissipated power causes the temperature of the oil to increase, which, in turn, leads to heat transfer to the housing and a rise in its temperature. With the increase in temperature of the hardware, the dissipated energy is then transferred as heat to the surroundings. The fractional loss of power is given by

$$\frac{\dot{W}_p - \dot{W}_s}{\dot{W}_p} = 1 - \eta = 1 - \frac{\Omega_s}{\Omega_p} = s,$$

and this gives an alternative meaning for slip. In steady operation, efficiency of a fluid coupling reaches 96–98%. During transients slip increases, and so does the loss. This is of secondary importance, because the coupling was invented to transmit power smoothly precisely during such transients.

■ EXAMPLE 12.1

A prime mover delivers power to a fluid coupling at 140 kW, with a shaft rotating at 1800 rpm, and with a slip of 3%. (a) What is the shaft torque? (b) What is the power flow in the output shaft? (c) Find the rotational speed of the driven shaft. (d) At what rate is energy dissipated as heat to the surroundings?

Solution:

(a) Torque on the shaft is

$$T = \frac{\dot{W}_p}{\Omega_p} = \frac{140000 \cdot 30}{1800 \pi} = 742.7 \text{ N m}$$

(b) The efficiency of the coupling at this operating point is

$$\eta = \frac{\Omega_s}{\Omega_p} = 1 - s = 1 - 0.03 = 0.97$$

and the power delivered is

$$\dot{W}_s = \eta \dot{W}_p = 0.97 \cdot 140 = 135.8 \text{ kW}$$

(c) The output shaft rotates at

$$\Omega_s = 0.97 \Omega_p = 1746 \text{ rpm}$$

(d) The power dissipation rate is

$$\dot{W}_d = (1 - \eta) \dot{W}_p = 0.03 \cdot 140 = 4.2 \text{ kW}$$

■

The two half-toroids making up the fluid coupling are each fitted with a set of radial blades. A typical number is 30 blades, but in order to avoid resonance vibrations, each half has a slightly different number. Better guidance is obtained by increasing the number of blades, but this comes at the cost of increased frictional losses and thus a slower circulating flow rate for the oil in the coupling. The flow rate is an operating characteristic of a coupling and needs to be estimated. This is carried out next.

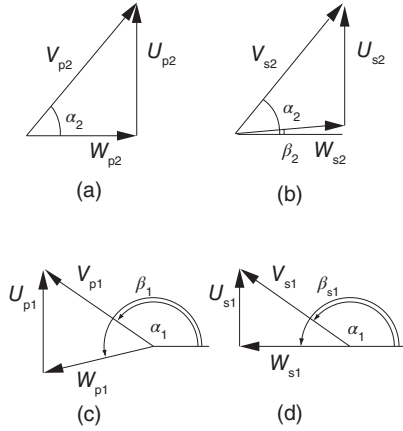


Figure 12.2 Velocity triangles for a fluid coupling. (a) Pump outlet, (b) turbine inlet, (c) pump inlet, and (d) turbine outlet.

12.1.2 Flow rate and hydrodynamic losses

Analysis of fluid couplings can be carried out by methods familiar from the analysis of centrifugal pumps and radial inflow turbines. The vector diagrams are shown in Figure 12.2. Since the relative velocity leaving the turbine and that leaving the pump are radial, the equation for the torque can be written as

$$T = \rho Q (\Omega_p r_2^2 - \Omega_s r_1^2) \quad (12.1)$$

where

$$r_1 = \frac{1}{2}(R_i + R_o) \quad r_2 = R_o - \frac{1}{2}b$$

according to the labels in Figure 12.1. The power dissipation in the coupling is $T(\Omega_p - \Omega_s)$. This can be estimated by noting that the losses consist of the losses at the inlets to the pump and the turbine and the frictional losses along the flow passage.

Analysis of inlet losses is left as an exercise. It is based on destruction of the difference in the tangential component of the velocity [69]. When carried out, it shows that at the inlet to the turbine the tangential component of velocity undergoes a change equal to $(\Omega_p - \Omega_s)r_2$. Hence, the kinetic energy change is equal to $(\Omega_p - \Omega_s)^2 r_2^2 / 2$ per unit mass. This kinetic energy is dissipated into internal energy of the fluid by turbulent mixing. Similarly, at the entrance to the pump, the kinetic energy change is $(\Omega_p - \Omega_s)^2 r_1^2 / 2$. Hence, the shock losses in the coupling amount to $(\Omega_p - \Omega_s)^2 (r_1^2 + r_2^2) / 2$.

Inside the coupling, owing to skin friction, losses, as in pipe flow, are proportional to the square of the meridional velocity. If the effective friction factor is denoted by f , the losses can be expressed as $f L Q^2 / 2 D_h A^2$ in which L is the length of the flow path, A is the cross-sectional area, and D_h is the hydraulic diameter $D_h = 4A/C$. In this expression, C is the circumference of the toroidal cross section. For fully turbulent flows, f is practically constant. The losses can now be expressed as

$$T(\Omega_p - \Omega_s) = \frac{1}{2} \rho Q \left[(\Omega_p - \Omega_s)^2 (r_1^2 + r_2^2) + f \frac{L}{D_h} \frac{Q^2}{A^2} \right] \quad (12.2)$$

Eliminating the torque between Eqs. (12.1) and (12.2) gives for the flow rate the expression

$$Q = A\Omega_p r_2 \sqrt{\frac{D_h}{fL}} \sqrt{\left(1 - \frac{\Omega_s^2}{\Omega_p^2}\right) \left(1 - \frac{r_1^2}{r_2^2}\right)} \quad (12.3)$$

Substituting this into the equation for torque gives

$$T = \rho A \Omega_p^2 r_2^3 \sqrt{\frac{D_h}{fL}} \sqrt{\left(1 - \frac{\Omega_s^2}{\Omega_p^2}\right) \left(1 - \frac{r_1^2}{r_2^2}\right)} \left(1 - \frac{r_1^2}{r_2^2} \frac{\Omega_s}{\Omega_p}\right) \quad (12.4)$$

This shows that the torque varies as the square of the rotational speed of the driver shaft. Increasing the load on the driven shaft increases the torque as well, up to a maximum value, which corresponds to such a large load that the driven shaft stops turning. The maximum torque is given by

$$T_m = \rho A \Omega_p^2 r_2^3 \sqrt{\frac{D_h}{fL}} \sqrt{1 - \frac{r_1^2}{r_2^2}}$$

The equation for torque can now be expressed as

$$T = T_m \sqrt{1 - \frac{\Omega_s^2}{\Omega_p^2}} \left(1 - \frac{r_1^2}{r_2^2} \frac{\Omega_s}{\Omega_p}\right)$$

The power delivered is $\dot{W}_s = T\Omega_s$, so that it can be written as

$$\dot{W}_s = \Omega_s T_m \sqrt{1 - \frac{\Omega_s^2}{\Omega_p^2}} \left(1 - \frac{r_1^2}{r_2^2} \frac{\Omega_s}{\Omega_p}\right)$$

or in nondimensional form as

$$\frac{\dot{W}_s}{T_m \Omega_p} = \frac{\Omega_s}{\Omega_p} \sqrt{1 - \frac{\Omega_s^2}{\Omega_p^2}} \left(1 - \frac{r_1^2}{r_2^2} \frac{\Omega_s}{\Omega_p}\right)$$

The performance curves are shown in Figure 12.3. If the load on the driven shaft is very large, the coupling will experience a large slip and only a small amount of power will be transmitted to the driven shaft. Similarly, for light loads, the torque is small and a small amount of power is needed to turn the shaft. Here again, the power flow is low. Hence, there is a maximum for some intermediate value, which depends on the dimensions of the coupling. For the characteristics shown $r_1/r_2 = 0.6$, and the maximum is at $\Omega_s/\Omega_p = 0.642$. The range $0.6 < r_1/r_2 < 0.8$ is typical.

By dimensional analysis, a torque coefficient can be defined, and it depends on the slip, the Reynolds number, and geometric parameters, the most important of which is the ratio of the volume \mathcal{V} of the space occupied by the working fluid and the cube of the outer diameter. These dependencies can be written as

$$C_T = \frac{T}{\rho \Omega_p^2 D^5} = f \left(s, \frac{\rho \Omega_p D^2}{\mu}, \frac{\mathcal{V}}{D^3} \right)$$

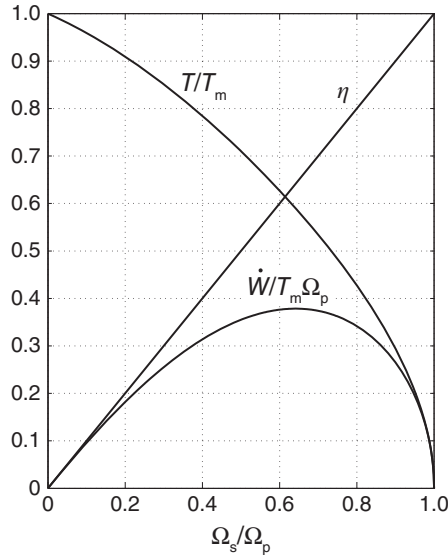


Figure 12.3 Characteristics of a fluid coupling with $r_1/r_2 = 0.6$.

The flow through a coupling, as in other turbomachines, is dominated by inertial forces and the influence of the Reynolds number on the torque coefficient is much weaker than that caused by the slip. The only other parameter that needs to be investigated is the volume ratio.

12.1.3 Partially filled coupling

It was observed early in the development of fluid couplings that the torque could be reduced by filling the coupling only partially with fluid. Modern couplings have chambers into which some of the fluid can be drawn. Similarly, extra fluid can be added into the coupling. This provides a smooth start, and the amount of fluid can be adjusted to obtain the best efficiency during the nominal operating conditions.

The performance of a partially filled coupling is shown in Figure 12.4, where the parameter $\mathcal{V}/\mathcal{V}_m$ is the ratio of the actual volume of the fluid to that in a fully filled coupling. One way to see that torque must decrease in a partially filled coupling is to note that when some of the flow channels are starved for fluid, they are not effective in providing a full force into the turbine blades. Although such a fluid distribution is possible in principle, it is more likely that the fluid distribution is such that each channel is only partially filled and then the fluid is crowded to the pressure side of each blade in a pump, with the suction side lacking its share. Now the loading of the turbine blades is similar to that in an impulse turbine, but since the blades are flat, they do not perform well under this loading. As a consequence, an equally large pressure increase is not possible in the pump as in a completely filled coupling, and the torque is reduced. The graphs in this figure were drawn to match the results shown in Pfleiderer [69]. For couplings in use today, such performance data are obtained from manufacturers' catalogs.

In addition to steady rotation, torsional vibrations may be present in the input shaft. Such torsional motions do not influence the flow in the coupling greatly, so they are not transmitted to the output shaft. The vibrations can be further suppressed by placing the coupling near the node of such a vibrational motion in the shaft, if it is not possible to

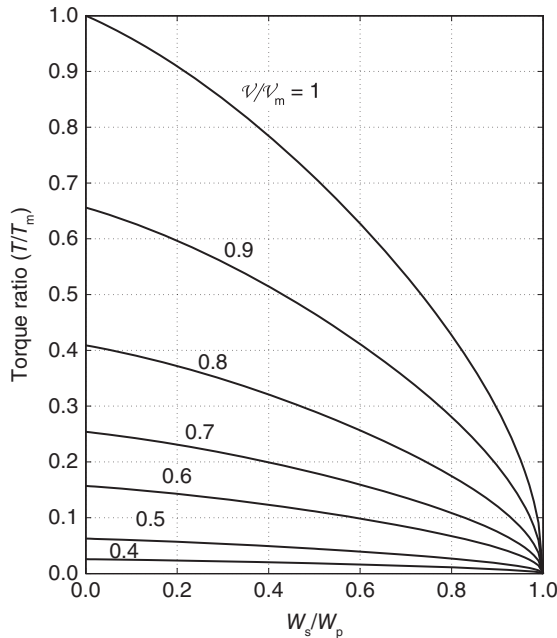


Figure 12.4 Partially filled coupling characteristics.

change the natural frequency of the load. Fluid couplings vary in size, with small ones handling about 1 kW. For those in the 2000 kW range, the outer diameter reaches over 1 m. They contain over 100 L of oil and have a mass approaching 2000 kg.

12.2 TORQUE CONVERTERS

The torque converter was also invented by H. Föttinger, while working at Vulcan Shipbuilding, where he was interested in finding an efficient way of connecting steam turbines to marine propellers. As the name suggests, *torque converter* changes and usually increases the input torque to a different output value. In order to achieve this, a set of guide vanes, fixed to the frame, direct the fluid into an impeller, which rotates with the input shaft. On the output shaft is a set of runner, or turbine, blades. To obtain the larger output torque, the blade shapes must be such that the fluid experiences a larger change in the tangential velocity through the turbine than through the pump. A torque converter with a single-stage radial outflow turbine is shown in Figure 12.5. More complicated designs having three turbine stages and two stationary guide vane stages exist. They have a wider operating range of high efficiency.

12.2.1 Fundamental relations

In order to keep the analysis general, the velocity triangles in Figure 12.6 are also drawn to depict the general situation. The equation for the output torque from the turbine is

$$T_s = \rho Q(r_2 V_{u2} - r_3 V_{u3})$$

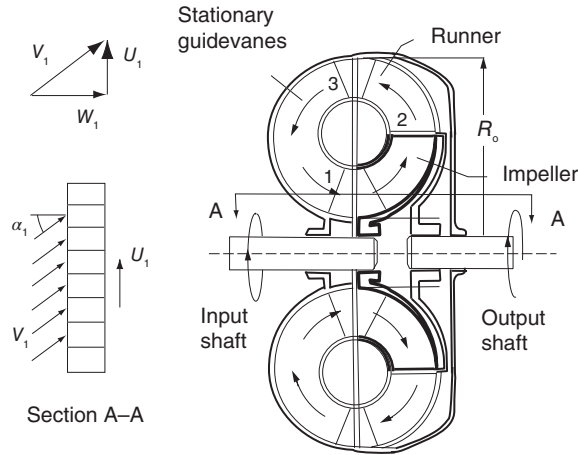


Figure 12.5 Sketch of a torque converter.

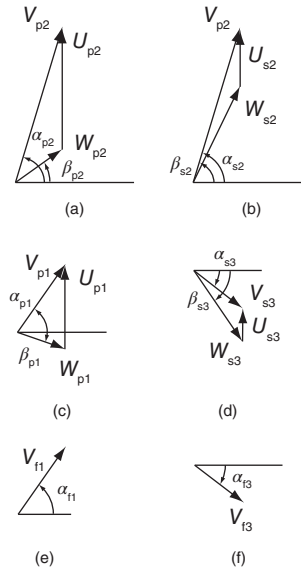


Figure 12.6 Velocity triangles for a torque converter. (a) Pump exit, (b) turbine inlet, (c) pump inlet, (d) turbine exit, (e) fixed exit, and (f) fixed inlet.

and the torque in the input shaft is

$$T_p = \rho Q (r_2 V_{u2} - r_1 V_{u1})$$

For the fixed member the equation is

$$T_f = \rho Q (r_1 V_{u1} - r_3 V_{u3})$$

Adding the last two shows that

$$T_s = T_p + T_f$$

Examination of the velocity diagrams shows that at the inlet to the turbine, the velocities are similar to those of an impulse turbine. Namely, the absolute velocity is at a steep angle to the axial direction. As the fluid flows through the turbine, its relative velocity is changed first toward the axis and then beyond it to a negative angle. Since at the exit of the turbine, the axial velocity is in the direction exactly opposite to that at the inlet of the pump, the velocity diagram on the bottom part of the figure has been reflected about the vertical axis to show this. Also, at the inlet to the turbine, the absolute velocity is identical to the absolute velocity at the exit of the pump and the blade speed is lower than that of the pump.

A configuration of a torque converter that more closely reflects a centrifugal pump and a radial inflow turbine would have these two components as mirror images across the vertical centerline. The fixed member would then occupy only the lower part of the converter. In this case, for a symmetric fixed member, the exit of the turbine would be at the same radius as the inlet to the pump.

The power in the input shaft is $\dot{W}_p = T_p \Omega_p$ and in the output shaft it is $\dot{W}_s = T_s \Omega_s$. The efficiency, given by

$$\eta = \frac{\dot{W}_s}{\dot{W}_p}$$

must be less than unity owing to irreversibilities. To obtain a large increase in torque, the output shaft must rotate substantially slower than the input shaft. For sufficiently large output load, the output shaft can be stopped. Under this situation, the efficiency of the torque converter drops to zero and the irreversibilities cause its temperature to rise considerably. The irreversibilities are now mainly *shock losses*, although frictional loss is still substantial. A light load on the output shaft gives no torque multiplication at all, and as the shock losses vanish, the small losses are now almost entirely frictional losses.

■ EXAMPLE 12.2

A torque converter, when operating with a slip equal to 0.8, multiplies the torque in the ratio of 2.5 : 1. The circulatory flow rate in the converter is 140 kg/s. For the primary element, the ratio of inner to outer mean radii is 0.55 and the blade speed of the primary at the outer mean radius is 50 m/s. The axial velocity remains constant throughout the flow circuit. The absolute velocity at inlet to the primary and the relative velocity at the exit of the primary are both axially directed. Evaluate the power developed by the secondary element in this torque converter.

Solution: Let the inlet to the impeller be denoted by 1, the inlet to the runner by 2, and the inlet to the guide vanes as 3. The design and operation is such that the tangential velocity at the inlet to the impeller is zero and the tangential component of the relative velocity to the runner vanishes also. For this reason, the velocity diagrams are as shown in Figure 12.7.

Since the inlet angular momentum to the primary is zero, the torque is $T_p = \rho Q r_2 V_{u2}$ and the input power is $\dot{W}_p = T \Omega_p$. Therefore,

$$\dot{W}_p = \rho Q U_2 V_{u2} = \rho Q U_2^2 = 140 \cdot 50^2 = 350.0 \text{ kW}$$

Since the torque ratio is 2.5 and the slip is 0.8, it follows that

$$\frac{\dot{W}_s}{\dot{W}_p} = \frac{T_s \Omega_s}{T_p \Omega_p} = 2.5 \cdot 0.2 = 0.5$$

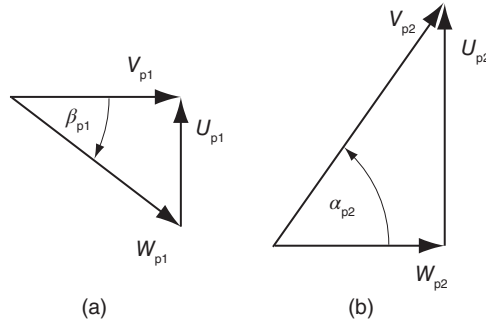


Figure 12.7 Velocity triangles for Example 12.2. (a) Primary inlet and (b) primary exit.

and $\dot{W}_s = 0.5 \cdot 350.0 = 175.0$ kW. There is a large irreversibility in the flow as the large torque multiplication requires heavily loaded blades. (Note that the ratio of the radii was not needed.) ■

12.2.2 Performance

To illustrate how the general analysis may proceed, consider the torque converter shown in Figure 12.5. Assume that the blades are radial at the exit of the primary so that the angles at which the relative velocity leaves is zero, and similarly for the flow at the exit of the secondary. Then, since the velocity does not change in magnitude or direction as the flow leaves the primary and enters the secondary, at the inlet of the secondary, the angular momentum is $r_2 V_{su2} = r_2 V_{pu2} = r_2^2 \Omega_p$. On the basis of what has been learned of the turbomachines studied so far, if the deviation is ignored, the exit angles of the relative velocity leaving the primary and the secondary do not change during the operation, and neither does the angle of the absolute velocity at the exit of the fixed member. Then dimensional analysis of this particular torque converter, which also has fixed value for the diameter ratio, shows that the torque of the primary is related to the angular speed ratio and Reynolds number as

$$C_p = \frac{T_p}{\rho \Omega_p^2 D^5} = f_1 \left(\frac{\Omega_s}{\Omega_p}, Re \right) \quad (12.5)$$

where the Reynolds number is $Re = \rho \Omega_p D^2 / \mu$. Similarly for the secondary

$$C_s = \frac{T_s}{\rho \Omega_p^2 D^5} = f_2 \left(\frac{\Omega_s}{\Omega_p}, Re \right) \quad (12.6)$$

Dividing these gives

$$\frac{T_s}{T_p} = f \left(\frac{\Omega_s}{\Omega_p}, Re \right) \quad (12.7)$$

The efficiency is also a function of the same nondimensional groups

$$\eta = g \left(\frac{\Omega_s}{\Omega_p}, Re \right) \quad (12.8)$$

Again, the influence of the Reynolds number is much weaker than the angular velocity ratio [48].

Typical plots of the torque ratio and efficiency are shown in Figure 12.8. Experimental evidence suggests that the torque coefficient of the primary C_p is independent of the speed ratio; that is, the amount of slip taking place in the torque converter influences mainly the downstream components. The primary torque is given by the angular momentum balance

$$T_p = \rho Q (\Omega_p r_2^2 - r_1 V_{u1})$$

With $V_{u1} = V_{x1} \tan \alpha_1 = Q \tan \alpha_1 / A$, the torque coefficient of the primary is then

$$C_p = \frac{T_p}{\rho \Omega_p^2 r_3^5} = \frac{Q}{\Omega_p r_3^3} \left(\frac{r_2^2}{r_3^2} - \frac{Q r_1 \tan \alpha_1}{A r_3^3 \Omega_p} \right)$$

The reaction torque of the secondary is given by

$$T_s = \rho Q (\Omega_p r_2^2 - \Omega_s r_3^2)$$

and the torque coefficient of the secondary is

$$C_s = \frac{T_s}{\rho \Omega_p^2 r_3^5} = \frac{Q}{\Omega_p r_3^3} \left(\frac{r_2^2}{r_3^2} - \frac{\Omega_s}{\Omega_p} \right)$$

The torque ratio becomes

$$\frac{T_s}{T_p} = \frac{r_2^2/r_3^2 - \Omega_s/\Omega_p}{r_2^2/r_3^2 - Q r_1 \tan \alpha_1 / A \Omega_p r_3^2} \quad (12.9)$$

The efficiency of the torque converter is then

$$\eta = \frac{T_s \Omega_s}{T_p \Omega_p} = \frac{(r_2^2/r_3^2 - \Omega_s/\Omega_p) \Omega_s / \Omega_p}{r_2^2/r_3^2 - Q r_1 \tan \alpha_1 / A r_3^2 \Omega_p} \quad (12.10)$$

Since C_p is assumed to be constant, it follows that Q/Ω_p is constant, and for a given torque converter, the torque ratio is seen to decrease linearly with the speed ratio Ω_s/Ω_p . The efficiency then varies parabolically, being zero when the secondary shaft either is fixed or rotates at the value given by

$$\frac{\Omega_s}{\Omega_p} = \frac{r_2^2}{r_3^2}$$

At the point of maximum efficiency, the speed ratio decreases to about one-half of this value. That the experimental curves of Figure 12.8 do not follow this theory exactly is caused by variation of C_p with the speed ratio.

Another design is shown in Figure 12.9. The output shaft is concentric with the input one, and the inlet mean radius of the fixed member is the same as its exit radius. This design is analyzed in the next example.

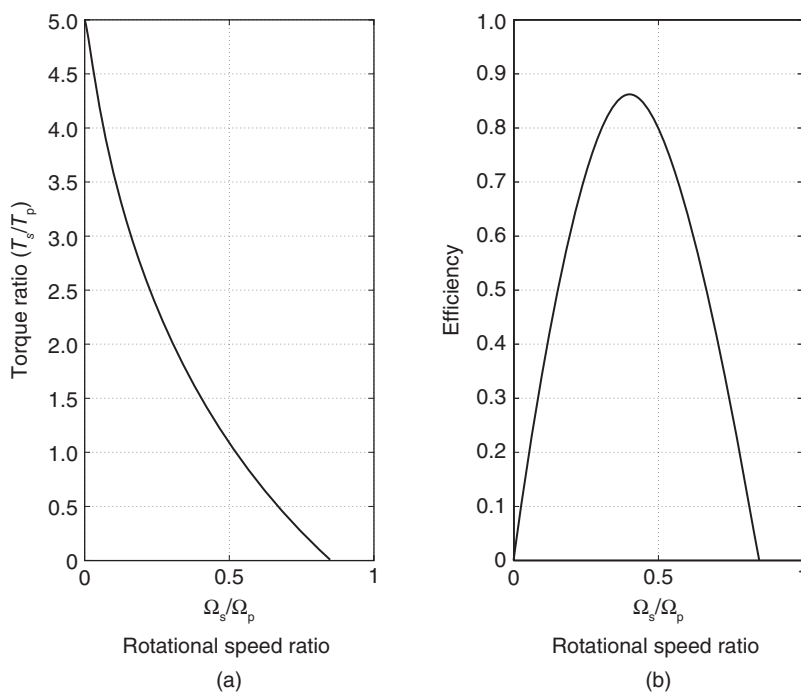


Figure 12.8 Performance curves for a torque converter. (a) Torque ratio and (b) efficiency.

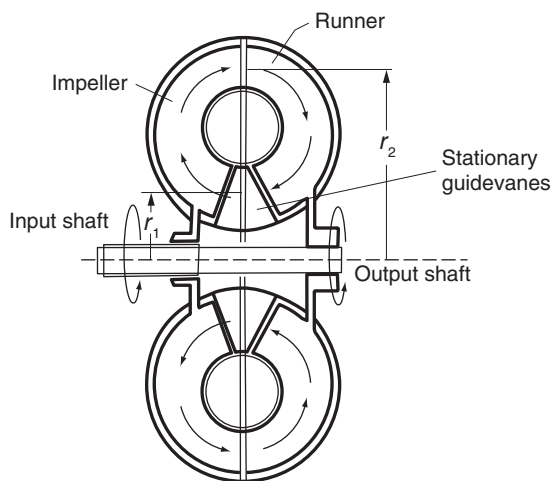


Figure 12.9 Torque converter with concentric shafts.

■ EXAMPLE 12.3

The mean radii of a torque converter of the type shown in Figure 12.9 are $r_1 = 10$ cm and $r_2 = 15$ cm. The primary operates with $\Omega_p = 2500$ rpm, and the secondary rotates at $\Omega_s = 1200$ rpm. The blades of the primary are oriented such that the angle of the relative flow at the exit is $\beta_{p2} = 35^\circ$. The exit angle of the relative velocity of the secondary is $\beta_{s3} = -56^\circ$. The fixed blades are shaped such that the exit velocity

from them is at the angle $\alpha_{f1} = 55^\circ$. The axial velocity is constant throughout the converter, and its value is $V_x = 15$ m/s. Determine the flow angles and calculate the torque ratio T_s/T_p and the efficiency of the torque converter.

Solution: The blade speeds are first determined as

$$U_{p1} = r_1 \Omega_p = \frac{0.10 \cdot 2500 \cdot \pi}{30} = 26.78 \text{ m/s}$$

$$U_{p2} = r_3 \Omega_p = \frac{0.15 \cdot 2500 \cdot \pi}{30} = 39.27 \text{ m/s}$$

$$U_{s2} = r_2 \Omega_s = \frac{0.15 \cdot 1200 \cdot \pi}{30} = 18.85 \text{ m/s}$$

$$U_{s3} = r_3 \Omega_p = \frac{0.10 \cdot 1200 \cdot \pi}{30} = 12.57 \text{ m/s}$$

Next, the tangential velocity at the exit of the primary is determined. Since the flow angle of the relative flow is given, the tangential component W_{pu2} is

$$W_{pu2} = V_x \tan \beta_{p2} = 15 \tan(35^\circ) = 10.50 \text{ m/s}$$

and the tangential component of the absolute velocity is

$$V_{pu2} = U_{p2} + W_{pu2} = 39.27 + 10.50 = 49.77 \text{ m/s}$$

The flow angle is therefore

$$\alpha_{p2} = \tan^{-1} \left(\frac{V_{pu2}}{V_x} \right) = \tan^{-1} \left(\frac{49.77}{15.00} \right) = 73.23^\circ$$

The absolute velocity and its flow angle at the inlet of the secondary are the same as those leaving the primary. Hence, $V_{su2} = 49.77$ m/s. The relative velocity entering the secondary has the tangential component

$$W_{su2} = V_{su2} - U_{s2} = 49.77 - 18.85 = 30.92 \text{ m/s},$$

and its flow angle is

$$\beta_{s2} = \tan^{-1} \left(\frac{W_{su2}}{V_x} \right) = \tan^{-1} \left(\frac{30.92}{15.00} \right) = 64.12^\circ$$

At the exit of the secondary, the tangential velocity component of the relative velocity is

$$W_{su3} = V_x \tan \beta_{s3} = 15 \tan(-56^\circ) = -22.24 \text{ m/s}$$

so that the component of the absolute velocity and its flow angle are

$$V_{su3} = W_{su2} + U_{s3} = -22.24 + 12.57 = -9.67 \text{ m/s}$$

$$\alpha_{s3} = \tan^{-1} \left(\frac{V_{su3}}{V_x} \right) = \tan^{-1} \left(\frac{-9.67}{15.00} \right) = -32.81^\circ$$

The flow enters the fixed member at the same velocity as it leaves the secondary. Hence, $V_{fu3} = -9.67$ m/s. At the exit of the fixed member,

$$V_{fu1} = V_x \tan \alpha_{f1} = 15 \tan(55^\circ) = 21.42 \text{ m/s}$$

The flow enters the primary with this tangential velocity and angle, so that $V_{pu1} = 21.24$ m/s. The relative velocity at the inlet of the primary is then

$$W_{pu1} = V_{pu1} - U_{p1} = 21.42 - 26.18 = -4.76 \text{ m/s}$$

The torques are

$$T_s = \rho Q(r_2 V_{su2} - r_3 V_{su3}) = 8.43 \rho Q$$

$$T_p = \rho Q(r_2 V_{pu2} - r_1 V_{pu1}) = 5.32 \rho Q$$

$$T_f = \rho Q(r_1 V_{fu1} - r_3 V_{fu3}) = 3.11 \rho Q$$

Hence,

$$\frac{T_s}{T_p} = \frac{8.43}{5.32} = 1.58 \quad \eta = \frac{T_s \Omega_s}{T_p \Omega_p} = 1.58 \frac{1200}{2500} = 0.761 \quad \blacksquare$$

The velocity triangles for the preceding example are close to what are shown in Figure 12.6.

EXERCISES

12.1 A fluid coupling operates with oil flowing in a closed circuit. The device consists of two elements, the primary and secondary, each making up one-half of a torus, as shown in Figure 12.1. The input power is 100 hp, and input rotational speed is 1800 rpm. The output rotational speed is 1200 rpm. (a) Evaluate both the efficiency and output power of this device. (b) At what rate must energy as heat be transferred to the cooling system, to prevent a temperature rise of the oil in the coupling? [Ans: (a) 2/3, 66.7 hp, (b) 24.86 kW]

12.2 (a) Carry out the algebraic details to show that the expression for the flow rate through a fluid coupling is given by Eq. (12.3) and assuming that for a low value of slip the friction factor is related to the flow rate by an expression

$$f = \frac{c}{Re} = \frac{c\mu A}{\rho Q D}$$

find the dependence of the flow rate on the slip for small values of s . (b) Carry out the algebraic details to show that the expression for the torque of a fluid coupling is given by Eq. (12.4). What is the appropriate form for this equation for low values of slip? [Ans: $C_T = 2s(1 - r_1^2/r_2^2)^2 \rho A D^2 \omega_p / c\mu L r_2$]

12.3 A fluid coupling operates with an input power of 200 hp, 5% slip, and a circulatory flow rate of 1500 L/s. (a) What is the rate at which energy as heat must be transferred from the coupling in order for its temperature to remain constant? (b) What would be the temperature rise of the coupling over a period of 30 minutes, assuming that no heat is transferred from the device and that it has a mass of 45 kg, consisting of 70% metal with

a specific heat 840 J/(kg K), and 30% oil with a specific heat 2000 J/(kg K)? [Ans: (a) 7.46 kW, (b) 251 °C]

12.4 In the fluid coupling shown in Figure 12.1 fluid circulates in the direction indicated, while the input and output shafts rotate at 2000 and 1800 rpm, respectively. The fluid is an oil having a specific gravity of 0.88 and viscosity 0.25 kg/(m s). The outer mean radius of the torus is $r_2 = 15$ cm and the inner mean radius is $r_1 = 7.5$ cm. The radial height is $b = 2r_2/15$. The axial flow area around the torus is the same as the flow area at the outer clearance between the primary and secondary rotors. Given that the relative roughness of the flow conduit is 0.01, find the volumetric flow rate and the axial velocity. [Ans: 247.6 L/s, 13.13 m/s]

12.5 Show that the kinetic energy loss model at the inlet to the turbine given by

$$\frac{1}{2}r_2^2(\Omega_p - \Omega_s)^2$$

is based on the conversion of the change in the one-half of the tangential component of the velocity squared, irreversibly into internal energy. To show this, note that the incidence of the relative velocity at the inlet to the turbine is β_2 since the blades are radial. This leads to a leading-edge separation, after which the flow reattaches to the blade. After this reattachment, the radial component of the relative velocity is the same as in the flow incident on the blade.

12.6 For a fluid coupling for which $r_1/r_2 = 0.7$, develop an expression from which by differentiation the value of the slip at which the power is maximum may be obtained. [Ans: 0.395]

12.7 A torque converter operates with oil flowing in a closed circuit. It consists of a torus with a pump, a turbine, and a stator. The input and output rotational speeds are 4000 and 1200 rpm, respectively. At this operating condition, the torque exerted on the stator is twice that exerted on the pump. Evaluate (a) the output to input torque ratio and (b) the efficiency. [Ans: (a) 3, (b) 0.9]

12.8 A torque converter is designed to provide torque multiplication ratio of 3.3 to 1. The circulating oil flow rate is 500 kg/s. The oil enters the fixed vanes in the axial direction at 10 m/s, and leaves at an angle 60° in the direction of the blade motion. The axial flow area is constant. Find the torque that the primary exerts on the fluid and the torque by the fluid on the blades of the secondary. The inlet and outlet radii of fixed vanes are 15 cm. [Ans: 565 N m, 1864 N m]

12.9 Develop the Eqs. (12.7) and (12.10). At what ratio of the rotational speeds is the efficiency maximum? From this and the experimental curves shown in the text, estimate (a) the ratio r_2/r_3 , (b) the value of $Qr_1 \tan \alpha_1 / Ar_3^2 \Omega_p$, and (c) efficiency. [Ans: (a) 0.92, (b) 0.584, (c) 0.68. Note that estimated efficiency is quite a bit lower than what is plotted.]

CHAPTER 13

WIND TURBINES

A brief history of wind turbines was given in Chapter 1. The early uses for grinding grain and lifting water have been replaced by the need to generate electricity. For this reason, the designation *windmill* has been dropped and it has been replaced by a *wind turbine*. Wind turbines, such as are shown in Figure 13.1, are the most rapidly growing renewable energy technology, but as they provide for only 2.5% of the primary energy production in the world, it will take a long time before their contribution becomes significant. Since the installed base of wind turbines is still relatively small, even a large yearly percentage increase in their use does not result in a large increase in the net capacity. But the possibility of growing wind capacity is large. China leads the world in installed capacity, followed by the United States, Germany, India, and Spain. The most windy regions of the United States are in the North and South Dakotas. These states, as well as the mountain ridges of Wyoming, the high plains of Texas, and the mountain passes of California, have seen the early gains in the number of wind turbines.

In countries such as Denmark and Germany, the growth of wind turbine power has been quite rapid. The winds from the North Sea provide particularly good wind prospects both onshore and offshore in Denmark's Jutland. In fact, during the year 2015, 42% of Denmark's electricity was generated from wind, and the entire power needs of western Denmark are provided by its windfarms on the windiest days. The installed capacity at the end of year 2015 was 5070 MW. The capacity factor is a modest 23% cent, owing to the intermittency of wind.

In Germany, during the years 2001–2004 wind turbines were put into operation at the rate of two each day. The installed capacity reached 55600 MW at the end of year 2017, and



Figure 13.1 A Darrieus rotor (a) and a windfarm of modern wind turbines (b).

this was based on some 26800 units. They provided about 18.7% of Germany's electricity that year.

The cost of generating electricity from wind has dropped greatly since the 1980s. With the rising costs of fossil fuels and nuclear energy, it is now competitive with the plants using these fuels as sources of power.

13.1 HORIZONTAL-AXIS WIND TURBINE

Aerodynamic theory of wind turbines is similar to that of airplane propellers. Propeller theory, in turn, originated from efforts to explain the propulsive power of marine propellers. The first ideas for them were advanced by W. J. M. Rankine in 1865 [73]. They are based on what has come to be called the *momentum theory of propellers*. It ignores the blades completely and replaces them by an *actuator disk*. The flow through the disk is separated from the surrounding flow by a streamtube, which is called a *slipstream* downstream of the disk. For a wind turbine, as energy is drawn from the flow, the axial velocity in the slipstream is lower than that of the surrounding fluid. Some of the energy is also converted into the rotational motion of the wake.

The next advance was by W. Froude in 1878 [28]. He considered how a *screw propeller* imparts a torque and a thrust on the fluid that flows across an *element of a blade*. This *blade element theory* was developed further by S. Drzewieci at the beginning of the twentieth century. During the same period contributions were made by N. E. Joukowski in Russia, A. Betz and L. Prandtl in Germany, and F. W. Lancaster in Great Britain. These studies were compiled into a research monograph on *airscrews* by H. Glauert [31]. He also made important contributions to the theory at a time when aerodynamic research took on great urgency with the development of airplanes. In addition to marine propellers, aircraft propellers, and wind turbines, the theory of screw propellers can also be used in the study of helicopter rotors, hovercraft propulsion, unducted fans, axial pumps, and propellers in hydraulic turbines. The discussion below begins by following Glauert's presentation.

The aim of theoretical study of wind turbines is to determine what the length of blades should be for nominal wind conditions at a chosen site, and how the chord, angle of twist, and shape should vary along the span of the blade to give the blade the best aerodynamical performance. Thickness of the cross section of the blade is determined primarily by

structural considerations, but a well-rounded leading edge performs better at variable wind conditions than a thin blade, so the structural calculations and aerodynamic analysis are complementary tasks.

13.2 MOMENTUM THEORY OF WIND TURBINES

In momentum theory, an airscrew is replaced by an *actuator disk*. When it functions as a propeller, it imparts energy to the flow; when it represents the blades of a wind turbine, it draws energy from the flow.

13.2.1 Axial momentum

To analyze the performance of a windmill by momentum theory, consider the control volume shown in Figure 13.2. The lateral surface of this control volume is that of a streamtube that divides the flow into a part that flows through the actuator disk and an external stream. Assuming that the flow is incompressible and applying the mass balance to this control volume gives

$$A_a V = A V_d = A_b V_b$$

in which A_a is the inlet area and A_b is the outlet area. The approach velocity of the wind is V and the downstream velocity is V_b . The disk area is A , and the velocity at the disk is V_d .

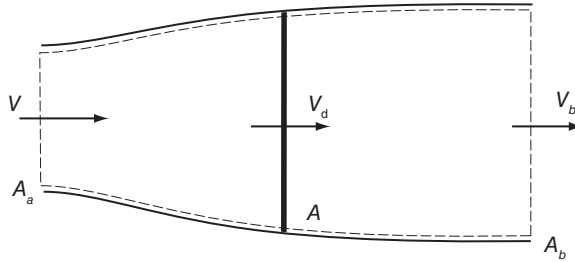


Figure 13.2 Control volume for application of the momentum theory for a wind turbine.

If there is *no rotation* in the slipstream, and velocity and pressure at the inlet and exit are uniform, then an energy balance applied to the control volume gives

$$\dot{m} \left(\frac{p_a}{\rho} + \frac{1}{2} V^2 \right) = \dot{W} + \dot{m} \left(\frac{p_a}{\rho} + \frac{1}{2} V_b^2 \right) \quad (13.1)$$

which gives for the specific work the expression

$$w = \frac{1}{2} (V^2 - V_b^2) \quad (13.2)$$

Introducing the stagnation pressures

$$p_{0+} = p_a + \frac{1}{2} \rho V^2 \quad p_{0-} = p_a + \frac{1}{2} \rho V_b^2$$

into Eq. (13.1), gives for the specific work the alternate form

$$w = \frac{p_{0+} - p_{0-}}{\rho} \quad (13.3)$$

and the specific work is evidently uniform across the disk. Making use of the fact that velocity V_d at the disk is the same on both sides, this can also be written as

$$w = \frac{p_+ - p_-}{\rho} \quad (13.4)$$

in which p_+ and p_- are the corresponding static pressures. Force balance across the disk gives

$$F_d = (p_+ - p_-)A \quad (13.5)$$

The force on the disk is also obtained by applying the momentum theorem to the control volume and assuming that the pressure along its lateral boundaries has a uniform value p_a . This yields

$$F_d = \int_A \rho V_d (V - V_b) dA = \rho A V_d (V - V_b) \quad (13.6)$$

and F_d here and in Eq. (13.5) is the force that the disk exerts on the fluid. It has been taken to be positive when it acts in the upstream direction. Equating Eq. (13.6) to Eq. (13.5) and making use of Eq. (13.3) gives

$$\rho V_d (V - V_b) = p_+ - p_- = \rho w$$

Substituting Eq. (13.2) for work gives

$$V_d (V - V_b) = \frac{1}{2} (V^2 - V_b^2) = \frac{1}{2} (V - V_b)(V + V_b)$$

from which it follows that

$$V_d = \frac{1}{2} (V + V_b)$$

Velocity at the disk is seen to be the arithmetic mean of the velocities in the free stream and in the far wake. Changes in velocity, total pressure, kinetic energy, and static pressure in the axial direction are shown in Figure 13.3.

A consequence of this analysis is that power delivered by the turbine is

$$\dot{W} = \rho A V_d w = A V_d (p_{0+} - p_{0-}) = A V_d (p_+ - p_-) = F_d V_d$$

This is a curious result, for in the previous chapters, the work delivered by a turbine was always related to a change in the tangential velocity of the fluid, which produces a torque on a shaft. To reconcile this, one may imagine the actuator disk to consist of two sets of blades rotating in opposite directions such that the flow enters and leaves the set axially. Each rotor extracts energy from the flow with the total power delivered as given above. Also, since the velocity entering and leaving the disk is the same, it is seen that work extracted is obtained by the reduction in static pressure across the disk. This sudden drop in static pressure is shown schematically in Figure 13.3.

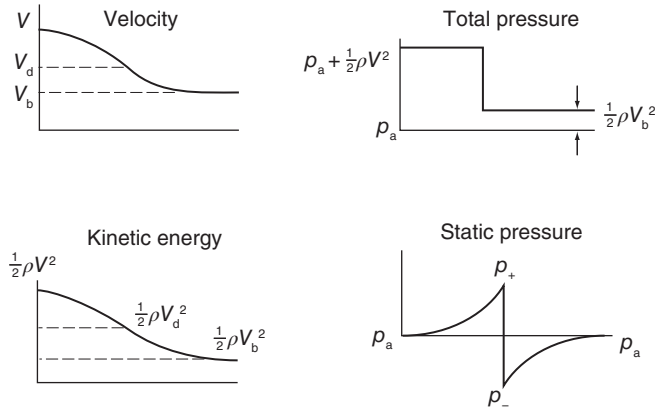


Figure 13.3 Variation of the different flow variables in the flow.

It is customary to introduce an *axial induction*, or *interference factor*, defined as

$$a = \frac{V - V_d}{V}$$

so that the velocities at the disk and far downstream are

$$V_d = (1 - a)V \quad V_b = (1 - 2a)V \quad (13.7)$$

The second of these equations shows that if $a > \frac{1}{2}$, there will be reverse flow in the wake and simple momentum theory has broken down. The axial force on the blades is given by

$$F_d = \rho V_d (V - V_b) A = 2a(1 - a)\rho A V^2 \quad (13.8)$$

A force coefficient defined as

$$C_x = \frac{F_d}{\frac{1}{2}\rho V^2} = 4a(1 - a) \quad (13.9)$$

is seen to depend on the induction factor. The power delivered to the blades is

$$\dot{W} = \frac{1}{2}\rho V_d A (V^2 - V_b^2) = 2a(1 - a)^2 \rho A V^3 \quad (13.10)$$

from which the power coefficient, defined as

$$C_p = \frac{\dot{W}}{\frac{1}{2}\rho A V^3} = 4a(1 - a)^2 \quad (13.11)$$

is also a function of the induction factor only. Maximum power coefficient is obtained by differentiating this with respect to a , which gives

$$4(1 - a)(1 - 3a) = 0 \quad \text{so that} \quad a = \frac{1}{3}$$

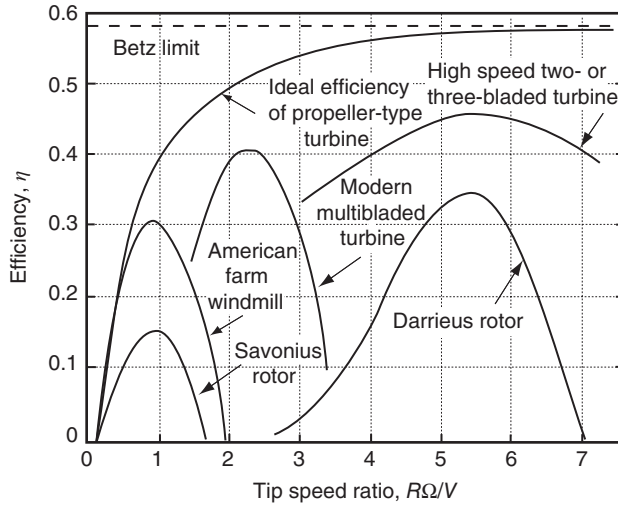


Figure 13.4 Efficiencies of various wind turbines.

If the efficiency is defined as the ratio of power delivered to that in the stream moving with speed V over an area A , which is $\rho AV^3/2$, then the efficiency and power coefficient are defined by the same equation. The maximum efficiency is seen to be

$$\eta = \frac{16}{27} = 0.593$$

This is called the *Betz limit*. Efficiencies of various wind turbines are shown in Figure 13.4.

Depending on their design, modern wind turbines operate at tip speed ratios $R\Omega/V$ in the range 1–6. In the upper part of this range, the number of blades is from one to three, and in the lower end, wind turbines are constructed with up to two dozen blades, as is shown in the American wind turbine in Figure 1.4.

The flow through the actuator disk and its wake patterns have been studied for propellers, wind turbines, and helicopters. Helicopters, in particular, operate under a variety of conditions, for the flow through the rotor provides a thrust at climb and a brake during descent. The various flow patterns are summarized in the manner of Eggleston and Stoddard [27] in Figure 13.5. The representation of the axial force coefficient was extended by Wilson and Lissaman [98] to the brake range $a > 1$, by rewriting it as

$$C_x = 4a|1 - a|$$

This explains the discontinuity in the slope at $a = 1$. For $a < 0$, the airscrew operates as a propeller. The limit of vanishing approach velocity corresponds to a tending to a large negative value at a rate that keeps V_d finite, while V tends to zero. Under this condition, the airscrew functions as an unducted axial fan. Since the flow leaves the fan as a jet, pressure is atmospheric short distance into the wake, and with a pressure increase across the fan, pressure will be lower than atmospheric at the inlet to the fan. This low pressure causes the ambient air to accelerate toward the front of the fan. At a given rotational speed, proper orientation of the blades gives a smooth approach. A slipstream forms downstream of the fan, separating the wake from the external flow. The wake is in angular rotation, and

vorticity that is shed from the blades forms a cylindrical vortex sheet that constitutes the boundary of the slipstream. As a consequence, at the slipstream boundary, velocity changes discontinuously from the wake to the surrounding fluid. This discontinuous change and rotation are absent in the flow upstream of the disk where the flow is axial, if the small radial component near the disk is neglected.

As the approach velocity increases to some small value V , the airscrew functions as a propeller, in which case V can be taken to be the velocity of an airplane flying through still air. The continuity equation now shows that the mass flow rate \dot{m} across the propeller comes from an upstream cylindrical region of area A_a , given by $A_a = \dot{m}/\rho V$, and the area decreases as the velocity V increases.

A further increase in the approach velocity leads to a condition at which $a = 0$. At this state, no energy is imparted to, or extracted from, the flow, and the slipstream neither expands nor contracts. As the velocity V increases from this condition, the angle of attack changes to transform what was the pressure side of the blade into the suction side, and the airscrew then extracts energy from the flow. The airscrew under this condition operates as a wind turbine. The blades are naturally redesigned so that they function optimally when they are used to extract energy from the wind. In a wind turbine, pressure increases as it approaches the plane of the blades and drops across them. The diameter of the slipstream, in contrast to that of a propeller, increases in the downstream direction.

For $a > \frac{1}{2}$, the slipstream boundary becomes unstable and forms vortex structures that mix into the wake. This is shown in Figure 13.5 as the *turbulent wake* state. The theoretical curve in the figure no longer holds, and an empirical curve of Glauert gives the value of the force coefficient in this range. At the condition $a = 1$, the flow first enters a *vortex ring* state and for large values, a *brake state*. Flows in these regions are sufficiently complex that they cannot be analyzed by elementary methods.

The aim of wind turbine theory is to explain how the induction factors change as a result of design and operating conditions. When the theory is developed further, it will be seen that wind turbines operate in the range $0 < a < \frac{1}{2}$, which is consistent with the momentum theory.

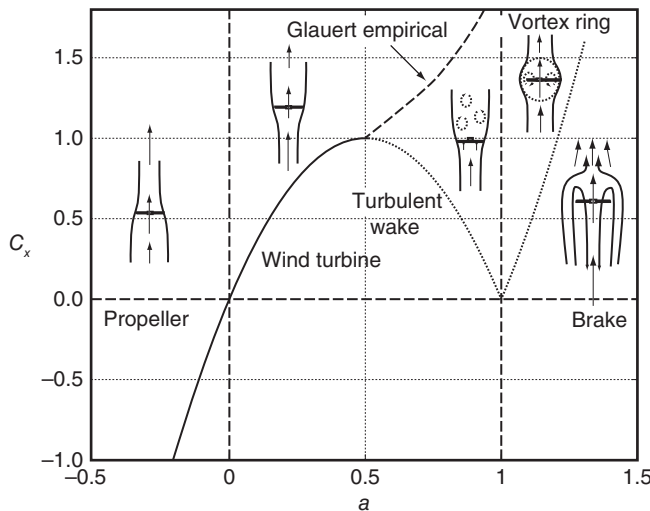


Figure 13.5 Operational characteristics of an airscrew. Source: After Eggleston and Stoddard [27].

13.2.2 Ducted wind turbine

Insight can be gained by repeating the analysis for a wind turbine placed in a duct and then considering the limit as the duct radius tends to infinity. Such an arrangement is shown in Figure 13.6. Applying the momentum equation to the flow through the control volume containing the slipstream gives

$$F_d - \int_{A_b} \rho V_b (V_b - V) dA_b = R + p_a A_a - p_b A_b \quad (13.12)$$

in which R is the x component of the net pressure force that the fluid outside the streamtube (consisting of the slipstream and its upstream extension) exerts on the fluid inside. For the flow outside this streamtube, the momentum balance leads to

$$p_a (A_e - A_a) - p_b (A_e - A_b) - R = \rho V_c (V_c - V) (A_e - A_b)$$

which can be recast as

$$R = p_a (A_b - A_a) + (p_a - p_b) (A_e - A_b) + \rho V (V - V_c) (A_e - A_a)$$

The pressure difference $p_a - p_b$ can be eliminated by using the Bernoulli equation

$$p_a + \frac{1}{2} \rho V^2 = p_b + \frac{1}{2} \rho V_c^2,$$

which transforms the expression for R into

$$R = p_a (A_b - A_a) - \frac{1}{2} \rho (V^2 - V_c^2) (A_e - A_b) + \rho V (V - V_c) (A_e - A_a)$$

or

$$R = p_a (A_b - A_a) - \frac{1}{2} \rho (V - V_c) [(V + V_c) (A_e - A_b) - 2V (A_e - A_a)]$$

The continuity equation for the flow outside the slipstream yields

$$V_c (A_e - A_b) = V (A_e - A_a)$$

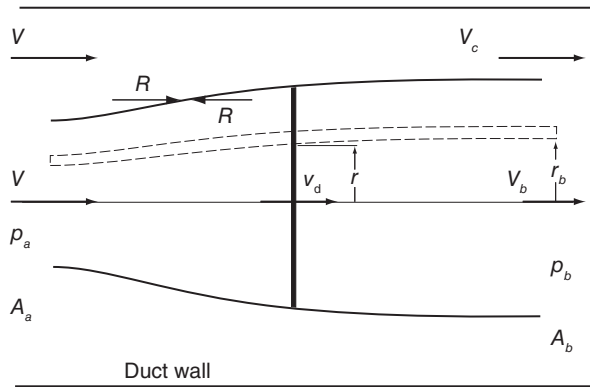


Figure 13.6 A ducted wind turbine.

so that

$$V - V_c = V \frac{A_a - A_b}{A_e - A_b} \quad V + V_c = V \frac{2A_e - A_a - A_b}{A_e - A_b}$$

Substituting these into the equation for R leads to

$$R = p_a(A_b - A_a) - \frac{1}{2}\rho V^2 \frac{(A_b - A_a)^2}{A_e - A_b}$$

This shows that, as A_e becomes large in comparison to A_a and A_b , then

$$R = p_a(A_b - A_a)$$

The extra term then accounts for the variable pressure along the streamtube boundary. That the pressure is not exactly atmospheric along this boundary is also clear by noting that whenever streamlines are curved, pressure increases in the direction from the concave to the convex sides. Also, as the axial velocity decreases, pressure increases, but this is compensated partly by the flow acquiring a small radial velocity as the area of the streamtube increases downstream.

Equation (13.12) for the force on the blades now takes the form

$$\begin{aligned} F_d - \int_{A_b} \rho V_b (V_b - V) dA_b &= R + p_a A_a - p_b A_b \\ &= (p_a - p_b) A_b - \frac{1}{2}\rho V^2 \frac{(A_b - A_a)^2}{A_e - A_b} \\ &= \frac{1}{2}\rho (V_c^2 - V^2) A_b - \frac{1}{2}\rho V^2 \frac{(A_b - A_a)^2}{A_e - A_b} \end{aligned}$$

Since

$$V_c^2 - V^2 = (V_c - V)(V_c + V) = V^2 \left(\frac{A_b - A_a}{A_e - A_b} \right) \left(\frac{2A_e - A_a - A_b}{A_e - A_b} \right)$$

this can be written as

$$F_d - \int_{A_b} \rho V_b (V_b - V) dA_b = \frac{1}{2}\rho V^2 \frac{(A_b - A_a)}{(A_e - A_b)^2} [A_e(A_a + A_b) - 2A_a A_b]$$

For large A_e , this reduces to

$$F_d = \int_{A_b} \rho V_b (V - V_b) dA_b \quad (13.13)$$

This is equivalent to Eq. (13.6) obtained above. It is now assumed that this equation is also valid for each annular element of the streamtube shown in Figure 13.6. The differential form can be written as

$$dF_d = \rho V_b (V - V_b) dA_b = \rho V (V - V_b) dA$$

The analysis based on this equation is called a *blade element analysis* and is justified if no interactions take place between adjacent annular elements. This assumption has been criticized by Goorjian [33], but evidently in many applications of the theory, the error is small.

13.2.3 Wake rotation

Wake rotation was included in the theory by Joukowsky in 1918, and its presentation can be found in Glauert [31]. This theory is considered next.

The continuity equation for an annular section of the slipstream gives

$$V_{dx} dA = V_{bx} dA_b \quad \text{or} \quad V_{dx} r dr = V_{bx} r_b dr_b \quad (13.14)$$

The axial component of velocity at the disk is denoted by V_{dx} and in the far wake is V_{bx} . The value of the radial location r_b far downstream depends on the radial location r at the disk. Since no torque is applied on the flow in the slipstream after it has passed through the disk, moment of momentum balance for the flow yields

$$r V_{du} V_{dx} 2\pi r dr = r_b V_{bu} V_{bx} 2\pi r_b dr_b$$

in which V_{du} is the tangential component of velocity just behind the disk and V_{bu} is its value in the distant wake. Using Eq. (13.14), this reduces to

$$r V_{du} = r_b V_{bu} \quad (13.15)$$

This means that the angular momentum remains constant. If the rotation rate is defined by $\omega = V_u/r$, then this can be written as

$$r^2 \omega = r_b^2 \omega_b \quad (13.16)$$

Velocity triangles for the flow entering and leaving the blades are shown in Figure 13.7. The rotation in the wake is in the direction opposite to blade rotation. Since trothalpy is constant across the blades, it follows that

$$h_+ + \frac{1}{2} W_+^2 = h_- + \frac{1}{2} W_-^2$$

and for isentropic incompressible flow, this reduces to

$$p_+ + \frac{1}{2} \rho (V_{dx}^2 + r^2 \Omega^2) = p_- + \frac{1}{2} \rho [V_{dx}^2 + (r\Omega + r\omega)^2]$$

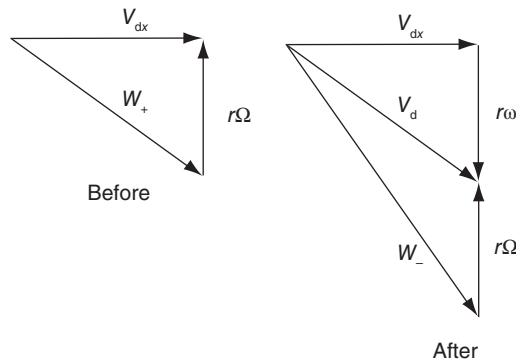


Figure 13.7 A velocity triangle for the flow leaving the blades of a wind turbine.

which simplifies to

$$p_+ = p_- + \rho \left(\Omega + \frac{1}{2} \omega \right) r^2 \omega \quad (13.17)$$

The Bernoulli equation upstream of the disk yields

$$\frac{p_a}{\rho} + \frac{1}{2} V^2 = \frac{p_+}{\rho} + \frac{1}{2} V_{dx}^2$$

and downstream it gives

$$\frac{p_-}{\rho} + \frac{1}{2} V_{dx}^2 + \frac{1}{2} r^2 \omega^2 = \frac{p_b}{\rho} + \frac{1}{2} V_{bx}^2 + \frac{1}{2} r_b^2 \omega_b^2$$

Adding the last two equations and using Eq. (13.17) to eliminate the pressure difference $p_+ - p_-$ leads to

$$\frac{p_a}{\rho} - \frac{p_b}{\rho} = \frac{1}{2} (V_{bx}^2 - V^2) + \left(\Omega + \frac{1}{2} \omega_b \right) r_b^2 \omega_b \quad (13.18)$$

Differentiating this with respect to r_b gives

$$-\frac{1}{\rho} \frac{dp_b}{dr_b} = \frac{1}{2} \frac{d}{dr_b} (V_{bx}^2 - V^2) + \frac{d}{dr_b} \left[\left(\Omega + \frac{1}{2} \omega_b \right) r_b^2 \omega_b \right]$$

Since the radial pressure variation in the downstream section is also given by

$$\frac{1}{\rho} \frac{dp_b}{dr_b} = \frac{V_{bu}^2}{r_b} = r_b \omega_b^2$$

equating these two pressure gradients produces

$$\frac{1}{2} \frac{d}{dr_b} (V_{bx}^2 - V^2) = -\frac{d}{dr_b} \left[\left(\Omega + \frac{1}{2} \omega_b \right) r_b^2 \omega_b \right] - r_b \omega_b^2$$

or

$$\begin{aligned} \frac{1}{2} \frac{d}{dr_b} (V_{bx}^2 - V^2) &= -\Omega \frac{dr_b^2 \omega_b}{dr_b} - r_b \omega_b^2 - r_b^2 \omega_b \frac{d\omega_b}{dr_b} - r_b \omega_b^2 \\ &= -\Omega \frac{dr_b^2 \omega_b}{dr_b} - \omega_b \left(2r_b \omega_b + r_b^2 \frac{d\omega_b}{dr_b} \right) \\ &= -(\Omega + \omega_b) \frac{dr_b^2 \omega_b}{dr_b} \end{aligned} \quad (13.19)$$

Momentum balance for the streamtube containing the flow through the disk yields

$$\int_{A_b} \rho V_{bx} (V_{bx} - V) dA_b = \int_{A_b} (p_a - p_b) dA_b - F_d$$

Assuming that this is also valid for an annular element yields

$$dF_d = \rho V_{bx} (V - V_{bx}) dA_b + (p_a - p_b) dA_b$$

This elemental force is related to the pressures difference across the disk, which according to Eq. (13.17) can be related to rotation as

$$dF_d = (p_+ - p_-)dA = \rho \left(\Omega + \frac{1}{2}\omega \right) r^2 \omega dA$$

When Eq. (13.14) is used, this takes the form

$$dF_d = \rho \left(\Omega + \frac{1}{2}\omega \right) r^2 \omega \frac{V_{bx}}{V_{dx}} dA_b$$

Therefore, the momentum balance for an elemental annulus becomes

$$\rho V_{bx}(V - V_{bx}) + p_a - p_b = \rho \left(\Omega + \frac{1}{2}\omega \right) r^2 \omega \frac{V_{bx}}{V_{dx}}$$

Eliminating the pressure difference $p_a - p_b$ by making use of Eq. (13.18) gives

$$V_{bx}(V - V_{bx}) - \frac{1}{2}(V^2 - V_{bx}^2) + \left(\Omega + \frac{1}{2}\omega_b \right) r_b^2 \omega_b = \left(\Omega + \frac{1}{2}\omega \right) r^2 \omega \frac{V_{bx}}{V_{dx}}$$

which simplifies to

$$\frac{(V - V_{bx})^2}{2 V_{bx}} = \frac{(\Omega + \frac{1}{2}\omega_b)r_b^2\omega_b}{V_{bx}} - \frac{(\Omega + \frac{1}{2}\omega)r^2\omega}{V_{dx}} \quad (13.20)$$

This is the main result of Joukowski's analysis. If ω_b is now specified, then Eq. (13.19) can be solved for $V_{bx}(r_b)$. After this, from Eq. (13.16), rotation $\omega(r, r_b)$ at the disk can be obtained as a function of r and r_b . The axial velocity $V_{dx}(r, r_b)$ at the disk is then obtained from Eq. (13.20). Substituting these into the continuity equation [Eq. (13.14)] gives a differential equation that relates r_b to r . Appropriate boundary conditions fix the values for the integration constants.

13.2.4 Irrotational wake

The analysis of the previous section is valid for an arbitrary rotational velocity distribution in the wake. An important special case is to assume the wake to be irrotational. Then $r^2\omega = r_b^2\omega_b = k$ is constant. Equation (13.19) then shows that V_{bx} is constant across the wake, and Eq. (13.20) can be recast into the form

$$\frac{V_{dx}}{V_{bx}} \left[\frac{1}{2}(V - V_{bx})^2 - \left(\Omega + \frac{k}{2r_b^2} \right) k \right] = - \left(\Omega + \frac{k}{2r^2} \right) k \quad (13.21)$$

Writing Eq. (13.14) as

$$\frac{V_{dx}}{V_{bx}} = \frac{r_b}{r} \frac{dr_b}{dr}$$

and making use of it in Eq. (13.21) leads to

$$\left[\frac{1}{2}(V - V_{bx})^2 - \Omega k \right] r_b dr_b - \frac{k^2}{2} \frac{dr_b}{r_b} = -\Omega k r dr - \frac{k^2}{2} \frac{dr}{r}$$

Integrating this gives

$$\left[\frac{1}{2}(V - V_{bx})^2 - \Omega k \right] \frac{r_b^2}{2} - \frac{k^2}{2} \ln \frac{r_b}{\epsilon R_b} = -\Omega k \frac{r^2}{2} - \frac{k^2}{2} \ln \frac{r}{\epsilon R}$$

where R is the disk radius and R_b the downstream slipstream radius. Owing to the logarithmic singularity, the lower limits of integration were taken to be ϵR and ϵR_b , so that as ϵ tends to zero and the ratio $\epsilon R/\epsilon R_b$ tends to R/R_b . Thus the solution takes the form

$$\frac{1}{2}(V - V_{bx})^2 - \Omega k \left(1 - \frac{r^2}{r_b^2} \right) = r_b^2 \omega_b^2 \ln \left(\frac{r_b R}{r R_b} \right)$$

The most reasonable way to satisfy this equation is to choose the r dependence of r_b to be

$$r_b = \frac{R_b}{R} r$$

for the logarithmic term then vanishes and the second term is a constant, which balances the first constant term. Thus an equation is obtained that relates the far wake axial velocity to the slipstream radius R_b

$$\frac{1}{2}(V - V_{bx})^2 = \Omega k \left(1 - \frac{R^2}{R_b^2} \right) \quad (13.22)$$

Furthermore, the following ratios are obtained:

$$\frac{r^2}{r_b^2} = \frac{\omega_b}{\omega} = \frac{V_{bx}}{V_{dx}} = \frac{R^2}{R_b^2} \quad (13.23)$$

Following Glauert's notation [31], the previous equation can be put into a nondimensional form by introducing the parameters

$$\lambda = \frac{V}{R\Omega} \quad \mu = \frac{V_{dx}}{R\Omega} \quad \mu_b = \frac{V_{bx}}{R\Omega} \quad \frac{q}{\mu} = \frac{k}{R^2\Omega}$$

In terms of these parameters, Eq. (13.22) can be written as

$$q = \frac{\mu^2}{2} \frac{(\lambda - \mu_b)^2}{(\mu - \mu_b)} \quad (13.24)$$

Equation (13.18), namely

$$\frac{p_a}{\rho} - \frac{p_b}{\rho} = \frac{1}{2}(V_{bx}^2 - V^2) + \left(\Omega + \frac{1}{2}\omega_b \right) r_b^2 \omega_b$$

evaluated at the edge of the slipstream, where $p_b = p_a$, gives

$$\frac{1}{2}(V^2 - V_{bx}^2) = \left(\Omega + \frac{k}{2R_b^2} \right) k = \left(\Omega + \frac{k}{2R^2} \frac{V_{bx}}{V_{dx}} \right) k$$

In terms of the nondimensional parameters, this can be transformed into

$$\frac{1}{2}(\lambda^2 - \mu_b^2) = \left(1 + \frac{q}{2\mu} \frac{\mu_b}{\mu} \right) \frac{q}{\mu} \quad (13.25)$$

Eliminating q between this and Eq. (13.24) gives

$$4(\mu - \mu_b)(2\mu - \mu_b - \lambda) = \mu(\lambda - \mu_b)^3 \quad (13.26)$$

Equations (13.25) and (13.26) determine μ and μ_b in terms of ratio λ and q . Equation (13.26) can be written as

$$\mu = \frac{1}{2}(\lambda + \mu_b) + \frac{\mu(\lambda - \mu_b)^3}{8(\mu - \mu_b)} \quad (13.27)$$

or in dimensional variables as

$$V_{dx} = \frac{1}{2}(V + V_{bx}) + \frac{V_{dx}(V - V_{bx})^3}{8(V_{dx} - V_{bx})\Omega^2 R^2}$$

This shows that

$$V_{dx} > \frac{1}{2}(V + V_{bx})$$

Since rotation of the flow takes place only in the wake, this means that the axial velocity in the wake V_{bx} is smaller than its value in a nonrotating wake.

Introducing the induction factors a and b by equations

$$\mu = \lambda(1 - a) \quad \mu_b = \lambda(1 - b)$$

and substituting them into Eq. (13.27) gives

$$a = \frac{1}{2}b \left[1 - \lambda^2 \frac{(1 - a)b^2}{4(b - a)} \right] \quad (13.28)$$

which, when solved for a , gives

$$a = \frac{3b}{4} \left[1 - \frac{1}{12}\lambda^2 b^2 - \frac{1}{3}\sqrt{\left(1 - \frac{1}{4}\lambda^2 b^2\right)^2 + (2 - b)\lambda^2 b} \right]$$

It is customary in wind turbine analysis to replace the *advance ratio* λ by its reciprocal $X = R\Omega/V$, the tip speed ratio, and plot the values of b as a function of a with the tip speed ratio as a parameter. The curves, shown in Figure 13.8, clearly indicate that for X greater than 3, the approximation $b = 2a$ is quite accurate.

For large values of X , the induction factor a can be approximated by

$$a = \frac{b}{2} - \frac{b^2}{4} \left(1 - \frac{b}{2} \right) \frac{1}{X^2} + O\left(\frac{1}{X^4}\right)$$

Writing this as

$$b = 2a + \frac{b^2}{2} \left(1 - \frac{b}{2} \right) \frac{1}{X^2} + O\left(\frac{1}{X^4}\right)$$

and after replacing b by $2a$ in the higher-order terms, gives

$$b = 2a \left[1 + \frac{a(1 - a)}{X^2} \right] + O\left(\frac{1}{X^4}\right)$$

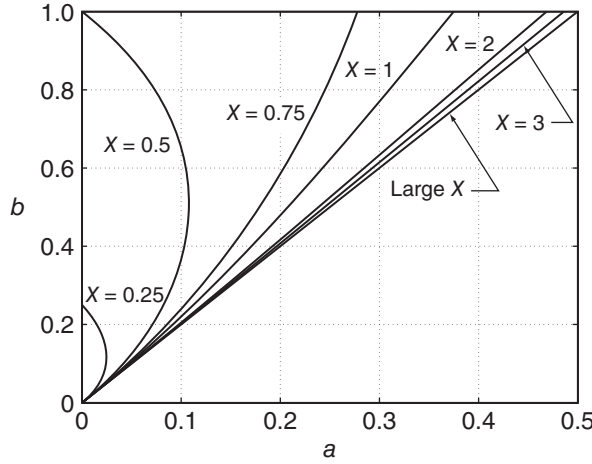


Figure 13.8 Induction factors for an irrotational wake.

This formula gives an estimate of the extent to which the axial velocity in the wake has been reduced as a result of wake rotation.

The expression for torque is

$$dT = 2\pi\rho V_{dx}rV_{du}r dr = 2\pi\rho V_{dx}kr dr,$$

which when integrated over the span gives

$$T = \rho AV_{dx}k$$

Hence, the torque coefficient

$$C_T = \frac{T}{\rho A \Omega^2 R^3} = \frac{V_{dx}k}{\Omega^2 R^3} = q$$

is given by the parameter q . With $\dot{W} = T\Omega$, the power coefficient becomes

$$C_p = \frac{T\Omega}{\rho V A \frac{1}{2} V^2} = \frac{2q}{\lambda^3} = \frac{b^2(1-a)^2}{b-a}$$

Since $r^2\omega$ is constant, the rate of rotation in an irrotational wake increases with decreasing radius, and for small enough radius, the rotation rate becomes unreasonably large. This leads to an infinite value for the power coefficient. To remedy this, the wake structure needs modification, and a reasonable model is obtained by making it a combination of solid body rotation at small radii and free vortex flow over large radii. The power coefficient for this, called the *Rankine combined vortex*, was stated by Wilson and Lissaman to be

$$C_p = \frac{b(1-a)^2}{b-a} [2aN + b(1-N)]$$

in which $N = \Omega/\omega_{\max}$. The details on how to develop this are not in their report, and it appears that in order to develop it, some assumptions need to be made [98].

13.3 BLADE ELEMENT THEORY

The blade forces can be calculated at each location of the span by the blade element analysis. This is carried out for an annular slice of thickness dr from the disk, as is shown in Figure 13.9. Across each blade element, airflow is assumed to be the same as that for an isolated airfoil. The situation in which wake rotation is ignored is considered first. Then the general analysis including wake rotation and Prandtl's tip loss model is discussed.

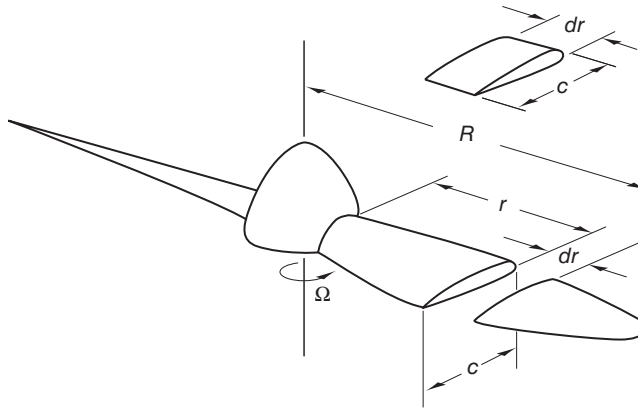


Figure 13.9 Illustration of a blade element.

13.3.1 Nonrotating wake

If the wake rotation is ignored, the velocity triangle at the midchord is as shown in Figure 13.10. The approach velocity at the disk is $(1 - a)V$ and the blade element moves at the tangential speed $r\Omega$. The broken (dashed) line gives the direction of the chord and thus defines the blade pitch angle θ , which is measured from the plane of the disk. The angle of attack is α , and the flow angle of the relative velocity is $\phi = \alpha + \theta$, also measured from the plane of the disk.

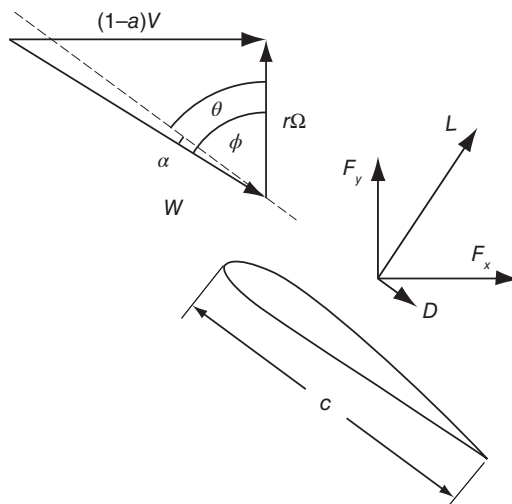


Figure 13.10 Illustration of the relative velocity across a blade.

The x and y components of the blade forces, expressed in terms of lift and drag, are

$$dF_x = (L \cos \phi + D \sin \phi) dr \quad dF_y = (L \sin \phi - D \cos \phi) dr$$

For small angles of attack, the lift coefficient is

$$C_L = 2\pi \sin \alpha = 2\pi \sin(\phi - \theta) = 2\pi(\sin \phi \cos \theta - \cos \phi \sin \theta)$$

From the velocity triangle

$$\sin \phi = \frac{(1-a)V}{W} \quad \cos \phi = \frac{r\Omega}{W},$$

so the lift coefficient can be written as

$$C_L = 2\pi \left[\frac{(1-a)V}{W} \cos \theta - \frac{r\Omega}{W} \sin \theta \right]$$

On an element of the blade of width dr , if drag is neglected, the x component of the force on the blade is

$$dF_x = L \cos \phi \, dr = \frac{1}{2} \rho W^2 c \, C_L \cos \phi \, dr$$

or

$$dF_x = \pi \rho c [(1-a)V \cos \theta - r\Omega \sin \theta] r \Omega \, dr$$

so that the blade force coefficient is

$$C_x = \frac{dF_x}{\frac{1}{2} \rho V^2 2\pi r \, dr} = \frac{r\Omega}{V} \frac{c}{r} \left[(1-a) \cos \theta - \frac{r\Omega}{V} \sin \theta \right]$$

The ratio c/r is part of the definition of solidity, which is defined as $\sigma = c \, dr / 2\pi r \, dr = c / 2\pi r$. With $x = r\Omega/V$, the blade speed ratio, the blade force coefficient becomes

$$C_x = 2\pi \sigma x [(1-a) \cos \theta - x \sin \theta] \quad (13.29)$$

The blade force coefficient can also be written as

$$C_x = 4a(1-a) = 4a|1-a| \quad (13.30)$$

where the absolute value signs have been inserted so that the propeller brake mode, for which the induction factor is larger than unity, is also taken into account. Following Wilson and Lissaman [98], the values of C_x from both Eqs. (13.29) and (13.30) are plotted in Figure 13.11. The operating state of the wind turbine is at the intersection of these curves. The straight-lines from Eq. (13.29) have a negative slope that depends mainly on the solidity times the blade speed ratio and weakly on angle θ . For $\theta = 0$, the blade force coefficient becomes zero at $a = 1$. The line for which $\theta_1 = \tan^{-1}(1/x)$ has the force coefficient zero at the value $a = 0$. Increasing the blade pitch angle further from this changes the operation from a wind turbine to a propeller. At $a = 0$, loading on the blades vanishes.

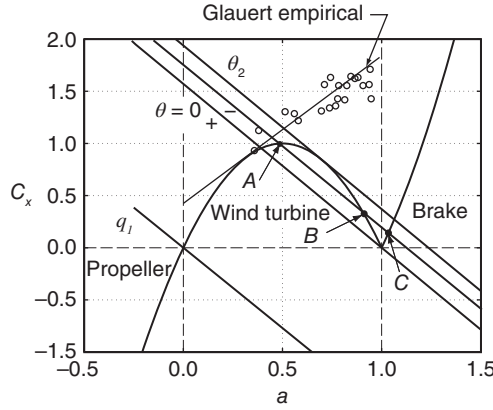


Figure 13.11 Blade force coefficient for different values of the interference factor. Source: Drawn after Wilson and Lissaman [98].

For $a = 1$, the blade angle becomes negative and the wind turbine operates as a propeller brake on the flow; that is with a propeller turning in one direction and the wind attempting to turn it in an opposite direction, the result is a braking action on the flow. This is best understood from the operation of helicopters. As they descend, their rotors attempt to push air into the direction in which they move and thereby cause a braking action on their descending motion.

Since in the far wake, the axial velocity is $(1 - 2a)V$, for states in the range $\frac{1}{2} < a < 1$, the simple momentum theory predicts a flow reversal somewhere between the disk and the far wake. Volkovitch [93] has shown that this anomaly disappears for yawed windmills, and momentum theory is still valid. Blade angles for a working range can be obtained by equating the two expressions for the blade force coefficient and solving the resulting equation for the interference factor. This gives

$$a = \frac{1}{4} [2 + \pi \sigma x \cos \theta \pm \sqrt{(2 - \pi \sigma x \cos \theta)^2 + 8 \pi \sigma x^2 \sin \theta}]$$

The two solutions of this equation are at points A and B, with point B corresponding to plus sign of the square root. The solution on this branch is unstable and can be ignored. The angle θ_2 is that for which the discriminant vanishes, and it can be determined as a root of

$$(2 - \pi \sigma x \cos \theta_2)^4 - 64 \pi^2 \sigma^2 x^4 (1 - \cos^2 \theta_2) = 0 \quad (13.31)$$

For a wind turbine at the span position where $\sigma = 0.03$ and blade speed ratio is $x = 4$, this comes out to be $\theta_2 = 12.76^\circ$.

The experimental curve of Glauert is for free-running rotors, which thus have a power coefficient zero. These correspond to states of autorotation of a helicopter. A line drawn through the data gives $C_{xe} = C_1 - 4(\sqrt{C_1} - 1)(1 - a)$, in which $C_1 = 1.8$ is the value of the blade force coefficient at $a = 1$, as obtained from the experimental data. The straight-line touches the parabola at $a^* = 1 - \frac{1}{2} \sqrt{C_1} = 0.33$.

■ EXAMPLE 13.1

Develop a MATLAB script to establish the value of θ_2 in Eq. (13.31) for various values of solidity and tip speed ratio.

Solution: The discriminant given by Eq. (13.31) is a fourth-order polynomial in $\cos \theta_2$; hence, the MATLAB procedure `roots` can be used to find the roots of this polynomial. Two of the roots are complex and can be disregarded. There is also an extraneous root, which arose when the expressions were squared. The script below gives the algorithm to calculate the roots:

```
sigma=0.03; x=4;
c(1)=(pi*sigma*x)^4; c(2)=-8*(pi*sigma*x)^3;
c(3)=24*(pi*sigma*x)^2*(1+8*x^2/3);
c(4)=-32*pi*sigma*x; c(5)=16-64*(pi*sigma*x^2)^2;
r=roots(c);
theta=min(acos(r)*180/pi);
```

For $\sigma = 0.03$ and $x = 4$, this gives $\theta_2 = 12.76^\circ$. ■

13.3.2 Wake with rotation

Figure 13.12 shows a schematic of a flow through a set of blades. As the blades turn the flow, the tangential velocity increases. If its magnitude is taken to be $2a'r\Omega$ after the blade, at some location as flow crosses the blade, it takes the value $a'r\Omega$. It is *assumed* that this coincides with the location at which relative velocity is parallel to the chord.¹

When drag is included, the axial force is given by

$$dF_x = (L \cos \phi + D \sin \phi) dr$$

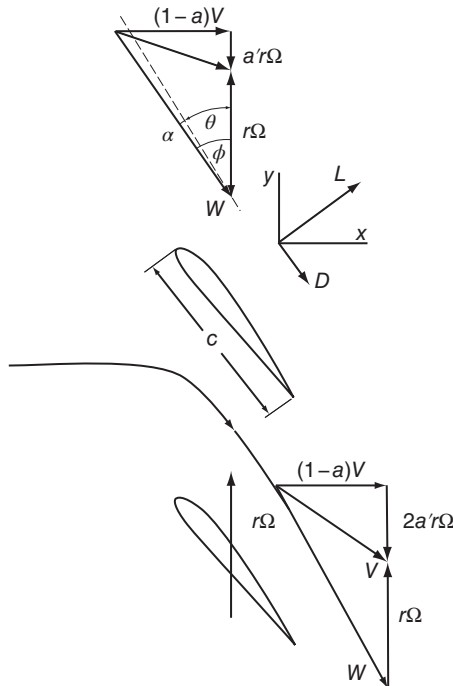


Figure 13.12 Illustration of the increase in tangential velocity across the disk.

¹This assumption is based on the examination of the induced velocity by the vortex structure in the wake.

and the torque is $dT = r dF_y$, or

$$dT = r(L \sin \phi - D \cos \phi) dr$$

Denoting the number of blades by Z , these can be expressed as follows:

$$dF_x = \frac{1}{2} \rho W^2 Z c (C_L \cos \phi + C_D \sin \phi) dr \quad (13.32)$$

$$dT = \frac{1}{2} \rho W^2 Z c r (C_L \sin \phi - C_D \cos \phi) dr \quad (13.33)$$

If the influence of wake rotation on the value of the static pressure at the exit is neglected, the momentum equation applied to an annular streamtube gives

$$dF_x = (V - V_b) \rho 2\pi r V_d dr = 4a(1-a)V^2 \rho \pi r dr$$

Equating this to dF_x in Eq. (13.32) gives

$$\frac{1}{2} W^2 Z c (C_L \cos \phi + C_D \sin \phi) = 4\pi r a(1-a)V^2 \quad (13.34)$$

The velocity diagram at the *mean chord position* is shown on the upper part of Figure 13.12. The relationships between the flow angle, relative velocity, and the axial and tangential components of absolute velocity are

$$\sin \phi = \frac{(1-a)V}{W} \quad \cos \phi = \frac{(1+a')r\Omega}{W} \quad (13.35)$$

With solidity defined now as $\sigma = Zc/2\pi r$, Eq. (13.34) can be recast as

$$\frac{a}{1-a} = \frac{\sigma(C_L \cos \phi + C_D \sin \phi)}{4 \sin^2 \phi} \quad (13.36)$$

Similarly, angular momentum balance applied to the elementary annulus gives

$$dT = r V_u d\dot{m} = r V_u \rho V_d 2\pi r dr = 4a'(1-a)\rho V \Omega r^3 \pi dr$$

and equating this to dT in Eq. (13.33) and making use of Eq. (13.35) yields

$$\frac{a'}{1+a'} = \frac{\sigma(C_L \sin \phi - C_D \cos \phi)}{4 \cos \phi \sin \phi} \quad (13.37)$$

Equations (13.36) and (13.37) can now be used to calculate the relationship between the parameters as follows. For a given blade element at location r/R , tip speed ratio $X = R\Omega/V$, and pitch angle θ , the solidity is $\sigma = Zc/2\pi r$ and the local blade speed ratio is $x = Xr/R = r\Omega/V$. With *assumed* values for a and a' , the angle ϕ , as seen from Figure 13.12, is calculated from

$$\tan \phi = \frac{1-a}{1+a'} \frac{1}{x} \quad (13.38)$$

and the angle of attack can then be determined from $\alpha = \phi - \theta$.

After this, the lift coefficient can be calculated from the theoretical relation $C_L = 2\pi \sin \alpha$ and the value of the drag coefficient is found from experimental data. It is often given in the form $C_D = \varepsilon C_L$ with ε having a value in the range of $0.003 < \varepsilon < 0.015$ as C_L increases toward 1.2. After this the value of a is calculated from Eq. (13.36) and a' from Eq. (13.37). With these new estimates, the calculations are repeated until the induction factors have converged. These calculations are demonstrated in the next example.

■ EXAMPLE 13.2

A three-bladed wind turbine with a rotor diameter of 40 m operates at the tip speed ratio 4. The blade has a constant chord of 1.2 m and a pitch angle of 12° . The drag-to-lift ratio is 0.005. Calculate the axial and angular induction factors at $r/R = 0.7$.

Solution: For given α , the lift and drag coefficients are calculated from

$$C_L = 2\pi \sin \alpha \quad C_D = \varepsilon C_L$$

The rest of the solution is carried out by iterations. First, for initial guesses for a and a'

$$\tan \phi = \frac{1 - a}{1 + a' x} \frac{1}{x}$$

is solved for ϕ . Then the axial and tangential force coefficients are defined as

$$C_x = C_L \cos \phi + C_D \sin \phi \quad C_y = C_L \sin \phi - C_D \cos \phi$$

and the axial and tangential induction factors are calculated from

$$\frac{a}{1 - a} = \frac{\sigma C_x}{4 \sin^2 \phi} \quad \frac{a'}{1 + a'} = \frac{\sigma C_y}{4 \cos \phi \sin \phi}$$

or in explicit form, from

$$a = \frac{\sigma C_x}{4 \sin^2 \phi + \sigma C_x} \quad a' = \frac{\sigma C_y}{4 \cos \phi \sin \phi - \sigma C_y}$$

These give new values for a and a' , and the process is repeated. After the iterations have converged, the final value of the angle of attack is determined from

$$\alpha = \phi - \theta$$

A MATLAB script gives the steps to carry out the calculations:

```
X=4; rR=0.7; R=20; theta=12*pi/180;
Z=3; c=1.2; ep=0.005; a(1)=0; ap(1)=0;
x=rR*X;
phi(1)=atan((1-a(1))/((1+ap(1))*x));
alpha(1)=phi(1)-theta;
CL(1)=2*pi*sin(alpha(1)); CD(1)=ep*CL(1);
Cx(1)=CL(1)*cos(phi(1))+CD(1)*sin(phi(1));
Cy(1)=CL(1)*sin(phi(1))-CD(1)*cos(phi(1));
```

```

sigma=Z*c/(2*pi*R*rR); imax=5;
for i=2:imax
    a(i)=sigma*Cx(i-1)/(4*sin(phi(i-1))^2+sigma*Cx(i-1));
    ap(i)=sigma*Cy(i-1)/(4*sin(phi(i-1))*cos(phi(i-1))-sigma*Cy(i-1));
    phi(i)=atan((1-a(i))/(1+ap(i))*x);
    alpha(i)=phi(i)-theta;
    CL(i)=2*pi*sin(alpha(i));    CD(i)=ep*CL(i);
    Cx(i)=CL(i)*cos(phi(i))+CD(i)*sin(phi(i));
    Cy(i)=CL(i)*sin(phi(i))-CD(i)*cos(phi(i));
end
fid=fopen('induction','w'); i=[1:imax];
fprintf(fid,'%12i%12.8f%12.8f\n',[i;a;ap]);
fclose(fid);

```

Convergence of the induction factors a and a' are given as follows:

| i | a | a' |
|-----|---------|----------|
| 1 | 0.00000 | 0.000000 |
| 2 | 0.06665 | 0.009046 |
| 3 | 0.06366 | 0.007349 |
| 4 | 0.06389 | 0.007451 |
| 5 | 0.06387 | 0.007443 |

■

The induction factor for the wake rotation is seen to be one order of magnitude smaller than that for axial flow. Were the tip speed ratio smaller, the wake rotation would be more pronounced. The next example extends the analysis to the entire span.

■ EXAMPLE 13.3

A three-bladed wind turbine with a rotor diameter of 40 m operates at the tip speed ratio 4. The blade has a constant chord of 1.2 m and the blades are at 4° angle of attack. The drag-to-lift ratio is 0.005. Calculate the pitch angle along the span from $r/R = 0.2$ to 1.0.

Solution: The procedure for calculating the local parameters is the same as in the previous example. An outer loop needs to be inserted to extend the calculations to all the span locations. Results are shown in the table below.

| r/R | ϕ | θ | a | a' |
|-------|--------|----------|--------|--------|
| 0.2 | 50.17 | 46.17 | 0.0169 | 0.0250 |
| 0.3 | 38.85 | 34.85 | 0.0204 | 0.0135 |
| 0.4 | 31.13 | 27.13 | 0.0246 | 0.0092 |
| 0.5 | 25.74 | 21.74 | 0.0292 | 0.0069 |
| 0.6 | 21.81 | 17.81 | 0.0340 | 0.0056 |
| 0.7 | 18.86 | 14.86 | 0.0391 | 0.0047 |
| 0.8 | 16.57 | 12.57 | 0.0443 | 0.0040 |
| 0.9 | 14.74 | 10.74 | 0.0496 | 0.0036 |
| 1.0 | 13.25 | 9.25 | 0.0550 | 0.0032 |

■

Examination of Figure 13.12 shows that as the blade speed increases toward the tip, the pitch angle decreases as the tip is approached. This also causes the flow angle ϕ to decrease and the lift force to tilt toward the axial direction. This means that the tangential component of lift, which is the force that provides the torque on the shaft, diminishes. The same effect comes from the increase in induction factor along the span, for then the axial velocity across the blades at large radii is low, and this causes the lift force to tilt toward the axis. Another way to think about this is that an increase in the induction factor leads to lower mass flow rate and thus to lower work done on the blade elements near the tip.

The induction factor also varies in the angular direction, because in a two- or three-bladed wind turbine much of the flow does not come close to the blades at all, and hence, this part of the stream is not expected to slow down substantially. Thus the induction factor in this part of the flow deviates from the factor that holds for an actuator disk.

The azimuthal variation of the induction factor has been calculated by Burton et al. [13] at four radial locations for a three-bladed wind turbine with the tip speed ratio of six. Their results are shown in Figure 13.13.

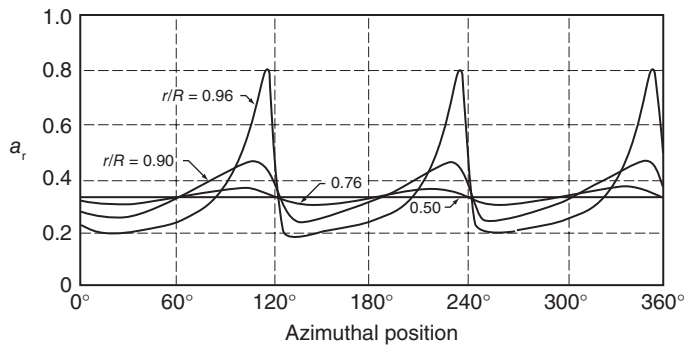


Figure 13.13 Azimuthal variation of induction factors for a three-bladed turbine at four radial locations. Source: Drawn after Burton et al. [13].

The axial force and torque can now be calculated for the entire disk from

$$F_x = 4\pi\rho V^2 \int_0^R a(1-a)r \, dr \quad (13.39)$$

$$T = 4\pi\rho\Omega V \int_0^R a'(1-a)r^3 \, dr \quad (13.40)$$

The power is then obtained as $\dot{W} = T\Omega$. A performance calculation for an actual wind turbine is given in the next example.

■ EXAMPLE 13.4

A three-bladed wind turbine with a rotor diameter of 40 m operates at the tip speed ratio 4. The blade has a constant chord of 1.2 m, and the blades are at 4° angle of attack. The drag-to-lift ratio is 0.005. The wind speed is $V = 10$ m/s, and air density can be taken to be $\rho = 1.2$ kg/m³. Only the blade along $r/R = 0.2$ –1.0 is to be used to calculate the total force and torque.

Solution: The calculation proceeds as in the previous example. After the results have been stored for various radial locations, the integrals can be evaluated by using the trapezoidal rule:

$$\int_a^b f(x)dx = \frac{\Delta r}{2} \sum_{i=1}^{n-1} (f(x_i) + f(x_{i+1})) = \Delta r \left[\sum_{i=1}^{n-1} f(x_i) + \frac{1}{2}(f(x_1) + f(x_n)) \right]$$

The part of the blade close to the hub is ignored and in the numerical integrations of Eqs. (13.39) and (13.40) the lower limit of integration is replaced by $r/R = 0.2$. The result of the integration gives the values

$$F_x = 14175 \text{ N} \quad T = 66149 \text{ Nm} \quad \dot{W} = 132.3 \text{ kW}$$

for the blade force, torque, and power. ■

13.3.3 Ideal wind turbine

Glauert [31] developed relations from which the pitch angle can be calculated for a wind turbine with the highest value for the power coefficient. Simple relations are obtained if drag is neglected. Under this assumption Eq. (13.36) becomes

$$\frac{a}{1-a} = \frac{Zc C_L \cos \phi}{8\pi r \sin^2 \phi}$$

and Eq. (13.37) reduces to

$$\frac{a'}{1+a'} = \frac{Zc C_L}{8\pi r \cos \phi}$$

Dividing the second by the first gives

$$\tan^2 \phi = \left(\frac{1-a}{1+a'} \right) \frac{a'}{a} \quad (13.41)$$

The velocity diagram at midchord shows that

$$\tan \phi = \frac{(1-a)}{(1+a')x}$$

in which the blade speed ratio is $x = r\Omega/V$. Making use of this expression reduces Eq. (13.41) to

$$a'(1+a')x^2 = a(1-a) \quad (13.42)$$

The power delivered by the turbine is

$$\dot{W} = \int_0^R \Omega dT = 4\pi\rho V\Omega^2 \int_0^R (1-a)a'r^3 dr$$

and the power coefficient can be written as

$$C_p = \frac{8}{X^2} \int_0^X (1-a)a'x^3 dx \quad (13.43)$$

Since the integrand is positive, the maximum power coefficient can be obtained by maximizing the integrand, subject to the constraint Eq. (13.42).² Hence, differentiating the integrand and setting it to zero gives

$$(1-a)\frac{da'}{da} = a$$

and the same operation on the constraint leads to

$$(1+2a')x^2\frac{da'}{da} = 1-2a$$

Eliminating the derivative between these gives

$$(1-a)(1-2a) = a'(1+2a')x^2 \quad (13.44)$$

Solving Eq. (13.42) for x^2 and substituting into this gives

$$\frac{1+2a'}{1+a'} = \frac{1-2a}{a}$$

from which

$$a' = \frac{1-3a}{4a-1} \quad (13.45)$$

This equation shows that for $\frac{1}{4} < a < \frac{1}{3}$, the value of a' is positive, and that as $a \rightarrow \frac{1}{4}$, then $a' \rightarrow \infty$. Also, as $a \rightarrow \frac{1}{3}$, then $a' \rightarrow 0$. Substituting $1+a'$ from Eq. (13.45) into Eq. (13.42) yields

$$a'x^2 = (1-a)(4a-1)$$

This shows that for $a = \frac{1}{4}$, the product $a'x^2 = 0$ and that for $a = \frac{1}{3}$, the value is $a'x^2 = \frac{2}{9}$.

The power coefficient can now be determined by integrating

$$C_p = \frac{8}{X^2} \int_0^X (1-a)a'x^3 dx$$

for various tip speed ratios X . The results for this calculation are presented in the graph in Figure 13.14. For high tip speeds, when $a = \frac{1}{3}$ and $a'x^2 = \frac{2}{9}$ the Betz limit $C_p = \frac{16}{27} = 0.593$ is approached.

With the coefficients a and a' known at various radial positions, both the relative velocity and the angle ϕ can be determined. From these, the blade pitch angle for a given angle of attack can be calculated.

²A problem of this kind is solved by methods of variational calculus and Lagrange multipliers. Owing to the form of the integrand, the direct method used above works.

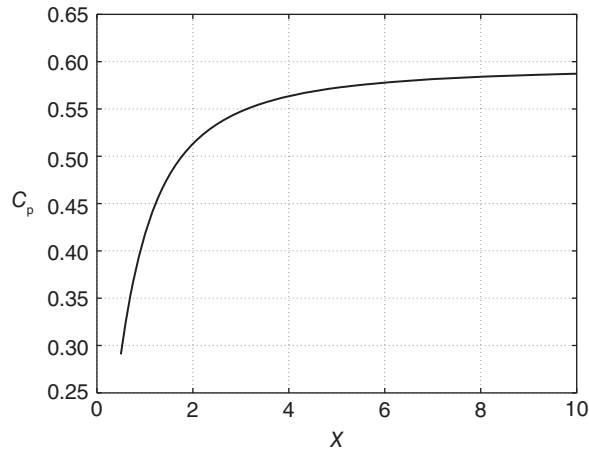


Figure 13.14 Power coefficient for optimum wind turbine.

13.3.4 Prandtl's tip correction

It has been seen that lift generated by a flow over an airfoil can be related to circulation around the airfoil. An important advance in the aerodynamic theory of flight was developed independently by Kutta and Joukowski, who showed that the magnitude of the circulation that develops around an airfoil is such that the rear stagnation point moves to the trailing edge. The action is a result of viscous forces, and the flow in the viscous boundary layers leaves the airfoil into the wake as a *free shear* layer with vorticity. The vorticity distribution in the wake is unstable and rolls into a *tip vortex*. In such a flow, it is possible to replace the blade by *bound* vorticity along the span of the blade and dispense with the blade completely. For such a model, vortex filaments exist in an inviscid flow, and according to the vortex theorems of Helmholtz, they cannot end in the fluid, but must either extend to infinity or form closed loops. This is achieved by connecting the bound vortex into the tip vortex, which extends far downstream.

For a wind turbine with an infinite number of blades, the vortex system in the wake consists of a cylindrical sheet of vorticity downstream from the edge of an actuator disk, as shown in Figure 13.15, and bound vorticity along radial lines starting from the center. From there, an axial vortex filament is directed downstream. The angular velocity in the

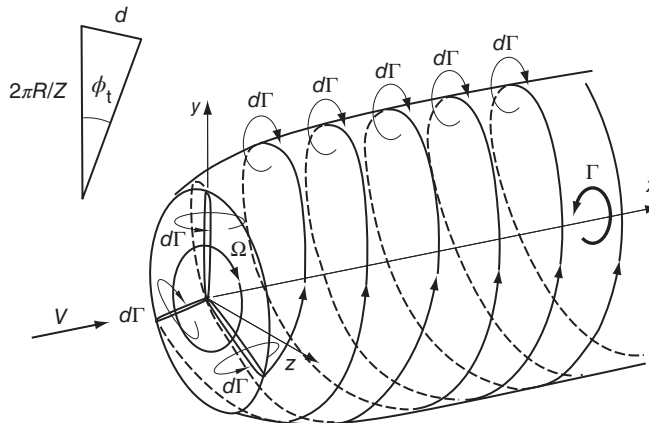


Figure 13.15 Wake vorticity. Source: Drawn after Burton et al. [13].

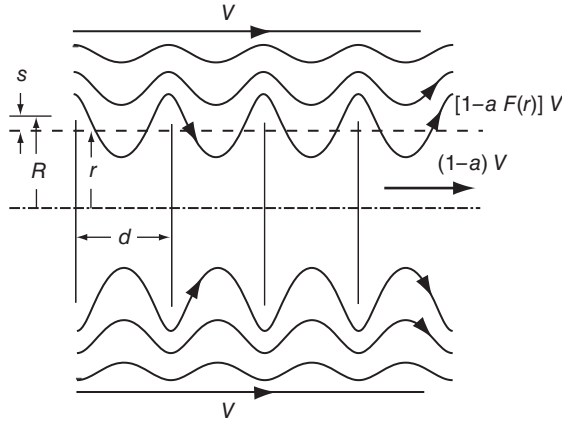


Figure 13.16 Prandtl's tip loss factor.

wake in this model is a result of the induced velocity of this *hub vortex*, and it explains why an *irrotational vortex* flow in the wake is a reasonable model.

When the number of blades is finite, vorticity leaves the blades of a wind turbine in a twisted helical sheet owing to rotation of the blades. One model is to assume that it organizes itself into a cylindrical vortex sheet. The twisted sheets are separated since the blades are discrete. Prandtl [71] and Goldstein [32] developed ways to take into account the influence of this vorticity, which now is assumed to be shed from the blade tips.

Prandtl's model is based on flow over the edges of a set of vortex sheets distance d apart, as shown in Figure 13.16. As the sheets move downstream, they induce a periodic flow near their edges. This leads to lower transfer of energy to the blades.³

Prandtl's analysis results in the introduction of factor F , given by

$$F = \frac{2}{\pi} \cos^{-1} \left[\exp \left(-\frac{\pi(R-r)}{d} \right) \right]$$

into the equation for the blade force of an elemental annulus. The distance d between helical sheets is given by

$$d = \frac{2\pi R}{Z} \sin \phi_t$$

as the diagram in Figure 13.16 shows. The sine of the flow angle at the tip is

$$\sin \phi_t = \frac{(1-a)V}{W_t}$$

so that

$$\frac{\pi(R-r)}{d} = \frac{1}{2} Z \left(\frac{R-r}{R} \right) \frac{W_t}{(1-a)V}$$

³The origin of the xy -coordinate system is at the tip of a blade with y increasing to the right and x vertically. With $z = x + iy$, a complex variable the solution is $z = \frac{d}{\pi} \ln \left(\cos \frac{d(\Phi + i\Psi)}{\pi} \right)$, with Φ the velocity potential and Ψ , the stream function. Equating the real and imaginary parts and eliminating Φ gives $x = -\frac{d}{2\pi} \ln \left(\frac{\cosh^2 \pi y/d}{\cosh^2 d\psi/\pi} + \frac{\sinh^2 \pi y/d}{\sinh^2 d\psi/\pi} \right)$, from which the streamlines may be calculated.

Following Glauert and assuming that

$$\frac{W_t}{R} = \frac{W}{r}$$

yields

$$\frac{\pi(R-r)}{d} = \frac{1}{2}Z \left(\frac{R-r}{r} \right) \frac{W}{(1-a)V}$$

The relative velocity is

$$W = \sqrt{(1-a)^2 V^2 + (r\Omega)^2}$$

so that

$$\frac{W}{(1-a)V} = \sqrt{1 + \frac{(r\Omega)^2}{(1-a)^2 V^2}} = \sqrt{1 + \frac{X^2}{(1-a)^2} \frac{r^2}{R^2}}$$

which gives

$$\frac{\pi(R-r)}{d} = \frac{1}{2}Z \left(\frac{R}{r} - 1 \right) \sqrt{1 + \frac{X^2}{(1-a)^2} \frac{r^2}{R^2}}$$

The tip loss correction factor is then given by

$$F = \frac{2}{\pi} \cos^{-1} \left[\exp \left(-\frac{1}{2}Z \left(\frac{R}{r} - 1 \right) \sqrt{1 + \frac{X^2}{(1-a)^2} \frac{r^2}{R^2}} \right) \right] \quad (13.46)$$

The tip loss factor calculated for four tip speed ratios is shown in Figure 13.17 for a two-bladed wind turbine. As the expression in Eq. (13.46) shows, decreasing the number of blades moves the curves in the same direction as decreasing the tip speed ratio. Both of these increase the spacing d and make the winding of the helix looser. Conversely, an actuator disk with an infinite number of blades results in $F = 1$. The blade force is thus

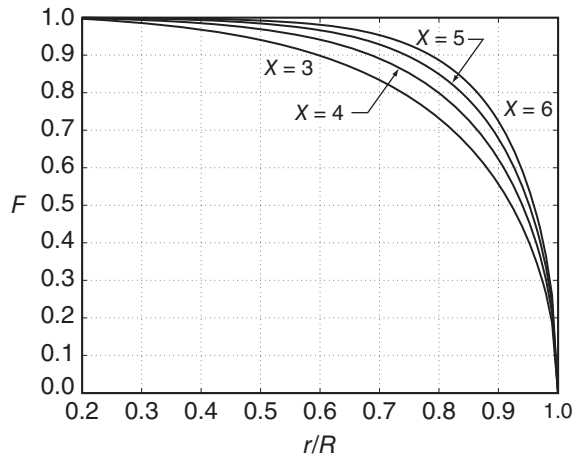


Figure 13.17 Prandtl's tip loss factor for two-bladed wind turbine with tip speed ratios $X = 3, 4, 5, 6$ at various radial positions r/R .

reduced by factor F for a wind turbine with a discrete number of blades. The axial force and torque are given by

$$dF_x = 4\rho\pi V^2 a(1-a)F r \, dr \quad dT = 4\rho\pi\Omega V a'(1-a)F r^3 \, dr$$

and in terms of the axial and tangential force coefficients, these are

$$dF_x = \frac{1}{2}\rho W^2 Z_c C_x \, dr \quad dT = \frac{1}{2}\rho W^2 Z_c C_y \, r \, dr$$

Equating these gives

$$8\pi a(1-a)V^2 F = Z_c W^2 C_x \quad 8\pi a'(1-a)V\Omega r^2 F = Z_c W^2 C_y$$

Making use of

$$\cos \phi = \frac{(1-a)V}{W} \quad \sin \phi = \frac{(1+a')r\Omega}{W}$$

and solving for a and a' then gives

$$a = \frac{\sigma C_x}{4F \sin^2 \phi + \sigma C_x} \quad a' = \frac{\sigma C_y}{4F \cos \phi \sin \phi - \sigma C_y} \quad (13.47)$$

These can now be used to calculate the wind turbine design and performance parameters. For the data given in the previous examples (with angle of attack 4°), the pitch angle and induction factors are as shown in table below. The results differ slightly from those in which the tip correction was neglected. As Figure 13.17 show, the factor F drops quickly as the tip of the blade is approached, and this accounts for the increase in a' at $r/R = 0.9$.

| r/R | ϕ | θ | a | a' |
|-------|--------|----------|--------|--------|
| 0.20 | 50.17 | 46.17 | 0.0169 | 0.0250 |
| 0.30 | 38.85 | 34.85 | 0.0204 | 0.0136 |
| 0.40 | 31.13 | 27.72 | 0.0248 | 0.0093 |
| 0.50 | 25.72 | 21.72 | 0.0298 | 0.0071 |
| 0.60 | 21.78 | 17.78 | 0.0357 | 0.0056 |
| 0.70 | 18.78 | 14.78 | 0.0430 | 0.0051 |
| 0.80 | 16.39 | 12.39 | 0.0541 | 0.0049 |
| 0.90 | 14.30 | 10.30 | 0.0777 | 0.0053 |

13.4 TURBOMACHINERY AND FUTURE PROSPECTS FOR ENERGY

In some sections of this book, the reader's attention has been drawn to how the present primary energy resources of the world are used and how important turbomachines are in converting the energy in fossil fuels into shaft work. Turbomachines powered by water and wind are the main kind of machines that contribute to significant forms of renewable energy in this mix. It is unfortunate that they still account for such a small fraction of the world's energy supply, because the fossil energy resources will be mostly exhausted during the next 80 years. During the first two decades of this century, oil prices have been

quite high, even if the tight oil production in North America with hydraulic fracturing technology caused a sufficient surge in production to bring prices down during the years 2014–2018. Nevertheless, the decline rate of the old aging giant fields is reported to be about 4.5% per year, which means that since the world petroleum liquids production is now 100 million barrels a day, to offset this, new production needs to be brought online at the rate of 4.5 million barrels a year. The new discoveries amount only two months of the world consumption. It is difficult to see how oil production can be increased much above the present level to keep up with the demand of the world's growing population (which in 2018 reached 7.5 billion). The production curves for oil, natural gas, and coal are bell-shaped, and the significant event on the road to their exhaustion is when each production peak will be passed. After that, the world will need to get by with less of these nonrenewable fuels. The peak production for world's oil is likely to occur during the next decade, and the production peaks for natural gas and coal will not be far behind. Coal, which is thought to be the most abundant of the three, has seen its reserve-to-production ratio drop from 227 years to the present 134 years during the first two decades of the present century. A 134-life for the existing reserve might seem like a long time, but the 93-year drop during this time interval indicates that the rate at which the reserves decrease is quite rapid. In addition, the reserve-to-production ratio gives a misleading number, as it assumes that production stays flat until the resource is completely exhausted.

In the United States, coal became the primary source of energy in the late 1800s overtaking biomass, which met the energy needs of the early settlers. It took some 40 years for coal's share to rise from 1% to 10% of the mix, and the historical record shows similar timespans for the rise of oil and natural gas as well. Nuclear energy's share, after 60 years of effort, is still less than 10% of the energy supply in the United States. The prospects for renewable forms to offset the decline of fossil fuels and the growing demand of the expanding population are exceedingly slim. Decisions to launch a comprehensive strategy for coping with the exhaustion of fossil fuels have been delayed many times despite warnings throughout the last century [11, 46]. Still installed wind energy capacity is increasing rapidly, and wind power offers the best possibility of becoming a significant source of energy in the United States, China, and India. Denmark and Germany, in particular, have demonstrated that wind power can make up a sizeable fraction of a country's energy supply with a continuous and sustained effort.

EXERCISES

13.1 Use a cylindrical control volume of cross sectional area A_e and develop the expression

$$F_d = \rho A_b V_b (V - V_b)$$

for the axial force on the blades. Note that it is in agreement with Eq. (13.6).

13.2 The nondimensional pressure difference can be expressed as

$$\frac{p_+ - p_a}{\frac{1}{2}\rho V^2}$$

in which the pressure difference is that just upstream the disk and the free stream. (a) Use the momentum theory for a wind turbine to express this relationship in terms of the

interference factor a . For which value of a is this maximum? Interpret this physically. (b) Develop a similar relationship for the expression

$$\frac{p_a - p_-}{\frac{1}{2}\rho V^2}$$

and determine for which value of a is this the maximum? [Ans: (a) $a = 1$, (b) $a = 1/3$]

13.3 A wind turbine operates at wind speed of $V = 12$ m/s. Its blade radius is $R = 20$ m and its tip speed radius $R\Omega/V = 4$. It operates at the condition $C_p = 0.3$. Find (a) the rate of rotation of the blades, (b) the power developed by the turbine, (c) the value of the interference factor a using the momentum theory, and (d) the pressure on the front of the actuator disk, assuming that the free stream pressure is 101.3 kPa and the temperature is 25 °C. [Ans: (a) 22.9 rpm, (b) 397.4 kW, (c) 0.0907, (d) 101.315 kPa]

13.4 Using the axial momentum theory, calculate the ratio of the slipstream radius to that of the disk radius in terms of the interference factor a . If the wind turbine blades are 80 m long, what is the radius of the slipstream far downstream for $a = 1/3$? What is the radius of the streamtube far upstream? [Ans: (a) 113 m, (b) 65.3 m]

13.5 In a wind with speed $V = 8.7$ m/s and air density $\rho = 1.2$ kg/m³, a wind turbine operates at a condition when the axial induction factor is $a = 0.11$. Find the blade length, assuming that the power of the turbine is $\dot{W} = 250$ kW. [Ans: 24 m]

13.6 Write a computer program to carry out the calculations associated with Example 13.4.

13.7 Write a computer program to carry out the calculations associated with Example 13.3 and which include the Prandtl tip correction.

13.8 Consider a three-bladed wind turbine with blade radius of $R = 35$ m and constant chord of $c = 80$ cm, which operates with a rotational speed of $\Omega = 10$ rpm. The wind speed is $V = 12$ m/s. (a) Find the axial and tangential induction factors at $r = 10$ m, assuming that the angle of attack is 6° and $C_D = 0.01C_L$. (b) Find the axial force and the torque, assuming the air density is $\rho = 0.12$ kg/m³. (c) Calculate the axial force and the torque by assuming that the induction factors are uniform and equal to their values at $r/R = 0.6$. [Ans: (a) 0.0117, 0.0033, (b) 21.67 kN m, 236.8 kN m, (c) 15.33 kN, 234.6 kN m]

Appendix A

Streamline Curvature and Radial Equilibrium

A.1 STREAMLINE CURVATURE METHOD

In this appendix, the governing equations for the streamline curvature method are developed. The derivation of the acceleration terms follows that of Cumpsty [18]. The blade surfaces may be highly curved, but it is useful to visualize locally flat surface patches in them. This method has been implemented into commercial CFD software, such as ANSYS-Fluent.

A.1.1 Fundamental equations

The acceleration of a fluid particle is given by its substantial derivative

$$\mathbf{a} = \frac{\partial \mathbf{V}}{\partial t} + \mathbf{V} \cdot \nabla \mathbf{V}$$

in which the unsteady term vanishes in steady flow. The second term represents the spatial acceleration of the flow. In cylindrical coordinates, the gradient operator can be written as

$$\nabla = \mathbf{e}_r \frac{\partial}{\partial r} + \frac{\mathbf{e}_\theta}{r} \frac{\partial}{\partial \theta} + \mathbf{e}_z \frac{\partial}{\partial z}$$

By defining the meridional component as

$$\mathbf{V}_m = V_m \mathbf{e}_m = V_r \mathbf{e}_r + V_z \mathbf{e}_z$$

the velocity vector can also be written as

$$\mathbf{V} = V_m \mathbf{e}_m + V_\theta \mathbf{e}_\theta$$

The scalar product of the unit vector in the direction of \mathbf{e}_m on the meridional plane and the gradient operator gives the directional derivative in the direction of the unit vector:

$$\mathbf{e}_m \cdot \nabla = \frac{\partial}{\partial m} = (\mathbf{e}_m \cdot \mathbf{e}_r) \frac{\partial}{\partial r} + (\mathbf{e}_m \cdot \mathbf{e}_z) \frac{\partial}{\partial z}$$

The term in the tangential direction has dropped out because the vector \mathbf{e}_m is orthogonal to \mathbf{e}_θ .

The angle between the directions of \mathbf{e}_m and \mathbf{e}_z is denoted by ϕ . In terms of this angle the partial derivatives may be written as

$$\frac{\partial}{\partial m} = \sin \phi \frac{\partial}{\partial r} + \cos \phi \frac{\partial}{\partial z}$$

and the gradient operator takes the form

$$\nabla = \mathbf{e}_m \frac{\partial}{\partial m} + \frac{\mathbf{e}_\theta}{r} \frac{\partial}{\partial \theta}$$

The acceleration of a fluid particle can now be expressed as

$$\mathbf{a} = (V_m \mathbf{e}_m + V_\theta \mathbf{e}_\theta) \cdot \left(\mathbf{e}_m \frac{\partial}{\partial m} + \mathbf{e}_\theta \frac{1}{r} \frac{\partial}{\partial \theta} \right) (V_m \mathbf{e}_m + V_\theta \mathbf{e}_\theta)$$

which leads to

$$\mathbf{a} = V_m \frac{\partial}{\partial m} (V_m \mathbf{e}_m + V_\theta \mathbf{e}_\theta) + \frac{V_\theta}{r} \frac{\partial}{\partial \theta} (V_m \mathbf{e}_m + V_\theta \mathbf{e}_\theta)$$

When this is expanded, it reduces to

$$\mathbf{a} = \mathbf{e}_m V_m \frac{\partial V_m}{\partial m} - \mathbf{e}_n \frac{V_m^2}{R} + \mathbf{e}_\theta V_m \frac{\partial V_\theta}{\partial m} - \mathbf{e}_r \frac{V_\theta^2}{r}$$

To arrive at these relations, the formulas

$$\frac{\partial \mathbf{e}_m}{\partial m} = -\frac{\mathbf{e}_n}{R} \quad \frac{\partial \mathbf{e}_m}{\partial \theta} = 0 \quad \frac{\partial \mathbf{e}_\theta}{\partial m} = 0 \quad \frac{\partial \mathbf{e}_\theta}{\partial \theta} = -\mathbf{e}_r$$

were used. The radius of curvature of a streamline on the meridional plane is denoted by R and is taken as positive when the streamline is concave away from the z axis. The direction of the unit vector \mathbf{e}_n is perpendicular to the direction of vector \mathbf{e}_m on the meridional plane in such a way that a right-handed triple $(\mathbf{e}_n, \mathbf{e}_\theta, \mathbf{e}_m)$ is retained. Since this was obtained by rotation by the angle ϕ about the axis of \mathbf{e}_θ , the n direction coincides with the radial direction and the m direction coincides with z direction, when the angle ϕ is zero.

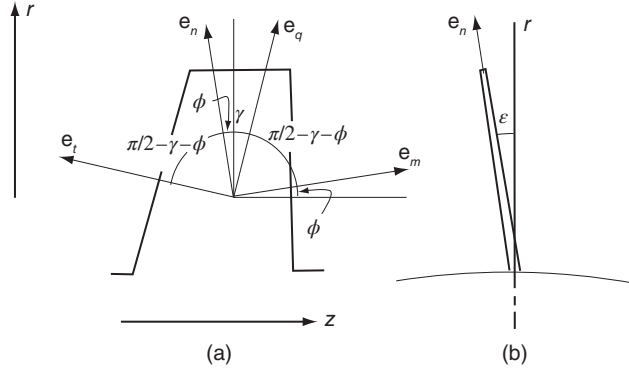


Figure A.1 Unit vectors on the meridional plane (a) and the angle of lean (b).

Consider next a direction specified by the unit vector \mathbf{e}_q on the meridional plane. It is inclined to the radial direction by angle γ . This and other angles are shown in Figure A.1. The angle γ is the *sweep* angle of the blade at its leading edge. It is positive for a sweep toward the positive z direction. The angle between direction \mathbf{e}_q and the m axis is $\pi/2 - (\gamma + \phi)$. Hence, the component of acceleration in the direction \mathbf{e}_q is

$$a_q = (\mathbf{e}_q \cdot \mathbf{e}_m) V_m \frac{\partial V_m}{\partial m} - (\mathbf{e}_q \cdot \mathbf{e}_n) \frac{V_m^2}{R} + (\mathbf{e}_q \cdot \mathbf{e}_\theta) V_m \frac{\partial V_\theta}{\partial m} - (\mathbf{e}_q \cdot \mathbf{e}_r) \frac{V_\theta^2}{r}$$

This reduces to

$$a_q = \sin(\gamma + \phi) V_m \frac{\partial V_m}{\partial m} - \cos(\gamma + \phi) \frac{V_m^2}{R} - \cos \gamma \frac{V_\theta^2}{r} \quad (\text{A.1})$$

Next, let the unit vector \mathbf{e}_t denote a direction normal to \mathbf{e}_q on the meridional plane. The component of acceleration in this direction is given by

$$a_t = (\mathbf{e}_t \cdot \mathbf{e}_m) V_m \frac{\partial V_m}{\partial m} - (\mathbf{e}_t \cdot \mathbf{e}_n) \frac{V_m^2}{R} + (\mathbf{e}_t \cdot \mathbf{e}_\theta) V_m \frac{\partial V_\theta}{\partial m} - (\mathbf{e}_t \cdot \mathbf{e}_r) \frac{V_\theta^2}{r}$$

which reduces to

$$a_t = \cos(\gamma + \phi) V_m \frac{\partial V_m}{\partial m} + \sin(\gamma + \phi) \frac{V_m^2}{R} - \sin \gamma \frac{V_\theta^2}{r}$$

Finally, the acceleration component in the tangential direction can be written as

$$a_\theta = V_m \frac{\partial V_\theta}{\partial m}$$

If the blades lean at an angle ε from the meridional plane, in the direction opposite to θ , the acceleration components \mathbf{a}_q and \mathbf{a}_θ can be used to construct new components that lie on the plane containing a blade with this lean angle. The transformation to this plane is equivalent to rotation of the surface about the axis containing the unit vector \mathbf{e}_t . With \mathbf{e}_e denoting the unit vector obtained by rotating \mathbf{e}_q by angle ε counterclockwise, the acceleration component in the direction of \mathbf{e}_e is given by

$$a_e = (\mathbf{e}_e \cdot \mathbf{e}_q) a_q + (\mathbf{e}_e \cdot \mathbf{e}_\theta) a_\theta + (\mathbf{e}_e \cdot \mathbf{e}_t) a_t$$

which reduces to

$$a_e = \cos \varepsilon a_q - \sin \varepsilon a_\theta$$

The Euler equation for an inviscid flow in vector notation is

$$\mathbf{a} = -\frac{1}{\rho} \nabla p + \frac{\mathbf{F}}{\rho} \quad (\text{A.2})$$

The components of this equation in any direction can now be obtained by taking its scalar product with a unit vector in the chosen direction. The component in the direction of \mathbf{e}_e is

$$a_e = -\frac{1}{\rho} \frac{\partial p}{\partial e} + \frac{F_e}{\rho}$$

and its component in the direction of \mathbf{e}_q is

$$a_q = -\frac{1}{\rho} \frac{\partial p}{\partial q} + \frac{F_q}{\rho} \quad (\text{A.3})$$

The acceleration component a_q is the acceleration in the q direction. The pressure term on the right side of Eq. (A.3) can be modified by making use of the Tds relation

$$T \frac{\partial s}{\partial q} = \frac{\partial h}{\partial q} - \frac{1}{\rho} \frac{\partial p}{\partial q} \quad (\text{A.4})$$

The directional derivative of the stagnation enthalpy

$$h_0 = h + \frac{1}{2}(V_m^2 + V_\theta^2) \quad (\text{A.5})$$

in the q direction is

$$\frac{\partial h}{\partial q} = \frac{\partial h_0}{\partial q} - V_m \frac{\partial V_m}{\partial q} - V_\theta \frac{\partial V_\theta}{\partial q} \quad (\text{A.6})$$

Using this in the expression for the pressure gradient in Eq. (A.4) leads to

$$-\frac{1}{\rho} \frac{\partial p}{\partial q} = T \frac{\partial s}{\partial q} - \frac{\partial h_0}{\partial q} + V_m \frac{\partial V_m}{\partial q} + V_\theta \frac{\partial V_\theta}{\partial q} \quad (\text{A.7})$$

Substituting this into Eq. (A.3) gives

$$\begin{aligned} & \sin(\gamma + \phi) V_m \frac{\partial V_m}{\partial m} - \cos(\gamma + \phi) \frac{V_m^2}{R} - V_m \frac{\partial V_m}{\partial q} \\ &= T \frac{\partial s}{\partial q} - \frac{\partial h_0}{\partial q} + \cos \gamma \frac{V_\theta^2}{r} + V_\theta \frac{\partial V_\theta}{\partial q} + \frac{F_q}{\rho} \end{aligned} \quad (\text{A.8})$$

With $q = \frac{r}{\cos \gamma}$, terms involving V_θ on the RHS can be combined to yield:

$$\frac{\partial V_m^2}{\partial q} + P(q) V_m^2 = T(q) \quad (\text{A.9})$$

where the functions $P(q)$ and $T(q)$ are defined as

$$P(q) = 2 \left[-\frac{\cos(\gamma + \phi)}{R} - \frac{\sin(\gamma + \phi)}{V_m} \frac{\partial V_m}{\partial m} \right] \quad (\text{A.10})$$

$$T(q) = 2 \left[\frac{\partial h_0}{\partial q} - T \frac{\partial s}{\partial q} - \frac{1}{2q^2} \frac{\partial}{\partial q} (q^2 V_\theta^2) - \frac{F_q}{\rho} \right] \quad (\text{A.11})$$

In a flow passage of constant height, the meridional direction is the z direction and q can be replaced by r . In addition, the streamlines do not bend in the direction of the axis z , so that the radius of curvature R tends to infinity. If there is no sweep γ is zero, and if the stagnation enthalpy and entropy do not vary across the channel, then, in the absence of a blade force, this equation reduces to

$$\frac{\partial V_z^2}{\partial r} + \frac{V_\theta}{r} \frac{\partial}{\partial r} (r V_\theta) = 0 \quad (\text{A.12})$$

This is the simple radial equilibrium equation used in Chapters 7 and 8.

A.1.2 Formal solution

Since Eq. (A.9) is nonlinear, it must be solved numerically. One way to carry this out is to first find its formal solution. Ignoring the nonlinearity and treating $P(q)$ and $T(q)$ as functions of q , the equation

$$\frac{\partial V_m^2}{\partial q} + P(q) V_m^2 = T(q) \quad (\text{A.13})$$

becomes a first-order differential equation with variable coefficients. Its solution can then be obtained by using an integrating factor, or by variation of parameters.

To simplify the notation, first the variable V_m^2 is replaced by U and the homogeneous solution of Eq. (A.13) is seen to be

$$U_h = C e^{-\int P(q) dq} \quad (\text{A.14})$$

To obtain the particular solution to Eq. (A.13), the solution is assumed to have the form

$$U_p = H(r) e^{-\int P(x) dx}$$

which, when inserted into the equation and after rearrangement, yields

$$\frac{\partial U_p}{\partial q} + P(q) U_p = \frac{\partial H}{\partial q} e^{-\int_{q_0}^q P(q') dq'}$$

Comparing this to Eq. (A.13) shows that

$$T = \frac{\partial H}{\partial q} e^{-\int_{q_0}^q P(q') dq'}$$

or

$$\frac{\partial H}{\partial q} = T e^{\int_{q_0}^q P(q') dq'}$$

Integrating leads to

$$H(q) = \int_{q_0}^q T(q') e^{\int_{q_0}^{q'} P(q'') dq''} dq'$$

Therefore, the particular solution is

$$U_p = e^{-\int_{q_0}^q P(q') dq'} \int_{q_0}^q e^{\int_{q_0}^{q'} P(q'') dq''} T(q') dq' \quad (\text{A.15})$$

The complete solution in the original variable is

$$V_m^2(q) = V_M^2 e^{-\int_{q_0}^q P(q') dq'} + e^{-\int_{q_0}^q P(q') dq'} \int_{q_0}^q e^{\int_{q_0}^{q'} P(q'') dq''} T(q') dq' \quad (\text{A.16})$$

If the sweep angle γ is zero, the q direction is the r direction. In such a case, integrations in Eq. (A.13) are with respect to r . With the lower limit of integration the middle streamline, the solution becomes

$$V_m^2(r) = V_M^2 e^{-\int_{r_M}^r P(r') dr'} + e^{-\int_{r_M}^r P(r') dr'} \int_{r_M}^r e^{\int_{r_M}^{r'} P(r'') dr''} T(r') dr' \quad (\text{A.17})$$

and the integration constant is identified as the meridional velocity squared on the middle streamline, $V_M^2 = V_m^2(r_M)$. The streamlines are then laid out such that each streamtube has the same mass flow rate, and grid is set up on the qz plane, with grid points on the streamlines a specified distance apart. The solution then proceeds by iteration. The simplest situation is to consider the intergap region so that the blades are not present. The quasiorthogonals q can be spaced and oriented such that the first one is aligned with the trailing edge of a blade and the last one with the leading edge of the next blade row. The curvature is calculated at the grid locations, and the velocity gradients are determined by finite-difference approximations. This fixes the values of P and T . Integration of Eq. (A.17) from the central streamline toward the hub and the casing gives the velocity field. Next, the mass flow rates are calculated for each streamtube. The residual is examined, and the streamlines are adjusted so that the fluid again flows at the same rate through each streamtube. The process is repeated until convergence for the location of the streamlines is obtained. This requires the use of relaxation.

Appendix B

Thermodynamic Tables

Table B.1 Thermodynamic properties of saturated steam, temperature table.

| T (°C) | p (bar) | $v_f \cdot 10^3$ (m ³ /kg) | v_g (m ³ /kg) | u_f (kJ/kg) | u_g (kJ/kg) | h_f (kJ/kg) | h_g (kJ/kg) | s_f (kJ/kg K) | s_g (kJ/kg K) |
|-------------|--------------|--|-------------------------------|------------------|------------------|------------------|------------------|--------------------|--------------------|
| 0.01 | 0.00611 | 1.0002 | 206.136 | 0.00 | 2375.3 | 0.01 | 2501.3 | 0.0000 | 9.1562 |
| 1 | 0.00657 | 1.0002 | 192.439 | 4.18 | 2375.9 | 4.183 | 2502.4 | 0.0153 | 9.1277 |
| 2 | 0.00706 | 1.0001 | 179.762 | 8.40 | 2377.3 | 8.401 | 2504.2 | 0.0306 | 9.1013 |
| 3 | 0.00758 | 1.0001 | 168.016 | 12.61 | 2378.7 | 12.61 | 2506.0 | 0.0459 | 9.0752 |
| 4 | 0.00814 | 1.0001 | 157.126 | 16.82 | 2380.0 | 16.82 | 2507.9 | 0.0611 | 9.0492 |
| 5 | 0.00873 | 1.0001 | 147.024 | 21.02 | 2381.4 | 21.02 | 2509.7 | 0.0763 | 9.0236 |
| 6 | 0.00935 | 1.0001 | 137.647 | 25.22 | 2382.8 | 25.22 | 2511.5 | 0.0913 | 8.9981 |
| 7 | 0.01002 | 1.0001 | 128.939 | 29.41 | 2384.2 | 29.42 | 2513.4 | 0.1063 | 8.9729 |
| 8 | 0.01073 | 1.0002 | 120.847 | 33.61 | 2385.6 | 33.61 | 2515.2 | 0.1213 | 8.9479 |
| 9 | 0.01148 | 1.0002 | 113.323 | 37.80 | 2386.9 | 37.80 | 2517.1 | 0.1361 | 8.9232 |
| 10 | 0.01228 | 1.0003 | 106.323 | 41.99 | 2388.3 | 41.99 | 2518.9 | 0.1510 | 8.8986 |
| 11 | 0.01313 | 1.0004 | 99.808 | 46.17 | 2389.7 | 46.18 | 2520.7 | 0.1657 | 8.8743 |
| 12 | 0.01403 | 1.0005 | 93.740 | 50.36 | 2391.1 | 50.36 | 2522.6 | 0.1804 | 8.8502 |
| 13 | 0.01498 | 1.0006 | 88.086 | 54.55 | 2392.4 | 54.55 | 2524.4 | 0.1951 | 8.8263 |
| 14 | 0.01599 | 1.0008 | 82.814 | 58.73 | 2393.8 | 58.73 | 2526.2 | 0.2097 | 8.8027 |

Table B.1 (continued)

| T (°C) | p (bar) | $v_f \cdot 10^3$ (m ³ /kg) | v_g (m ³ /kg) | u_f (kJ/kg) | u_g (kJ/kg) | h_f (kJ/kg) | h_g (kJ/kg) | s_f (kJ/kg K) | s_g (kJ/kg K) |
|-------------|--------------|--|-------------------------------|------------------|------------------|------------------|------------------|--------------------|--------------------|
| 15 | 0.01706 | 1.0009 | 77.897 | 62.92 | 2395.2 | 62.92 | 2528.0 | 0.2242 | 8.7792 |
| 16 | 0.01819 | 1.0011 | 73.308 | 67.10 | 2396.6 | 67.10 | 2529.9 | 0.2387 | 8.7560 |
| 17 | 0.01938 | 1.0012 | 69.023 | 71.28 | 2397.9 | 71.28 | 2531.7 | 0.2532 | 8.7330 |
| 18 | 0.02064 | 1.0014 | 65.019 | 75.47 | 2399.3 | 75.47 | 2533.5 | 0.2676 | 8.7101 |
| 19 | 0.02198 | 1.0016 | 61.277 | 79.65 | 2400.7 | 79.65 | 2535.3 | 0.2819 | 8.6875 |
| 20 | 0.02339 | 1.0018 | 57.778 | 83.83 | 2402.0 | 83.84 | 2537.2 | 0.2962 | 8.6651 |
| 21 | 0.02488 | 1.0020 | 54.503 | 88.02 | 2403.4 | 88.02 | 2539.0 | 0.3104 | 8.6428 |
| 22 | 0.02645 | 1.0023 | 51.438 | 92.20 | 2404.8 | 92.20 | 2540.8 | 0.3246 | 8.6208 |
| 23 | 0.02810 | 1.0025 | 48.568 | 96.38 | 2406.1 | 96.39 | 2542.6 | 0.3388 | 8.5990 |
| 24 | 0.02985 | 1.0027 | 45.878 | 100.57 | 2407.5 | 100.57 | 2544.5 | 0.3529 | 8.5773 |
| 25 | 0.03169 | 1.0030 | 43.357 | 104.75 | 2408.9 | 104.75 | 2546.3 | 0.3670 | 8.5558 |
| 26 | 0.03363 | 1.0033 | 40.992 | 108.93 | 2410.2 | 108.94 | 2548.1 | 0.3810 | 8.5346 |
| 27 | 0.03567 | 1.0035 | 38.773 | 113.12 | 2411.6 | 113.12 | 2549.9 | 0.3949 | 8.5135 |
| 28 | 0.03782 | 1.0038 | 36.690 | 117.30 | 2413.0 | 117.30 | 2551.7 | 0.4088 | 8.4926 |
| 29 | 0.04008 | 1.0041 | 34.734 | 121.48 | 2414.3 | 121.49 | 2553.5 | 0.4227 | 8.4718 |
| 30 | 0.04246 | 1.0044 | 32.896 | 125.67 | 2415.7 | 125.67 | 2555.3 | 0.4365 | 8.4513 |
| 31 | 0.04495 | 1.0047 | 31.168 | 129.85 | 2417.0 | 129.85 | 2557.1 | 0.4503 | 8.4309 |
| 32 | 0.04758 | 1.0050 | 29.543 | 134.03 | 2418.4 | 134.04 | 2559.0 | 0.4640 | 8.4107 |
| 33 | 0.05033 | 1.0054 | 28.014 | 138.22 | 2419.8 | 138.22 | 2560.8 | 0.4777 | 8.3906 |
| 34 | 0.05323 | 1.0057 | 26.575 | 142.40 | 2421.1 | 142.41 | 2562.6 | 0.4914 | 8.3708 |
| 35 | 0.05627 | 1.0060 | 25.220 | 146.58 | 2422.5 | 146.59 | 2564.4 | 0.5050 | 8.3511 |
| 40 | 0.07381 | 1.0079 | 19.528 | 167.50 | 2429.2 | 167.50 | 2573.4 | 0.5723 | 8.2550 |
| 45 | 0.09593 | 1.0099 | 15.263 | 188.41 | 2435.9 | 188.42 | 2582.3 | 0.6385 | 8.1629 |
| 50 | 0.12345 | 1.0122 | 12.037 | 209.31 | 2442.6 | 209.33 | 2591.2 | 0.7037 | 8.0745 |
| 55 | 0.1575 | 1.0146 | 9.5726 | 230.22 | 2449.2 | 230.24 | 2600.0 | 0.7679 | 7.9896 |
| 60 | 0.1993 | 1.0171 | 7.6743 | 251.13 | 2455.8 | 251.15 | 2608.8 | 0.8312 | 7.9080 |
| 65 | 0.2502 | 1.0199 | 6.1996 | 272.05 | 2462.4 | 272.08 | 2617.5 | 0.8935 | 7.8295 |
| 70 | 0.3118 | 1.0228 | 5.0446 | 292.98 | 2468.8 | 293.01 | 2626.1 | 0.9549 | 7.7540 |
| 75 | 0.3856 | 1.0258 | 4.1333 | 313.92 | 2475.2 | 313.96 | 2634.6 | 1.0155 | 7.6813 |
| 80 | 0.4737 | 1.0290 | 3.4088 | 334.88 | 2481.6 | 334.93 | 2643.1 | 1.0753 | 7.6112 |
| 85 | 0.5781 | 1.0324 | 2.8289 | 355.86 | 2487.9 | 355.92 | 2651.4 | 1.1343 | 7.5436 |
| 90 | 0.7012 | 1.0359 | 2.3617 | 376.86 | 2494.0 | 376.93 | 2659.6 | 1.1925 | 7.4784 |
| 95 | 0.8453 | 1.0396 | 1.9828 | 397.89 | 2500.1 | 397.98 | 2667.7 | 1.2501 | 7.4154 |
| 100 | 1.013 | 1.0434 | 1.6736 | 418.96 | 2506.1 | 419.06 | 2675.7 | 1.3069 | 7.3545 |
| 105 | 1.208 | 1.0474 | 1.4200 | 440.05 | 2512.1 | 440.18 | 2683.6 | 1.3630 | 7.2956 |
| 110 | 1.432 | 1.0515 | 1.2106 | 461.19 | 2517.9 | 461.34 | 2691.3 | 1.4186 | 7.2386 |
| 115 | 1.690 | 1.0558 | 1.0370 | 482.36 | 2523.5 | 482.54 | 2698.8 | 1.4735 | 7.1833 |
| 120 | 1.985 | 1.0603 | 0.8922 | 503.57 | 2529.1 | 503.78 | 2706.2 | 1.5278 | 7.1297 |
| 125 | 2.320 | 1.0649 | 0.7709 | 524.82 | 2534.5 | 525.07 | 2713.4 | 1.5815 | 7.0777 |
| 130 | 2.700 | 1.0697 | 0.6687 | 546.12 | 2539.8 | 546.41 | 2720.4 | 1.6346 | 7.0272 |
| 135 | 3.130 | 1.0746 | 0.5824 | 567.46 | 2545.0 | 567.80 | 2727.2 | 1.6873 | 6.9780 |
| 140 | 3.612 | 1.0797 | 0.5090 | 588.85 | 2550.0 | 589.24 | 2733.8 | 1.7394 | 6.9302 |
| 145 | 4.153 | 1.0850 | 0.4464 | 610.30 | 2554.8 | 610.75 | 2740.2 | 1.7910 | 6.8836 |
| 150 | 4.757 | 1.0904 | 0.3929 | 631.80 | 2559.5 | 632.32 | 2746.4 | 1.8421 | 6.8381 |
| 160 | 6.177 | 1.1019 | 0.3071 | 674.97 | 2568.3 | 675.65 | 2758.0 | 1.9429 | 6.7503 |
| 170 | 7.915 | 1.1142 | 0.2428 | 718.40 | 2576.3 | 719.28 | 2768.5 | 2.0421 | 6.6662 |
| 180 | 10.02 | 1.1273 | 0.1940 | 762.12 | 2583.4 | 763.25 | 2777.8 | 2.1397 | 6.5853 |
| 190 | 12.54 | 1.1414 | 0.1565 | 806.17 | 2589.6 | 807.60 | 2785.8 | 2.2358 | 6.5071 |
| 200 | 15.55 | 1.1564 | 0.1273 | 850.58 | 2594.7 | 852.38 | 2792.5 | 2.3308 | 6.4312 |

| T (°C) | p (bar) | $v_f \cdot 10^3$ (m ³ /kg) | v_g (m ³ /kg) | u_f (kJ/kg) | u_g (kJ/kg) | h_f (kJ/kg) | h_g (kJ/kg) | s_f (kJ/kg K) | s_g (kJ/kg K) |
|-------------|--------------|--|-------------------------------|------------------|------------------|------------------|------------------|--------------------|--------------------|
| 210 | 19.07 | 1.1726 | 0.1044 | 895.43 | 2598.7 | 897.66 | 2797.7 | 2.4246 | 6.3572 |
| 220 | 23.18 | 1.1900 | 0.0862 | 940.75 | 2601.6 | 943.51 | 2801.3 | 2.5175 | 6.2847 |
| 230 | 27.95 | 1.2088 | 0.0716 | 986.62 | 2603.1 | 990.00 | 2803.1 | 2.6097 | 6.2131 |
| 240 | 33.45 | 1.2292 | 0.0597 | 1033.1 | 2603.1 | 1037.2 | 2803.0 | 2.7013 | 6.1423 |
| 250 | 39.74 | 1.2515 | 0.0501 | 1080.4 | 2601.6 | 1085.3 | 2800.7 | 2.7926 | 6.0717 |
| 260 | 46.89 | 1.2758 | 0.0422 | 1128.4 | 2598.4 | 1134.4 | 2796.2 | 2.8838 | 6.0009 |
| 270 | 55.00 | 1.3026 | 0.0356 | 1177.4 | 2593.2 | 1184.6 | 2789.1 | 2.9751 | 5.9293 |
| 280 | 64.13 | 1.3324 | 0.0302 | 1227.5 | 2585.7 | 1236.1 | 2779.2 | 3.0669 | 5.8565 |
| 290 | 74.38 | 1.3658 | 0.0256 | 1279.0 | 2575.7 | 1289.1 | 2765.9 | 3.1595 | 5.7818 |
| 300 | 85.84 | 1.4037 | 0.0217 | 1332.0 | 2562.8 | 1344.1 | 2748.7 | 3.2534 | 5.7042 |
| 310 | 98.61 | 1.4473 | 0.0183 | 1387.0 | 2546.2 | 1401.2 | 2727.0 | 3.3491 | 5.6226 |
| 320 | 112.8 | 1.4984 | 0.0155 | 1444.4 | 2525.2 | 1461.3 | 2699.7 | 3.4476 | 5.5356 |
| 340 | 145.9 | 1.6373 | 0.0108 | 1569.9 | 2463.9 | 1593.8 | 2621.3 | 3.6587 | 5.3345 |
| 360 | 186.6 | 1.8936 | 0.0070 | 1725.6 | 2352.2 | 1761.0 | 2482.0 | 3.9153 | 5.0542 |
| 374.12 | 220.9 | 3.1550 | 0.0031 | 2029.6 | 2029.6 | 2099.3 | 2099.3 | 4.4298 | 4.4298 |

Table B.2 Thermodynamic properties of saturated steam, pressure table.

| p (bar) | T (°C) | $v_f \cdot 10^3$ (m ³ /kg) | v_g (m ³ /kg) | u_f (kJ/kg) | u_g (kJ/kg) | h_f (kJ/kg) | h_g (kJ/kg) | s_f (kJ/kg K) | s_g (kJ/kg K) |
|--------------|-------------|--|-------------------------------|------------------|------------------|------------------|------------------|--------------------|--------------------|
| 0.06 | 36.17 | 1.0065 | 23.737 | 151.47 | 2424.0 | 151.47 | 2566.5 | 0.5208 | 8.3283 |
| 0.08 | 41.49 | 1.0085 | 18.128 | 173.73 | 2431.0 | 173.74 | 2576.0 | 0.5921 | 8.2272 |
| 0.10 | 45.79 | 1.0103 | 14.693 | 191.71 | 2436.8 | 191.72 | 2583.7 | 0.6489 | 8.1487 |
| 0.12 | 49.40 | 1.0119 | 12.377 | 206.82 | 2441.6 | 206.83 | 2590.1 | 0.6960 | 8.0849 |
| 0.16 | 55.30 | 1.0147 | 9.4447 | 231.47 | 2449.4 | 231.49 | 2600.5 | 0.7718 | 7.9846 |
| 0.20 | 60.05 | 1.0171 | 7.6591 | 251.32 | 2455.7 | 251.34 | 2608.9 | 0.8318 | 7.9072 |
| 0.25 | 64.95 | 1.0198 | 6.2120 | 271.85 | 2462.1 | 271.88 | 2617.4 | 0.8929 | 7.8302 |
| 0.30 | 69.09 | 1.0222 | 5.2357 | 289.15 | 2467.5 | 289.18 | 2624.5 | 0.9438 | 7.7676 |
| 0.40 | 75.85 | 1.0263 | 3.9983 | 317.48 | 2476.1 | 317.52 | 2636.1 | 1.0257 | 7.6692 |
| 0.50 | 81.31 | 1.0299 | 3.2442 | 340.38 | 2483.1 | 340.43 | 2645.3 | 1.0908 | 7.5932 |
| 0.60 | 85.92 | 1.0330 | 2.7351 | 359.73 | 2488.8 | 359.79 | 2652.9 | 1.1451 | 7.5314 |
| 0.70 | 89.93 | 1.0359 | 2.3676 | 376.56 | 2493.8 | 376.64 | 2659.5 | 1.1917 | 7.4793 |
| 0.80 | 93.48 | 1.0385 | 2.0895 | 391.51 | 2498.1 | 391.60 | 2665.3 | 1.2327 | 7.4342 |
| 0.90 | 96.69 | 1.0409 | 1.8715 | 405.00 | 2502.0 | 405.09 | 2670.5 | 1.2693 | 7.3946 |
| 1.00 | 99.61 | 1.0431 | 1.6958 | 417.30 | 2505.5 | 417.40 | 2675.1 | 1.3024 | 7.3592 |
| 2.00 | 120.2 | 1.0605 | 0.8865 | 504.49 | 2529.2 | 504.70 | 2706.5 | 1.5301 | 7.1275 |
| 2.50 | 127.4 | 1.0672 | 0.7193 | 535.12 | 2537.0 | 535.39 | 2716.8 | 1.6073 | 7.0531 |
| 3.00 | 133.5 | 1.0731 | 0.6063 | 561.19 | 2543.4 | 561.51 | 2725.2 | 1.6719 | 6.9923 |
| 3.50 | 138.9 | 1.0785 | 0.5246 | 584.01 | 2548.8 | 584.38 | 2732.4 | 1.7276 | 6.9409 |
| 4.00 | 143.6 | 1.0835 | 0.4627 | 604.38 | 2553.4 | 604.81 | 2738.5 | 1.7768 | 6.8963 |
| 5.00 | 151.8 | 1.0925 | 0.3751 | 639.74 | 2561.1 | 640.29 | 2748.6 | 1.8608 | 6.8216 |
| 6.00 | 158.8 | 1.1006 | 0.3158 | 669.96 | 2567.2 | 670.62 | 2756.7 | 1.9313 | 6.7602 |
| 7.00 | 165.0 | 1.1079 | 0.2729 | 696.49 | 2572.2 | 697.27 | 2763.3 | 1.9923 | 6.7081 |
| 8.00 | 170.4 | 1.1147 | 0.2405 | 720.25 | 2576.5 | 721.14 | 2768.9 | 2.0462 | 6.6627 |
| 9.00 | 175.4 | 1.1211 | 0.2150 | 741.84 | 2580.1 | 742.85 | 2773.6 | 2.0947 | 6.6224 |
| 10.00 | 179.9 | 1.1272 | 0.1945 | 761.67 | 2583.2 | 762.80 | 2777.7 | 2.1387 | 6.5861 |
| 11.00 | 184.1 | 1.1329 | 0.1775 | 780.06 | 2585.9 | 781.31 | 2781.2 | 2.1791 | 6.5531 |
| 12.00 | 188.0 | 1.1384 | 0.1633 | 797.23 | 2588.3 | 798.60 | 2784.3 | 2.2165 | 6.5227 |

Table B.2 (continued)

| p (bar) | T (°C) | $v_f \cdot 10^3$ (m ³ /kg) | v_g (m ³ /kg) | u_f (kJ/kg) | u_g (kJ/kg) | h_f (kJ/kg) | h_g (kJ/kg) | s_f (kJ/kg K) | s_g (kJ/kg K) |
|--------------|-------------|--|-------------------------------|------------------|------------------|------------------|------------------|--------------------|--------------------|
| 13.00 | 191.6 | 1.1437 | 0.1513 | 813.37 | 2590.4 | 814.85 | 2787.0 | 2.2514 | 6.4946 |
| 14.00 | 195.1 | 1.1488 | 0.1408 | 828.60 | 2592.2 | 830.21 | 2789.4 | 2.2840 | 6.4684 |
| 15.00 | 198.3 | 1.1538 | 0.1318 | 843.05 | 2593.9 | 844.78 | 2791.5 | 2.3148 | 6.4439 |
| 16.00 | 201.4 | 1.1586 | 0.1238 | 856.81 | 2595.3 | 858.66 | 2793.3 | 2.3439 | 6.4208 |
| 17.00 | 204.3 | 1.1633 | 0.1167 | 869.95 | 2596.5 | 871.93 | 2795.0 | 2.3715 | 6.3990 |
| 18.00 | 207.1 | 1.1678 | 0.1104 | 882.54 | 2597.7 | 884.64 | 2796.4 | 2.3978 | 6.3782 |
| 19.00 | 209.8 | 1.1723 | 0.1047 | 894.63 | 2598.6 | 896.86 | 2797.6 | 2.4230 | 6.3585 |
| 20.00 | 212.4 | 1.1766 | 0.0996 | 906.27 | 2599.5 | 908.62 | 2798.7 | 2.4470 | 6.3397 |
| 25.00 | 224.0 | 1.1973 | 0.0800 | 958.92 | 2602.3 | 961.92 | 2802.2 | 2.5543 | 6.2561 |
| 30.00 | 233.9 | 1.2165 | 0.0667 | 1004.59 | 2603.2 | 1008.2 | 2803.3 | 2.6453 | 6.1856 |
| 35.00 | 242.6 | 1.2348 | 0.0571 | 1045.26 | 2602.9 | 1049.6 | 2802.6 | 2.7250 | 6.1240 |
| 40.00 | 250.4 | 1.2523 | 0.0498 | 1082.18 | 2601.5 | 1087.2 | 2800.6 | 2.7961 | 6.0690 |
| 45.00 | 257.5 | 1.2694 | 0.0441 | 1116.14 | 2599.3 | 1121.9 | 2797.6 | 2.8607 | 6.0188 |
| 50.00 | 264.0 | 1.2861 | 0.0394 | 1147.74 | 2596.5 | 1154.2 | 2793.7 | 2.9201 | 5.9726 |
| 55.00 | 270.0 | 1.3026 | 0.0356 | 1177.39 | 2593.1 | 1184.6 | 2789.1 | 2.9751 | 5.9294 |
| 60.00 | 275.6 | 1.3190 | 0.0324 | 1205.42 | 2589.3 | 1213.3 | 2783.9 | 3.0266 | 5.8886 |
| 65.00 | 280.9 | 1.3352 | 0.0297 | 1232.06 | 2584.9 | 1240.7 | 2778.1 | 3.0751 | 5.8500 |
| 70.00 | 285.9 | 1.3515 | 0.0274 | 1257.52 | 2580.2 | 1267.0 | 2771.8 | 3.1211 | 5.8130 |
| 75.00 | 290.6 | 1.3678 | 0.0253 | 1281.96 | 2575.1 | 1292.2 | 2765.0 | 3.1648 | 5.7774 |
| 80.00 | 295.0 | 1.3843 | 0.0235 | 1305.51 | 2569.6 | 1316.6 | 2757.8 | 3.2066 | 5.7431 |
| 85.00 | 299.3 | 1.4009 | 0.0219 | 1328.27 | 2563.8 | 1340.2 | 2750.1 | 3.2468 | 5.7097 |
| 90.00 | 303.4 | 1.4177 | 0.0205 | 1350.36 | 2557.6 | 1363.1 | 2742.0 | 3.2855 | 5.6771 |
| 95.00 | 307.3 | 1.4348 | 0.0192 | 1371.84 | 2551.1 | 1385.5 | 2733.4 | 3.3229 | 5.6452 |
| 100.0 | 311.0 | 1.4522 | 0.0180 | 1392.79 | 2544.3 | 1407.3 | 2724.5 | 3.3592 | 5.6139 |
| 105.0 | 314.6 | 1.4699 | 0.0170 | 1413.27 | 2537.1 | 1428.7 | 2715.1 | 3.3944 | 5.5830 |
| 110.0 | 318.1 | 1.4881 | 0.0160 | 1433.34 | 2529.5 | 1449.7 | 2705.4 | 3.4288 | 5.5525 |
| 115.0 | 321.5 | 1.5068 | 0.0151 | 1453.06 | 2521.6 | 1470.4 | 2695.1 | 3.4624 | 5.5221 |
| 120.0 | 324.7 | 1.5260 | 0.0143 | 1472.47 | 2513.4 | 1490.8 | 2684.5 | 3.4953 | 5.4920 |
| 125.0 | 327.9 | 1.5458 | 0.0135 | 1491.61 | 2504.7 | 1510.9 | 2673.4 | 3.5277 | 5.4619 |
| 130.0 | 330.9 | 1.5663 | 0.0128 | 1510.55 | 2495.7 | 1530.9 | 2661.8 | 3.5595 | 5.4317 |
| 135.0 | 333.8 | 1.5875 | 0.0121 | 1529.31 | 2486.2 | 1550.7 | 2649.7 | 3.5910 | 5.4015 |
| 140.0 | 336.7 | 1.6097 | 0.0115 | 1547.94 | 2476.3 | 1570.5 | 2637.1 | 3.6221 | 5.3710 |
| 145.0 | 339.5 | 1.6328 | 0.0109 | 1566.49 | 2465.9 | 1590.2 | 2623.9 | 3.6530 | 5.3403 |
| 150.0 | 342.2 | 1.6572 | 0.0103 | 1585.01 | 2455.0 | 1609.9 | 2610.0 | 3.6838 | 5.3091 |
| 155.0 | 344.8 | 1.6828 | 0.0098 | 1603.55 | 2443.4 | 1629.6 | 2595.5 | 3.7145 | 5.2774 |
| 160.0 | 347.4 | 1.7099 | 0.0093 | 1622.17 | 2431.3 | 1649.5 | 2580.2 | 3.7452 | 5.2450 |
| 165.0 | 349.9 | 1.7388 | 0.0088 | 1640.92 | 2418.4 | 1669.6 | 2564.1 | 3.7761 | 5.2119 |
| 170.0 | 352.3 | 1.7699 | 0.0084 | 1659.89 | 2404.8 | 1690.0 | 2547.1 | 3.8073 | 5.1777 |
| 175.0 | 354.7 | 1.8033 | 0.0079 | 1679.18 | 2390.2 | 1710.7 | 2529.0 | 3.8390 | 5.1423 |
| 180.0 | 357.0 | 1.8399 | 0.0075 | 1698.88 | 2374.6 | 1732.0 | 2509.7 | 3.8714 | 5.1054 |
| 185.0 | 359.3 | 1.8801 | 0.0071 | 1719.17 | 2357.7 | 1754.0 | 2488.9 | 3.9047 | 5.0667 |
| 190.0 | 361.5 | 1.9251 | 0.0067 | 1740.22 | 2339.3 | 1776.8 | 2466.3 | 3.9393 | 5.0256 |
| 195.0 | 363.7 | 1.9762 | 0.0063 | 1762.34 | 2319.0 | 1800.9 | 2441.4 | 3.9756 | 4.9815 |
| 200.0 | 365.8 | 2.0357 | 0.0059 | 1785.94 | 2296.2 | 1826.7 | 2413.7 | 4.0144 | 4.9331 |
| 205.0 | 367.9 | 2.1076 | 0.0055 | 1811.76 | 2269.7 | 1855.0 | 2381.6 | 4.0571 | 4.8787 |
| 210.0 | 369.9 | 2.1999 | 0.0050 | 1841.25 | 2237.5 | 1887.5 | 2343.0 | 4.1060 | 4.8144 |
| 215.0 | 371.8 | 2.3362 | 0.0045 | 1878.57 | 2193.9 | 1928.8 | 2291.0 | 4.1684 | 4.7299 |
| 220.9 | 374.1 | 3.1550 | 0.0316 | 2029.60 | 2029.6 | 2099.3 | 2099.3 | 4.4298 | 4.4298 |

Table B.3 Thermodynamics properties of superheated steam.

| T (°C) | v (m ³ /kg) | u (kJ/kg) | h (kJ/kg) | s (kJ/kg K) | T (°C) | v (m ³ /kg) | u (kJ/kg) | h (kJ/kg) | s (kJ/kg K) |
|----------------|-----------------------------|----------------|----------------|------------------|----------------|-----------------------------|----------------|----------------|------------------|
| $p = 0.06$ bar | | | | | $p = 0.35$ bar | | | | |
| 36.17 | 23.739 | 2424.0 | 2566.5 | 8.3283 | 72.67 | 4.531 | 2472.1 | 2630.7 | 7.7148 |
| 80 | 27.133 | 2486.7 | 2649.5 | 8.5794 | 80 | 4.625 | 2483.1 | 2645.0 | 7.7553 |
| 120 | 30.220 | 2544.1 | 2725.5 | 8.7831 | 120 | 5.163 | 2542.0 | 2722.7 | 7.9637 |
| 160 | 33.303 | 2602.2 | 2802.0 | 8.9684 | 160 | 5.697 | 2600.7 | 2800.1 | 8.1512 |
| 200 | 36.384 | 2660.9 | 2879.2 | 9.1390 | 200 | 6.228 | 2659.9 | 2877.9 | 8.3229 |
| 240 | 39.463 | 2720.6 | 2957.4 | 9.2975 | 240 | 6.758 | 2719.8 | 2956.3 | 8.4821 |
| 280 | 42.541 | 2781.2 | 3036.4 | 9.4458 | 280 | 7.287 | 2780.6 | 3035.6 | 8.6308 |
| 320 | 45.620 | 2842.7 | 3116.4 | 9.5855 | 320 | 7.816 | 2842.2 | 3115.8 | 8.7707 |
| 360 | 48.697 | 2905.2 | 3197.4 | 9.7176 | 360 | 8.344 | 2904.8 | 3196.9 | 8.9031 |
| 400 | 51.775 | 2968.8 | 3279.5 | 9.8433 | 400 | 8.872 | 2968.5 | 3279.0 | 9.0288 |
| 440 | 54.852 | 3033.4 | 3362.6 | 9.9632 | 440 | 9.400 | 3033.2 | 3362.2 | 9.1488 |
| 500 | 59.468 | 3132.4 | 3489.2 | 10.134 | 500 | 10.192 | 3132.2 | 3488.9 | 9.3194 |
| $p = 0.7$ bar | | | | | $p = 1.0$ bar | | | | |
| 89.93 | 2.368 | 2493.8 | 2659.5 | 7.4793 | 99.61 | 1.6958 | 2505.5 | 2675.1 | 7.3592 |
| 120 | 2.5709 | 2539.3 | 2719.3 | 7.6370 | 120 | 1.7931 | 2537.0 | 2716.3 | 7.4665 |
| 160 | 2.8407 | 2599.0 | 2797.8 | 7.8272 | 160 | 1.9838 | 2597.5 | 2795.8 | 7.6591 |
| 200 | 3.1082 | 2658.7 | 2876.2 | 8.0004 | 200 | 2.1723 | 2657.6 | 2874.8 | 7.8335 |
| 240 | 3.3744 | 2718.9 | 2955.1 | 8.1603 | 240 | 2.3594 | 2718.1 | 2954.0 | 7.9942 |
| 280 | 3.6399 | 2779.8 | 3034.6 | 8.3096 | 280 | 2.5458 | 2779.2 | 3033.8 | 8.1438 |
| 320 | 3.9049 | 2841.6 | 3115.0 | 8.4498 | 320 | 2.7317 | 2841.1 | 3114.3 | 8.2844 |
| 360 | 4.1697 | 2904.4 | 3196.2 | 8.5824 | 360 | 2.9173 | 2904.0 | 3195.7 | 8.4171 |
| 400 | 4.4342 | 2968.1 | 3278.5 | 8.7083 | 400 | 3.1027 | 2967.7 | 3278.0 | 8.5432 |
| 440 | 4.6985 | 3032.8 | 3361.7 | 8.8285 | 440 | 3.2879 | 3032.5 | 3361.3 | 8.6634 |
| 480 | 4.9627 | 3098.6 | 3446.0 | 8.9434 | 480 | 3.4730 | 3098.3 | 3445.6 | 8.7785 |
| 520 | 5.2269 | 3165.4 | 3531.3 | 9.0538 | 520 | 3.6581 | 3165.2 | 3531.0 | 8.8889 |
| $p = 1.5$ bar | | | | | $p = 3.0$ bar | | | | |
| 111.37 | 1.1600 | 2519.3 | 2693.3 | 7.2234 | 133.55 | 0.6060 | 2543.4 | 2725.2 | 6.9923 |
| 160 | 1.3174 | 2594.9 | 2792.5 | 7.4660 | 160 | 0.6506 | 2586.9 | 2782.1 | 7.1274 |
| 200 | 1.4443 | 2655.8 | 2872.4 | 7.6425 | 200 | 0.7163 | 2650.2 | 2865.1 | 7.3108 |
| 240 | 1.5699 | 2716.7 | 2952.2 | 7.8044 | 240 | 0.7804 | 2712.6 | 2946.7 | 7.4765 |
| 280 | 1.6948 | 2778.2 | 3032.4 | 7.9548 | 280 | 0.8438 | 2775.0 | 3028.1 | 7.6292 |
| 320 | 1.8192 | 2840.3 | 3113.2 | 8.0958 | 320 | 0.9067 | 2837.8 | 3109.8 | 7.7716 |
| 360 | 1.9433 | 2903.3 | 3194.8 | 8.2289 | 360 | 0.9692 | 2901.2 | 3191.9 | 7.9057 |
| 400 | 2.0671 | 2967.2 | 3277.2 | 8.3552 | 400 | 1.0315 | 2965.4 | 3274.9 | 8.0327 |
| 440 | 2.1908 | 3032.0 | 3360.6 | 8.4756 | 440 | 1.0937 | 3030.5 | 3358.7 | 8.1536 |
| 480 | 2.3144 | 3097.9 | 3445.1 | 8.5908 | 480 | 1.1557 | 3096.6 | 3443.4 | 8.2692 |
| 520 | 2.4379 | 3164.8 | 3530.5 | 8.7013 | 520 | 1.2177 | 3163.7 | 3529.0 | 8.3800 |
| 560 | 2.5613 | 3232.9 | 3617.0 | 8.8077 | 560 | 1.2796 | 3231.9 | 3615.7 | 8.4867 |

Table B.3 (continued)

| T (°C) | v (m ³ /kg) | u (kJ/kg) | h (kJ/kg) | s (kJ/kg K) | T (°C) | v (m ³ /kg) | u (kJ/kg) | h (kJ/kg) | s (kJ/kg K) |
|-------------|-----------------------------|----------------|----------------|------------------|-------------|-----------------------------|----------------|----------------|------------------|
| p = 5 bar | | | | | p = 7 bar | | | | |
| 151.86 | 0.3751 | 2561.1 | 2748.6 | 6.8216 | 164.97 | 0.2729 | 2572.2 | 2763.3 | 6.7081 |
| 180 | 0.4045 | 2609.5 | 2811.7 | 6.9652 | 180 | 0.2846 | 2599.6 | 2798.8 | 6.7876 |
| 220 | 0.4449 | 2674.9 | 2897.4 | 7.1463 | 220 | 0.3146 | 2668.1 | 2888.4 | 6.9771 |
| 260 | 0.4840 | 2738.9 | 2980.9 | 7.3092 | 260 | 0.3434 | 2733.9 | 2974.2 | 7.1445 |
| 300 | 0.5225 | 2802.5 | 3063.7 | 7.4591 | 300 | 0.3714 | 2798.6 | 3058.5 | 7.2970 |
| 340 | 0.5606 | 2866.3 | 3146.6 | 7.5989 | 340 | 0.3989 | 2863.2 | 3142.4 | 7.4385 |
| 380 | 0.5985 | 2930.7 | 3229.9 | 7.7304 | 380 | 0.4262 | 2928.1 | 3226.4 | 7.5712 |
| 420 | 0.6361 | 2995.7 | 3313.8 | 7.8550 | 420 | 0.4533 | 2993.6 | 3310.9 | 7.6966 |
| 460 | 0.6736 | 3061.6 | 3398.4 | 7.9738 | 460 | 0.4802 | 3059.8 | 3395.9 | 7.8160 |
| 500 | 0.7109 | 3128.5 | 3483.9 | 8.0873 | 500 | 0.5070 | 3126.9 | 3481.8 | 7.9300 |
| 540 | 0.7482 | 3196.3 | 3570.4 | 8.1964 | 540 | 0.5338 | 3194.9 | 3568.5 | 8.0393 |
| 560 | 0.7669 | 3230.6 | 3614.0 | 8.2493 | 560 | 0.5741 | 3229.2 | 3612.2 | 8.09243 |
| p = 10 bar | | | | | p = 15 bar | | | | |
| 179.91 | 0.1945 | 2583.2 | 2777.7 | 6.5861 | 198.32 | 0.1318 | 2593.9 | 2791.5 | 6.4439 |
| 220 | 0.2169 | 2657.5 | 2874.3 | 6.7904 | 220 | 0.1405 | 2638.1 | 2849.0 | 6.5630 |
| 260 | 0.2378 | 2726.1 | 2963.9 | 6.9652 | 260 | 0.1556 | 2712.6 | 2945.9 | 6.7521 |
| 300 | 0.2579 | 2792.7 | 3050.6 | 7.1219 | 300 | 0.1696 | 2782.5 | 3036.9 | 6.9168 |
| 340 | 0.2776 | 2858.5 | 3136.1 | 7.2661 | 340 | 0.1832 | 2850.4 | 3125.2 | 7.0657 |
| 380 | 0.2970 | 2924.2 | 3221.2 | 7.4006 | 380 | 0.1965 | 2917.6 | 3212.3 | 7.2033 |
| 420 | 0.3161 | 2990.3 | 3306.5 | 7.5273 | 420 | 0.2095 | 2984.8 | 3299.1 | 7.3322 |
| 460 | 0.3352 | 3057.0 | 3392.2 | 7.6475 | 460 | 0.2224 | 3052.3 | 3385.9 | 7.4540 |
| 500 | 0.3541 | 3124.5 | 3478.6 | 7.7622 | 500 | 0.2351 | 3120.4 | 3473.1 | 7.5699 |
| 540 | 0.3729 | 3192.8 | 3565.7 | 7.8721 | 540 | 0.2478 | 3189.2 | 3561.0 | 7.6806 |
| 580 | 0.3917 | 3262.0 | 3653.7 | 7.9778 | 580 | 0.2605 | 3258.8 | 3649.6 | 7.7870 |
| 620 | 0.4105 | 3332.2 | 3742.7 | 8.0797 | 620 | 0.2730 | 3329.4 | 3739.0 | 7.8894 |
| p = 20 bar | | | | | p = 30 bar | | | | |
| 212.42 | 0.0996 | 2599.5 | 2798.7 | 6.3397 | 233.90 | 0.06667 | 2603.2 | 2803.3 | 6.1856 |
| 240 | 0.1084 | 2658.8 | 2875.6 | 6.4937 | 240 | 0.06818 | 2618.9 | 2823.5 | 6.2251 |
| 280 | 0.1200 | 2735.6 | 2975.6 | 6.6814 | 280 | 0.07710 | 2709.0 | 2940.3 | 6.4445 |
| 320 | 0.1308 | 2807.3 | 3068.8 | 6.8441 | 320 | 0.08498 | 2787.6 | 3042.6 | 6.6232 |
| 360 | 0.1411 | 2876.7 | 3158.9 | 6.9911 | 360 | 0.09232 | 2861.3 | 3138.3 | 6.7794 |
| 400 | 0.1512 | 2945.1 | 3247.5 | 7.1269 | 400 | 0.09935 | 2932.7 | 3230.7 | 6.9210 |
| 440 | 0.1611 | 3013.4 | 3335.6 | 7.2539 | 440 | 0.10618 | 3003.0 | 3321.5 | 7.0521 |
| 480 | 0.1708 | 3081.9 | 3423.6 | 7.3740 | 480 | 0.11287 | 3073.0 | 3411.6 | 7.1750 |
| 520 | 0.1805 | 3150.9 | 3511.9 | 7.4882 | 520 | 0.11946 | 3143.2 | 3501.6 | 7.2913 |
| 560 | 0.1901 | 3220.6 | 3600.7 | 7.5975 | 560 | 0.12597 | 3213.8 | 3591.7 | 7.4022 |
| 600 | 0.1996 | 3291.0 | 3690.2 | 7.7024 | 600 | 0.13243 | 3285.0 | 3682.3 | 7.5084 |
| 640 | 0.2091 | 3362.4 | 3780.5 | 7.8036 | 640 | 0.13884 | 3357.0 | 3773.5 | 7.6105 |

| T (°C) | v (m ³ /kg) | u (kJ/kg) | h (kJ/kg) | s (kJ/kg K) | T (°C) | v (m ³ /kg) | u (kJ/kg) | h (kJ/kg) | s (kJ/kg K) |
|-------------|-----------------------------|----------------|----------------|------------------|-------------|-----------------------------|----------------|----------------|------------------|
| p = 40 bar | | | | | p = 60 bar | | | | |
| 250.38 | 0.04978 | 2601.5 | 2800.6 | 6.0690 | 276.62 | 0.03244 | 2589.3 | 2783.9 | 5.8886 |
| 280 | 0.05544 | 2679.0 | 2900.8 | 6.2552 | 280 | 0.03317 | 2604.7 | 2803.7 | 5.9245 |
| 320 | 0.06198 | 2766.6 | 3014.5 | 6.4538 | 320 | 0.03874 | 2719.0 | 2951.5 | 6.1830 |
| 360 | 0.06787 | 2845.3 | 3116.7 | 6.6207 | 360 | 0.04330 | 2810.6 | 3070.4 | 6.3771 |
| 400 | 0.07340 | 2919.8 | 3213.4 | 6.7688 | 400 | 0.04739 | 2892.7 | 3177.0 | 6.5404 |
| 440 | 0.07872 | 2992.3 | 3307.2 | 6.9041 | 440 | 0.05121 | 2970.2 | 3277.4 | 6.6854 |
| 480 | 0.08388 | 3064.0 | 3399.5 | 7.0301 | 480 | 0.05487 | 3045.3 | 3374.5 | 6.8179 |
| 520 | 0.08894 | 3135.4 | 3491.1 | 7.1486 | 520 | 0.05840 | 3119.4 | 3469.8 | 6.9411 |
| 560 | 0.09392 | 3206.9 | 3582.6 | 7.2612 | 560 | 0.06186 | 3193.0 | 3564.1 | 7.0571 |
| 600 | 0.09884 | 3278.9 | 3674.3 | 7.3687 | 600 | 0.06525 | 3266.6 | 3658.1 | 7.1673 |
| 640 | 0.10372 | 3351.5 | 3766.4 | 7.4718 | 640 | 0.06859 | 3340.5 | 3752.1 | 7.2725 |
| 680 | 0.10855 | 3424.9 | 3859.1 | 7.5711 | 680 | 0.07189 | 3414.9 | 3846.3 | 7.3736 |
| p = 80 bar | | | | | p = 100 bar | | | | |
| 295.04 | 0.02352 | 2569.6 | 2757.8 | 5.7431 | 311.04 | 0.01802 | 2544.3 | 2724.5 | 5.6139 |
| 320 | 0.02681 | 2661.7 | 2876.2 | 5.9473 | 320 | 0.01925 | 2588.2 | 2780.6 | 5.7093 |
| 360 | 0.03088 | 2771.9 | 3018.9 | 6.1805 | 360 | 0.02330 | 2728.0 | 2961.0 | 6.0043 |
| 400 | 0.03431 | 2863.5 | 3138.0 | 6.3630 | 400 | 0.02641 | 2832.0 | 3096.1 | 6.2114 |
| 440 | 0.03742 | 2946.8 | 3246.2 | 6.5192 | 440 | 0.02911 | 2922.3 | 3213.4 | 6.3807 |
| 480 | 0.04034 | 3026.0 | 3348.6 | 6.6589 | 480 | 0.03160 | 3005.8 | 3321.8 | 6.5287 |
| 520 | 0.04312 | 3102.9 | 3447.8 | 6.7873 | 520 | 0.03394 | 3085.9 | 3425.3 | 6.6625 |
| 560 | 0.04582 | 3178.6 | 3545.2 | 6.9070 | 560 | 0.03619 | 3164.0 | 3525.8 | 6.7862 |
| 600 | 0.04845 | 3254.0 | 3641.5 | 7.0200 | 600 | 0.03836 | 3241.1 | 3624.7 | 6.9022 |
| 640 | 0.05102 | 3329.3 | 3737.5 | 7.1274 | 640 | 0.04048 | 3317.9 | 3722.7 | 7.0119 |
| 680 | 0.05356 | 3404.9 | 3833.4 | 7.2302 | 680 | 0.04256 | 3394.6 | 3820.3 | 7.1165 |
| 720 | 0.05607 | 3480.9 | 3929.4 | 7.3289 | 720 | 0.04461 | 3471.6 | 3917.7 | 7.2167 |
| p = 120 bar | | | | | p = 140 bar | | | | |
| 324.75 | 0.01426 | 2513.4 | 2684.5 | 5.4920 | 336.75 | 0.01148 | 2476.3 | 2637.1 | 5.3710 |
| 360 | 0.01810 | 2677.1 | 2894.4 | 5.8341 | 360 | 0.01421 | 2616.0 | 2815.0 | 5.6579 |
| 400 | 0.02108 | 2797.8 | 3050.7 | 6.0739 | 400 | 0.01722 | 2760.2 | 3001.3 | 5.9438 |
| 440 | 0.02355 | 2896.3 | 3178.9 | 6.2589 | 440 | 0.01955 | 2868.8 | 3142.5 | 6.1477 |
| 480 | 0.02576 | 2984.9 | 3294.0 | 6.4161 | 480 | 0.02157 | 2963.1 | 3265.2 | 6.3152 |
| 520 | 0.02781 | 3068.4 | 3402.1 | 6.5559 | 520 | 0.02343 | 3050.3 | 3378.3 | 6.4616 |
| 560 | 0.02976 | 3149.0 | 3506.1 | 6.6839 | 560 | 0.02517 | 3133.6 | 3485.9 | 6.5940 |
| 600 | 0.03163 | 3228.0 | 3607.6 | 6.8029 | 600 | 0.02683 | 3214.7 | 3590.3 | 6.7163 |
| 640 | 0.03345 | 3306.3 | 3707.7 | 6.9150 | 640 | 0.02843 | 3294.5 | 3692.5 | 6.8309 |
| 680 | 0.03523 | 3384.3 | 3807.0 | 7.0214 | 680 | 0.02999 | 3373.8 | 3793.6 | 6.9392 |
| 720 | 0.03697 | 3462.3 | 3906.0 | 7.1231 | 720 | 0.03152 | 3452.8 | 3894.1 | 7.0425 |
| 760 | 0.03869 | 3540.6 | 4004.8 | 7.2207 | 760 | 0.03301 | 3532.0 | 3994.2 | 7.1413 |

Table B.3 (*continued*)

| T (°C) | v (m ³ /kg) | u (kJ/kg) | h (kJ/kg) | s (kJ/kg K) | T (°C) | v (m ³ /kg) | u (kJ/kg) | h (kJ/kg) | s (kJ/kg K) |
|-------------|-----------------------------|----------------|----------------|------------------|-------------|-----------------------------|----------------|----------------|------------------|
| p = 160 bar | | | | | p = 180 bar | | | | |
| 347.44 | 0.00931 | 2431.3 | 2580.2 | 5.2450 | 357.06 | 0.00750 | 2374.6 | 2509.7 | 5.1054 |
| 360 | 0.01105 | 2537.5 | 2714.3 | 5.4591 | 360 | 0.00810 | 2418.3 | 2564.1 | 5.1916 |
| 400 | 0.01427 | 2718.5 | 2946.8 | 5.8162 | 400 | 0.01191 | 2671.7 | 2886.0 | 5.6872 |
| 440 | 0.01652 | 2839.6 | 3104.0 | 6.0433 | 440 | 0.01415 | 2808.5 | 3063.2 | 5.9432 |
| 480 | 0.01842 | 2940.5 | 3235.3 | 6.2226 | 480 | 0.01596 | 2916.9 | 3204.2 | 6.1358 |
| 520 | 0.02013 | 3031.8 | 3353.9 | 6.3761 | 520 | 0.01756 | 3012.7 | 3328.8 | 6.2971 |
| 560 | 0.02172 | 3117.9 | 3465.4 | 6.5133 | 560 | 0.01903 | 3101.9 | 3444.5 | 6.4394 |
| 600 | 0.02322 | 3201.1 | 3572.6 | 6.6390 | 600 | 0.02041 | 3187.3 | 3554.8 | 6.5687 |
| 640 | 0.02466 | 3282.6 | 3677.2 | 6.7561 | 640 | 0.02173 | 3270.5 | 3661.7 | 6.6885 |
| 680 | 0.02606 | 3363.1 | 3780.1 | 6.8664 | 680 | 0.02301 | 3352.4 | 3766.5 | 6.8008 |
| 720 | 0.02742 | 3443.3 | 3882.1 | 6.9712 | 720 | 0.02424 | 3433.7 | 3870.0 | 6.9072 |
| 760 | 0.02876 | 3523.4 | 3983.5 | 7.0714 | 760 | 0.02545 | 3514.7 | 3972.8 | 7.0086 |
| p = 200 bar | | | | | p = 240 bar | | | | |
| 365.81 | 0.00588 | 2296.2 | 2413.7 | 4.9331 | | | | | |
| 400 | 0.00995 | 2617.9 | 2816.9 | 5.5521 | 400 | 0.00673 | 2476.0 | 2637.5 | 5.2365 |
| 440 | 0.01223 | 2775.2 | 3019.8 | 5.8455 | 440 | 0.00929 | 2700.9 | 2923.9 | 5.6511 |
| 480 | 0.01399 | 2892.3 | 3172.0 | 6.0534 | 480 | 0.01100 | 2839.9 | 3103.9 | 5.8971 |
| 520 | 0.01551 | 2993.1 | 3303.2 | 6.2232 | 520 | 0.01241 | 2952.1 | 3250.0 | 6.0861 |
| 560 | 0.01688 | 3085.5 | 3423.2 | 6.3708 | 560 | 0.01366 | 3051.8 | 3379.5 | 6.2456 |
| 600 | 0.01817 | 3173.3 | 3536.7 | 6.5039 | 600 | 0.01480 | 3144.6 | 3499.8 | 6.3866 |
| 640 | 0.01939 | 3258.2 | 3646.0 | 6.6264 | 640 | 0.01587 | 3233.3 | 3614.3 | 6.5148 |
| 680 | 0.02056 | 3341.6 | 3752.8 | 6.7408 | 680 | 0.01690 | 3319.6 | 3725.1 | 6.6336 |
| 720 | 0.02170 | 3424.0 | 3857.9 | 6.8488 | 720 | 0.01788 | 3404.3 | 3833.4 | 6.7450 |
| 760 | 0.02280 | 3505.9 | 3961.9 | 6.9515 | 760 | 0.01883 | 3488.2 | 3940.2 | 6.8504 |
| 800 | 0.02388 | 3587.8 | 4065.4 | 7.0498 | 800 | 0.01976 | 3571.7 | 4046.0 | 6.9508 |
| p = 280 bar | | | | | p = 320 bar | | | | |
| 400 | 0.00383 | 2221.7 | 2328.8 | 4.7465 | 400 | 0.00237 | 1981.0 | 2056.8 | 4.3252 |
| 440 | 0.00712 | 2613.5 | 2812.9 | 5.4497 | 440 | 0.00543 | 2509.0 | 2682.9 | 5.2325 |
| 480 | 0.00885 | 2782.7 | 3030.5 | 5.7472 | 480 | 0.00722 | 2720.5 | 2951.5 | 5.5998 |
| 520 | 0.01019 | 2908.9 | 3194.3 | 5.9592 | 520 | 0.00853 | 2863.4 | 3136.2 | 5.8390 |
| 560 | 0.01135 | 3016.8 | 3334.6 | 6.1319 | 560 | 0.00962 | 2980.6 | 3288.4 | 6.0263 |
| 600 | 0.01239 | 3115.1 | 3462.1 | 6.2815 | 600 | 0.01059 | 3084.9 | 3423.8 | 6.1851 |
| 640 | 0.01336 | 3207.9 | 3582.0 | 6.4158 | 640 | 0.01148 | 3182.0 | 3549.4 | 6.3258 |
| 680 | 0.01428 | 3297.2 | 3697.0 | 6.5390 | 680 | 0.01232 | 3274.6 | 3668.8 | 6.4538 |
| 720 | 0.01516 | 3384.4 | 3808.8 | 6.6539 | 720 | 0.01312 | 3364.3 | 3784.0 | 6.5722 |
| 760 | 0.01600 | 3470.3 | 3918.4 | 6.7621 | 760 | 0.01388 | 3452.3 | 3896.4 | 6.6832 |
| 800 | 0.01682 | 3555.5 | 4026.5 | 6.8647 | 800 | 0.01462 | 3539.2 | 4006.9 | 6.7881 |

Table B.4 Thermodynamic properties of air.

| T (K) | h (kJ/kg) | s^0 (kJ/(kg K)) | p_r | v_r | T (K) | h (kJ/kg) | s^0 (kJ/(kg K)) | p_r | v_r |
|------------|----------------|----------------------|--------|--------|------------|----------------|----------------------|-------|--------|
| 200 | 199.97 | 1.29559 | 0.3363 | 1707.0 | 450 | 451.80 | 2.11161 | 5.775 | 223.6 |
| 210 | 209.97 | 1.34444 | 0.3987 | 1512.0 | 460 | 462.02 | 2.13407 | 6.245 | 211.4 |
| 220 | 219.97 | 1.39105 | 0.4690 | 1346.0 | 470 | 472.24 | 2.15604 | 6.742 | 200.1 |
| 230 | 230.02 | 1.43557 | 0.5477 | 1205.0 | 480 | 482.49 | 2.17760 | 7.268 | 189.5 |
| 240 | 240.02 | 1.47824 | 0.6355 | 1084.0 | 490 | 492.74 | 2.19876 | 7.824 | 179.7 |
| 250 | 250.05 | 1.51917 | 0.7329 | 979.0 | 500 | 503.02 | 2.21952 | 8.411 | 170.6 |
| 260 | 260.09 | 1.55848 | 0.8405 | 887.8 | 510 | 513.32 | 2.23993 | 9.031 | 162.1 |
| 270 | 270.11 | 1.59634 | 0.9590 | 808.0 | 520 | 523.63 | 2.25997 | 9.684 | 154.1 |
| 280 | 280.13 | 1.63279 | 1.0889 | 738.0 | 530 | 533.98 | 2.27967 | 10.37 | 146.7 |
| 285 | 285.14 | 1.65055 | 1.1584 | 706.1 | 540 | 544.35 | 2.29906 | 11.10 | 139.7 |
| 290 | 290.16 | 1.66802 | 1.2311 | 676.1 | 550 | 554.74 | 2.31809 | 11.86 | 133.1 |
| 295 | 295.17 | 1.68515 | 1.3068 | 647.9 | 560 | 565.17 | 2.33685 | 12.66 | 127.0 |
| 300 | 300.19 | 1.70203 | 1.3860 | 621.2 | 570 | 575.59 | 2.35531 | 13.50 | 121.2 |
| 305 | 305.22 | 1.71865 | 1.4686 | 596.0 | 580 | 586.04 | 2.37348 | 14.38 | 115.7 |
| 310 | 310.24 | 1.73498 | 1.5546 | 572.3 | 590 | 596.52 | 2.39140 | 15.31 | 110.6 |
| 315 | 315.27 | 1.75106 | 1.6442 | 549.8 | 600 | 607.02 | 2.40902 | 16.28 | 105.8 |
| 320 | 320.29 | 1.76690 | 1.7375 | 528.6 | 610 | 617.53 | 2.42644 | 17.30 | 101.2 |
| 325 | 325.31 | 1.78249 | 1.8345 | 508.4 | 620 | 628.63 | 2.44356 | 18.36 | 96.92 |
| 330 | 330.34 | 1.79783 | 1.9352 | 489.4 | 630 | 638.63 | 2.46048 | 19.84 | 92.84 |
| 340 | 340.42 | 1.82790 | 2.149 | 454.1 | 640 | 649.22 | 2.47716 | 20.64 | 88.99 |
| 350 | 350.49 | 1.85708 | 2.379 | 422.2 | 650 | 659.84 | 2.49364 | 21.86 | 85.34 |
| 360 | 360.58 | 1.88543 | 2.626 | 393.4 | 660 | 670.47 | 2.50985 | 23.13 | 81.89 |
| 370 | 370.67 | 1.91313 | 2.892 | 367.2 | 670 | 681.14 | 2.52589 | 24.46 | 78.61 |
| 380 | 380.77 | 1.94001 | 3.176 | 343.4 | 680 | 691.82 | 2.54175 | 25.85 | 75.50 |
| 390 | 390.88 | 1.96633 | 3.481 | 321.5 | 690 | 702.52 | 2.55731 | 27.29 | 72.56 |
| 400 | 400.98 | 1.99194 | 3.806 | 301.6 | 700 | 713.27 | 2.57277 | 28.80 | 69.76 |
| 410 | 411.12 | 2.01699 | 4.153 | 283.3 | 710 | 724.04 | 2.58810 | 30.38 | 67.07 |
| 420 | 421.26 | 2.40142 | 4.522 | 266.6 | 720 | 734.82 | 2.60319 | 32.02 | 64.53 |
| 430 | 431.43 | 2.06533 | 4.915 | 251.1 | 730 | 745.62 | 2.61803 | 33.72 | 62.13 |
| 440 | 441.61 | 2.08870 | 5.332 | 236.8 | 740 | 756.44 | 2.63280 | 35.50 | 59.82 |
| 750 | 769.29 | 2.64737 | 37.35 | 57.63 | 1300 | 1395.97 | 3.27345 | 330.9 | 11.275 |
| 760 | 778.18 | 2.66176 | 39.07 | 55.54 | 1320 | 1419.76 | 3.29160 | 352.5 | 10.747 |
| 770 | 789.11 | 2.67595 | 41.31 | 53.39 | 1340 | 1443.60 | 3.30959 | 375.3 | 10.247 |
| 780 | 800.03 | 2.69013 | 43.35 | 51.64 | 1360 | 1467.49 | 3.32724 | 399.1 | 9.780 |
| 790 | 810.99 | 2.70100 | 45.55 | 49.86 | 1380 | 1491.44 | 3.34474 | 424.2 | 9.337 |
| 800 | 821.95 | 2.71787 | 47.75 | 48.08 | 1400 | 1515.42 | 3.36200 | 450.5 | 8.919 |
| 820 | 843.98 | 2.74504 | 52.59 | 44.84 | 1420 | 1539.44 | 3.37901 | 478.0 | 8.526 |
| 840 | 866.08 | 2.77170 | 57.60 | 41.85 | 1440 | 1563.51 | 3.39586 | 506.9 | 8.153 |
| 860 | 888.27 | 2.79783 | 63.09 | 39.12 | 1460 | 1587.63 | 3.41217 | 537.1 | 7.801 |
| 880 | 910.56 | 2.82344 | 68.98 | 36.61 | 1480 | 1611.79 | 3.42892 | 568.8 | 7.468 |
| 900 | 932.93 | 2.84856 | 75.29 | 34.31 | 1500 | 1635.97 | 3.44516 | 601.9 | 7.152 |
| 920 | 955.39 | 2.87324 | 82.05 | 32.18 | 1520 | 1660.23 | 3.46120 | 636.5 | 6.854 |
| 940 | 977.92 | 2.89748 | 89.28 | 30.22 | 1540 | 1684.51 | 3.47712 | 672.8 | 6.569 |
| 960 | 1000.55 | 2.92128 | 97.00 | 28.40 | 1560 | 1708.82 | 3.49276 | 710.5 | 6.301 |
| 980 | 1023.25 | 2.94469 | 105.2 | 26.73 | 1580 | 1733.17 | 3.50829 | 750.0 | 6.046 |

Table B.4 (continued)

| T (K) | h (kJ/kg) | s^0 (kJ/(kg K)) | p_r | v_r | T (K) | h (kJ/kg) | s^0 (kJ/(kg K)) | p_r | v_r |
|------------|----------------|----------------------|-------|--------|------------|----------------|----------------------|-------|-------|
| 1000 | 1046.04 | 2.96770 | 114.0 | 25.17 | 1600 | 1757.57 | 3.52364 | 791.2 | 5.804 |
| 1020 | 1068.89 | 2.99034 | 123.4 | 23.72 | 1620 | 1782.00 | 3.53879 | 834.1 | 5.574 |
| 1040 | 1091.85 | 2.99034 | 123.4 | 22.39 | 1640 | 1806.46 | 3.55381 | 878.9 | 5.355 |
| 1060 | 1114.86 | 3.03449 | 143.9 | 21.12 | 1660 | 1830.96 | 3.56867 | 925.3 | 5.147 |
| 1080 | 1137.89 | 3.05608 | 155.2 | 19.98 | 1680 | 1855.50 | 3.58355 | 974.2 | 4.949 |
| 1100 | 1161.07 | 3.07732 | 167.1 | 18.896 | 1700 | 1880.1 | 3.5979 | 1025 | 4.761 |
| 1120 | 1184.28 | 3.09825 | 179.7 | 17.886 | 1750 | 1941.6 | 3.6336 | 1161 | 4.328 |
| 1140 | 1207.57 | 3.11883 | 193.1 | 16.946 | 1800 | 2003.3 | 3.6681 | 1310 | 3.944 |
| 1160 | 1230.92 | 3.13916 | 207.2 | 16.064 | 1850 | 2065.3 | 3.7023 | 1475 | 3.601 |
| 1180 | 1254.34 | 3.15916 | 222.2 | 15.241 | 1900 | 2127.4 | 3.7354 | 1655 | 3.295 |
| 1200 | 1277.79 | 3.17888 | 238.0 | 14.170 | 1950 | 2189.7 | 3.7677 | 1852 | 3.022 |
| 1220 | 1301.31 | 3.19834 | 254.7 | 13.747 | 2000 | 2252.1 | 3.7994 | 2068 | 2.776 |
| 1240 | 1324.93 | 3.21751 | 272.3 | 13.069 | 2050 | 2314.6 | 3.8303 | 2303 | 2.555 |
| 1260 | 1348.55 | 3.21751 | 281.3 | 12.435 | 2100 | 2377.4 | 3.8605 | 2995 | 2.356 |
| 1280 | 1372.24 | 3.25510 | 310.4 | 11.835 | 2150 | 2440.3 | 3.8901 | 2837 | 2.175 |
| | | | | | 2200 | 2503.2 | 3.9191 | 3138 | 2.012 |
| | | | | | 2250 | 2566.4 | 3.9474 | 3464 | 1.864 |

Table B.5 Specific heats of common gases.

| T (K) | CO (kJ/kg K) | CO ₂ (kJ/kg K) | H ₂ (kJ/kg K) | H ₂ O (kJ/kg K) | O ₂ (kJ/kg K) | N ₂ (kJ/kg K) |
|------------|-----------------|------------------------------|-----------------------------|-------------------------------|-----------------------------|-----------------------------|
| 250 | 1.0404 | 0.7957 | 14.1961 | 1.8498 | 0.9094 | 1.0416 |
| 300 | 1.0400 | 0.8482 | 14.3169 | 1.8629 | 0.9178 | 1.0408 |
| 350 | 1.0425 | 0.8961 | 14.4000 | 1.8805 | 0.9289 | 1.0428 |
| 400 | 1.0476 | 0.9398 | 14.4553 | 1.9018 | 0.9421 | 1.0475 |
| 450 | 1.0548 | 0.9796 | 14.4914 | 1.9263 | 0.9565 | 1.0548 |
| 500 | 1.0640 | 1.0156 | 14.5160 | 1.9534 | 0.9717 | 1.0647 |
| 550 | 1.0746 | 1.0482 | 14.5354 | 1.9827 | 0.9871 | 1.0772 |
| 600 | 1.0863 | 1.0777 | 14.5549 | 2.0136 | 1.0022 | 1.0922 |
| 650 | 1.0989 | 1.1044 | 14.5787 | 2.0458 | 1.0167 | 1.1097 |
| 700 | 1.1120 | 1.1285 | 14.6099 | 2.0790 | 1.0304 | 1.1296 |
| 750 | 1.1253 | 1.1504 | 14.6504 | 2.1128 | 1.0430 | 1.1520 |
| 800 | 1.1385 | 1.1702 | 14.7011 | 2.1472 | 1.0545 | 1.1769 |
| 850 | 1.1513 | 1.1884 | 14.7616 | 2.1819 | 1.0648 | 1.2042 |
| 900 | 1.1634 | 1.2051 | 14.8306 | 2.2167 | 1.0741 | 1.2341 |
| 950 | 1.1746 | 1.2207 | 14.9054 | 2.2518 | 1.0823 | 1.2666 |
| 1000 | 1.1846 | 1.2355 | 14.9825 | 2.2870 | 1.0899 | 1.3016 |

Table B.6 Molar specific heats of common gases.

| T (K) | CO (kJ/(kg mol K)) | CO ₂ (kJ/(kg mol K)) | H ₂ (kJ/(kg mol K)) | H ₂ O (kJ/(kg mol K)) | O ₂ (kJ/(kg mol K)) | N ₂ (kJ/(kg mol K)) |
|------------|--------------------------|---------------------------------------|--------------------------------------|--|--------------------------------------|--------------------------------------|
| 250 | 29.1421 | 35.0193 | 28.6194 | 33.3337 | 29.1004 | 29.1760 |
| 300 | 29.1294 | 37.3292 | 28.8628 | 33.5702 | 29.3683 | 29.1533 |
| 350 | 29.1996 | 39.4394 | 29.0304 | 33.8866 | 29.7249 | 29.2086 |
| 400 | 29.3419 | 41.3622 | 29.1419 | 34.2710 | 30.1457 | 29.3399 |
| 450 | 29.5459 | 43.1103 | 29.2148 | 34.7124 | 30.6086 | 29.5453 |
| 500 | 29.8015 | 44.6961 | 29.2642 | 35.2010 | 31.0944 | 29.8234 |
| 550 | 30.0989 | 46.1320 | 29.3033 | 35.7277 | 31.5863 | 30.1727 |
| 600 | 30.4285 | 47.4306 | 29.3426 | 36.2847 | 32.0704 | 30.5923 |
| 650 | 30.7811 | 48.6044 | 29.3906 | 36.8650 | 32.5355 | 31.0816 |
| 700 | 31.1478 | 49.6658 | 29.4535 | 37.4628 | 32.9729 | 31.6401 |
| 750 | 31.5199 | 50.6273 | 29.5352 | 38.0732 | 33.3769 | 32.2677 |
| 800 | 31.8892 | 51.5014 | 29.6374 | 38.6922 | 33.7443 | 32.9646 |
| 850 | 32.2475 | 52.3006 | 29.7594 | 39.3170 | 34.0744 | 33.7310 |
| 900 | 32.5872 | 53.0374 | 29.8984 | 39.9457 | 34.3696 | 34.5679 |
| 950 | 32.9008 | 53.7242 | 30.0493 | 40.5775 | 34.6347 | 35.4761 |
| 1000 | 33.1812 | 54.3736 | 30.2048 | 41.2125 | 34.8772 | 36.4569 |

Table B.7 MATLAB- or GNU/OCTAVE-function for thermodynamic properties of air.

```
% Thermodynamic properties of Air based on the ideal gas model with
% variable specific heats.
%
% By Seppo Korpela
% The code is free on "as is" basis. It is meant for educational purposes.
% Commercial software exists that provides similar functionality.
% I take no responsibility for any errors or if its use causes damage.
% You are free to use, modify and distribute the code as long as you
% acknowledge its authorship.
% Please notify me at korpela.1@osu.edu if you make improvements in it.
%*****
%
% YAir takes two arguments, that are:
% YAir('T',T)
% YAir('h',h)
% YAir('pr',pr)
% YAir('vr',vr)
% YAir('s0',s0)
% It returns the vector [T,h,u,s0,pr,vr] in this order.
% From the calling program this function is invoked by the command, e.g.
%*****
% T1=500;
% [T1,h1,u1,s01,pr1,vr1]=YAir('T',T1)
%
```

Table B.7 (continued)

```

% or
%
% pr1=1.3860;
% [T2s,h2s,u2s,s02,pr2,vr2]=YAir('pr',pr1)
%
% The correlations for the specific heat at constant pressure, c_p(T),
% are from the report by E. W. Lemmon, R. T. Jacobsen, S. Penoncello and
% D. G. Friend, Thermodynamic Properties of Air and Mixtures of Nitrogen,
% Argon, and Oxygen from 60 to 2000 K at pressures to 2000 Mpa, Journal of
% Physical and Chemical Reference Data, 29, 331 (2000).
%*****
function [T,h,u,s0,pr,vr] = YAir(fun,In)
    fun = lower(fun);
    tol=10^-16;
    Tref=300; href=300.19; s0ref=1.70203; pref=1.3860; vref=621.2;
    Rbar=8.31447; M=28.943; R=Rbar/M;
    switch fun
        case 't'
            [T,h,u,s0,pr,vr] = XAir(In);
        case 'h'
            Tf(1)=200; Tf(2)=1500;
            f(1)=href+integral(@cpa,Tref,Tf(1))-In;
            f(2)=href+integral(@cpa,Tref,Tf(2))-In;
            i=2;
            while i < 30
                i=i+1;
                Tf(i)=Tf(i-1)-(f(i-1))*((Tf(i-1)-Tf(i-2))/(f(i-1)-f(i-2)));
                f(i)=href+integral(@cpa,Tref,Tf(i))-In;
                Ta=Tf(i);
                if abs(f(i)-f(i-1)) < tol
                    break
                end
            end
            [T,h,u,s0,pr,vr]=XAir(Ta);
        %
        case 'pr'
            %Secant method
            Tf(1)=200; Tf(2)=1500;
            s0(1)=s0ref+integral(@cpad,Tref,Tf(1));
            s0(2)=s0ref+integral(@cpad,Tref,Tf(2));
            f(1)=pref*exp(s0(1)/R-s0ref/R)-In;
            f(2)=pref*exp(s0(2)/R-s0ref/R)-In;
            i=2;
            while i < 30
                i=i+1;
                Tf(i)=Tf(i-1)-f(i-1))*((Tf(i-1)-Tf(i-2))/(f(i-1)-f(i-2)));
                s0(i)=s0ref+integral(@cpad,Tref,Tf(i));
                f(i)=pref*exp(s0(i)/R-s0ref/R)-In;
                if abs(f(i)-f(i-1)) <= tol
                    break

```

```

        end
        Ta=Tf(i);
    end
    [T,h,u,s0,pr,vr]=XAir(Ta);
%
case 'vr'
%Secant method
    Tf(1)=200; Tf(2)=1000;
    s0(1)=s0ref+integral(@cpad,Tref,Tf(1));
    s0(2)=s0ref+integral(@cpad,Tref,Tf(2));
    pr(1)=pref*exp(s0(1)/R-s0ref/R);
    pr(2)=pref*exp(s0(2)/R-s0ref/R);
    f(1)=vref*(Tf(1)*pref)/(Tref*pr(1))-ln;
    f(2)=vref*(Tf(2)*pref)/(Tref*pr(2))-ln;
    i=2;
    while i < 30
        i=i+1;
        Tf(i)=Tf(i-1)-(f(i-1))*((Tf(i-1)-Tf(i-2))/(f(i-1)-f(i-2))));
        s0(i)=s0ref+integral(@cpad,Tref,Tf(i));
        pr(i)=pref*exp(s0(i)/R-s0ref/R);
        f(i)=vref*(Tf(i)*pref)/(Tref*pr(i))-ln;
        if abs(f(i)-f(i-1)) <= tol
            break
        end
        Ta=Tf(i);
    end
    [T,h,u,s0,pr,vr] = XAir(Ta);
%
case 's0'
    Tf(1)=200; Tf(2)=1500;
    f(1)=s0ref+integral(@cpad,Tref,Tf(1))-ln;
    f(2)=s0ref+integral(@cpad,Tref,Tf(2))-ln;
    i=2;
    while i < 30
        i=i+1;
        Tf(i)=Tf(i-1)-(f(i-1))*((Tf(i-1)-Tf(i-2))/(f(i-1)-f(i-2))));
        f(i)=s0ref+integral(@cpad,Tref,Tf(i))-ln;
        if abs(f(i)-f(i-1)) < tol
            break
        end
        Ta=Tf(i);
    end
    [T,h,u,s0,pr,vr]=XAir(Ta);
%
case 'u'
    Tf(1)=200; Tf(2)=1500;
    f(1)=href+integral(@cpa,Tref,Tf(1))-R*Tf(1)-ln;
    f(2)=href+integral(@cpa,Tref,Tf(2))-R*Tf(2)-ln;

```

```

        i=2;
        while i < 30
            i=i+1;
            Tf(i)=Tf(i-1)-(f(i-1))*((Tf(i-1)-Tf(i-2))/((f(i-1)-f(i-2)))));
            f(i)=href+integral(@cpa,Tref,Tf(i))-R*Tf(i)-In;
            if abs(f(i)-f(i-1))< tol
                break
            end
            Ta=Tf(i);
        end
        [T,h,u,s0,pr,vr]=XAir(Ta);
    otherwise
        error(['Unknown calling function to XAir, ',fun, '...
        See help XAir for valid calling functions\n']);
    end
end
%
function [T,h,u,s0,pr,vr] = XAir(In)
    Rbar=8.314510; M=28.9586; R=Rbar/M;
    Tref=300; href=300.19; s0ref=1.70203; pref=1.3860; vref=621.2;
    T=In;
    s0=s0ref+integral(@cpad,Tref,T);
    h=href+integral(@cpa,Tref,T);
    pr=pref*exp(s0/R-s0ref/R);
    vr= vref*(T*pref)/(Tref*pr);
    u=h-R*T;
end
%
function cp = cpa(T)
    Rbar=8.314510; M=28.9586; R=Rbar/M;
    N1=3.490888032;      N2=2.395525583e-6;
    N3=7.172111248e-9;   N4=-3.115413101e-13;
    N5=0.223806688;      N6=0.791309509;
    N7=0.212236768;      N8=0.197938904;
    N9=3364.011;          N10=2242.45;
    N11=11580.4;
    u= N9./T; v= N10./T; w= N11./T;
    cp = R*(N1+N2*T+N3*T.*T+N4*T.^3+N5*T.^(-1.5)+ ...
        N6*u.^2.*exp(u)./(exp(u)-1).^2+N7*v.^2.*exp(v)./(exp(v)-1).^2+ ...
        (2/3)*N8*w.^2.*exp(-w)./((2/3)*exp(-w)+1).^2);
end
%
function cpd=cpad(T)
    cpd=cpa(T)./T;
end

```

References

1. Agricola, G. (1950). *De Re Metallica* (trans. H.C. Hoover and L.H. Hoover). New York: Dover.
2. Ainley, D.G. (1948). Performance of axial flow turbines. *Proceedings of the Institute of Mechanical Engineers* 159: 230–244.
3. Ainley, D.G. and Mathieson, G.C.R. (1957). A Method for Performance Estimation for Axial-Flow Turbines. Aeronautical Research Council, Reports and Memoranda No. 2974. London: Her Majesty's Stationary Office.
4. Arakeri, V. (1999). Contributions to some cavitation problems in turbomachinery. *Proceedings Academy of Engineering Sciences, India* 24: 454–483.
5. Balje, O.E. (1981). *Turbo Machines: A Guide to Selection and Theory*. New York: Wiley.
6. Baskharone, E.A. (2006). *Principles of Turbomachinery in Air-Breathing Engines*. Cambridge: Cambridge University Press.
7. Bathie, W.W. (1984). *Fundamentals of Gas Turbines*. New York: Wiley.
8. Binnie, A.M. and Woods, M.W. (1938). The pressure distribution in a convergent-divergent steam nozzle. *Proceedings of the Institute of Mechanical Engineers* 138: 229–266.
9. Brennen, C.E. (1994). *Hydrodynamics of Pumps*. White River Junction, VT: Concepts NREC and Oxford University Press.
10. Brennen, C.E. (1995). *Cavitation and Bubble Dynamics*. Oxford University Press.
11. Brown, H. (1954). *The Challenge of Man's Future*. New York: The Viking Press.
12. Burstall, A.F. (1965). *A History of Mechanical Engineering*. Cambridge, MA: MIT Press.
13. Burton, T., Sharpe, D., Jenkins, N., and Bossanyi, E. (2001). *Wind Energy Handbook*. New York: Wiley.

14. Carter, A.D.S. (1950). The Low Speed Performance of Related Airfoils in Cascade. Aeronautical Research Council, CP 29.
15. Cohen, H., Rogers, G.F.C., and Saravanamuttoo, H.I.H. (1972). *Gas Turbine Theory*, 3e. London: Longman Scientific & Technical.
16. Craig, H.R.M. and Cox, H.J.A. (1970). Performance estimation of axial-flow turbines. *Proceedings of the Institute of Mechanical Engineers* 185: 407–424.
17. Csanady, G.T. (1964). *Theory of Turbomachines*. New York: McGraw-Hill.
18. Cumpsty, N.A. (1989). *Compressor Aerodynamics*. London: Longman Scientific & Technical.
19. Cumpsty, N.A. (2003). *Jet Propulsion*. Cambridge: Cambridge University Press.
20. Daugherty, R.L. (1937). *Hydraulics*. New York: McGraw-Hill.
21. Denton, J.D. (1993). Loss mechanisms in turbomachines. *Journal of Turbomachinery* 115: 621–653.
22. Dibelius, G. and Stoff, H. (2011). Strömungsmaschinen. In: *Dubbel, Taschenbuch für Maschinenbau*, 23. Auflage (ed. K.-H. Grote and J. Feldhusen). Springer.
23. Dick, E. (2015). *Fundamentals of Turbomachines*. Dordrecht: Springer.
24. Dixon, S.L. (2005). *Thermodynamics and Fluid Dynamics of Turbomachinery*, 5e. Oxford: Elsevier.
25. Drbal, L.F., Boston, P.G., and Westra, K.L. (1995). *Power Plant Engineering*. Berlin: Springer-Verlag.
26. Dunham, J. and Came, P.M. (1970). Improvements to the Ainley–Mathieson Method of Turbine Performance Prediction, ASME paper 70-GT-2.
27. Eggleston, D.M. and Stoddard, F.S. (1987). *Wind Turbine Engineering Design*. New York: Van Nostrand Reinhold.
28. Froude, W. (1878). On the elementary relation between pitch, slip and propulsive efficiency. *Transactions of the Institute of Naval Architects* 19: 47–57.
29. Fullermann, J. (1962). Centrifugal compressors. In: *Advances in Petroleum Chemistry and Refining, Engineering*, Chapter 8 (ed. J. McKetta). New York: Interscience Publishers.
30. Glassman, A.J. (1976). Computer Program for Design and Analysis of Radial Inflow Turbines. TN-8164. NASA.
31. Glauert, H. (1963). Airplane propellers. In: *Aerodynamic Theory, A General Review of Progress*, vol. 4 (ed. W.F. Durand). New York: Dover.
32. Goldstein, S. (1929). On the vortex theory of screw propellers. *Proceedings of the Royal Society of London Series A* 123: 440–465.
33. Goorjian, P.M. (1972). An invalid equation in the general momentum theory of actuator disk. *AIAA Journal* 10: 543–544.
34. Guha, A. (1992). Jump conditions across normal shock waves in pure vapour-droplet flows. *Journal of Fluid Mechanics* 241: 349–369.
35. Guha, A. (1994). A unified theory of aerodynamic and condensation shock waves in vapor-droplet flows with or without a carrier gas. *Physics of Fluids* 6: 1893–1913.
36. Guha, A. (2007). Shock waves in fluids with interphase transport of mass, momentum and energy (Vapour-droplet mixtures and solid-particle-laden gases. In: *Shock Wave Science and Technology Reference Library*, vol. 1 (ed. M.E.H. van Dongen), 136–186. Berlin, Heidelberg: Springer.

37. Gyarmathy, G. (1966). *Grundlagen Einer Theorie das Nassdampfturbine*, Mitteilung Nr. 6. Institut für Thermische Turbomaschinen, Federal Technical University, Zurich, 1962. English translation by the Foreign Technology Division, FTD-TT-63-785, Air Force Systems Command, Wright Patterson Air Force Base, Ohio.
38. de Haller, P. (1953). Das Verhalten von Tragflügelgittern in Axialverdichtern und in Windkanal. *Bernstoff-Wärmer-Kraft* 5 (10).
39. Hau, E. (2006). *Wind Turbines, Fundamentals, Technologies, Application, Economics*. Berlin: Springer-Verlag.
40. Hawthorne, W.R. (1957). *Elements of Turbine and Compressor Theory*. Gas Turbine Laboratory Note, MIT (quoted by Horlock, in Axial Flow Turbines [41].)
41. Horlock, J.H. (1958). *Axial Flow Compressors*. London: Butterworth & Co.
42. Horlock, J.H. (1966). *Axial Flow Turbines*. London: Butterworth & Co.
43. Howell, A.R. (1942). The Present Basis of Axial Flow Compressor Design, Part I, Cascade Theory and Performance. Aeronautical Research Council, Reports and Memoranda No. 2095. London: Her Majesty's Stationary Office.
44. Howell, A.R. (1945). Design of axial compressors. *Proceedings of the Institution of Mechanical Engineers* 153: 452–462.
45. Howell, A.R. and Bonham, R.P. (1950). Overall and stage characteristics of axial-flow compressors. *Proceedings of the Institution of Mechanical Engineers* 163: 235–248.
46. Hubbert, M.K. (1945). Energy from fossil fuels. *Science* 109: 103–109.
47. Hugoniot, H. (1887). Propagation des mouvements dans les corps et spécialement dans les gaz parfaits. *Journal de l'Ecole Polytechnique* 57: 3.
48. Hunsaker, J.C. and Rightmire, B.G. (1947). *Engineering Applications of Fluid Mechanics*. New York: McGraw-Hill.
49. Huntington, R.A. (1985). Evaluation of polytropic calculation methods for turbomachinery analysis. *ASME Journal of Engineering for Gas Turbines and Power* 107: 872–879.
50. Jackson, R. and Davidson, B.J. (1983). An equation set for non-equilibrium two phase flow, and an analysis of some aspects of choking, acoustic propagation, and losses in low pressure wet steam. *International Journal of Two-Phase Flows* 9: 494–510.
51. Kadambi, V. and Prasad, M. (1977). *An Introduction to Energy Conversion, Vol. III Turbomachinery*. New Delhi: New Age International Publishers.
52. Karrasik, I.J., Messina, J.P., Cooper, P., and Heald, C.C. (2007). *Pump Handbook*. New York: McGraw-Hill.
53. Kearton, W.J. (1931). *Steam Turbine Theory and Practice*. Bath: Pitman and Sons.
54. Keenan, J.H. (1971). *Thermodynamics*. Cambridge: MIT Press.
55. Khalil, I.M., Tabakoff, W., and Hamed, A. (1976). Losses in a radial inflow turbine. *Journal of Fluids Engineering* 98: 364–372.
56. Kirillov, I.I. and Yablonik, R.M. (1968). Fundamentals of the Theory of Turbines Operating On Wet Steam. NASA Technical Translation, NASA TT F-611. Leningrad: Mashinostroyeniye Press.
57. Lewis, R.I. (1996). *Turbomachinery Performance Analysis*. Oxford: Elsevier.
58. Lieblein, S. and Roudebush, W.H. (1956). Theoretical Loss Relation for Low-Speed 2D Cascade Flow. TN 3662. NASA.

59. Logan, E. Jr. (1981). *Turbomachinery; Basic Theory and Applications*. New York: Marcel-Dekker.
60. Lugaresi, A. and Massa, A. (1987). Designing Francis turbines: trends in the last decade. In: *Water Power & Dam Construction*, 23–28. International Water Power and Dam Construction.
61. Maddison, A. (2004). Contours of world economy and the art of macro-measurement 1500–2001, Rugglers lecture. IARIW 28th General Conference, Cork, Ireland.
62. Mallen, M. and Saville, G. (1977). Polytropic Processes in the Performance Prediction of Centrifugal Compressors. Paper C183/77, 89–96. Institution of Mechanical Engineers.
63. Marble, F.E. (1969). Some gasdynamic problems in the flow of condensing vapors. *Astronautica Acta* 14: 585–614.
64. Moody, L.F. *Handbook of Applied Hydraulics*, Section 66, 3e (ed. C.V. Davis and K.E. Sorensen). New York: McGraw-Hill.
65. Moody, L.F. and Zowski, T. (1969). Fluid machinery. In: *Handbook of Applied Hydraulics*, 3e (ed. C.V. Davis and K.W. Sorenson). New York: McGraw-Hill.
66. Mouton, C.A. (2007). Transition between regular and mach reflection in the dual-solution domain. PhD dissertation. California Institute of Technology.
67. Nechleba, M. (1957). *Hydraulic Turbines, Their Design and Equipment*. Prague, Czechoslovakia: Artia.
68. Patel, Y., Patel, G., and Turunen-Saaresti, T. (2015). Influence of turbulence modeling on non-equilibrium condensing flows in nozzle and turbine cascade. *International Journal of Heat and Mass Transfer* 88: 165–180.
69. Pfleiderer, C. *Die Wasserturbinen, mit einem Anhang über Strömungsgetriebe*. Hannover: Wolfenbütteler Verlag-Anst.
70. Pfleiderer, C. and Petermann, H. (1986). *Strömungsmaschinen*. Berlin: Springer-Verlag.
71. Prandtl, L. (1919). Schraubenpropeller mit geringstem Energieverlust, Nachrichten Mathematischphysikalische Klasse, Göttingen, Germany (Appendix to the article of A. Betz).
72. Prasad, U.S., Ajay, V.S., Rajat, R.H., and Samanya, S. (2017). Aerodynamics analysis over double wedge airfoil, *Frontiers in Automobile and Mechanical Engineering. IOP Conference Series: Materials Science and Engineering* 197: 012076.
73. Rankine, W. (1865). On the mechanical principles of propellers. *Transactions of the Institute of Naval Architects* 6: 13–30.
74. Rankine, W. (1870). On the thermodynamic theory of waves of finite longitudinal disturbances. *Philosophical Transactions of the Royal Society of London* 160: 27.
75. Rodgers, C. and Geiser, R. (1987). Performance of a high-efficiency radial/axial turbine. *ASME Journal of Turbomachinery* 109: 151–154.
76. Rohlik, H. (1975). Radial-inflow turbines. In: *Turbine Design and Applications*, SP290 (ed. A.J. Glassman), 31–58. NASA.
77. Rolls Royce (2005). *The Jet Engine*. London: Rolls-Royce plc.
78. Rotty, R.M. (1962). *Introduction to Gas Dynamics*. New York: Wiley.
79. Rudinger, G. (1964). Some properties of shock relations in gas flows carrying small particles. *Physics of Fluids* 7: 658–663.
80. Savonius, S.J. (1931). The S-rotor and its applications. *Mechanical Engineering* 53 (5): 333–338.
81. Schweiger, F. and Gregory, J. (1987). *Developments in the Design of Kaplan Turbines*. Water Power & Dam Construction.

82. Shepherd, D.G. (1995). Historical development of the windmill. In: *Wind Turbine Technology* (ed. D.A. Spera). New York: ASME Press.
83. Shultz, J.M. (1962). The polytropic analysis of centrifugal compressors. *ASME Journal of Engineering for Power* 84 (1): 69–82.
84. Smith, S.F. (1965). A simple correlations of turbine efficiency. *Journal of Royal Aeronautical Society* 69: 467–470.
85. Smith, L.H. Jr. (1970). Casing boundary layers in multistage compressors. In: *Proceedings of the Symposium on Flow Research on Blading* (ed. L.S. Dzung). Burlington, MA: Elsevier.
86. Soderberg, C.R. (1948). *Unpublished Notes of the Gas Turbine Laboratory*. Cambridge, MA: MIT (quoted by Horlock [42]).
87. Stanitz, J.D. (1952). Some theoretical aerodynamic investigations of impellers in radial and mixed-flow centrifugal compressors. *ASME Transactions, Series A* 74: 473–497.
88. Starzmann, J., Casey, M.V., and Meyer, J.F. (2011). Unsteady numerical study of wet steam flow in a low pressure steam turbine. In: *High Performance Computing in Science and Engineering '11* (ed. W.E. Nagel, D.B. Kroner, and M.M. Resch), 437–450. Springer-Verlag.
89. Stodola, A. (1945). *Steam and Gas Turbines*, 6e. New York: P. Smith.
90. Traupel, W. (1971). *Thermische Turbomachinen*, 2e. Springer.
91. US-DOE (2017). International Energy Outlook 2017, Released (14 September).
92. Vincenti, W.G. and Kruger, C.H. (1967). *Introduction to Physical Gas Dynamics*. New York: Wiley.
93. Volkovitch, J. (1973). Analytical prediction of vortex ring boundaries for helicopters in steep descents. *Journal of American Helicopter Society* 17 (3): 13–19.
94. Whitfield, A. (1990). The preliminary design of radial inflow turbines. *Journal of Turbomachinery* 112 (1): 50.
95. Whitfield, A. and Baines, N.C. (1990). *Design of Radial Turbomachines*. Essex: Longman Scientific and Technical.
96. Wiesner, F.J. (1967). A review of slip factors for centrifugal compressors. *Journal of Engineering Power* 89: 558–572.
97. Wilson, D.G. and Korakianitis, T. (1998). *Design of High-Efficiency Turbomachinery and Gas Turbines*, 2e. Upper Saddle River, NJ: Prentice-Hall.
98. Wilson, R.E. and Lissaman, P.B.E. (1974). *Applied Aerodynamics of Wind Power Machines*. Oregon State University.
99. Wirzenius, A. (1978). *Keskipakopumput (Centrifugal Pumps*, 3e. Finland: Kustannusyhymä, Tampere (in Finnish).
100. Wislicenus, G.F. (1965). *Fluid Mechanics of Turbomachinery*, vol. 1, 2e. Dover.
101. World Energy Council (2016). World Energy Resources - 2016. www.worldenergy.org (accessed 29 December 2019).
102. Wróblewski, W., Dykas, S., and Gardzilewicz, A. (2009). Numerical and experimental investigations in the LP part of a large power turbine. *Journal of Fluids Engineering* 131: 041301–041311.
103. Yeoh, C.C. and Young, J.B. (1984). Nonequilibrium throughflow analyses of low-pressure, wet steam turbines. *Journal of Engineering for Gas Turbines and Power* 106: 716–724.
104. Young, J.B. (1992). Two-dimensional, non-equilibrium, wet steam calculations for nozzles and turbine cascades. *Journal of Turbomachinery* 114: 569–579.

105. Young, J.B. and Guha, A. (1991). Normal shock-wave structure in two-phase vapor-droplet flows. *Journal of Fluid Mechanics* 228: 243–274.
106. Young, J.B., Yau, K.K., and Walters, P.T. (1988). Fog droplet deposition and coarse water formation in low-pressure steam turbines: a combined experimental and theoretical analysis. *Journal of Turbomachinery* 110: 163–172.
107. Zhang, G., Zhang, S., Zhou, Z., Li, Y., Wang, L., Liu, C. (2017). Numerical study of condensing flow based on the modified method. *Applied Thermal Engineering* 127: 1206–1214.
108. Zimmerman, R.H. (1989). *Lecture Notes on Turbomachinery*. Columbus, OH: The Ohio State University.
109. Zweifel, O. (1945). The spacing of turbomachinery blading, especially with large angular deflection. *Brown Boveri Review* 32: 12.

Index

- actuator disk, 508
- advance ratio, 520
- Ainley–Mathieson correlation
 - profile losses, 293
 - secondary losses, 295
- air tables, 30
- axial compressor
 - 50% reaction, 317
 - blade-loading coefficient, 312
 - cascade, 343
 - deflection, 318
 - de Haller criterion, 318
 - design deflection, 3, 231
 - diffusion factor, 333
 - flow angles, 317
 - flow coefficient, 312
 - flow deviation, 349
 - free vortex defined, 326
 - free vortex design, 319, 327
 - illustration of a modern multistage, 12
 - Lieblein diffusion factor, 334
 - multistage reheat factor, 351
 - off-design operation, 324
 - optimum diffusion, 349
 - other losses, 339, 348
 - performance characteristics, 324
 - polytropic efficiency, 351
 - pressure ratio, 311, 314
 - radial equilibrium, 326
 - reaction, 315
 - solidity, 323
 - stage efficiency, 341
 - stage stagnation temperature rise, 313
 - static enthalpy loss coefficients, 341
 - tangent-difference formula, 323
 - typical range for blade-loading coefficient, 312
 - typical range of flow coefficient, 312
 - work-done factor for multistage compressors, 352
- axial turbine
 - 0% reaction stage, 262
 - 50% reaction stage, 258
 - Ainley–Mathieson correlation, 253, 254
 - constant mass flux, 274
 - fixed nozzle angle, 273
 - flow angles, 255
 - flow coefficient, 254
 - free vortex design, 269
 - hub-to-casing ratio, 216
 - multistage reheat factor, 303
 - off-design operation, 264
 - performance characteristics, 285
 - polytropic efficiency, 304
 - pressure ratio, 280
 - radial equilibrium, 267
 - reaction, 254
 - secondary losses, 296
 - Smith chart, 285
 - Soderberg loss coefficients, 276
 - stage, 249
 - stage efficiency, 277
 - stage stagnation temperature drop, 265
 - stagnation pressure losses for a stage, 280
 - Zweifel correlation, 291

- balance principle defined, 46
- blade element theory, 312, 316
 - axial turbine, 254
 - defined, 184
- blade shapes
 - axial compressor, 344
 - Francis turbine, 478
 - single-stage steam turbine, 231
- boundary layer
 - displacement thickness, 335
 - momentum thickness, 335
- British gravitational units, 13
- buckets, 232
- bulb turbine, 466
 - specific speed, 467
- casing, 248
- cavitation
 - hydraulic turbines, 486
 - pumps, 404
- centrifugal compressor
 - blade height, 386
 - characteristics, 382
 - choking of inducer, 379
 - diffusion ratio, 385
 - history, 12
 - inducer, 364
 - natural-gas transmission, 5
 - optimum inducer angle, 375
 - slip, 366
 - vaneless diffuser, 387
- centrifugal pump
 - cavitation, 404
 - Cordier diagram, 395
 - efficiency, 392, 394
 - flow and loading coefficients, 395
 - history, 12
 - industrial uses, 6
 - specific diameter, 395
 - specific speed, 395
 - total head, 391
 - vaneless diffuser, 407
 - volute design, 407
- choking, 71, 87
 - axial compressor, 325
- chord and axial chord, 248
- Colebrook formula for friction, 82, 472
- combustion
 - specific heat of gases, 36
 - theoretical air, 35
- compressible flow
 - area change, 68
 - choked flow, 71
 - converging–diverging nozzle, 87
 - converging nozzle, 72
 - Fanno flow with area change, 83
 - friction in nozzle flow, 73
 - Mach waves, 100
 - over-expanded, 88
 - speed of sound, 64
 - underexpanded, 88
- compressor
 - characteristics of a radial inflow turbine, 209
 - choking, 209
 - computer software EES, 22
 - condensation shocks, 167
 - conservation principle defined, 46
 - Cordier diagram, 205, 395
 - corrected flow rate, 208
- Dalton's model for a mixture of ideal gases, 33
- Darcy friction factor, 82
- diffusion ratio
 - centrifugal compressor, 385
 - radial inflow turbine, 454
- double-suction pump, 394
- efficiency
 - axial compressor stage, 316
 - axial turbine stage, 277
 - centrifugal compressor, 371
 - centrifugal pump, 392
 - hydraulic turbine, 467
 - nozzle, 81
 - polytropic, 73, 304, 351
 - pressure-compounded steam turbine stage, 230
 - radial inflow turbine, 417, 422
 - Rankine cycle, 215
 - rotor, 219
 - steam power plant, 217
 - total-to-static, 38, 219
 - total-to-total, 37
- electricity production, 2
- endwalls, 248
- energy engineering, 2
- energy resources
 - biomass, 1
 - fossil fuels, 1
 - hydraulic, 463
 - wind energy, 507
- enthalpy
 - relative stagnation, 316
 - stagnation, 17
- Euler equation for turbomachinery, 182
- fan angle, 115
- Fanning friction factor, 82, 83
- Fanno flow, 82
 - stagnation pressure loss, 85
- fifty percent (50%) reaction stage, 258
- flow coefficient, 184, 199
 - axial compressor, 316
 - axial turbine, 254
- flow function, 69
- flow work, 17
- fluid coupling
 - advantages, 491
 - efficiency, 493
 - flow rate, 494
 - losses, 494
 - partially filled, 496

- primary, 491
- secondary, 491
- toroidal shape, 492
- torque coefficient, 496
- Francis turbine, 466, 475
 - specific speed, 467
- friction factor
 - Colebrook, 82
 - Darcy, 82
 - Fanning, 82
- gas turbine
 - electricity generation, 4
 - industrial, 11
 - jet engine history, 10
- Gibbs–Dalton model for ideal gases, 34
- Helmholtz vortex theorem, 532
- hub, 248
- hydraulic turbine
 - bulb turbine, 466
 - capacity factor, 4
 - crossflow or Banki–Mitchell turbine, 486
 - effective head, 464
 - electricity generation, 5
 - Francis turbine, 466, 475, 478
 - gross head, 464
 - history, 8
 - Kaplan turbine, 466, 483, 484
 - mechanical efficiency, 465
 - overall efficiency, 464
 - Pelton wheel, 466
 - pit turbine, 475
 - power-specific speed, 466
 - synchronous speed, 467
 - turgo, 486
 - volumetric efficiency, 465
- IFR-turbine, 416
- incompressible fluid
 - internal energy and irreversibility, 36
 - stagnation pressure, 36, 46
- induced and forced draft, 41
- induction factor, 511
- internal heating, 44
- jet engine
 - gas generator, 311
 - history, 11
 - spool, 311
- Kaplan turbine, 466
 - number of blades, 484
 - specific speed, 467
- kinetic theory of specific heats for gases, 28
- Lieblein diffusion factor, 334
- Mach number, 65
- manometer formula, 200
- mass conservation principle, 16
- meridional velocity, 178
- mixing and pressure change, 56
- Mollier diagram, 24
- moment of momentum balance, 181
- momentum equation, 48
- nondimensional groups, 199
- normal shock, 88, 90
- nozzle
 - efficiency, 81
 - polytropic process, 74
 - static enthalpy loss coefficient, 77
 - velocity coefficient, 77
- nuclear fuels—uranium and thorium, 1
- oblique shock, 88
- off-design operation of an axial turbine, 264
- overexpanded flow, 88
- Pelton wheel, 466
 - number of buckets, 468
 - specific speed, 467
- Pfleiderer correlation for pumps, 394
- pitch, 248
- polytropic efficiency, 304, 351
- positive-displacement machine, 2
- power-absorbing machine, 2
- power coefficient, 201
- power-producing machine, 2
- power ratio of a radial inflow turbine, 417
- power-specific speed, 466
- Prandtl–Meyer theory, 112
- pressure compounding, 226
- pressure ratio
 - axial compressor, 314
 - axial turbine, 258
 - steam turbine, 216
- pressure recovery partial, 53
- pressure side of blade, 333
- primary energy production
 - wind energy, 507
- radial equilibrium
 - axial compressor, 326
 - axial turbine, 258
 - constant mass flux, 274
 - first power exponent for axial compressor, 331
 - fixed nozzle angle, 273
 - zero-power exponent, 330
- radial inflow turbine, 415, 416
 - Balje diagram, 426
 - blade height, 455
 - characteristics, 210
 - efficiency, 422
 - gap loss coefficients, 436
 - minimum exit Mach number, 450
 - number of blades, 456
 - optimum incidence, 456
 - optimum inlet, 442

- radius ratio, 453
- recommended diffusion, 454
- specific diameter, 426
- specific speed, 426
- stator flow, 432
- stator loss coefficients, 436
- typical design parameters, 431
- Rankine combined vortex wake, 521
- reaction
 - axial compressor, 316
 - axial turbine, 254
 - definition, 189
 - in terms of kinetic energies, 189
- reheat factor
 - axial compressor, 351
 - axial turbine, 303
- relaxation times for steam, 144
- renewable energy, 1
- Reynolds number, 199
- rothalpy, 187
- rotor efficiency
 - centrifugal compressor, 368
- scale effect, 199
- scaling analysis, 198
- shape parameter, 202
- shock
 - normal, 88, 90
 - Rankine–Hugoniot relations, 95
 - shock relations, 93
 - strength, 97
 - wet steam, 161
- similitude, 198
- slip, 366
- slip stream, 508
- sonic state, 69
- specific diameter
 - centrifugal pump, 395
 - radial inflow turbine, 426
- specific speed, 202
 - centrifugal pump, 395
 - hydraulic turbines, 466, 467
 - radial inflow turbine, 426
- speed of sound, 65, 146
 - influence of molecular mass, 65
 - influence of relaxation in wet steam, 149
- spouting velocity, 419
- stage
 - axial compressor, 313
 - axial turbine, 249
 - normal, 184, 249, 254, 266
 - repeating, 184, 254, 266
- stagnation density, 66
- stagnation pressure, 66
 - low Mach number, 66
- stagnation pressure loss and entropy, 47
- stagnation pressure losses
 - axial turbine, 280
 - profile losses for axial compressor, 338
- stagnation state
 - defined, 37
- stagnation temperature, 65
- static enthalpy loss coefficients, 222
- steam
 - computer software EES, 22
 - equation of state, 22
 - MATLAB, 22
 - Mollier diagram, 24
 - supersaturation, 25
 - Wilson line, 25, 168
 - Zeuner equation, 29, 135
- steam tables, 22
- steam turbine, 3
 - blade shape, 232
 - electricity production, 2
 - history, 10
 - nozzle coefficient, 218
 - pressure compounding, 226
 - rotor efficiency, 219
 - single-stage impulse, 217
 - single-stage optimum blade speed, 224
 - Soderberg correlation, 241
 - types, 216
 - velocity compounding, 233
 - zero-reaction stage, 239
- streamline curvature method, 539
- subsonic flow defined, 65
- suction side of blade, 248, 333
- supercritical and ultra-supercritical steam cycle, 3
- supersaturation, 168
- supersonic flow defined, 65
- swirl velocity, 250
- thermodynamics
 - compressed liquid, 26
 - equation of state for air, 29
 - equation of state for steam, 22
 - first law, 17
 - Gibbs equations, 20
 - ideal gas, 27
 - ideal gas mixtures, 32
 - incompressible fluid, 36
 - second law, 19
- three-dimensional flow
 - axial compressor, 326
 - axial turbine, 267
- tip clearance and leakage flow, 249
- torque converter
 - efficiency, 499, 501
 - torque multiplication, 497
- transonic flow defined, 65
- trothalpy, 187
- turbocharger, 208
- turbomachine
 - definition of, 2
 - history, 7
 - household use, 6
 - names of components, 2
- Tygun formula, 468
- undercooled
 - subcooled, 168
- underexpanded flow, 88

- unloading of a blade, 333
- utilization
 - definition, 191
 - maximum, 192
 - relation to reaction, 192
- variable specific heats, 29, 42
- velocity compounding, 233
- velocity triangle, 178
 - flow angles of absolute and relative velocity, 178
 - law of cosines, 179
 - law of sines, 179
- ventilating blower, 41
- volute, 407
- water wheel history, 7
- Wilson line, 25
- wind energy
 - capacity factor, 507
 - Denmark, 507
 - Germany, 507
 - installed capacity, 5
 - United States, 507
- windmill, 507
- wind turbine, 507
 - actuator disk, 509
 - American windmill, 9
 - axial induction factor, 511
 - Betz limit, 512
 - blade element theory, 522
 - blade element theory of W. Froude, 508
 - blade forces for a nonrotating wake, 522
 - capacity factor, 5
 - Darrieus rotor, 9
 - ducted turbine, 514
 - Glauert theory for an ideal turbine, 530
 - history, 8
 - induction factors for an irrotational wake, 521
 - momentum theory, 509
 - momentum theory of W. J. M. Rankine, 508
 - operation as a propeller, 513
 - power coefficient, 511
 - Prandtl's tip correction, 532
 - pressure drop across the actuator disk, 510
 - Savonius rotor, 9
 - tip speed ratio, 512, 520
 - turbine efficiencies, 512
 - velocity at the actuator disk, 510
 - wake rotation, 516, 525
- work coefficient, 200
- zero percent (0%) reaction, 239, 262
- Zweifel correlation, 291

WILEY END USER LICENSE AGREEMENT

Go to www.wiley.com/go/eula to access Wiley's ebook EULA.